ISSN 0021-9673

VOL. 475 JULY 28, 1989
COMPLETE IN ONE ISSUE

including
Int. Symp. on Chromatography
Rehovot, November 14–17, 1988

JOURNAL OF CHROMATOGRAPHY

INTERNATIONAL JOURNAL ON CHROMATOGRAPHY, ELECTROPHORESIS AND RELATED METHODS

JOURNAL OF CHROMATOGRAPHY

Scope. The *Journal of Chromatography* publishes papers on all aspects of chromatography, electrophoresis and related methods. Contributions consist mainly of research papers dealing with chromatographic theory, instrumental development and their applications. The section *Biomedical Applications*, which is under separate editorship, deals with the following aspects: developments in and applications of chromatographic and electrophoretic techniques related to clinical diagnosis or alterations during medical treatment; screening and profiling of body fluids or tissues with special reference to metabolic disorders; results from basic medical research with direct consequences in clinical practice; drug level monitoring and pharmacokinetic studies; clinical toxicology; analytical studies in occupational medicine.

Submission of Papers. Papers in English, French and German may be submitted, in three copies. Manuscripts should be submitted to: The Editor of *Journal of Chromatography*, P.O. Box 681, 1000 AR Amsterdam, The Netherlands, or to: The Editor of *Journal of Chromatography, Biomedical Applications*, P.O. Box 681, 1000 AR Amsterdam, The Netherlands. Review articles are invited or proposed by letter to the Editors. An outline of the proposed review should first be forwarded to the Editors for preliminary discussion prior to preparation. Submission of an article is understood to imply that the article is original and unpublished and is not being considered for publication elsewhere. For copyright regulations, see below.

Subscription Orders. Subscription orders should be sent to: Elsevier Science Publishers B.V., P.O. Box 211, 1000 AE Amsterdam, The Netherlands, Tel. 5803 911, Telex 18582 ESPA NL. The *Journal of Chromatography* and the *Biomedical Applications* section can be subscribed to separately.

Publication. The *Journal of Chromatography* (incl. *Biomedical Applications*) has 37 volumes in 1989. The subscription prices for 1989 are:

J. Chromatogr. + *Biomed. Appl.* (Vols. 461–497):
Dfl. 6475.00 plus Dfl. 999.00 (p.p.h.) (total *ca.* US$ 3737.00)

J. Chromatogr. only (Vols. 461–486):
Dfl. 5200.00 plus Dfl. 702.00 (p.p.h.) (total *ca.* US$ 2951.00)

Biomed. Appl. only (Vols. 487–497):
Dfl. 2200.00 plus Dfl. 297.00 (p.p.h.) (total *ca.* US$ 1248.50).

Our p.p.h. (postage, package and handling) charge includes surface delivery of all issues, except to subscribers in Argentina, Australia, Brasil, Canada, China, Hong Kong, India, Israel, Malaysia, Mexico, New Zealand, Pakistan, Singapore, South Africa, South Korea, Taiwan, Thailand and the U.S.A. who receive all issues by air delivery (S.A.L. — Surface Air Lifted) at no extra cost. For Japan, air delivery requires 50% additional charge; for all other countries airmail and S.A.L. charges are available upon request. Back volumes of the *Journal of Chromatography* (Vols. 1–460)are available at Dfl. 195.00 (plus postage). Claims for missing issues will be honoured, free of charge, within three months after publication of the issue. Customers in the U.S.A. and Canada wishing information on this and other Elsevier journals, please contact Journal Information Center, Elsevier Science Publishing Co. Inc., 655 Avenue of the Americas, New York, NY 10010. Tel. (212) 633-3750.

Abstracts/Contents Lists published in Analytical Abstracts, ASCA, Biochemical Abstracts, Biological Abstracts, Chemical Abstracts, Chemical Titles, Chromatography Abstracts, Current Contents/Physical, Chemical & Earth Sciences, Current Contents/Life Sciences, Deep-Sea Research/Part B: Oceanographic Literature Review, Excerpta Medica, Index Medicus, Mass Spectrometry Bulletin, PASCAL-CNRS, Referativnyi Zhurnal and Science Citation Index.

See inside back cover for Publication Schedule, Information for Authors and information on Advertisements.

0021-9673/89/$03.50

Printed in The Netherlands

CONTENTS

(Abstracts/Contents Lists published in Analytical Abstracts, ASCA, Biochemical Abstracts, Biological Abstracts, Chemical Abstracts, Chemical Titles, Chromatography Abstracts, Current Contents/Physical, Chemical & Earth Sciences, Current Contents/Life Sciences, Deep-Sea Research/Part B: Oceanographic Literature Review, Excerpta Medica, Index Medicus, Mass Spectrometry Bulletin, PASCAL-CNRS, Referativnyi Zhurnal and Science Citation Index)

INTERNATIONAL SYMPOSIUM ON CHROMATOGRAPHY, REHOVOT, NOVEMBER 14–17, 1988

(Continued overleaf)

(Continued overleaf)

Contents (continued)

In articles with more than one author, the name of the author to whom correspondence should be addressed is indicated in the article heading by a 6-pointed asterisk (*)

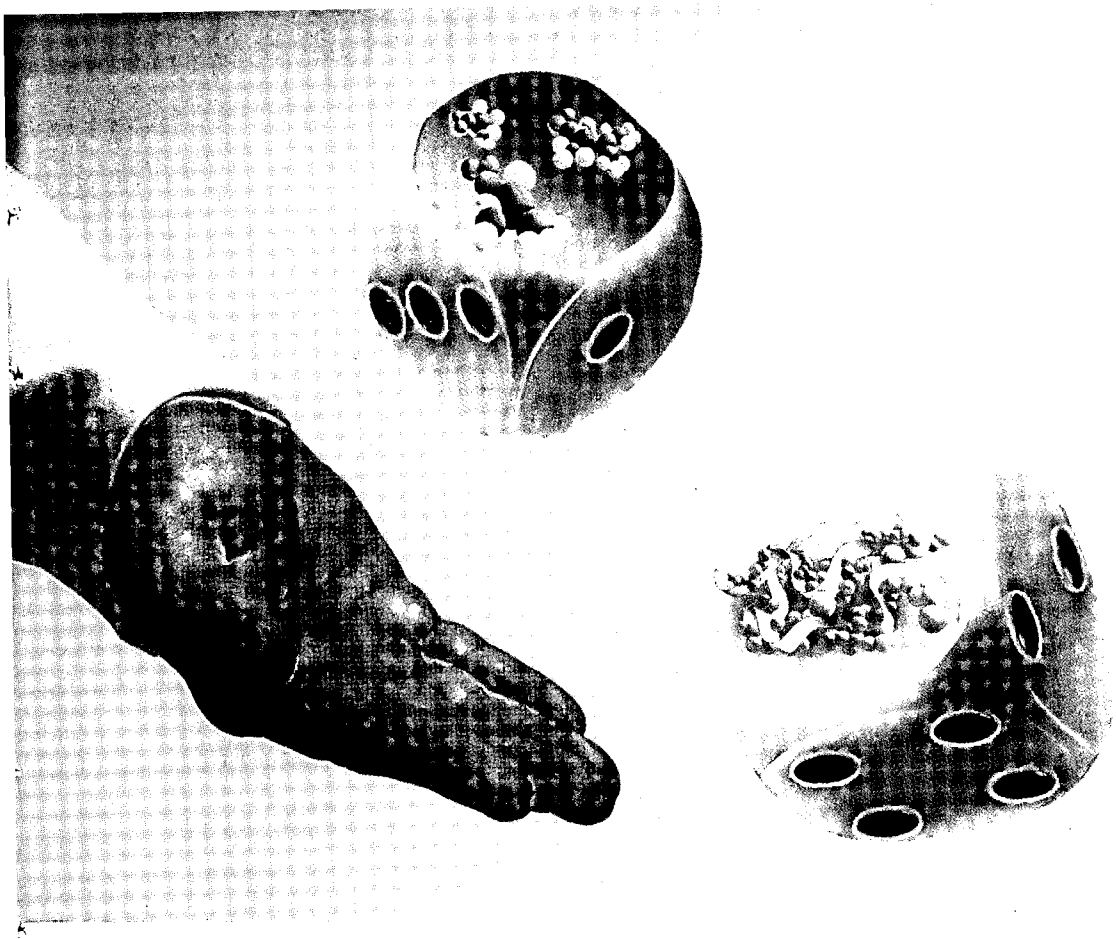

Why gamble with your biomolecules?

Why take chances with your biomolecular separations when you can invest in the new HPLC systems and products Designed for the Biochemist?

By meeting the rigid requirements of the biochemical working environment, which demands minimal maintenance and maximum sensitivity and recovery, DfB takes the risk out of biomolecule separation.

Reliable, reproducible results are assured, because HPLC DfB sets the highest possible standard for the separation of biomolecules, such as peptides and amino acids. Advanced, new detection technology and low pulsation pumps provide the high sensitivity that this work demands.

Inert solvent delivery assures reliability, and the new HPLCmanager software provides total system control and ease of use. HPLC DfB is also the perfect complement to our toprated FPLC® System for protein chromatography.

Contact your nearest representative and ask about the new DfB systems. It's a safe investment that you won't regret.

We help you manage biomolecules.

Pharmacia

Pharmacia LKB Biotechnology

1110

Head office Sweden Tel 46 (018) 163000. **Australia** Tel (02) 8883622. **Austria** Tel (0222) 6866250. **Belgium** Tel (02) 2424660. **Brazil** Tel 55-11 284 5815/289 8967. **Canada** Tel (514) 457 6661. **Denmark** Tel (02) 265200. **East Europe** Tel 43 (0222) 921607. **Federal Republic of Germany** Tel (0761) 49030. **Finland** Tel (90) 5021077. **France** Tel (01) 30643400. **Great Britain** Tel (0908) 661101. **Holland** Tel (031) 348077911. **India** Tel (0812) 29634. **Italy** Tel (02) 25324844/26700475. **Japan** Tel (03) 4929181. **Norway** Tel (02) 549095. **Soviet Union** Tel 46 (08) 799800. **Spain** Tel (34)-3675 44 11. **Sweden** Tel (08) 799800. **Switzerland** Tel (01) 821 1816. **United States** Tel (201) 457 8000. **Far East** Tel 852 (5) 814 8421. **Middle East** Tel 30 (1) 894 7396. **Other countries** Tel 46 (08) 799800. *(8904)*

JOURNAL OF CHROMATOGRAPHY

VOL. 475 (1989)

JOURNAL *of* CHROMATOGRAPHY

INTERNATIONAL JOURNAL ON CHROMATOGRAPHY, ELECTROPHORESIS AND RELATED METHODS

ELSEVIER

AMSTERDAM — OXFORD — NEW YORK — TOKYO

Part of map of Asian Turkey, made in 1748 by Robert. The biblical Rehovot (Gen. 26, 22) was 1000 km further to the south than the present city. However, the main centre of learning was moved after the destruction of the second temple (in the year 70 A.D.) from Jerusalem to a small city called Yavne, which is just a few kilometres to the west of modern Rehovot. Thus, this geographical location (some 15 km to the southeast of Jaffa, which is shown on the map) has been connected with learning for nearly two millenia.

0021-9673/89/$03.50

Printed in The Netherlands

SYMPOSIUM ISSUE

INTERNATIONAL SYMPOSIUM ON CHROMATOGRAPHY

Rehovot (Israel), November 14–17, 1988

Guest Editor

E. GIL-AV
(Rehovot)

CONTENTS

INTERNATIONAL SYMPOSIUM ON CHROMATOGRAPHY, REHOVOT, NOVEMBER 14–17, 1988

Journal of Chromatography, 475 (1989) 1–11
Elsevier Science Publishers B.V., Amsterdam — Printed in The Netherlands

CHROM. 21 201

STUDY OF THE REPRESENTATION OF COMPETITIVE ISOTHERMS AND OF THE INTERSECTION BETWEEN ADSORPTION ISOTHERMS

BINGCHANG LIN, ZIDU MA, SADRODDIN GOLSHAN-SHIRAZI and GEORGES GUIOCHON*
**Department of Chemistry, University of Tennessee, Knoxville, TN 37996-1600, and Division of Analytical Chemistry, Oak Ridge National Laboratory, Oak Ridge, TN 37831-6120 (U.S.A.)*

SUMMARY

Theoretical investigations of the separation of the components of a mixture by preparative liquid chromatography require a knowledge of the competitive equilibrium isotherms of the components of the mixture between the two phases of the chromatographic system. In many instances the set of competitive Langmuir equations provide a satisfactory model. When the competitive isotherms of the two components of a binary mixture intersect each other, however, the Langmuir model becomes unsuitable. This model postulates constant selectivity for the equilibrium between the two phases of a chromatographic system.

A modified Langmuir model is proposed, using the ratio between two second-degree polynomials. This model is supported by general results from statistical mechanics. It accounts well for some experimental data that could not be explained in terms of the Langmuir isotherm.

INTRODUCTION

Recently, the competitive adsorption isotherms of *cis*- and *trans*-androsterone between silica (Partisil-10; Whatman, Clifton, NJ, U.S.A.) modified with a pH 6.8 phosphate buffer[1] and acetonitrile–chloroform (10:90, 15:85 and 20:80) solutions were determined at 5, 15 and 25°C[2]. The single-component isotherms and the chromatographic behaviour of mixtures of these isomers were studied by Gonzalez *et al.*[3]. When the measurements were carried out at constant relative concentrations of the two isomers, and for a certain range of composition of the isomer mixture and of the mobile phase, the isotherms intersected each other. This phenomenon may explain the unusual band profiles observed when the column is strongly overloaded. Depending on the sample size and composition, the elution order is different. With relatively small sample sizes *cis*-androsterone is eluted first, whereas with large sample sizes it is eluted last.

This phenomenon may not be exceptional. When two compounds are closely eluted in a given chromatographic system, it is the larger, bulkier and/or heavier one that interacts more strongly with the stationary phase. Hence the slope of its adsorption isotherm is larger, and it is the more retained at low concentrations.

0021-9673/89/$03.50

However, at higher concentrations, it is the same larger, heavier compound that occupies the greatest area on the adsorbent surface, and hence for which the column capacity is the smaller. Consequently, for two closely related compounds of different shape, the larger (or the flatter) molecule tends to exhibit the isotherm with the steeper tangent at the origin and the lower asymptote. As a consequence, the isotherms must cross each other at some point, and we have a situation comparable to that experienced with the androsterone isomers.

In such an event, the classical Langmuir isotherm cannot account correctly for the experimental results[2]. We propose here an improved Langmuir model, based on the assumption that the kinetics of adsorption and desorption are a linear function of each of the concentrations of the two compounds in the mobile phase. The experimental data obtained previously for *cis*- and *trans*-androsterone are fitted on the equation obtained.

THEORY

The classical Langmuir model for multi-component isotherms is as follows:

$$q_i = \frac{a_i c_i}{1 + \sum_{j=1}^{n} b_j c_j} \qquad i = 1, 2, \ldots, n \tag{1}$$

where q_i and c_i are the concentrations of the compounds studied in the stationary phase and the mobile phase, respectively.

For two components, the selectivity, α, of the phase equilibrium is defined as

$$\alpha = \frac{q_2/c_2}{q_1/c_1} \tag{2}$$

Obviously, for a Langmuir isotherm the selectivity is constant and equal to the ratio a_2/a_1. Consequently, the Langmuir model cannot account for experimental results where the selectivity changes with increasing concentration of the components of the mixture in the mobile phase. It certainly cannot account for changes in the selectivity order observed when the isotherms determined at constant relative concentration, c_2/c_1, cross each other at a certain intermediate value of the concentration. Another approach is necessary and a more complex isotherm than the classical Langmuir model must be used.

General statistical mechanics background

The following derivation (see the next section) can be justified by some general considerations of statistical thermodynamics[4]. It is well known that the concentration of the solute in the stationary phase, q_i, is proportional to the average number of molecules present in the stationary phase at equilibrium, *i.e.*, to N_i. It has been shown[4] that this number is given by

$$N_i = \lambda_i \cdot \frac{\partial \ln \Xi}{\partial \lambda_i} \tag{3}$$

where Ξ is the grand partition function of the system:

$$\Xi = \sum_{N_1} \ldots \sum_{N_k} Q(N_1, N_2, \ldots, N_k) \prod_{j=1}^{k} \lambda_j^{N_j} \tag{4}$$

Accordingly, the competitive isotherms are best represented by the ratio of two polynomials. When $k = 2$, *i.e.*, with two components,

$$\Xi = 1 + Q_1\lambda_1 + Q_2\lambda_2 + Q_{12}\lambda_1\lambda_2 + Q_{11}\lambda_1^2 + Q_{22}\lambda_2^2 + \ldots \tag{5}$$

where Q_i and Q_{ij} are canonical partition functions and λ_i is the activity of component i. If the activity is small, Ξ can be approximated by a second-order polynomial. Obviously $\lambda_i(\partial\Xi/\partial\lambda_i)$ is also a polynomial. From the above discussion, for multi-component systems the denominator of the competitive isotherm equation for each component should be the same.

Hence on a general basis, statistical mechanics predicts that competitive isotherms for multi-component systems are best represented by the ratio of two polynomials. The denominators of the isotherms are the same for all compounds. A set of second-degree polynomials is probably the best compromise between model errors (which decrease with increasing degree of the polynomial) and adjustment errors (which become significant in the fitting of experimental data with equations that have too many parameters).

The modified Langmuir model

To account for competitive multi-component adsorption, we propose to modify the Langmuir model by assuming that the rates of adsorption and desorption of each of the compounds studied are linear functions of the concentrations of both compounds in the stationary phase (rate of adsorption) and in the mobile phase (rate of desorption). This assumption permits molecular interactions in both the solution and the sorbed monolayer to be taken into account.

The corresponding kinetic equations for the two compounds involved are written as follows[5]:

$$\frac{\partial q_1}{\partial t} = K_{a1}(q_s - \alpha_{11}q_1 - \alpha_{12}q_2)c_1 - K_{d1}(c_s - \beta_{11}c_1 - \beta_{12}c_2)q_1 \tag{6}$$

$$\frac{\partial q_2}{\partial t} = K_{a2}(q_s - \alpha_{21}q_1 - \alpha_{22}q_2)c_2 - K_{d2}(c_s - \beta_{21}c_1 - \beta_{22}c_2)q_2 \tag{7}$$

where K_a and K_d are the rates of adsorption and desorption, respectively, q_i and c_i are the concentrations of the two components of the mixture used in the stationary phase and the mobile phase, respectively, q_s and c_s are the saturation concentrations in the stationary and mobile phase, respectively, and t is time.

The values of α_{ij} and β_{ij} depend on the size of the molecules of the solvent(s) and solutes involved and on the strength of the interactions between these molecules. The classical case of the competitive Langmuir isotherm corresponds to $\alpha_{ij} = 1$ and $\beta_{ij} = 0$, for all combinations of i and j.

Equilibrium between the mobile phase and the stationary phase is reached when the concentrations of the two compounds are constant. Thus, we have

$$\frac{\partial q_i}{\partial t} = 0 \qquad i = 1, 2 \tag{8}$$

Combination of eqns. 6–8 gives a system of two linear equations with two unknowns, q_1 and q_2. The classical solution of this system is

$$q_1 = \frac{\Delta_1}{\Delta}; \qquad q_2 = \frac{\Delta_2}{\Delta} \tag{9}$$

where Δ, Δ_1 and Δ_2 are the three determinants of the coefficients of the system of equations:

$$\Delta = b_0 + b_1 c_1 + b_2 c_2 + b_{11} c_1^2 + b_{22} c_2^2 \tag{10}$$

$$\Delta_1 = a_1 c_1 + a_{12} c_1 c_2 + a_{11} c_1^2 \tag{11}$$

and

$$\Delta_2 = a_2 c_2 + a_{21} c_1 c_2 + a_{22} c_1^2 \tag{12}$$

The values of the different coefficients in these three equations are the following:

$$b_0 = K_{d1} K_{d2} c_s^2 \tag{13a}$$

$$b_1 = K_{a1} K_{d2} \alpha_{11} c_s - K_{d1} K_{d2} \beta_{21} c_s - K_{d1} K_{d2} \beta_{11} c_s \tag{13b}$$

$$b_2 = K_{a2} K_{d1} \alpha_{22} c_s - K_{d1} K_{d2} \beta_{12} c_s - K_{d1} K_{d2} \beta_{22} c_s \tag{13c}$$

$$b_{12} = K_{a1} K_{a2} (\alpha_{11} \alpha_{22} - \alpha_{12} \alpha_{21}) + K_{d1} K_{d2} \beta_{11} \beta_{22} + K_{d1} K_{d2} \beta_{12} \beta_{21} - K_{a1} K_{d2} \alpha_{11} \beta_{22} - K_{a2} K_{d1} \alpha_{22} \beta_{11} \tag{13d}$$

$$b_{11} = K_{d1} K_{d2} \beta_{11} \beta_{21} - K_{a1} K_{d2} \alpha_{11} \beta_{21} \tag{13e}$$

$$b_{22} = K_{d1} K_{d2} \beta_{12} \beta_{22} - K_{d1} K_{a2} \beta_{12} \alpha_{22} \tag{13f}$$

$$a_1 = K_{a1} K_{d2} c_s q_s \tag{14a}$$

$$a_{12} = K_{a1} K_{a2} q_s \alpha_{22} - K_{a1} K_{a2} \alpha_{12} q_s - K_{a1} K_{d2} q_s \beta_{22} \tag{14b}$$

$$a_{11} = -K_{a1} K_{d2} q_s \beta_{21} \tag{14c}$$

$$a_2 = K_{a2} K_{d1} c_s q_s \tag{14d}$$

$$a_{21} = K_{a1}K_{a2}q_s\alpha_{11} - K_{a1}K_{a2}\alpha_{21}q_s - K_{a2}K_{d1}q_s\beta_{11} \tag{14e}$$

$$a_{22} = -K_{a2}K_{d1}q_s\beta_{12} \tag{14f}$$

If one divides all the coefficients in the sets 10 and 11 above by the first coefficient, b_0, and let

$$K_{ij} = \frac{k_{ij}}{b_0} \tag{15}$$

where k_{ij} represents any of the coefficients a_i, a_{ij}, b_i or b_{ij}, except b_0, we may now write the equations for the two competitive isotherms of the modified Langmuir equation:

$$q_1 = \frac{A_1c_1 + A_{12}c_1c_2 + A_{11}c_1^2}{1 + B_1c_1 + B_2c_2 + B_{12}c_1c_2 + B_{11}c_1^2 + B_{22}c_2^2} \tag{16}$$

and

$$q_2 = \frac{A_2c_2 + A_{21}c_1c_2 + A_{22}c_2^2}{1 + B_1c_1 + B_2c_2 + B_{12}c_1c_2 + B_{11}c_1^2 + B_{22}c_2^2} \tag{17}$$

When $\alpha_{ij} = 1$ and $\beta_{ij} = 0$. eqns. 16 and 17 reduce to eqn. 1, the conventional Langmuir isotherm. In the general case, the two isotherm equations depend on eleven parameters, which is too many for most practical applications. It becomes very difficult to determine these parameters accurately using the conventional fitting techniques. Convergence is not assured and is rarely achieved. It would be useful, for most practical applications, to reduce the number of independent parameters in eqns. 16 and 17. We observe that four of these parameters, A_{11}, A_{22}, B_{11} and B_{22}, depend only on the original coefficients β_{12} and β_{21} and become zero if these coefficients of the kinetic equation are zero. These coefficients account for the influence of the concentration of one component of the binary mixture on the rate of desorption of the other; we can neglect this interaction, as a first approximation. We then obtain the following extension of the Langmuir equations:

$$q_1 = \frac{A_1c_1 + A_{12}c_1c_2}{1 + B_1c_1 + B_2c_2 + B_{12}c_1c_2} \tag{18}$$

and

$$q_2 = \frac{A_2c_2 + A_{21}c_1c_2}{1 + B_1c_1 + B_2c_2 + B_{12}c_1c_2} \tag{19}$$

This system is simpler than the previous one. Nevertheless, it contains seven constants, which cannot be predicted from first principles and have to be determined by a least-square fitting of the experimental data on eqns. 18 and 19. In addition to the terms of the classical Langmuir equations, it contains only cross terms, accounting for

interactions between the two components of the mixture studied. The coefficients depend on the rate constants of the adsorption and the desorption of the two components, and on the α and β coefficients, which account for molecular interactions.

One of the major advantages of the isotherm equations derived above (eqns. 16 and 17) is that the coefficients in these equations are related to the rate constants (eqns. 6 and 7). This relationship also justifies the simplification which leads from eqns. 16 and 17 to eqns. 18 and 19.

Least-square fitting

We discuss here the fitting procedure of the experimental data with eqns. 18 and 19. We have taken the data regarding the competitive adsorption isotherms of *cis*- and *trans*-androsterone measured previously[2], and fitted them with eqns. 18 and 19. The least-square fitting of data on a non-linear model for a multi-component system can be considered as a multi-variant, multi-objective, non-linear programming problem. Although the field of theoretical results in non-linear programming is rich and many methods are available, solving practical problems remains difficult.

TABLE I

FITTING OF THE FIRST COMPOUND

Note: convergence criterion met.

Non-linear least-squares summary statistics; dependent variable Q_1:

Source	*Degrees of freedom*	*Sum of squares*	*Mean square*
Regression	5	110763.94687	22152.78937
Residual	18	5.84413	0.32467
Uncorrected total	23	110769.79100	
Corrected total	22	50460.28589	

Parameter	*Estimate*	*Asymptotic std. error*	*Asymptotic 95% confidence interval*	
			Lower	*Upper*
A_1	8.5604	0.1041	8.3417	8.7791
A_{12}	−0.0031	0.0233	−0.0520	0.0457
B_1	0.0160	0.0012	0.0135	0.0185
B_2	0.0157	0.0042	0.0068	0.0246
B_{12}	0.0001	0.0001	−0.0001	0.0003

Asymptotic correlation matrix of the parameters:

Correlation	A_1	A_{12}	B_1	B_2	B_{12}
A_1	1.0000	0.1521	0.6052	0.3757	−0.2676
A_{12}	0.1521	1.0000	−0.6304	0.9646	0.8617
B_1	0.6052	−0.6304	1.0000	−0.4415	−0.8980
B_2	0.3757	0.9646	−0.4415	1.0000	0.7102
B_{12}	−0.2676	0.8617	−0.8980	0.7102	1.0000

We have defined our problem as the search for the set of parameters which minimizes the value of the following function:

$$\sum_{k=1}^{n} [y_{1,k} - F_1(a_i,b_i) + y_{2,k} - F_2(a_i,b_i)]^2 \tag{20}$$

where $y_{i,k}$ ($i = 1, 2$) is the concentration of component i in the stationary phase, determined during the measurement number k, n is the number of experimental points and $F_i(a_i,b_i)$ is the right-hand side of eqn. 17 ($i = 1$) or 15 ($i = 2$).

The reason for selecting this criterion is as follows. Let

$$y_1 = F_1(a_i,b_i) + \varepsilon_1 \tag{21}$$

and

$$y_2 = F_2(a_i,b_i) + \varepsilon_2 \tag{22}$$

where ε_i ($i = 1,2$) are the errors made in the estimate of the concentration in

TABLE II

FITTING OF THE SECOND COMPOUND

Note: convergence criterion met.

Non-Linear least squares summary statistics; dependent variable Q_2:

Source	*Degrees of freedom*	*Sum of squares*	*Mean square*
Regression	2	92218.884725	46109.442362
Residual	21	108.826675	5.182223
Uncorrected total	23	92327.711400	
Corrected total	22	39940.694774	

Parameter	*Estimate*	*Asymptotic std. error*	*Asymptotic 95% confidence interval*	
			Lower	*Upper*
A_2	8.7174	0.1502	8.4050	9.0298
A_{21}	−0.0195	0.0075	−0.0351	−0.0039

Asymptotic correlation matrix of the parameters:

Correlation	A_2	A_{21}
A_2	1.000	−0.909
A_{21}	−0.909	1.000

the stationary phase. The condition chosen is equivalent to the minimization of $\sum_{k=1}^{n} (\varepsilon_{1,k} + \varepsilon_{2,k})^2$.

From the experimental procedure[2], it is obvious that both sets of errors, $\varepsilon_{1,k}$ and $\varepsilon_{2,k}$, which have the same origin, are statistically equivalent. Accordingly, the procedure followed here will give an estimate of the parameters of the isotherm equations which is statistically equivalent to that obtained by minimizing the error made in the estimate for each component separately.

RESULTS

The results are reported in Tables I and II and Figs. 1–4. They were obtained using the SAS computer program package.

Tables I and II show the results determined by the SAS program for the isotherm of the first and second components, respectively. Using the values of the parameters in these tables, we calculated the theoretical isotherms corresponding to the three sets of

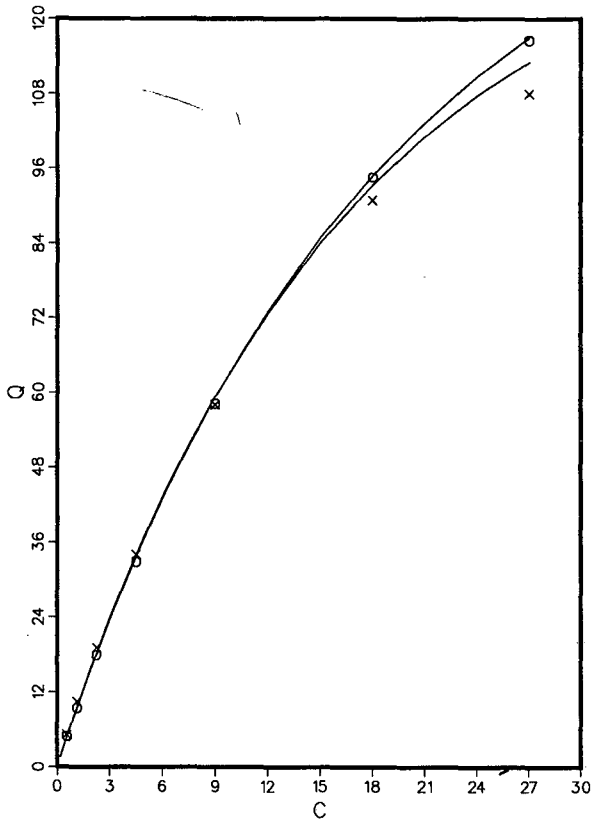

Fig. 1. Comparison between the experimental isotherm data (points) measured by frontal analysis, using solutions of constant relative composition of the two isotherms, and the result of the least-square fitting of these data with eqns. 18 and 19. O, *cis*-; +, *trans*-Androsterone. Relative concentrations, *cis*- to *trans*-androsterone = 1:1. Concentrations in mg/ml.

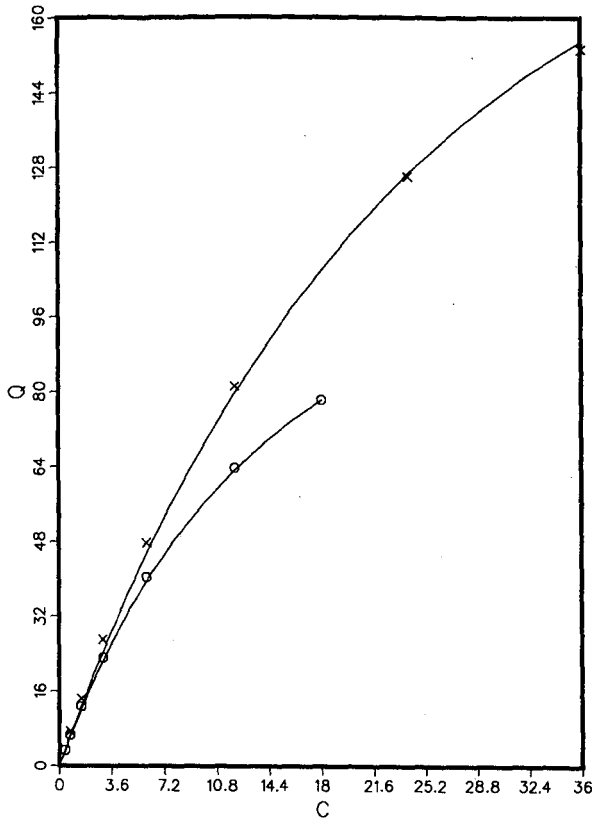

Fig. 2. As Fig. 1 with relative concentrations *cis*- to *trans*-androsterone = 1:2.

data points which had been determined previously[2]. These sets are obtained by frontal analysis[6], using increasingly concentrated steps of binary mixtures of the two isomers with constant relative concentrations of the two isomers (2:1, 1:1 and 1:2).

The calculated isotherms and the data points are plotted on Figs. 1–3. There is good agreement between the experimental data and the calculated isotherms (see the statistical data in the tables and figures). The model permits a good representation of the experimental results obtained at high concentrations, which is not surprising with 7 degrees of freedom instead of 4 for a Langmuir isotherm. The agreement between the model and the experimental data is less good at low concentrations, however. The relative retention determined from the retention times of very small size samples of the two androsterones isomers is 1.2; the model gives $\alpha_2/\alpha_1 = 1.02$ instead. All attempts at forcing the least-square fit procedure to give a larger ratio A_2/A_1 in order to obtain a larger relative retention at low concentrations gave poor fits of the experimental data at high concentrations. This lack of a good fit between the experimental data and the model would create problems in the simulation of the elution and separation of large-size samples of binary mixtures of these isomers.

Fig. 4 shows a three-dimensional plot of the two isotherms, in a space (C_1, C_2,

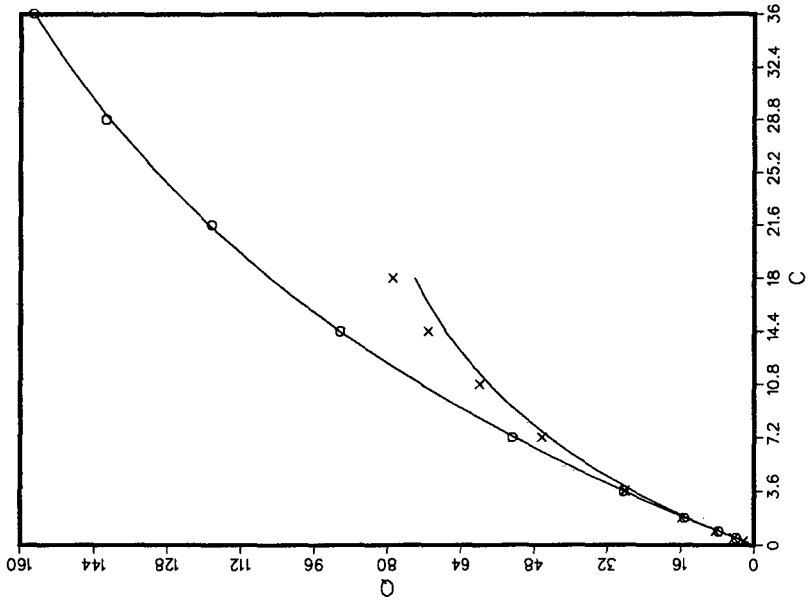

Fig. 3. As Fig. 1 with relative concentrations *cis*- to *trans*-androsterone = 2:1.

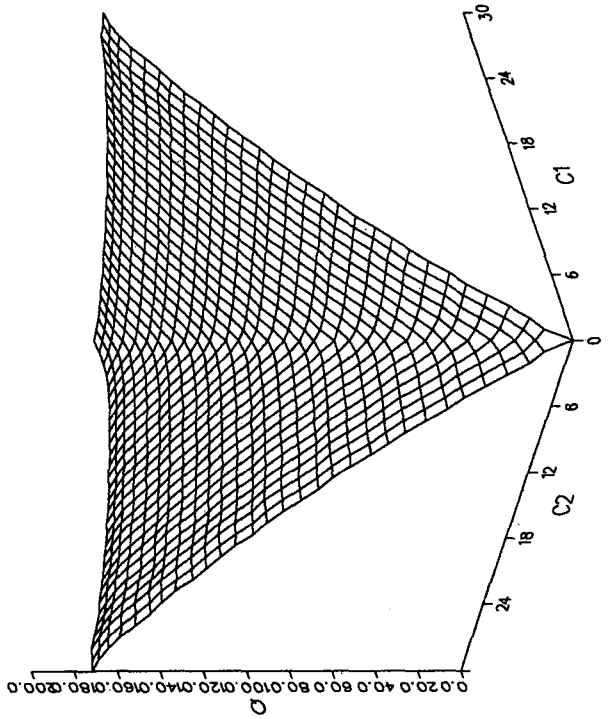

Fig. 4. Three-dimensional plot of the two component isotherms, showing the slightly twisted intersection line.

Q_i). The isotherms of the two isomers in a vertical plane ($C_2/C_1 = a$) intersect because the curve which is the intersection between the two isotherm surfaces is twisted and not planar. The Langmuir isotherm predicts a planar intersection between these two surfaces and could not be used to account for experimental results in this instance[2].

REFERENCES

1 R. Schwarzenbach, *J. Chromatogr.*, 202 (1980) 397.
2 J. X. Huang and G. Guiochon, *J. Colloid Interface Sci.*, 128 (1989) 577.
3 M. J. Gonzalez, A. Jaulmes, P. Valentin and C. Vidal-Madjar, *J. Chromatogr.*, 386 (1986) 333.
4 T. L. Hill, *An Introduction of Statistical Thermodynamics*, Addison-Wesley, London, 1962.
5 G. B. Whitham, *Linear and Non-linear Waves*, Wiley, New York, 1974.
6 S. Golshan-Shirazi, S. Ghodbane and G. Guiochon, *Anal. Chem.*, 60 (1988) 2630.

Journal of Chromatography, 475 (1989) 13–21
Elsevier Science Publishers B.V., Amsterdam — Printed in The Netherlands

CHROMSYMP. 1622

MICROCOLUMN LIQUID CHROMATOGRAPHY OF SMALL NUCLEIC ACID CONSTITUENTS

J. FRED BANKS, Jr. and MILOS V. NOVOTNY*
Department of Chemistry, Indiana University, Bloomington, IN 47405 (U.S.A.)

SUMMARY

Mixtures of small nucleic acid fragments were separated by reversed-phase microcolumn liquid chromatography. By using a miniaturized UV detector, a detection limit of 10 pg with a signal-to-noise ratio of 2 for individual nucleosides was achieved. Various mixtures of nucleobases, nucleosides, nucleotides, and cyclic nucleotides were separated. Using tetrabutylammonium hydrogensulfate as an ion-pairing reagent, the negatively charged mono-, di-, and triphosphate nucleotides were also resolved. As an application for nucleic acid research, the separation of the enzymatic hydrolysis products from a 100-ng sample of tRNA-Phe is shown.

INTRODUCTION

Recent advances in genetic and biochemical research mandate improved methods for the separation and analysis of nucleic acid fragments, including their basic constituents, such as nucleobases, nucleosides, and nucleotides. Liquid chromatography (LC) with UV detection has been utilized for the analysis of low-molecular-weight nucleic acid fragments. The powerful role of this method is evidenced by a number of reviews on the subject[1–3]. While conventional high-performance liquid chromatography (HPLC) has obviously been very useful for the research on nucleic acids, there are instances where its miniaturized version, microcolumn LC, can facilitate further advances in terms of high efficiency and increased mass sensitivity for sample-limited situations. The general analytical advantages of microcolumn LC have been pointed out in recent review articles[4–7]. The purpose of this communication is to demonstrate, on several selected examples, certain merits of this method in the chromatographic analysis of nucleobases, nucleosides, and nucleotides.

The simultaneous separation of nucleobases, nucleosides, and nucleotides, representing a considerable range of polarity, has presented a challenge to LC for some time. All three of the classes are frequently present in biological samples, so that a single analysis step with minimal sample preparation seems desirable. However, due to the limited efficiency of conventional LC, most proposed separation schemes have consisted of the combination of sample fractionation steps with the separate LC analyses of these classes of compounds. In attempts to solve the problems of simulta-

0021-9673/89/$03.50

neous analysis by the mobile phase effects[8], very polar nucleotides are still eluted in the very early part of a chromatogram, making their quantitation a difficult task. Alternatively, column switching techniques have been employed[9]. As shown in this communication, slurry-packed capillary columns, featuring 70 000–100 000 theoretical plates per analytical column in the reversed-phase mode are capable of such simultaneous analysis. Similarly, the same reversed-phase microcolumn has been utilized in an efficient ion-pairing separation of mono-, di-, and triphosphate nucleosides, which are important biochemicals in cell bioenergetics as well as enzymatic and hormonal regulatory systems. One of the important advantages of LC microcolumns —an increased mass sensitivity of the concentration-sensitive detectors— will be demonstrated on the analysis of an enzymatic digest of ribonucleic acid (RNA). While analyzing nucleic acids by classical schemes, the assumption is made that only the four major nucleotides uridine 5′-monophosphate [(UMP) or thymidine 5′-monophosphate (TMP), cytidine 5′-monophosphate (CMP), guanosine 5′-monophosphate (GMP), and adenosine 5′-monophosphate (AMP)] are present. In the tRNAs and, to a lesser extent, the rRNAs and mRNAs, extensive modification of the nucleotide units may occur. The most common of these is methylation. Unlike electrophoretic methods, LC has the general capability of separating the modified nucleotide units. However, since the natural concentration of these nucleic acids in cells may be quite low, isolation procedures can be lengthy. In exploring the merits of microcolumn LC with respect to its superior mass detection sensitivity, small samples of tRNA-Phe have been analyzed in this work. Efficient separation of the major and modified nucleosides present is also demonstrated.

The limits of detection with the miniaturized UV-absorbance detector are demonstrated on yet another important class of compounds, the cyclic nucleotides. Due to their important roles in neurotransmission and hormonal regulation[10–12], the ability to quantitate these substances is critical in a number of research problems. Natural concentrations of cyclic nucleotides are frequently in the picomolar range, so that microcolumn LC may become a very useful analytical tool in this area.

EXPERIMENTAL

Apparatus

The pump used for mobile phase delivery was a syringe-type ISCO μLC-500, (Lincoln, NE, U.S.A.). In order to deliver step gradients, a laboratory-built device, previously described[13], was employed. Injection was accomplished by either moving-loop[14] or stopped-flow injection[13]. With the moving loop, a helium-actuated C14W Valco injection valve with a high-speed switching kit and a modified digital valve sequence programmer[15,16] were used (Valco Instruments, Houston, TX, U.S.A.). The analytical columns were fabricated from 50 and 250 μm I.D. fused silica (Polymicro Technologies, Phoenix, AZ, U.S.A.). The reversed-phase packing material used in all columns was Capcell Pak C_{18} (Shiseido, Tokyo, Japan). The detector used in all cases was an ISCO μLC-10, operated at a wavelength of 254 nm, with a miniaturized 1.0-mm pathlength UV-absorbance cell (ISCO) of the Z-type configuration.

Materials

All nucleobase, nucleoside, and nucleotide standards were obtained from Sig-

ma (St. Louis, MO, U.S.A.), as was bacterial alkaline phosphatase type III-R. tRNA-Phe and nuclease Pl were obtained from Boehringer (Indianapolis, IN, U.S.A.). Methanol used for the gradient steps was purchased from Burdick & Jackson Labs. (McGraw Park, IL, U.S.A.). Water was purified with a Milli-Q system, from Millipore (Bedford, MA, U.S.A.). Water, organic solvents, and buffer solutions were filtered through Nylon-66 membranes from Anspec (Ann-Arbor, MI, U.S.A.).

The nucleic acid standards were dissolved in water at 1 mg/ml. Dilutions were then made as needed prior to analysis. The less soluble nucleobases were sonicated in water for 1 h to assure complete dissolution. In some cases, pH adjustments were necessary. Standards were kept frozen at −20°C.

Procedure

Methanol gradients were prepared from aqueous 0.03 *M* KH_2PO_4 and methanol. After mixing, 0.1 *M* KOH or 0.1 *M* HCl was added dropwise until the pH was 5.60.

The tRNA hydrolysis and analysis were performed in the following manner, as adapted from Gehrke *et al.*[17,18] and Davis *et al.*[19]. The original 1-mg/ml solution of tRNA-Phe was diluted to 100 ng/μl. A volume of 1 μl (100 ng of tRNA) of this solution was then transferred to a 400-μl microcentrifuge tube. This was immersed in boiling water for 3 min in order to remove some of the tertiary structure of the tRNA. Next, 500 nl of bacterial alkaline phosphatase and 500 nl of nuclease Pl were added. The entire solution was then incubated for 3.5 h, at which time the sample was lyophilized and frozen at −20°C until analysis was performed. When ready for use, the sample was thawed and dissolved in 400 nl of water. This solution was removed from the tube by capillary action and injected into the column by the stopped-flow injection technique[13].

RESULTS AND DISCUSSION

Separation of nucleobases, nucleosides and nucleotides

The simultaneous separation of the nucleobases, nucleosides, and nucleotides related to uracil, cytosine, guanine, adenine, and thymine is shown in Fig. 1. On a 1 m × 250 μm I.D., efficiently slurry-packed microcolumn, all fifteen components were adequately resolved in a period of 2 h. While the standard mixture injected represents 1 ng amounts per component, the detection limit for a single nucleotide, AMP, was determined to be 10 pg at a signal-to-noise ratio (S/N) of 2. This compares favorably with the results of other investigators[3,8], who typically report detection limits of 50 pmol per nucleotide, or 17 ng in the case of AMP. As an example of the benefits of increased mass detection sensitivity, a 100-ng sample of tRNA-Phe was subjected to enzymatic hydrolysis, as described above. Fig. 2 shows the separation of the major and modified nucleosides resulting from the hydrolysis procedure. By employing the stopped-flow injection technique[13], the entire sample could be utilized. The minor components (modified nucleosides), which are effectively separated from the major constituents, are estimated to be well below the nanogram level. This compares very favorably with the results reported by Gehrke *et al.*[17], where a minimum of 5 μg of tRNA-Phe was required for hydrolysis and subsequent chromatographic analysis.

Increased concentrations of certain modified nucleosides in urine and tissue

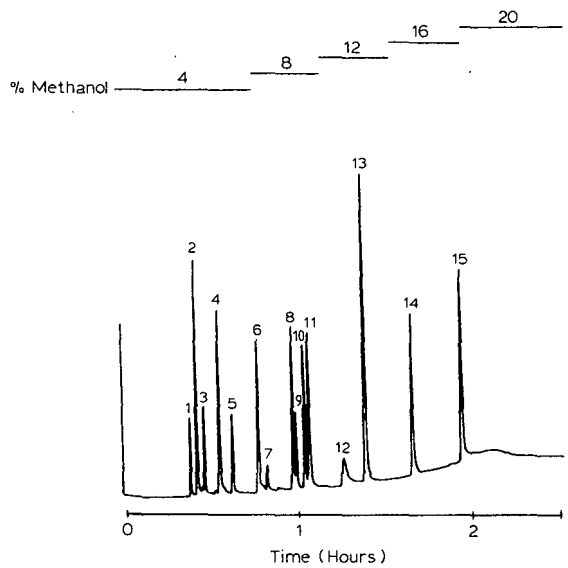

Fig. 1. Separation of the nucleobases, nucleosides, and nucleotides. Gradient from 0 to 20% methanol in 0.03 *M* KH_2PO_4 at pH 5.6 in 2 h by step gradients, as shown. Elution order: (1) CMP, (2) cytosine, (3) UMP, (4) uracil, (5) GMP, (6) cytidine, (7) guanine, (8) uridine, (9) TMP, (10) thymine, (11) AMP, (12) adenine, (13) guanosine, (14) thymidine, (15) adenosine.

Fig. 2. Separation of the major and minor nucleosides from the hydrolysis of 100 ng of tRNA-Phe. The gradient is the same as in Fig. 1. Elution order: (1) pseudouridine, (2) cytidine, (3) 5-methylcytidine, (4) uridine, (5) 5-methylguanosine, (6) 2′-O-methylcytidine, (7) 5-methyluridine, (8) 1-methyladenosine, (9) adenosine, (10) 2′-O-methylguanosine, (11) N^2-methylguanosine, (12) guanosine, (13) N^2,N^2-dimethylguanosine.

have been associated with various neoplastic disorders[20,21]. These diseases are known to alter various enzyme functions that affect tRNA metabolism, resulting in elevated amounts of the methylated nucleotides in the urine[22,23]. Again, the sensitivity afforded by microcolumns may be beneficial in studies of such compounds in physiological fluids and tissues.

Separation of cyclic nucleotides

In view of the recently realized importance of the cyclic nucleotides and their very low natural concentrations, considerable effort has been exerted towards the development of more sensitive detection of these compounds. Our results are shown in Fig. 3 as the isocratic separation of cUMP, cCMP, cGMP, and cAMP in just over 30 min. The column used in this case was 60 cm × 250 μm I.D. and the mobile phase consisted of 15% methanol in 0.03 *M* KH_2PO_4. Each peak represents 150 pg per component, with an average detection limit of 20 pg at S/N = 2. Earlier work by Krstulovic *et al.*[12] produced a similar separation of cUMP, cCMP, cGMP, cIMP, and cAMP in 25 min, with a reported detection limit of 40 pmol, or approximately 10 ng per component.

Potential applications to this class of compounds include the quantitation of cyclic nucleotides in brain tissue. Recent work by Fayolle *et al.*[24] has demonstrated

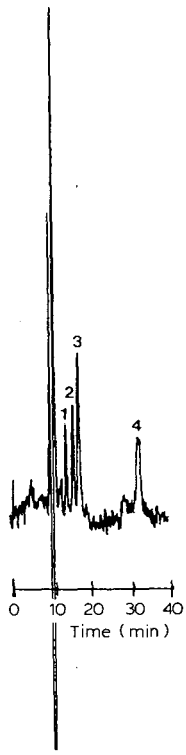

Fig. 3. Separation of cyclic nucleotides. Mobile phase, 15% methanol in 0.03 *M* KH_2PO_4 (pH 5.60); column length, 60 cm; compounds at 150 pg each in the elution order: (1) cCMP, (2) cUMP, (3) cGMP, (4) cAMP.

the detection of cAMP in rat brain cortex with a detection limit of 10 pmol (*ca.* 3 ng). Once again, our microcolumns represent an increase in sensitivity for these compounds of over 2 orders of magnitude as compared to conventional LC.

Separation of the mono-, di-, and triphosphate nucleosides

The use of ion-pairing chromatography to separate the phosphorylated nucleosides was first demonstrated by Hoffman and Liao[25], who investigated the effects of mobile phase pH, buffer concentration, buffer type, and percent methanol on retention of these compounds. In their work, the mono-, di-, and triphosphate nucleosides of uridine, cytidine, guanosine, and adenosine, as well as cAMP were separated in 36 min on a conventional reversed-phase column with a chloride ion/methanol gradient in 0.025 *M* tetrabutylammonium hydrogensulfate. The smallest amount of sample studied in their work represented 100 pmol per component. Due to the complexity of this type of mobile phase, column re-equilibration time required, and an interest in maintaining mobile-phase consistency at extremely sensitive UV-absorbance levels, an isocratic separation scheme was explored. Fig. 4 shows the separation of 1-ng amounts each of the mono-, di- and triphosphates of uridine, cytidine, guanosine, and

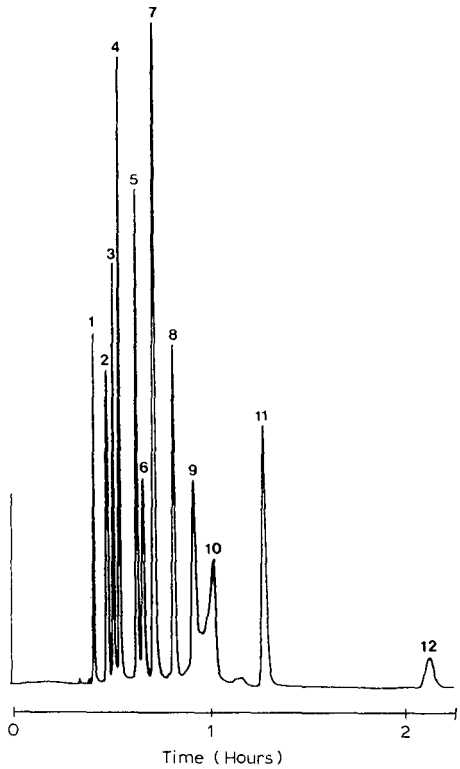

Fig. 4. Separation of mono-, di-, and triphosphate nucleoside analogues. Mobile phase, 0.025 *M* tetrabutylammonium hydrogensulfate–0.13 *M* NH_4Cl–0.03 *M* KH_2PO_4 at pH 6.10. Elution order: (1) CMP, (2) UMP, (3) CDP, (4) GMP, (5) UDP, (6) CTP, (7) GDP, (8) AMP, (9) UTP, (10) GTP, (11) ADP, (12) ATP.

adenosine in 2 h on a 1 m × 250 μm I.D. microcolumn. Detection limits at S/N = 2 for the mono-, di-, and triphosphate nucleosides of adenosine are 10, 25, and 50 pg, respectively. The optimized mobile phase consisted of a solution which was 0.03 *M* KH_2PO_4, 0.13 *M* NH_4Cl, and 0.025 *M* tetrabutylammonium hydrogensulfate adjusted to pH 6.10 with 5 *M* KOH. In order to obtain reproducible retention behavior, it was necessary to condition the column for 2 h with the ion-pairing mobile phase.

In order to optimize the separation of this mixture, the effect of mobile phase chloride ion concentration as NH_4Cl was investigated, while the ion-pairing reagent

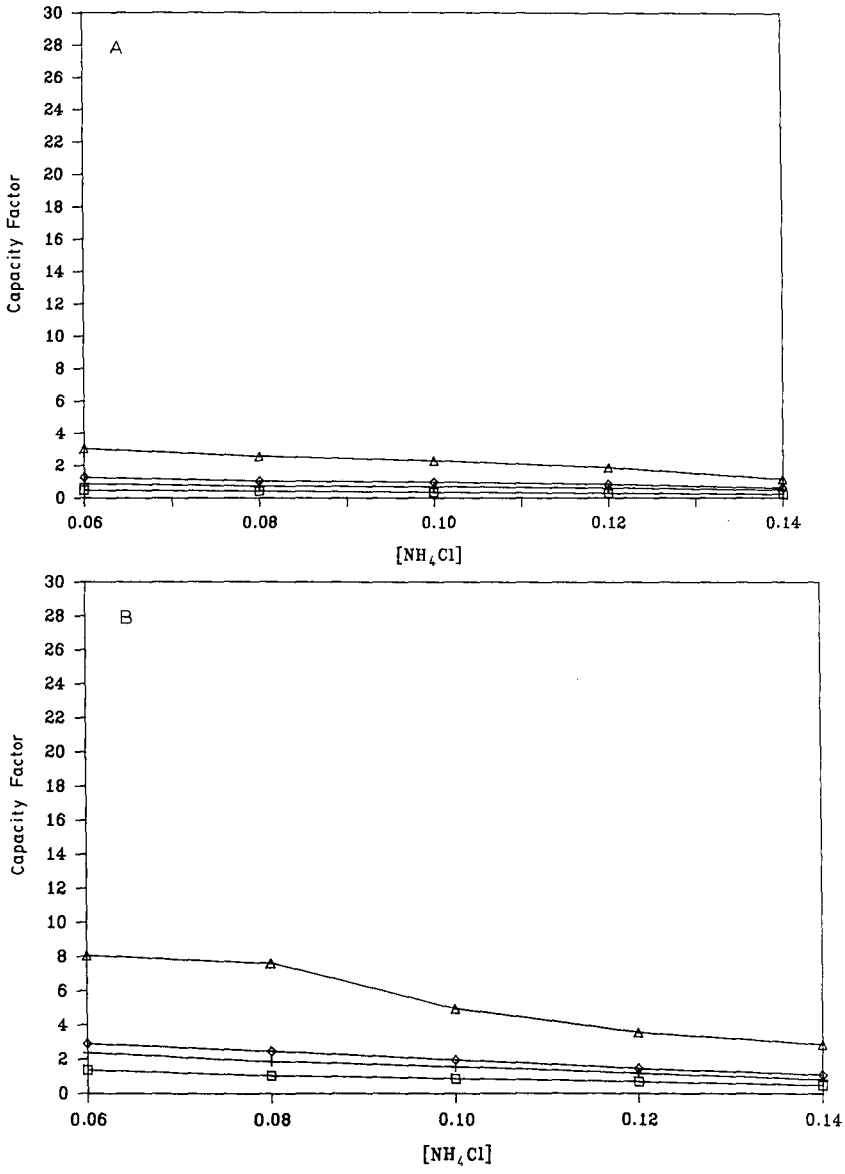

Fig. 5.

(*Continued on p. 20*)

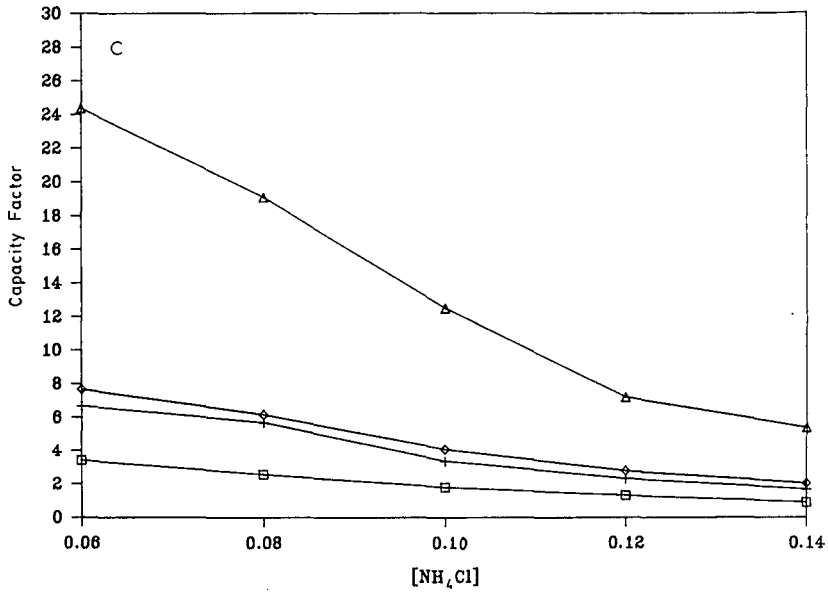

Fig. 5. Effect of NH_4Cl concentration on capacity factor for nucleotides. (A) Nucleoside monophosphates: (□) CMP, (+) UMP, (◇) GMP, (△) AMP. (B) Nucleoside diphosphates: (□) CDP, (+) UDP, (◇) GDP, (△) ADP. (C) Nucleoside triphosphates: (□) CTP, (+) UTP, (◇) GTP, (△) ATP.

concentration and phosphate buffer concentrations were held constant. Fig. 5 illustrates the effect of [NH_4Cl] on the capacity factor values, k, for the mono-, di-, and triphosphate nucleosides, respectively. Immediately obvious is the correlation between the [NH_4Cl] effect on k and the number of terminal phosphate groups present in a nucleoside. Clearly, the sensitivity of k to [NH_4Cl] increases dramatically with the number of phosphates. For this reason, it is possible to alter the elution positions in a somewhat selective fashion. That is, a slight change in [NH_4Cl] may substantially shift the k value for a triphosphate nucleoside while having little or no effect on the

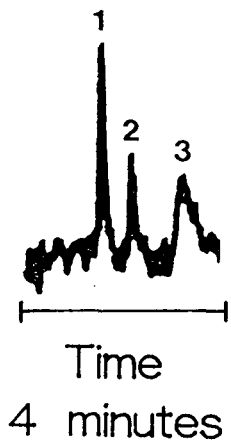

Fig. 6. Separation of (1) AMP, (2) ADP, and (3) ATP at 100 pg per component. Mobile phase, 0.03 M KH_2PO_4–0.16 M NH_4Cl–0.025 M tetrabutylammonium hydrogensulfate at pH 6.00.

mono- or diphosphate nucleoside. This behavior was critical in optimizing the mobile phase conditions for this separation.

The mono-, di-, and triphosphate adenosine nucleosides are of particular interest due to their vital role in bioenergetics. Several groups of researchers have developed rapid and sensitive assays for the determination of AMP, ADP, and ATP in such samples as brain tissue[26,27], myocardial tissue[28–31], intestinal cells[32], and bone marrow cells[32]. In these reports, the detection limits are not better than 20 pmol per component. Fig. 6 shows the isocratic separation of AMP, ADP, and ATP in 4 min on a 10 cm × 250 μm I.D. column, with detection limits of 10, 25, and 50 pg, respectively.

In summary, we believe that microcolumn LC provides certain analytical advantages over conventional HPLC in the area of research on nucleic acids and their metabolism. With a wider acceptance of microcolumn instrumental systems, these advantages are likely to be utilized in biochemical applications where greater mass detection sensitivity and chromatographic resolution are needed.

ACKNOWLEDGEMENT

This work was supported by a grant from the Amoco Technology Company.

REFERENCES

1 R. A. Hartwick, S. P. Assenza and P. R. Brown, *J. Chromatogr.*, 186 (1979) 647.
2 R. A. Hartwick, A. M. Krstulovic and P. R. Brown, *J. Chromatogr.*, 186 (1979) 659.
3 R. C. Simpson and P. R. Brown, *J. Chromatogr.*, 379 (1986) 269.
4 M. Novotny, *Anal. Chem.*, 50 (1988) 500A.
5 M. Novotny, in P. Kucera (Editor), *Microcolumn High Performance Liquid Chromatography*, Elsevier, Amsterdam, 1984, p. 194.
6 M. Novotny, in I. Wainer (Editor), *Liquid Chromatography in Pharmaceutical Development: An Introduction*, Aster, Springfield, OR, 1988, p. 5.
7 M. Novotny, in F. Bruner (Editor), *The Science of Chromatography*, Elsevier, Amsterdam, 1985, p. 305.
8 R. A. Hartwick and P. R. Brown, *J. Chromatogr.*, 126 (1976) 679.
9 P. R. Brown (Editor), *HPLC in Nucleic Acid Research: Methods and Applications* (*Chromatographic Science Series*, Vol. 28), Marcel Dekker, New York, 1984, p. 235.
10 J. W. Kababian, Y. C. Clement-Cormier, G. L. Petzold and P. Greengard, *Adv. Neurol.*, 9 (1975) 1.
11 G. A. Robison, R. W. Butcher and E. W. Sutherland, *Cyclic AMP*, Academic Press, New York, 1971.
12 A. M. Krstulovic, R. A. Hartwick and P. R. Brown, *Clin. Chem.*, 25 (1979) 235.
13 Y. Hirata and M. Novotny, *J. Chromatogr.*, 186 (1979) 521.
14 M. C. Harvey and S. D. Stearns, *J. Chromatogr. Sci.*, 21 (1983) 473.
15 M. C. Harvey, S. D. Stearns and J. P. Averette, *LC Liq. Chromatogr. HPLC Mag.*, 3 (1985) 434.
16 M. C. Harvey and S. D. Stearns, *Anal. Chem.*, 56 (1984) 837.
17 C. W. Gehrke, K. C. Kuo, R. A. McCune and K. O. Gerhardt, *J. Chromatogr.*, 23 (1982) 297.
18 C. W. Gehrke, K. C. Kuo and R. W. Zumwalt, in P. F. Agris and R. A. Kopper (Editors), *The Modified Nucleosides of Transfer RNA II*, Alan R. Liss, New York, 1983, p. 59.
19 G. E. Davis, C. W. Gehrke, K. C. Kuo and P. F. Agris, *J. Chromatogr.*, 173 (1979) 281.
20 G. E. Davis, R. D. Suits, K. C. Juo, C. W. Gehrke, P. Waalkes and E. Borek, *Clin. Chem.*, 23 (1977) 1427.
21 C. W. Gehrke, K. C. Kuo, G. Davis, R. D. Suits, T. P. Waalkes and E. Borek, *J. Chromatogr.*, 150 (1978) 455.
22 C. W. Gehrke, K. C. Kuo and R. W. Zumwalt, *J. Chromatogr.*, 188 (1980) 129.
23 S. J. Kerr, *Cancer Res.*, 35 (1975) 2969.
24 C. Fayolle and G. Fillion, *J. Chromatogr.*, 426 (1988) 177.

25 N. E. Hoffman and J. C. Liao, *Anal. Chem.*, 49 (1977) 2231.
26 K. Morimoto, K. Tagawa, T. Kayakawa, F. Watanabe and H. Mogami, *J. Neurochem.*, 38 (1982) 833.
27 D. F. Hammer, D. V. Unverferth, R. E. Kelley, P. A. Harvan and R. A. Altschuld, *Anal. Biochem.*, 169 (1988) 300.
28 E. Juengling and H. Kammermeier, *Anal. Biochem.*, 102 (1980) 358.
29 O. C. Ingebretsen, A. M. Bakken, L. Segadal and M. Farstad, *J. Chromatogr.*, 242 (1982) 119.
30 E. Harmsen, P. Ph. De Tombe and J. W. De Jong, *J. Chromatogr.*, 230 (1982) 131.
31 E. A. Hull-Ryde, R. G. Cummings and J. E. Lowe, *J. Chromatogr.*, 275 (1983) 411.
32 J. L.-S. Au, M.-H. Su and M. G. Wientjes, *J. Chromatogr.*, 423 (1987) 308.

Journal of Chromatography, 475 (1989) 23–44
Elsevier Science Publishers B.V., Amsterdam — Printed in The Netherlands

CHROMSYMP. 1616

EVALUATION OF NICKEL(II) BIS[α-(HEPTAFLUOROBUTANOYL)-TERPENEKETONATES] AS CHIRAL STATIONARY PHASES FOR THE ENANTIOMER SEPARATION OF ALKYL-SUBSTITUTED CYCLIC ETHERS BY COMPLEXATION GAS CHROMATOGRAPHY

V. SCHURIG*, W. BÜRKLE[a], K. HINTZER[b] and R. WEBER[c]
Institut für Organische Chemie, Universität Tübingen, D-7400 Tübingen (F.R.G.)

SUMMARY

A method is described which permits the determination of thermodynamic data for molecular association, as well as the enantioselectivity $-\Delta_{R,S}(\Delta G^\circ)$, from relative retention data by complexation gas chromatography. Thus, the solute–solvent association equilibria between two achiral, and fifteen chiral alkyl-substituted cyclic ethers and twelve non-racemic nickel(II) bis[α-(heptafluorobutanoyl)terpeneketonates] in squalane have been measured at 60°C. The selectivity of the solute–solvent association between alkyl-substituted oxiranes and the twelve nickel terpeneketonates follows a common trend which is rationalized in terms of opposing electronic and steric effects of the Lewis bases. The origin of the striking influence of ring size of cyclic ethers on the association strength with the twelve nickel terpeneketonates, which varies by two orders of magnitude, is unknown. Improved chiral stationary phases for the enantiomer separation of alkyl-substituted cyclic ethers have been found. The highest enantiomeric bias on racemic oxiranes is induced by nickel(II) bis[3-(heptafluorobutanoyl)-(1*R*,2*S*)-pinan-4-onate], containing a bicyclic terpene structure, and by nickel(II) bis[5-(heptafluorobutanoyl)-(*S*)-carvonate], containing a monocyclic terpene structure, respectively. The enantioselectivity, $-\Delta_{R,S}(\Delta G^\circ)$, is generally high when the solute–solvent interaction is intermediate. For chiral alkyl-substituted oxiranes a consistent relationship between molecular configuration and the order of elution is observed for almost all of the twelve nickel terpeneketonates used as solvent. The synthesis of these solvents is described in detail.

INTRODUCTION

Chiral bis[3-(heptafluorobutanoyl)-(1*R*)-camphorates] of manganese(II), cobalt(II) and nickel(II)[1,2] have been successfully employed as enantioselective stationary phases for the gas chromatographic (GC) separation of underivatized racemic

[a] Present address: Hoechst AG, Produktentwicklung, Ökologie, D-6230 Frankfurt/Main 80, F.R.G.
[b] Present address: Hoechst AG, Werk Gendorf, D-8269 Burgkirchen, F.R.G.
[c] Present address: Degussa AG, ZN Wolfgang, D-6450 Hanau, F.R.G.

0021-9673/89/$03.50

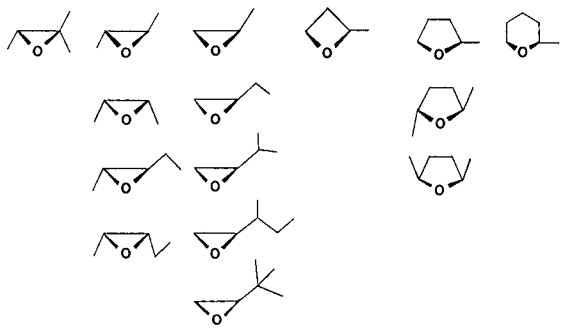

Scheme 1. Alkyl-substituted cyclic ethers as solutes for complexation GC.

Lewis bases, such as cyclic ethers and thio ethers, N-chloroaziridines, acetals, esters, lactones, ketones and alcohols[3–7]. Various applications associated with the precise determination of enantiomeric ratios (enantiomeric excess, ee) and absolute configurations have been reported by our own laboratory and by other groups[8,9].

In extension of these studies, a number of non-racemic nickel(II) bis[α-(heptafluorobutanoyl)terpeneketonates] have now been synthesized, and the influence of constitutional and configurational modifications on the enantiomer discrimination of fifteen racemic cyclic ethers (*cf.*, Scheme 1) has been scrutinized. Only mono- and bicyclic terpeneketones, which were readily available from natural sources in essentially enantiomerically pure form and which lent themselves to a regioselective α-acylation followed by bis chelation with the nickel(II) ion, were selected in the present investigation (*cf.*, Scheme 2).

The unique molecular architectures displayed by terpeneketoenolates have previously been utilized by Mc Creary *et al.*[10] in an effort to optimize chiral lanthanide "shift reagents", *e.g.*, paramagnetic europium(III) tris[α-(heptafluorobutanoyl)ter-

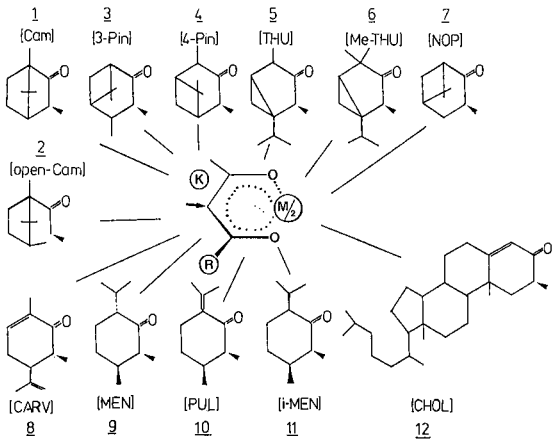

Scheme 2. A selection of mono- and bicyclic terpeneketones as chiral constituents of nickel(II) β-ketoenolates. R = $-C_3F_7$; M = Ni.

pene ketonates], for the discrimination of enantiomers by NMR spectroscopy. The chemical shift anisochrony of enantiotopic nuclei, rendered diastereotopic in the presence of a non-racemic chiral shift reagent, arises from at least two, mutually dependent, contributions which are related to the stability and geometry of the resulting diastereomeric association complexes in solution[11]. Because the individual contributions to chemical shift non-equivalence are indistinguishable, meaningful thermodynamic data, describing chiral recognition as well as simple correlations of absolute configuration with the sense of induced shifts, are not readily available from NMR studies using lanthanide "shift reagents"[11], despite the general utility of chiral solvating agents for the elucidation of donor–acceptor interactions[12].

The separation of enantiomers by complexation GC entirely depends on the difference in the stabilities of the diastereomeric 1:1 association complexes between the racemic substrate (hereafter called "solute") and the non-racemic metal bis chelate (hereafter called "solvent", the complexing agent), allowing a somewhat more straightforward interpretation of the thermodynamic data for chiral recognition. Furthermore, thermodynamic parameters of molecular association can readily be obtained from GC retention data[13,14] and, when applied to enantiomer separation[15], the difference in the free enthalpy change for molecular association between the solute and the solvent, *i.e.*, $-\Delta_{R,S}(\Delta G^\circ)$ (*vide infra*), provides valuable information on the enantioselectivity of the donor–acceptor interaction between the racemic solute and the non-racemic metal bis chelate. The determination of the elution order of the solute on a GC column containing a solvent of predefined chirality in the stationary phase must necessarily complement the assessment of chiral recognition, $-\Delta_{R,S}(\Delta G^\circ)$. It is important to establish the true sign of $-\Delta_{R,S}(\Delta G^\circ)$ and to detect peak inversions, which may arise from reversal of enantioselectivities caused by the inherent thermodynamics of chiral recognition[16] for solutes that are members of homologous series of compounds. In the present study, therefore, both the magnitude and the sign of enantiomer discrimination is determined between alkyl-substituted cyclic ethers and various chiral metal bis chelates. Structural elements of the solvent necessary for efficient chiral recognition are systematically investigated.

The procedures described were designed for the purpose of obtaining correct thermodynamic data for enantioselectivity. For practical enantiomer analysis, the use of vitreous open-tubular columns in connection with polysiloxane solvents was found to be more advantageous in complexation GC[6,7].

EXPERIMENTAL

Instrumentation

A Carlo Erba (Hofheim/Taunus, F.R.G.) Fractovap 2101 gas chromatograph, equipped with a flame ionization detector and suitable for operation with metal open-tubular columns, was used. High-purity-grade nitrogen was used as the carrier gas. The injector temperature was 120°C. The splitting device was set to 1:100. The solutes were injected together with methane, and the reference standard, *n*-octane, as air-diluted vapours. In order to avoid overloading, which results in peak tailing and broadening, the instrument was set to its highest sensitivity at a tolerable signal-to-noise ratio ($>1:10$). The split line and detector exhaust gases should be ventinaled into a hood.

Open-tubular columns

Nickel open-tubular columns (100 m × 0.5 mm I.D. and 75 m × 0.5 mm I.D., 200 seamless tubing, 99.53% Ni, 0.24% Mn), obtained from Handy and Harman Tube Co. (Norristown, PA, U.S.A.), were used. Prior to use, the columns were washed with *n*-hexane, chloroform, acetone and water. The rinsing was then repeated in the reverse order.

Coating of the columns[17]

The columns were coated dynamically. In a typical coating procedure, 15.1 mg of compound **1** and 200 mg of squalane [0.1 *m* (molality) of **1**] were dissolved in 3.5 ml of chloroform. [It is important for thermodynamic measurements to produce a film thickness of 1.0–1.5 μm. Therefore, concentrated coating solutions, *ca.* 10% (w/w), were used.] The solution was transferred to a laboratory-made coating device, fashioned entirely from PTFE. Approximately 0.6 bar of nitrogen overpressure were used to force the solution through the column. The nitrogen pressure was maintained for 5 h after the solution had passed the column. The column was connected to the gas chromatograph and conditioned at 0.3 bar nitrogen with a temperature programme of 30–80°C at 2°/min and 80°C (isothermal) for 24 h. After conditioning, the carrier gas pressure was raised to 1.5 bar and *ca.* 5 cm of the column end were heated with a flame in order to remove volatiles. Before starting the thermodynamic measurements the column was conditioned at 60°C for 24 h.

Calculation of the retention increase, R', and of the free enthalpy difference for enantiomer discrimination, $\Delta_{R,S}(\Delta G°)$[17]

Methane was used to measure the gas hold-up (dead-volume); its finite but negligible short retention time did not falsify the thermodynamic parameters calculated from adjusted retention times. Commercial *n*-octane was used as an inert reference standard to determine relative retentions, *r*. Adjusted retention times, t'_{sol}, were measured as the distance between the maximum peak heights of the solute, and the methane peak; t'_{sol} was then related to t'_{ref} of the non-coordinating reference standard, *n*-octane, which was simultaneously injected, *i.e.*, $t'_{sol}/t'_{ref} = r$ the relative retention of a solute with respect to *n*-octane. The relative retention of a solute, obtained from a column containing the solvent in squalane, *r*, and that of the same solute obtained from a column containing pure squalane, r_0, were used to calculate R' according to $R' = (r - r_0)/r_0$. The ratio of R' for the respective enantiomers was then used to calculate the enantioselectivity according to $-\Delta_{R,S}(\Delta G°) = RT \cdot \ln(R'_R/R'_S)$ (for derivation, *vide supra*). Graphic acquisition of retention data proved to be as reliable, *i.e.*, $r = \pm 0.005$, as data processing with a conventional integrating system (time interval: 0.1 s).

Solutes

The solutes were commercially available or were prepared from the alkenes by epoxidation with *m*-chloroperbenzoic acid[17]. Optically active reference compounds

with established stereochemistries used for peak assignment were prepared as described[18,19]. Oxiranes were handled with the appropriate care in closed systems.

Solvents 1–12

Strict adherence to the mode of preparation of solvents is recommended. Solvents prepared and purified by alternative routes may exhibit different physical and chromatographic properties[7].

Nomenclature

For simplicity and clarity the configuration of the solvents is specified as follows. The symbols *R* or *S*, respectively, which precede the conventional name of the terpenone, specify the chirality of the starting material regardless of descriptor reversals that may arise in subsequent chemical modifications (an ambiguity in specifying enol or keto forms of certain β-diketones).

The numbering of the carbon atoms of terpenones is that adopted in ref. 20. The thermodynamic data were extrapolated to ee = 100% for solvents which were not enantiomerically pure.

(1*R*)-Camphor, (1*S*)-thujan-3-one (containing the epimer), (*S*)-carvone, (1*R*)-menthone and (*R*)-pulegone were obtained from Haarmann and Reimer (Holzminden, F.R.G.). (1*R*)-Campholylmethane was obtained from (1*R*)-campholic acid[10], (1*R*,2*R*)-pinan-3-one from (1*R*,2*R*,3*R*)-pinan-3-ol (isopinocampheol) and (1*R*,2*S*)-pinan-4-one from (1*R*)-pin-2-en-4-one[(−)-verbenone][19]. (1*S*)-4-Methylthujan-3-one was obtained from (1*S*,4*R*)-thujan-3-one[18,21] and (1*R*,5*S*)-nopinone from (1*S*)-β-pinene[10].

General procedure for (heptafluorobutanoyl)terpeneketones[10]

The reaction was carried out in a nitrogen atmosphere, using a dry, three-necked, round-bottom flask, equipped with a nitrogen inlet, dropping funnel, a low-temperature thermometer and an efficient mechanical stirrer. The calculated amount of methyl-lithium (170 ml of a 0.8 *M* solution, 136 mmol) was diluted in 100 ml of dry diethyl ether and cooled to −20°C. An equimolar quantity of N,N-diisopropylamine (19 ml, 136 mmol) was added dropwise (evolution of methane!). After stirring for 30 min at −20°C, an equimolar amount of ketone (136 mmol), dissolved in 20 ml of dry diethyl ether, was slowly added. The mixture was stirred for 20 min at −20°C and then cooled to −60°C. An equimolar amount of heptafluorobutanoyl chloride (20 ml, 136 mmol) (Fluka, Buchs, Switzerland), dissolved in 20 ml of dry diethyl ether, was added at such a rate as to keep the temperature below −50°C. The reaction mixture was stirred for 1 h at −50°C and was subsequently allowed to warm to room temperature within 2 h. For work-up, the mixture was poured into 100 g of ice-water and acidified with hydrochloric acid to pH\2; the aqueous phase was repeatedly extracted with diethyl ether. The pooled organic layers were washed with aqueous sodium bicarbonate and brine, dried over sodium sulphate and then concentrated. The residue was purified by column chromatography on silica and fractional distillation. [Upon chromatography of the β-diketones on silica, the formation of a red product,

believed to be an iron(III) tris chelate, was generally observed. To increase the yield of the diketone, the concentrated eluates were diluted in ethanol, and a few ml of a 20% aqueous solution of sodium cyanide were added to remove iron ions. The mixture was diluted in water, acidified to pH 2–3 with cold 1 *M* sulphuric acid and the aqueous phase was extracted with ethyl acetate. The diketone was recovered in the usual manner.]

In the following, the polarimetric measurements refer to optical rotations, α, rather then to specific rotations, $[\alpha]$, of neat liquids (which require knowledge of the density) measured with a 1-dm cell. The elemental analysis and spectroscopic data corresponded to those expected for the β-diketones and the solutes derived therefrom.

3-Heptafluorobutanoyl-(1R)-camphor[15]

Prior to chromatography, unreacted camphor was removed by sublimation at 35°C (14 Torr). Chromatography on silica gel with benzene–light petroleum (b.p. 60–90°C) (2:3, v/v). Yield: 23%, b.p. 57°C (0.05 Torr), α_D^{20} + 170.8° (neat).

Heptafluorobutanoyl-(1R)-campholylmethane

Yield: 32%, b.p. 70°C (0.07 Torr), α_D^{20} + 50.5° (neat).

4-Heptafluorobutanoyl-(1R,2R)-pinan-3-one

Chromatography on silica gel with chloroform–light petroleum (b.p. 60–90°C) = (2:3, v/v). Yield: 8%, b.p. 65°C (0.4 Torr), α_D^{20} + 36.3° (neat).

3-Heptafluorobutanoyl-(1R,2S)-pinan-4-one

Chromatography on silica gel with chloroform–light petroleum (b.p. 60–90°C) (2:3, v/v). Yield: 15%, b.p. 59°C (0.15 Torr), α_D^{20} + 10.8° (neat).

2-Heptafluorobutanoyl-(1S,4R)-thujan-3-one

Chromatography on silica gel with chloroform–light petroleum (b.p. 60–90°C) (2:3, v/v). Yield: 22%, b.p. 70°C (0.7 Torr), α_D^{20} − 11.2° (neat).

2-Heptafluorobutanoyl-(1S)-4-methylthujan-3-one

Chromatography on silica gel with dichloromethane–light petroleum (b.p. 60–90°C) (2:3, v/v). Yield: 26%, b.p. 74°C (0.4 Torr), α_D^{20} − 145.2° (neat).

3-Heptafluorobutanoyl-(1R,5S)-nopinone

Chromatography on silica gel with chloroform–light petroleum (b.p. 60–90°C) (2:3, v/v). Yield: 38%, b.p. 70°C (0.5 Torr), α_D^{20} + 22.9° (neat).

5-Heptafluorobutanoyl-(R)-carvone

Chromatography on silica gel with dichloromethane–light petroleum (b.p. 60–90°C) (2:3, v/v). Yield: 27%, b.p. 80°C (0.2 Torr), α_D^{20} + 184.2° (neat).

2-Heptafluorobutanoyl-(1*R*)-menthone and 2-heptafluorobutanoyl-(1*R*)-isomenthone were prepared by acylation of an epimeric mixture and subsequent separation by column chromatography of the β-diketones.

Epimerization of (1R)-menthone

A mixture of concentrated sulphuric acid (150 ml) and water (15 ml) was cooled to −30°C. (1*R*)-Menthone (26 g) was added, and the reaction mixture was allowed to warm to 30°C with mechanical stirring. The yellow reaction mixture was transferred in ice–water and was extracted with diethyl ether. The organic phase were dried with sodium sulphate, concentrated and distilled to give 19 g of isomenthone–menthone (2:3), α_D^{20} + 29.7° (neat). After acylation, the residue was distilled to remove unreacted ketones. The fraction boiling at 60–75°C (0.02 Torr) was repeatedly chromatographed on silica [benzene–light petroleum (b.p. 60–90°C) (2:3)] to give the following compounds.

2-Heptafluorobutanoyl-(1R)-menthone. Yield: 4.7 g (20%), b.p. 69°C (0.02 Torr), m.p. 38°C, $[\alpha]_D^{20}$ + 80° (*c* 1,3, $CHCl_3$); $[\alpha]_D^{20}$ + 83.5° (*c* 1, $CHCl_3$) for the β-diketone prepared directly from menthone without prior epimerization.

2-Heptafluorobutanoyl-(1R)-isomenthone. Yield: 2.1 g (9%), b.p. 68°C (0.02 Torr), α_D^{20} + 148° (neat), $[\alpha]_D^{20}$ + 115.7° (*c* 3, $CHCl_3$). Chromatography on silica gel with chloroform–light petroleum (b.p. 60–90°C) (2:3, v/v). Yield 26%, b.p. 70°C (0.4 Torr), α_D^{20} + 12.4° (neat).

6-Heptafluorobutanoyl-(R)-pulegone. Yield: 26%, b.p. 87°C (0.5 Torr), α_D^{20} −62.1° (neat).

*2-Heptafluorobutanoyl-(+)-cholest-4-en-2-one*As the lithium salt of the ketone precipitated at −60°C, dry tetrahydrofuran was added to the reaction mixture[18]. The reaction mixture was extracted with ethyl acetate. Chromatography on silica gel with dichloromethane–light petroleum (b.p. 60–90°C) (2:3, v/v). Yield: 36%.

General procedure for nickel(II) bis[3-(heptafluorobutanoyl)terpeneketonates]1–12

The nickel bis chelates were prepared via the corresponding sodium salts of the β-diketonates[15]:

Sodium (heptafluorobutanoyl)terpeneketonates

In a nitrogen atmosphere, *ca.* 0.3 g of a sodium hydride suspension in paraffin (80%, w/w) were freed from paraffin by repeatedly washing with dry toluene. The sodium hydride (0.24 g, 10 mmol) was suspended in toluene and transferred to a Schlenk tube. The β-diketone (7 mmol) was dissolved in toluene and added dropwise to the suspension (evolution of hydrogen!). After stirring for 2 h, the excess of sodium hydride was removed by filtration or decanting and was repeatedly washed with solvent. The pooled filtrates were concentrated *in vacuo*. The resulting glassy products (yield: 80–95%) were dried in an high vacuum and were employed without further purification.

Nickel(II) bis[3-(heptafluorobutanoyl)terpeneketonates] 1–12

Stoichiometric amounts of the sodium β-diketonate and nickel(II) dichloride hexahydrate were dissolved in ethanol, and the mixture was refluxed for 1 h. The sodium chloride formed was filtered off and the green solution was concentrated *in vacuo*. Further purification was carried out with accompanying loss of product by sublimation at 150–200°C at high vacuum (0.01 Torr). Yield: 30–80% of a green solid, soluble in most organic solvents.

Nickel(II) bis[3-(heptafluorobutanoyl)-(1R)-camphorate] **1**. $[\alpha]_D^{20}$ + 129.3° (*c*

0.7, $CHCl_3$). Mass spectrum [*m/e* (rel. int.)]: 754(46), 753(35), 752(100), 724(79), 696(24).

Nickel(II) bis[(heptafluorobutanoyl)-(1R)-campholylmethanate] **2**. Mass spectrum [*m/e* (rel. int.)]: 784(42), 765(4), 701(12), 504(17), 420(100), 125(46).

Nickel(II) bis[4-(heptafluorobutanoyl)-(1R,2R)-pinan-3-onate] **3**. $[\alpha]_D^{20}$ +86.6° (*c* 0.2, $CHCl_3$). Mass spectrum [*m/e* (rel. int.)]: 752(46), 737(16), 709(62), 404(100), 333(55), 305(10).

Nickel(II) bis[3-(heptafluorobutanoyl)-(1R,2S)-pinan-4-onate] **4**. $[\alpha]_D^{20}$ +4.3° (*c* 0.23, $CHCl_3$). Mass spectrum [*m/e* (rel. int.)]: 752(2), 709(2), 404(2), 333(8), 305(100), 265(19), 177(21), 149(63), 83(81).

Nickel(II) bis[2-(heptafluorobutanoyl)-(1S,4R)-thujan-3-onate] **5**. Field desorption mass spectrum: base peak *m/e* = 753.

Nickel(II) bis([2-heptafluorobutanoyl)-(1S)-4-methylthujan-3-one] **6**. $[\alpha]_D^{20}$ −92.1° (*c* 0.37, $CHCl_3$). Mass spectrum [*m/e* (rel. int.)]: 781(18), 481(17), 346(42), 331(47), 69(100).

Nickel(II) bis[3-(heptafluorobutanoyl)-(R)-nopinonate] **7**. $[\alpha]_D^{20}$ −51° (*c* 0.47, $CHCl_3$). Mass spectrum [*m/e* (rel. int.)]: 724(100), 709(17), 682(55), 390(91), 362(42), 348(42).

Nickel(II) bis[5-(heptafluorobutanoyl)-(S)-carvonate] **8**. $[\alpha]_D^{20}$ +400° (*c* 0.6, $CHCl_3$). Mass spectrum [*m/e* (ref. int.)]: 748(85), 707(100), 665(18), 551(26), 403(23), 346(18).

Nickel(II) bis[2-(heptafluorobutanoyl)-(1R)-menthonate] **9**. $[\alpha]_D^{20}$ −28.0° (*c* 0.4, $CHCl_3$). Mass spectrum [*m/e* (rel. int.)]: 756(13), 741(40), 406(5), 350(20), 55(100).

Nickel(II) bis[6-(heptafluorobutanoyl)-(R)-pulegone] **10**. $[\alpha]_D^{20}$ −25.9° (*c* 0.15, $CHCl_3$). Mass spectrum [*m/e* (rel. int.)]: 752(23), 737(10), 404(30), 348(16), 149(100).

Nickel(II) bis[2-heptafluorobutanoyl)-(1R)-isomenthonate] **11**. $[\alpha]_D^{20}$ −110.2° (*c* 0.4, $CHCl_3$). Mass spectrum [*m/e* (rel. int.)]: 756(44), 406(4), 350(28), 55(100).

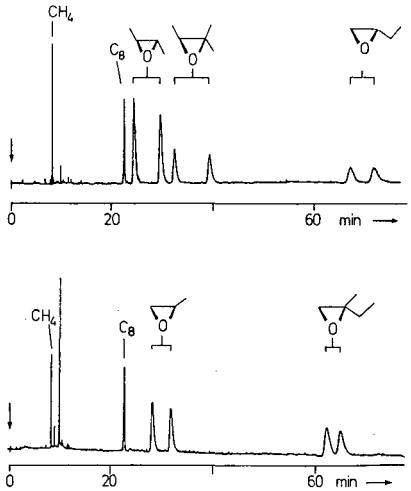

Fig. 1. Enantiomer separation of racemic oxiranes on nickel(II) bis[3-(heptafluorobutanoyl)-(1*R*)-camphorate] (0.1 *m* in squalane) at 60°C by complexation GC. Nickel open-tubular column, 100 m × 0.5 mm I.D.; 2.5 ml/min N_2 (0.55 bar). Reference standard: *n*-octane. Lower chromatogram: methyloxirane; 2,2-ethylmethyloxirane. Upper chromatogram: *trans*-2,3-dimethyloxirane; trimethyloxirane; ethyloxirane.

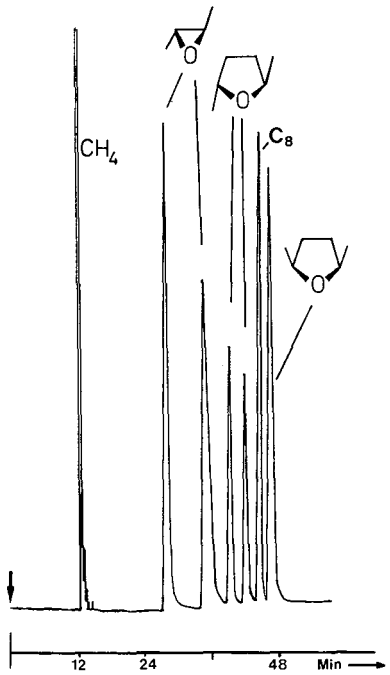

Fig. 2. Enantiomer separation of α,α'-dimethyl-substituted cyclic ethers on nickel(II) bis[3-(heptafluorobutanoyl)-(1*R*)-camphorate] (0.1 *m* in squalane) at 60°C by complexation GC. Nickel open-tubular column, 75 m × 0.5 mm I.D.; 0.8 bar N_2. Elution order: methane; enantiomers of *trans*-2,3-dimethyloxirane; enantiomers of *trans*-2,5-dimethyltetrahydrofuran; *n*-octane (reference standard) and *cis*-2,5-dimethyltetrahydrofuran (achiral).

Nickel(II) bis[2-heptafluorobutanoyl)-(+)-cholest-4-en-2-onate] **12**. $[\alpha]_D^{20}$ −108.7° (*c* 0.46, $CHCl_3$). Mass spectrum [*m/e* (rel. int.)]: 1216(5), 580(12), 281(35), 207(22), 57(100).

RESULTS AND DISCUSSION

Enantiomer separation of racemic alkyl-substituted cyclic ethers on metal(II) bis[3-(perfluoroacyl)-(1*R*)-camphorates] **1** (*cf.*, representative chromatograms in Figs. 1 and 2) has previously been examined by variation (i) of the central metal ion, *i.e.*, manganese(II), cobalt(II) and nickel(II)[15], and (ii) of the 3-perfluoroacyl residue, *i.e.*, –C(O)R, with R = CF_3, *n*-C_3F_7, *n*-C_7F_{15} and C_6F_5[19]. These studies revealed that the solute–solvent interaction, $-\Delta G°$, and the observed enantioselectivity, $-\Delta_{R,S}(\Delta G°)$, are greatly dependent on the composition of compound **1**. Thus, while the acceptor properties of the metal ion in **1** toward cyclic ethers increases markedly in the order manganese(II) < cobalt(II) ≪ nickel(II) spanning a factor up to 50, no such dramatic effect was noted in the observed enantioselectivity. Strong donor–acceptor interactions, as found for nickel(II), are not a prerequisite for efficient enantiomer discrimination. This is confirmed by the observation that, *e.g.*, isopropyloxirane is not separated by nickel(II) bis[3-(heptafluorobutanoyl)-(1*R*)-camphorate] but is quantitatively resolved by the weakly coordinating manganese(II) bis[3-(heptafluorobuta-

noyl)-(1*R*)-camphorate[6,15]. Lengthening the perfluoroalkyl side chain in **1** [M = manganese(II)] leads to a pronounced increase in enantiomer discrimination when going from R = CF_3 to *n*-C_3F_7 without further improvement when going to *n*-C_7F_{15}.

Preliminary screenings showed that the composition of the metal bis chelates markedly determined the strength of the donor–acceptor interaction as well as the observed enantioselectivity. Since the extent of coordination may sometimes be quite low, we used the strong acceptor, nickel(II), as the central metal ion. Furthermore, in the present study, all terpeneketones were converted into β-diketones via heptafluorobutanoyl acylation (R = C_3F_7).

In Scheme 2, *constitutional formulae* of the nickel(II) bis[α-(heptafluorobutanoyl)terpene ketonates] **1–12**, which have been prepared and investigated as chiral stationary phases for enantiomer separation of alkyl-substituted cyclic ethers, are depicted. The structural elements selected in the present study involve: (i) bicyclic terpene moieties, rigidly fused with the metal chelate ring, *i.e.*, [CAM], [NOP], [3-PIN], [4-PIN], [THU] and [Me-THU]; (ii) monocyclic terpene moieties, rigidly fused with the metal chelate ring, *i.e.*, [MEN], [i-MEN], [PUL], [CARV], [CHOL] and (iii) a monocyclic terpene moiety, non-rigidly attached to the metal chelate ring, *i.e.*, [open-CAM].

In Scheme 3 *configurational formulae* of the nickel(II) bis[α-(heptafluorobutanoyl)terpeneketonates] **1–12**, prepared from terpeneketones of specified configuration and high enantiomeric purity, are shown for comparison.

Enantiomer separation by complexation GC can be used as a versatile tool for the determination of thermodynamic parameters for chiral recognition. The GC enantiomer separation of racemic Lewis base solutes on chiral non-racemic Lewis acid metal coordination compounds requires (i) that the stabilities of the diastereomeric donor–acceptor association complexes are different, (ii) that complex formation is reversible and (iii) that the equilibrium is established rapidly, with respect to the GC time-scale.

While the chemical interaction between the solute and the solvent is expressed by the association constant, K, or the free enthalpy of association, $-\Delta G^\circ$, the difference in $-\Delta G^\circ$ for a pair of enantiomers, $-\Delta_{R,S}(\Delta G^\circ)$ (R and S denote oppositely configurated enantiomers), represents a thermodynamic quantity for enantiomer discrimination.

It has previously been shown that thermodynamic data describing chiral recognition may readily be obtained from relative retention data by complexation GC[15]. Thus, when a Lewis base B is chromatographed on a stationary phase containing the solution of a Lewis acid A, *e.g.*, a metal coordination compound in an inert solvent, *e.g.*, squalane, the retention of B is not only dependent on the physical partition equilibrium between the gaseous and liquid phases but is also determined by the reversible and rapid chemical association equilibrium in the liquid phase

$$A + B \rightleftharpoons AB$$

leading to a retention increase, R'. The latter is related to the association constant, K, and to the activity of A in S, a_A, by the linear relationship[13,14]

$$K \cdot a_A = \frac{r - r_0}{r_0} = R' \qquad (1)$$

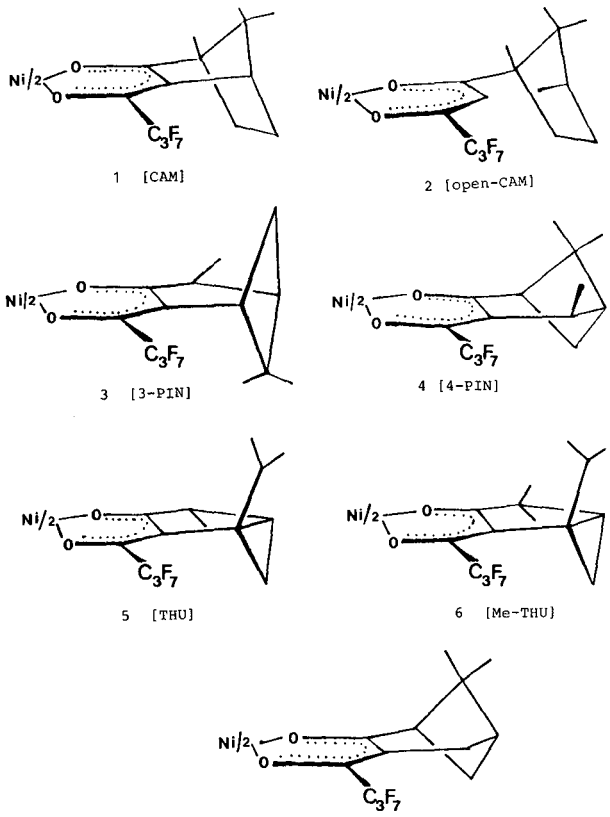

1 [CAM]

2 [open-CAM]

3 [3-PIN]

4 [4-PIN]

5 [THU]

6 [Me-THU]

7 [NOP]

BICYCLIC

8 [CARV]

9 [MEN]

10 [PUL]

11 [i-MEN]

MONOCYCLIC

12 [CHOL]

POLYCYCLIC

Scheme 3. Configurational formulae of nickel(II) bis[α-(heptafluorobutanoyl)terpeneketonates] **1–12**.

R' can be calculated from the readily accessible relative retention data, r_0 and r, where r = relative adjusted (= corrected for the dead-volume of the column) retention of B with respect to an inert reference standard, not interacting with A, on a column containing the activity a_A in S, and r_0 = relative adjusted retention of B with respect to the inert reference standard on a reference column containing the pure solvent, S.

With

$$K = a_{AB}/a_A a_B \tag{2}$$

it follows from eqn. 1 that the retention increase, R', defines the activity fraction of the complexed *vs.* uncomplexed solute B in the liquid phase (A in S), *i.e.*:

$$R' = a_{AB}/a_B \tag{3}$$

Because only a trace of solute B (approximately 10^{-8} g) as well as dilute solutions of A in S (0.05–0.1 *m*; note that the molality concentration scale is chosen because *m* is temperature independent and the weight rather than the volume of S is determined for practical purposes) are used in complexation GC, eqns. 1 and 3 can be simplified to:

$$K_{(m)} m_A = \frac{r - r_0}{r_0} = \frac{m_{AB}}{m_B} = R' \tag{4}$$

K and $-\Delta G°$, and, by measurements at different temperatures, the corresponding Gibbs–Helmholtz parameters $-\Delta H°$ and $\Delta S°$, can be obtained from eqn. 4. When R' is distinct for a pair of enantiomers on a chiral metal chelate A, peak separation will occur according to eqns. 5 and 6:

$$\frac{R'_R}{R'_S} = \frac{K_R}{K_S} = \frac{r_R - r_0}{r_S - r_0} \tag{5}$$

$$-\Delta_{R,S}(\Delta G°) = RT \cdot \ln \frac{R'_R}{R'_S} \tag{6}$$

Thus, the thermodynamic quantities for enantiomer discrimination, $-\Delta_{R,S}(\Delta G°)$, and, by measurements at different temperatures, the corresponding Gibbs–Helmholtz parameters, $\Delta_{R,S}(\Delta H°)$ and $\Delta_{R,S}(\Delta S°)$, are accessible from the differences in the retention increases, R', of the enantiomers. Note that r_0 is alike for enantiomers and that the concentration of the metal bis chelate, m_A, does not need to be known, eliminating possible errors in $-\Delta_{R,S}(\Delta G°)$.

In the present investigations, as well as in previous studies, the retention increase, R', rather than K or $-\Delta G°$, is consulted as criterion for the solute–solvent association, because this quantity is not biased by errors in m_A. It should be noted that the validity of eqn. 4 as well as the high precision of $-\Delta_{R,S}(\Delta G°)$ have previously been verified in an investigation of four racemic alkyl-substituted oxiranes at five concentrations of manganese(II) bis[3-(heptafluorobutanoyl)-(1*R*)-camphorate] in squalane (m = 0.05–0.15)[6].

The ratio R'_R/R'_S of a solute depends on the enantiomeric composition (enantiomeric excess, ee) of the solvent. In the present study, $-\Delta_{R,S}(\Delta G^\circ)$ always refers to enantiomer discrimination caused by an enantiomerically pure (ee = >99%) nickel(II) bis chelate. When the metal bis chelate was not obtained in an enantiomerically pure form, *e.g.*, [3-PIN] and [4-PIN], the relative retention, r_{ee} (measured with the metal bis chelate of given ee), was extrapolated to r_{100} (corresponding to ee = 100%) via eqns. 7 and 8[22]:

$$r_{R100} = \frac{1}{2}(r_{Ree} + r_{See}) + \frac{50}{ee}(r_{Ree} - r_{See}) \tag{7}$$

$$r_{S100} = \frac{1}{2}(r_{Ree} + t_{See}) - \frac{50}{ee}(r_{Ree} - r_{See}) \tag{8}$$

with

$$ee(\%) = \frac{R - S}{R + S} \cdot 100 \tag{9}$$

Note that in eqns. 7 and 8, for ee $\rightarrow$ 0, $r_R - r_S \rightarrow 0$.

The solute–solvent association equilibria between two achiral and fifteen chiral alkyl-substituted cyclic ethers and twelve non-racemic nickel(II) bis[α-(heptafluorobutanoyl)terpeneketonates] **1–12** in squalane have been measured at 60°C. The results are shown in the table. Listed therein are the retention increases, R', for the respective enantiomers and the measure of enantioselectivity, $-\Delta_{R,S}(\Delta G^\circ)$, derived therefrom. The elution order of the individual enantiomers is also reported.

According to eqn. 1, both K and $-\Delta G^\circ$ can be calculated from R' from a knowledge of the concentration of the solvent in squalane at the very moment of the measurement. Due to uncertainties, such as partial insolubility and decomposition of the metal bis chelate as well as losses of stationary phase during the GC experiment, absolute values of R', K and $-\Delta G^\circ$ may involve an unacceptable systematic error. However, the relative comparison of the quantities $RT \cdot \ln(R_R/R'_S) = RT \cdot \ln(K_R/K_S) = -\Delta_{R,S}(\Delta G^\circ)$ becomes independent of the concentration of the solvent when the screening of the solutes is performed at the same time or in very close succession. It is important to note that $-\Delta_{R,S}(\Delta G^\circ)$ for each individual solute is not affected by errors in m, since enantiomer separation is the result of a single chromatographic experiment. Nevertheless, the magnitude of the absolute retention increase, R', will also be considered in order to allow the distinction between (i) the ability of the solutes to undergo association with the solvent, as expressed by R', K and $-\Delta G^\circ$, on the one hand, and (ii) the extent to which the association equilibria differ for a pair of enantiomers, as expressed by $-\Delta_{R,S}(\Delta G^\circ)$, on the other hand. It has already been demonstrated[6,15,19] that the intuitive assumption that a strong donor–acceptor interaction is a necessary requirement for efficient enantiomer discrimination is incorrect and that small interactions may cause high "chiral recognition factors", $\chi = -\Delta_{R,S}(\Delta G^\circ)/-\Delta G^\circ$.

TABLE I

RETENTION INCREASE, R', AND $\Delta_{R,S}(\Delta G°)$ FOR CYCLIC ETHERS AND **1–12** AT 60°C

First row: R'[a] and elution order of enantiomers *R,S*. Second row: $\Delta_{R,S}(\Delta G°)$.

Solute	*[CAM]* **1**		*[open-CAM]* **2**		*[3-PIN]* **3**		*[4-PIN]* **4**		*[THU]* **5**	
Methyloxirane	53.40 (*R*) 63.88 (*S*)	0.12	20.46 (*R*) 25.22 (*S*)	0.14	9.24[b]		10.46 (*R*) 13.51 (*S*)	0.16	49.24 (*S*) 63.39 (*R*)	0.17
Ethyloxirane	54.46 (*R*) 59.00 (*S*)	0.05	16.03 (*R*) 19.46 (*S*)	0.13	9.09 (*R*) 11.04 (*S*)	0.13	12.06 (*R*) 20.76 (*S*)	0.36	37.06 (*S*) 40.85 (*R*)	0.07
Isopropyloxirane	56.74[b]	[c]	15.35[b]	[c]	10.29 (*R*) 11.92 (*S*)	0.10	11.98 (*R*) 24.45 (*S*)	0.48	47.76 (*S*) 56.64 (*R*)	0.08
erythro-sec.-Butyloxirane	[b]		[b]		[b]		[b]		[b]	
threo-sec.-Butyloxirane	[b]		[b]		[b]		[b]		[b]	
tert.-Butyloxirane	38.70 (*R*) 43.43 (*S*)	0.08	14.81 (*R*) 17.48 (*S*)	0.11	7.21[b]	[c]	13.41 (*R*) 24.61 (*S*)	0.40	26.80 (*S*) 29.87 (*R*)	0.07
2,2-Ethylmethyloxirane	35.01 (*S*) 36.56 (*R*)	0.03	13.64[b]	[c]	4.30[b]	[c]	6.92[b] 10.07[b]	0.25	29.65[b] 33.76[b]	0.09
trans-2,3,Dimethyloxirane	22.47 (2*R*) 30.25 (2*S*)	0.20	16.22 (2*R*) 24.14 (2*S*)	0.26	5.18 (2*R*) 6.64 (2*S*)	0.16	6.22 (2*R*) 11.36 (2*S*)	0.40	33.03 (2*S*) 55.25 (2*R*)	0.35
cis-2,3-Dimethyloxirane	112.6		22.33		23.79		29.00		20.88	
trans-2-Ethyl-3-methyloxirane	7.79 (2*R*) 9.32 (2*S*)	0.12	8.49[b] 12.69[b]	0.26	3.90[b] 5.43[b]	0.22	5.94[b] 12.50[b]	0.49	26.13[b] 39.89[b]	0.28
cis-2-Ethyl-3-methyloxirane	42.54 (2*R*) 45.46 (2*S*)	0.05	39.87[b] 40.74[b]	0.01	22.01[b]	[c]	28.03[b] 32.54[b]	0.10	11.77[b]	[c]
2,2,3-Trimethyloxirane	19.00 (3*R*) 24.89 (3*S*)	0.18	15.85 (3*R*) 26.42 (3*S*)	0.34	4.28 (3*R*) 5.05 (3*S*)	0.11	4.97 (3*R*) 6.42 (3*S*)	0.17	25.77 (3*S*) 42.31 (3*R*)	0.33
2-Methyloxetane	[d]		[d]		34.44[b] 67.60[b]	0.45	42.53[b] 87.82[b]	0.48	[d]	
2-Methyltetrahydrofuran	56.63 (*S*) 60.33 (*R*)	0.04	8.16[b] 8.57[b]	0.03	8.44[b] 13.14[b]	0.30	20.89[b] 29.60[b]	0.23	60.4[b] 101.4[b]	0.35
trans-2,5-Dimethyltetrahydrofuran	2.25[b] 2.64[b]	0.10	1.28[b] 1.50[b]	0.11	0.22[b] 0.64[b]	0.70	0.69[b] 2.42[b]	0.83	1.78[b] 2.39[b]	0.20
cis-2,5-Dimethyltetrahydrofuran	6.21		2.29		2.35		9.50		11.54	
2-Methyltetrahydropyran	13.84 (*S*) 14.47 (*R*)	0.03	0.45	[c]	0.22[b] 0.31[b]	0.22	0.47[b] 0.77[b]	0.32	2.54[b] 3.21[b]	0.15

[a] Measured at, or extrapolated to, 0.1 *m* (molality) solvent in squalane. Extrapolated to ee = 100%, if necessary.

[b] Not measured.

[c] No separation detectable.

[d] Exceedingly high retention.

[Me-THU] **6**	*[NOP]* **7**	*[CARV]* **8**	*[MEN]* **9**	*[PUL]* **10**	*[i-MEN]* **11**	*[CHOL]* **12**
8.73 (*S*) 0.33 14.35 (*R*)	2.69 [c]	1.97 (*S*) 0.06 2.17 (*R*)	1.76 [c]	0.44 (*S*) 0.25 0.64 (*R*)	1.71 (*S*) 0.22 2.39 (*R*)	1.56 [c]
9.56 (*S*) 0.33 15.83 (*R*)	3.11 [c]	1.81 (*S*) 0.28 2.76 (*R*)	1.63 [c]	0.41 (*S*) 0.20 0.55 (*R*)	1.28 (*S*) 0.38 2.27 (*R*)	1.82 [c]
8.90 (*S*) 0.32 14.49 (*R*)	3.42 (*R*) 0.06 3.72 (*S*)	1.58 (*S*) 0.38 2.79 (*R*)	1.10 [c]	0.38 (*S*) 0.11 0.45 (*R*)	0.72 (*S*) 0.58 1.73 (*R*)	1.39 [c]
5.33 (2*R*) 0.22 7.45 (2*S*)	2.81 (2*R*) 0.14 3.48 (2*S*)	1.28 (2*S*) 0.33 2.10 (2*R*)	0.89 [c]	1.82 [b] 0.03 1.89 [b]	0.57 [b] 0.03 0.89 [b]	1.13 [c]
9.71 (2*R*) 0.35 16.44 (2*S*)	3.51 (2*R*) 0.10 4.07 (2*S*)	1.80 (2*S*) 0.45 3.54 (2*R*)	1.13 [c]	1.89 [b] 0.05 2.03 [b]	0.78 [b] 0.64 2.06 [b]	1.32 [c]
4.97 (*R*) 0.28 7.60 (*S*)	2.85 (*R*) 0.11 3.37 (*S*)	1.09 (*S*) 0.29 1.68 (*R*)	0.65 (*R*) 0.07 0.72 (*S*)	0.24 (*R*) 0.26 0.35 (*S*)	0.42 (*S*) 0.52 0.93 (*R*)	1.12 [c]
4.69 (*R*) 0.15 5.92 (*S*)	2.24 (2*S*) 0.13 2.72 (2*R*)	0.66 [b] 0.08 0.74 [b]	0.42 [b] 0.02 0.43 [b]	0.13 [c]	0.31 [c]	0.53 [c]
4.45 (2*S*) 0.28 6.78 (2*R*)	2.11 (2*R*) 0.09 2.41 (2*S*)	0.85 (2*S*) 0.13 1.04 (2*R*)	0.41 (2*S*) 0.26 0.60 (2*R*)	0.15 (2*S*) 0.51 0.33 (2*R*)	0.49 (2*S*) 0.62 1.23 (2*R*)	0.66 [c]
11.68	7.23	2.59	3.56	0.66	1.63	3.67
3.30 (2*S*) 0.18 4.32 (2*R*)	2.06 (2*R*) 0.04 2.18 (2*S*)	0.60 [b] 0.17 0.77 [b]	0.26 (2*S*) 0.18 0.34 (2*R*)	0.10 [b] 0.34 0.18 [b]	0.31 (2*S*) 0.61 0.80 (2*R*)	0.54 [c]
11.02 (2*R*) 0.02 11.28 (2*S*)	7.87 (2*R*) 0.03 8.25 (2*S*)	2.70 [b] 0.02 2.79 [b]	2.51 [b] 0.02 2.60 [b]	0.55 [c]	1.42 (2*S*) 0.08 1.61 (2*R*)	3.60 [c]
3.49 (3*S*) 0.04 3.72 (3*R*)	2.42 (3*S*) 0.04 2.59 (3*R*)	0.73 [c]	0.38 [b] 0.13 0.46 [b]	0.15 [c]	0.46 [c]	0.92 [c]
89.6 (*S*) 0.33 147.3 (*R*)	47.5 (*S*) 0.26 70.8 (*R*)	21.4 (*S*) 0.18 28.0 (*R*)	9.50 (*S*) 0.27 14.25 (*R*)	2.27 (*S*) 0.12 2.74 (*R*)	7.58 (*S*) 0.22 10.53 (*R*)	16.53 [c]
6.70 (*S*) 0.02 6.93 [b]	7.82 (*R*) 0.20 10.55 (*S*) [b]	2.09 [b] 0.04 2.22 [b] [b]	0.77 (*S*) 0.22 1.08 (*R*) [b]	0.23 [c] [b]	0.67 [c] [b]	2.20 [c] [b]
[b]	[b]	[b]	[b]	[b]	[b]	[b]
0.42 [c]	0.27 [c]	0.15 [c]	0.05 [c]	0.03 [c]	0.06 [c]	0.14 (*S*) 0.12 0.17 (*R*)

Selectivity of solute–solvent association (horizontal comparison)

The interaction between cyclic ethers and the nickel bis chelates **1–12** show remarkable differences. As shown for methyloxirane, the interaction with **1–12**, when normalized to $m = 0.1$ mol/kg, decreases in the order:

[CAM] > [THU] > [open-CAM] > [4-PIN] > [3-PIN] > [Me-THU] >

[NOP] > [CARV] > [CHOL] > [MEN] > [i-MEN] > [PUL]

Despite the dramatic differences in donor–acceptor association, whereby [CAM] shows the strongest and [PUL] the weakest coordination of methyloxirane, respectively, the measure for chiral recognition, $-\Delta_{R,S}(\Delta G^\circ)$, differs only by a factor of 2 from the weakly interacting [PUL], including an higher enantiomer discrimination than that of [CAM]. This result is also of practical interest, because efficient enantiomer separation already caused by a rather weak solute–solvent interaction permits rapid enantiomer analyses via short retention times. In general, the nickel bis chelates containing bicyclic terpene moieties exhibit much stronger acceptor properties than those containing monocyclic terpene structures. While the decrease in interaction by a factor of 10 upon going from [THU] to [Me-THU] may be rationalized by steric arguments, the reverse situation, *i.e.* , the increase of interaction when going from [NOP] to [Me-NOP = 4-PIN] is difficult to comprehend. It should be mentioned that any interpretation of the selectivity of association between a single solute with different solvents (horizontal comparison) can only be very tentative, because the nickel bis chelates may possess different molecular structures, such as coordination geometries and/or different states of self-association, etc. (*vide infra*).

Selectivity of solute–solvent association (vertical comparison)

The vertical comparison of the retention increase, R', between cyclic ethers, differing in alkyl substitution, E/Z geometry and ring size, with one particular nickel bis chelate **1–12** directly reveals steric, electronic and any strain effects of the solute–solvent association. For studying these effects [CHOL] is a useful test compound, because the retention increase, R', is identical for both enantiomers, $-\Delta_{R,S}(\Delta G^\circ) = 0$.

The effect of alkyl substitution at the α-carbon atom of cyclic ethers on the donor–acceptor association equilibrium is thought to arise mainly from electronic and steric factors. Unfortunately, these contributions to association selectivity cannot readily be separated from each other. Moreover, the electronic and steric effects of alkyl groups will oppose each other, because the +I-effect of the alkyl substituent tends to increase the donor properties of the lone pairs of oxygen and will be counterbalanced by steric hindrance, created by bulky alkyl groups. Thus, the donor–acceptor association of monoalkyl-substituted oxiranes with [CHOL] slightly increases upon going from methyl- to ethyloxirane and then steadily decreases with increasing steric hindrance, whereby interestingly the configuration of the *sec*-butyl group shows a remarkable steric effect. Introduction of a second alkyl group in a geminal- or *trans*-position leads to a strong steric destabilization of association, because one alkyl group is disposed in a position *syn* to the coordinating lone pair of oxygen. Contrarily, *cis*-dialkyl substitution entails an increase in interaction compared to monoalkyl substitution, and this is clearly due to an electronic effect, because the alkyl substituents may adopt a position *anti* to the lone pair of oxygen. As might have been expected, the trialkyl-substituted oxirane (trimethyloxirane) shows an association behaviour intermediate between those of *cis*- and *trans*-dialkyloxiranes. Allowing for some small individual changes owing to the compositional diversity of the solvents,

the general trend of association selectivity between oxiranes and [CHOL] is also observed for all other nickel bis chelates, regardless of the overall strength of the association equilibria. It follows then that the small degree to which this general trend fluctuates for the individual enantiomers of the solute determines the extent of chiral recognition caused by the solvent, as expressed by $-\Delta_{R,S}(\Delta G^\circ)$ (*vide supra*).

An high selectivity of the association equilibria, differing by two orders of magnitude, is observed as the result of changing the ring size of α-methyl-substituted cyclic ethers. Thus, while methyloxirane and 2-methyltetrahydrofuran exhibit a comparable association strength with [CHOL], that of 2-methyloxetane is stronger by a factor of ten and that of 2-methyltetrahydropyran is weaker by approximately the same factor. This remarkable influence of ring size upon coordination with nickel bis chelates

$$\text{oxane} < \text{oxolane} \leqslant \text{oxirane} \ll \text{oxetane}$$

is evident for all solvents investigated and was previously discovered for [CAM][15]. The exceedingly strong interaction of oxetanes and nickel bis chelates may give rise to extreme retention times, preventing the acquisition of thermodynamic data for donor–acceptor association.

Enantioselectivity

While the donor–acceptor association selectivity between alkyl-substituted cyclic ethers and the nickel bis chelates **1–12** follows the same trend (vertical comparison), regardless of the strength of interaction (horizontal comparison), remarkable differences are observed for the individual enantiomers of the solute, as expressed by $-\Delta_{R,S}(\Delta G^\circ)$. Thus, inspection of the table reveals that

$$[\text{CHOL}] \ll [\text{NOP}] < [\text{MEN}] < [\text{3-PIN}]$$

entail negligible chiral recognition, while

$$[\text{CARV}] < [\text{Me-THU}] < [\text{4-PIN}] < [\text{i-MEN}]$$

display the highest enantioselectivity for oxiranes. The largest figure for oxiranes, $-\Delta_{R,S}(\Delta G^\circ) = 0.60$–$0.65$ kcal/mol, has been observed with [i-MEN], while $-\Delta_{R,S}(\Delta G^\circ) = 0.83$ kcal/mol was found for *trans*-2,5-dimethyltetrahydrofuran and [4-PIN] at 60°C.

The unique molecular architectures displayed by the terpene backbones of the nickel bis chelates **1–12** offer interesting insights into trends of enantiomer discrimination.

Variation of conformational flexibility by formal opening of the chelate terpene fusion: [CAM] vs. [open-CAM]. This comparison shows that a rigid polycyclic structure is not a prerequisite for efficient chiral recognition. Quite unexpectedly, a slightly higher enantiomeric bias is observed for the conformationally flexible solvent [open-CAM]. A similar observation has been made by McCreary *et al.*[10] with europium(III) tris chelates containing ketoenolates related to [open-CAM] which

showed efficient chemical shift differences of enantiotopic protons by NMR spectroscopy.

Variation of ring size in the bicyclic terpene moiety: [CAM], [PIN] and [THU]. This comparison does not demonstrate any significant influence of strained rings in the terpene moiety on enantiomer discrimination.

Inversion of the bicyclic terpene moiety with respect to the metal chelate ring: [4-PIN] vs. [3-PIN]. This comparison reveals a remarkable difference of chiral recognition for bulky monoalkyl-substituted oxiranes, whereby [3-PIN] shows none or only negligible enantiodifferentiation, indicating that the position of the cyclobutane unit in pinanone, juxtaposed *syn* to the perfluoroalkyl residue, impairs enantiomer discrimination. No such effect is noted for cyclic ethers containing four-, five- and six-membered rings.

Increase in steric constraint by methyl substitution: [Me-THU] vs. [THU] and [4-PIN] vs. [NOP]. This comparison shows that methyl substitution of the terpene moiety significantly increases enantiomer discrimination for monoalkyl-substituted oxiranes. [NOP] exhibits consistently lower enantiodifferentiation as compared to [4-PIN]. However, the stronger enantioselectivity of [THU] as compared to [Me-THU] for trimethyloxirane and 2-methyltetrahydrofuran should be noted, stressing the complexity of chiral recognition phenomena in complexation GC.

Transformation of bicyclic to monocyclic terpene moieties by formal ring opening between C_1 and C_6: [3-PIN] vs. [CARV] and [4-PIN] vs. [i-MEN]. This comparison shows that solvents with monocyclic terpene moieties are as efficient as, and in some cases even superior to, their bicyclic counterparts with respect to enantiomer discrimination. This result implies again that steric rigidity is not a precondition for efficient chiral recognition.

Variation of the geometric relationship between the 1,4-dialkylcyclohexane substituents in monocyclic terpene moieties: [MEN] vs. [PUL] vs. [i-MEN]. This comparison should illuminate the effect of the position of the isoprop(en)yl group (*trans*, *cis*, planar) with respect to the methyl group at the carbon atom with fixed stereochemistry. For oxiranes, with the exception of trimethyloxirane, efficient enantiomer discrimination is found with [i-MEN] and to a lesser extent with [PUL] but not with [MEN], indicating a pronounced effect of the relative geometry of the 1,4-dialkylcyclohexane substituents on $-\Delta_{R,S}(\Delta G^\circ)$. With increasing bulk or ring size of the cyclic ethers, chiral recognition is induced also by [MEN]. As expected, [PUL], possessing a configuration between that of [MEN] and [i-MEN], exhibits also an enantiomer discrimination intermediate between those of these stereoisomers.

Inversion of the 1,4-dialkyl(idene)cyclohexane substituents in monocyclic terpene moieties: [PUL] vs. *[CARV].* This comparison should shed light on the rôle of an alkyl group juxtaposed *syn* to the perfluoroalkyl group. However, the results allow no clear-cut decision on the influence of steric bulk at the chiral centre of C_4, because either [CARV] or [PUL] shows a moderate chiral recognition effect for a particular solute. In keeping with the observations made with the series of solvents [i-MEN], [PUL] and [MEN], it can be predicted that [CARV] will entail an intermediate enantiomer discrimination as compared to either one of the nickel bis chelates obtained from α-heptafluorobutanoyl-carvomenthonate [CARVMEN] **13** and -iso-carvomenthonate [i-CARVMEN] **14**. Unfortunately, these terpene ketones are not readily accessible in epimerically and enantiomerically pure form.

Planarization through incorporation of unsaturation into the terpene moiety with concomitant π-orbital conjugation with the quasiaromatic metal chelate ring: [PUL] and [CARV]. The comparison of solvents containing an essentially planar conjugated π system, [CARV] and [PUL], with solvents containing bulky bicyclic terpene moieties, *e.g.*, [CAM] or [3-PIN], with regard to their ability to induce enantioselectivity towards alkyl-substituted cyclic ethers reiterates once again that chiral recognition may be brought about by rather simple molecular architectures.

Correlation between absolute configuration and order of elution

The correlation between the molecular configuration of the enantiomers of the solute and their relative order of elution from the solvent of defined chirality ought to give additional insight into the mechanisms of enantiomer discrimination by complexation GC. In this study, the absolute configuration of the enantiomeric fractions which are eluted as the first or second peak, respectively, for most cyclic ethers and the nickel(II) bis chelates **1–12** has been determined by simultaneous coinjection of enantiomers with known stereochemistry[18]. This study aimed at recognizing certain trends of chiral recognition between solutes belonging to a class of homologous compounds and solvents representing different constitutional (*cf.*, Scheme 1) and/or configurational (*cf.*, Scheme 2) compositions. It has previously been found that *S*-methyloxirane and (2*S*,3*S*)-2,3-dimethyloxirane exhibit a stronger interaction with nickel(II) bis[3-(heptafluorobutanoyl)-(1*R*)-camphorate] **1**, obtained from natural (+)-D-(1*R*)-camphor, and were therefore eluted as the second peak[23]. This observation led to the formulation of a quadrant rule, which empirically predicts the elution order of alkyl-substituted three-membered heterocycles from GC column, containing **1**, derived from (1*R*)-camphor.

Thus, when the heterocycle is viewed from the heteroatom X in the direction of the horizontal C–C bond, the absolute configuration of the enantiomer eluted as the second peak from (1*R*)-**1** (M = Ni) is that in which the bulkier group(s) is (are) situated on the upper left at C_1 and/or the lower right at C_2. Although in most cases the validity of the quadrant rule was confirmed, a number of exceptions were found when it was extended to other solvents or solutes with larger ring sizes[7,15].

Inconsistency of the quadrant rule may have its origin not only in structural requirements but also in the temperature-dependent reversal of enantioselectivity due to the inherent thermodynamics of chiral recognition which leads to a change of the sign of $\Delta_{R,S}(\Delta G^\circ)$ at the isoenantioselective temperature[16]. With this in mind, it is surprising to find that the elution order of cyclic ethers on all nickel bis chelates **1–12** shows a rather consistent trend, save for some exceptional cases, lending further support to the justification of formulating rules which correlate absolute configurations of the solute with its retention behaviour on metal bis chelates of predefined chirality in complexation GC. Inspection of Tables I and II shows that a consistent elution order for members of homologous solutes is observed on solvents that induce a large enantiomer discrimination, $-\Delta_{R,S}(\Delta G^\circ)$. The following discussion will focus on solvents that entail a strong enantiomer discrimination. It will be seen that an high degree of consistency between the molecular configuration and the elution order for mono-, di- and trialkyl-substituted oxiranes is observed (*cf.*, the table). The following trends are noteworthy.

Variation of conformational flexibility by formal opening of the chelate terpene

fusion: [(1R)-CAM] vs. [(1R)-open-CAM]. This comparison shows that opening of the camphor skeleton between C_3 and C_4 slightly improves the degree of enantiomer discrimination, but does not change its sign for monoalkyl-substituted oxiranes.

Increase of steric constraint and introduction or removal, respectively, of a new chiral centre by methyl substitution: [Me-THU] vs. [THU] and [4-PIN] vs. [NOP]. This comparison shows that methyl substitution, which either destroys or creates a chiral centre, has no influence on the sign of $\Delta_{R,S}(\Delta G°)$, which is obviously governed by the chirality of the equivalent bicycle terpene skeleton. It should be noted that [THU] used in this study actually represented a mixture of epimers with regard to C_4 with an unknown molar ratio, and [Me-THU] may be thought to produce the same overall effect as a mixture of the epimeric [THU]s. The inverse retention behaviour of *trans*-2,3-dimethyloxirane on [4-PIN] *vs.* [NOP] is noteworthy, but insignificant, in view of the poor enantiomer discrimination of the latter.

Inversion of the bicyclic terpene moiety of equivalent stereochemistry with respect to the metal chelate ring: [4-PIN] vs. [3-PIN]. This comparison does not reveal any change in the sign of $\Delta_{R,S}(\Delta G°)$, suggesting that the equivalent chirality of the positional isomers (1*R*,2*S*)-pinan-4-one and (1*R*,2*R*)-pinan-3-one determines the elution order for alkyl-substituted oxiranes, irrespective of their inverted fusion with the β-diketonate ring.

Transformation of bicyclic to monocyclic terpene moieties of equivalent stereochemistry by formal ring opening between C_1 and C_8: [4-PIN] vs. [i-MEN]. This comparison shows that formal ring opening of the bicyclic terpene moiety to the monocyclic terpene structure with the same chirality on the carbon atoms does not lead to an identical elution order for any of the solutes investigated.

Transformation of bicyclic to monocyclic terpene moieties of equivalent stereochemistry at the carbon atom carrying the isoprop(en)yl substituent: [Me-THU] and [THU] vs. [CARV]. This comparison indicates that the consistency of the elution order for mono-, *trans*-di and trisubstituted oxiranes as well as 2-methyloxetane is governed by the (equivalent) chirality of the carbon atom carrying the bulky isoprop(en)yl group, juxtaposed *syn* to the perfluoroalkyl group.

Inversion of the p-menthane moiety with equivalent stereochemistry at the carbon atom carrying the isoprop(en)yl substituent: [CARV] vs. [i-MEN]. This comparison indicates that the consistency of the elution order for mono-, *trans*-di and trisubstituted oxiranes, as well as 2-methyloxetane is governed by the (equivalent) chirality of the carbon atom carrying the bulky isoprop(en)yl group residing in different positions with respect to the perfluoroacyl group.

Variation of the geometric relationship between the 1,4-dialkylcyclohexane substituents in monocyclic terpene moieties, [MEN] vs. [PUL] vs. [i-MEN], and their inverted order: [PUL] vs. [CARV]. This comparison shows that changing the chirality of the carbon atom carrying the isopropyl group in [MEN] *vs.* [i-MEN] changes the elution order for *tert.*-butyloxirane but not for *trans*-2,3-dimethyloxirane and 2-methyloxetane. Having the bulky isopropylidene group in a planar position [PUL] causes a reversed elution order for *tert.*-butyloxirane compared to [i-MEN]. The identical elution orders for *trans*-2,3-dimethyloxirane and 2-methyloxetane on [i-MEN], [PUL] and [MEN] can be explained only by assuming that for these solutes the chirality carrying the methyl group juxtaposed *syn* to the perfluoroalkyl group is important in determining the sign of $\Delta_{R,S}(\Delta G°)$, irrespective of the relative geometry of the bulky isopropyl(idene) group.

CONCLUSIONS

The results of this investigation may be summarized as follows:

The selectivity of the solute–solvent association (vertical comparison) between alkyl-substituted oxiranes and compounds **1–12** follows a common trend, which is rationalized in terms of opposing electronic and steric effects of the Lewis bases.

The origin of the striking influence of the ring size of cyclic ethers on the association strength with **1–12** which varies by two orders of magnitude, *i.e.* oxane < oxolane ⩽ oxirane ⩽ oxetane remains elusive.

There is no clear-cut relationship between the strength of solute–solvent association and the magnitude of enantiomer discrimination, *i.e.*, the chiral recognition factor, $\chi = -\Delta_{R,S}(\Delta G^\circ)/-\Delta G^\circ$. varies at random, although, in general, enantioselectivity is high when the donor–acceptor interaction is impaired on steric grounds.

For chiral alkyl-substituted oxiranes, a consistent relationship between molecular configuration and the order of elution is observed for almost all solvents **1–12**. The reliability of empirical rules that correlate configuration and peak emergence improves as the propensity of the solvent to induce enantiomer discrimination increases.

The magnitude and the sign of enantioselectivity, $-\Delta_{R,S}(\Delta G^\circ)$, between alkyl-substituted cyclic ethers and **1–12** can neither be predicted nor rationalized by simple molecular models, owing to the complexity of the nature of the solvent under the conditions of the GC experiment.

The present study has revealed improved chiral stationary phases for the enantiomer separation of alkyl-substituted cyclic ethers. The highest enantiomeric bias of solvents with a bicyclic terpene structure is induced by [4-PIN] and of those with a monocyclic terpene structure by [CARV].

The preparation of the solvents **1–12** possessing interesting molecular architectures will stimulate further investigations of enantiomer separation of other classes of compounds by complexation GC and by substitution of nickel(II) by lanthanide(III) ions may complement[11] the arsenal of chiral lanthanide shift reagents for the NMR spectroscopic discrimination of enantiotopic nuclei.

While the conditions of the use of the solvents **1–12** were chosen to obtain reliable thermodynamic data for solute–solvent association, the employment for practical purposes of high-resolution glass and fused-silica columns as well as polysiloxanes as co-solvents for **1–12**[6,24] has greatly improved the state of the art of enantiomer separation by complexation GC and various applications have been reported[4,7,8]. Thus, [NOP] and [4-PIN] have been used as versatile solvents for the enantiomer separation of diols as their acetonides or *n*-butylboronates[25], and [PUL] has been employed, *inter alia*, for the enantiomer separation of the pheromone chalcogran (2-ethyl-1,6-dioxaspiro[4.4]nonane)[26] and [Me-THU] for that of the pheromone of the olive fly, 1,7-dioxaspiro[5.5]undecane[27]. Finally, [CARV] has recently been employed as a versatile stationary phase for the first semipreparative enantiomer separation of spiroketals by complexation GC[28].

REFERENCES

1 V. Schurig, *Inorg. Chem.*, 11 (1972) 736.
2 V. Schurig, *J. Coord. Chem.*, 6 (1976) 63.
3 V. Schurig, *Chromatographia*, 13 (1980) 263.
4 V. Schurig and R. Weber, *Angew. Chem. Suppl.*, (1983) 1130.
5 V. Schurig, in J. D. Morrison (Editor), *Asymmetric Synthesis*, Vol. 1, Academic Press, New York, 1983, p. 59.
6 V. Schurig and R. Weber, *J. Chromatogr.*, 289 (1984) 321.
7 V. Schurig, *J. Chromatogr.*, 441 (1988) 135.
8 V. Schurig, *Kontakte (Darmstadt)*, No. 1 (1986) 3 and references therein.
9 V. Schurig, in P. Schreier (Editor), *Bioflavour '87*, Walter de Gruyter, Berlin, New York, 1988, p. 35 and references therein.
10 M. D. Mc Creary, D. W. Lewis, D. L. Wernick and G. M. Whitesides, *J. Am. Chem. Soc.*, 96 (1974) 1038.
11 V. Schurig, *Kontakte (Darmstadt)*, (1985, 2) 22.
12 W. H. Pirkle and D. J. Hoover, *Top. Stereochem.*, 13 (1982) 263.
13 V. Schurig, R. C. Chang, A. Zlatkis and B. Feibush, *J. Chromatogr.*, 99 (1974) 147.
14 V. Schurig, *Inorg. Chem.*, 25 (1986) 945.
15 V. Schurig and W. Bürkle, *J. Am. Chem. Soc.*, 104 (1982) 7573.
16 V. Schurig, J. Ossig and R. Link, *Angew. Chem., Int. Ed. Engl.*, 28 (1989) 197.
17 V. Schurig and R. Weber, *J. Chromatogr.*, 217 (1981) 51.
18 K. Hintzer, *Thesis*, University of Tübingen, 1983.
19 R. Weber, *Thesis*, University of Tübingen, 1983.
20 *Beilsteins Handbuch der Organischen Chemie*, E III, Vol. 7.
21 C. H. Brieskorn and W. Schwack, *Chem. Ber.*, 114 (1981) 1993.
22 U. Beitler and B. Feibush, *J. Chromatogr.*, 123 (1976) 149.
23 V. Schurig, B. Koppenhoefer and W. Bürkle, *Angew. Chem., Int. Ed. Engl.*, 17 (1978) 937.
24 V. Schurig, U. Leyrer and R. Weber, *J. High Resolut. Chromatogr. Chromatogr. Commun.*, 8 (1985) 459.
25 V. Schurig and D. Wistuba, *Tetrahedron Lett.*, 25 (1984) 5633.
26 B. Koppenhoefer, K. Hintzer, R. Weber and V. Schurig, *Angew. Chem., Int. Ed. Engl.*, 19 (1980) 471.
27 G. Haniotakis, W. Francke, W. K. Mori, H. Redlich and V. Schurig, *J. Chem. Ecol.*, 12 (1986) 1559.
28 V. Schurig, *Naturwissenschaften*, 74 (1987) 190.

Journal of Chromatography, 475 (1989) 45–53
Elsevier Science Publishers B.V., Amsterdam — Printed in The Netherlands

CHROMSYMP. 1614

OCCURRENCE OF D-AMINO ACIDS IN FOOD

DETECTION BY CAPILLARY GAS CHROMATOGRAPHY AND BY REVERSED-PHASE HIGH-PERFORMANCE LIQUID CHROMATOGRAPHY WITH L-PHENYLALANINAMIDES AS CHIRAL SELECTORS

GERARDO PALLA*, ROSANGELA MARCHELLI, ARNALDO DOSSENA and GIUSEPPE CASNATI
Istituto di Chimica Organica dell'Università, viale delle Scienze, 43100 Parma (Italy)

SUMMARY

The presence of D-amino acids was investigated in dairy products, in raw ham and in roasted coffee. The analysis was carried on by capillary gas chromatography, using a very stable tetraamidic selector derived from L-phenylalanine, which allowed the detection of D-alanine, D-aspartic acid, D-glutamic acid and other D-amino acids. Moreover, D-glutamic acid and D-alanine were detected also by reversed-phase high-performance liquid chromatography, using L-phenylalaninamide and copper(II) acetate as chiral additives to the eluent. The presence of D-amino acids may be ascribed to thermal racemization or to microbial activity.

INTRODUCTION

Amino acids in proteins are generally assumed to occur as L-enantiomers. However, D-amino acids are quite common in nature as constituents of bacterial cell walls (D-alanine, D-glutamate) and of several antibiotics[1]. In addition, heat and alkali treatments, used for food processing, have been shown to produce racemization of "natural" L-amino acids[2–5], thus affecting the food quality by decreasing the nutritional value, or producing xenobiotics of unknown biological properties.

In the last few years we have been involved in the study of the mechanism of chiral recognition by both gas chromatography (GC)[6] and high-performance liquid chromatography (HPLC)[7]. In particular, we synthesized a novel series of chiral tetraamidic selectors containing L-phenylalanine, which enabled good separations of N-trifluoroacetyl (TFA) alkyl esters of D,L-amino acids by GC[8], and devised new copper(II) complexes as chiral additives to the eluent, which yielded good separations of D,L-dansyl (Dns) amino acids in HPLC on a C_{18} column[9,10].

In a general project aimed at studying the presence of xenobiotics in food, we have investigated the occurrence of D-amino acids in processed foods, in particular those which undergo a severe heat treatment such as roasted coffee, ultra-high temperature (UHT) milk and in products obtained by fermentation processes (yoghurt

0021-9673/89/$03.50

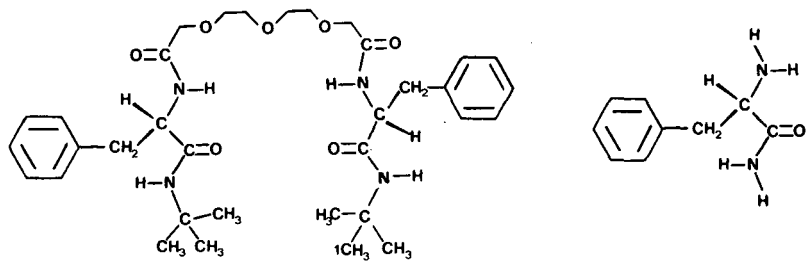

1 2

Fig. 1. Structure of the chiral selectors L-Phe-3-O-TA (**1**) and L-Phe-A (**2**).

and cheese). For this work we used the selector trioxaundecanoyl tetramide, **1** (L-Phe-3-O-TA), as a stationary phase for GC analysis, and L-phenylalaninamide, **2** (L-Phe-A), with copper acetate as a chiral additive for the HPLC eluent (Fig. 1).

EXPERIMENTAL

Gas chromatography

GC analyses were carried out with a Dani 8500 instrument, from Dani (Monza, Italy), equipped with a flame ionization detector, using wall-coated open-tubular (WCOT) fused-silica columns (0.25 mm × 20–25 m I.D.), injector and detector at 250°C, with helium as the carrier gas at a pressure of 0.75 bar. Bare silica columns (Supelco, Bellefonte, PA, U.S.A.) were leached with 20% HCl at 120°C, deactivated with barium carbonate[11] and then statically wall-coated with a dichloromethane solution of the chiral tetraamide L-Phe-3-O-TA (0.15%) and of the commercial silicone gum OV-101 (0.15%) (Carlo Erba, Italy). Other columns were statically coated with the same procedure, using tetraamide L-Phe-3-O-TA and Carbowax 20M (Carlo Erba), instead of OV-101. Columns were conditioned for 10 h at 180°C. The numbers of effective theoretical plates per metre, N/m, were calculated under isothermal conditions at 120°C and 0.75 atm, with split injection of *n*-dodecane for OV-101 columns and of methyl dodecanoate for Carbowax 20M columns.

Derivatization of standard D,L-amino acids for GC

N-TFA-amino acid methyl, isopropyl or butyl esters were prepared as follows: 10 mg of D,L-amino acid were dissolved in 2 ml of 1 *M* HCl in alcohol (methanol, 2-propanol or butanol respectively) and kept in a sealed tube at 90°C for 1 h. The sample was evaporated, the residue was dissolved in dry dichloromethane (4 ml) and treated with trifluoroacetic anhydride (0.5 ml) in a sealed or a screw-capped tube at 70°C for 1 h. After cooling, the tube was opened with care, the solvent was evaporated and the residue was redissolved in dichloromethane and analyzed. No racemization of pure L-enantiomers was observed during this treatment.

Liquid chromatography

Chromatographic analyses were carried out with a Waters 440 Model liquid

TABLE I

ELUTION PROGRAMME USED FOR THE SEPARATION OF D,L-DNS-AMINO ACIDS BY HPLC

t (min)	*Flow-rate (ml/min)*	*Buffer A (22% acetonitrile)*	*Buffer B (50% acetonitrile)*
0	0.5	100	0
68	0.5	68	32
85	0.8	57	43
110	0.8	0	100
130	0.2	100	0

chromatograph, equipped with a UK-6 septumless injector, a 6000 A pump, a Model 420 fluorescence detector and a Waters recorder (Waters Assoc., Milford, MA, U.S.A.). A C_{18} Novapak (4 μm, 15 cm × 0.4 cm) column (Waters Assoc.) was used. Two aqueous solutions containing 4 m*M* L-phenylalaninamide, 2 m*M* copper acetate and 0.3 *M* sodium acetate were prepared, the former (A) containing 22% of acetonitrile, the latter (B) 50%. The eluent was filtered and degassed under reduced pressure. The pH was adjusted to 7.3 with concentrated sodium hydroxide. The mixing was performed by means of a Waters automated gradient apparatus, according to the program shown in Table I.

Derivatization of standard D,L-amino acids for HPLC

To 50 μl of a 10 m*M* sample of the amino acids, 150 μl of an acetonitrile solution containing dansyl chloride (Dns-Cl) (3 mg/ml) and 300 μl of an aqueous solution of Li_2CO_3 (40 m*M*, pH 9.5) were rapidly added. The mixture was gently shaken until the turbidity disappeared and then allowed to stand at room temperature for 35–40 min, in the dark. The reaction was quenched by adding 50 μl of ethylamine. The reaction mixture can either be injected directly or dried with nitrogen and redissolved in doubly distilled water.

Extraction and derivatization of free amino acids from milk

A 20-ml volume of milk was diluted to 100 ml with distilled water, treated under stirring with 5 ml of trifluoroacetic acid to remove proteins and then centrifuged at 3000 *g* for 10 min. The supernatant was concentrated under vacuum to remove the trifluoroacetic acid, the residue was dissolved with 50 ml of water and extracted twice with 50 ml of diethyl ether to remove fats. The aqueous phase was filtered, evaporated to remove the organic solvent and passed through an ion-exchange column (30 cm × 1.5 cm) filled with a cation-exchange resin (Dowex 50W-X2), freshly regenerated with 60 ml of 2 *M* HCl. Amino acids were then eluted from the resin with 60 ml of 2 *M* HCl. The eluate was divided into two fractions, one for GC and the other for HPLC analysis, and evaporated to dryness. One fraction was dissolved in 1 *M* HCl in 2-propanol and treated according to the procedure reported for the derivatization of standard amino acids in GC. The fraction for HPLC analysis was dissolved in 2 ml of distilled water and ultrafiltered through a Millipore PLGC cellulose filter (Millipore, Milford, MA, U.S.A.) to remove proteins. A 1-ml volume of the ultrafiltered sample was diluted to 2 ml by adding a 30% aqueous methanol solution containing 0.1%

trifluoroacetic acid, and then passed through a Sep-Pak C_{18} cartridge (Waters Assoc.), previously conditioned by washing with 10 ml of HPLC-grade methanol, 10 ml of 0.1% trifluoroacetic acid in water and 10 ml of 0.1% trifluoroacetic acid in 20% aqueous methanol. The sample eluted from the cartridge was dried, redissolved in 0.1 *M* LiOH and 40 m*M* Li_2CO_3 to pH 7.5 and brought to a final volume of 4 ml. The derivatization procedure was performed on 50 μl of the sample at a time, by adding 150 μl of the acetonitrile solution of Dns-Cl (3 mg/ml) and 300 μl of the 40 m*M* Li_2CO_3 aqueous solution.

Extraction and derivatization of free amino acids from cheese

A 1-g of grated cheese was dissolved in 50 ml of distilled water, treated with 5 ml of trifluoroacetic acid and stirred for 2 min. The sample was centrifuged for 10 min at 3000 *g*, the supernatant was evaporated to remove trifluoroacetic acid, then diluted with 20 ml of water and extracted twice with 50 ml of diethyl ether to remove fats. The aqueous fraction was recovered, divided into two parts and evaporated to dryness. The first part was dissolved in 1 *M* HCl in methanol and treated according to the derivatization procedure for standard amino acids in GC. The second fraction was ultrafiltered and derivatized as reported for HPLC analysis of milk samples.

Extraction and derivatization of free amino acids from yoghurt

A 10-g amount of yoghurt was dissolved in 50 ml of distilled water, treated with 2 ml of trifluoroacetic acid, stirred for 2 min and centrifuged at 3000 *g* for 10 min. The supernatant was evaporated to remove the acid, diluted with water to 100 ml and extracted three times with 50 ml of dichloromethane. The aqueous fraction was evaporated to remove the organic solvent and was passed through a cation-exchange resin in the acid form, as reported for the milk treatment. Amino acids were recovered from the resin by eluting with 2 *M* HCl and were derivatized as reported for milk amino acids.

Extraction and derivatization of free amino acids from coffee

A 5-g amount of roasted coffee (Brasilian) was stirred for 2 min with 20 ml of hot water and filtered. The filtrate was evaporated to dryness and 0.5 g of residue were dissolved in 50 ml of methanol, filtered and evaporated to dryness. A 50-mg amount of the new residue was dissolved in 10 ml of 1 *M* HCl in methanol and kept at 80°C for 1 h in a screw-capped test-tube. The solution was evaporated, and the residue was dissolved in dichloromethane (3 ml) and derivatized with trifluoroacetic anhydride for GC. Green coffee was analyzed in the same way, starting with 5 g of a milled sample.

Extraction and derivatization of free amino acids from raw ham

A 5-g amount of raw ham, aged for 18 months (Parma technology), was homogenized for 5 min in 20 ml of warm water containing 2 ml of trifluoroacetic acid, and then centrifuged at 3000 *g* for 10 min. The supernatant was concentrated to dryness, dissolved in 50 ml of water and extracted with diethyl ether. The aqueous fraction was concentrated under vacuum and the residue was dissolved in 10 ml of 1 *M* HCl in methanol and derivatized for GC analysis as reported for standard amino acids.

TABLE II

COLUMN CHARACTERISTICS AND RESOLUTION FACTORS FOR N-TFA-D,L-AMINO ACID METHYL ESTERS

Column	*N/m*	*Length (m)*	*I.D. (mm)*	*Film (μm)*	*Resolution factors,* $r = t'_L/t'_D$							
					Ala	*Val*	*Leu*	*Nleu*	*Asp*	*Met*	*Phe*	*Glu*
A	1200	20	0.25	0.21	1.084	1.102	1.090	1.067	1.015	1.018	1.017	1.016
B	1850	25	0.25	0.15	1.037	1.050	1.043	1.034	1.006	1.011	1.010	1.009

RESULTS AND DISCUSSION

Food analysis of D,L-amino acids by capillary GC

The two chiral columns used were characterized by different polarities: A, less polar, carrying L-Phe-3-O-TA (**1**) on OV-101 silicone gum; B, more polar with L-Phe-3-O-TA on Carbowax 20M. The column properties and performance, with resolution factors $r = t'_L/t'_D$ of N-TFA-D,L-amino acid methyl esters, are reported in Table II.

The resolution, r, was obtained at 0.75 bar helium, with a temperature programme of 110–170°C at 3°/min, after an initial hold at 110°C for 4 min. The r values obtained with columns A and B for N-TFA-D,L-valine 2-propyl ester at 90°C were 1.130 and 1.095, respectively, and were considered satisfactory. Column A shows higher resolution, but B is more efficient.

In Fig. 2 gas chromatograms of a cheese sample, obtained with columns A and B, respectively, are compared. In many cases, the reversed elution order for alanine and valine, and for glycine and leucine, recorded on the two columns, was of help for identification. The resolution of D,L-valine and D,L-alanine is higher with column B, while D,L-aspartic and D,L-glutamic acids are better resolved on column A. Both columns can easily be fitted and used on gas chromatography–mass spectrometry (GC–MS) quadrupole instruments (Finnigan 1050, Hewlett-Packard 5970B), with operating parameters similar to those used for GC.

Milk. Samples of cow's milk, new, pasteurized, ultra-high temperature treated (UHT) milk and dried milk were tested. D,L-Norleucine was used as the internal standard for quantitative analysis. Because of their low amount in milk (60–200 ppm), the free amino acids were derivatized to 2-propyl esters, thus obtaining an higher response to the flame ionization detector than the methyl esters. Several amino acids were identified by their retention volumes and by GC–MS. The presence of alanine, valine, glycine, leucine, proline, aspartic acid, methionine, glutamic acid and phenylalanine was confirmed by comparison with the fragmentation patterns reported in the NBS library (of the Finnigan 1050 quadrupole). The most abundant amino acid detected was glutamic acid (40–130 mg/l), which derives also from the hydrolysis of glutamine during the derivatization step. A typical gas chromatogram of milk amino acids (as N-TFA-2-propyl esters) is shown in Fig. 3.

The percentages of racemization of free amino acids detected in milk, cheese, yoghurt, ham and coffee samples are summarized in Table III.

The presence of D-glutamic acid (3–5%) and D-aspartic acids (1–3%) was ob-

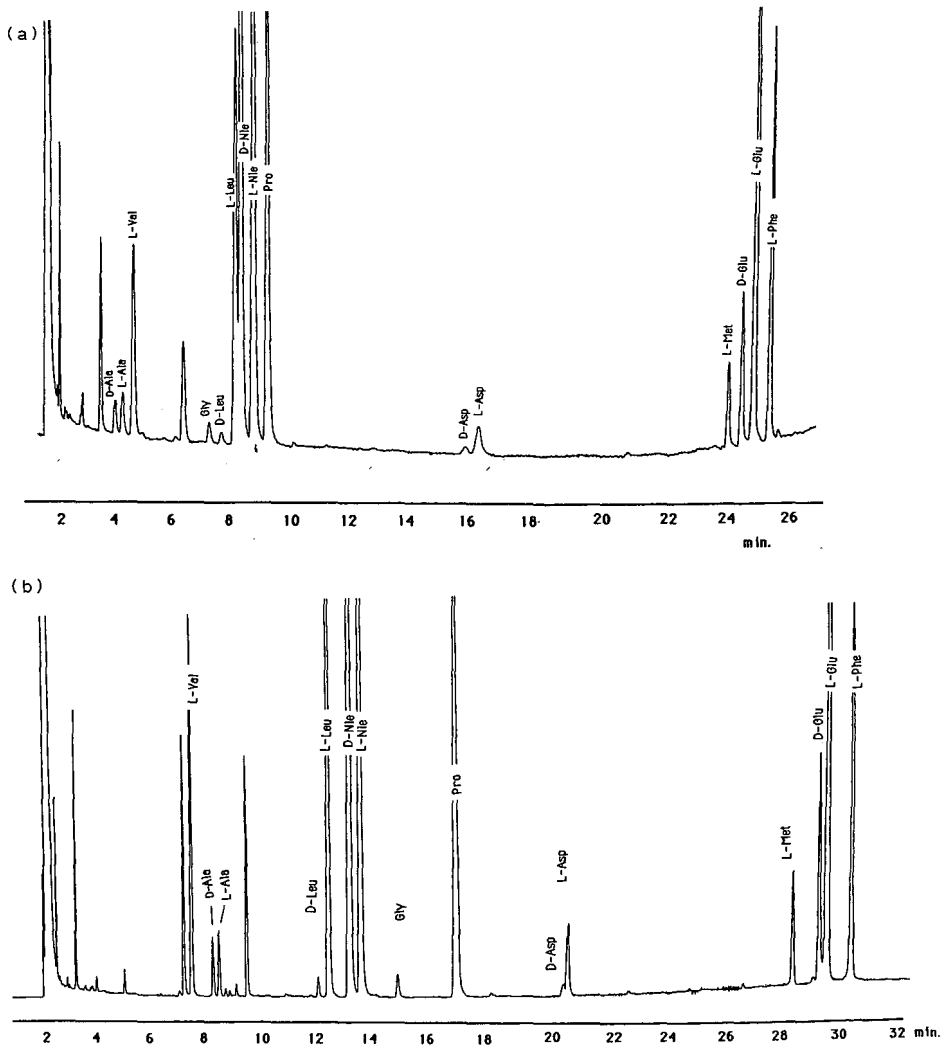

Fig. 2. Gas chromatograms of the enantiomeric separation of free amino acids (as N-TFA methyl esters) from aged cheese, recorded with a 20 m × 0.25 mm I.D. fused-silica column wall-coated with the chiral phase Phe-3-O-TA/OV-101 (a) and with a 25 m × 0.25 mm I.D. fused-silica column wall-coated with Phe-3-O-TA/CW (b). Temperature programme: 100–180°C at 4°/min after an initial hold at 100°C for 4 min.

served in each sample of new, pasteurized and UHT milk examined (twelve samples). Surprisingly, the percentage of D-derivatives was not influenced by the temperature of the thermal treatment. Only samples of dried milk showed more D-aspartic acid (4–5%), and D-alanine (8–12%). This is in contrast to previous reports on heated (60°C) dried milk[2–5]. In order to determine whether D-amino acids were also present in milk proteins, a sample of casein was precipitated with trifluoroacetic acid, and hydrolyzed with 6 *M* HCl at 100°C for 6 h. The hydrolyzate was derivatized and analyzed as reported for standard D,L-amino acids. In this case, the amounts (< 1%)

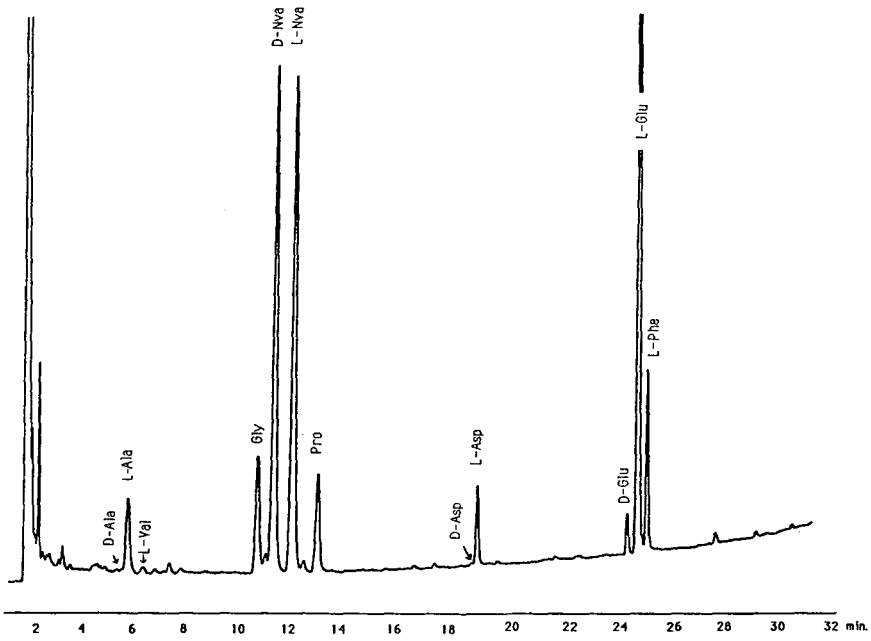

Fig. 3. Gas chromatogram of the enantiomeric separation of free amino acids (as N-TFA 2-propyl esters) from dried milk, recorded with a 20 m × 0.25 mm I.D. fused-silica column wall-coated with the chiral phase Phe-3-O-TA/OV-101. Temperature programme: as in Fig. 2.

of D-glutamic and D-aspartic acids detected were minimal, probably arising from the racemization induced by hydrolysis.

Yoghurt. An higher content of D-amino acids was detected in yoghurt samples, where the amount of D-alanine and D-glutamic acid was in some cases higher than that of the L-isomer (Table III). Amino acids were isolated by the same procedure as

TABLE III

RACEMIZATION OF FREE AMINO ACIDS IN COW'S MILK AND OTHER FOODS, DETECTED BY CAPILLARY GC WITH THE CHIRAL PHASE L-Phe-3-O-TA

Food	*Degree of racemization, D/D+L (%)*				
	Ala	*Leu*	*Asp*	*Glu*	*Phe*
New milk	3–4		2–3	2–3	
Pasteurized milk	3–4		1–2	3–5	
UHT milk	4–6		2–3	3–5	
Dried milk	8–12		4–5	3–4	
Yoghurt	64–68		20–32	53–66	
Aged cheese	20–45	2–7	8–35	5–22	2–13
Raw ham	0–1	<0.2		0–0.5	0–0.3
Roasted coffee			23–38	32–41	9–12
Green coffee				<0.2	

reported for milk, and derivatized to N-TFA 2-propyl esters. The amino acid pattern and the percentage of the D-enantiomers changed from sample to sample, probably on account of different strains of microorganisms.

Cheese. Microbial action is probably responsible for the presence of D-amino acids in aged cheese, which shows considerable amount of D-alanine, D-glutamic and D-aspartic acid. Minor quantities of D-leucine and D-phenylalanine were also detected, as shown in Table III.

Raw ham. Free amino acids, isolated from raw ham (Parma ham), were derivatized with 1 *M* HCl in methanol and then with trifluoroacetic anhydride. Only trace amounts of D-glutamic acid and D-phenylalanine (less than 0.5% as D/D+L) and about 1% of D-alanine were detected (Table III).

Roasted coffee. Chromatograms of roasted coffee were very much complicated by the presence of aroma components, and only aspartic acid, glutamic acid and phenylalanine were dependably determined, with D/D+L % values ranging from 10 to 40%. Several methods were employed in attempts to obtain clean GC profiles, including chromatography on ion exchangers, absorption with active carbons and solvent extraction. The best method was the simplest one; it is described in the Experimental section.

Analysis by HPLC with chiral eluents

D-Amino acids were determined as dansyl derivatives by HPLC on a C_{18} reversed-phase column, using L-phenylalaninamide/Cu(II) as a chiral eluent. Cheese, milk and yoghurt have been examined so far. A chromatogram of a cheese extract is presented in Fig. 4.

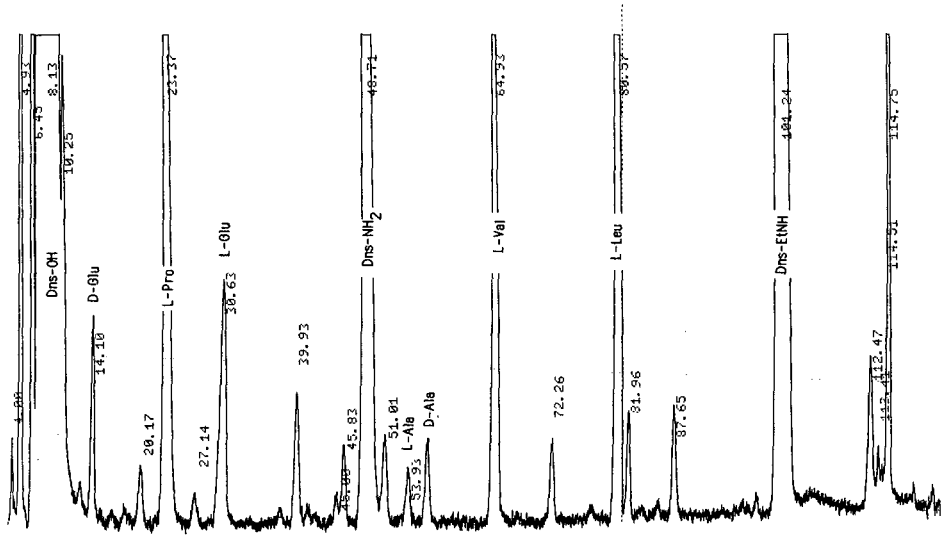

Fig. 4. HPLC chromatogram of the enantiomeric separation of free amino acids (as dansyl derivatives) from aged cheese, with the chiral additive L-Phe-A/Cu(II). Conditions: 4 m*M* L-Phe-A, 2 m*M* copper acetate, 0.3 *M* sodium acetate, pH 7.3 in acetonitrile and water; Novapak C_{18} column; gradient as reported in the Experimental.

Although many interfering substances were present in the matrix, which complicated the chromatograms, D-amino acids were detected and identified by comparison with authentic samples. In cheese, D-alanine and D-glutamic acid were quantified by HPLC and the results were found to be consistent with the GC data. In milk and yoghurt the analyses are still being carried out.

Undoubtedly, the present results raise questions concerning the quality of the food products examined and their sensory, nutritional and toxicological properties[12], which will be discussed in a more suitable context. In the present paper, we wish to point out that D-amino acids are surprisingly present not only in harshly treated foods, such as roasted coffee, but also in fermentation products, such as cheese and yoghurt, while high-temperature short-time treatments do not affect the D/D+L values, *cf.*, *e.g.*, UHT milk. Finally, it must be stressed that, when approaching the analysis of complex mixtures such as those present in biological systems, the combination of different chromatographic techniques allows cross-checks of the results so as to avoid pitfalls of single methods or derivatization procedures.

ACKNOWLEDGEMENTS

This work was supported by the C.N.R. (Consiglio Nazionale delle Ricerche), Roma, Progetto strategico "Characterization, Control and Analysis of Food".

REFERENCES

1 J. S. Davies in B. Weinstein (Editor), *Chemistry and Biochemistry of Amino Acids, Peptides, and Proteins*, Vol. 4, Marcel Dekker, New York, 1977, p. 1.
2 L. Liardon and R. F. Hurrell, *J. Agric. Food Chem.*, 31 (1983) 432.
3 S. Bunjampamai, R. R. Mahoney and I. S. Fagerson, *J. Food Sci.*, 47 (1982) 1229.
4 R. Hayashi and I. Kemada, *Agric. Biol. Chem.*, 44 (1980) 891.
5 M. Friedman, J. C. Zahnley and P. M. Masters, *J. Food Sci.*, 46 (1981) 127.
6 A. Spisni, R. Corradini, R. Marchelli and A. Dossena, *J. Org. Chem.*, 54 (1989) 684.
7 R. Marchelli, A. Dossena, G. Casnati, F. Dallavalle and S. Weinstein, *Angew. Chem., Int. Ed. Engl.*, 24 (1985) 336.
8 G. Palla, A. Dossena and R. Marchelli, *J. Chromatogr.*, 349 (1985) 9.
9 E. Armani, A. Dossena, R. Marchelli and R. Virgili, *J. Chromatogr.*, 441 (1988) 275.
10 E. Armani, L. Barazzoni, A. Dossena and R. Marchelli, *J. Chromatogr.*, 441 (1988) 287.
11 K. Grob, G. Grob and K. Grob, Jr., *Chromatographia*, 10 (1977) 181.
12 L. R. Tovar and D. E. Schwass, *ACS Symp. Ser.*, 234 (1983), 169; and references cited therein.

END OF SYMPOSIUM PAPERS

Journal of Chromatography, 475 (1989) 57–74
Elsevier Science Publishers B.V., Amsterdam — Printed in The Netherlands

CHROM. 21 528

RETENTION PREDICTION OF ANALYTES IN REVERSED-PHASE HIGH-PERFORMANCE LIQUID CHROMATOGRAPHY BASED ON MOLECULAR STRUCTURE

I. MONOSUBSTITUTED AROMATIC COMPOUNDS

ROGER M. SMITH* and CHRISTINA M. BURR
Department of Chemistry, Loughborough University of Technology, Loughborough, Leics. LE11 3TU (U.K.)

(First received September 28th, 1988; revised manuscript received February 13th, 1989)

SUMMARY

A system has been developed to predict retentions in reversed-phase high-performance liquid chromatography based on the molecular structure of the analyte. The retentions are calculated as retention indices, on the alkyl aryl ketone scale, by the summation of a value for a parent compound, increments for the individual substituents and contributions for interactions between the substituents. In this paper the coefficients of the quadratic equations are reported, which define the increments for a range of 17 substituents on an aromatic ring over the eluent ranges 40–80% methanol in buffer and 30–80% acetonitrile in buffer.

INTRODUCTION

In many laboratories the development of a high-performance liquid chromatographic (HPLC) method for a new analyte is a process of trial and error coupled with experience of similar or closely related compounds. The first stage is the selection of a suitable eluent composition to give retentions within a reasonable time span. This has led to computer based prediction techniques, which can rapidly suggest suitable conditions for an isocratic elution based on an initial gradient elution[1]. In addition if more than one analyte is involved, the conditions for a suitable resolution can take a considerable time to achieve. As a consequence, there has been considerable interest in recent years in methods to aid the development of a separation according to predetermined resolution criteria[2,3]. Both these approaches combine experimental observation with calculation but in neither case is the structure of the analyte taken into account. Although these approaches have advantages for unknown compounds or impurities, the structure of most analytes is known. It should therefore be possible to make use of a knowledge of the elution strength and selectivity of the eluent towards different structural features to predict a potentially suitable eluent.

The primary aim of the present study has been to develop a method which can

predict the retention of a compound, based on its structure by the summation of contributions from the carbon skeleton and any substituents and thus suggest a suitable initial eluent for examination. Potentially this approach could also suggest the optimum conditions to achieve a particular resolution between two analytes but because the interactions between substituents are not fully understood particularly on heterocyclic and aromatic ring systems, it will probably not be possible to make accurate predictions for complex molecules. However, if the experimental retentions of a core molecule are known then it should be possible to predict the relative retentions of closely related compounds containing different substituents. Any deviations found in subsequent experiments could be used to examine the interactions between the functional groups.

The concept that individual substituents contribute to retention in a definable way has been studied in a number of laboratories. However, only in a few previous studies have attempts been made to use these relationships to predict retentions and in most of these cases only a limited range of substituents have been included.

Jandera[4–8] recorded values for the polar and non-polar contribution of different groups to retention and has discussed a method of predicting retention based on interaction indices[9]. In initial studies he described changes in test compounds with eluent composition and showed that the expressions could be used to predict the retention of these compounds. He compared the retentions with the *n*-alkylbenzenes which were considered to only possess significant "non-polar" interactions and each substituent was then identified by two parameters, a non-polar contribution (n_{ce}) and a specific or polar contribution (q_i). The n_{ce} values were found to be dependent on the parent compound while the q_i contributions were reported to be virtually independent of the nature of the rest of the molecule[7]. The resulting values were used to successfully predict capacity factors for a range of substituted benzenes and phenylurea and triazine herbicides.

There has also been a wide range of studies which have examined the effect of different substituents of the retention of analytes. These quantitative structure–retention relationships (QSRR) have been discussed in detail by Kaliszan[10]. Similar concepts have long been used as the basis of log partition coefficient (log P) calculations in quantitative structure–activity relationships (QSAR) studies. Hansch and Leo[11] have successfully shown that octanol–water partition coefficients can be calculated in an additive manner from the value of a parent compound, plus contributions for each substituent (π) and a similar approach by Rekker[12] has used fragmental constants (f factors). There is often a good correlation between the octanol–water partition coefficient and retention, particularly for structurally related compounds. However, this relationship is relatively poor if compounds containing different functional groups are compared. Kaliszan[10] listed over 100 studies relating log P to retention in either thin-layer chromatography (TLC) or HPLC. These studies include work by Hanai and co-workers[13–19] who have used the linear relationship between log P calculated using Rekker f constants and log k' to predict the relative retention of several different types of compounds including bases[13], phenols[14,15] and, in combination with dissociation constants, to predict the retention times of acids[16–19]. For each type of compound a separate regression equation was used to calculate the retention times of "unknown" members of a family of compounds. Octanol–water partition coefficients calculated using π values have also been used by Jinno and Kawasaki[20,21] to predict

the capacity factors of alkylbenzenes and polynuclear aromatic compounds. In a proposed general prediction method Jinno and co-workers[22–24] have used the π values as one of several descriptors which include molecular connectivity indices, number of electron donating/accepting groups and Hammett constants to calculate the capacity factors of a range of substituted benzenes. However, most of the studies of the relationship of retention and log P have been aimed at using HPLC to predict log P values rather than using log P to predict retentions.

One of the most commonly reported structure–retention relationships in HPLC is the linear relationship between carbon number and log k' and this forms the basis of most retention index scales proposed for HPLC[25] and be used to express the contribution of different groups to retention. Baker using a retention scale based on 2-ketoalkanes[26] showed a close linear relationship between the retention index values and log P of structurally related drug compounds[27]. Baker used this to develop a prediction method for the retention index of a compound from the measured index of a "parent" compound and a weighted value from the substituent Hansch substituent constant (π). The method was used to calculate retention indices of a number of drug compounds including barbiturates[27], anthranilic acid analogues[27], narcotic analgesic[28], steroids[29] and urushiols[30]. He also noted that the addition of groups such as the glucuronides to drug molecules caused predictable constant increments in the measured retention indices[31].

A small number of other workers have suggested the use of substituent contributions derived from retention indices to predict the retention of related compounds. Shalaby *et al.*[32] used the retention index scale to suggest a system to predict the retention indices of nitrogen bridged compounds based on measured log P values. Magg and Ballschmiter[33] derived functional group contributions for ergot alkaloids using the 2-ketoalkane scale and found that, although the retention indices of the compounds varied between columns, differences were not dependent on the column. However, the work was not extended to predict the retention indices of unknown compounds. Morishita *et al.*[34] have suggested a method of predicting retention indices, on an alkane scale, in which substituent contributions were calculated from monosubstituted benzenes. These were used in combination with terms to account for interactions between substituents to predict the retention indices of polysubstituted benzenes. This was a limited study and the group contributions were only determined at a single eluent composition. Popl and co-workers[35–37] have used a scale based on the number of aromatic rings to predict the retention of a range of "unknown" phenolic oxidants.

Rather than relate retention to log P or retention indices a number of workers have attempted to predict retentions from molecular structure by the use of a substituent or group contributions to capacity factors[38,39]. The definition of the "group effect" differs but is usually the difference between the retention of a substituted and unsubstituted compound and substituent contributions have been derived using many different "parent" species and experimental conditions. The compounds which have been examined include coumarins[40], catecholamines[41,42], 2-phenylethylamine derivatives[43], purines[39,44], chromonoid compounds[45], and substituted benzenes[46]. As the majority of the papers used substituent contributions based on log k' the contributions will depend on the separation conditions although it has been suggested that the derived values can be transferred from one ODS column to another[39].

Prediction method

The basis of the prediction system examined in the present study is that the retention index of an analyte in a selected eluent can be calculated by the summation of the retention index of a parent compound (*PI*), substituent index values (*SI*) for each substituent plus terms required to describe interactions between substituents (interaction indices *II*, *i.e.*, hydrogen bonding, steric and electronic interactions). The retention index of a compound can then be determined as

$$RI = PI + SI_R + \Sigma SI_{Ar-X} + \Sigma SI_{R-X} + \Sigma II_{YZ}$$

where *PI* represents the retention index value of a parent compound; SI_R the retention index contribution from saturated aliphatic carbons; ΣSI_{Ar-X} the substituent index values for substituents on an aromatic ring; ΣSI_{R-X} the substituent index values for substituents on saturated aliphatic carbons (these will include olefin and carbonyl groups); and ΣII_{YZ} the interaction index values between substituents to account for H-bonding, and electronic effects.

The values of the retention indices and the increments will be dependent on the composition of the mobile phase. For most compounds it has been shown that there is a nearly linear relationship between percentage of composition and log k' but that a closer correlation can usually be obtained with a quadratic relationship particularly if a wide range of eluent compositions is being considered[47]. Consequently, for each different modifier, each of the terms in the prediction system will need to be defined as an experimentally determined quadratic equation of the form

$$I = ax^2 + bx + c$$

where x is the percentage of organic modifier in the eluent. It will be therefore possible to sum the a, b and c coefficients of the different components of the prediction equation to give an overall quadratic equation for each modifier

$$RI = \Sigma ax^2 + \Sigma bx + \Sigma c$$

Benzene was selected as the parent compound because all its substituted derivatives could be readily detected spectroscopically. A wide range of derivatives are also readily available, substituted both directly on the aromatic ring and on aliphatic side chains, which means that both types of substituents can be studied. In future work it is hoped to make the system more general so that other parent groups could be used.

It was decided to base the study on retention indices using the alkyl aryl ketone scale[48] rather than capacity factors or log capacity factors, because in previous studies in these laboratories, retention indices have been shown to be much more reproducible over time and are much less susceptible to small changes in the operating conditions (eluent composition, temperature and flow-rates) such as could occur between separations carried out on different occasions or on different equipment[49]. The retention indices of most compounds are also much less affected by the differences between brands of stationary phases than are capacity factors[50] and the intention was to develop a prediction system which would be generally applicable in other laboratories and if possible on other columns. The retention indices of the alkyl aryl

ketone standards are directly related to their capacity factors. Consequently, as long as the capacity factors of the alkyl aryl ketones are known on a particular column, the predicted retention indices of analytes can be converted to the corresponding estimated capacity factors. The alkyl aryl ketone scale has already been widely used in this laboratory for the study of the reproducibility of assay of drug compounds of forensic interest[25] and has been shown to be applicable to eluents containing methanol[48], acetonitrile[51], and tetrahydrofuran[51] and has been recently adopted in other laboratories as the basis of collections of retention values for drugs[52] and mycotoxins[53].

In this first part of the study retention parameters of benzene as the parent compound have been measured and the parameters, which describe the changes in retention due to the presence of single substituents on the aromatic ring have been determined. The robustness of the measurements, long-term precision studies, and the methods adopted to ensure reproducible results are described in the following paper[54]. In future papers the determination of expressions for substituents on aliphatic carbons, for isomers and for the interactions between groups in multisubstituted compounds will also be examined. A database of these expressions has been linked to an expert system (CRIPES, chromatographic retention index prediction expert system)[55] to provide a user friendly interface for the calculation of retention indices.

EXPERIMENTAL

Chemicals and eluents

Retention index alkyl aryl ketone standards (acetophenone, propiophenone, butyrophenone, valerophenone, hexanophenone and heptanophenone) and model aromatic compounds were purchased from various sources. Methanol and acetonitrile, HPLC grade, and sodium nitrate, A.R. grade, and disodium hydrogenorthophosphate and sodium dihydrogenorthophosphate, reagent grade, were from FSA Laboratory Supplies (Loughborough, U.K.).

Buffer solutions

Buffer solutions of pH 7 were prepared by adding disodium hydrogenorthophosphate (1.37 g) and sodium dihydrogenorthophosphate dihydrate (1.58 g) to 1000 ml of deionised water. For eluents containing 90% organic modifier the buffer was diluted ten-fold with water to avoid precipitation.

Sample solutions

Solutions of the retention index standards and model aromatic compounds were prepared in the mobile phases at a dilution which gave a signal at 254 nm using a 10-μl injection. The void volume marker was prepared as an aqueous solution containing 6 mg ml^{-1} of sodium nitrate.

HPLC equipment

HPLC separations were performed using a Pye-Unicam PU 4010 pump and a Pye-Unicam PU 4025 UV detector set at 254 nm. Injections of the samples (10 μl) were made using a Rheodyne 7125 valve fitted with a 20-μl loop. The column (100 × 5 mm I.D.) was packed with Spherisorb ODS-2, 5-μm (Batch 23/151, Phase Separations, Queensferry, U.K.). The column was maintained at a constant temperature

by enclosing it in a glass water jacket and circulating water at 30°C from a thermostated bath. Retention times were recorded on a Shimadzu Chromatopac C-R3A integrator.

Experimental procedure

Each set of separations consisted of the injection of solutions containing in turn, a mixture of the alkyl aryl ketones (acetophenone to heptanophenone), followed by three standard compounds (phenol, benzene and toluene), the individual model compounds and finally aqueous sodium nitrate (6 mg ml^{-1}) as a column void volume marker. This procedure was carried out in triplicate for each set of model compounds. Whenever possible the three runs were completed on a single day, however with eluents containing low organic modifier concentrations this was not practical even if higher flow-rates were used. The retention times were determined in a range of eluent compositions, methanol–buffer, pH 7.0 (40:60 to 90:10, v/v) and acetonitrile–buffer, pH 7.0 (30:70 to 90:10, v/v). Each set of data was collected using a single batch of eluent which was recycled.

Calculations of retention values

Capacity factors were calculated from the arithmetic mean of the triplicate retention times of each of the solutes using $k' = (t_R - t_0)/t_0$. To ensure consistency, the retention times (in min) were taken from the integrator to three decimal places and capacity factors were rounded to two decimal places. These were used to calculate retention indices (as integers), using the capacity factors of the alkyl aryl ketones included within the same set of injections as the model compounds. The least squares linear correlation between the log k' and the carbon number $\times$ 100 of the alkyl aryl ketones (acetophenone to heptanophenone) was determined as described previously[48] and the retention indices of the standard and model compounds were calculated by substitution into the regression equation.

RESULTS AND DISCUSSION

In order to determine the substituent contribution of different functional groups directly attached to an aromatic ring the capacity factors of the retention index scale alkyl aryl ketones (acetophenone to heptanophenone), the parent compound benzene and 16 mono-substituted aromatic model compounds were measured in a range of different eluent combinations of methanol–buffer, pH 7 (40:60 to 90:10) and acetonitrile–buffer, pH 7 (30:70 to 90:10) (Tables I and II). The monosubstituted model compounds covered a wide range of functional groups, however, it was not possible to examine carboxylic and sulphonic acids groups as they would be ionised in the buffer. Some of the groups could be considered as mixed alkyl aryl compounds (Ph–O–R, Ph–CO–R, Ph–CO_2–R and Ph–R) and in each case only the smallest homologue [R = methyl (Me)] was included in this study to derive a value for the aromatic functional group (Ph–X–). The effects of changes in the alkyl groups will be discussed in later papers.

The capacity factors were collected over a two year period and during this time the column had to be repacked a number of times with new stationary phase because the efficiency had deteriorated. Individual results may therefore have been obtained

TABLE I

CAPACITY FACTORS OF ALKYL ARYL KETONE STANDARDS AND MONOSUBSTITUTED MODEL COMPOUNDS IN ELUENTS CONTAINING METHANOL

Mobile phase, methanol–buffer, pH 7.

Compound	*Capacity factor*					
	Methanol (%)					
	40	*50*	*60*	*70*	*80*	*90*
Retention index standards						
Acetophenone	6.79	3.23	1.63	0.99	0.58	0.42
Propiophenone	15.74	6.61	2.93	1.58	0.83	0.52
Butyrophenone	34.56	12.92	5.01	2.40	1.12	0.62
Valerophenone	82.41	27.25	9.16	3.86	1.57	0.79
Hexanophenone	206.6	59.44	16.76	6.35	2.26	1.00
Heptanophenone	536.1	132.4	32.52	10.61	3.30	1.30
Monosubstituted model compounds						
Aniline	1.73	1.09	0.68	0.49	0.33	0.25
Anisole	12.23	6.08	3.33	1.85	1.05	–
Benzaldehyde	4.65	2.42	1.37	0.86	0.56	–
Benzamide	1.18	0.68	0.42	0.33	0.25	0.21
Benzene	11.49	7.37	3.58	2.00	1.08	0.64
Benzonitrile	5.01	2.83	1.37	0.86	0.50	0.35
Benzyl alcohol	2.31	1.31	0.79	0.56	0.41	0.24
Benzyl bromide	31.54	13.41	6.01	2.86	1.56	0.49
Benzyl chloride	24.56	10.90	5.04	2.48	1.24	0.49
Benzyl cyanide	4.79	2.28	1.20	0.70	0.48	0.26
Biphenyl	204.0	62.3	22.21	8.29	3.26	–
Bromobenzene	41.82	19.74	7.67	3.70	1.67	0.88
Chlorobenzene	32.52	15.79	6.44	3.16	1.46	0.79
Methyl benzoate	14.16	6.69	2.94	1.61	0.85	0.53
Nitrobenzene	8.12	4.67	2.32	1.35	0.74	0.46
Phenol	2.27	1.27	0.78	0.49	0.34	0.25
Toluene	29.57	13.66	6.81	3.38	1.68	0.86

on different columns under slightly different conditions and may not be directly comparable. No correction or standardisation was applied at this stage because this role will be provided by the conversion to retention indices. At high proportions of methanol or acetonitrile the capacity factors of many of the model compounds and standards are very small ($k' < 0.5$) so that their accuracy is likely to be sensitive to minor errors in the measurement of the retention times. Consequently these capacity factors may have a greater degree of uncertainty than results based on longer retention times.

The capacity factors for the alkyl aryl ketones, acetophenone to heptanophenone, in both sets of eluent combinations showed linear correlations between log k' and the retention index (carbon number × 100). The correlations were consistently good across the composition ranges (Table III, based on the corresponding capacity factors in Tables I and II) in agreement with earlier studies[48,51].

TABLE II

CAPACITY FACTORS OF ALKYL ARYL KETONE STANDARDS AND MONOSUBSTITUTED MODEL COMPOUNDS IN ELUENTS CONTAINING ACETONITRILE

Mobile phase, acetonitrile–buffer, pH 7.

Compound	*Capacity factor*						
	Acetonitrile (%)						
	30	*40*	*50*	*60*	*70*	*80*	*90*
Retention index standards							
Acetophenone	5.25	2.91	1.69	1.10	0.74	0.57	0.36
Propiophenone	11.94	5.71	2.89	1.71	1.07	0.75	0.45
Butyrophenone	25.06	10.31	4.57	2.49	1.47	0.96	0.55
Valerophenone	55.00	19.18	7.42	3.69	2.04	1.24	0.68
Hexanophenone	124.04	36.42	12.27	5.59	2.90	1.64	0.85
Heptanophenone	282.27	69.47	20.44	8.55	4.17	2.21	1.09
Monosubstituted model compounds							
Aniline	2.21	1.63	1.01	0.73	0.52	0.43	0.22
Anisole	13.43	6.85	3.43	1.98	1.17	0.81	–
Benzaldehyde	5.28	3.10	1.79	1.16	0.77	0.44	–
Benzamide	0.83	0.61	0.43	0.35	0.28	0.33	0.20
Benzene	12.52	6.57	3.42	2.04	1.27	0.87	0.45
Benzonitrile	5.86	3.27	1.82	1.15	0.74	0.55	0.28
Benzyl alcohol	1.76	1.15	0.80	0.57	0.43	0.39	0.32
Benzyl bromide	34.10	13.08	5.69	2.84	1.67	1.11	0.62
Benzyl chloride	27.63	11.05	4.97	2.53	1.50	0.94	0.42
Benzyl cyanide	6.88	3.50	1.93	1.13	0.75	0.53	0.36
Biphenyl	154.5	46.07	14.89	6.49	3.10	1.82	–
Bromobenzene	35.34	14.60	6.34	3.38	1.97	1.24	0.63
Chlorobenzene	28.58	12.32	5.51	3.01	1.77	1.13	0.57
Methyl benzoate	10.72	5.19	2.81	1.63	1.03	0.73	0.38
Nitrobenzene	9.08	4.70	2.43	1.45	0.89	0.62	0.30
Phenol	2.54	1.47	0.99	0.63	0.44	0.35	0.20
Toluene	30.63	11.95	6.29	3.02	1.86	1.23	0.58

Calculation of retention indices

The retention indices of the model compounds (Tables IV and V) were calculated from their capacity factors and those of the alkyl aryl ketones run as part of that same test set (usually on the same day). As expected, the retention indices of acetophenone (which has a defined retention index of 800), when calculated as a model monosubstituted compound (Ph–CO–Me) has experimental retention indices very close to this value with both organic modifiers. The small constant deviations in methanol eluents may suggest a small systematic error but this was not considered to be significant. To ensure consistency the defined value of $RI = 800$ has been used in subsequent stages in the calculations. Although retention indices of analytes are affected to only a small extent by small changes in the eluent conditions and composition[49], they do show some changes across relatively wide composition ranges. As expected the relative changes were considerably less than the corresponding changes

TABLE III

CORRELATION BETWEEN LOG k' AND CARBON NUMBER OF THE ALKYL ARYL KETONES

Log k' = a(100 × carbon number) + b.

	Correlation coefficient	*Slope* ($\times 10^3$)	*Intercept*
Methanol–buffer (v/v, %)			
40:60	0.9994	3.778	−2.132
50:50	0.9995	3.214	−2.080
60:40	0.9995	2.581	−1.865
70:30	0.9995	2.053	−1.658
80:20	0.9994	1.492	−1.434
90:10	0.9985	0.985	−1.179
Acetonitrile–buffer (v/v, %)			
30:70	0.9999	3.441	−2.033
40:60	0.9999	2.734	−1.718
50:50	0.9998	2.143	−1.481
60:40	0.9998	1.757	−1.359
70:30	0.9997	1.478	−1.308
80:20	0.9994	1.164	−1.179
90:10	0.9994	0.955	−1.213

TABLE IV

RETENTION INDICES OF MODEL COMPOUNDS IN METHANOL ELUENTS

Compound	*Retention index*					
	Methanol (%)					
	40	*50*	*60*	*70*	*80*	*90*
Acetophenone[a]	805	806	803	803	804	809
Aniline	650	658	657	659	639	579
Anisole	884	904	917	934	954	–
Benzaldehyde	774	777	777	775	784	–
Benzamide	605	589	578	570	551	514
Benzene	888	915	937	958	985	999
Benzene[b]	885	913	938	961	982	
Benzonitrile	776	788	775	774	760	736
Benzyl alcohol	689	691	698	684	675	610
Benzyl bromide	991	1004	1019	1030	1059	917
Benzyl chloride	962	976	992	992	994	915
Benzyl cyanide	773	766	763	738	722	658
Biphenyl	1205	1222	1231	1247	1270	–
Bromobenzene	1027	1051	1065	1088	1110	1139
Chlorobenzene	998	1021	1036	1051	1072	1090
Methyl benzoate	899	904	904	910	914	917
Nitrobenzene	851	857	864	874	874	853
Phenol	685	683	680	671	650	582
Toluene	987	1019	1039	1065	1095	1132

[a] Defined value 800.

[b] Parent index values for benzene values derived from quadratic regression equation (Table VI).

TABLE V

RETENTION INDICES OF MODEL COMPOUNDS IN ACETONITRILE ELUENTS

Compound	*Retention index*						
	Acetonitrile (%)						
	30	*40*	*50*	*60*	*70*	*80*	*90*
Acetophenone[a]	800	798	798	798	799	803	805
Aniline	691	706	694	695	691	696	656
Anisole	900	908	912	915	917	913	–
Benzaldehyde	781	786	786	788	788	779	–
Benzamide	568	549	521	511	509	593	636
Benzene	910	927	940	951	957	960	962
Benzene[b]	910	927	940	951	958	963	
Benzyl alcohol	654	640	630	624	636	645	690
Benzyl bromide	1026	1025	1020	1011	1002	986	985
Benzyl chloride	999	999	993	983	973	956	813
Benzyl cyanide	825	817	804	789	774	751	741
Benzonitrile	814	817	813	808	799	788	749
Biphenyl	1201	1198	1196	1195	1194	1195	–
Bromobenzene	1041	1054	1065	1074	1084	1093	1109
Chlorobenzene	1014	1027	1037	1045	1053	1058	1070
Methyl benzoate	890	890	900	894	894	897	894
Nitrobenzene	869	874	871	864	853	836	797
Phenol	695	687	674	660	639	645	671
Toluene	1005	1022	1036	1046	1054	1061	1072

[a] Defined value 800.

[b] Parent index values for benzene values derived from quadratic regression equation (Table VI).

in capacity factors. The effects were systematic up to 80% modifier but particularly for the acetonitrile separations, they were often non-linear (Fig. 1). The sharp changes in the retention indices for some compounds, such as the benzyl halides, aniline and phenol, in eluents containing 90% of organic modifier are apparently due to changes in the effective eluent conditions. The change to the lower buffer strength used with the highest proportions of organic modifier eluents should not be the cause of these effects as it has been found that the ionic strength has no effect on the retention indices of test compounds at 70% modifier[54]. Katz *et al.*[56] have suggested that there is a change in the active eluent composition at 90% methanol, which may result in a selectivity change in the system. As a consequence of these non-systematic changes it was decided to restrict the study to the composition ranges up to 80% and the results for the 90% proportion of modifiers have been omitted from the calculations. The measured values at 90% modifier are in any case rather uncertain because the corresponding retention times and capacity factors are so small.

Rather than use the retention indices for benzene in each eluent composition as the reference values for the database, it was decided to base the study on smoothed values (parent indices *PI*), calculated from the quadratic least squares relationship between the experimental retention index of benzene and the proportion of modifier in the eluent (up to 80% modifier, Table VI and Fig. 2).

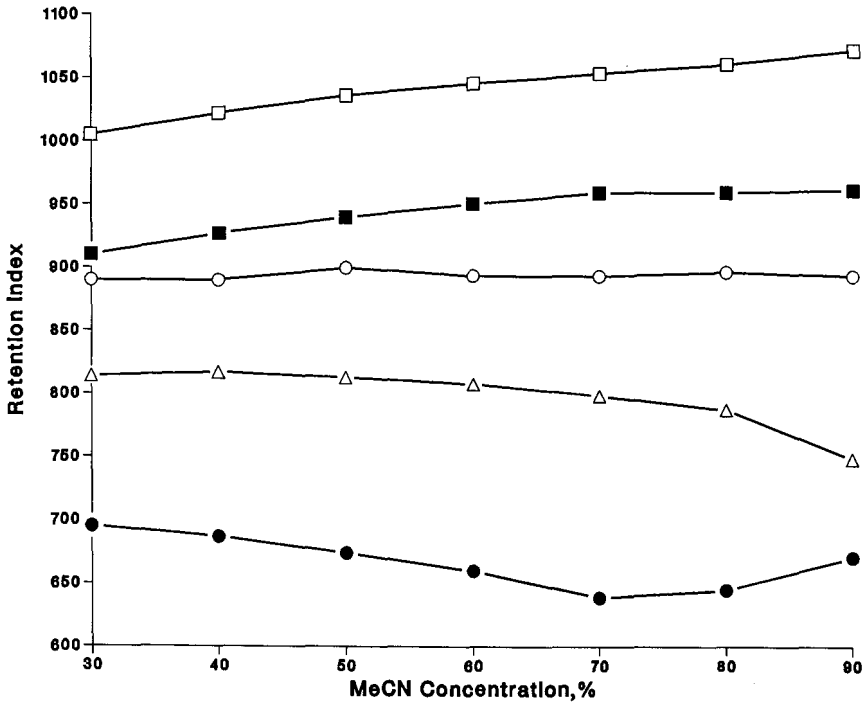

Fig. 1. Changes of retention indices of selected substituted aromatic compounds with percentage of acetonitrile (MeCN). Compounds: □, benzene; ■, toluene; ○, phenol; ●, methyl benzoate; △, benzonitrile.

Determination of substituent index equations

Using the calculated parent index (*PI*) values for benzene (given in Tables IV and V), the effects of each of the substituents can be calculated as the retention index increments (increment = $RI_{Ph-X} - PI_{Ph-H}$, Tables VII and VIII). Between 40 to 80% methanol and 30 to 80% acetonitrile the changes in the retention index increments for all the substituents are effectively systematic. The results for the methyl group were close to the defined value for the methylene increment of 100 units.

With each eluent the coefficients of the quadratic equation between the retention index increment and the percentage of composition were obtained (Table IX). If

TABLE VI

COEFFICIENTS OF PARENT INDEX EQUATIONS FOR BENZENE IN METHANOL AND ACETONITRILE CONTAINING ELUENTS

$PI = ax^2 + bx + c$. x = Percentage of modifier.

Organic modifier	*Range (%)*	*Coefficient*		
		a	*b*	*c*
Methanol	40–80	−0.0121	3.887	748
Acetonitrile	30–80	−0.0154	2.761	841

TABLE VII

RETENTION INDEX INCREMENTS FOR SUBSTITUENTS ON AN AROMATIC RING IN METHANOL ELUENTS

Increment = $RI_{\text{Model compound}} - PI$. PI = calculated parent index value for benzene (Table IV).

Substituent	*Hansch and Leo*[11] *π value*	*Retention index increment*				
		Methanol (%)				
		40	*50*	*60*	*70*	*80*
$CONH_2$	−1.49	−280	−324	−360	−391	−431
NH_2	−1.23	−235	−255	−281	−302	−343
CH_2OH	−1.03	−196	−222	−240	−277	−307
OH	−0.67	−205	−230	−258	−290	−332
CHO	−0.65	−111	−136	−161	−186	−198
CH_2CN	−0.57	−112	−147	−175	−223	−260
CN	−0.57	−109	−133	−163	−187	−222
$COCH_3$[a]	−0.55	−85	−113	−138	−161	−182
NO_2	−0.28	−34	−56	−74	−87	−108
OCH_3	−0.02	−1	−9	−20	−27	−28
CO_2CH_3	−0.01	14	−9	−34	−51	−68
H	0.00	0	0	0	0	0
CH_2Cl	0.17	77	63	54	31	12
CH_3[b]	0.56	102	106	101	104	113
Cl	0.71	113	108	98	90	90
CH_2Br	0.79	106	91	81	69	77
Br	0.86	142	138	127	127	128
Phenyl	1.96	320	309	293	286	288

[a] Based on defined values of RI = 800.
[b] Defined value = 100.

the variation in the increment across the composition range was less than 10 units a single mean value was included instead of a quadratic expression. Values for the aromatic substituent (Ph–X–) of the mixed alkyl aryl substituents (Ph–X–R), were calculated by excluding the contributions from the aliphatic group (–Me, SI = 100). These coefficients will be used in the prediction scheme to calculate the substituent index (SI) values as $SI = ax^2 + bx + c$.

Prediction of retention indices

The substituent index equation coefficients can now be used to calculate the predicted substituent indices and the retention indices for the model compounds. The correspondence between the experimental and the calculated substituent indices is close (Fig. 3) and should be sufficiently accurate for reliable prediction calculations. However, the calculated indices should not be extrapolated to compositions outside the measured regions as the values will be unreliable.

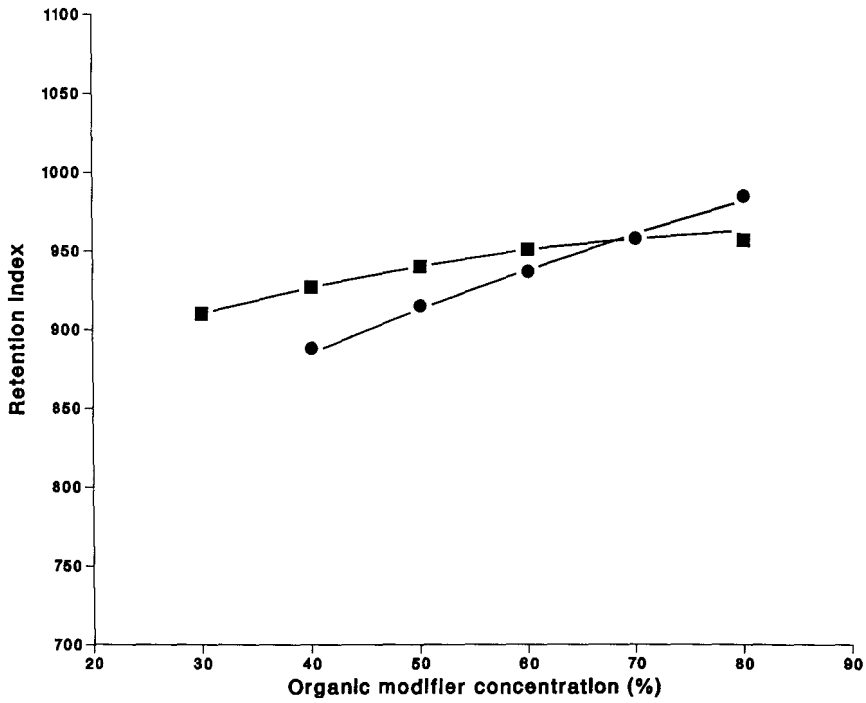

Fig. 2. Comparison of experimental retention indices of benzene in methanol–buffer and acetonitrile–buffer eluents with calculated values of parent index values derived from quadratic relationships (Table VI). Eluents: ●, methanol–buffer; ■, acetonitrile–buffer. Points are measured retention indices and curves are calculated values.

Relationship between substituent indices and octanol–water partition substituent increments

Within groups of closely related compounds, log k' of analytes in reversed-phase (RP)-HPLC has frequently been linearly correlated with the octanol–water partition coefficient (log P) (ref. 10) which are calculated in an additive manner from the Hansch substituent constants (π) and the octanol–water log P value of a parent. The values for the substituent indices should be thus related to the increments reported for the prediction of octanol–water partition coefficients, although the exact values will differ because of the different organic phases involved. This relationship could provide an mechanism by which estimated SI values could be obtained for substituents not determined experimentally (*e.g.*, the non-ionised carboxylic acid group). However, care must be taken as this approach would be expected give much less reliable values than the experimental data as the interactions occurring in an RP-HPLC separation are not always directly comparable to those in the octanol–water partition system.

The correlations between the π values for the aromatic substituents (listed in Table VII and VIII) and the corresponding SI values at different eluent compositions have therefore been determined (Table X). These results suggest that the relationship is approximately linear in both methanol and acetonitrile containing eluents. A com-

TABLE VIII

RETENTION INDEX INCREMENTS FOR SUBSTITUENTS ON AN AROMATIC RING IN ACETONITRILE ELUENTS

Increment = $RI_{\text{Model compound}} - PI$. PI = calculated parent index value for benzene (Table V).

Substituent	*Hansch and Leo*[11] *π value*	*Retention index increment*					
		Acetonitrile (%)					
		30	*40*	*50*	*60*	*70*	*80*
$CONH_2$	−1.49	−342	−378	−419	−440	−449	−370
NH_2	−1.23	−219	−221	−246	−256	−267	−267
CH_2OH	−1.03	−256	−287	−310	−327	−322	−318
OH	−0.67	−215	−240	−266	−291	−319	−318
CHO	−0.65	−129	−141	−154	−163	−170	−184
CH_2CN	−0.57	−85	−110	−136	−162	−184	−212
CN	−0.57	−96	−110	−127	−143	−151	−175
$COCH_3$[a]	−0.55	−110	−127	−140	−151	−158	−163
NO_2	−0.28	−41	−53	−69	−87	−105	−127
OCH_3	−0.02	−10	−19	−28	−36	−41	−50
CO_2CH_3	−0.01	−20	−37	−40	−57	−64	−66
H	0	0	0	0	0	0	0
CH_2Cl	0.17	89	72	53	32	15	−7
CH_3[b]	0.56	95	95	96	94	95	95
Cl	0.71	104	100	97	94	95	95
CH_2Br	0.79	116	98	80	60	44	23
Br	0.86	131	127	125	123	126	130
Phenyl	1.96	291	271	256	244	236	232

[a] Based on defined values of RI = 800.
[b] Defined value = 100.

parison of the values for SI in methanol–buffer (40:60) and π values (Fig. 4) showed a good correlation, with only one major outlier which was identified as the phenolic hydroxyl group. The equivalent curves for acetonitrile–buffer (40:60) (Fig. 5) suggested three outliers, the phenolic hydroxyl, benzyl hydroxyl and the carboxamide groups, again all are hydrogen bonding species. Differences in the relationship between log P and log k' particularly between hydrogen bonding species and non-hydrogen bonding species have been noted previously[57]. The overall pattern for acetonitrile was more scattered suggesting that the octanol–water partition is a poorer model of the interactions on HPLC. The values are closely related to those used for the prediction of octanol–water partition constants.

CONCLUSIONS

The parent retention indices for benzene and substituent indices for 17 aromatic substituents have been determined and expressed as quadratic equations covering a

TABLE IX

COEFFICIENTS OF SUBSTITUENT INDEX EQUATIONS FOR SUBSTITUENTS ON AN AROMATIC RING

Methanol–buffer (40:60 to 80:20) and acetonitrile–buffer (30:70 to 80:20). $SI = ax^2 + bx + c$.

Substituent Ph–X	*Methanol–buffer*			*Acetonitrile–buffer*		
	a	*b*	*c*	*a*	*b*	*c*
$CONH_2$	0.0093	−4.804	−104	0.1260	−14.878	2
NH_2	−0.0264	0.541	−215	0.0118	−2.405	−153
CH_2OH	−0.0193	−0.456	−148	0.0513	−6.872	−95
OH	−0.0271	0.117	−167	0.0218	−4.616	−93
CHO	0.0186	−4.469	39	0.0025	−1.335	−92
CH_2CN	−0.0171	−1.663	−18	0.0002	−2.543	−9
CN	−0.0114	−1.429	−34	−0.0025	−1.251	−57
$COCH_3$	0.0114	−3.791	48	0.0150	−2.704	−43
CO-R[a]	0.0114	−3.791	−52	0.0150	−2.704	−143
NO_2	0.0050	−2.390	53	−0.0104	−0.586	−14
OCH_3	0.0129	−2.263	70	0.0029	−1.097	20
O-R[a]	0.0129	−2.263	−30	0.0029	−1.097	−80
CO_2CH_3	0.0143	−3.774	143	0.0105	−2.096	33
CO_2-R[a]	0.0143	−3.774	43	0.0105	−2.096	−67
H	0	0	0	0	0	0
CH_2Cl	−0.0171	0.437	86	−0.0030	−1.586	140
CH_3[b]	0	0	100	0	0	100
Cl	0.0086	−1.669	167	0	0	98
CH_2Br	0.0314	−4.571	240	−0.0012	−1.711	168
Br	0.0150	−2.190	207	0	0	127
Phenyl	0.0250	−3.870	436	0.0193	−3.299	372

[a] Values exclude the contribution from the saturated aliphatic R group (Me = 100).
[b] Defined value.

TABLE X

REGRESSION COEFFICIENTS FOR π COMPARED TO CALCULATED SUBSTITUENT INDICES

$SI = a\pi + b$.

	Coefficients		*Correlation coefficient*
	a	*b*	
Methanol (%)			
40	−7.97	178	0.9849
50	−26.62	185	0.9839
60	−44.52	195	0.9816
70	−62.00	207	0.9787
80	−70.58	222	0.9607
Acetonitrile (%)			
30	−18.95	180	0.9739
40	−35.32	189	0.9661
50	−55.54	194	0.9573
60	−58.91	199	0.9588
70	−70.04	197	0.9622
80	−77.64	194	0.9627

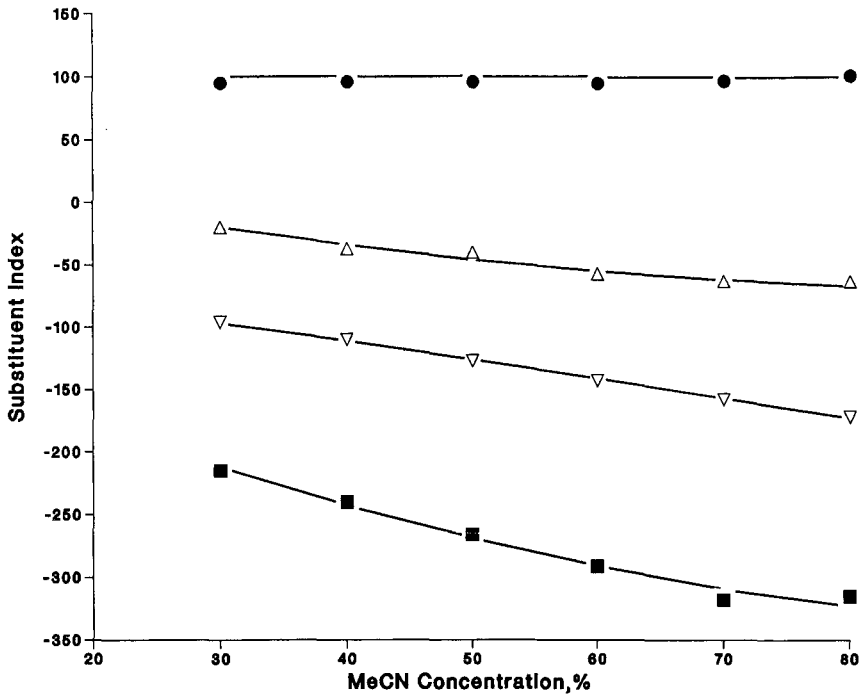

Fig. 3. Comparison of experimental values of retention index increments and calculated values of substituent indices in acetonitrile (MeCN)–buffer. Points are experimental values and curves are calculated substituent indices. Compounds: ■, phenol; ●, toluene; △, methyl benzoate; ▽, benzonitrile.

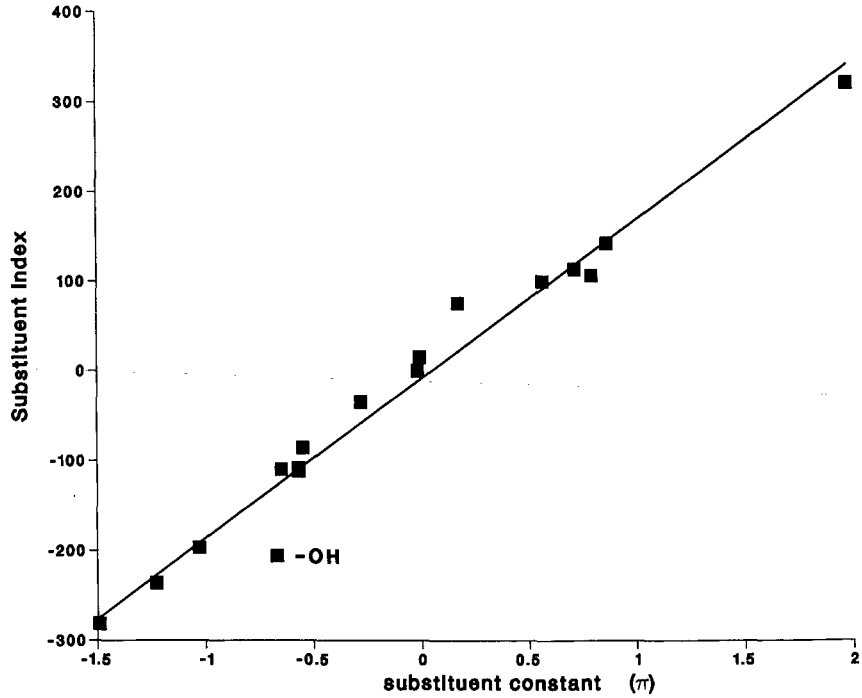

Fig. 4. Comparison of Hansch π values for substituents and calculated substituent indices in methanol–buffer (40:60).

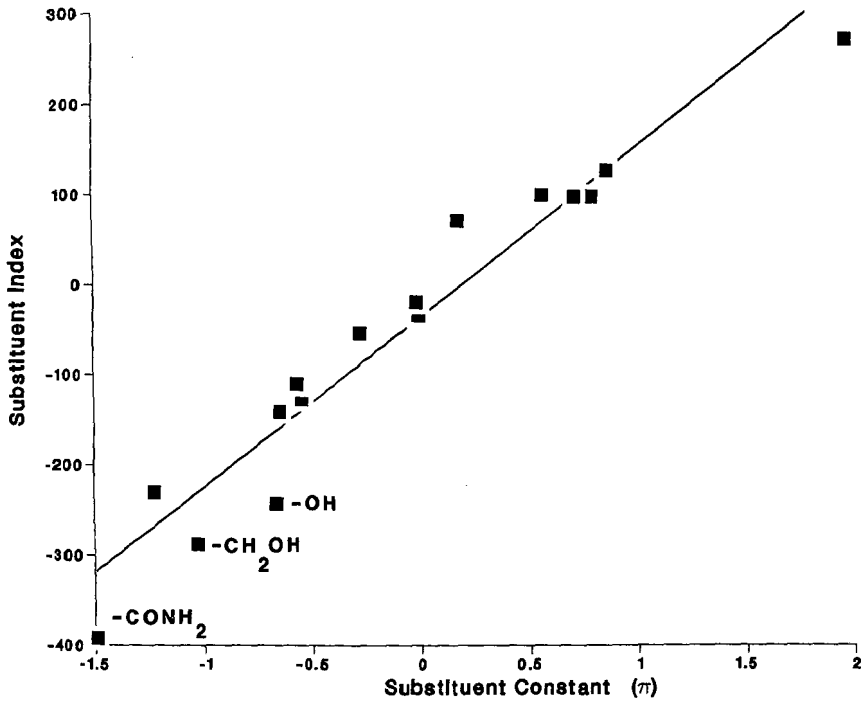

Fig. 5. Comparison of Hansch π values for substituents and calculated substituent indices in acetonitrile–buffer (40:60).

wide range of methanol and acetonitrile containing eluents, which can be used to predict retention in multisubstituted compounds.

ACKNOWLEDGEMENTS

Thanks are expressed to the Science and Engineering Research Council for a research grant and for a studentship to C.M.B. and to Phase Separations Ltd., U.K., for a gift of Spherisorb ODS-2.

REFERENCES

1 L. R. Snyder, J. L. Glajch and J. J. Kirkland, *Practical HPLC Method Development*, Wiley-Interscience, New York, 1988, pp. 239–245.
2 J. C. Berridge, *Techniques for the Automated Optimization of HPLC Separations*, Wiley, Chichester, 1985.
3 P. J. Schoenmakers, *Optimization of Chromatographic Selectivity (Journal of Chromqtography Library*, Vol. 35), Elsevier, Amsterdam, 1986.
4 P. Jandera, *J. Chromatogr.*, 314 (1984) 13.
5 P. Jandera, *J. Chromatogr.*, 352 (1986) 91.
6 P. Jandera, *J. Chromatogr.*, 352 (1986) 111.
7 P. Jandera and M. Špaček, *J. Chromatogr.*, 366 (1986) 107.
8 P. Jandera, *Chromatographia*, 19 (1984) 101.
9 H. Colin, G. Guiochon and P. Jandera, *Anal. Chem.*, 55 (1983) 442.

10 R. Kaliszan, *Quantitative Structure–Chromatographic Retention Relationships* (*Chemical Analysis*, Vol. 93), Ed. J. D. Winefordner, Wiley, New York, 1987.
11 C. Hansch and A. Leo, *Substituent Constants for Correlation Analysis in Chemistry and Biology*, Wiley, New York, 1979.
12 R. F. Rekker, *The Hydrophobic Fragmental Constant*, Elsevier, Amsterdam, 1977.
13 T. Hanai and J. Hubert, *J. Liq. Chromatogr.*, 8 (1985) 2463.
14 T. Hanai and J. Hubert, *J. High Resolut. Chromatogr. Chromatogr. Commun.*, 6 (1983) 20.
15 T. Hanai, C. Tran and J. Hubert, *J. High Resolut. Chromatogr. Chromatogr. Commun.*, 4 (1981) 454.
16 T. Hanai, K. C. Tran and J. Hubert, *J. Chromatogr.*, 239 (1982) 385.
17 T. Hanai and J. Hubert, *J. Chromatogr.*, 239 (1982) 527.
18 T. Hanai and J. Hubert, *J. High Resolut. Chromatogr. Chromatogr. Commun.*, 7 (1984) 524.
19 T. Hanai, *J. Chromatogr.*, 332 (1985) 189.
20 K. Jinno and K. Kawasaki, *Anal. Chim. Acta*, 152 (1983) 25.
21 K. Jinno and K. Kawasaki, *Chromatographia*, 17 (1983) 337.
22 K. Jinno and M. Kuwajima, *Chromatographia*, 21 (1986) 541.
23 K. Jinno and K. Kawasaki, *J. Chromatogr.*, 316 (1984) 1.
24 K. Jinno and K. Kawasaki, *J. Chromatogr.*, 298 (1984) 326.
25 R. M. Smith, *Adv. Chromatogr.*, 26 (1987) 277.
26 J. K. Baker and C.-Y. Ma, *J. Chromatogr.*, 169 (1979) 107.
27 J. K. Baker, *Anal. Chem.*, 51 (1979) 1693.
28 J. K. Baker, R. E. Skelton, T. N. Riley and J. R. Bagley, *J. Chromatogr. Sci.*, 18 (1980) 153.
29 J. K. Baker and E. K. Fifer, *J. Pharm. Sci.*, 69 (1980) 590.
30 C.-Y. Ma, M. A. Elsohly and J. K. Baker, *J. Chromatogr.*, 200 (1980) 163.
31 J. K. Baker, *J. Liq. Chromatogr.*, 4 (1981) 271.
32 A. Shalaby, Zs. Budvári-Bríny and Gy. Szász, *J. Liq. Chromatogr.*, 7 (1984) 1133.
33 H. Magg and K. Ballschmiter, *J. Chromatogr.*, 331 (1985) 245.
34 F. Morishita, H. Kakihana and T. Kojima, *Anal. Lett.*, 17 (1984) 2385.
35 M. Popl, V. Dolanský and J. Mostecký, *J. Chromatogr.*, 91 (1974) 649.
36 M. Popl, V. Dolanský and J. Mostecký, *J. Chromatogr.*, 117 (1976) 117.
37 M. Popl, I. Vít and F. Šmejkal, *J. Chromatogr.*, 213 (1981) 363.
38 V. Ya. Davydov, *J. Chromatogr.*, 365 (1986) 123.
39 S. P. Assenza and P. R. Brown, *J. Chromatogr.*, 282 (1983) 477.
40 K. Glowniak and M. L. Bieganowska, *J. Chromatogr.*, 370 (1986) 281.
41 I. Molnár and Cs. Horváth, *J. Chromatogr.*, 145 (1978) 371.
42 B.-K. Chen and Cs. Horváth, *J. Chromatogr.*, 171 (1979) 15.
43 R. Gill, S. P. Alexander and A. C. Moffat, *J. Chromatogr.*, 218 (1981) 639.
44 P. R. Brown and E. Grushka, *Anal. Chem.*, 52 (1980) 1210.
45 J. Borda, V. Szabó and J. Kelemen, *J. Chromatogr.*, 286 (1984) 113.
46 E. Tomlinson, H. Poppe and J. C. Kraak, *Int. J. Pharm.*, 7 (1981) 225.
47 P. J. Schoenmakers, H. A. H. Billiet and L. de Galan, *J. Chromatogr.*, 185 (1979) 179.
48 R. M. Smith, *J. Chromatogr.*, 236 (1982) 313.
49 R. M. Smith, T. G. Hurdley, R. Gill and A. C. Moffat, *Chromatographia*, 19 (1987) 401.
50 R. M. Smith, *Anal. Chem.*, 56 (1984) 256.
51 R. M. Smith, G. A. Murilla and C. M. Burr, *J. Chromatogr.*, 388 (1987) 37.
52 D. W. Hill and K. J. Langner, *J. Liq. Chromatogr.*, 10 (1987) 377.
53 J. C. Frisvad and U. Thrane, *J. Chromatogr.*, 404 (1987) 195.
54 R. M. Smith and C. M. Burr, *J. Chromatogr.*, 475 (1989) 75.
55 C. M. Burr and R. M. Smith, *Anal. Proc.*, 26 (1989) 26.
56 E. D. Katz, K. Ogan and R. P. W. Scott, *J. Chromatogr.*, 352 (1986) 67.
57 K. Miyake, N. Mizuno and H. Terada, *Chem. Pharm. Bull.*, 34 (1986) 4787.

Journal of Chromatography, 475 (1989) 75–83
Elsevier Science Publishers B.V., Amsterdam — Printed in The Netherlands

CHROM. 21 529

RETENTION PREDICTION OF ANALYTES IN REVERSED-PHASE HIGH-PERFORMANCE LIQUID CHROMATOGRAPHY BASED ON MOLECULAR STRUCTURE

II. LONG TERM REPRODUCIBILITY OF CAPACITY FACTORS AND RETENTION INDICES

ROGER M. SMITH* and CHRISTINA M. BURR
Department of Chemistry, Loughborough University of Technology, Loughborough, Leics. LE11 3TU (U.K.)
(First received September 28th, 1988; revised manuscript received February 13th, 1989)

SUMMARY

As part of the compilation of a database of substituent parameters for the prediction of retention indices in reversed-phase high-performance liquid chromatography, the reproducibility of retention measurements over a two-year period has been determined. Care was taken to ensure constant mobile phase and operating conditions and all the work was carried out using a single batch of stationary phase. Retention indices, based on the alkyl aryl ketones, were found to be much more consistent than capacity factors for recording retentions.

INTRODUCTION

Many methods have been proposed for the prediction of retention in high-performance liquid chromatography (HPLC) based either on comparisons with known compounds or by extrapolation from gradient elution but most do not take into account the nature of the analyte. As described in the preceding paper[1], a method has been developed to predict the retention of a compound in reversed-phase (RP) HPLC from its molecular structure and the composition of the mobile phase. The calculation is based on the summation of the retention index of a parent structure and contributions from the substituents and any interactions between the substituents.

The initial stages of the study have involved the accumulation of a database of values for substituent and interaction contributions based on experimental retention indices of model compounds[1–3]. To be useful for retention prediction all the values which contribute to the database must form a consistent data set. The individual retentions and the selectivity of the separation must therefore remain constant over the period of the study. Thus the measurement of retention must be reproducible and robust to minor changes, such as might occur in the preparation of eluents on different days, on repacking columns or to minor differences in the design of chromatographs. Because capacity factors are very susceptible to changes in the operating

conditions, retention indices based on the alkyl aryl ketones[4] were used as the basis of the study. These have been used in earlier studies to compare the reproducibility of collaborative studies[5] and the repeatability of drug assays under controlled conditions[6].

The present paper reports a study of the variations in the retentions of a number of test compounds in a wide range of eluent compositions over a two-year period using a number of replicate columns. In particular the effects of the determination of the column void volume have been examined and the use of capacity factors and retention indices as methods for recording retentions have been compared. Few previous studies have examined the robustness of HPLC retentions over a prolonged period and frequently collections of retention values have been reported without any indication of the reliability and consistency or of the expected uncertainty margins around the results.

EXPERIMENTAL

The equipment, chemicals and methods were as described in the preceding paper[1].

DISCUSSION

In the measurement of the retention values of model compounds for the prediction system, a number of steps were taken to control the experimental separation conditions to enhance long term reproducibility. The column temperature was maintained at 30°C as the capacity factors (k') of most analytes are inversely proportional to the temperature of the column[7]. Although retention indices are more robust to changes in temperature, some variations can occur due to changes in the selectivity of the separation[6]. However, in many laborartories separations are carried out at ambient temperature even though the variations within a working day can cause major changes in retention times.

The retention of ionisable compounds is dependent on the pH and ionic strength of the mobile phase. In order to control ionisation, the aqueous phase component of the mobile phase was a phosphate buffer with pH 7, which was prepared by weight from solid components to ensure constant ionic strength and pH. Most compounds, including aromatic amines and phenols are not ionised at this pH but it was not possible to examine the retention of carboxylic or sulphonic acid groups. The retentions of neutral compounds were largely unaffected on changing the strength of the buffer in steps from 0.00 to 0.02 M in methanol–buffer (70:30) and acetonitrile–buffer (70:30) eluents so that the exact buffer concentration would not be a critical factor. However, the retentions of strongly basic primary amines decreased considerably with increases in ionic strength (3-phenylpropylamine, pK_a = 10.39, in acetonitrile–buffer (70:30); 0.001 M, k' = 24.23; 0.005 M, k' = 8.79; 0.02 M, k' = 4.44). These changes suggested that the amines were partially or fully protonated and were being retained by an ion-exchange interaction with the acidic silanols on the surface of the silica rather than a reversed-phase partition mechanism[8]. The aliphatic amino group was therefore also not included in the present study, although it is planned in the future to examine the unionised acidic and basic groups by using different pH buffers.

Large changes in capacity factors and to a lesser extent retention indices have been reported for separations on different brands of nominally equivalent column packing materials and significant differences can also occur when different batches of the same manufacturer's packing material have been used[6]. To ensure consistent results within the study, a single batch of Spherisorb ODS-2 was used throughout. So far five columns (A–E) have been used, they were repacked with fresh stationary phase as soon as the peak shapes started to deteriorate or the retentions of standard compounds altered. The capacity factors of a number of compounds were examined in the same eluent on three of the columns. These showed some moderate variations [relative standard deviations (R.S.D.) of up to 9%] but the corresponding retention indices were more consistent with a variation of less than three units for rapidly eluted compounds and approximately one unit for well retained compounds (Table I). These variations in retention indices were no greater than the differences between individual replicate separations on a single day.

TABLE I

CAPACITY FACTORS OF A SELECTION OF COMPOUNDS DETERMINED ON THREE COLUMNS USED IN THE STUDY

Eluent: methanol–buffer (60:40).

Compound	*Capacity factor*			*Mean*	*S.D.*	*Retention index*			*Mean*	*S.D.*
	Column					*Column*				
	A	*B*	*C*			*A*	*B*	*C*		
Acetophenone	1.59	1.59	1.54	1.57	0.03					
Propiophenone	2.88	2.96	2.74	2.86	0.11					
Butyrophenone	4.93	5.18	4.64	4.92	0.27					
Valerophenone	8.94	9.62	8.40	8.99	0.61					
Hexanophenone	16.61	18.23	15.57	16.80	1.34					
Heptanophenone	31.70	34.85	29.38	31.98	2.74					
Phenylacetamide	0.52	0.46	0.47	0.48	0.03	605	600	603	603	2.5
Benzyl alcohol	0.82	0.79	0.78	0.80	0.02	694	689	689	691	2.9
Benzyl cyanide	1.21	1.20	1.15	1.19	0.03	758	756	755	756	1.5
Methyl phenylacetate	2.53	2.30	2.15	2.33	0.19	861	863	862	862	1.0
Toluene	6.52	6.76	6.08	6.45	0.35	1041	1038	1039	1039	1.5
Benzyl bromide	5.74	6.01	5.44	5.73	0.29	1020	1019	1020	1020	0.6

Column void volume

Capacity factors are calculated from the equation $k' = (t_R - t_0/t_0)$. However, small variations in the measured column void volume could significantly alter the calculated capacity factors but despite its importance, there is still no agreed standard method for its determination. Numerous suggestions have been compared but no single method is generally applicable[9,10]. In contrast, we have previously noted that the value of column void volume has only a small effect on the retention indices if the analyte is eluted within the calibrated range[11].

In the present study a 10-μl injection of dilute aqueous solution of sodium nitrate (6 mg ml^{-1}) has been used to determine the column void volume. This marker

compound is readily detectable spectroscopically but it has previously been noted that a fixed concentration should be used[12,13]. This was confirmed using 10 μl injections of aqueous sodium nitrate solutions containing 1–24 mg ml^{-1} sodium nitrate, corresponding to molar concentrations of 0.01–0.28 *M* sodium nitrate. As the concentration increased, the retention times measured at the peak maximum increased from 0.843 to 0.922 min with methanol–buffer (70:30) and from 0.749 to 0.818 min with acetonitrile–buffer (70:30). If the eluent buffer strength was altered there were only minor changes.

There is reported to be a direct relationship between the retention of a series of homologues and retention such that the zero retention index should represent the column void volume[9]. Therefore as an alternative to the direct measurement of the column void volume, two calculation methods have been examined using the homologous alkyl aryl ketone standards. The first is a method proposed by Berendsen *et al.*[14] and the second an iterative procedure developed by Smith and Garside[15]. However, in both cases the results were very erratic and often the calculated column void volume was greater than the retention times of rapidly eluting analytes.

In order to determine how much variation could be expected in the final retention results as a consequence of differences in the measurement of the column void volume, the individual experimental values at each eluent composition during the two years of the study have been evaluated. In each case there were between 20 and 30 measurements and they showed variations of up to 20% from the mean value [*i.e.*, methanol–buffer (50:50), t_0 ranged from 0.568 to 0.678 min with an R.S.D. of 15%]. To determine the effects of variations of this magnitude the capacity factors and retention indices for a number of compounds using high (90%) and low (40%) percentage of modifier were recalculated from the experimental retention times by assuming the mean column void volume and values which were 15% higher and lower. The compounds covered the range of alkyl aryl ketones and included compounds eluting before and within the calibrated region of the retention index scale (Table II). As expected, the calculated capacity factors were very dependent on the value of the column void volume, particularly when the retention times were similar to the column void volume. This confirmed the sensitivity of capacity factors to the exact value of the column void volume and their susceptibility to different methods of measurement and consequently low reliability for comparison studies.

The retention indices (*RI*) in 40% modifier were generally robust and even for the rapidly eluted compound, phenylacetamide, varied by only seven units. With 90% organic modifier the retention indices for all the rapidly eluted compounds with retentions shorter than acetophenone and therefore outside the calibration region, showed marked variations (phenylacetamide from $RI = 605$ to 455 and 3-phenyl-1-propanol from 755 to 719). However, for all these compounds the capacity factors were less than 0.5. Thus at these very low retentions any minor variations in the measured column void volume could have a marked effect on the reproducibility of retention indices. Similar results were obtained for the corresponding eluents containing acetonitrile as the modifier.

These calculations represent the worst possible examples and indicate the maximum extent of expected variations. Clearly if the capacity factors of analytes are small (particularly if the retention indices are less than 700) there is likely to be a considerable uncertainty in the values. Thus the use of retention indices while largely

TABLE II

EFFECT OF CHANGES IN THE VALUE OF THE COLUMN VOID VOLUME USED TO CALCULATE CAPACITY FACTORS AND RETENTION INDICES

Compound	*Capacity factor*			*Retention index*		
	Assumed column void volume			*Assumed column void volume*		
	−15%	*Mean*	*+15%*	*−15%*	*Mean*	*+15%*
Column void volume (min)[a]	0.341	0.401	0.461	0.341	0.401	0.461
Acetophenone	9.29	7.75	6.61	804	804	803
Hexanophenone	270.04	229.49	199.49	1197	1197	1197
Phenylacetamide	2.37	1.87	1.49	645	638	631
Benzyl alcohol	3.74	3.03	2.50	698	694	691
2-Phenylethanol	6.31	5.22	4.41	759	758	756
3-Phenyl-1-propanol	12.67	10.62	9.11	840	840	840
4-Phenylbutyronitrile	22.22	18.74	16.17	906	906	906
Toluene	93.85	79.66	69.16	1074	1074	1075
Column void volume (min)[b]	1.404	1.652	1.900	1.404	1.652	1.900
Acetophenone	0.75	0.48	0.29	810	804	795
Hexanophenone	1.52	1.15	0.87	1196	1197	1199
Phenylacetamide	0.51	0.28	0.12	605	560	455
Benzyl alcohol	0.57	0.33	0.16	665	635	574
2-Phenylethanol	0.61	0.37	0.19	705	683	643
3-Phenyl-1-propanol	0.67	0.42	0.24	755	741	719
Methyl 3-phenylpropionate	0.94	0.65	0.43	809	803	794
Toluene	1.31	0.96	0.70	1113	1117	1122

[a] Eluent: Methanol–pH 7 buffer (40:60) (2 ml min^{-1}).
[b] Eluent: Methanol–pH 7 buffer (90:10) (0.5 ml min^{-1}).

compensating for variations in capacity factors does not totally overcome the problem of the reproducibility of the measurements of the column void volume. On elution with 90% modifier many analytes had particularly low capacity factors (often $k' < 0.5$) and these often required extrapolation beyond the range of retention index standards. In addition, there was doubt that the retentions at the high organic proportions could be directly related to lower compositions[1]. Consequently, the range of the study has been limited to eluents up to 80% modifier. In addition, in subsequent work the retentions of compounds with capacity factors lower than 0.15 in any eluent have also been excluded from the calculations.

Long term reproducibility

Despite controlling as many factors as feasible, experimental variation cannot be totally eliminated. This will be reflected in the uncertainty in any determined value and therefore in the accuracy which could be expected from the predicted retention indices. To examine the success of the precautions taken to produce reproducible retentions and to determine the anticipated uncertainty in an individual retention index value, an investigation of the long term reproducibility was undertaken.

Apart from the earliest part of the work on the first column, the retention times

TABLE III

LONG TERM REPRODUCIBILITY OF CAPACITY FACTORS AND RETENTION INDICES OF TOLUENE, BENZENE AND PHENOL OVER A TWO-YEAR PERIOD

Methanol–buffer	*Capacity factor*				*Retention index*			
	Mean	*Max.*	*Min.*	*S.D.*	*Mean*	*Max.*	*Min.*	*S.D.*
Phenol								
40:60	2.24	2.80	2.02	0.21	691	704	685	5.4
50:50	1.26	1.29	1.14	0.10	689	695	681	7.0
60:40	0.71	0.83	0.75	0.02	683	689	679	2.7
70:30	0.53	0.57	0.50	0.02	673	679	669	3.2
80:20	0.34	0.39	0.33	0.02	654	663	648	5.4
Benzene								
40:60	12.27	13.22	11.38	0.60	885	891	883	5.6
50:50	6.56	6.99	5.91	0.50	913	917	909	4.0
60:40	3.55	3.86	3.22	0.15	936	941	933	2.0
70:30	1.97	2.09	1.75	0.07	956	962	952	2.0
80:20	1.11	1.21	1.06	0.04	980	986	977	2.8
Toluene								
40:60	29.83	31.80	27.25	1.07	986	989	979	5.7
50:50	13.92	16.07	12.32	0.90	1015	1022	1012	3.7
60:40	7.13	7.81	5.54	0.84	1036	1045	1031	4.3
70:30	3.24	3.46	2.40	0.28	1063	1065	1059	1.8
80:20	1.66	1.80	1.56	0.07	1091	1097	1088	2.9
Acetonitrile–buffer								
Phenol								
30:70	2.46	2.84	1.84	0.21	695	697	688	2.2
40:60	1.51	1.64	1.38	0.07	688	696	682	3.2
50:50	0.96	1.09	0.84	0.18	672	682	664	4.4
60:40	0.65	0.68	0.63	0.02	660	661	658	1.2
70:30	0.44	0.47	0.42	0.01	641	642	638	2.1
80:20	0.31	0.39	0.24	0.05	625	652	611	11.6
Benzene								
30:70	13.76	15.38	11.99	1.02	905	910	899	3.9
40:60	6.90	7.79	6.14	0.57	926	932	923	4.4
50:50	3.70	4.27	2.98	0.37	939	941	931	2.9
60:40	2.14	2.28	2.03	0.10	949	952	944	2.2
70:30	1.31	1.40	1.29	0.05	956	959	951	3.5
80:20	0.84	0.95	0.74	0.06	962	969	958	3.8
Toluene								
30:70	29.75	31.98	25.27	2.19	1003	1008	999	2.9
40:60	12.78	14.37	11.31	1.20	1019	1026	1017	3.8
50:50	6.12	7.01	4.94	0.59	1031	1037	1024	4.4
60:40	3.18	3.41	3.01	0.15	1043	1047	1039	2.6
70:30	1.87	1.98	1.73	0.08	1051	1057	1049	3.5
80:20	1.13	1.26	1.09	0.09	1061	1065	1055	3.2

of three standard compounds, phenol, benzene and toluene were measured as part of every set of separations. This resulted in 20–30 individual measurements at each eluent composition over the two-year period depending on the number of times each eluent was used. These standard compounds were chosen to represent both polar and non-polar analytes and the two homologues could be used to check the consistency of the methylene selectivity. The range, mean and standard deviations from the mean of the capacity factors were determined for the standards (Table III). Although the capacity factors on each column were reasonably consistent, there were significant differences between the columns even though they were all packed with the same batch of Spherisorb ODS 2 (Fig. 1). Despite the precautions taken to ensure that the experimental conditions remained as constant as possible, there is still considerable variation in the results of up to 18% from the mean values. Although much of this variation is due to the different columns, there are also variations resulting from uncertainties in measuring both the retention times and the column void volume.

Generally the retention indices of the three standards were more consistent and suggest that retention indices can be expressed with a high degree of confidence as the measured value ± 10 units (twice the standard deviation) (Table III). No significant differences could be seen in the results from the different columns (Fig. 2).

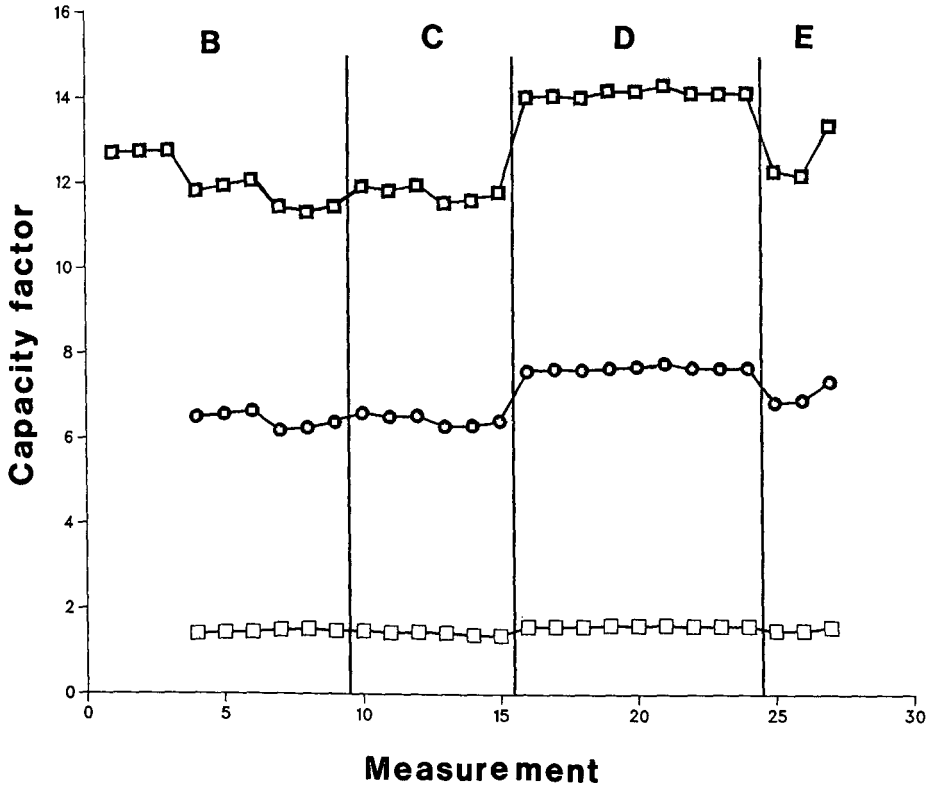

Fig. 1. Individual measurements of capacity factors of phenol (□), benzene (●) and toluene (■) throughout the study using acetonitrile–buffer (40:60) as the mobile phase on four different columns (B–E) packed with the same batch of Spherisorb ODS-2.

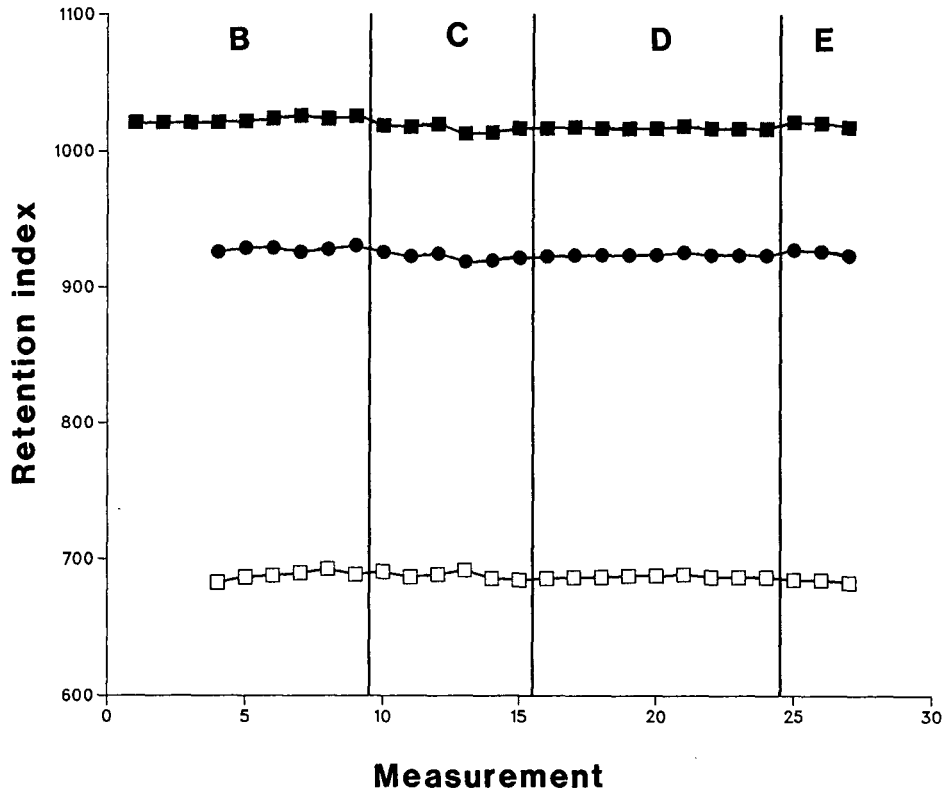

Fig. 2. Individual measurements of retention indices of phenol (□), benzene (●) and toluene (■) throughout the study using acetonitrile–buffer (40:60) as the mobile phase on four different columns (B–E) packed with the same batch of Spherisorb ODS-2.

CONCLUSION

The variation in the capacity factors over a prolonged period even under closely controlled chromatographic conditions is considerable and is emphasised by variations in the measurement of the column void volume. However, the use of relative measurements expressed as retention indices can eliminate much of the variation and can act as an efficient method for standardisation. The retention indices of many compounds can probably be expressed with high confidence to within 10 retention index units. This gives a guide to the expected precision of predicted retentions based on this data depending on the number of contributions that are included.

These conclusions have considerable relevance for other large collections of chromatographic data as even using the same batch of packing material and controlled experimental conditions, capacity factors are likely to have varied considerably unless some form of correction has been applied throughout the period of the study.

REFERENCES

1 R. M. Smith and C. M. Burr, *J. Chromatogr.*, 475 (1989) 57.
2 C. M. Burr and R. M. Smith, *Anal. Proc.*, 26 (1989) 24.
3 C. M. Burr and R. M. Smith, *Anal. Proc.*, 25 (1988) 46.
4 R. M. Smith, *J. Chromatogr.*, 236 (1982) 313.
5 R. Gill, A. C. Moffat, R. M. Smith and T. G. Hurdley, *J. Chromatogr. Sci.*, 24 (1986) 153.
6 R. M. Smith, T. G. Hurdley, R. Gill and A. C. Moffat, *Chromatographia*, 19 (1984) 401.
7 E. Grushka, H. Colin and G. Guiochon, *J. Chromatogr.*, 248 (1982) 325.
8 G. B. Cox and R. W. Stout, *J. Chromatogr.*, 384 (1987) 315.
9 R. J. Smith, C. S. Nieass and M. S. Wainwright, *J. Liq. Chromatogr.*, 9 (1986) 1387.
10 R. A. Djerki and R. J. Laub, *J. Liq. Chromatogr.*, 10 (1987) 1749.
11 R. M. Smith, *Anal. Chem.*, 56 (1984) 256.
12 K. Jinno, N. Ozaki and T. Sato, *Chromatographia*, 17 (1983) 341.
13 M. C. Hennion and R. Rosset, *Chromatographia*, 25 (1988) 43.
14 G. E. Berendsen, P. J. Schoenmakers, L. de Galan, G. Vigh, Z. Varga-Puchony and J. Inczedy, *J. Liq. Chromatogr.*, 3 (1980) 1669.
15 R. M. Smith and D. R. Garside, *J. Chromatogr.*, 407 (1987) 19.

Journal of Chromatography, 475 (1989) 85–94
Elsevier Science Publishers B.V., Amsterdam — Printed in The Netherlands

CHROM. 21 490

PROGRAMMING OF PRESSURE AND MOBILE PHASE COMPOSITION AT CONSTANT FLOW-RATE USING A SELF-ADJUSTING VALVE IN SUPERCRITICAL-FLUID CHROMATOGRAPHY

STEPHAN KÜPPERS, BENNO LORENSCHAT, FRANZ PETER SCHMITZ* and ERNST KLESPER
Lehrstuhl für Makromolekulare Chemie, RWTH Aachen, Worringerweg, D-5100 Aachen (F.R.G.)
(First received January 31st, 1989; revised manuscript received March 13th, 1989)

SUMMARY

Programming of pressure and mobile phase composition were compared for the separation of styrene oligomers on silica. At a constant flow-rate, *i.e.*, constant pump feed rate, composition gradients were found to be superior to pressure gradients, the latter being produced by means of a self-adjusting valve. For optimization the two types of gradient may be combined. Additionally, it is shown that optimized resolution can also be obtained by superimposing a negative pressure gradient on a composition gradient.

INTRODUCTION

Recently, supercritical-fluid chromatography (SFC) has become a rapidly expanding technique, owing especially to the steadily growing interest of applications chemists looking for a chromatographic technique complementary to gas (GC) and liquid chromatography (LC). As has been demonstrated [1–4], a need for such a technique actually exists, and a growing number of application "niches" for SFC are being found with regard to the solution of problems that are very difficult or even impossible to solve by either GC or LC.

A unique feature of SFC is the greater variety of gradient techniques, which have a large effect on the separation: temperature programming with increasing temperature, as in GC, or with decreasing temperature; composition programming, as in LC; flow programming, as in GC or LC; and pressure/density programming (unique to SFC). These different gradient techniques can be used either as single gradients or as coupled multiple gradients (for a detailed discussion, see recent reviews[5–8]). So far, however, coupled gradients have often been used involuntarily, that is, a gradient of one variable was produced by changing a second variable. As an example, pressure programming is most frequently effected by increasing the feed rate of the pump against a non-adjustable flow resistance (restrictor), regardless of the effect of the changing linear flow-rate in the column on the separation.

In this paper we present results obtained using pressure and/or composition

0021-9673/89/$03.50

gradients. The feed rate of the pumps was kept constant, using a self-adjusting valve at the outlet for changing the pressure. The self-adjustment was based on a pressure feedback loop. The optimization of the separation of a styrene oligomer sample under these conditions is demonstrated.

EXPERIMENTAL

The chromatographic instrumentation used was similar to that described previously[9]. The central part of the SFC instrument was an HP 1084B chromatograph (Hewlett-Packard, Waldbronn, F.R.G.), which provides a constant volume flow-rate of liquid eluent, irrespective of the system pressure or of the relative flow pumped by either of the two pumps, *i.e.*, irrespective of the mobile phase composition. The mobile phase compositions given with the chromatograms refer to the volume feed ratio for the two liquid mobile phase components. The carbon dioxide eluent (99.995%; Messer Griesheim, Köln, F.R.G.) was fed to one pump from a cylinder added to the original HP 1084B, prepressurized by helium, and turned upside down. The 1,4-dioxane eluent was delivered from the storage bottles provided with the chromatograph. Column heating was as described previously[9], and the column (25 cm × 4.6 mm I.D.) was packed with LiChrosorb Si 100 (10 μm) using a slurry packing procedure[10]; the column was conditioned with 1,4-dioxane in order to produce a uniform silica surface with improved resolution characteristics[11]. The detector and pressure regulators, which were different to the design previously described[9], are described in more detail below.

The UV detector used in these experiments was a Model LC 75 (Perkin-Elmer, Düsseldorf, F.R.G.) equipped with a pressure-resistant detector cell. However, when working with low-boiling mobile phases, leaks frequently occurred, and retightening of the cell assembly often resulted in destruction of the cell window. Therefore, the

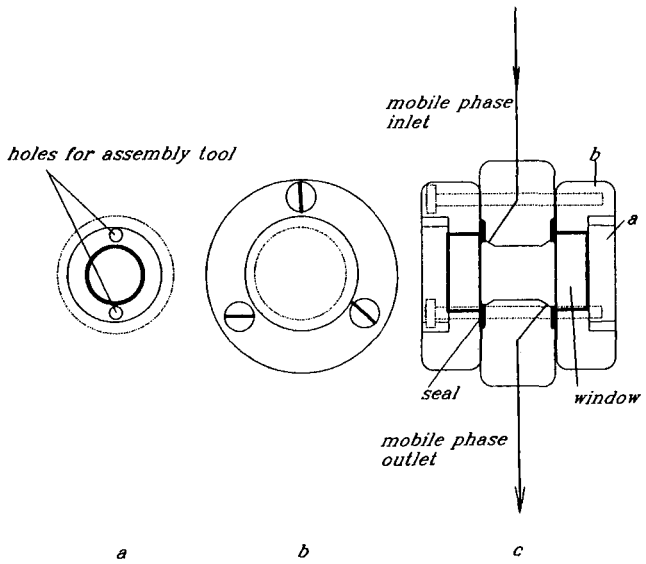

Fig. 1. Design of the UV detector cell. (a) Screw; (b) cover (front view); (c) cell assembly.

cell assembly was redesigned in order to prevent breakage of the windows. This assembly is shown schematically in Fig. 1. The window is pressed against the seal by means of the central screw, and thus the pressure applied is distributed nearly equally. This permits very effective tightening of the cell assembly and therefore the application of high working pressures (*ca.* 350 bar) for long periods of time without leaks.

The pressure regulation was performed downstream of the detector, using an electronically regulated valve of the back-pressure regulating type (HITEC P732; Bronkhorst, Ruurlo, The Netherlands, distributed by Mättig Mess- und Regeltechnik, Unna, F.R.G.). The valve assembly contains a pressure sensor, a feedback loop and the valve proper, which consists of a plunger oscillating in a solenoid. The strength of the magnetic field is controlled by the feedback loop, which compares the actual value from the pressure sensor with an external preset value. This external value can be obtained from a personal computer, in our case from an IBM AT (IBM, Stuttgart, F.R.G.) via a D/A interface. Hence the pressure can not only be held constant but can also be programmed via a simple BASIC program. With the applied flow-rate of 1 ml min^{-1} (liquid), the regulating times are short, which allows the use of steeply ramped pressure programmes. Problems will arise, however, from the high dead volume of the regulating valve (a few millilitres) when distinctly lower flow-rates are used, as is commonly done with microbore or even open-tubular capillary columns.

Pressure programming by means of the PC is demonstrated by the screen hardcopy shown in Fig. 2. Trace A (shifted to lower pressure by 10 pixels for the sake of better inspection) shows a calculated pressure programme from 230 to 300 bar within 75 min, corresponding to a linear pressure ramp of 0.93 bar min^{-1}, and in trace B the

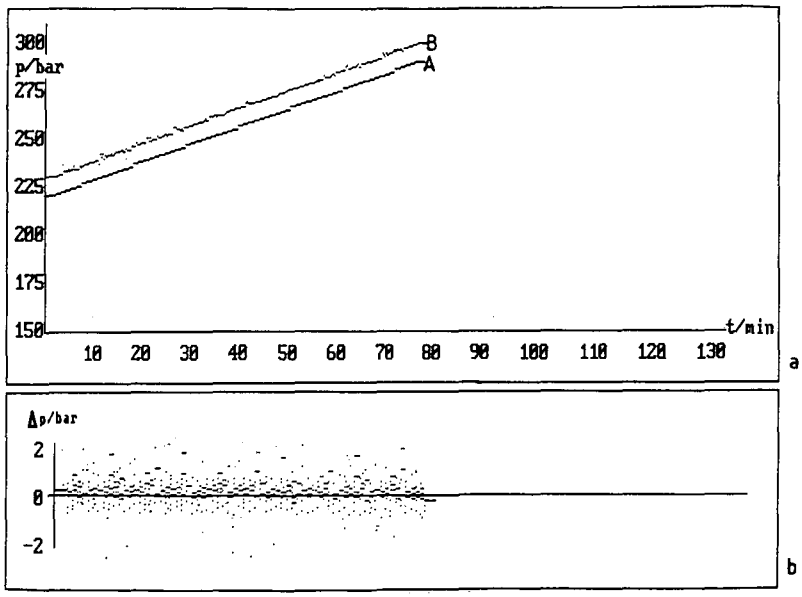

Fig. 2. Hardcopy of pressure-control screen. (a) Pressure programme (A) and actual gradient (B). For better inspection, trace A is arbitrarily shifted to lower values. (b) Actual pressure difference between programme and resulting gradient (the short lines are series of points).

actual data as measured by the pressure sensor of the valve assembly are given. In Fig. 2b actual pressure differences between traces A and B in Fig. 2a are shown, measured at a frequency of 1 s^{-1}. The pressure variations are seen to be in the range of ± 2 bar.

As the analyte we chose an oligostyrene sample (polystyrene PS 800 from Pressure Chemical, obtained from Pfannenschmidt, Hamburg, F.R.G.). The sample concentration was 65 mg ml^{-1}, the solvent being 1,4-dioxane. The sample was injected by means of a Rheodyne 7125 valve equipped with a 20-μl sample loop. The injection time was manually controlled at 3 s, which can prevent the occurrence of double peaks[12]. For all chromatograms shown here the temperature was kept at 150°C; this proved to be reasonably near the optimum of resolution in preliminary experiments based on data from fundamental studies with mobile phases composed of carbon dioxide and 1,4-dioxane[13]. The flow-rate was 1 ml min^{-1} (liquid), as measured by the flow controllers provided with the HP 1084B.

RESULTS

The reasons for the choice of sample, mobile phase and stationary phase were as follows. First, styrene oligomers were selected as the analyte because of their ready availability as highly standardized samples. Further, the separation of oligomers has become a domain of SFC owing to its advantages over GC and LC. Second, a mobile phase composed of carbon dioxide and 1,4-dioxane was chosen as this combination has proved suitable for the separation of styrene oligomers[14]. Finally, experimental data[13] are available for this eluent combination and its chromatographic behaviour with respect to pressure, temperature and 1,4-dioxane content with silica as the stationary phase.

Separations using composition gradients

Applying a composition gradient of 5 to 40% (v/v) 1,4-dioxane with a linear increase of the volume ratio[10] within 80 min, chromatograms were obtained at pressures of 230, 265 and 300 bar (Fig. 3). The pressure was kept above 220 bar because at lower pressures mobile phase demixing must be considered when the 1,4-dioxane content exceeds 30%[13]. The chromatograms show decreasing analysis times with increasing pressure, and baseline separations were obtained except at the lowest pressure. The effect of increasing pressure on retention differences appears more pronounced for the lower members of the homologous series and thus more equal spacing results over the entire chromatogram; at the end of the chromatogram, the unresolved peaks at lowest pressure (Fig. 3a) become baseline resolved at 265 bar (Fig. 3b). A further increase in pressure to 300 bar then reduces the analysis time required for separating fifteen oligomers by an additional 10 min (Fig. 3c), maintaining the good resolution obtained at 265 bar. With increasing pressure, the 1,4-dioxane content needed for eluting an individual oligomer is reduced, and this effect seems to improve the quality for this specific separation.

Separations using pressure gradients

Pressure-programmed separations with a linear gradient from 230 to 300 bar within 75 min were performed at constant dioxane contents of 5, 15, 20, 25 and 30% (v/v). The resulting chromatograms are shown in Fig. 4. At the lowest 1,4-dioxane

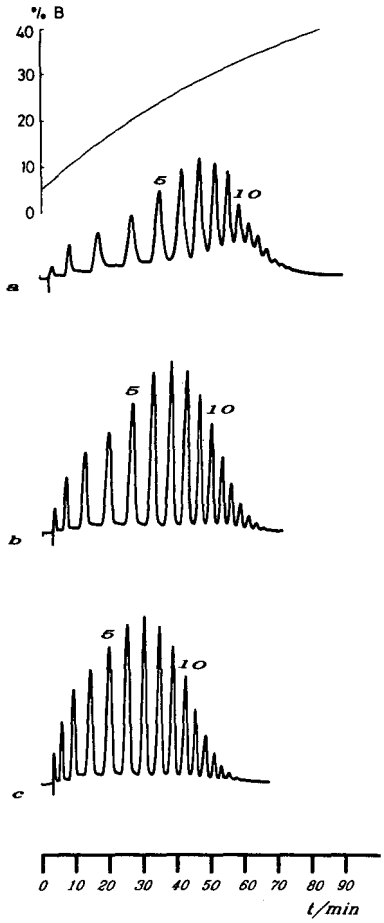

Fig. 3. Composition-gradient separation of styrene oligomers; 5–40% (v/v) 1,4-dioxane in carbon dioxide within 80 min at a constant pressure of (a) 230, (b) 265 and (c) 300 bar. Temperature, 150 °C; flow-rate, 1 ml min^{-1}. For further details, see Experimental.

content the pressure programme elutes only six oligomers within 2 h. Increasing the 1,4-dioxane content reduces the retention times substantially. However, 1,4-dioxane contents exceeding 25% are not suitable for a pressure gradient separation in this instance as is evident from the inferior resolution in Fig. 4e.

The quality of the pressure-gradient separations is poorer than those of the composition-gradient separations in Fig. 3; in fact, in the present instance, pressure gradients are not very effective. This is evident from Fig. 5, showing a comparison between an isocratic pressure-programmed separation (Fig. 5a) and an isocratic–isobaric separation (Fig. 5b). Although the effect of the pressure gradient is clearly visible (*e.g.*, by comparison of retention times for the decamer, $n = 10$), this effect is not very large. Extending the pressure gradient to higher pressures would yield a further reduction in retention, but as the gain in density for a given pressure interval

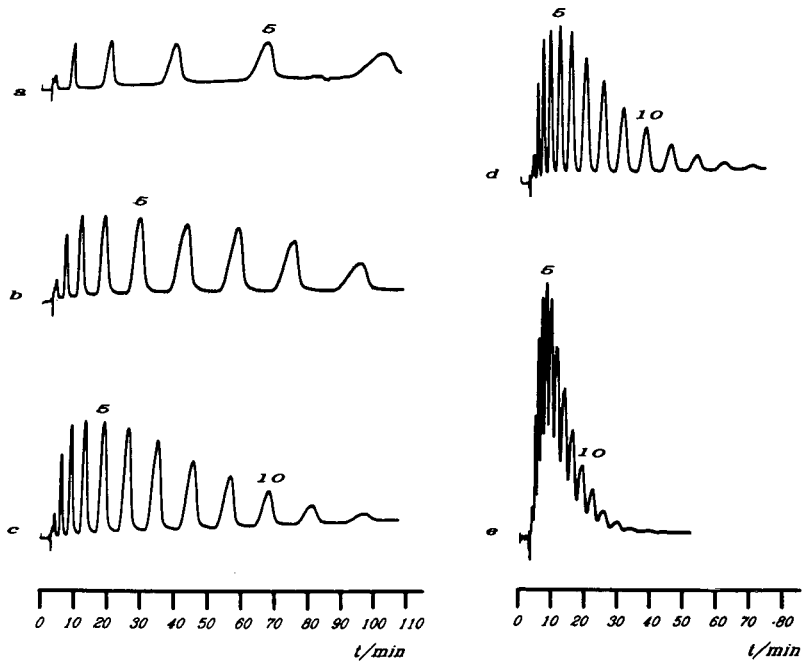

Fig. 4. Pressure-gradient separation of styrene oligomers; 230–300 bar linear increase within 75 min with a constant 1,4-dioxane content of (a) 5, (b) 15, (c) 20, (d) 25 and (e) 30% (v/v) in carbon dioxide. Other conditions as in Fig. 3.

becomes smaller at increasing pressure levels, it can be predicted that for separating higher oligomers pressure gradients will be less effective with this chromatographic system of solute, mobile phase and stationary phase, at a constant flow-rate.

Frequently, non-linear pressure gradients have been applied for oligomer separations. With the pressure-control device used in this work, the use of non-linear gradients is also possible. Such a separation is shown in Fig. 6. With this "asymptotically shaped" pressure gradient, a pressure of 350 bar is obtained after 45 min. It is

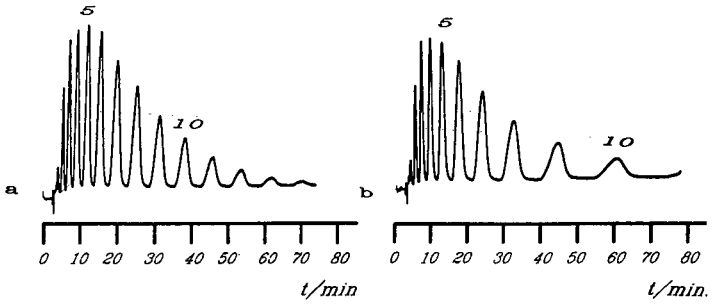

Fig. 5. Comparison of (a) isocratic pressure-programmed separation (*cf.*, Fig. 4d) with (b) isobaric–isocratic separation of styrene oligomers. Mobile phase, carbon dioxide–dioxane (75:25, v/v); pressure, 230 bar (b), 230–300 bar (a). Other conditions as in Fig. 3.

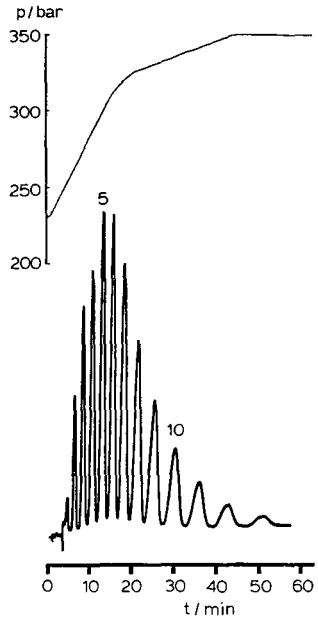

Fig. 6. Separation of styrene oligomers with an "asymptotic" pressure gradient from 230 to 350 bar. Mobile phase, carbon dioxide–1,4-dioxane (80:20, v/v). Other conditions as in Fig. 3.

seen that the more steeply ramped gradient combined with a higher final pressure yields a considerable decrease in retention (*cf.*, Fig. 4c). Nevertheless, this pressure effect appears insufficient for eluting species of higher molecular weight within a reasonable analysis time.

Multiple gradient separations

Superimposing pressure and composition gradients results in a combined effect of reduction of retention times, as demonstrated several years ago[9,10]. Fig. 7 shows a separation obtained by the simultaneous application of the composition gradient used for the separations shown in Fig. 3 and the pressure gradient in Fig. 4. The combined effects are obvious, but the peak spacing is unequal with large inter-peak distances in the first part and unresolved peaks in the second part of the chromatogram.

Better results are obtained when at least one of the two gradients is modified. Fig. 8 shows an example. Here the composition gradient is modified and increases, after a 5-min isocratic period, from 20% to 40% within 50 min, keeping the pressure gradient unchanged as in Figs. 4 and 7. The chromatogram shows an almost baseline separation for sixteen oligomers within 45 min.

Alternatively, negative pressure gradients (*i.e.*, gradients of decreasing pressure) can be used for refinement of a composition gradient. This appeared possible as the reduction in retention times with increasing pressure was more pronounced for the lower than for the higher oligomers (*cf.*, Fig. 3). Accordingly, a decrease in pressure during the separation resulted in only a slight increase in analysis time, as shown in

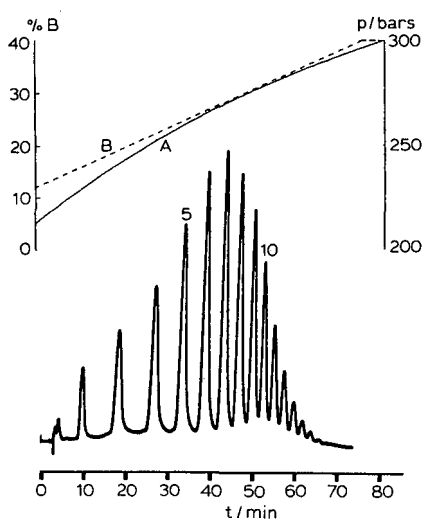

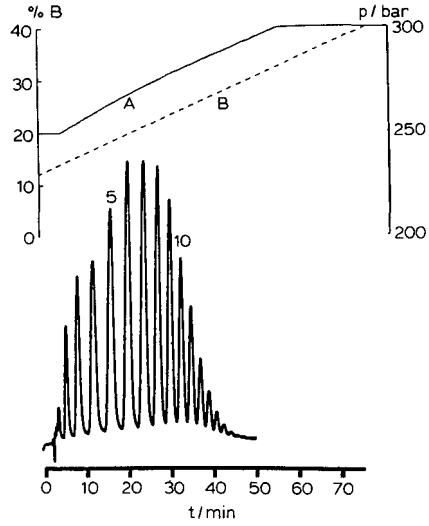

Fig. 7. Separation of styrene oligomers with combined composition (full line, A) and pressure (broken line, B) gradients as used for separations in Figs. 3 and 4. Other conditions as in Fig. 3.

Fig. 8. Separation of styrene oligomers with pressure gradient (broken line, A) as in Fig. 4 and modified composition gradient (full line, B): 5 min isocratic with carbon dioxide–1,4-dioxane (80:20), then from 20 to 40% (v/v) 1,4 dioxane within 50 min. Other conditions as in Fig. 3.

Fig. 9 for a composition gradient as in Figs. 3 and 7 but with a negative pressure gradient from 290 to 230 bar within 75 min. Compared with Fig. 3c, which was obtained at a constant pressure of 300 bar, the peak widths are identical, but the spacing between the peaks is increased in Fig. 9. In other words, the chromatogram in Fig. 9 shows a higher resolution than that in Fig. 3c. This may be of interest for the separation of more complex samples than the styrene oligomer sample separated here.

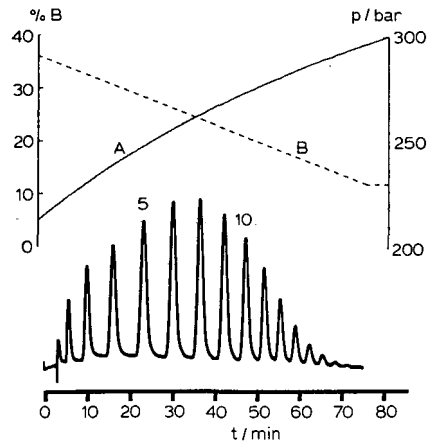

Fig. 9. Separation of styrene oligomers with composition gradient (full line, A) as in Fig. 3 and negative (linear) pressure gradient (broken line, B) from 290 to 230 bar within 75 min. Other conditions as in Fig. 3.

DISCUSSION

The results demonstrate that programming of pressure or density is less suitable for the separation of styrene oligomers on a polar silica stationary phase and with a mobile phase of carbon dioxide plus a constant amount of modifier if the (liquid) volume flow-rate (or the mass flow-rate) is kept constant throughout the run. Composition gradients and combinations of composition and pressure gradients were found to yield distinctly better results.

One reason for this partial failure of single pressure gradients may be the decrease in linear velocity in the separation column, as indicated by the corresponding change in dead time, if the pressure is increased at a constant mass flow-rate or at a constant volume flow-rate (which is virtually identical with a constant mass flow-rate with moderate pressure changes and pumping of the mobile phase in the liquid state). Hence an improvement in the effectiveness of pressure gradients may be possible if the decrease in the linear velocity in the column is counteracted or even balanced by a continuous change in the mobile phase feed rate, *i.e.*, by a flow gradient. However, previous results with combined pressure–flow gradients[15] do not seem promising. With composition gradients, changes in linear velocity in the column at a constant pump feed rate are only small and can be neglected to a first approximation.

By means of the pressure-control system used in this study, pressure control was very easy to achieve and pressure changes could be carried out instantaneously. It also provides high flexibility for pressure and density programming. These statements are valid as long as flow-rates are applied that are typical for normal-bore packed columns, *i.e.*, around 1 ml min^{-1}. With substantially lower flow-rates the large dead volume of the valve assembly may cause serious problems. For such low flow-rates a valve assembly as described by Saito and co-workers[16,17] might be more suitable. This valve, being similar in principle to that used in this study, is stated to have a very low dead volume of only a few microlitres. Nevertheless, the use of both valves is restricted to post-detector regulation, such as with UV (or IR or fluorescence) detection. For use upstream of the detector, as is necessary, *e.g.*, with flame ionization detection, the dead volumes of both valves are too high; also, a substantial reduction in dead volumes might be inevitable for pre-column use.

ACKNOWLEDGEMENT

Financial support by the Arbeitsgemeinschaft Industrieller Forschungsvereinigungen (AIF) is gratefully acknowledged.

REFERENCES

1 B. A. Charpentier and M. R. Sevenants (Editors), *Supercritical Fluid Extraction and Chromatography. Techniques and Applications* (*ACS Symposium Series*, No. 366), American Chemical Society, Washington, DC, 1988.
2 R. M. Smith (Editor), *Supercritical Fluid Chromatography*, Royal Society of Chemistry, London, 1988.
3 C. M. White (Editor), *Modern Supercritical Fluid Chromatography*, Hüthig, Heidelberg, Basle, New York, 1988.
4 M. Yoshioka, S. Parvez, T. Miyazaki and H. Parvez (Editors), *Supercritical Fluid Chromatography and Micro-HPLC* (*Progress in HPLC*, Vol. 4), VSP, Utrecht, 1988.

5 E. Klesper and F. P. Schmitz, in C. M. White (Editor), *Modern Supercritical Fluid Chromatography*, Hüthig, Heidelberg, Basle, New York, 1988, p.1.
6 F. P. Schmitz and E. Klesper, *J. Chromatogr.*, 388 (1987) 3.
7 E. Klesper and F. P. Schmitz, *J. Chromatogr.*, 402 (1987) 1.
8 E. Klesper and F. P. Schmitz, *J. Supercrit. Fluids*, 1 (1988) 45.
9 F. P. Schmitz, H. Hilgers and E. Klesper, *J. Chromatogr.*, 267 (1983) 267.
10 F. P. Schmitz, H. Hilgers, B. Lorenschat and E. Klesper, *J. Chromatogr.*, 346 (1985) 69.
11 F. P. Schmitz, D. Leyendecker and D. Leyendecker, *J. Chromatogr.*, 389 (1987) 245.
12 D. Thiebaut, M. Caude and R. Rosset, *Analusis*, 15 (1987) 528.
13 D. Leyendecker, D. Leyendecker, F. P. Schmitz, B. Lorenschat and E. Klesper, *J. Chromatogr.*, 398 (1987) 105.
14 F. P. Schmitz, D. Leyendecker, D. Leyendecker and B. Gemmel, *J. Chromatogr.*, 395 (1987) 111.
15 F. P. Schmitz, *Chromatographie mit überkritischen verdichteten Gasen zur Trennung von Oligomeren und Polymeren*, Profil, Munich, 1988.
16 M. Saito, T. Hondo and Y. Yamauchi, in R. M. Smith (Editor), *Supercritical Fluid Chromatography*, Royal Society of Chemistry, London, 1988, p. 203.
17 M. Saito, Y. Yamauchi, H. Kashiwazaki and M. Sugawara, *Chromatographia*, 25 (1988) 801.

Journal of Chromatography, 475 (1989) 95–112
Elsevier Science Publishers B.V., Amsterdam — Printed in The Netherlands

CHROM. 21 534

RETENTION BEHAVIOUR OF SOME CLASSES OF PHARMACEUTICAL PRODUCTS ON CHEMICALLY MODIFIED THIN-LAYER CHROMATOGRAPHIC PLATES

J. DINGENEN*
Department of Chemical Development, Janssen Pharmaceutica, Turnhoutseweg 30, B-2340 Beerse (Belgium)
and
A. PLUYM
Department of Analytical Research, Janssen Pharmaceutica, B-2340 Beerse (Belgium)
(First received July 12th, 1988; revised manuscript received March 22nd, 1989)

SUMMARY

In order to widen the application of chemically modified plate materials in the analysis of drug substances, the characteristics of such commercially available precoated polar and non-polar modified layers have been studied using a series of butyrophenones and benzimidazol-2-ones as model compounds, and normal as well as reversed-phase conditions. The influence of different types of salts, salt concentrations, organic modifier content, the use of ion-pair reagents and the influence of pH on the retention behaviour have been examined. The most suitable layers for reversed-phase thin-layer chromatography of the compounds investigated are the cyano-, RP-2 and RP-18W (completely wettable RP-18 layer) high-performance plates. Because of the low wettability with water-rich solvent mixtures, and hence a long development time and more diffuse spots, the RP-8 and RP-18 layers are less suitable. The high-performance amino-modified precoated plate, used under normal-phase conditions, is very suitable for chromatography of the alkaline compounds investigated.

INTRODUCTION

Up to a few years ago, most problems related to thin-layer chromatography (TLC) were solved in our laboratories by means of normal-phase chromatography on silica gel as the stationary phase. After the introduction of the first commercially available, chemically modified, plate materials in 1977–1978 (Whatman, Antec, Merck, Macherey-Nagel, etc.), and partly under the influence of high-performance liquid chromatography (HPLC) technology, in which reversed-phase packing materials were being used quite generally at that time, more TLC methods were systematically developed on chemically modified plate materials. At present in our laboratories the ratio of silica gel/chemically modified phase TLC applications is approximately 20:80.

TLC, using silica gel as a stationary phase, is still used quite frequently for pilot investigations and partial optimization of chromatographic parameters for preparative column chromatographic separations. Both for quality-control applications, in which minute percentages of starting materials and by-products have to be determined in a pharmaceutical substance, and for process-control purposes, in which measurements have to be performed within a wide concentration range, we initially opted for the KC_{18} plate material supplied by Whatman. Using this material, we were able to achieve a good compromise between the hR_F value, spot shape and running time by means of relatively simple eluent combinations, usually consisting of a 0.5–1 *M* salt solution (sodium chloride, ammonium acetate) and 1,4-dioxane, tetrahydrofuran, methanol or a mixture of these organic modifiers. In order further to improve the separation we later started to use high performance (HP) TLC plate materials (RP-18, Merck). However, when we introduced the smaller 10 cm × 10 cm HPTLC plates, a number of major advantages soon became apparent. In comparison to the normal quality TLC plates, separation times appeared to be shorter, spots were less diffuse and less solvent was consumed. Thus, we continued to use systematically the 10 cm × 10 cm TLC quality plates, as if they were HPTLC plates. This implied the application of smaller amounts, the use of shorter migration distances and development in smaller chambers. The results were very successful, since separations could usually be transferred quite easily from the 20 cm × 20 cm to the 10 cm × 10 cm plates. Rarely had the mobile phase composition to be modified, whilst the detection limit of the impurities relative to the main component remained almost constant. For a number of semiquantitative analyses, cutting up the 20 cm × 20 cm TLC plates was (and still is) a valuable alternative to the use of the more expensive HPTLC quality plates.

Nevertheless, at present we are still using real HPTLC plates most of the time, since a greater variety of plate types[1–8] is available. Moreover, because of the finer surface structure of the layer, this type of plates permits a much better detection of smaller quantities of product by means of *in situ* scanning equipment (improved signal-to-noise ratio).

To acquire an insight into the retention behaviour of diverse product classes on the available modified plate materials, systematic research is required. For this purpose we have composed a number of series comprising our most frequently occurring product classes. Each series contains starting materials, isomeric compounds, analogous structures, decomposition products and by-products. Such a series thus represents a realistic model of a normal analytical problem. For product series we chose the butyrophenones and benzimidazol-2-ones. The composition of both series with the chemical structure of each component is given in Tables I and II.

EXPERIMENTAL

All experiments were carried out on HPTLC precoated plates from Merck (Darmstadt, F.R.G.). Plate types used: RP-2 F_{254s} (Art. 13726); RP-8 F_{254s} (Art. 13725); RP-18 F_{254s} (Art. 13724); NH_2 F_{254s} (Art. 15647); CN F_{254s} (Art. 16464); RP-18 WF_{254s} (Art. 13124). Due to visualization problems with certain products, 500 ng was used as a standard application aliquot.

A Camag twin-trough chamber was used for development, one trough containing 10 ml of the eluent. The water used for the preparation of the salt solutions was purified via reverse osmosis prior to use. All solvents and reagents used were of analytical grade quality or were purified by us prior to use. Reflection measurements were performed on a Camag TLC scanner II, linked with an HP 9816 computer (Camag software 1986, revision 7.01).

The major parameters investigated were: effect of the type of salt[3,7] and its molar concentration on the retention behaviour and the spot shape; use of ion-pair reagents[1,5]; pH effects (addition of inorganic acids/bases, or the use of buffer solutions); influence of choice of organic modifier[6] on the selectivity.

The salts used were lithium chloride, ammonium chloride, ammonium acetate and sodium chloride (1, 0.5, 0.25, 0.1 and 0.05 *M*), the organic modifiers were methanol, acetone, 1,4-dioxane and 2-propanol and the ion-pair reagents were 1-butane-, 1-hexane- or 1-octanesulphonic acid sodium salt in buffered (pH 3.5) and non-buffered media (1, 0.5, 0.25 and 0.1 *M*).

RESULTS AND DISCUSSION

A detailed discussion of all experiments performed is obviously not possible. Therefore, we shall restrict ourselves to the most important observations.

TABLE I

COMPOSITION OF THE BUTYROPHENONE SERIES

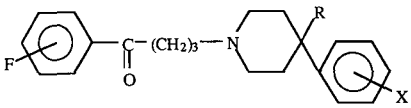

Compound	*Research No.*	*Position of F atom*	*R*	*X*
1	R 1616	4	OH	4-F
2	R 1625	4	OH	4-Cl
3	R 1658	4	OH	4-CH_3
4	R 1838	4	OH	4-H
5	R 2498	4	OH	3-CF_3
6	R 8719	3	OH	4-Cl
7	R 9298	4	OH	3-CF_3 4-Cl
8	R 11333	4	OH	4-Br
9	R 13672	4	–C–*n*-C_9H_{19} ‖ O	4-Cl
10	R 46541	4	–C–*n*-C_9H_{19} ‖ O	4-Br
11	R 65996	2	OH	3-CF_3
12	R 72265	2	OH	4-CH_3

TABLE II

COMPOSITION OF THE BENZIMIDAZOL-2-ONE SERIES

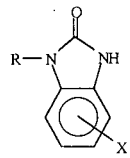

Compound	*Research No.*	*R*	*X*
1	R 4748	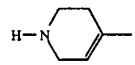	H
2	R 30507	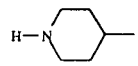	H
3	R 29676	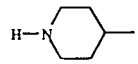	5-Cl
4	R 4730	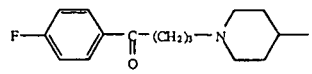	H
5	R 4749	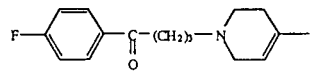	H
6	R 6238	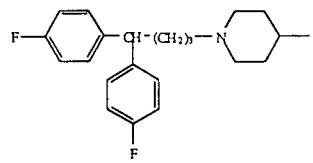	H
7	R 6413	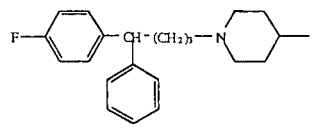	H
8	R 29764	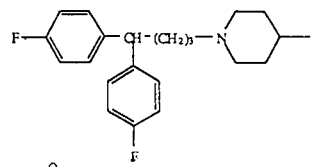	5-Cl
9	R 33812	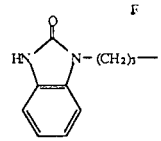	5-Cl
10	R 34009	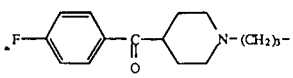	5-Cl
11	R 34301	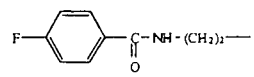	5-Cl

TABLE II (*continued*)

Compound	*Research No.*	*R*	*X*
12	R 34315	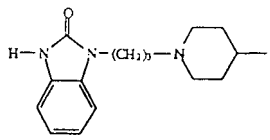	H
13	R 35443	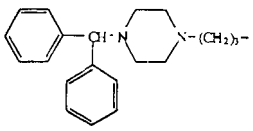	H

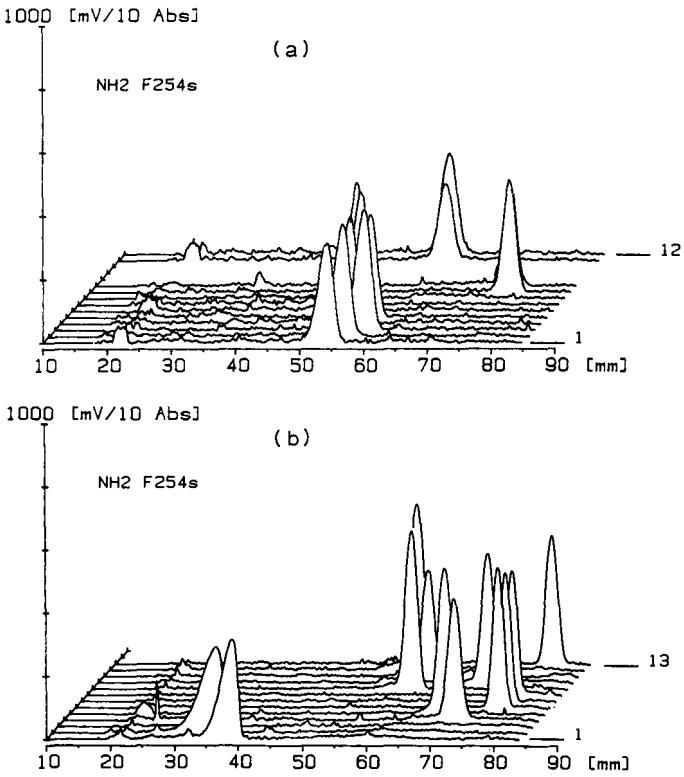

Fig. 1. Normal-phase chromatography on amino-modified HPTLC plates, NH_2 F_{254s}; (a) butyrophenones, mobile phase cyclohexane–1,4-dioxane (70:30, v/v); (b) benzimidazol-2-ones, mobile phase cyclohexane–2-propanol (70:30, v/v).

Amino plate

For both product classes none of the reversed-phase conditions tested (mixtures of water and organic modifiers in a ratio of 40:60, v/v) yielded good results on the NH_2 phase. The products were mostly eluted as "front-running" spots. Under normal-phase conditions (mixtures of cyclohexane and polar modifiers in different ratios), on the other hand, the retention is well controllable both for the butyrophenones and the benzimidazol-2-ones and a good spot shape is observed in virtually all cases (Fig. 1). In general, we have observed for our products that, in order to obtain a certain separation, the composition of the eluents on the NH_2 plate material is much more simple than that required for an equivalent result on silica gel as the stationary phase. Separations on an amino phase are also more reproducible than on silica gel. Due to the less polar character of the former plate type, the retention seems to be influenced to a smaller extent by the relative humidity.

In most cases, a smaller amount of the polar component is required, which obviously has a beneficial effect on the prevention of solvent separation or, in other words, multifront formation. The favourable results obtained under normal-phase conditions on this type of plate are presumably the consequence of the alkaline characteristics of the alkylamino groups present on the plate. The effect of the polar component in the eluent on the retention behaviour is illustrated in Fig. 2.

The low hR_F values observed for the benzimidazol-2-one derivatives, when acetone and dioxane are used as polar components in the mobile phase, are probably

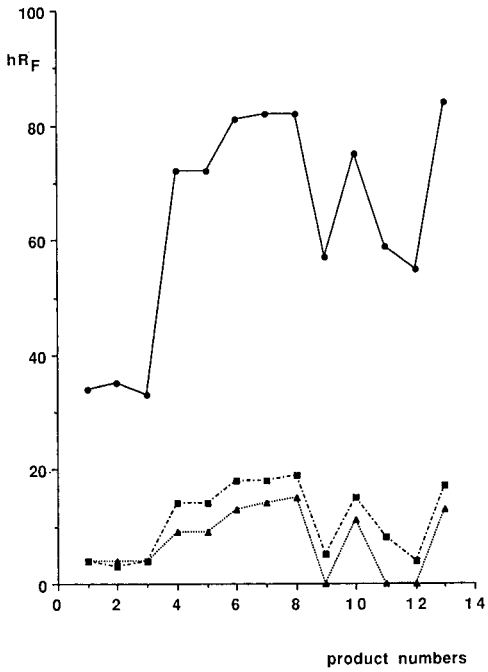

Fig. 2. Effect of the polar component in the mobile phase on the retention of benzimidazol-2-ones (see Table II for product numbers) on NH_2 F_{254s}. Mobile phases: ▲ = cyclohexane–acetone (70:30, v/v); ■ = cyclohexane–1,4-dioxane (70:30, v/v); ● = cyclohexane–2-propanol (70:30, v/v).

the result of strong interactions between the somewhat acidic secondary amide hydrogen of the benzimidazol-2-one and the alkaline alkylamino groups on the plate. Therefore, a stronger eluent will probably be required to displace these products.

Ion-pair reagents

On the plate types investigated (RP-2, CN and RP-18W), ion-pair reagents have a particularly positive effect on the spot shape for both product series (Fig. 3).

For the various ion-pair reagents applied, the results obtained in a buffered medium are comparable to those obtained in a non-buffered medium. This may presumably be ascribed to the pH value of the ion-pair reagent used. For the ion-pair reagent dissolved in buffer pH 3.5, as well as for the reagent dissolved in water, the pH values were always found to be approximately 4–5 units lower than the pK_a values of most of the products investigated, so that we can be sure that ion-pair formation occurs in both cases. When ion-pair reagents dissolved in buffer pH 3.5 are used, the spots formed are usually smaller than in experiments carried out under identical circumstances in the non-buffered medium.

For both product classes, the lowest hR_F values are obtained at a concentration of 0.1 *M* of the ion-pair reagents investigated, which may be regarded as a logical consequence of increasing dissociation of the reagent at lower concentrations, so that the chance of ion-pair formation increases. In general, however, the spot size increases with decreasing concentration of ion-pair reagent. At a concentration of 0.1 *M*, the spots usually become longer on the CN phase. Fig. 4 shows the effect of the different ion-pair reagents on the retention behaviour of the butyrophenones on an RP-2 plate. The hR_F values obtained under identical chromatographic conditions for a 0.25 *M* sodium chloride solution were used as a reference. This curve clearly demonstrates that the hydrophobicity of the ion pairs formed increases with increasing chain length of the reagent used.

In general, on the RP-2 and RP-18W material, the effect on the retention behaviour is rather small for butanesulphonic acid. The greatest differences from the reference curve were observed for octanesulphonic acid. As regards the spot shape, butanesulphonic acid yields the best results.

Owing to the presence of a polar functional group, the cyano plate has a more polar character than the RP-2 and RP-18W plate types. This is clearly visible: in contrast to the observations on the RP-2 and RP-18W material, the hR_F values measured for the reference solution (0.25 *M* NaCl) are lower for both product series than in those cases where an ion-pair reagent was applied. On the basis of this observation, we expect a decrease in the hR_F values in the order octyl, hexyl, butyl as a result of an increasing hydrophobicity of the ion pairs formed with increasing chain length of the ion-pair reagent used. This appeared to be the case for none of the product classes investigated. The highest retention was always observed for the ion pairs formed with octanesulphonic acid. Therefore, both the adsorptive and the distributive characteristics of the layer can be utilized on the cyano plate.

Effect of salts

As is generally known, the addition of inorganic salts to the aqueous phase, in reversed-phase TLC, considerably improves the spot shape. However, our experiments demonstrated that addition of inorganic salts to the mobile phase may also exert a number of other effects on the TLC behaviour of the compounds investigated.

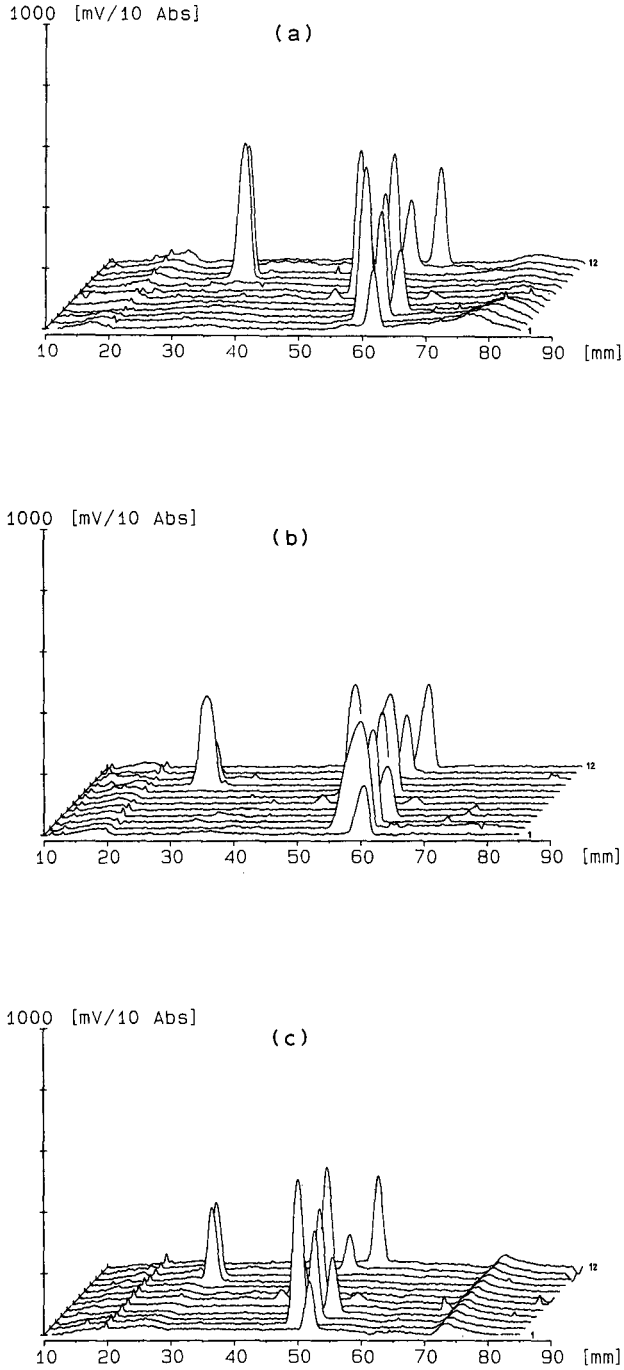

Fig. 3. Effect of ion-pair reagents on the spot shape of butyrophenones on: RP-18 WF_{254s}. Mobile phases: (a) 1,4-dioxane–0.25 *M* sodium chloride (60:40, v/v); (b) 1,4-dioxane–buffer pH 3.5 (60:40, v/v); (c) 1,4-dioxane–0.25 *M* octanesulphonic acid sodium salt in buffer pH 3.5 (60:40, v/v).

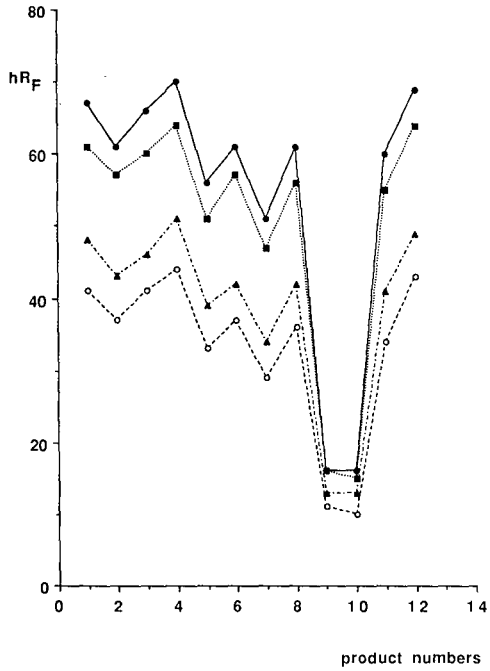

Fig. 4. Effect of ion-pair reagents on the retention behaviour or butyrophenones (see Table I for product numbers) on RP-2 F_{254s}. Mobile phases: 1,4-dioxane–aqueous phase (60:40, v/v); (●) 0.25 *M* sodium chloride, (■) 0.25 *M* sodium 1-butanesulphonate–buffer pH 3.5, (▲) 0.25 *M* sodium 1-hexanesulphonate–buffer pH 3.5, (○) 0.25 *M* sodium 1-octanesulphonate–buffer pH 3.5.

Influence of the salt concentration on the retention behaviour and spot shape. Table III summarizes for the different plate types the influence of the salt concentration on the retention behaviour of the product classes investigated. Ammonium, lithium as well as sodium chloride yield good results as tailing reducers. For these salts,

TABLE III

BENZIMIDAZOL-2-ONES AND BUTYROPHENONES: INFLUENCE ON PRODUCT RETENTION OF THE SALT CONCENTRATION IN THE RANGE 0.05–1 *M*

–, Almost no effect, or only a very limited effect; +, distinct effect.

Salt	*Plate type*				
	RP-2	*RP-8*	*RP-18*	*RP-18W*	*CN*
Lithium chloride Ammonium chloride Sodium chloride	–	–	–	–	–
Ammonium acetate	+	+	+	+	+
Ammonium hydroxide	+	+	+	+	+

concentration changes within the range tested have only a very limited effect on the retention behaviour.

Ammonium acetate, on the other hand, shows a strongly deviating behaviour in comparison to the other salts. When the salt concentration is lowered, the retention of most compounds increases considerably (Fig. 5). A comparable effect is observed when dilute ammonia solutions are used as the aqueous phase. The fact that alkaline compounds are sometimes strongly retained on chemically modified phases can be explained by interactions between these compounds and residual acidic silanol groups in the packing material. In salt-containing mobile phases, the cation present will play a major role in suppressing silanol interactions. Although the phenomenon of "silanol effects" is still somewhat obscure, it is highly probable that the interaction between cations from the mobile phase, acidic silanol groups and protonated alkaline compounds occurs via an ion-exchange mechanism[9]:

$$\equiv SiO^- M^+ + R\text{–}NH_3^+ \rightleftharpoons \equiv SiO^- R\text{–}NH_3^+ + M^+ \quad (1)$$

For the product classes investigated, changes in salt concentration have little effect on the retention behaviour when lithium chloride, sodium chloride and ammonium chloride are used. It is likely that, with these salts, sufficient cations are present in the mobile phase, even at low concentrations, to shield the acidic silanol groups, or, in other words, to force eqn. 1 completely to the left.

When ammonium acetate solutions are used as the aqueous phase, it is clear that at low concentrations the alkaline compounds to be analyzed are preferably bound to the acidic silanol groups. Although the dissociation rate of a weak electrolyte increases when its concentration is lowered, there are, from an absolute point of view, more ions present in the solution at higher concentrations. As a result, upon increasing the salt concentrations the equilibrium in eqn. 1 will shift more and more to the left so that the retention due to silanol interactions decreases. The influence of ammonium hydroxide solutions on the retention behaviour of the compounds investigated can be explained in a similar fashion. Nevertheless, it should be noted that in such solutions most of the products tested are no longer present in a protonated form. In principle, however, these free bases are also able to bind to the acidic silanol groups without ion-exchange effects.

Table IV summarizes for the butyrophenones and the benzimidazol-2-ones the influence of salt concentration on the spot shape. Ammonium, lithium and sodium chloride, up to a concentration of 0.25 *M*, usually result in a good spot shape on all plate types tested. On RP-8 and RP-18, the spots formed are usually more diffuse than on CN, RP-2 and RP-18W plate material.

Over the entire concentration range, the smallest spots are observed on RP-18W plates. For our products, salt solutions of 0.1 *M* result in problems with regard to spot shape in many cases. Elongation of the spots with decreasing salt concentration is manifested most clearly on the CN phase; spherical spots are observed on this plate type only at the highest concentrations (Fig. 6).

Ammonium acetate as a tailing reducer results in a good spot shape for both product series at higher salt concentrations (1–0.5 *M*). Ammonium hydroxide as the aqueous phase mostly yields, for the plate types tested (CN, RP-2, RP-18W), a very good spot shape at higher concentrations (1, 0.5, 0.25 *M*). However, for reasons of reproducibility, the use of dilute ammonia solutions is less suitable in practice.

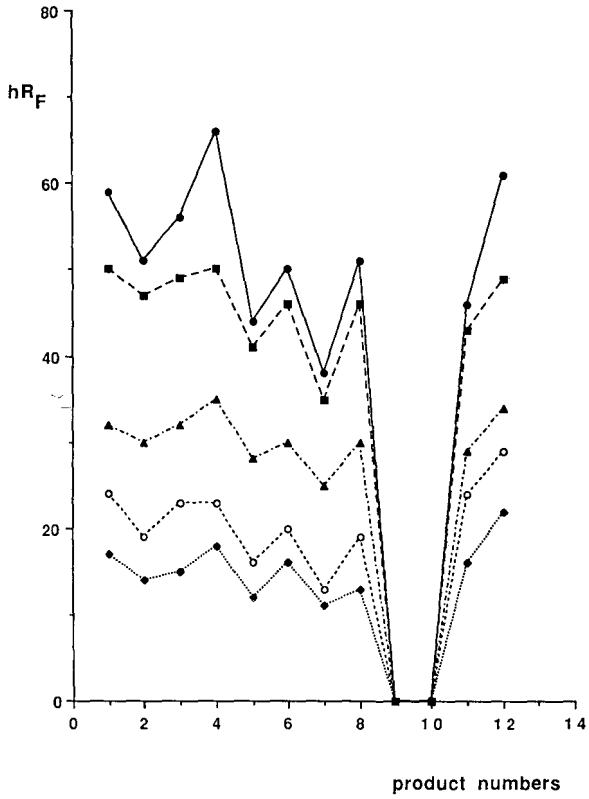

Fig. 5. Effect of ammonium acetate concentration on the retention behaviour of butyrophenones (Table I) on RP-18 F_{254s}. Mobile phases: 1,4-dioxane–aqueous ammonium acetate (60:40, v/v); (●) 1, (■) 0.5, (▲) 0.25, (○) 0.1, (◆) 0.05 *M*.

TABLE IV

BENZIMIDAZOL-2-ONES AND BUTYROPHENONES: INFLUENCE OF THE NATURE AND CONCENTRATION OF THE SALT SOLUTION USED ON THE SPOT SHAPE

+, Good spot shape; +(D), good spot shape, but rather diffuse spots; + +, round, well formed spots; + + +, minute round spots; −, mostly poor spot shape (fronting, tailing, formation of stripes); −(E), distinctly elongated spots; NI, not investigated.

Salt	*Concentration*	*Plate type*				
		RP-2	*RP-8*	*RP-18*	*RP-18 W*	*CN*
Lithium chloride Ammonium chloride Sodium chloride	High	+ +	+(D)	+(D)	+ + +	+
	Low	−	−	−	+ +	−(E)
Ammonium acetate	High	+ +	+(D)	+(D)	+ + +	+
	Low	−	−	−	+ +	−(E)
Ammonium hydroxide	High	+ +	NI	NI	+ + +	+
	Low	+	NI	NI	+ +	−(E)

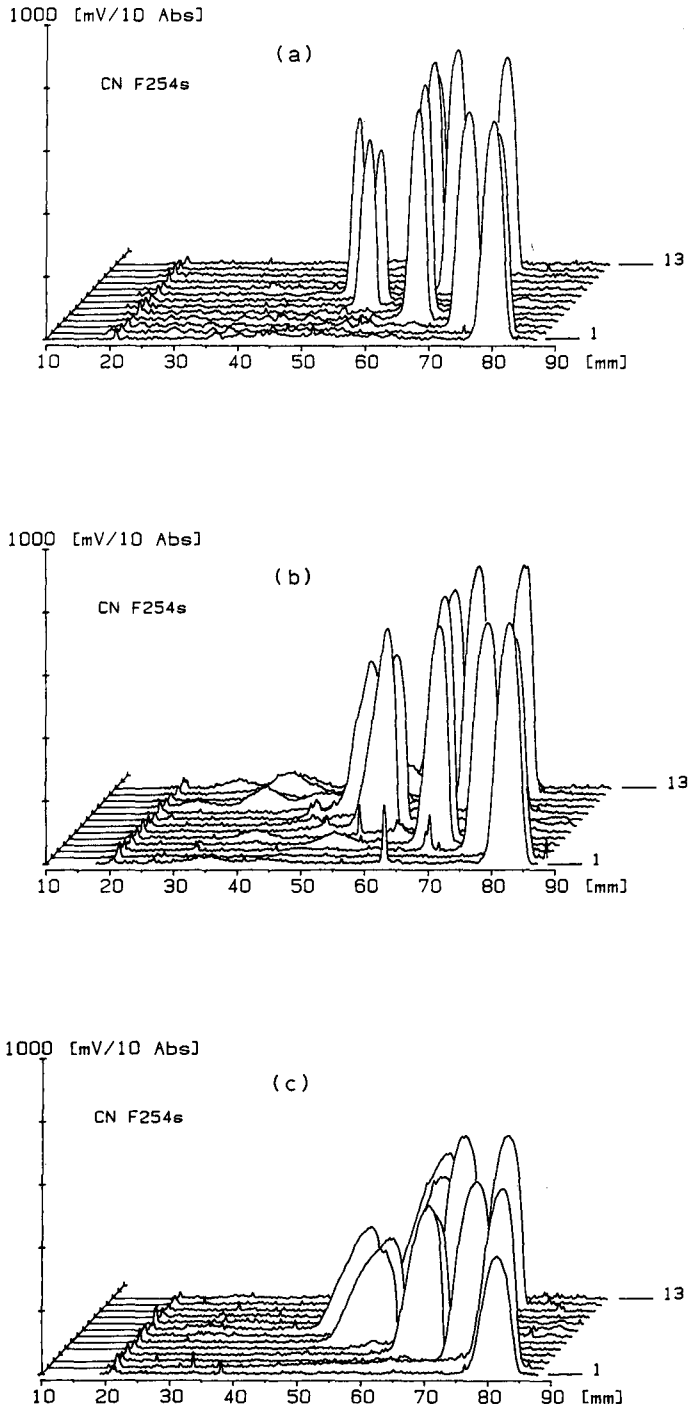
1000 [mV/10 Abs]
(a)
CN F254s
13
1
10 20 30 40 50 60 70 80 90 [mm]
1000 [mV/10 Abs]
(b)
CN F254s
13
1
10 20 30 40 50 60 70 80 90 [mm]
1000 [mV/10 Abs]
(c)
CN F254s
13
1
10 20 30 40 50 60 70 80 90 [mm]

Fig. 6.

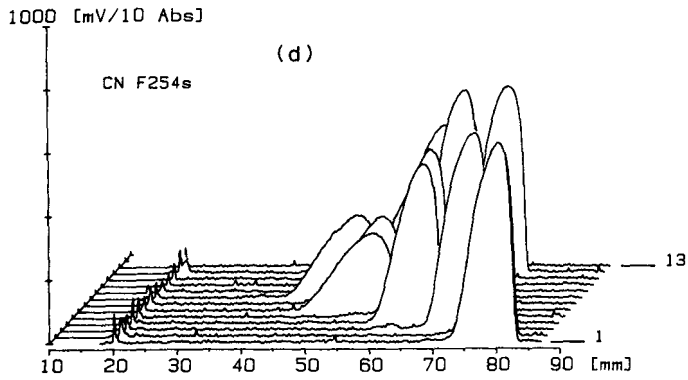

Fig. 6. Effect of inorganic salt concentration on the spot shape of benzimidazol-2-ones on CN F_{254s}. Mobile phases: 1,4-dioxane–aqueous ammonium chloride (60:40, v/v); (a) 1, (b) 0.5, (c) 0.1, (d) 0.05 *M*.

Effects on the spot shape which result from the combined effects of the kind of organic modifier and the nature and concentration of the salt solution used. For the product classes investigated, ammonium, lithium and sodium chloride in combination with the solvents tested (methanol, acetone, 2-propanol and 1,4-dioxane) result, at higher salt concentrations, in a good spot shape on all plate types. At salt concentrations of 0.1 *M*, problems with the spot shape are frequently encountered. A concentration of 0.05 *M* does not result in a good spot shape with any of the salt solution–organic modifier combinations. The spot shape remains relatively good at the lowest salt concentration only on the RP-18W plate.

Ammonium acetate, in combination with the solvents tested, results in a good spot shape for both product series at higher salt concentrations (1 and 0.5 *M*). In the more dilute solutions, fronting was observed on several plate types with methanol, 2-propanol and 1,4-dioxane as the organic modifiers. On the RP-18 plate, even stripes were seen over the entire migration distance. A good spot shape was obtained at lower salt concentrations only when acetone was used as the solvent.

Furthermore. according to the eluent composition, we often noted secondary fronts when using ammonium acetate. Moreover, the fact that the zone containing the salt rapidly turns yellow is often regarded as a nuisance, particularly for reflection measurements.

Ammonium hydroxide as an aqueous phase in combination with the various solvents investigated mostly resulted, for the plate types tested (CN, RP-2, RP-18W), in a very good spot shape at higher concentrations (1, 0.5, 0.25 *M*). Particularly on the CN phase, lower concentrations yield poorer results.

In general, 1,4-dioxane in combination with the different salt solutions furnishes the best spot shape and the most diffuse spots are observed with methanol as the organic modifier. An additional phenomenon for water–methanol mixtures is tailing of relatively apolar compounds (*e.g.*, R 13672, a basic substance with a large hydrophobic moiety incorporated within the molecule), presumably a direct result of the poorer solubility of such products in polar solvents. Our experience shows that salt formation, as a result of which the solubility of these products in polar solvents increases, may solve this problem.

Correlation between the retention behaviour and the polarity of the plate type used. For ammonium, lithium as well as for sodium chloride as tailing reducers, the retention behaviour for both product series may be correlated quite well with the polarity of the plate types tested. The lowest hR_F values are almost always found on RP-18W, the highest on RP-18. The hR_F values on RP-2 and RP-8 are situated, with a few exceptions, at predictable positions between these two extremes (Fig. 7).

The results obtained on the CN phase are somewhat more difficult to categorize, based only on the polarity of the material. As mentioned before, several mechanisms presumably determine the retention behaviour on this plate type.

As regards the selectivity, under identical chromatographic circumstances, there are no pronounced differences between the respective plate types.

When ammonium acetate is used the retention behaviour of the compounds investigated on the various plate types is less easy to predict, particularly for the benzimidazol-2-ones (Fig. 8). In this series the retention behaviour is so random that no sensible relationship can be established with the polarity of the plate type tested.

For dilute ammonium hydroxide solutions in combination with an organic modifier, the retention behaviour of the compounds investigated correlates well with the polarity of the plate types tested, with only a few exceptions (for example the polar secondary amines R 4748, R 30507, R 29676 which are strongly retained on RP-18W particularly due to additional silanol interactions on this material) (Fig. 9).

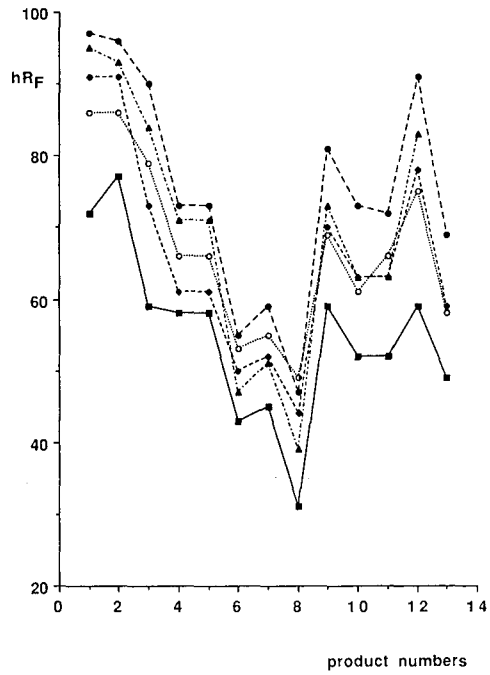

Fig. 7. Influence of the inorganic salt and different reversed-phase stationary phases on the retention of benzimidazol-2-ones (Table II). Plates: ○ = CN F_{254s}; ◆ = RP-2 F_{254s}; ▲ = RP-8 F_{254s}; ● = RP-18 F_{254s}; ■ = RP-18 WF_{254s}. Mobile phase: 1,4-dioxane–1 *M* lithium chloride (60:40, v/v).

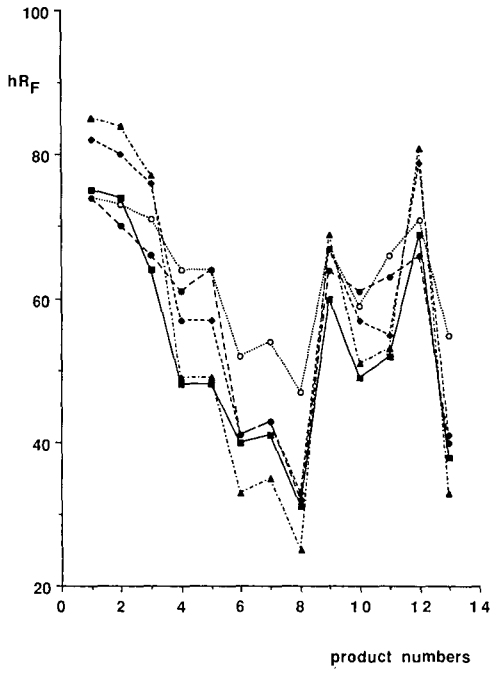

Fig. 8. Influence of ammonium acetate and different reversed-phase stationary phases on the retention of benzimidazol-2-ones (Table II). Plates: as in Fig. 7. Mobile phase: 1,4-dioxane–1 *M* ammonium acetate (60:40, v/v).

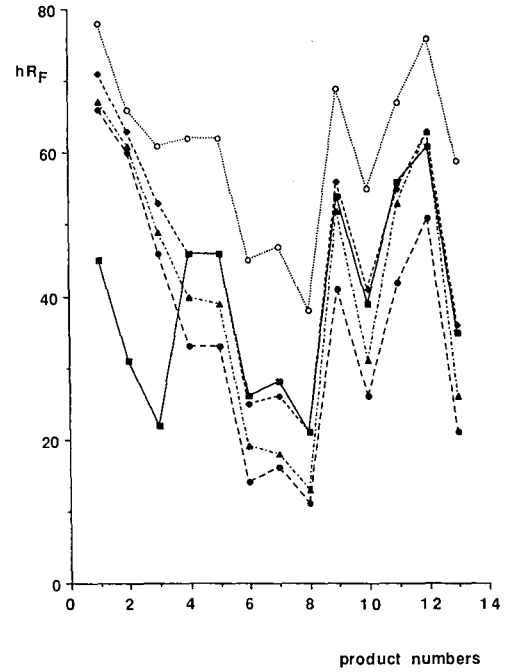

Fig. 9. Influence of ammonia and different reversed-phase stationary phases on the retention of benzimidazol-2-ones (Table II). Plates: as in Fig. 7. Mobile phase: 1,4-dioxane–1 *M* ammonia (60:40, v/v).

pH effect

pH control in the acidic range by the addition of hydrogen chloride to the chloride salt solutions used as part of the eluent has, for our products, no effect on the retention behaviour. This may be considered logical, since the pH values of the salt solutions used are usually sufficiently low to produce protonated forms of the substances to be subjected to chromatography.

Retention control in the alkaline range, on the other hand, is possible by using ammonium salts and pH control by means of concentrated ammonia or sodium hydroxide solutions. The influence on the retention behaviour by adding inorganic bases is certainly not a pure pH effect, since, for a neutral salt (0.25 *M* NaCl) practically no shifts in retention occur upon addition of sodium hydroxide or ammonia.

Ammonium chloride, on the other hand, adjusted to the desired pH with 10 *M* NaOH does show a certain shift of retention. The most sizeable effects on retention are observed for ammonium salts in combination with ammonia (Fig. 10).

The difference in effect observed upon addition of an inorganic base to a sodium chloride or ammonium chloride solution may perhaps be explained by changes in the ionic composition of the aqueous phase. When a sodium chloride solution is used as the aqueous phase the addition of small amounts of sodium hydroxide or ammonia will hardly have any effect on the ionic equilibrium. However, with the acidic salt ammonium chloride there is an effect. The pronounced interference with the retention behaviour, when ammonium chloride–ammonia is used, is probably to be ascribed to

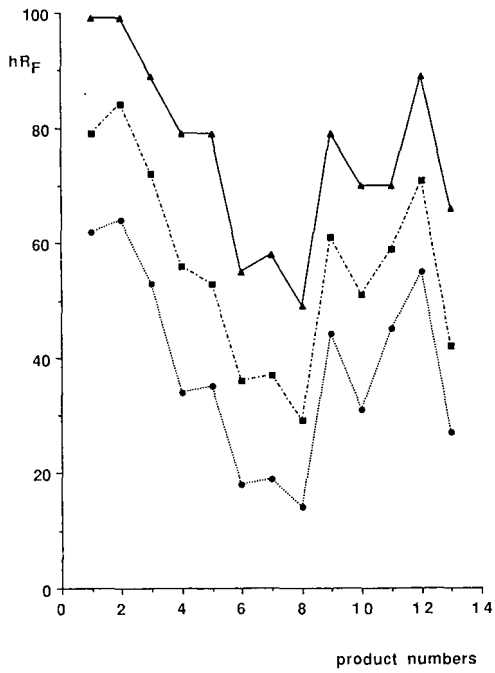

Fig. 10. pH effect on the retention of benzimidazol-2-ones (Table II). Plate: RP-2 F_{254s}. Mobile phases: ▲ = 1,4-dioxane–0.25 *M* ammonium chloride (60:40, v/v); ■ = addition of sodium hydroxide to pH 10; ● = addition of ammonia to pH 10.

the aforementioned strong effect on the retention behaviour upon use of dilute ammonium hydroxide solutions.

An interesting observation is that ammonium chloride solutions, adjusted with NaOH, have an additional effect on the selectivity compared with identical solutions adjusted with ammonia (Fig. 11). At pH 8–9 or 10, no separation of the three analogous compounds R 29676, R 30507 and R 4748 was obtained on any of the plate types investigated (RP-2, CN, RP-18W), when ammonium chloride solutions were used which had been adjusted with sodium hydroxide. For ammonium chloride solutions whose pH had been adjusted with ammonia, there was, at pH 10, a baseline separation for these three components, on RP-18W as well as on the cyano plate. For the product series investigated, pH control by means of ammonia hence has a more pronounced effect on the selectivity than a pH adjusted with sodium hydroxide. However, similar tests on other product series from the benzimidazol-2-one group have demonstrated that the selectivity is sometimes influenced more by pH control with sodium hydroxide than by the addition of ammonia. Therefore, the example shown should certainly not be considered as a general rule.

CONCLUSIONS

It is possible to summarize the results of our investigations as follows.

For our alkaline compounds, cyano, RP-18W and RP-2 are the most interesting plate materials under reversed-phase conditions; RP-18W generally yields the best spot shape.

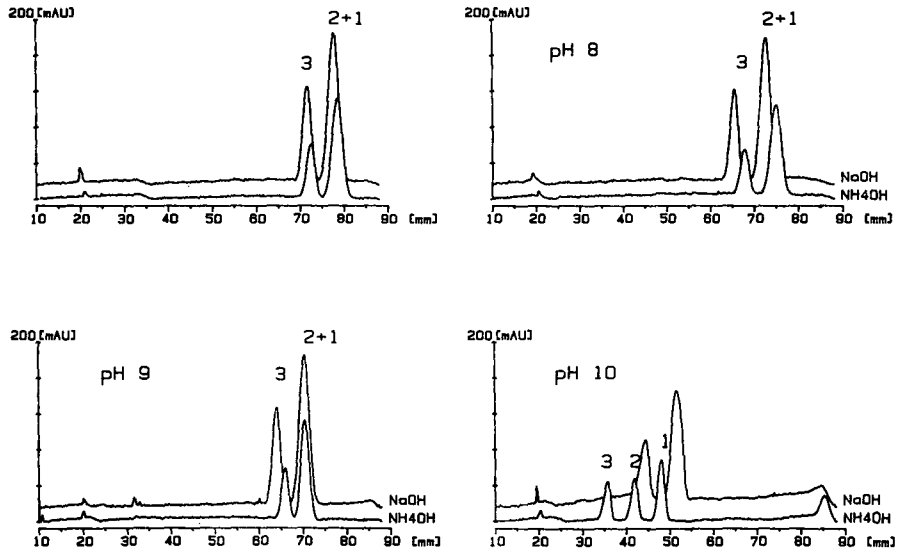

Fig. 11. Effect of pH control with ammonia or sodium hydroxide on the selectivity for benzimidazol-2-ones: 1 = R 29676; 2 = R 30507; 3 = R 4748. Plate: RP-18 WF_{254s}. Mobile phase: 1,4-dioxane–0.25 *M* ammonium chloride (60:40, v/v) adjusted to different pH values with ammonia or sodium hydroxide.

The amino phase, when used under normal-phase conditions, is also very suitable for our applications.

Improvement of the spot shape may be achieved by adding salts in which there is little difference in retention behaviour, if any, when using ammonium, lithium or sodium chloride. For these salts, concentration changes have only a limited effect on retention behaviour. The spot size usually increases with decreasing salt concentration. Ammonium acetate shows a behaviour which is totally different from those of the other salts. For this salt the retention of most compounds increases considerably with decreasing salt concentration, and no sensible relationship can be established with the polarity of the plate types investigated.

Retention can be strongly influenced by adding ammonia, particularly if this occurs in combination with an ammonium salt.

When using ion-pair reagents, a distinct improvement of the spot shape is achieved, and the selectivity can also be influenced.

ACKNOWLEDGEMENTS

The authors gratefully thank Ms. E. Ausloos, Ms. L. Minnen and Mrs. C. Schroyen for their participation in the experimental work. We also thank Mrs. G. Roes for her expedient and accurate handling of the manuscript.

REFERENCES

1 C. Gonnet, M. Marichy and A. Naghizadeh, *Analusis*, 8 (1980) 243.
2 W. Jost and H. E. Hauck, *Anal. Biochem.*, 135 (1983) 120.
3 U. A. Th. Brinkman and G. De Vries, *J. Chromatogr.*, 258 (1983) 43.
4 W. Jost and H. E. Hauck, *J. Chromatogr.*, 261 (1983) 235.
5 W. Jost and H. E. Hauck, *J. Chromatogr.*, 264 (1983) 91.
6 U. A. Th. Brinkman and G. De Vries, *J. Chromatogr.*, 265 (1983) 105.
7 C. Gonnet and M. Marichy, in R. E. Kaiser (Editor), *Instrumental HPTLC*, Institute for Chromatography, Bad Dürkheim, 1985, p. 49.
8 W. Jost and H. E. Hauck, in R. E. Kaiser (Editor), *Instrumental HPTLC*, Institute for Chromatography, Bad Dürkheim, 1985. p. 83.
9 D. Chan Leach, M. A. Stadalius, J. S. Berus and L. R. Snyder, *LC · GC Int., Mag. Liq. Gas Chromatogr.*, 1 (1988) 23.

Journal of Chromatography, 475 (1989) 113–123
Elsevier Science Publishers B.V., Amsterdam — Printed in The Netherlands

CHROM. 21 536

IDENTIFICATION OF ALKYLBENZENES UP TO C_{12} BY CAPILLARY GAS CHROMATOGRAPHY AND GAS CHROMATOGRAPHY–MASS SPECTROMETRY

II. RETENTION INDICES ON OV-101 COLUMNS AND RETENTION–MOLECULAR STRUCTURE CORRELATIONS

E. MATISOVÁ*, E. KOVAČIČOVÁ and PHAM THI HA
Department of Analytical Chemistry, Faculty of Chemical Technology, Slovak Technical University, Radlinského 9, 812 37 Bratislava (Czechoslovakia)
E. KOLEK
Department of Environment Production, Slovnaft, 824 12 Bratislava (Czechoslovakia)
and
W. ENGEWALD
Section of Chemistry, Karl-Marx University, 7010 Leipzig (G.D.R.)
(First received December 8th, 1988; revised manuscript received March 28th, 1989)

SUMMARY

Synthesized multicomponent mixtures of alkylbenzenes with carbon atom numbers greater than ten were analyzed by capillary gas chromatography on the poly(dimethyl silicone) stationary phase OV-101 and gas chromatography–mass spectrometry with electron impact ionization. From the mass spectra acquired, the molecular weights were determined and the alkyl substituents specified. The assignment of the positions of the alkyl substituents of C_{11} and C_{12} alkylbenzenes was based on correlations between the retention data and molecular structures of alkylbenzenes arranged into homologous series. Retention indices on OV-101 at 100°C and temperature coefficients, dI/dT, are given for 34 C_7–C_{10}, 34 C_{11} and 42 C_{12} alkylbenzenes. The regularities of the chromatographic retention behaviour of alkylbenzenes are summarized.

INTRODUCTION

High-resolution capillary gas chromatography (HRCGC) is the most generally useful method for the analysis of complex hydrocarbon mixtures when the ultimate aim is to separate and identify or at least classify all the components. Several GC methods are available for the detailed analysis of C_7–C_{10} alkylbenzenes and of some alkylbenzenes up to C_{15} in petroleum samples and distillates[1]. In a recently published review article on alkylbenzenes[2] it was shown that the best interlaboratory reproducibility of isothermal retention data was achieved on the non-polar stationary phases

0021-9673/89/$03.50

squalane and silicones. However, due to the low temperature stability of squalane and therefore the long analysis time for the analysis of alkylbenzenes with more than nine carbon atoms, the non-polar silicones OV-101 and SE-30 are much more preferable. There are published isothermal retention indices on OV-101[3–5] and SE-30[6,7] for alkylbenzenes with carbon atom numbers up to C_{10}. For higher alkylbenzenes, particularly isomers with several short alkyl chains in the aromatic ring, there are very few published retention data on non-polar silicones[3,5,7].

Chromatographic techniques are often insufficient for the positive identification of components in a multicomponent mixture. Obtaining both retention index and spectrometric data by capillary gas chromatography–mass spectrometry (CGC–MS) has greatly improved the identification of unknown individual components in complex hydrocarbon mixtures[8]. The most widely used technique, CGC–MS with electron-impact (EI) ionization, can unambiguously detect alkylbenzenes in hydrocarbon mixtures[9–12]. However, because of some drawbacks with this technique in the differentiation of structural isomers, the lack of standard materials and the low precision of calculation methods for predicting retention data[6], structure–retention correlations based on precise measurements for alkylbenzenes of lower molecular weight may be justified for the identification of alkylbenzenes of higher molecular weight[13].

The GC retention parameters of hydrocarbons are usually determined in particular by intermolecular van der Waals forces, specifically by dispersion forces if the separation occurs in a column containing a non-polar liquid stationary phase. The retention index value is determined by the structural characteristics of the compounds analyzed, by the type and position of the functional groups, the position of the double bond and by steric effects[14–24]. The dependence of the retention behaviour of alkylbenzenes on their molecular structure has been studied for various stationary phases: non-polar, squalane[24–30], OV-101[3,30,31], SE-30[6]; slightly polar, UCON LB-550[28,32], UCON HP-250[28], Citroflex A-4[25–27]; polar, Carbowax 20M[28,32], 6000[33], 400[33,34], TCEP[25–27]. Physico-chemical properties and structural parameters were also utilized for the calculation and prediction of retention indices of alkylbenzenes[35–38].

The aim of the present paper was to increase the number of published retention indices of alkylbenzenes with carbon atom numbers greater than ten on the non-polar silicone stationary phase OV-101 and to broaden the knowledge of retention behaviour of alkylbenzenes in connection with their molecular structure. Owing to the lack of standard higher alkylbenzenes, mixed samples were prepared by alkylation reactions of benzene or alkylbenzenes using alkyl halogenides described previously (Part I)[39]. The characterization of the alkylbenzenes with carbon atom numbers > 10 and without published retention indices was performed on the basis of GC–MS results, correlation between retention data and molecular structure and by application of quantum chemistry methods for studying the stability of isomers formed during synthesis and for interpretation of retention data of alkylbenzenes.

Alkylbenzenes were identified in 25 synthesized mixed samples prepared by various Friedel-Crafts alkylation reactions described in our previous paper[39] using glass capillary columns (50 m × 0.25 mm I.D.) statically coated with the stationary phase OV-101.

EXPERIMENTAL

GC measurements were performed on a Carlo Erba gas chromatograph (Model 2350, Milan, Italy) equipped with a flame ionization detector and a stream splitter, using nitrogen as the carrier gas at a linear velocity of about 10 cm/s under isothermal conditions at 100 and 120°C. Methane was used for the determination of the gas hold-up time. The elution time was measured with a digital stop-watch Time calculator RM 4111 (Tesla Rožnov, Czechoslovakia).

GC–MS measurements with EI ionization were performed using an HP 5995 instrument under temperature-programmed conditions (initial temperature 80°C, increased at 1°C/min, final temperature 190°C with the isothermal experiment) in an HP column Ultra 2 (50 m × 0.2 mm I.D.) with the chemically bonded phase SE-54. Helium was used as the carrier gas.

RESULTS AND DISCUSSION

Samples of alkylbenzenes obtained by Friedel-Crafts alkylation reactions with the aim of preparing C_{12} alkylbenzenes with two or more small alkyl substituents in the benzene ring comprised multicomponent mixtures due to the formation of C_{14} and C_{15} alkylbenzenes and as the result of isomerization, disproportionation and transalkylation reactions[39]. All the components of 25 samples were characterized by their retention indices at 100°C and their temperature coefficients, dI/dT, measured on OV-101 capillary columns with a film thickness of 0.35 μm which should be sufficient for the measurement of reproducible retention data[40]. The efficiency of the columns used was N_e = 127 866 for k = 5. The separation of several isomers did not improve significantly when using a more efficient system (N_e = 395 720, k = 4.4).

After GC–MS analysis in EI ionization mode, from collected mass spectra it was possible to determine the molecular weights of individual alkylbenzenes (from the molecular ions), the type and number of alkyl groups[2]. In several cases, however, when the concentration of the solute analyzed was small and therefore the quality of the spectra acquired was low, it was not possible to determine the type and number of alkyls in the ring, only the number of carbon atoms. For alkylbenzenes with carbon numbers > 10, for which there are no literature retention and mass spectral data, the most probable structures were proposed by interpretation of the mass spectra acquired (according to the characteristic fragment ions), however without determination of the positions of the alkyl substituents.

The assignment of the final structure (position of substituents) of alkylbenzenes was based mainly on structure–retention correlations. First we used the dependences of the retention indices, I, selective indices, I^* (ref. 41) and homeomorph factors, H (refs. 15–17) on the number of carbon atoms (nC) of the alkylbenzenes arranged in homologous series[42]. The dependences of I on nC were linear for series with narrow (straight) alkyl substituents (see Fig. 1), and for in all other series studied the correlation coefficients of the dependences were very close to 1 as the scale on the y axis (700–1500 i.u.) was significantly different compared to the scale on the x axis (nC = 7–15). The precision of these dependences for the assignment of structure to the given alkylbenzenes is not sufficient. The largest differences between the measured retention indices and those calculated by linear regression were found for *n*-propyl-

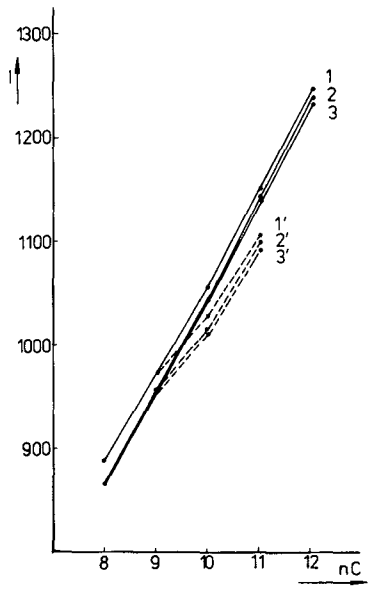

Fig. 1. The dependence of Kováts indices, I, on the number of carbon atoms (nC) for homologous series 1–3 and 1'–3'. Series: (1) 1,2-DiMeB, 1-Me-2-EtB, 1-Me-2-*n*-PrB, 1-Me-2-*n*-BuB, 1-Me-2-*n*-PeB; (2) 1,4-DiMeB, 1-Me-4-EtB, 1-Me-4-*n*-PrB, 1-Me-4-*n*-BuB, 1-Me-4-*n*-PeB; (3) 1,3-DiMeB, 1-Me-3-EtB, 1-Me-3-*n*-PrB, 1-Me-3-*n*-BuB, 1-Me-3-*n*-PeB; (1') 1,2-DiMeB, 1-Me-2-EtB, 1-Me-2-*iso*-PrB, 1-Me-2-*sec*.-BuB; (2') 1,4-DiMeB, 1-Me-4-EtB, 1-Me-4-*iso*-PrB, 1-Me-4-*sec*.-BuB; (3') 1,3-DiMeB, 1-Me-3-EtB, 1-Me-3-*iso*-PrB, 1-Me-3-*sec*.-BuB. See Table I for abbreviations.

benzene (about 5 i.u.) which is connected with the so-called propyl effect[25–27]. The measured and calculated retention indices for some homologous series are given in Table I.

For a particular solute the retention behaviour is determined by the magnitude of the intermolecular forces involved in its interaction with the stationary phase. With *n*-alkanes these forces are exclusively dispersion forces which are additive and increase with molecular weight. As heteroatoms and multiple bonds are introduced into a molecule, polar forces contribute increasingly to the overall retention. The retention behaviour of any solute is dependent upon its size, shape and functionality. The homeomorph factors, H, and selective indices, I^*, reflect the combined effects of molecular shape and functionality the values of which are closely related to molecular structure[15–17,28,41]. According to definition, they are calculated from

$$H = I - I_n(\text{alkane}) \tag{1}$$

where I = measured retention index of an analyte and I_n(alkane) = index of *n*-alkane having the same carbon skeleton as that of the analyte, and

$$I^* = I - I_M \tag{2}$$

where I_M = the retention index of an hypothetical *n*-alkane having the same molecular weight as that of the analyte and defined by the expression $I_M = (M - 2.016)/$

TABLE I

MEASURED, y, AND LINEAR REGRESSION CALCULATED, Y, RETENTION INDICES FOR THREE HOMOLOGOUS SERIES FROM THE EQUATION

$y = a + bx$, where x = nC. $L_{1,2}$ = Confidence intervals. B = Benzene; Me = methyl; Et = ethyl; Pr = propyl; Bu = butyl; Pe = pentyl.

Homologous series	*Substance*	x	y	Y	L_1	L_2
1	1,2-DiMeB	8	888.8	884.2	870.3	898.1
	1-Me-2-EtB	9	973.2	974.2	964.4	984.0
	1-Me-2-*n*-PrB	10	1057.0	1064.2	1056.2	1072.2
	1-Me-2-*n*-BuB	11	1153.3	1154.2	1144.4	1164.0
	1-Me-2-*n*-PeB	12	1248.7	1244.2	1230.3	1258.1
	$y = 164.3 + 89.99x$; $r = 0.99941$; $s_{y,x} = 5.63$					
2	1,4-DiMeB	8	865.8	863.1	853.7	872.5
	1-Me-4-EtB	9	957.1	957.1	950.5	963.7
	1-Me-4-*n*-PrB	10	1045.6	1051.1	1045.7	1056.5
	1-Me-4-*n*-BuB	11	1145.5	1145.1	1138.6	1151.7
	1-Me-4-*n*-PeB	12	1241.5	1239.1	1229.7	1248.5
	$y = 111.3 + 93.98x$; $r = 0.99975$; $s_{y,x} = 3.81$					
3	1,3-DiMeB	8	865.8	862.8	852.9	872.7
	1-Me-3-EtB	9	954.8	955.2	948.2	962.2
	1-Me-3-*n*-PrB	10	1041.9	1047.5	1041.8	1053.2
	1-Me-3-*n*-BuB	11	1140.1	1139.9	1132.9	1146.9
	1-Me-3-*n*-PeB	12	1235.1	1232.4	1222.5	1242.3
	$y = 123.64 + 92.39x$; $r = 0.9997$; $s_{y,x} = 4.03$					

0.14026. With alkylbenzenes, extension of the π-electron system increases selectivity on an apolar phase. In the case of alkyl substitution, the values of H and I^* appear to be dependent upon the nature and position of the substituent groups. For the individual homologous series of alkylbenzenes (1–3) studied, characteristic dependences were obtained for both these parameters. The courses of the dependences were similar (Figs. 2 and 3).

For the identification of individual alkylbenzenes with nC > 10, homeomorph factors were utilized. Alkylbenzenes with narrow or branched substituents were arranged into homologous series, and from the measured retention data the homeomorph factors were calculated. The characteristic dependences of H on nC were used for assignment of the positions of the alkyl substituents in isomers of all C_{11} and many C_{12} alkylbenzenes studied and of some higher alkylbenzenes. Examples of the dependences of H on nC for several homologous series are given in Figs. 3–5. In series of alkylbenzenes with increasing numbers of methyl groups in the benzene ring the homeomorph factors increase with increasing number of carbon atoms, Fig. 4 (homologous series 4–8). In alkylbenzenes with increasing alkyl chain length, in homologous series the homeomorph factor decreases and is approximately constant (Figs. 3 and 5). When the homologous series starts with a relatively high number of carbon atoms (10) it was not possible to propose a structure for C_{11}, C_{12} or higher alkylben-

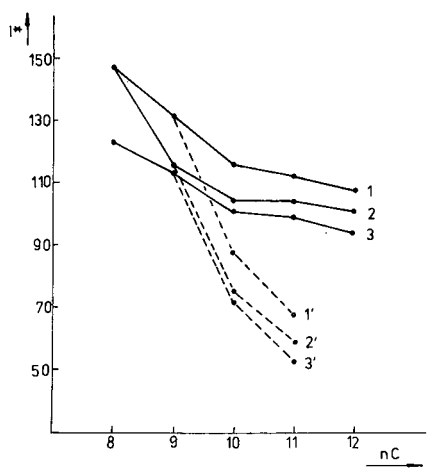

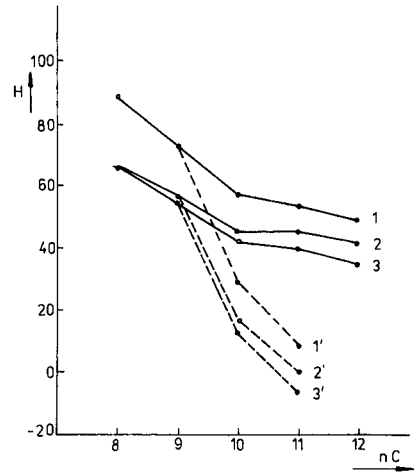

Fig. 2. The dependence of selectivity indices, I^*, on nC for homologous series 1–3 and 1′–3′ (the same as in Fig. 1).

Fig. 3. The dependence of homeomorph factors, H, on nC for homologous series 1–3 and 1′–3′ (the same as in Fig. 1).

zenes. Instead the structures of some isomers of C_{11}, C_{12} alkylbenzenes were assigned by application of a quantum chemistry method for compound identification by studying the stability of the isomers and the probability of their formation during synthesis[43]. Quantum chemistry was further used for the interpretation of retention data of alkylbenzenes with the aim of finding and interpreting relationships between reten-

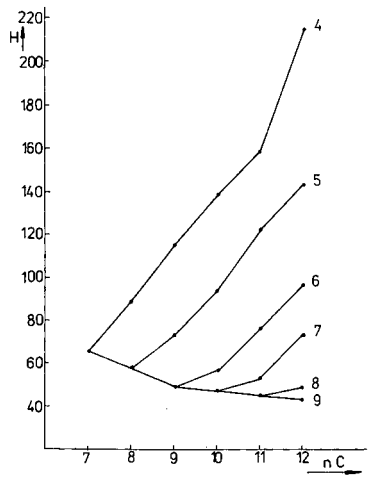

Fig. 4. The dependence of homeomorph factors, H, on nC for homologous series 4–9. Series: (4) MeB, 1,2-DiMeB, 1,2,3-TriMeB, 1,2,3,4-TetraMeB, 1,2,3,4,5-PeMeB, 1,2,3,4,5,6-HeMeB; (5) EtB, 1-Me-2-EtB, 1,2-DiMe-3-EtB, 1,2,3-TriMe-4-EtB, 1,2,3,4-TetraMe-5-EtB; (6) *n*-PrB, 1-Me-2-*n*-PrB, 1,2-DiMe-3-*n*-PrB, 1,2,3-TriMe-4-*n*-PrB; (7) *n*-BuB, 1-Me-2-*n*-BuB, 1,2-DiMe-3-*n*-BuB; (8) *n*-PeB, 1-Me-2-*n*-PeB; (9) MeB, EtB, *n*-PrB, *n*-BuB, *n*-PeB, *n*-HeB.

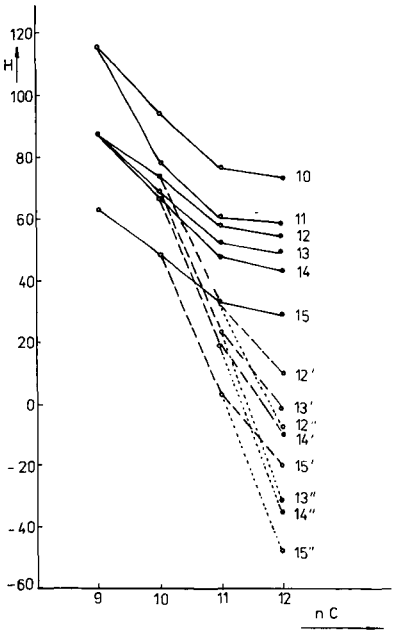

Fig. 5. The dependence of homeomorph factors, H, on nC for homologous series 10–15, 12′–15′ and 12″–15″. Series: (10) 1,2,3-TriMeB, 1,2-DiMe-3-EtB, 1,2-DiMe-3-*n*-PrB, 1,2-DiMe-3-*n*-BuB; (11) 1,2,3-TriMeB, 1,3-DiMe-2-EtB, 1,3-DiMe-2-*n*-PrB, 1,3-DiMe-2-*n*-BuB; (12) 1,2,4-TriMeB, 1,2-DiMe-4-EtB, 1,2-DiMe-4-*n*-PrB, 1,2-DiMe-4-*n*-BuB; (13) 1,3,4-TriMeB, 1,3-DiMe-4-EtB, 1,3-DiMe-4-*n*-PrB, 1,3-DiMe-4-*n*-BuB; (14) 1,2,4-TriMeB, 1,4-DiMe-2-EtB, 1,4-DiMe-2-*n*-PrB, 1,4-DiMe-2-*n*-BuB; (15) 1,3,5-TriMeB, 1,3-DiMe-5-EtB, 1,3-DiMe-5-*n*-PrB, 1,3-DiMe-5-*n*-BuB; (12′) 1,2,4-TriMeB, 1,2-DiMe-4-EtB, 1,2-DiMe-4-*iso*-PrB, 1,2-DiMe-4-*sec*.-BuB; (13′) 1,3,4-TriMeB, 1,3-DiMe-4-EtB, 1,3-DiMe-4-*iso*-PrB, 1,3-DiMe-4-*sec*.-BuB; (14′) 1,2,4-TriMeB, 1,4-DiMe-2-EtB, 1,4-DiMe-2-*iso*-PrB, 1,4-DiMe-2-*sec*.-BuB; (15′) 1,3,5-TriMeB, 1,3-DiMe-5-EtB, 1,3-DiMe-5-*iso*-PrB, 1,3-DiMe-5-*sec*.-BuB; (12″) 1,2,4-TriMeB, 1,2-DiMe-4-EtB, 1,2-DiMe-4-*iso*-PrB, 1,2-DiMe-4-*tert*.-BuB; (13″) 1,3,4-TriMeB, 1,3-DiMe-4-EtB, 1,3-DiMe-4-*iso*-PrB, 1,3-DiMe-4-*tert*.-BuB; (14″) 1,2,4-TriMeB, 1,4-DiMe-2-EtB, 1,4-DiMe-2-*iso*-PrB, 1,4-DiMe-2-*tert*.-BuB; (15″) 1,3,5-TriMeB, 1,3-DiMe-5-EtB, 1,3-DiMe-5-*iso*-PrB, 1,3-DiMe-5-*tert*.-BuB.

tion indices and calculated interaction energies (between partitioned substances and the stationary phase) and to use the obtained correlation equations for the prediction of retention data. Alkylbenzenes (C_{11}, C_{12}) with defined structure, their retention indices, I, and temperature coefficients, dI/dT, on OV-101 are given in Table II. Also included are data for alkylbenzenes with nC $\leqslant$ 10 for interlaboratory comparison of retention data of alkylbenzenes of lower molecular weight.

The regularities in the chromatographic retention of alkylbenzenes on the poly(dimethyl silicone) stationary phase OV-101 were studied and explained by Gerasimenko and Nabivach[3]. The differences in retention indices of aromatic hydrocarbons between OV-101 and squalane are 10–12 i.u. and higher. The order of elution of alkylbenzenes corresponds to their boiling points; the dependence of the Kováts retention indices of lower alkylbenzenes on their boiling points is given in Fig. 6. Aromatic compounds possess systems of delocalized π-electrons which are capable of electron pair donor–acceptor interactions. Alkyl substituents as strong σ-donors evoke deformation of the electronic state of the benzene ring and therefore influence

TABLE II

RETENTION INDICES, *I*, OF ALKYLBENZENES ON OV-101 STATIONARY PHASE AT 100°C AND THEIR TEMPERATURE COEFFICIENTS, d*I*/d*T*

Compound	*I*	*dI/dT*	*Compound*	*I*	*dI/dT*
C_{7-10}					
MeB	765.5	0.260	1-Me-2-*iso*-PrB	1029.1	0.292
EtB	857.7	0.245	1-Me-3-*n*-PrB	1041.9	0.272
1,3-DiMeB	865.8	0.245	1,3-DiEtB	1039.5	0.244
1,4-DiMeB	865.8	0.250	1-Me-4-*n*-PrB	1045.6	0.280
1,2-DiMeB	888.8	0.290	*n*-BuB	1047.4	0.270
iso-PrB	919.5	0.275	1,4-DiEtB	1046.0	0.265
n-PrB	949.3	0.265	1,3-DiMe-5-EtB	1048.4	0.240
1-Me-3-EtB	954.8	0.246	1,2-DiEtB	1051.4	0.310
1-Me-4-EtB	957.1	0.254	1-Me-2-*n*-PrB	1057.0	0.334
1,3,5-TriMeB	963.0	0.240	1,4-DiMe-2-EtB	1067.2	0.300
1-Me-2-EtB	973.2	0.305	1,3-DiMe-4-EtB	1069.0	0.310
1,2,4-TriMeB	987.3	0.310	1,2-DiMe-4-EtB	1074.3	0.318
tert.-BuB	986.8	0.310	1,3-DiMe-2-EtB	1078.5	0.330
sec.-BuB	1005.2	0.310	1,2-DiMe-3-EtB	1094.1	0.360
1-Me-3-*iso*-PrB	1012.7	0.235	1,2,4,5-TetraMeB	1106.0	0.347
1,2,3-TriMeB	1015.5	0.370	1,2,3,5-TetraMeB	1109.3	0.375
1-Me-4-*iso*-PrB	1016.5	0.263	1,2,3,4-TetraMeB	1139.0	0.440
C_{11}					
1-Et-3-*iso*-PrB	1092.5	0.230	1,4-DiMe-2-*n*-PrB	1147.5	0.297
1-Me-3-*sec.*-BuB	1093.5	0.281	1,3-DiEt-4-MeB	1149.1	0.305
1-Et-2-*iso*-PrB	1098.2	0.314	1,3-DiMe-4-*n*-PrB	1152.1	0.302
1-Me-4-*sec.*-BuB	1100.0	0.282	1-Me-2-*n*-BuB	1153.3	0.328
1-Et-4-*iso*-PrB	1103.5	0.260	1,2-DiEt-4-MeB	1154.2	0.315
1,3-DiMe-5-*iso*-PrB	1102.8	0.214	1,3-DiEt-2-MeB	1156.9	0.370
1-Me-2-*sec.*-BuB	1108.7	0.341	1,2-DiMe-4-*n*-PrB	1157.9	–
1,4-DiMe-2-*iso*-PrB	1118.7	0.252	1,3-DiMe-2-*n*-PrB	1160.5	0.303
1,3-DiMe-4-*iso*-PrB	1123.4	0.276	1,2-DiEt-3-MeB	1170.3	–
1-Et-3-*n*-PrB	1124.1	0.258	1,2,4-TriMe-5-EtB	1173.0	0.315
1,3-DiEt-5-MeB	1129.8	0.240	1,2-DiMe-3-*n*-PrB	1176.5	0.371
1,2-DiMe-4-*iso*-PrB	1130.4	0.287	1,3,5-TriMe-2-EtB	1182.8	0.324
1,3-DiMe-5-*n*-PrB	1132.6	0.235	1,2,5-TriMe-3-EtB	1184.3	0.329
1-Et-2-*n*-PrB	1133.5	0.284	1,2,3-TriMe-5-EtB	1193.2	0.340
1-Me-3-*n*-BuB	1140.1	0.249	1,2,4-TriMe-3-EtB	1215.1	0.431
1,4-DiEt-2-MeB	1143.7	0.300	PentaMeB	1259.9	0.435
1-Me-4-*n*-BuB	1145.5	0.280	1,2,3-TriMe-4-EtB	1222.4	–
C_{12}					
1-*iso*-Pr-2-*n*-PrB	1179.8	0.275	1-Me-2-*n*-PeB	1248.7	0.310
1-Et-4-*sec.*-BuB	1184.6	0.310	1,3-DiMe-4-*n*-BuB	1248.8	0.280
1-*iso*-Pr-4-*n*-PrB	1190.1	0.268	1,2,4-TriMe-5-*n*-PrB	1251.7	0.340
1,4-DiMe-2-*sec.*-BuB	1190.6	0.260	1,2-DiMe-4-*n*-BuB	1254.0	–
1,2-DiMe-4-*tert.*-BuB	1192.4	0.310	1,3-DiMe-2-*n*-BuB	1258.3	0.293
1,3-DiMe-4-*sec.*-BuB	1198.4	0.312	1,3,5-TriMe-2-*n*-PrB	1263.2	0.346
1,3,5-TriEtB	1206.2	0.118	1,2-DiMe-3-*n*-BuB	1273.6	0.311
1,3-Di-*n*-PrB	1209.2	0.260	1,2,5-TriMe-3-*n*-PrB	1276.6	0.354
1,2-DiMe-4-*sec.*-BuB	1209.7	0.285	1,2,3-TriMe-5-*n*-PrB	1278.8	0.397
1,4-Di-*n*-PrB	1220.6	0.297	1,2,3-TriMe-4-*n*-PrB	1297.0	0.422

TABLE II (*continued*)

Compound	*I*	*dI/dT*	*Compound*	*I*	*dI/dT*
1-Et-3-*n*-BuB	1220.6	0.250	1,2,3,4-TetraMe-5-EtB	1344.2	–
1,3-Di-*iso*-PrB	1140.8	0.208	1,2,4-TriEtB	1222.7	0.294
1,2-Di-*iso*-PrB	1150.2	0.255	1,3-DiMe-5-*n*-BuB	1229.1	0.208
1,3-DiMe-5-*tert.*-BuB	1151.9	0.230	1-Et-4-*n*-BuB	1231.9	0.302
1,4-Di-*iso*-PrB	1159.6	0.248	1,2,4-TriMe-5-*iso*-PrB	1232.7	0.250
1,4-DiMe-2-*tert.*-BuB	1164.4	0.180	1-Me-3-*n*-PeB	1235.1	0.245
1,3-DiMe-4-*tert.*-BuB	1168.3	0.280	1,3,5-TriMe-2-*iso*-PrB	1238.5	0.265
1-Et-3-*sec.*-BuB	1170.5	0.272	1-Me-4-*n*-PeB	1241.5	0.267
1-*iso*-Pr-3-*n*-PrB	1175.7	0.238	1,4-DiMe-2-*n*-BuB	1243.2	0.257
1-Et-2-*sec.*-BuB	1177.5	–	1,2,3-TriEtB	1245.7	0.310
1,3-DiMe-5-*sec.*-BuB	1179.4	0.227	1,2,3-TriMe-5-*iso*-PrB	1245.5	0.295

the mutual interactions with the molecules of the stationary phase. According to the literature and our results, the following conclusions can be drawn about the retention of alkylbenzenes on OV-101.

(1) For monoalkylbenzenes the retention indices increase with increasing alkyl chain length. Substitution of the benzene ring by a methyl group results in an increase in retention indices of greater than 100 i.u. compared to benzene owing to increased solute–stationary phase interaction. For C_8, C_9 alkylbenzenes the increment I_{CH_2} decreases and is lower than 100 i.u. For *n*-propylbenzene a considerable decrease in retention index is connected with the propyl effect[25–27,44]. For C_{10} and higher alkyl-

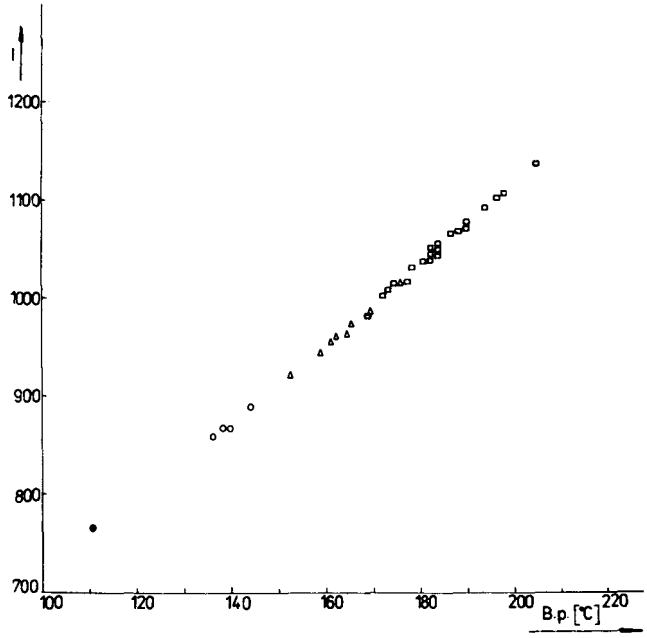

Fig. 6. The dependence of Kováts indices, *I*, on the boiling points for C_7 (●), C_8 (○), C_9 (△) and C_{10} (□) alkylbenzenes.

benzenes the sorption process is dominated by the alkyl substituent and therefore the value of I_{CH_2} approximates to 100 i.u. With branched substituents there is a decrease in retention compared to straight chain ones, the order of elution being *tert.*- < *iso*- < *sec.*- < *n*-alkyl. The temperature coefficients, dI/dT, slightly increase with increasing alkyl chain length, and are higher for branched substituents.

(2) For dialkylbenzenes the elution order corresponds to two groups of isomers. In the first group there are alkylbenzenes with one methyl substituent (dimethyl, methyl-ethyl, methyl-isopropyl, methyl-*n*-propyl, methyl-*sec.*-butyl, methyl-*n*-butyl, methyl-*n*-pentyl) and diethylbenzenes with the elution order of 1,3 < 1,4 < 1,2. The second group comprises alkylbenzenes with both alkyl substituents having nC > 1 (ethyl-isopropyl, ethyl-*n*-propyl, ethyl-*sec.*-butyl, ethyl-*n*-butyl, diisopropyl, isopropyl-*n*-propyl, di-*n*-propyl) with the elution order 1,3 < 1,2 < 1,4. These elution orders of the alkylbenzene isomers was explained by the change in electron density of the delocalized π-orbitals of the hydrocarbons studied upon substitution by the two alkyl groups[3]. On increasing the size of an alkylbenzene molecule by addition of a methyl group the increment I_{CH_2} is higher than 100 i.u., but on prolonging the alkyl chain length to C_5 the value of I_{CH_2} is lower than 100. For dialkylbenzene isomers, I_{CH_2} increases in the order of 1,3 < 1,4 < 1,2 when the substituent is methyl. Temperature coefficients of dialkylbenzene positional isomers with one methyl substituent and diethylbenzene increase in the order 1,3 < 1,4 < 1,2.

(3) For polyalkylbenzenes the number of possible isomers depends on the number and type of alkyl groups present in the benzene ring. As a general rule, among positional isomers, the most symmetrical molecules are eluted first; high retention is observed for molecules with adjacent substituents, the highest being for polymethylbenzenes with *ortho* methyl groups. In trialkylbenzenes with only one kind of substituents the order of elution of the three possible isomers is 1,3,5 < 1,2,4 < 1,2,3; the temperature coefficients increase in the same order, the highest values being found for trimethylbenzenes. Increase in the alkyl chain length results in decreasing I_{CH_2} and dI/dT values. For trialkylbenzenes with two different substituents, the order of elution of the six possible isomers is 1,3-5 < 1,4-2 < 1,3-4 < 1,2-4 < 1,3-2 < 1,2-3; the dI/dT values of these isomers increase in the same sequence.

For tetramethylbenzenes the retention indices increase in the order 1,2,4,5 < 1,2,3,5 < 1,2,3,4. Generally polymethylbenzenes have relatively high dI/dT values compared with other isomeric alkylbenzenes, the highest being those with the most methyl groups in *ortho* position. By prolonging one methyl group there is a slight decrease in the value of I_{CH_2}, dependent on its position. The retention of the six isomers increases in the order 1,2,4-5 < 1,3,5-2 < 1,2,5-3 < 1,2,3-5 < 1,3,4-2 < 1,2,3-4. The I_{CH_2} and dI/dT values of trimethylalkylbenzenes also increase in this order.

REFERENCES

1 B. Kumar, R. K. Kuchhal, P. Kumar and P. L. Gupta, *J. Chromatogr. Sci.*, 24 (1986) 99.
2 E. Matisová, *J. Chromatogr.*, 438 (1988) 131.
3 V. A. Gerasimenko and V. M. Nabivach, *Zh. Anal. Khim.*, 37 (1982) 110.
4 J. A. Lubeck and D. L. Sutton, *J. High Resolut. Chromatogr. Chromatogr. Commun.*, 6 (1983) 328.
5 W. Engewald, I. Topalova, N. Petsev and Chr. Dimitrov, *Chromatographia*, 23 (1987) 561.
6 V. Švob and D. Deur-Šiftar, *J. Chromatogr.*, 91 (1974) 677.

7 T. Tóth, *J. Chromatogr.*, 279 (1983) 157.
8 I. M. Whittemore, in K. H. Altgelt and T. H. Gouw (Editors), *Chromatography in Petroleum Analysis*, Marcel Dekker, New York, 1979, pp. 50–70.
9 S. Zadro, J. K. Haken and W. V. Pinczewski, *J. Chromatogr.*, 323 (1985) 305.
10 E. S. Gallegos, I. M. Whittemore and R. F. Klaver, *Anal. Chem.*, 46 (1974) 157.
11 L. V. S. Hood and C. M. Erikson, *J. High Resolut. Chromatogr. Chromatogr. Commun.*, 3 (1980) 516.
12 W. Bertsch, E. Anderson and G. Holzer, *J. Chromatogr.*, 126 (1976) 213.
13 J. Soják and J. A. Rijks, *J. Chromatogr.*, 119 (1976) 505.
14 A. Wehrli and E. Kovats, *Helv. Chim. Acta*, 42 (1959) 2709.
15 G. Schomburg, *J. Chromatogr.*, 14 (1964) 157.
16 G. Schomburg, *J. Chromatogr.*, 23 (1966) 1.
17 G. Schomburg, *J. Chromatogr.*, 23 (1966) 118.
18 G. Schomburg, *Anal. Chim. Acta*, 38 (1967) 45.
19 D. A. Tourres, *J. Chromatogr.*, 30 (1967) 357.
20 R. A. Hively and R. E. Hinton, *J. Gas Chromatogr.*, 6 (1968) 203.
21 M. B. Evans, *Chromatographia*, 2 (1969) 397.
22 L. S. Ettre, *Chromatographia*, 7 (1974) 39.
23 F. Vernon, W. E. Sharples and T. W. Kyffin, *J. Chromatogr.*, 111 (1975) 117.
24 S. Rang, K. Kuningas, A. Orov and O. Eisen, *J. Chromatogr.*, 128 (1976) 59.
25 L. Soják, J. Janák and J. A. Rijks, *J. Chromatogr.*, 135 (1977) 71.
26 L. Soják, J. Janák and J. A. Rijks, *J. Chromatogr.*, 138 (1977) 119.
27 L. Soják, J. Janák and J. A. Rijks, *J. Chromatogr.*, 142 (1977) 177.
28 W. Engewald and L. Wennrich, *Chromatographia*, 9 (1976) 540.
29 J. Macák, V. Nabivach, P. Buryan and S. Šindler, *J. Chromatogr.*, 234 (1982) 285.
30 V. M. Nabivach, P. Buryan and J. Macák, *Vopr. Khim. Khim. Tekhnol.*, 53 (1978) 64.
31 Jie Wu and Wanzhen Lu, *Sepu*, 1 (1984) 11; *C.A.*, 103 (1985) 24585r.
32 C. E. Döring, D. Estel and R. Fischer, *J. Prakt. Chem.*, 316 (1974) 1.
33 J. Krupčík, O. Liška and L. Soják, *J. Chromatogr.*, 51 (1970) 119.
34 L. Soják and J. Hrivnák, *Ropa Uhlie*, 11 (1969) 361.
35 J. Bermejo, J. J. Canga and O. M. Gayol, *Int. J. Environ. Anal. Chem.*, 11 (1982) 271.
36 J. Bermejo and M. D. Guillén, *Chromatographia*, 17 (1983) 664.
37 J. Bermejo, J. J. Canga, O. M. Gayol and M. D. Guillén, *J. Chromatogr. Sci.*, 22 (1984) 252.
38 Fuan Wang, *Sepu*, 4 (1986) 258; *C.A.*, 105 (1986) 218094s.
39 E. Matisová, M. Rukriglová, J. Krupčík, E. Kovačičová and Š. Holotík, *J. Chromatogr.*, 455 (1988) 301.
40 E. Matisová, J. Krupčík and J. Garaj, *Chromatographia*, 16 (1982) 169.
41 M. B. Evans, J. K. Haken and T. Tóth, *J. Chromatogr.*, 351 (1986) 155.
42 E. Matisová, J. Krupčík, J. Garaj, P. Čellár and E. Kolek, *Abstracts, 16th International Symposium on Chromatography, Groupement pour l'Avancement des Méthodes Spectroscopiques et Physicochimiques d'Analyse, Paris, September 21–26, 1986*, p. 53.
43 E. Matisová, S. Miertuš, V. Jakuš, E. Kovačičová and Pham Thi Ha, *Abstracts, 17th International Symposium on Chromatography, Vienna, September 25–30*, 1988, Poster Session II, p. 155 (p. II P 155).
44 L. Soják, I. Ostrovský and J. Janák, *J. Chromatogr.*, 406 (1987) 43.

Journal of Chromatography, 475 (1989) 125–134
Elsevier Science Publishers B.V., Amsterdam — Printed in The Netherlands

CHROM. 21 553

ADSORPTION EQUILIBRIUM OF HYDROGEN ISOTOPES ON ALUMINA ADSORBENTS FOR GAS–SOLID CHROMATOGRAPHY

TOSHIHIKO YAMANISHI and HIROSHI KUDO
Japan Atomic Energy Research Institute, Tokai-mura, Ibaraki-ken 319-11 (Japan)
(First received September 1st, 1988; revised manuscript received April 4th, 1989)

SUMMARY

The adsorption equilibrium of an alumina–hydrogen system was studied, in the context of the use of alumina adsorbents for hydrogen isotope separation by gas chromatography. Both the amount of hydrogen adsorbed at low equilibrium pressure and the heat of adsorption observed for an alumina adsorbent dried above 473 K increased due to the appearance of active adsorption sites associated with oxide (O^{2-}) and aluminium (Al^{3+}) ions. The surface of the alumina adsorbent was partially deactivated by coating with $MnCl_2$, but the deactivation effect was lost when the alumina was dried above 473 K, owing to the appearance of active adsorption sites. Chromatographic experiments performed on the alumina adsorbents with and without coating indicated that the separation performance of the column was strongly affected by the adsorption equilibrium of hydrogen isotopes on alumina. The retention time of hydrogen isotopes agreed approximately with the predicted time calculated from the adsorption equilibrium data obtained.

INTRODUCTION

A gas chromatograph is a simple and adequate tool in analytical chemistry of hydrogen isotopes. Six hydrogen isotopes (H_2, H^2H, H^3H, $^2H_2$, $^2H^3H$ and $^3H_2$) are sufficiently separated using alumina as well as molecular sieve adsorbents cooled with liquid nitrogen[1–9]. Recently, increasing interest has been showing this separation method for fuel processing in nuclear fusion reactors. A mixture of deuterium and tritium is used as a fuel of fusion reactors, and the control of the fuel composition and purification of the fuel exhaust are current problems to be solved. Although cryogenic separation of hydrogen isotopes is likely be used in the fuel processing system of fusion reactors, gas chromatography (GC) would be an attractive option in the process control and monitoring.

There is a possibility of applying GC to the enrichment of tritium fuel if a separation column capable of separating large volumes of hydrogen can be developed, *e.g.*, 1 g or 4 dm^3 of tritium gas. In this respect, efforts have been made to develop a rotating column with two-dimensional separation systems[10] and a separation column to be used for fairly large amounts of tritium gas[11].

For separation of hydrogen isotopes by gas–solid chromatography (GSC),

0021-9673/89/$03.50

alumina is a convenient column packing material and is commonly used at liquid nitrogen temperature[1–8]. Although it is practical to maintain the temperature sufficiently low and constant during the separation by immersing the column in liquid nitrogen, we have to use partially deactivated alumina adsorbents because highly activated alumina has too strong adsorbability for hydrogen at liquid nitrogen temperature[1,3–5]. One might use alumina adsorbents at a slightly higher temperature (≈ 100 K), but the temperature control would become difficult. A number of papers have been published on the partial deactivation of alumina adsorbents[2,5–8], and an alumina adsorbent coated with $MnCl_2$ was reported to be an excellent adsorbent for hydrogen isotope separation at liquid nitrogen temperature[12]. In addition, on alumina adsorbents coated with salts, the overlap of *ortho*-hydrogen and hydrogen deuteride bands in chromatograms due to the interconversion of nuclear spin isomers was eliminated[2,3,5,8]. However, detailed knowledge of the fundamental adsorption characteristics of the alumina adsorbents is not yet available, although there are some data on the adsorption equilibrium between alumina catalysts and hydrogen isotopes[13].

Since it is essential to understand the adsorption equilibrium of hydrogen on solid adsorbents in order to design and develop a sophisticated column packing material for separation of hydrogen isotopes by GSC, the present study aims to obtain insight into the adsorption equilibria of H_2 and $^2H_2$ on alumina adsorbents with and without a coating of $MnCl_2$ and to examine further the effect of coating, drying and deactivation of alumina adsorbents used in GC.

EXPERIMENTAL

Alumina adsorbents coated with 19% (w/w) of $MnCl_2$ (60–80 mesh) from Shimadzu (Kyoto, Japan) and the same adsorbents, from which the coating had been removed by washing with HCl were used after heat treatment in a vacuum. The alumina adsorbents were prepared by heating a mixture of activated alumina and $MnCl_2$ at 400 K. Hydrogen (99.99999% pure) and deuterium with 99.7% isotopic purity (99.99% chemical purity) were used after passing through a column packed with molecular sieves 5A cooled with liquid nitrogen. Argon gas (99.999% pure) was used after passing through a column packed with molecular sieves 5A at room temperature.

Thermogravimetry (TG) and differential thermal analysis (DTA) of these alumina adsorbents were carried out with a Seiko SSC/560GH TG–DTA system, the samples being heated in a stream of argon. Hydrogen and argon adsorption isotherms on alumina adsorbents were measured with a conventional volumetric apparatus, shown in Fig. 1, consisting of a gas burette, a constant-temperature bath, pressure gauges and an evacuation system. The volume of the apparatus enclosing the sample was 72 cm^3. The temperature of the sample was kept constant using the low-temperature bath filled with liquid nitrogen or mixtures such as isopentane–nitrogen (113 K), *n*-pentane–nitrogen (142 K), CS_2–N_2 (163 K), toluene–nitrogen (178 K) and solid carbon dioxide–acetone (196 K).

An Yanagimoto G-30 gas chromatograph with a thermal conductivity detector was used to examine the performance characteristics of alumina adsorbents as column packing materials. The stainless-steel column (2 m × 3 mm I.D.) packed with adsorbents was immersed in liquid nitrogen when used for the separation of hydrogen isotopes. Neon (99.99% pure) was used as the carrier gas.

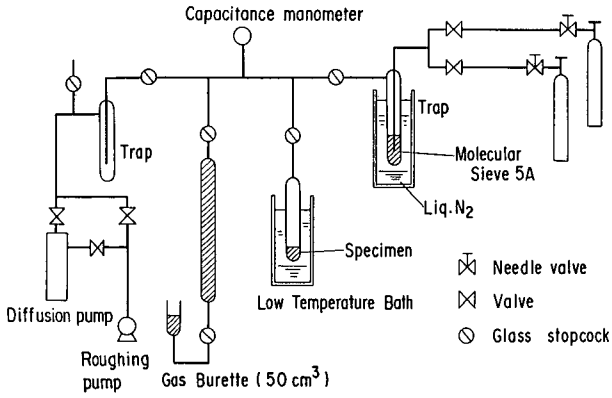

Fig. 1. Schematic diagram of the experimental apparatus.

RESULTS AND DISCUSSION

Effect of heat treatment on adsorption characteristics

The surface area of alumina adsorbents was found to change slightly depending upon the temperature of the heat treatment in a vacuum. Fig. 2 shows the variation of the surface area for the alumina adsorbents without coating, heated for 5 h at a prescribed temperature between 300 and 1100 K. The surface area determined from the BET equation for argon adsorption at liquid nitrogen temperature increased slightly with increasing temperature up to 900 K. It is generally known that alumina adsorbents chemisorb at least a monolayer of water when exposed to moisture at room temperature and that the water forms hydroxyl groups (OH^-) on the surface[14,15]. The hydroxyl groups might be removed by the heat treatment and the decrease in the amount of residual hydroxyl groups depended on the temperature of the heat treatment[14]. The change in the surface area was not attributed to the sintering of the sample but to removal of hydroxyl groups, because no particular signal was observed in the DTA measurement.

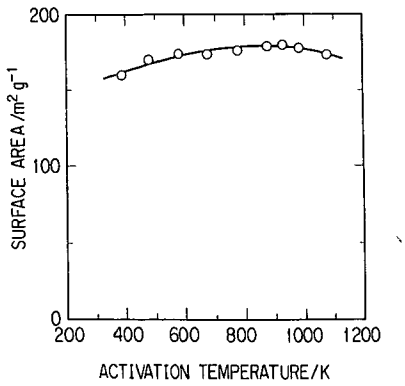

Fig. 2. Change in the surface area of an alumina adsorbent upon heat treatment.

Fig. 3 illustrates the hydrogen adsorption isotherms observed at liquid nitrogen temperature for alumina adsorbents dried at 383, 473 and 773 K. The Freundlich equation is commonly used for adsorption isotherms of gases[13]; however the present results did not obey this. Namely, relationship between the logarithm of the amount of adsorbed hydrogen and that of the equilibrium pressure was not linear. In the present study, therefore, an equation derived by Suwanayuen and Danner[16] based on vacancy solution theory was applied to the adsorption equilibrium data

$$P = [n_1^{s,\infty}/K(1-\theta)]f(\Lambda_{13},\Lambda_{31},\theta) \tag{1}$$

with $\theta = n_1^s/n_1^{s,\infty}$ where P is the pressure of the gas phase, K the Henry law constant, n_1^s the number of moles of component 1 on the surface, $n_1^{s,\infty}$ the maximum number of moles of component 1 on the surface, θ the fractional coverage and Λ_{13} and Λ_{31} the Wilson equation parameters for surface interaction between components 1 and 3 (adsorbent). The four independent parameters, $n_1^{s,\infty}$, K, Λ_{13} and Λ_{31}, were obtained by fitting the isotherm equation to the observed data using a simplex method. The calculated curve, the solid line in Fig. 3, was well superimposed on the experimental values over a wide range of the equilibrium pressure. This indicates that physisorption of hydrogen was dominant on the surface of alumina adsorbents dried below 383 K.

On the other hand, the hydrogen adsorption isotherms observed for alumina adsorbents dried at 473 and 773 K did not necessarily agree with the calculated isotherms in the low equilibrium pressure range (1–100 Pa). The amounts of hydrogen adsorbed in the low equilibrium pressure range were larger than expected from the calculation and increased with drying temperature up to 1073 K. The amounts of

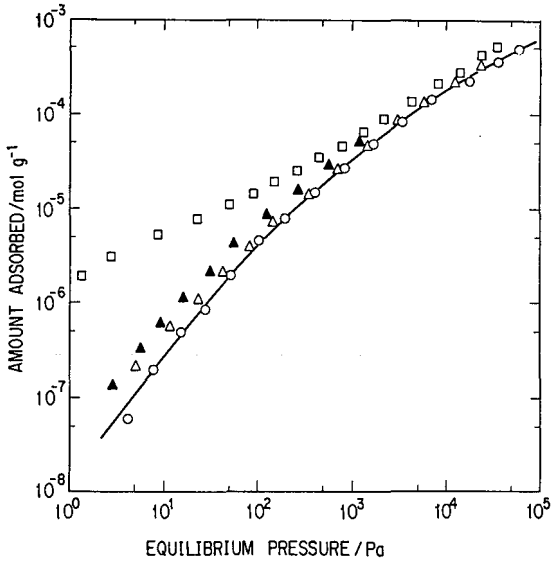

Fig. 3. Adsorption isotherms of H_2 and D_2 on alumina adsorbents: ○, H_2 on alumina dried at 383 K; △, H_2 on alumina dried at 473 K; □, H_2 on alumina adsorbent dried at 773 K; ▲, $^2H_2$ on alumina dried at 473 K. The continuous line is the predicted curve.

deuterium adsorbed on the alumina adsorbents were larger than that of hydrogen. The same tendency was observed for the effect of the drying temperature. A comparison of the adsorption equilibria between H_2 and D_2 is also shown in Fig. 3 for an alumina adsorbent dried at 473 K.

These results suggest that a stronger effect than physisorption is involved in the hydrogen adsorption on alumina adsorbents dried at temperatures above 473 K. Namely, it is implied that the appearance of both oxide (O^{2-}) and aluminium ions (Al^{3+}) on the surface of alumina adsorbents associated with the removal of hydroxyl groups[13] through the heat treatment above 473 K played important roles in the hydrogen adsorption in the low equilibrium pressure range.

The heat of adsorption of hydrogen evaluated from the Clausis–Clapeyron equation at constant volume adsorbed is shown in Fig. 4. The values obtained for alumina adsorbents dried at 773 K were about ten times as large as the latent heat of vaporization (0.9 kJ/mol)[17] and decreased with increasing amount of adsorbed hydrogen. These phenomena were not observed for alumina dried at 383 K. The results also reveal that active adsorption sites for hydrogen (O^{2-} and Al^{3+}) were formed by the removal of hydroxyl groups.

Effect of coating with $MnCl_2$ on adsorption characteristics

Table I shows the amount of hydrogen adsorbed on alumina adsorbents with and without coating. Table II shows the BET surface areas and the parameters of the isotherm equation of Suwanayuen and Danner obtained by fitting the adsorption equilibrium data for hydrogen on the alumina adsorbents with and without coating, dried at 383 K. The BET surface area of the coated alumina adsorbent was the same as that of the alumina adsorbent without coating. However, the latter adsorbed larger amounts of hydrogen when dried at 383 K. In addition, all the values of the parameters in eqn. 1 decreased upon coating; a remarkable difference was observed especially for the Henry law constant, which is a parameter related to the adsorption characteristics at low equilibrium pressure. The heat of adsorption of hydrogen was also measured for the coated alumina adsorbent. The values obtained were smaller than those for the

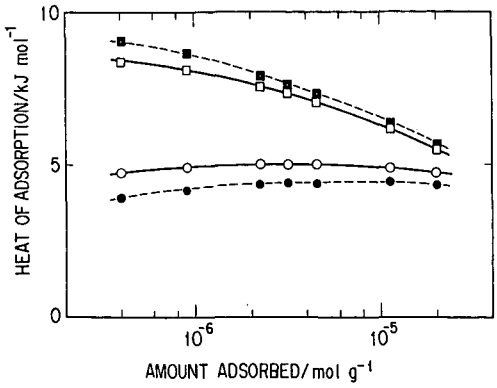

Fig. 4. Effect of the activation temperature and coating by $MnCl_2$ on the heat of adsorption of hydrogen on alumina adsorbents: ○, alumina adsorbent without coating dried at 383 K; ●, adsorbent with coating dried at 383 K; □, adsorbent without coating dried at 773 K; ■, adsorbent with coating dried at 773 K.

TABLE I

AMOUNTS OF HYDROGEN ADSORBED ON ALUMINA ADSORBENTS WITH AND WITHOUT COATING WITH $MnCl_2$

	Drying temperature (K)	*Amount of hydrogen adsorbed (mol/g alumina)*	*Equilibrium pressure (kPa)*
Without coating	383	0.40	0.013
		5.5	0.133
		40	1.33
		190	13.3
With coating	383	0.36	0.013
		3.5	0.133
		26	1.33
		150	13.3
Without coating	473	0.58	0.013
		5.8	0.133
		41	1.33
		220	13.3
With coating	473	0.54	0.013
		5.0	0.133
		35	1.33
		230	13.3

alumina adsorbent without coating when the drying temperature was 383 K as shown in Fig. 4. These results indicate that the adsorption site for hydrogen on the surface of alumina is deactivated by the coating with $MnCl_2$.

As seen in Table I, no apparent difference was observed in the amount of hydrogen adsorbed when the alumina adsorbents were dried at 473 K before measurement. As shown in Fig. 4, the heat of adsorption of hydrogen on the coated alumina adsorbent dried at 773 K was slightly larger than that on the alumina adsorbent without coating. As described in the preceding section, the O^{2-} and Al^{3+} formed by the heat treatment would govern the adsorption behaviour of hydrogen on alumina adsorbents dried above 473 K. Alternatively, the coating with $MnCl_2$ did not inhibit the removal of hydroxyl groups as well as the appearance of the active adsorption sites on the surface when dried above 473 K.

TABLE II

PARAMETERS OF THE ADSORPTION ISOTHERM EQUATION FOR HYDROGEN ON ALUMINA ADSORBENTS WITH AND WITHOUT COATING WITH $MnCl_2$ DRIED AT 383 K

	Without coating	*With coating*
$n_1^{s,\infty}$ (mmol/g alumina)	4.91	3.37
K (mol/g alumina kPa)	23.7	12.6
A_{13}	0.42	0.39
A_{31}	4.4	2.7
Surface area (m^2/g alumina)	161.1	169.1

Chromatographic performance and adsorption characteristics of hydrogen on alumina adsorbents

In a number of reports on chromatographic experiments, two simulation models have been used for the analysis of experimental data: (1) the series-of-stirred-tanks model[9] and (2) the dispersion model[18–20]. Applying these two models, we evaluated parameters for the separation performance such as the retention time.

The series-of-stirred-tanks model gives

$$v = K'V_s(N-1)/t'_R \tag{2}$$

$$t'_R = t_R - (t_R)_{inert} \tag{3}$$

$$(t_R)'_{inert} = (N-1)V_G/v \tag{4}$$

where v is the flow-rate of carrier gas, K' the Henry law constant of the alumina–hydrogen system in a neon carrier, V_s the hold-up of the adsorbent in a stage, N the total number of theoretical stages, t_R the mean residence time of the adsorbate gas, $(t_R)_{inert}$ the mean residence time of inert gas and V_G the hold-up of gas in a stage. From the dispersion model, a set of partial differential equations is derived for chromatograms[18–20]. A moment method[19] was used for modification of these equations because of its simplicity and adequate reliability for the analysis of chromatograms[21] in the present study

$$(t'_R - t_{oi}/2)/(\varepsilon_p/\varepsilon_b - \varepsilon_p) = (\rho_p K'/\varepsilon_p)(z\varepsilon_b/u) \tag{5}$$

$$t'_R = t_R - (t_R)_{inert} \tag{3}$$

$$(t_R)_{inert} = (1 + \varepsilon_p/\varepsilon_b - \varepsilon_p)(z\varepsilon_b/u) \tag{6}$$

where t_{oi} is the time required for injection of adsorbate, ε_p the void fraction of the adsorbent, ε_b the void fraction of the column, z the column length, u the superficial velocity of the carrier gas and ρ_p the apparent particle density of the adsorbent. In the derivation of eqns. 2 and 6, it was assumed that the adsorption isotherm expressed by eqn. 1 could be simplified to a linear relationship at low equilibrium pressure important for the chromatography

$$n_1^s = K'c \tag{7}$$

where c is the molar concentration of adsorbate.

The chromatograms for H_2 and $^2H_2$ on the alumina adsorbents with and without coating were measured at several flow-rates of the carrier gas. Fig. 5 shows an example. It is clear that the chromatographic performance was strongly affected by the adsorption equilibrium between the alumina adsorbents and hydrogen isotopes. The deactivation by the coating with $MnCl_2$ reduced the retention time and sharpened the peak in the chromatogram. Since the peaks in the chromatogram were approximately symmetric, the mean residence time in eqn. 2 and 5 would correspond to the retention time. A plot of v against $V_s(N-1)/t'_R$ shown in Fig. 6 is almost linear as suggested by

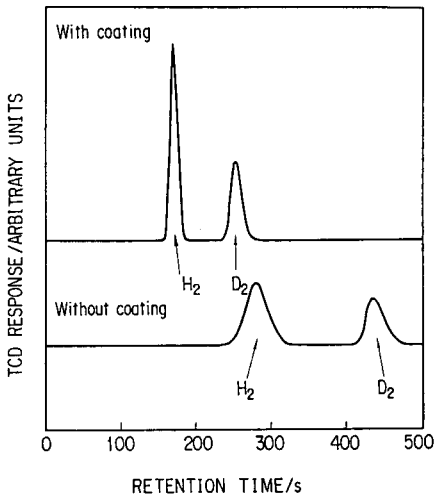

Fig. 5. Typical chromatogram of a mixture of H_2–$^2H_2$ and packing materials: alumina adsorbent and alumina adsorbent coated with $MnCl_2$ dried at 383 K. Packed weight: 11 g. Neon flow-rate: 1.933 cm^3/s. Sample volume: 0.02 cm^3 H_2 + 0.02 cm^3 $^2H_2$.

eqn. 2. Fig. 7 shows chromatographic data for H_2 and D_2 linearized by eqn. 5. Eqns. 2 and 5 seem to be valid for analysis of the chromatogram. The small deviation from the straight lines passing through the origin of the coordinate axes observed in both figures might be due to the error resulting from the assumption of eqn. 7 in which a linear approximation for the adsorption equilibrium was adopted. The degree of this deviation depended on the flow-rate of the carrier gas which affected the equilibrium pressure of adsorbate gas within the column.

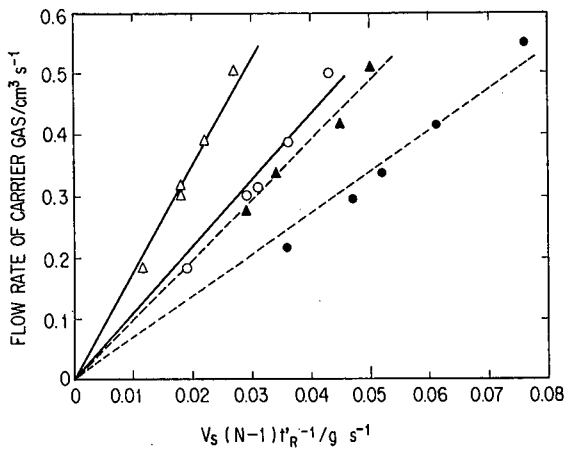

Fig. 6. Plots of the chromatographic parameters for H_2 and $^2H_2$ in the series-of-stirred-tanks model (eqn. 2). Relationship between the carrier gas and the total number of theoretical stages of the column: ○, H_2 on alumina adsorbent without coating; ●, H_2 on adsorbent coated with $MnCl_2$; △, $^2H_2$ on adsorbent without coating; ▲, $^2H_2$ on adsorbent coated with $MnCl_2$.

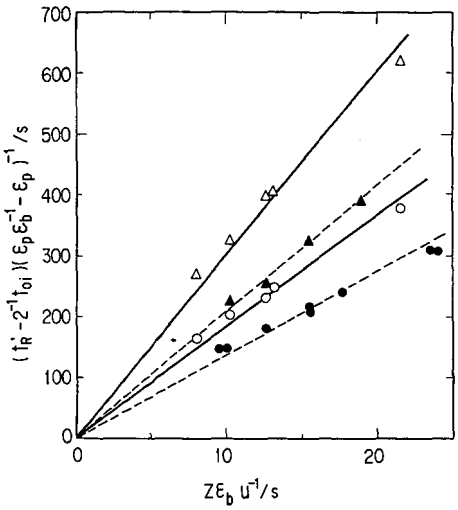

Fig. 7. Chromatographic parameters for H_2 and $^2H_2$ on alumina obtained from the moment method (eqn. 5). Dependence of the retention time on the flow-rate of carrier gas: ○, H_2 on alumina adsorbent without coating; ●, H_2 on adsorbent coated with $MnCl_2$; △, $^2H_2$ on adsorbent without coating; ▲, $^2H_2$ on adsorbent coated with $MnCl_2$.

The retention time can be calculated from eqns. 2 and 5 and the Henry law constants obtained in the present adsorption isotherm measurment. Table III lists the calculated and observed retention times under the analytical conditions used for the chromatograms shown in Fig. 5. No significant difference was observed between the retention times calculated with the series-of-stirred-tanks and dispersion models. The calculated retention time agreed approximately with the observed retention time,

TABLE III
RETENTION TIMES OF H_2 AND $^2H_2$ ON ALUMINA ADSORBENTS DRIED AT 383 K

		Retention time (s)	
		H_2	$^2H_2$
With coating	Experimental observation	171	252
	Calculated value using Henry law constant of adsorption equilibrium		
	Series-of-stirred-tanks model	173	309
	Dispersion model	174	310
Without coating	Experimental observation	276	435
	Calculated value using Henry law constant of adsorption equilibrium		
	Series-of-stirred-tanks model	347	526
	Dispersion model	351	532

although the chromatographic experiments were performed on the alumina adsorbents packed in the stainless-steel column with neon as the carrier gas under conditions different from those used for the adsorption isotherm measurement by the volumetric method.

CONCLUSIONS

Remarkable increases in both the amount of hydrogen adsorbed at low equilibrium pressure and the heat of adsorption observed for alumina dried above 473 K were ascribed to the formation of active adsorption sites due to the appearance of O^{2-} and Al^{3+} on the surface resulting from the removal of hydroxyl groups.

The coating of alumina adsorbents with $MnCl_2$ made the surface deactivated, and it was elucidated that such adsorbents were suitable column packing materials at liquid nitrogen temperature for the separation of hydrogen isotopes by GSC. However, the deactivation effect disappeared with the alumina adsorbent dried above 473 K, since active adsorption sites of O^{2-} and Al^{3+} were formed with drying above 473 K regardless of the coating.

The adsorption equilibrium of the alumina–hydrogen system was a key parameter which determined the chromatographic performance. The present data for the adsorption equilibrium would lead to the selection of optimum conditions for column treatment as well as the design of a new adsorbent for GSC.

ACKNOWLEDGEMENTS

The authors express their sincere thanks to Dr. K. Okuno for his useful discussion and Dr. M. Kinoshita for his assistance in the computer calculation.

REFERENCES

1 H. A. Smith and P. P. Hunt, *J. Phys. Chem.*, 64 (1960) 383.
2 W. R. Moore and H. R. Ward, *J. Phys. Chem.*, 64 (1960) 832.
3 P. P. Hunt and H. A. Smith, *J. Phys. Chem.*, 65 (1961) 87.
4 J. King, Jr., *J. Phys. Chem.*, 67 (1963) 1397.
5 E. H. Carter, Jr. and H. A. Smith, *J. Phys. Chem.*, 67 (1963) 1512.
6 M. Z. Gersh, *Anal. Chem.*, 37 (1965) 1786.
7 C. Genty and R. Schott, *Anal. Chem.*, 42 (1970) 7.
8 P. Urk and L. Linder, *Int. J. Appl. Radiat. Isot.*, 23 (1972) 239.
9 M. L. Conti and M. Lesimple, *J. Chromatogr.*, 29 (1967) 32.
10 M. Fujie, M. Kato and M. Tanase, *J. Appl. Radiat. Isot.*, 38 (1987) 1047.
11 H. Frischmuth, J. Perchermeier, A. Stimmelmayr and H. Weichselgartner, *Fifth Topical Meeting on the Technology of Fusion Energy, April 26–28, Knoxville, 1983,* p. 267.
12 K. Fujita and T. Kwan, *Bunseki Kakagu*, 12 (1963) 15.
13 W. S. Millman, F. H. Van Cauwelart and W. Keith Hall, *J. Phys. Chem.*, 83 (1979) 2764.
14 J. B. Peri, *J. Phys. Chem.*, 69 (1965) 211.
15 J. M. Bather and R. A. C. Gray, *J. Chromatogr.*, 156 (1978) 21.
16 S. Suwanayuen and R. P. Danner, *AIChE J.*, 26 (1980) 68.
17 R. B. Stewart and H. M. Roder, *Technology and Use of Liquid Hydrogen,* Pergamon, New York, 1964, Ch. 11, p. 379.
18 E. Kucera, *J. Chromatogr.*, 19 (1965) 237.
19 P. Schmeider and J. M. Smith, *AIChE J.*, 14 (1968) 762.
20 Y. W. Wong and F. B. Hill, *AIChE J.*, 25 (1979) 592.
21 R. S. Anderson and E. T. White, *Chem. Eng. Sci.*, 25 (1970) 1015.

Journal of Chromatography, 475 (1989) 135–144
Elsevier Science Publishers B.V., Amsterdam — Printed in The Netherlands

CHROM. 21 545

STUDIES ON IODINATED COMPOUNDS

VI. SEPARATION CHARACTERISTICS OF IODOHISTIDINES ON REVERSED-PHASE HIGH-PERFORMANCE LIQUID CHROMATOGRAPHY

MASAHIRO MIYASHITA and SABURO YAMASHITA*
Department of Clinical Chemistry, Hoshi College of Pharmacy, 2-4-41 Ebara, Shinagawa-ku, Tokyo 142 (Japan)
(Received February 6th, 1989)

SUMMARY

The separation of iodohistidines [monoiodohistidine (MIH) and diiodohistidine (DIH)] by reversed-phase high-performance liquid chromatography on octadecylsilylsilica columns was attempted in comparison with the separation of iodotyrosines. The retention of iodohistidines with the phosphate buffer used as the mobile phase was relatively small, and less pH dependent. However, the retention increased with the addition of hydrophobic ion-pairing agents to the mobile phase. When acetic acid was used in the mobile phase, DIH was eluted by reversed-phase elution, MIH by polar-phase elution. The separation of iodohistidines was largely dependent on the properties of the stationary phase, silanophilic interactions being influential. It may be concluded that the separation of iodohistidines will be best accomplished when an high ionic strength, low pH mobile phase containing an alkanesulphonate is used.

INTRODUCTION

Analyses of iodoamino acids are essential for the study of thyroid hormones[1–3] and iodination of proteins[4]. Iodinated derivatives of tyrosine (Tyr) and thyronine have been the main target of the investigation. There are two molecular species of iodotyrosines: that is, 3-iodotyrosine (MIT) and 3,5-diiodotyrosine (DIT). There are more molecular species of iodothyronines: triiodothyronine and thyroxine and many other isomers depending on the positions of iodine substitution in the thyronine. Recently, reversed-phase high-performance liquid chromatography (RP-HPLC) has been widely used for the separation of such iodoamino acids[5–7].

On the other hand, iodinated derivatives of histidine (His) are known. There are two molecular species of iodohistidines as in the case of iodotyrosines: that is, 4(5)-iodohistidine (MIH) and 2,4(5)-diiodohistidine (DIH) (Fig. 1). Separations of these iodohistidines were performed by paper chromatography[8], thin-layer chromatography[9] and open column chromatography[10,11], but HPLC separation has not been attempted. Therefore, the separation of these iodohistidines by HPLC was examined

0021-9673/89/$03.50

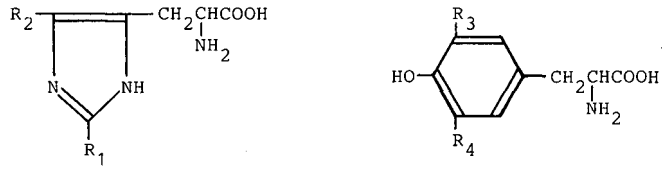

His: R_1= H, R_2= H
MIH: R_1= H, R_2= I
DIH: R_1= I, R_2= I

Tyr: R_3= H, R_4= H
MIT: R_3= I, R_4= H
DIT: R_3= I, R_4= I

Fig. 1. Structures of the compounds studied.

in the present study, since some physiologically activity of these compounds has been suggested[11,12]. Comparison of the separations of iodohistidines and iodotyrosines by HPLC may be of interest, since the imidazolyl group of His and the hydroxyphenyl group of Tyr have markedly different chemical properties. Thus in the present study, the separation of iodohistidines by RP-HPLC on an octadecylsilylsilica (ODS) column was attempted in comparison with the separation of iodotyrosines.

EXPERIMENTAL

Apparatus

The HPLC equipment consisted of a Waters Model 6000A pump, U6K universal injector and Model NS-310A variable-wavelength UV absorbance detector from Nippon Seimitsu Kagaku. The HPLC column was a Waters radial compression separation system, with cartridges of Radialpak Novapak C_{18} (NC_{18}) (100 mm × 8 mm I.D.), μBondapak C_{18} (MC_{18}) (100 mm × 8 mm I.D.) or C_{18} (RC_{18}) (100 mm × 8 mm I.D.).

Reagents

MIH (hydrochloride) and DIH (hydrochloride) were synthesized in our laboratory by the reported methods[13,14]. MIT and DIT were obtained from Sigma, His (hydrochloride, hydrate), potassium iodide (KI) and 0.5 *M* tetra-*n*-butylammonium hydroxide (TBAOH) solution from Wako and Tyr and 1-heptanesulphonic acid (HSA) (sodium salt) from Nakarai. Water used for the mobile phase component was deionized and distilled, and methanol and acetonitrile were of HPLC grade. Other reagents were of commercial guaranteed grade. Stock solutions of iodinated compounds were prepared by dissolving them in water or in 5 m*M* HCl: His, MIH and DIH (0.5 mg/ml in water); Tyr, MIT, DIT (0.5 mg/ml in 5 m*M* HCl) and KI (0.1 mg/ml in water).

Methods

HPLC was performed at room temperature (*ca.* 20°C). The flow-rate of the mobile phase was 2.5 ml/min when the NC_{18} column was used, and 3.0 ml/min when MC_{18} and RC_{18} were used. Detection of the solute was performed at 225 nm in general, and when an acetic acid-containing mobile phase was used, His was detected at 235 nm and other iodinated compounds at 254 nm. Ammonium phosphate buffer,

50 m*M*, used as the mobile phase was prepared by mixing 50 m*M* $NH_4H_2PO_4$, 50 m*M* $(NH_4)_2PO_4$ or 50 m*M* H_3PO_4, and the pH was adjusted using a pH meter. All solvents for the mobile phase were filtered through a 0.45-μm filter before use. Retention of compounds was determined by injecting 2–5 μl of the stock solutions. The capacity factor, k', was calculated by $k' = (V - V_0)/V_0$, where V is the retention volume of the solute, and V_0 is the hold up volume of the column. The hold up volume of the column was obtained from the retention volume of nitrate ion after injection of $NaNO_3$ using 60% acetonitrile as the mobile phase.

RESULTS AND DISCUSSION

Influence of the pH of the mobile phase

A solvent mixture of methanol (or acetonitrile)–water–phosphoric acid has been used as the mobile phase for RP-HPLC for the separation of iodotyrosines and iodothyronines[5,6]. The relationships between the retention of iodoamino acids with the above solvent mixture and their hydrophobicities, pH of the mobile phase and compositions of organic solvents have been reported[15–17]. Based on knowledge of the conditions for HPLC separation of these iodoamino acids, and the effect of the pH of mobile phase systems composed of methanol–50 m*M* ammonium phosphate buffer, the retention of iodohistidines was examined using three different ODS columns (Fig. 2).

The pH of the mobile phase was altered within the range allowed for the ODS column (pH 3.0–7.0). Under these conditions, the elution of iodohistidines was in the order of decreasing iodine substitution of the histidine, which might reflect that the hydrophobicity of histidine is increased, as in tyrosine, with increasing iodine substitution. The retention of iodohistidines and iodotyrosines having the same numbers of iodine groups was compared, and it was found that the retention of iodohistidine

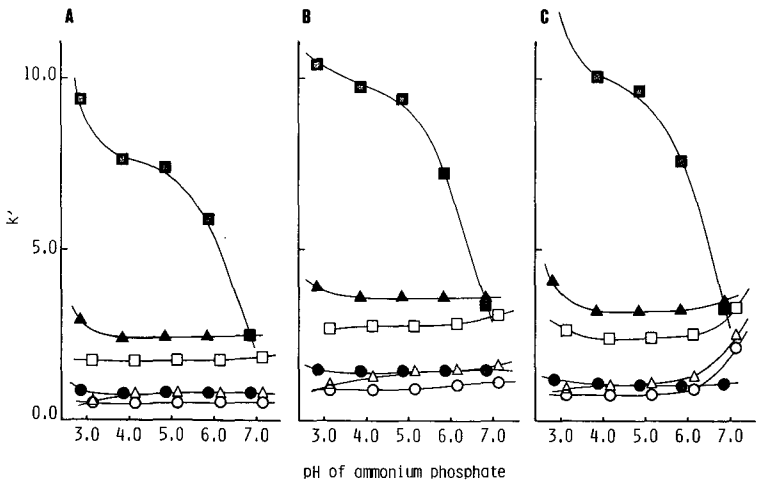

Fig. 2. Influence of pH on retention. Columns: (A) NC_{18}; (B) MC_{18}; (C) RC_{18}. Mobile phase: 25% methanol in 50 m*M* ammonium phosphate (pH 3.0–7.0). Compounds: ○, His; △, MIH; □, DIH; ●, Tyr; ▲, MIT; ■, DIT.

was less than that of the corresponding iodotyrosine. This may be due to the lower hydrophobicity of the histidine (imidazole moiety) than the tyrosine (hydroxyphenol moiety)[18]. No change in the retention behaviour of iodohistidines with the pH of the mobile phase was observed except in the case of the RC_{18} column. However, in general the retention of the solutes is dependent on the degree of solute ionization, so that the degree of ionization of iodohistidines at various pH should be taken into consideration. The degree of solute ionization, which is influenced by various factors, for example the organic solvent content in the mobile phase, may be assumed briefly from the pK_a value of the dissociable groups. There are three dissociable groups on iodohistidines, and the pK_a values of each were reported by Brunings[14] [although Brunings determined the pK_a of MIH for 2(5)-iodohistidine, the structure of MIH was corrected to 4(5)-iodohistidine by Bensusan and Naidu[19]] (Table I).

The pK_a value of the carboxyl group of His tends to be shifted toward lower values on iodination. However, the maximum pK_a of the carboxyl group of these compounds, which is the highest in His, is below 2.0, so that it may be assumed that the carboxyl group of the iodohistidines would be mostly dissociated in these pH regions. The pK_a value of the amino group of His will also be shifted to lower values on iodination. However, the lowest pK_a value of the amino group in these compounds, which is lowest in DIH, is above 8.0, thus the amino group of iodohistidines is assumed to be mostly dissociated in these pH regions. Therefore, the carboxyl and amino groups of His and iodohistidines are in the mostly ionized state, and no change in the retention behaviour due to a change of the extent of ionization of these groups is expected.

The influence of the pH of the mobile phase on the ionization of iodohistidines is marked for the third dissociable group, imidazolyl. The imidazolyl group is basic in nature, and its dissociation increases at pH lower than the pK_a value. The opposite is true for the hydroxyphenyl group of the iodotyrosines, which functions as an acid and its dissociation increases at pH higher than the pK_a value. However, the pK_a value of the imidazolyl of His is markedly lowered on iodination as in the case of Tyr. Therefore, the imidazolyl groups of His and MIH are mostly ionized at pH lower than 6.0 and 4.2, respectively, but the imidazolyl group of DIH would not be ionized within the pH range used in the present study. Based on such considerations, the

TABLE I

pK_a VALUES OF IODOAMINO ACIDS

Compound	pK_a[14,20,21]			
	Imidazolyl	*Hydroxyphenyl*	*-COOH*	$-NH_2$
His	6.00		1.82	9.17
MIH	4.18		1.72	8.62
DIH	2.72		–[a]	8.18
Tyr		10.13	2.20	9.11
MIT		8.20	–[a]	–[a]
DIT		6.48	2.12	7.82

[a] Not in literature.

ionization of the imidazolyl groups of His and MIH is expected to change the retention behaviour. However, no significant change in the retention as seen for DIT was observed on NC_{18} and MC_{18}, while the retention of DIT decreased at pH from 5.0 to 7.0 because of increasing dissociation of the hydroxyphenyl group. A change in the degree of ionization of the imidazolyl group might not contribute to the retention behaviour of iodohistidines since the hydrophobicity of the imidazolyl group is very small even when the imidazolyl group is not dissociated. Therefore, even if the dissocation of the imidazolyl group is suppressed at high pH in the mobile phase, a significant increase in the retention would not be expected. A high pH of the mobile phase poses a problem of the influence of the stationary phase as will be mentioned below.

Influence of the stationary phase

The separation of iodohistidines was not dependent on the nature of the stationary phase at lower pH of the mobile phase. However, as the pH of the mobile phase increased, the efficiency of the separation of iodohistidines became less, as in the case of iodotyrosines. This was seen mainly from the shape of the peaks: when the NC_{18} column was used, good peak shape was obtained for iodohistidines and iodotyrosines at pH 7, but when MC_{18} and RC_{18} columns were used, broadening and tailing of the peaks occurred. When the RC_{18} column was used the retention of iodohistidines was specifically increased as the pH of the mobile phase increased (Fig. 2C).

The properties of the column packings need to be known in order to discuss the difference in separation of iodohistidines ascribed to the stationary phase: particle sizes (NC_{18}, 4; MC_{18}, 10; RC_{18}, 10 μm); particle shapes (NC_{18}, spherical; MC_{18}, irregular; RC_{18}, spherical); modifications of the residual silanol groups (NC_{18}, endcapped; MC_{18}, endcapped; RC_{18}, non-endcapped); nominal pore sizes [range] (NC_{18}, 60 [60–100]; MC_{18}, 125 [50–300]; RC_{18}, 90 [60–175] Å) and carbon load (NC_{18}, 7; MC_{18}, 10; RC_{18}, 12%)[22]. The relatively small particle size and less carbon load of the NC_{18} column might be responsible for the good peak shape of iodohistidines and iodotyrosines at higher pH. Some ionic interactions between silanol groups on the stationary phase and iodohistidines might contribute to the increase in retention of iodohistidines on the RC_{18} column. The silanophilic interaction might be weak in acidic conditions because dissociation of the silanol groups may be suppressed, and the dissociation is increased as the pH is increased. Such an increase in the retention was not observed with iodotyrosines, so that the ionic interaction between iodoamino acids and silanol groups might be specific for the imidazolyl group on the iodohistidines.

Influence of organic solvent modifiers

The relationship between the ratio of organic solvent in the mobile phase and retention of iodohistidines on the NC_{18} column was examined using methanol–phosphate buffer (pH 3.0 or 7.0) as the mobile phase (Fig. 3).

As the ratio of methanol decreased at both pH values the retention of DIH as well as of iodotyrosines increased. However, little change was observed in the retention of His and MIH, which might imply that sufficient separation of His and MIH may not be accomplished with a lower ratio of the organic solvent modifier.

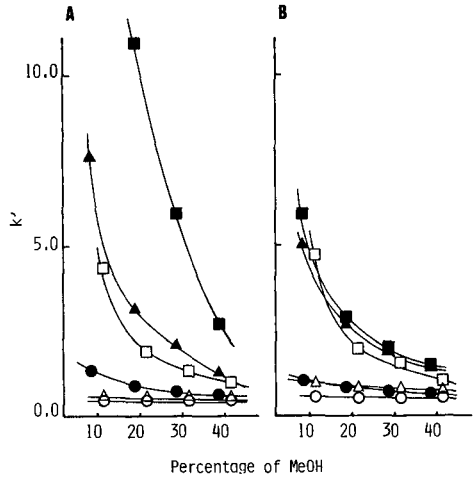

Fig. 3. Influence of the ratio of methanol on retention. Mobile phases: (A) methanol in 50 m*M* ammonium phosphate (pH 3.0), (B) methanol in 50 m*M* ammonium phosphate (pH 7.0). Column: NC_{18}. Compounds: as in Fig. 2.

When the ratio of the organic solvent modifiers was the same, less retention was obtained with acetonitrile (not shown) than with methanol.

Influence of hydrophobic ion-pairing agents

It is known that phosphate ions act as hydrophilic ion-pairing agents to decrease the retention of solutes when a mobile phase containing phosphates is used[5,23]. However, this property is not favourable for the separation of iodohistidines, the retention of which on the reversed stationary phase is weak. For the purpose of increasing the retention of iodohistidines, hydrophobic ion-pairing agents HSA and TBAOH were added to the mobile phase. The pH of the mobile phase was that generally used for HPLC (Table II).

When HSA was added to the mobile phase on the NC_{18} column an increase in the retention of iodohistidines was observed. As a result, a satisfactory separation of I^-, His, MIH and DIH was accomplished. A similar separation was observed with columns other than NC_{18} (Fig. 4).

Similarly, when TBAOH was added to the mobile phase on the NC_{18} column an increase in the retention of iodohistidines was observed. In this system, the retention of inorganic I^- together with iodoamino acids increased characteristically. The separation of I^- and iodoamino acids with a mobile phase containing alkylammonium will be reported elsewhere in detail. The separation of iodohistidines in the presence of TBAOH was largely dependent on the nature of the columns, as in the case of iodotyrosines (Fig. 5).

The shapes of the peak of iodohistidines were good when the NC_{18} column was used, but marked broadening and tailing were observed with other columns, and thus good separation was difficult. The effect of the stationary phase on the peak shapes was not dependent on the addition of TBAOH, but on the pH of the mobile phase, because the shapes were not affected by the addition of TBAOH at lower pH.

TABLE II

INFLUENCE OF ADDITION OF HYDROPHOBIC ION-PAIRING AGENTS

Mobile phase: A, 25% methanol in 50 m*M* ammonium phosphate (pH 3.0); A', 25% methanol in 50 m*M* ammonium phosphate (pH 3.0) containing 5 m*M* HSA; B, 25% methanol in 50 m*M* ammonium phosphate (pH 7.0); B', 25% methanol in 50 m*M* ammonium phosphate (pH 7.0) containing 5 m*M* TBAOH.

Compound	*k'*			
	A	*A'*	*B*	*B'*
I^-	0.55	0.34	0.59	3.30
His	0.49	1.54	0.54	0.74
MIH	0.59	1.99	0.80	1.24
DIH	1.74	4.09	1.84	3.09
Tyr	0.83	1.76	0.80	1.07
MIT	2.91	8.22	2.42	3.47
DIT	9.39	28.01	2.41	4.64

Retention behaviours in the presence of acetic acid

Acetic acid was added to the mobile phase in the place of phosphoric acid for the separation of iodotyrosines and iodothyronines[7]. Acetate ion behaves as a hydrophobic ion-pairing agent like alkanesulphonic acids[23]. Thus, an increase in the retention of iodohistidines was expected, and satisfactory separation should be accomplished. A mixture of methanol (or acetonitrile)–50 m*M* acetic acid, pH 3.0, was prepared as the mobile phase and the relationships between the ratio of organic

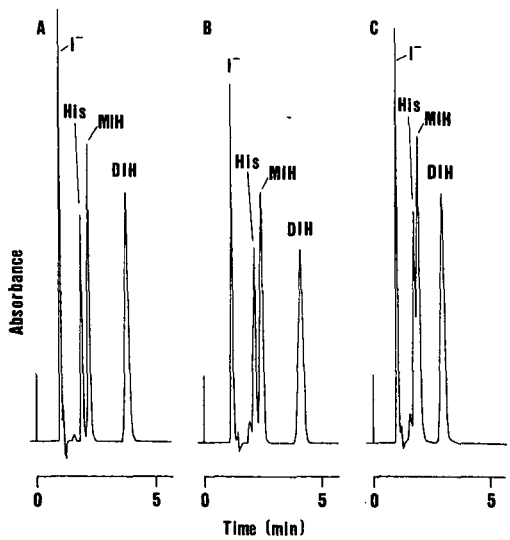

Fig. 4. HPLC separation of iodohistidines on different columns: (A) NC_{18}; (B) MC_{18}; (C) RC_{18}. Mobile phase: 25% methanol in 50 m*M* ammonium phosphate (pH 3.0) containing 5 m*M* HSA. Flow-rates: (A) 2.5; (B) 3.0; (C) 3.0 ml/min. Detector: wavelength, 225 nm; sensitivity, 0.1 a.u.f.s. Amounts injected: His, 1; MIH, 1; DIH, 1; I^-, 0.2 μg.

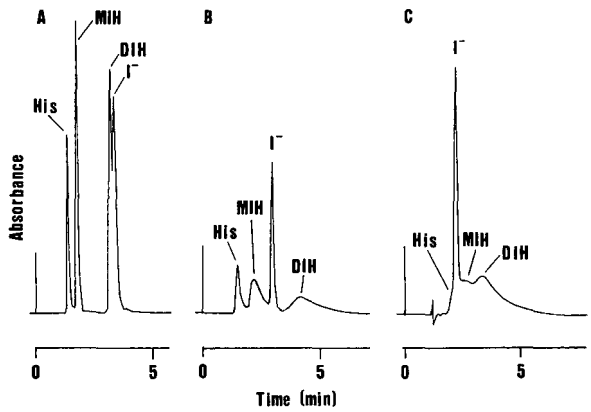

Fig. 5. HPLC separation of iodohistidines on different columns. Mobile phase: 25% methanol in 50 m*M* ammonium phosphate (pH 7.0) containing 5 m*M* TBAOH. Other conditions as in Fig. 4.

solvent modifier in the mobile phase and the retention of iodohistidines on the NC_{18} column were examined (Fig. 6).

The retention of DIH as well as iodotyrosines using the acetate mobile phase was larger than with the corresponding phosphate one, methanol (or acetonitrile)–50 m*M* phosphate buffer, pH 3.0, and an increase in the ratio of the organic solvent modifier resulted in a decrease in the retention, as generally observed in RP-HPLC. On the contrary, the retention behaviours of His and MIH with the acetate mobile phase was entirely different from that with the phosphate system. Thus, His and MIH showed an increase in retention when the ratio of organic solvent modifier was increased, and greater retention was obtained with acetonitrile than with methanol. When the mobile phase contained more than 40% methanol or more than 20% acetonitrile the elution sequence was entirely reversed, to DIH, MIH and His, which

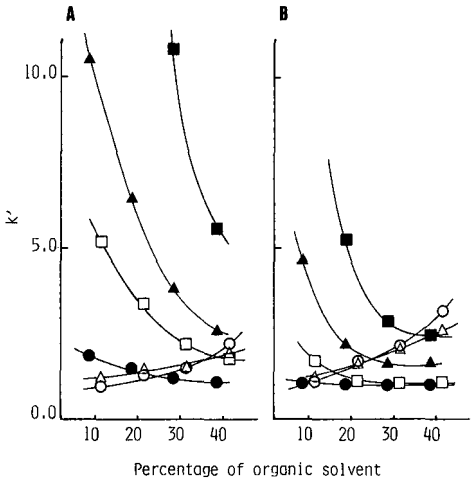

Fig. 6. Influence of the ratio of the organic solvent on retention. Mobile phases: (A) methanol in 50 m*M* acetic acid; (B) acetonitrile in 50 m*M* acetic acid. Column: NC_{18}. Compounds as in Fig. 2.

was unexpected based on the hydrophobicities of these compounds. The mode of retention of His and MIH was entirely different from that anticipated in the reversed-phase elution profile, and the elution pattern observed was that of a polar phase elution. Such retention behaviour was reported in the separation of iodotyrosines and iodothyronines with a mobile phase system containing a high ratio of organic solvent modifier[17]. It was also observed for His and MIH when a propionic acid-containing solution or methanol (or acetonitrile)–water without salt was used as the mobile phase. However, normal reversed-phase elution was observed when trifluoroacetic acid, having a dissociation constant higher than those of acetic acid and propionic acid, was used, or an inorganic salt like NaCl was added to the mobile phase, methanol (or acetonitrile)–50 m*M* acetic acid. Therefore, a polar phase elution mode might be observed in a mobile phase with low ionic strength.

The retention behaviour of iodohistidines was dependent on the nature of the stationary phase when the mobile phase containing acetic acid was used. The separation of iodohistidines was compared on three different columns using 30% acetonitrile in 50 m*M* acetic acid as the mobile phase (Fig. 7).

The retention of iodohistidines as well as iodotyrosines on the NC_{18} column was smaller than that on the RC_{18} column, and larger than that on the MC_{18} column. The marked increase in the retention of iodohistidines on RC_{18} might be due to strong ionic interaction between the silanol groups on the stationary phase and the iodohistidines. The different retention behaviours with phosphate and acetate are notable: that is, when 30% acetonitrile in 50 m*M* phosphate buffer, pH 3.0, was used as the mobile phase, the separation mode was little altered by the stationary phase,

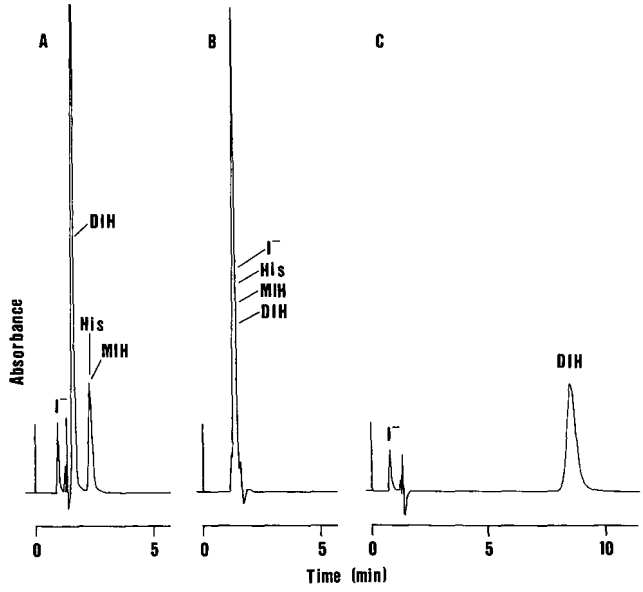

Fig. 7. HPLC separation of iodohistidines on different columns. Mobile phase: 30% acetonitrile in 50 m*M* acetic acid. Detector: wavelength, 254 nm; sensitivity, 0.02 a.u.f.s. The elution position of His was confirmed by separate injection and detection at 235 nm. Other conditions as in Fig. 4. His and MIH were not eluted within 10 min on the RC_{18} column.

while when acetate was used the separation was altered by the column used. Thus, the physicochemical properties of the stationary phase might be influential with a mobile phase solvent of low ionic strength at lower pH.

The relatively large retention of iodohistidines due to the polar phase elution mode or interaction with silanol groups is accompanied by broadening and tailing of the peaks, so that this system may not be adequate for practical purposes.

CONCLUSIONS

The separation characteristics of iodohistidines in RP-HPLC were investigated in comparison with iodotyrosines. A mobile phase composed of phosphate buffer did not give sufficient retention upon altering the pH and the ratio of the mobile phase solvents, so that satisfactory separation of iodohistidines was not achieved. Therefore, it is necessary to add adequate hydrophobic ion-pairing agents to increase the retention for a better separation. The characteristics of the stationary phase may be the influential factors when a mobile phase of about neutral pH or with low ionic strength is used. From the retention behaviours of iodohistidines in RP-HPLC, it may be concluded that an acidic mobile phase with high ionic strength, containing alkanesulphonic acid, should be the most suitable for the present purpose.

REFERENCES

1 S. B. Barker, in R. I. Dorfman (Editor), *Methods in Hormone Research*, Vol. 1, Academic Press, New York, 2nd ed., 1968, p. 411.
2 C. W. Turner, in R. I. Dorfman (Editor), *Methods in Hormone Research*, Vol. 2, Part A, Academic Press, New York, 2nd ed., 1969, p. 301.
3 J. Robbins and J. E. Rall, in C. H. Gray and V. H. T. James (Editors), *Hormones in Blood*, Vol. 1, Academic Press, London, 3rd ed., 1979, p. 575.
4 O. A. Roholt and D. Pressman, *Methods Enzymol.*, 25 (1972) 438.
5 M. T. W. Hearn, W. S. Hancock and C. A. Bishop, *J. Chromatogr.*, 157 (1978) 337.
6 M. T. W. Hearn and W. S. Hancock, *J. Liq. Chromatogr.*, 2 (1979) 217.
7 N. M. Alexander and M. Nishimoto, *Clin. Chem.*, 25 (1979) 1757.
8 J. Roche, S. Lissitzky and R. Michel, *Methods Biochem. Anal.*, 1 (1954) 243.
9 W. M. Goldberg, *J. Chromatogr.*, 134 (1977) 246.
10 P. Thomopoulos, *Anal. Biochem.*, 65 (1975) 600.
11 J. C. Savoie, P. Thomopoulos and F. Savoie, *J. Clin. Invest.*, 52 (1973) 106.
12 J. C. Savoie, J. P. Massin and F. Savoie, *J. Clin. Invest.*, 52 (1973) 116.
13 M. Miyashita, Y. Seyama, K. Kaji and S. Yamashita, *Chem. Pharm. Bull.*, 31 (1983) 386.
14 K. J. Brunings, *J. Am. Chem. Soc.*, 69 (1947) 205.
15 M. T. W. Hearn and W. S. Hancock. *J. Chromatogr. Sci.*, 18 (1980) 288.
16 S.-J. Su, B. Grego and M. T. W. Hearn, *J. Liq. Chromatogr.*, 4 (1981) 1709.
17 M. T. W. Hearn and B. Grego, *J. Liq. Chromatogr.*, 7 (1984) 1079.
18 R. F. Rekker, *The Hydrophobic Fragmental Constant*, Elsevier, Amsterdam, 1977, p. 301.
19 H. B. Bensusan and M. S. R. Naidu, *Biochemistry*, 6 (1967) 12.
20 H. Edelhoch, *J. Biol. Chem.*, 237 (1962) 2778.
21 E. D. Mooz, in G. D. Fasman (Editor), *Handbook of Biochemistry and Molecular Biology*, Vol. 1, CRC Press, Ohio, 3rd ed., 1976, p. 109.
22 *Waters Sourcebook for Chromatography Columns and Supplies*, Waters, Milford, MA, 1986.
23 M. T. W. Hearn, *Adv. Chromatogr. (N.Y.)*, 20 (1982) 21.

Journal of Chromatography, 475 (1989) 145–151
Elsevier Science Publishers B.V., Amsterdam — Printed in The Netherlands

CHROM. 21 509

EVALUATION OF SMALL DIAMETER CAPILLARY COLUMNS FOR GAS CHROMATOGRAPHY

G. P. CARTONI*, G. GORETTI, B. NERI and M. V. RUSSO
Department of Chemistry, "La Sapienza" University, P. le Aldo Moro 5, 00185 Rome (Italy)
(Received March 14th, 1989)

SUMMARY

Glass and fused silica capillary columns of inner diameter 50–200 μm were compared for their chromatographic characteristics and their application to the analysis of complex mixtures. The results show that columns of small diameter can be usefully employed in gas chromatography despite some instrumental difficulties.

INTRODUCTION

Until recently, an increase in the efficiency of gas chromatographic capillary columns depended on the possibility of utilizing longer columns. In recent years, research has been focused on the inner diameter (I.D.) and the liquid film thickness (d_f). The decrease in these two parameters, which appear as squared terms in the mass transfer term (C) in the numerator of the Van Deemter equation, suggested the possibility of obtaining a large number of theoretical plates with relatively short columns.

Several workers have prepared capillary columns of I.D. <200 μm and obtained promising results[1–8]. Cramers[9] provided some technical considerations to explain the chromatographic behaviour of these columns. However, their use is limited because of their relatively small sample loading capacity.

This work was aimed at determining experimentally the chromatographic performance of columns of I.D. 50–200 μm and assessing whether the kind of capillary, glass or fused silica, affects the chromatographic performance.

EXPERIMENTAL

Glass capillary columns were prepared in our laboratory with a drawing machine manufactured by Carlo Erba (Milan, Italy) from Duran glass tubing of O.D. and I.D. 7 and 2 mm, respectively, for columns of I.D. >100 μm and from tubing of I.D. 1 mm for columns with I.D. $\leqslant 100$ μm. The tubing was previously washed with a cleaning solution consisting of concentrated sulphuric acid and 0.1 M potassium dichromate and then with distilled water and acetone.

Fused-silica columns were obtained from SGE (Melbourne, Australia). Both

0021-9673/89/$03.50

the glass and fused-silica columns, after washing with dichloromethane, were leached with 20% hydrochloric acid at 175°C overnight, followed by successive washing with 1% hydrochloric acid, water and acetone; they were then dehydrated under pure nitrogen at 300°C for 3 h[10–12].

The columns were silanized at 400°C with diphenyldichlorosilane (Fluka, Buchs, Switzerland)[13] for 3 h followed by washing with dichloromethane and then hexamethyldisilazane (Fluka) overnight. The pure silanizing agents were passed through the columns at a rate of *ca.* 2.5 cm/s.

After each silanization, deactivation was checked by performing gas chromatography at 60°C on a standard mixture including *n*-decane, *n*-undecane and *n*-dodecane, octanol, 2,6-dimethylphenol (2,6-DMP) and 2,6-dimethylaniline (2,6-DMA). After silanization, all columns were washed successively with toluene, methanol and pentane.

The stationary phase was deposited statistically together with dicumyl peroxide (DCUP) and changing the relative concentrations according to the I.D. as shown in Table I.

TABLE I

SOLUTION CONCENTRATIONS FOR COLUMNS OF 0.20 μm FILM THICKNESS

I.D. (μm)	*% (w/v) (SE-54/pentane)*	*% (w/w) (DCUP/SE-54)*
200	0.4	0.25
100	0.8	1.2
75	1.1	2.0
50	1.6	3.0

Both ends of the columns were closed by melting, and curing was performed with temperature programming from 50 to 170°C at 3°C/min; the final temperature was maintained for 30 min.

After curing and conditioning at 280°C under hydrogen, the columns were washed with methanol, dichloromethane and pentane. The columns were evaluated by performing chromatography at 90°C on the above standard mixture; the carrier gas was hydrogen.

Each chromatographic parameter reported in Table II was assessed at the minimum point of the Van Deemter curves; the mass transfer term C was obtained by plotting $h \cdot \bar{u}$ against u^2, where h is height equivalent to a theoretical plate and $\bar{u}$ is the linear velocity of carrier gas. Comparison of the capacity factors (k') of *n*-dodecane obtained from columns prepared with SE-54 only and from cross-linked columns indicated that the reaction gave a 60–70% yield, in agreement with the literature[2,14]. This comparison also served as a basis for evaluating the actual thickness of the liquid film (d_f). Gas chromatographic measurements were performed using DANI 3900 and 6500 and Hewlett-Packard 5890 gas chromatographs with Shimazu C-R 3 and HP 339 A integrators.

TABLE II

GAS CHROMATOGRAPHIC CHARACTERISTICS OF THE COLUMNS

No.	*I.D.* *(μm)*	*Length* *(m)*	d_f *(μm)*	k' $(C_{12}H_{26})$	$\bar{u}$ *(cm/s)*	h_{min} *(μm)*	*h/I.D.*	*n/s*	*TZ/m*	η	$C \cdot 10^5$ *(s)*
1	200	6	0.14	10.2	35.0	171	0.86	2050	3.7	100	28
2[a]	200	13	0.14	10.3	37.0	173	0.87	2230	2.6	100	27
3	180	18	0.13	10.3	36.7	161	0.81	2280	2.4	100	21
4[a]	100	7	0.19	27.5	39.5	99	0.99	3980	4.9	93	15
5	100	7	0.22	31.6	40.5	99	0.99	4090	5.0	94	12
6[a]	100	4.5	0.22	32.1	41.0	115	1.15	3550	5.3	81	17
7	75	6.3	0.09	17.0	44.7	86	1.15	5210	5.5	86	9
8	75	5.7	0.15	29.8	44.0	91	1.20	4880	5.3	82	13
9	75	7.0	0.16	30.5	41.7	81	1.10	5140	5.0	87	12
10	75	6.0	0.24	35.0	42.1	98	1.30	4340	5.5	71	15
11	75	6.5	0.35	66.3	41.0	94	1.25	4380	5.4	75	27
12	50	6.0	0.13	37.0	43.6	56	1.12	8720	7.1	83	9
13	50	4.7	0.13	35.1	46.9	47	0.95	10 300	8.2	100	10

[a] Fused-silica columns.

RESULTS AND DISCUSSION

Fig. 1 shows the Van Deemter curves for *n*-dodecane ($C_{12}H_{26}$) obtained from four columns with I.D. decreasing from 200 to 50 μm; it clearly shows the increase in efficiency resulting from the decrease in I.D. The larger dispersion shown by the curve for the column of smallest I.D. can be attributed to the difficult introduction of the sample into the column at a rate sufficient to maximize its resolving power.

The results in Table II indicate that when the I.D. decreases the column efficiency increases (h_{min} from 171 to 56 μm) for columns having approximately the same d_f and length (6 m) such as Nos. 1 and 12; at the same time, the peak capacity per metre of column length (TZ/m) increases from 3.7 to 7.2; the same is true for the separation speed, n/s, which increases from about 2000 for larger diameter columns to 8000–10 000 for smaller diameter columns. The capacity factor, k', increases from about 10 (column of 200 μm I.D.) to over 35 (for 50 μm I.D. columns). This increase in k' is due, as expected, to the increased phase ratio ($V_f/V_m = 2\,d_f/r$); assuming d_f to be constant, it is inversely related to the capillary radius, r. However, this effect does not imply an increased analysis time; to achieve a given separation with smaller diameter columns it is possible to employ shorter columns or operate at a higher linear flow-rate, as is shown by the decrease in the C term, which falls from $28 \cdot 10^{-5}$ s for 200 μm I.D. columns to about $10 \cdot 10^{-5}$ s for columns of smaller I.D. with the same d_f. The coating efficiency (η) is quite good for almost all columns.

Table II also shows how the thickness of the liquid film affects the microcolumn efficiency (see columns 7–11 of 75 μm I.D.). In fact, when d_f increases from 0.09 to 0.35 μm, h_{min} increases from 86 to 94 μm whereas n/s decreases from 5200 to 4300 and TZ/m remains virtually unchanged.

In any case, the moderate decreases in efficiency observed in the d_f range examined allows columns with a relatively high phase load to be employed and the sample

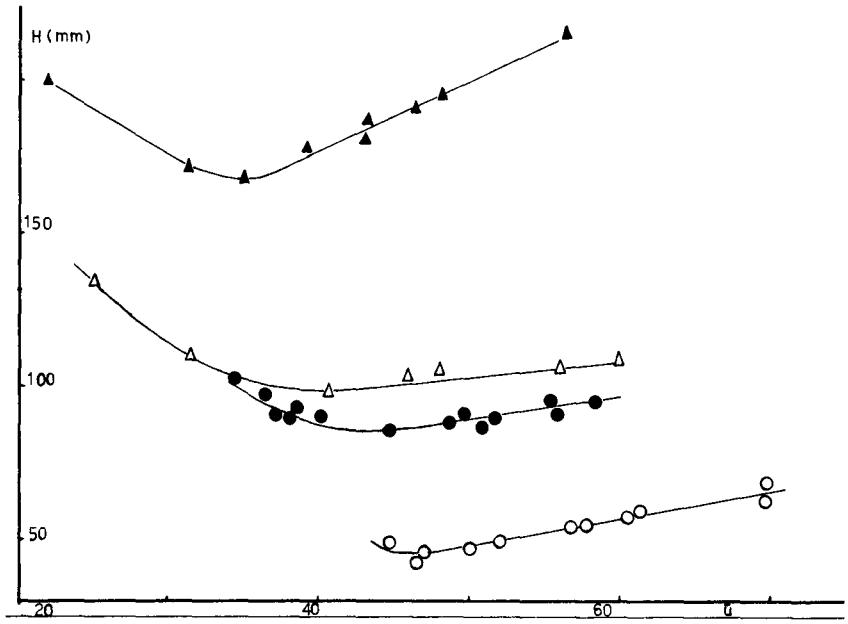

Fig. 1. Van Deemter plots: *n*-decane at 90°C, hydrogen as carrier gas. Column No.: ▲, 1; △, 5; ●, 7; ○, 13.

load to be kept within acceptable values. The *C* term is affected by an increase in d_f only at higher values (see columns 10 and 11). The values reported in Table II show that capillary columns with similar d_f and I.D. have equivalent properties, regardless of the kind of capillary (glass or fused silica).

Table III reports the retention indices for octanol, 2,6-DMP and 2,6-DMA determined using the same columns as in Table II. These values, which change by

TABLE III

RETENTION INDICES

Column No.	*n-Octanol*	*2,4-DMP*	*2,4-DMA*
1	1070	1106	1163
2[a]	1073	1109	1167
3	1076	1113	1170
4[a]	1072	1109	1167
5	1078	1111	1169
6[a]	1075	1111	1169
7	1073	1110	1167
8	1073	1109	1167
9	1071	1109	1166
10	1074	1111	1168
11	1076	1113	1170
12	1075	1113	1170
13	1078	1112	1169

[a] Fused-silica columns.

only a few units, show that the type of capillary and the various methods employed have only a very limited influence on the column polarity.

Some chromatographic determinations are presented in order to evaluate the performance of these columns. Columns of different I.D. were compared: with the same number of theoretical plates; with comparable lengths; and with comparable linear carrier gas flow-rates ($\bar{u}$).

Gas chromatograms obtained from two different columns with the same polycyclic aromatic hydrocarbon (PAH) standard are shown in Fig. 2. The two columns, of different length (23 and 7 m), had the same number of theoretical plates (about 74 000) and I.D.s of 300 and 100 μm, respectively. The two chromatograms were obtained isothermally at 240°C using hydrogen as the carrier gas with $\bar{u}$ = 40 cm/s for the first column and 60 cm/s for the second in order to obtain roughly the same number of plates. The separations were equivalent but the analysis time was 25 min with the first and less than 10 min with the second column.

Fig. 3 shows chromatograms obtained from columns having the same length, with I.D. 200 and 100 μm, analysing the same petit grain essential lemon oil and using for the second column a higher linear carrier gas flow-rate to obtain a similar analysis time (the temperature programme was the same for both columns). The column of smaller I.D. shows a better separation, especially for the peaks marked with asterisks.

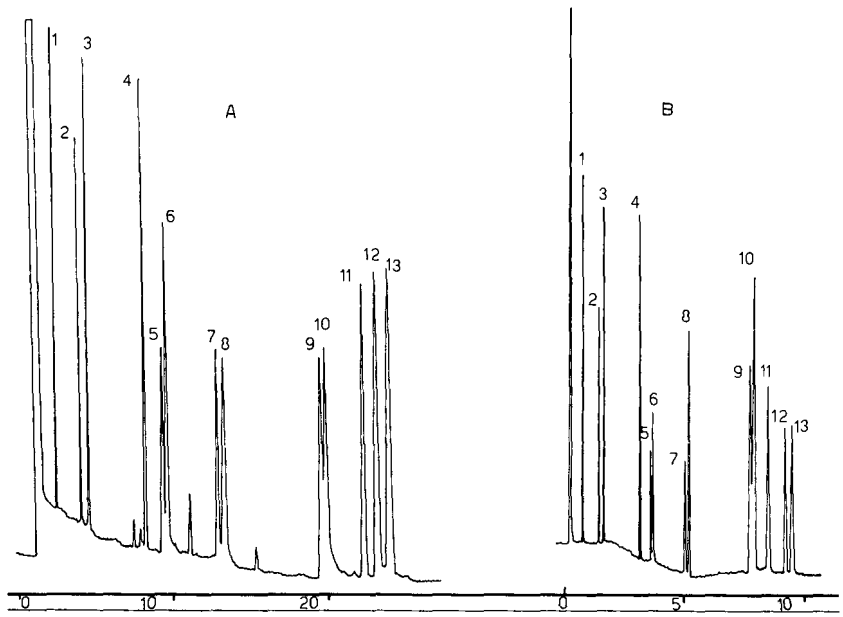

Fig. 2. Gas chromatograms of a standard PAH mixture at 240°C: (A) column length = 23.2 m, I.D. = 300 μm, $\bar{u}$ = 39 cm/s; (B) column length = 7.0 m, I.D. = 100 μm, $\bar{u}$ = 62 cm/s. Peaks: 1 = phenanthrene; 2 = fluoranthene; 3 = pyrene; 4 = benzo[*ghi*]fluoranthene; 5 = benzoanthracene; 6 = chrysene; 7 = 2-methylchrysene; 8 = 4-methylchrysene; 9 = benzo[*h*]fluoranthene; 10 = benzo[*k*]fluoranthene; 11 = n-C_{28}; 12 = benz[*e*]pyrene; 13 = benz[*c*]pyrene.

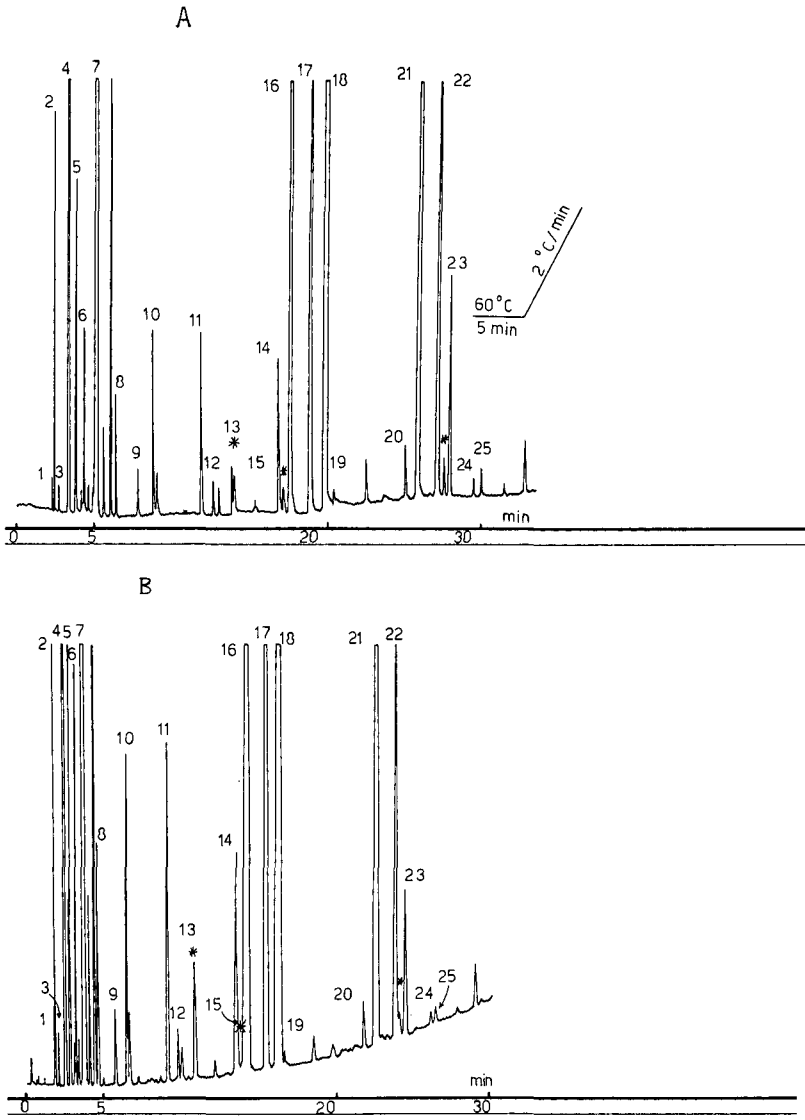

Fig. 3. Gas chromatograms of petit grain essential lemon oil on 7-m columns: (A) I.D. = 100 μm, $\bar{u}$ = 60 cm/s; (B) I.D. = 200 μm, $\bar{u}$ = 45 cm/s. Peaks: 1 = α-thujene; 2 = α-pinene; 3 = camphene; 4 = β-pinene + sabinene; 5 = myrcene; 6 = *p*-cymene; 7 = limonene; 8 = γ-terpinene; 9 = terpinolene; 10 = linalool; 11 = citronellal; 12 = 4-terpinolene; 13 = α-terpineol; 14 = nerol; 15 = citronellol; 16 = neral; 17 = linalyl acetate; 18 = geraniol; 19 = bornyl acetate; 20 = citronellyl acetate; 21 = neryl acetate; 22 = genaryl acetate; 23 = β-cariophyllene; 24 = bergamotene; 25 = humulene.

Fig. 4 shows chromatograms obtained by analysing Aroclor 1232 using columns of I.D. 100 and 50 μm; the temperature programme and linear carrier gas flow-rate (100 cm/s) were the same in each instance. The separations were roughly the same but the analysis time with the second column was 19 min compared with 27 min

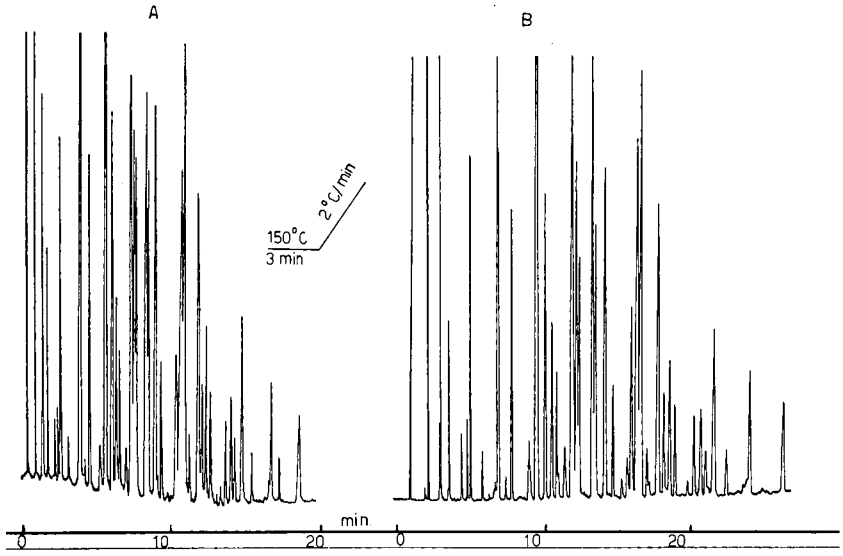

Fig. 4. Gas chromatograms of Aroclor 1232 on two columns: (A) length = 4.7 m, I.D. = 50 μm, $\bar{u}$ = 99 cm/s; (B) length = 7.0 m, I.D. = 100 μm, $\bar{u}$ = 101 cm/s.

for the first column; as a consequence, the elution temperature of the last peak is also markedly lower for the second column (about 180°C) than for the first (200°C).

ACKNOWLEDGEMENT

This work was supported by a grant from the Ministry of Education (40%) of Italy.

REFERENCES

1 R. C. Kong and M. L. Lee, *J. High Resolut. Chromatogr. Chromatogr. Commun.*, 6 (1983) 31.
2 R. C. Kong, S. M. Fields, W. P. Jackson and M. L. Lee, *J. Chromatogr.*, 289 (1984) 105.
3 C. L. Wolley, K. E. Markides, M. L. Lee and K. D. Bartle, *J. High Resolut. Chromatogr. Chromatogr. Commun.*, 9 (1986) 506.
4 A. Farbrot, S. Folestad and M. Larsson, *J. High Resolut. Chromatogr. Chromatogr. Commun.*, 9 (1986) 117.
5 A. Aerts, J. Rijks, A. Berngard and L. Blomberg, *J. High Resolut. Chromatogr. Chromatogr. Commun.*, 9 (1986) 49.
6 L. Wolley, B. J. Tarbet, K. D. Bartle, K. E. Markides, J. S. Brandshaw and M. L. Lee, in P. Sandra (Editor), *Eighth International Symposium on Capillary Chromatography, Riva del Garda, Italy*, Vol. I, Research Institute for Chromatography, University of Ghent, Ghent, 1987, p. 253.
7 G. Goretti, A. Liberti and G. Pili, *J. High Resolut. Chromatogr. Chromatogr. Commun.*, 1 (1978) 143.
8 G. Goretti, M. V. Russo and A. Liberti, *Essenze Deriv. Agrum.*, 54 (1984) 13.
9 C. A. Cramers, *J. High Resolut. Chromatogr. Chromatogr. Commun.*, 9 (1986) 676.
10 V. Pretorius and J. C. Davidz, *J. High Resolut. Chromatogr. Chromatogr. Commun.*, 2 (1979) 703.
11 G. Grob, K. Grob and K. Grob, Jr., *J. High Resolut. Chromatogr. Chromatogr. Commun.*, 2 (1979) 31.
12 G. Grob, K. Grob and K. Grob, Jr., *J. High Resolut. Chromatogr. Chromatogr. Commun.*, 2 (1979) 677.
13 R. Burrows, M. Cooke and D. G. Gillespie, *J. Chromatogr.*, 260 (1983) 168.
14 B. W. Wright, P. A. Peaden, M. L. Lee and T. J. Stark, *J. Chromatogr.*, 248 (1982) 17.

Journal of Chromatography, 475 (1989) 153–165
Elsevier Science Publishers B.V., Amsterdam — Printed in The Netherlands

CHROM. 21 489

DESIGN AND SYNTHESIS OF A CHIRAL STATIONARY PHASE CONTAINING A BENZ[*de*]ISOQUINOLINONE SKELETON

I. FIRST CHROMATOGRAPHIC RESULTS

M. SALLÉ, A. TAMBUTÉ* and A. BÉGOS
Direction des Recherches et Études Techniques, Centre d'Études du Bouchet, B.P. No. 3, Le Bouchet, 91710 Vert-le-Petit (France)
(First received December 20th, 1988; revised manuscript received March 13th, 1989)

SUMMARY

A chiral stationary phase (CSP) derived from 3-(4′-glycidyloxyphenyl)-2,3-dihydro-1*H*-benz[*de*]isoquinolin-1-one was designed and synthesized according to the reciprocality concept. A coplanar arrangement of possible attractive sites of interaction is due to the rigid conformation of the chiral selector. It was demonstrated that this CSP exhibits a good chiral discrimination ability towards families of racemates such as 3,5-dinitrobenzoyl derivatives of α-amino esters and α-aminoamides. Significant enhancements of selectivity were observed when chloroform was used instead of ethanol as a polar modifier in hexane, emphasizing the major contribution of the nature of the mobile phase to the chiral recognition process.

INTRODUCTION

Asymmetric synthesis is now applied to a great variety of organic compounds, and requires the development of analytical methods for the determination and control of enantiomeric purity. New methods able to resolve racemates, for both analytical and preparative purposes, have been developed. Among these, chromatography on chiral stationary phases (CSPs) is an efficient and reliable method for the determination of enantiomeric purity, using either high-performance liquid chromatography (HPLC)[1] or supercritical-fluid chromatography (SFC)[2]. CSPs can also be applied on a preparative scale, which is sometimes an interesting alternative, particularly for compounds devoid of suitable functional groups and which cannot be obtained with a high enantiomeric excess by conventional techniques such as asymmetric synthesis or fractional crystallization.

An example of such a CSP, developed recently in our laboratory, is illustrated by the (*S*)-thio-DNBTyr-A (CSP 1)[3,4] (Fig. 1). CSP 1 resolves various families of racemates, such as α-methylene-γ-butyrolactam derivatives (Fig. 2A), which are potential cytotoxic agents[5].

The ability of a CSP to resolve a racemate results from a combination of

0021-9673/89/$03.50

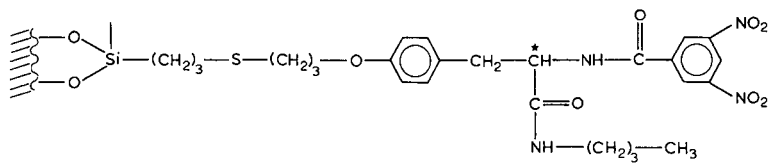

Fig. 1. Chiral stationary phase derived from (*S*)-tyrosine: (*S*)-thio-DNBTyr-A (CSP 1).

attractive interactions (such as hydrogen bonding, dipolar interactions, π–π charge-transfer overlap), and repulsive interactions such as steric hindrance effects). Several structural features of α-methylene-γ-butyrolactam are useful for chiral separation purposes: (a) the presence of a methylene group in the five membered ring, which confers a rigid quasi-planar structure to the molecule; (b) the *cis* disposition of the hydrogen atom and the carbonyl group in the amide dipole when R is a hydrogen atom (Fig. 2A); and (c) access to the chiral centre, which is limited to one side only owing to the presence of the bulky R′ moiety (Fig. 2A). A CSP whose chiral selector (CS) is structurally derived from α-methylene-γ-butyrolactam (Fig. 2A) should fulfil the requirements of an effective CSP.

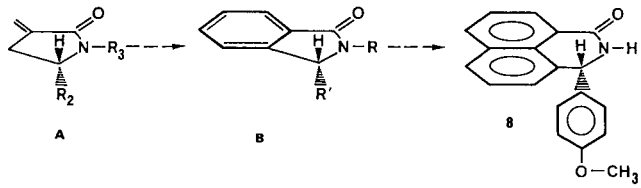

Fig. 2. Progress of the design of the chiral selector.

The synthesis of such a CSP takes into account the well known reciprocality concept[6], assuming that a resolved solute on a given CSP, such as some α-methylene-γ-butyrolactams on (*S*)-thio-DNBTyr-A, should be reciprocally operative as a chiral selector to resolve some amino acid derivatives on an α-methylene-γ-butyrolactam bonded phase. First, the optimization of the design of the CS is reported. Second, the separation of a diastereomeric mixture with respect to the carbon atom configuration in the lactam ring by preparative-scale chromatography on CSP 1 is described. Finally, the binding of one diastereomer on to LiChrosorb-NH_2, according to a previously published procedure[7], is discussed.

EXPERIMENTAL

Analytical chromatography

Analytical chromatography was performed with a modular liquid chromatograph (Gilson, Villiers-le-Bel, France) equipped with a Model 303 pump, a Model 802C manometric module, a Gilson 811 (1.5 ml) dynamic mixer and a Model 116 variable-wavelength UV detector (190–360 nm). All results were recorded with a Shimadzu CR3A integrator (Touzart et Matignon, Vitry-sur-Seine, France). Chiral stationary phases were packed into 150 × 4.6 mm I.D. stainless-steel columns by the usual slurry technique, at 400 bar with ethanol as pumping solvent. All chromato-

graphic determinations were carried out at room temperature with *n*-hexane–ethanol or *n*-hexane–chloroform as mobile phases (flow-rate 2 ml/min).

Preparative chromatography

Preparative chromatography was performed at room temperature with a Modulprep apparatus (Jobin-Yvon, Longjumeau, France). The (*S*)-thio-DNBTyr-A (CSP 1) (200 g, 7 μm) was packed into the column (40 mm I.D.) by axial compression at 15 bar. UV detection was carried out at 254 nm with a Model SM-25 variable-wavelength detector (195–370 nm) (Jobin-Yvon). The eluent inlet pressure was about 13 bar, which gave a flow-rate of *ca.* 30 ml/min.

Nuclear magnetic resonance spectra

^{1}H NMR spectra were recorded at 200 MHz on a Bruker-WP.200 spectrometer at 296 K, using tetramethylsilane (TMS) as internal standard and [^{2}H]chloroform or [$^2H_6$]dimethyl sulphoxide as solvent; values and constants are given in hertz.

Polarimetry

Optical rotations were measured on a Perkin-Elmer 141 micropolarimeter with a thermostated 1-dm quartz cell and using high-purity solvents (usually from Merck, Darmstadt, F.R.G.).

Physical data

The melting points were measured on a Büchi–Tottoli hot-stage apparatus and are uncorrected.

The compounds, listed with their empirical formulae, had elemental analyses consistent with their formulae to within ±0.3% (Service Central de Microanalyse du CNRS).

Materials

For analytical chromatography, *n*-hexane and ethanol were of LiChrosorb grade from Merck. Chloroform of analytical-reagent grade [stabilized with 0.6% (w/w) of ethanol] was from Prolabo (Paris, France). For preparative chromatography and packing of the columns, the solvents (*n*-hexane, ethanol) were of analytical-reagent grade, purchased from Prolabo. LiChrosorb-NH_2 γ-aminopropylsilica gel (particle diameter 5 or 7 μm) was purchased from Merck.

Classical column chromatographic purifications were carried out on Merck H-60 silica gel. Analytical thin-layer chromatography (TLC) was performed on Merck F-254 silica gel plates.

Syntheses

8-(4'-Anisoyl)-1-naphthoicacid (7). The keto acid **7** (Fig. 3) was prepared using a Grignard reaction between 1,8-naphthoic anhydride and *p*-anisylmagnesium bromide[8] instead of the procedure using aluminium chloride, which may cause several side reactions[9].

1,8-Naphthoic anhydride (Aldrich) (59.46 g, 0.3 mol) was partially dissolved in 750 ml of freshly distilled tetrahydrofuran (THF) and the Grignard reagent solution (10% excess) was slowly added through a dropping funnel, at room temperature. The

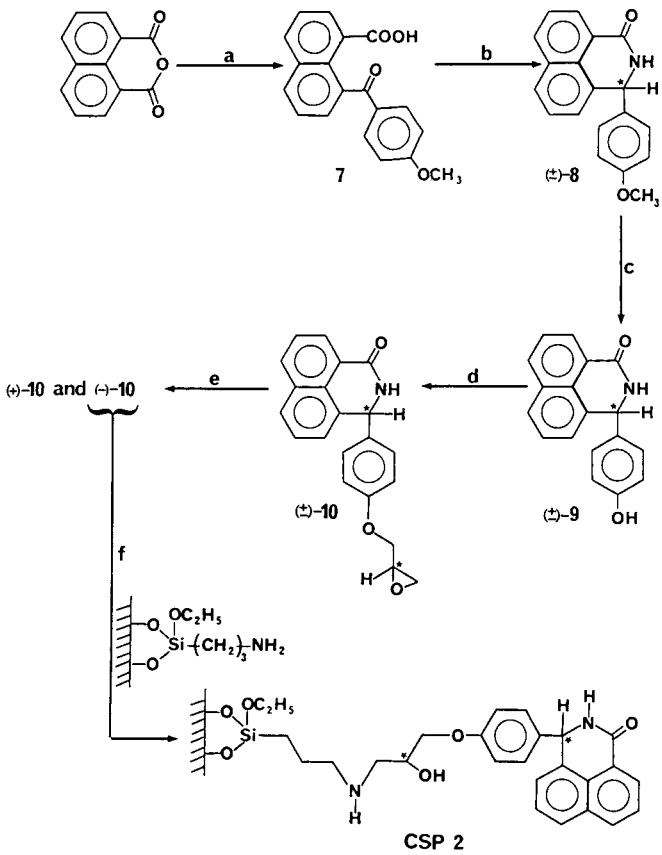

Fig. 3. Preparation of CSP 2. (a) *p*-Anisyl magnesium bromide, THF, 47% yield; (b) formamide, formic acid, reflux 2.5 h, 90% yield; (c) boron tribromide in methylene chloride, 96% yield; (d) potassium carbonate, epibromohydrin, acetonitrile, reflux 30 h, 66% yield; (e) preparative separation on CSP 1; (f) LiChrosorb-NH_2 (5 μm), triethylamine, benzene, reflux 44 h.

homogeneous solution was refluxed for 2.5 h then, after cooling, hydrolysed with a saturated solution of ammonium chloride. The mineral was filtered off on Celite and the filtrate partly evaporated. The crude product which appeared as a brown gum was filtered on a fine-pore sintered-glass funnel, rinsed with water and dried under vacuum. The solid residue was crystallized from methanol–benzene (5:1, v/v) to afford 43 g of a white solid (47%); m.p. 197–198.5°C. Analysis (C, H, O): $C_{19}H_{14}O_4$. ^1H NMR ([$^2H_6$]dimethyl sulphoxide): 3.84 (s, 3H, OCH_3), 7.02 (d, J = 10 Hz, 2H, aromatic), 7.51–7.68 (m, 4H, aromatic), 7.79 (d, J = 10 Hz, 2H, aromatic), 8.05–8.28 (m, 2H, aromatic).

*(±)-3-(4'-Anisyl)2,3-dihydro-1H-benz[de]isoquinolin-1-one (**8**).* A solution of **7** (21.4 g, 70 mmol) in freshly distilled formamide (56 ml, 1.4 mol) and formic acid (26 ml, 0.7 mol) were refluxed for 2.5 h at 140°C[10]. The reaction mixture was allowed to cool to room temperature and water (200 ml) was added. The pale brown precipitate was filtered through a fine-pore sintered-glass funnel, rinsed abundantly with water

and triturated in hot methanol (150 ml) to afford a colorless solid (18.2 g, 90% yield); m.p. 226.5–230°C. A sample, triturated twice in hot methanol, afforded **8** as a white solid; m.p. 229–231°C. Analysis (C, H, N, O) · $C_{19}H_{15}NO_2$. ^{1}H NMR ([$^2H_6$]dimethyl sulphoxide): 3.70 (s, 3H, OCH_3), 6.08 (s, 1H, C*H), 6.86 (d, J = 9 Hz, 2H, aromatic), 7.20 (d, J = 9 Hz, 2H, aromatic), 7.33–8.25 (m, 6H, aromatic), 8.71 (s, 1H, NH).

*3-(4'-Hydroxyphenyl)-2,3-dihydro-1H-benz[de]isoquinolin-1-one (**9**).* A solution of **8** (15.9 g, 55 mmol) in 1 l of dichloromethane was treated dropwise with 116 ml of 1 *M* boron tribromide in dichloromethane (Aldrich) at −18°C under nitrogen[7]. During addition, the solution became homogeneously dark. The resulting mixture was allowed to come to room temperature and was stirred overnight. The reaction mixture was hydrolysed by adding water, then neutralized with sodium hydrogencarbonate solution. The solid, collected by filtration under suction, was triturated in 100 ml of a hot chloroform–methanol (50:50, v/v) solution, and finally dried under vacuum at 50°C. In this way, **9** was obtained as a pink powder (14.5 g, 96% yield); m.p. 273–275°C (decomp.). Analysis (C, H, N, O): $C_{18}H_{13}NO_2$. ^{1}H NMR ([$^2H_6$]dimethyl sulphoxide): 6.02 (s, 1H, C*H), 6.69 (d, J = 8 Hz, 2H, aromatic), 7.08 (d, J = 8 Hz, 2H, aromatic), 7.32–8.24 (m, 6H, aromatic), 8.67 (s, 1H, NH), 9.42 (s, 1H, OH).

*3-(4'-Glycidyloxyphenyl)-2,3-dihydro-1H-benz[de]isoquinolin-1-one (**10**).* Potassium carbonate (4,5 g, 32 mmol) was added to a solution of **9** (6.88 g, 25 mmol) in 250 ml of acetonitrile. The resulting suspension was stirred magnetically for 3 h under nitrogen, then 4.11 g (30 mmol) of epibromohydrin were added and the mixture was refluxed for 30 h[7]. The solvent was evaporated and the organic material was extracted with chloroform and washed with water until neutrality, then washed with brine. The solvent was evaporated and 8.0 g of raw product resulted, which was purified by chromatography on silical gel with dichloromethane–ethyl acetate (78:22, then 75:25, v/v) as eluent. The solvent was evaporated. Trituration in hot acetonitrile (45 ml) afforded 5.5 g (66% yield) of **10** as a pale yellow powder; m.p. 177–178°C. Analysis (C, H, N, O): $C_{21}H_{17}NO_3$. ^{1}H NMR (C^2HCl_3): 2.74 (m) and 2.90 (t), terminal methylene, 3.33 (m, C*H glycidyloxy), 3.92 (ddd) and 4.21 (dt) for the other methylene, 6.06 (s, 1H, C*H), 6.35 (s, 1H, NH), 6.88 (d, J = 9 Hz, 2H, aromatic), 7.24 (d, J = 9 Hz, 2H, aromatic), 7.12–8.44 (m, 6H, aromatic).

The diastereomeric mixture (with regard to the glycidyloxy chirality) was separated by chiral preparative chromatography using an (*S*)-thio-DNBTyr-A (200 g) packed column (CSP 1)[3,4]. The composition of the mobile phase was determined from analytical optimization data: *n*-hexane–ethanol (65:35, v/v). UV detection was carried out at 254 nm; flow-rate, 30 ml/min; pressure, 13 bar; amount injected, 300 mg each run. The diastereomeric mixture (−)-**10**, eluted first, was obtained with 100% enantiomeric excess (e.e.), measured on analytical CSP 1 (Fig. 4); m.p. 154–156°C; $[\alpha]_D^{22} = -106.9°$ (c = 1, THF). (+)-**10** was obtained with 100% e.e.; m.p. 157–158°C; $[\alpha]_D^{22} = +113.9°$ (c = 1, THF) (Fig. 4).

Synthesis of CSP 2. Anhydrous benzene (50 ml), triethylamine (0.2 ml) and 0.66 g (2 mmol) of (−)-**10** were added to 5 g of LiChrosorb-NH_2 (5 μm). The mixture was stirred magnetically under reflux until the starting (−)-**10** has disappeared (TLC). CSP 2 was isolated by filtration on a fine-pore sintered-glass funnel and was abundantly rinsed with benzene, methanol and diethyl ether, then dried in air; 5.63 g of CSP 2 resulted. Analysis: found, C 23.20, H 3.10, N 1.21, Si 28.90%; calculated, 0.16 mmol of chiral moiety per gram of chiral phase (based on N).

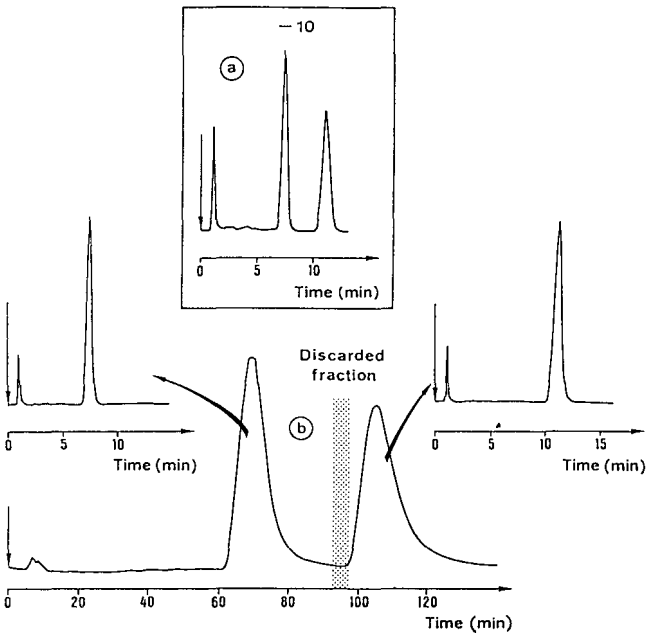

Fig. 4. (a) Analytical and (b) preparative resolution of compound **10** on CSP 1. Mobile phase: *n*-hexane–ethanol (65:35, v/v). Flow-rate: (a) 2 ml/min; (b) 30 ml/min. Amount injected, 300 mg per run; UV detection at 254 nm.

*(±)-N-(3,5-Dinitrobenzoyl)-α-aminobutylamide derivatives (**19–23**).* These compounds were prepared from the corresponding (±)-N-(3,5-dinitrobenzoyl)-α-aminomethyl ester derivatives[7], using the following procedure. The methyl ester (300 mg) was dissolved in a solution of butylamine (3 ml) in dry THF (15 ml). The reaction mixture was then stirred magnetically (about 30 days) at room temperature. Progress of the reaction was monitored by HPLC [CSP 2; mobile phase, hexane–ethanol (85:15, v/v)]. The solvent was evaporated under vacuum and the crude product obtained was purified by chromatography on silica gel with *n*-hexane–ethyl acetate as eluent. After work-up, **19** (m.p. 211.5–212.5°C), **20** (m.p. 198–199°C), **21** (m.p. 212–214°C), **22** (m.p. 130–132°C) and **23** (m.p. 174–176°C) were obtained [Table V, (70:30, v/v) except for compound 20 (75:25, v/v)].

Phthalic anhydride was a convenient precursor for the synthesis of compounds involved with the design optimization of CSP 2 (Fig. 5). Synthesis (reference) and physical data are given in Table I.

RESULTS AND DISCUSSION

Design of the chiral selector (CS)

In order to maximize the behaviour of the reciprocal CSP, we first optimized the design of the chiral moiety intended to be bound to LiChrosorb-NH_2. As compound A (Fig. 2A) is too reactive to be bound directly, the α-methylene unit was replaced with a 1,2-phenylene group combined in the 3,4 position of the lactam (Fig. 2A) to create

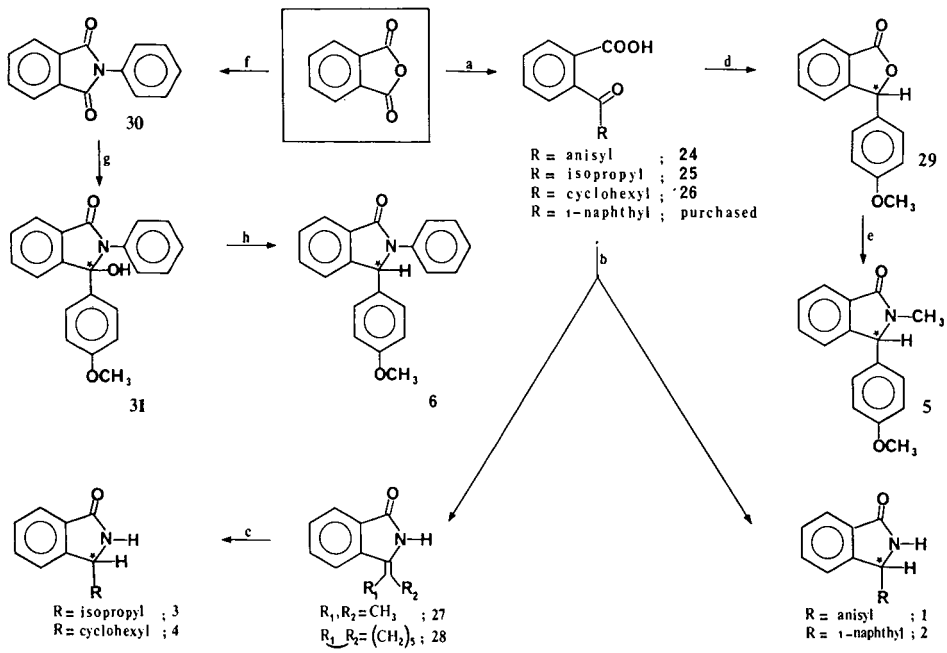

Fig. 5. Syntheses of compounds involved in the design study. (a) RMgBr, THF, reflux 2–3 h, 30–37% yield; (b) formamide, reflux 2.5 h, 52–62% yield; (c) H_2, Pd–$BaSO_4$, solvent ethyl acetate–methanol, 94–99% yield; (d) sodium borohydride, sodium hydroxide, 93% yield; (e) 40% methylamine, 190–200°C, 10 h, 9% yield [and 43% yield of demethylated product (OH)]; (f) aniline, *p*-cymene, reflux 12 h, 55% yield; (g) *p*-anisylmagnesium bromide, THF, 20% yield; (h) H_2, Pd–C, in acetic acid, 21% yield.

TABLE I

MELTING POINTS OF COMPOUNDS INVOLVED IN THE DESIGN OF THE CHIRAL SELECTOR

Compound	*m.p. (°C)*	*Ref.*[a]
1	167–168.5 (ref. 10: 165–166)	10
2	229–231.5	10
3	155.5–157	11
4	184–185.5	11
5	111–112	12
6	148–150	13
24	144–146 (ref. 9: 148)	9
25	122.5–124	9
26	Oil	9
27	220–222	10
28	218–220	10
29	115–115.5	6
30	204–207 (ref. 14: 200–210)	14
31	186–187.5	15

[a] References deal with the synthesis of analogues of the products mentioned.

the isoindolinone skeleton (Fig. 2B). Such a modification enhances the planar character of the CS candidate. With respect to the reciprocality concept, the best resolved derivative of structure B (Fig. 2) on CSP 1 will be expected to constitute the most suitable candidate to be the reciprocal CS. We studied the selectivity (α) of the separation of some B derivatives with respect to the nature of the R and R′ substituent groups (Table II).

Among the series, (±)-3-(4′-methoxyphenyl)isoindolin-1-one (**1**) appeared at this stage to be the most suitable candidate, as (a) **1** has the highest selectivity on CSP 1, which allows the isolation of enantiomers on a preparative scale by chiral chromatography and (b) as previously reported[7], the anisyl group allows easy binding of the chiral moiety to LiChrosorb-NH_2. Chromatographic results demonstrated that the driving force between CSP **1** and compounds **1–6** is governed by the dipolar interaction involving the CSP aliphatic amide dipole and the cyclic amide group (in the *Z* configuration), as no selectivity is observed for compounds **5** and **6**. It should be noted that the dipole moment of the *Z* form of an amide is lower than that of the *E* form[16].

The replacement of the *p*-anisyl moiety (R′) in **1** by an aliphatic group, such as the isopropyl group in **3** or the cyclohexyl group in **4**, leads to a decrease in selectivity. This result suggests that the mechanism for chiral recognition also involves the formation of a π–π charge-transfer complex between the anisyl group (π-electron donor) and the π-electron acceptor 3,5-dinitrobenzoyl group of CSP 1. Nevertheless, this interaction is less significant than the above-mentioned dipolar interaction, as we do not observe a complete loss of selectivity for aliphatic substitution (R′ group, Fig. 2B). More surprising is the fact that the selectivity decreases when R′ is 1-naphthyl (see compound **2**, Table II), whereas this group is considered to be more strongly π-basic than the anisyl group, and hence should be better resolved. In fact, we observed the opposite result, *i.e.*, the bulky character of 1-naphthyl group affects the dipole–dipole interaction developed by the adjacent amide bond. Chromatographic results for compound **2** (Table II) suggested that, in order to enhance the potential π-donating character of the CS candidate, an additional aromatic ring should be incorporated inside the molecule skeleton (see compound **8**, Fig. 2) rather than on the asymmetric centre. Indeed, a significant increase in selectivity is observed for compound **8** in comparison with compound **1** (Tables II and III).

Finally, the methoxy group in (±)-**8** was demethylated using boron tribromide to give the phenol (±)-**9**, then condensed with epibromohydrin to give the ether **10**, which introduces an additional asymmetric centre, thus leading to a mixture of four diastereomers. As racemate **8** is well separated on CSP 1, the separation into two peaks observed for the diastereomeric mixture **10** seems to be due to the same asymmetric centre located in the lactam ring. Therefore, the isolation of two mixtures of two diastereomers was performed by means of chiral preparative chromatography. Fig. 4 illustrates both analytical and preparative resolution of CS **10** on CSP 1. The first eluted fraction, (−)-**10**, is allowed to react with LiChrosorb-NH_2 to lead to CSP 2 (Fig. 3).

Preliminary chromatographic results

The π-basic CSP 2 provides separations of π-acid analytes such as N-(3,5-dinitrobenzoyl) derivatives of α-amino esters (Table IV) and α-aminoamides (Table

TABLE II

SEPARATION OF RACEMATES OF ISOINDOLINONE DERIVATIVES **1–6** ON CSP 1

Mobile phase: *n*-hexane–ethanol (90:10, v/v).

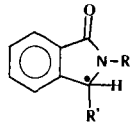

Compound	*R*	*R'*	k'_2[a]	α[b]
1	H	*p*-Anisyl	8.15	1.36
2	H	1-Naphthyl	9.70	1.08
3	H	Isopropyl	2.40	1.07
4	H	Cyclohexyl	2.67	1.15
5	CH_3	*p*-Anisyl	4.25	1.00
6	C_6H_5	*p*-Anisyl	6.29	1.00

[a] k'_2 is the capacity factor of the second eluted enantiomer, $k'_2 = (t_{R2}/t_0) - 1$, where t_{R2} is the retention time of the second eluted enantiomer and t_0 is the retention time of a non-retained solute.

[b] The selectivity, α, between two enantiomers is the ratio of their respective capacity factors (k'_2/k'_1).

TABLE III

SEPARATION OF RACEMATES **8–10** ON CSP 1

Mobile phase: *n*-hexane–ethanol (90:10, v/v).

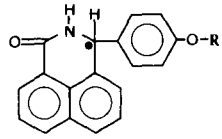

Compound	*R*	k'_2[a]	α[b]
8	CH_3	17.35	1.57
9	H	25.95	1.47
10	Glycidyloxy	48.03	1.61

[a,b] As defined in Table II.

V). Two different mobile phases were studied: *n*-hexane–ethanol and *n*-hexane–chloroform. The sensitive difference in selectivity observed with these two mobile phases clearly indicates how important for chiral recognition is the relative ability of a solvent to act as a proton acceptor (as defined by Snyder[17]), such as ethanol, or as a proton donor[17], such as chloroform. As selectivity is a direct consequence of various interactions between the CSP and each enantiomer, it is not surprising that any competing interaction occurring between the mobile phase and the CSP may alter or enhance chiral separations[18]. The results in Tables IV and V indicate that, regarding selectivity, chloroform is more suitable than ethanol in the mobile phase for the resolution of ester and amide derivatives (Fig. 6).

TABLE IV

SEPARATION OF RACEMATES OF N-(3,5-DINITROBENZOYL) DERIVATIVES OF α-AMINO ESTERS **11–18** ON CSP 2

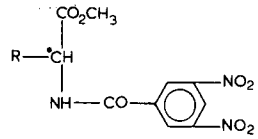

Compound	*R*	*n-Hexane–ethanol (85:15)*			*n-Hexane–chloroform (50:50)*		
		k'_2 [a]	α [b]	*Elution order* [c]	k'_2 [a]	α [b]	*Elution order* [c]
11	$CH_2C_6H_5$	7.44	1.10	*S*	6.23	1.19	*S*
12	C_6H_5	8.10	1.17	*S*	6.30	1.26	*S*
13	$CH_2CH(CH_3)_2$	4.09	1.15	*S*	8.11	1.32	*S*
14	$CH(CH_3)_2$	4.15	1.08	*S*	3.95	1.21	*S*
15	$CH_2CH_2SCH_3$	8.92	1.15	*S*	10.38	1.30	*S*
16	CH_3	6.39	1.15	*S*	10.57	1.31	*S*
17	p-$CH_2C_6H_4OCH_2CH=CH_2$	9.33	1.08	*S*	5.93	1.16	*S*
18	$CH_2CH_2CO_2CH_3$	9.80	1.13	*S*	6.80	1.26	*S*

[a,b] As defined in Table II.

[c] Absolute configuration of the first-eluted enantiomer.

The most important phenomenon is a reversal of elution order of enantiomers between α-amino esters **11–18** (*S,R* elution order, Table IV) and α-aminoamides **19–23** (*R,S* elution order, Table V). This indicates that the two families of racemates are resolved according to two different chiral recognition mechanisms. The presence of

TABLE V

SEPARATION OF RACEMATES OF N-(3,5-DINITROBENZOYL) DERIVATIVES OF α-AMINO-BUTYLAMIDES **19–23** ON CSP 2

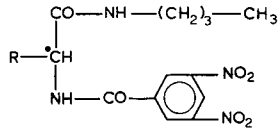

Compound	*R*	*n-Hexane–ethanol (90:10)*			*n-Hexane–chloroform (30:70)*		
		k'_2 [a]	α [b]	*Elution order* [c]	k'_2 [a]	α [b]	*Elution order* [c]
19	$CH_2C_6H_5$	9.71	1.13	*R*	9.37	1.48	*R*
20	C_6H_5	9.25	1.08	*R*	5.30	1.32	*R*
21	$CH_2CH(CH_3)_2$	5.12	1.33	*R*	8.4	1.92	*R*
22	$CH_2CH_2SCH_3$	10.06	1.08	*R*	8.79	1.49	*R*
23	p-$CH_2C_6H_4OCH_2CH=CH_2$	12.36	1.18	*R*	8.88	1.79	*R*

[a,b] As defined in Table II.

[c] Absolute configuration of the first-eluted enantiomer.

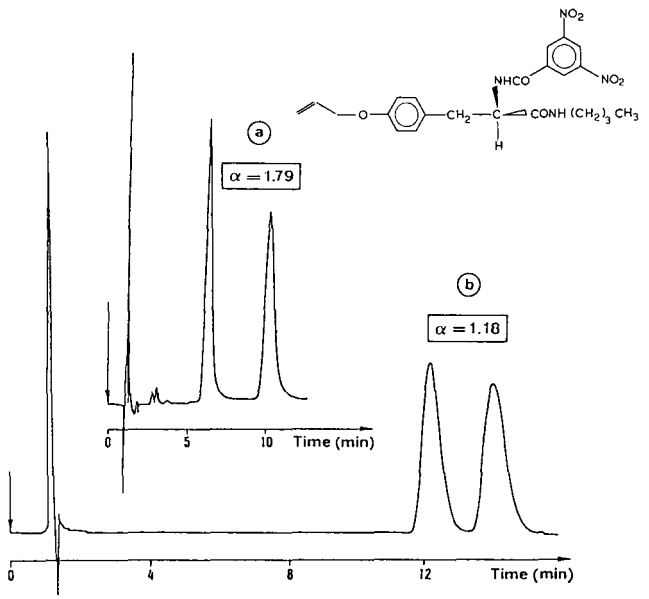

Fig. 6. Resolution of (±)-N-(3,5-dinitrobenzoyl)-O-allyltyrosine *n*-butylamide, (±)-**23**, on CSP 2. Mobile phase: (a) *n*-hexane–chloroform (30:70, v/v); (b) *n*-hexane–ethanol (90:10, v/v). Flow-rate, 2 ml/min; UV detection at 254 nm.

a second aliphatic amide dipole for solutes **19–23** influences the nature and/or the strength of interaction prevailing in the chiral recognition mechanism.

Two chiral recognition models can be proposed (Fig. 7) to account for possible interactions between CSP 2 (arbitrary *R* configuration) and amide or ester solutes. From steric considerations, the preferred approach of the solute towards the CSP

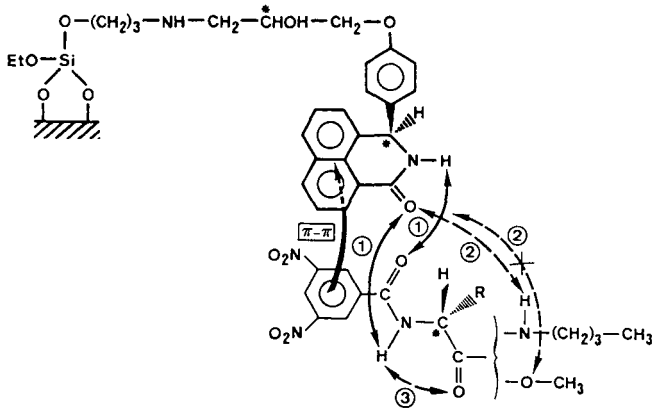

Fig. 7. Proposed chiral recognition model, showing the relative coplanar arrangement which provides several simultaneous interactions between CSP 2 (of arbitrary *R* configuration) and (*R*)-N-(3,5-dinitrobenzoyl) derivatives of α-amino methyl esters and *n*-butylamides. Interactions depicted are π–π charge-transfer complex; (1) dipole stacking between the two aromatic amide functional groups; (2) hydrogen bonding for *n*-butylamide only; (3) intramolecular hydrogen bonding.

occurs preferably on the side of the hydrogen atom, rather than on the side of the aromatic substituent.

Both mechanisms involve the formation of a π–π charge-transfer complex between the 1,8-naphthylene group of CSP 2 and the 3,5-dinitrophenyl group of α-amino ester or α-aminoamide derivatives. In mechanism (1), a stacking dipole interaction [Fig. 7, see (1)] is expected between the solute aromatic amide dipole and the CSP 2 amide group. In mechanism (2), a hydrogen-bonding interaction [Fig. 7, see (2)] is established between the aliphatic NH group of the solute and the carbonyl group of the CSP 2. α-Amino esters **11–18** can only be resolved according to mechanism (1), whereas α-aminoamides **19–23** can be resolved according to both mechanisms. From the examination of CPK models, these two mechanisms act in opposite stereochemical senses. As a reversal of elution order is observed between esters and amides, mechanism (2) seems to prevail for the resolution of α-aminoamides **19–23**. The study of the influence of the nature of the mobile phase on selectivity further confirms this assumption. In fact, owing to its acidic character, chloroform interacts with carbonyl groups of either ester or aliphatic amide groups. This competing interaction may lead to a decrease in the intramolecular hydrogen bonding [Fig. 7, see (3)] and may reinforce the acidic character of the hydrogen atom of the solute aliphatic amide. This may create stronger hydrogen bonding [Fig. 7, see (2)], thus leading to a noticeable increase in selectivity for amides **19–23**. Such a phenomenon cannot occur for esters **11–18**: the increase in the selectivity for the resolution of these solutes was observed to be of lesser importance when chloroform was used instead of ethanol as organic modifier (Table IV).

CONCLUSION

In this paper, the step-by-step optimization of the design of a new π-basic CSP derived from the benz[*de*]isoquinolinone skeleton has been presented. The choice of a chiral selector based on the reciprocality concept was described. This chiral selector was easily prepared with high optical purity by means of preparative-scale chromatography, and was easily bound to LiChrosorb-NH_2. First chromatographic results were presented. Once again, the nature of the polar modifier in the mobile phase (as defined by Snyder[17]) was found to be of great importance for the chiral recognition process[18,19]. *n*-Hexane–chloroform was shown to be more suitable than *n*-hexane–ethanol for the resolution of series of N-(3,5-dinitrobenzoyl) derivatives of α-aminoamides and α-amino esters. Two chiral recognition processes were finally proposed, depending on the chemical nature of the solute.

ACKNOWLEDGEMENTS

The authors are grateful to Michelle Lienne and Pierre Macaudière for useful discussions.

REFERENCES

1 M. Lienne, M. Caude, A. Tambuté and R. Rosset, *Analusis*, 15 (1987) 431.
2 P. Macaudière, A. Tambuté, M. Caude, R. Rosset, M. A. Alembik and I. W. Wainer, *J. Chromatogr.*, 371 (1986) 177.

3 A. Tambuté, A. Begos, M. Lienne, P. Macaudière, M. Caude and R. Rosset, *New J. Chem.*, in press.
4 A. Tambuté, M. Lienne, P. Macaudière, M. Caude and R. Rosset, paper presented at the *Twelfth International Symposium on Column Liquid Chromatography, Washington, DC, June 19–24, 1988.*
5 C. Belaud, C. Roussakis, Y. Letourneux, N. E. Alami and J. Villieras, *Synth. Commun.*, 15 (1985) 1233.
6 W. H. Pirkle and T. J. Sowin, *J. Chromatogr.*, 396 (1987) 83.
7 A. Tambuté, A. Begos, M. Lienne, M. Caude and R. Rosset, *J. Chromatogr.*, 396 (1987) 65.
8 M. S. Kharash and O. Reinmuth, *Grignard Reactions of Non-Metallic Substances*, Prentice Hall, New York, 1954, p. 846.
9 C. Weizmann, E. Bergmann and F. Bergmann, *J. Chem. Soc.*, (1935) 1367.
10 H. J. W. Vollmann, K. Bredereck and H. Bredereck, *Chem. Ber.*, 105 (1972) 2933.
11 E. Kupfer and W. Keller-Schierlein, *Helv. Chim. Acta*, 62 (1979) 1525.
12 W. Theilacker and W. Schmidt, *Justus Liebigs Ann. Chem.*, 597 (1955) 95.
13 D. M. Bailey and C. G. de Grazia, *J. Org. Chem.*, 35 (1970) 4093.
14 J. M. Chapman, P. J. Vorstad, G. H. Cocolas and I. H. Hall, *J. Med. Chem.*, 26 (1983) 237.
15 G. Wittig, G. Closs and F. Mindermann, *Justus Liebigs Ann. Chem.*, 594 (1955) 7.
16 S. Patai, *The Chemistry of Double-Bonded Functional Groups*, Vol. I, Wiley, Chichester, 1977, p. 68.
17 L. R. Snyder, *J. Chromatogr.*, 92 (1974) 223.
18 P. Macaudière, M. Lienne, M. Caude, R. Rosset and A. Tambuté, *J. Chromatogr.*, in press.
19 P. Pescher, M. Caude, R. Rosset and A. Tambuté, *J. Chromatogr.*, 371 (1986) 159.

Journal of Chromatography, 475 (1989) 167–175
Elsevier Science Publishers B.V., Amsterdam — Printed in The Netherlands

CHROM. 21 511

HIGH-PERFORMANCE CHROMATOFOCUSING OF PROTEINS ON AGAROSE COLUMNS

I. MACROPOROUS 15–20 μm BEADS

STELLAN HJERTÉN and JIN-PING LI[a]

Institute of Biochemistry, University of Uppsala, Biomedical Center, P.O. Box 576, S-751 23 Uppsala (Sweden)

(Received March 14th, 1989)

SUMMARY

The synthesis of a polyethyleneimine based anion exchanger is described. The titration capacity was highest at alkaline pH (14–16 mequiv. per 100 g agarose bed) and roughly constant in the interval pH 3–8 (8–10 mequiv. per 100 g agarose bed). The resolution has been determined as a function of flow-rate, concentration of the eluting buffer (Polybuffer™) and sample load. The mass recovery was about 100%, whereas the recovery of the enzymatic activity of β-galactosidase was slightly below 90%. Human serum albumin was isocratically eluted without tailing in 0.05 *M* Tris–HCl, pH 7.5, containing 0.5 *M* sodium chloride, indicating that the beads were hydrophilic. The focusing effect was demonstrated by photographing a separation of haemoglobins A, F, S and C and by application of a sample in different volumes and at different times during the course of the generation of the pH gradient (a sample volume 40-fold larger than the bed volume did not affect the resolution). The resolution increased upon dilution of the Polybuffer up to at least 160-fold; there is accordingly no need to use large amounts of this expensive buffer (a dilution greater than 1:80 is not recommended, since the concentration in the protein zones then becomes low).

INTRODUCTION

Since it was introduced in 1962 as a chromatographic support[1], agarose, a polysaccharide from red seaweed, has probably become the most widely used gel matrix for the fractionation of macromolecules by classical low pressure chromatography, including chromatofocusing. About 20 years later experiments with highly concentrated, cross-linked agarose beads suitable for high-performance liquid chromatography (HPLC) columns, were reported[2]. During the last few years various column packings based on agarose have been prepared and used successfully for HPLC of proteins: for instance, beds for molecular sieving[3–6], hydrophobic inter-

[a] Permanent address: Institute of Radiation Medicine, Beijing, China.

0021-9673/89/$03.50

action chromatography[7], ion-exchange chromatography[8,9], affinity chromatography[10] and boronate chromatography[11].

In this paper we describe the chromatographic properties of a macroporous agarose-based HPLC matrix for chromatofocusing.

MATERIALS AND METHODS

The macroporous, cross-linked 12% agarose beads (diameter: 15–20 μm) were a gift from Dr. Sten Porrvik, Casco Nobel, Sundsvall, Sweden. They were prepared by a modification of a method published previously[12] and were then cross-linked. Polyethyleneimine (molecular weight: 30 000) was obtained from Serva (Heidelberg, F.R.G.); Polybuffer™ from Pharmacia (Uppsala, Sweden); β-galactosidase from Boehringer (Mannheim, F.R.G.); haemoglobin A, F, S and C from Isolab (Akron, OH, U.S.A.); and sodium borohydride from E. Merck (Darmstadt, F.R.G.). Human serum albumin and human transferrin were gifts from KabiVitrum (Stockholm, Sweden). Other chemicals, including butanediol diglycidyl ether, Bis-Tris [bis(2-hydroxyethyl)iminotris(hydroxymethyl)methane], ovalbumin and *o*-nitrophenyl-D-galactopyranoside, were obtained from Sigma (St. Louis, MO, U.S.A.).

The Model 2150 HPLC pump, the Model 2152 HPLC controller, the Models 2138 and 2158 detectors and the Model 2210 recorder were from LKB-Products (Bromma, Sweden). The Model 7125 loop injectors were from Rheodyne (Berkely, CA, U.S.A.). The pH-monitor was from Pharmacia. The column tubes, made from Plexiglas, had an inner diameter of 6 mm (their design has been described in ref. 13). They were packed with agarose beads suspended in deionized water at a flow-rate of 1.0 ml/min.

EXPERIMENTAL AND RESULTS

Synthesis of the anion exchanger

The cross-linked agarose beads were treated with 1,4-butanediol diglycidyl ether essentially as described by Maisano *et al.*[14]. By this treatment the agarose chains became not only further cross-linked (in the case when both epoxide groups reacted with the agarose chains) but also activated (in the case where only one epoxide group reacted with the agarose; the other epoxide group was used later for coupling to polyethyleneimine). In brief, the activation (and attendant cross-linking) was performed as follows. Sedimented gel (1 g) was suspended in 1 ml of 0.6 *M* sodium hydroxide and mixed with 0.5 ml of 1,4-butanediol diglycidyl ether and 2 mg of sodium borohydride. After stirring for 15 h at room temperature, the beads were washed with water by centrifugation until the supernatant had a pH of 7–8. The agarose beads, thus activated, were suspended in 1 ml of 0.5 *M* sodium bicarbonate (pH 8.0) containing 6 mg of sodium borohydride[9]. An appropriate amount of polyethyleneimine was added and the suspension was stirred at room temperature for various periods of time. The beads were finally washed with water on a Büchner funnel. The reaction scheme is found in ref. 9.

If not otherwise stated, we used 0.5 ml of polyethyleneimine per gram sedimented agarose and a reaction time of 7 h. After each experiment the columns were cleaned with about 1 ml of a 2 *M* solution of sodium chloride prior to equilibration with the starting buffer.

Titration of the synthesized anion exchanger

The titration was performed essentially as described by Peterson and Sober[15]. A 3-g amount of the sedimented ion exchanger was suspended in 10 ml of a 0.5 *M* solution of sodium chloride prepared from boiled water for the removal of carbon dioxide. The titration capacity in different pH intervals is presented in Fig. 1 along with the total titration capacity as a function of the reaction time and volume of polyethyleneimine used for the synthesis.

Recovery

The column (30 mm × 6 mm I.D.) was equilibrated with 0.025 *M* Bis-Tris, pH 6.5. Ovalbumin (2 mg) was dissolved in 0.1 ml of this buffer and applied to the column. The protein was eluted with Polybuffer 74 (diluted 1:10)–HCl, pH 4, at a flow-rate of 1.0 ml/min. From measurements of the volume and absorption at 280 nm of both the applied sample and the eluted fractions, the mass recovery was estimated at 99%. For human serum albumin (1 mg) the recovery was 100%.

The recovery of enzymatic activity, using β-galactosidase as a sample, was determined in an analogous way to be 89%. When both the starting and eluting buffers contained 1% (w/v) G3707, or 10%, or 20% (v/v) ethylene glycol, the recovery was estimated at 88, 87 and 72%, respectively.

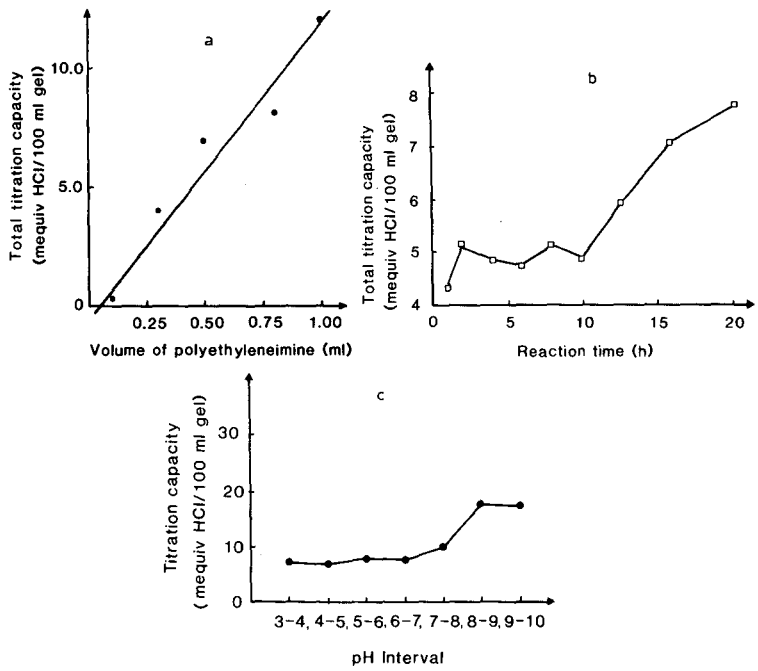

Fig. 1. The total titration capacity as a function of the amount of polyethyleneimine added (a) and as a function of reaction time (b). The titration capacity within different pH intervals is presented in (c). The reaction time in (a) and (c) was 7 h; 0.5 ml of polyethyleneimine per gram agarose were used in (b) and (c).

Resolution as a function of flow-rate

A Plexiglas column with an inner diameter of 6 mm was packed at a flow-rate of 1.2 ml/min to a height of 30 mm with the 12%, cross-linked 15–20 μm agarose beads. The bed was equilibrated with 0.025 *M* Bis-Tris–HCl, pH 6.5. The sample, 0.5 mg of human transferrin, was dissolved in 100 μl of the equilibration buffer (starting buffer). Elution was performed with Polybuffer 74 (diluted 1:20)–HCl, pH 5.0, at a flow-rate of 1.2 ml/min. The experiment was then repeated at the flow-rates 0.9, 0.6 and 0.24 ml/min. The resolution, R_s, between the two transferrin peaks obtained was calculated at the different flow-rates from the relationship.

$$R_s = \frac{t_2 - t_1}{0.5\ (t_{w2} + t_{w1})} \tag{1}$$

where t_1 and t_2 are the retention times of the tranferrin peaks and t_{w1} and t_{w2} are the peak widths (in time units) at half the peak heights. The results are presented in Fig. 2.

Resolution as a function of Polybuffer concentration

The experimental conditions were similar to those mentioned in the previous section with the exception that the flow-rate was kept constant, 0.6 ml/min, and the dilution of the Polybuffer 74 was varied (1:5, 1:10, 1:20, 1:40, 1:80 and 1:160). Fig. 3a shows a plot of the resolution against dilution. Some of the chromatograms are presented in Fig. 3b in order to give a visual impression of the variations in resolution with the dilution of the Polybuffer.

Resolution as a function of sample load

The column bed (30 mm × 6mm I.D.) was equilibrated with 0.025 *M* triethanolamine–HCl, pH 8.3 (starting buffer). After application of 0.25 mg of a mixture of haemoglobin C, S, A and F, dissolved in 100 μl of the starting buffer, the proteins were eluted at a flow-rate of 0.5 ml/min with Polybuffer 96 (diluted 1:10)–HCl, pH 7.0. The resolution was calculated for haemoglobins C and S according to eqn. 1. After washing with 2 *M* sodium chloride and equilibration of the column, the experiment was

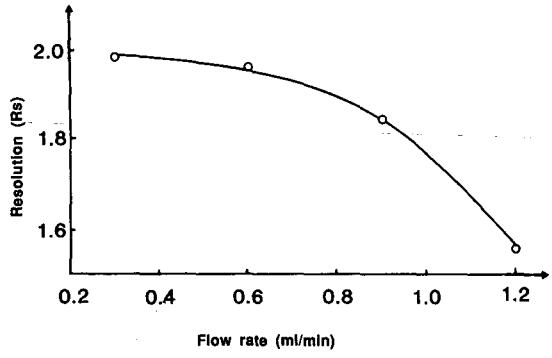

Fig. 2. Resolution as a function of flow-rate. A 0.5-mg amount of transferrin in 100 μl of starting buffer was applied to the column (30 mm × 6 mm) and eluted at flow-rates of 1.2, 0.9, 0.6 and 0.3 ml/min. The resolution between the two transferrin components obtained was calculated from eqn. 1.

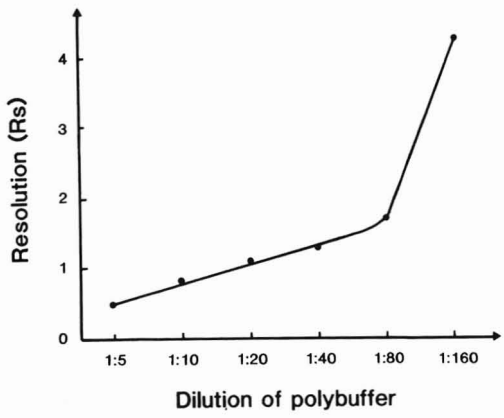

a

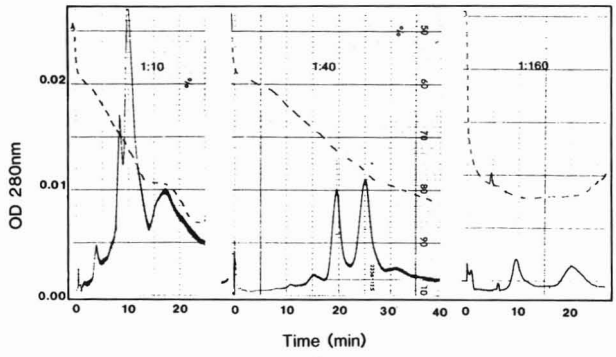

b

Fig. 3. Resolution as a function of dilution of Polybuffer. Transferrin (0.5 mg), dissolved in 100 μl of the starting buffer, was applied to the column and eluted with different concentrations of Polybuffer at a flow-rate of 0.6 ml/min. (a) A plot of resolution against dilution. The resolution between the two transferrin components obtained was calculated from eqn. 1. (b) Chromatograms obtained at different dilutions of Polybuffer. The dashed curve shows the shape of the pH gradient.

repeated with 0.5 mg of haemoglobin. Similar experiments were then performed with 0.75 and 1.0 mg of haemoglobin. Fig. 4 shows a plot of the resolution against the sample load.

Visual inspection of chromatofocusing of haemoglobins C, S, A and F

The dimensions of the agarose bed were 50 mm × 6 mm I.D. Starting and elution buffers were 0.025 *M* triethanolamine–HCl, pH 8.3 and Polybuffer 96 (diluted 1:20)–HCl, pH 7.0, respectively. The sample consisted of 100 μg of a mixture of haemoglobins A, F, S and C, dissolved in 100 μl of the starting buffer. The flow-rate was 1.0 ml/min. A photograph of the column with the focused haemoglobin zones is presented in Fig. 5.

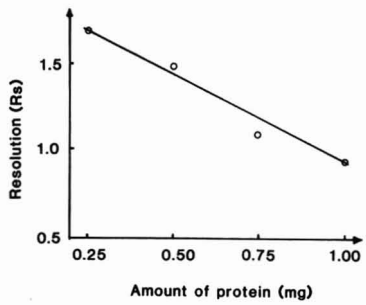

Fig. 4. Resolution as a function of sample load. Samples of Hb C, S, A and F (from 0.25 to 1.0 mg) were dissolved in 100 μl of starting buffer. Elution was performed at a flow-rate of 0.5 ml/min (column dimensions: 30 × 6 mm I.D.). The resolution was calculated for haemoglobins C and S with the aid of eqn. 1.

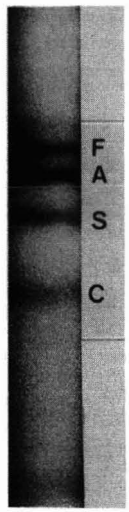

Fig. 5. Photograph of a separation of haemoglobins C, S, A and F by high-performance chromatofocusing. Conditions: column 50 × 6 mm I.D.; sample, 0.1 mg Hb C, S, A and F in 100 μl of starting buffer; flow-rate, 1.0 ml/min. The picture was taken 15 min after sample application.

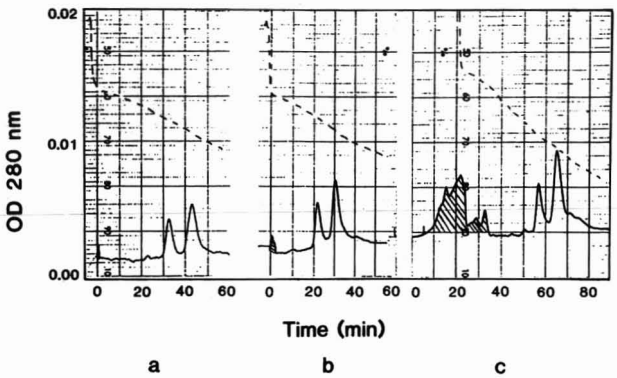

Fig. 6. Demonstration of the focusing effect by application of the sample in different volumes. A 0.5-mg amount of transferrin was dissolved in 0.01 (a), 1.0 (b) and 32 ml (c) of the starting buffer. Column dimensions: 30 mm × 6 mm I.D. Flow-rate: 0.6 ml/min. The shaded peaks are disturbances caused by the sample application. The dashed curves show the shape of the pH gradient. The figure illustrates that the separation pattern is independent of the sample volume.

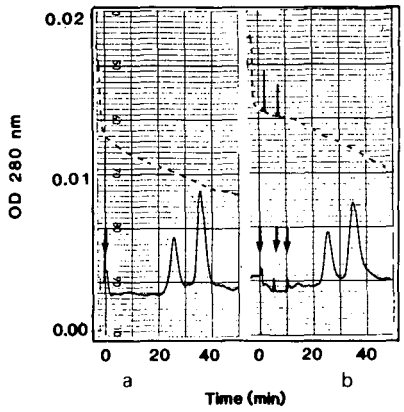

Fig. 7. Demonstration of the focusing effect by application of the sample at different times. (a) The sample (0.5 mg of transferrin) in 100 μl of starting buffer was applied in one injection. (b) The same sample was injected in three 33-μl aliquots at times indicated by arrows. For conditions, see Fig. 6. The dashed curves show the course of the pH gradient. A comparison of the two chromatograms indicates that the focusing pattern is independent of the time of application of the sample.

Demonstration of the focusing effect by application of the sample in different volumes and at different times

The experiments were performed under the same conditions as those given in *Resolution as a function of flow-rate* with the difference that the flow-rate was constant, 0.6 ml/min, and that the sample volumes were 0.01, 1.0 and 32 ml (the latter was injected in 0.6-ml portions every min; the total time for application of this sample was thus about 50 min). The amount of transferrin was 0.5 mg in each case. The chromatograms are presented in Fig. 6. The shaded peaks at the left in the chromatograms do not correspond to proteinaceous material.

The above experiment was then repeated with the exception that the sample was dissolved in 0.1 ml of the starting buffer (Fig. 7a). In another experiment this sample was injected in three aliquots (0.033 ml each) at the times indicated by arrows in the chromatogram (Fig. 7b).

DISCUSSION

Electrofocusing and chromatofocusing, two analogous separation methods

Electrophoresis and chromatography are analogous methods and therefore any electrophoretic method has its chromatographic counterpart and *vice versa*[16]. If more researchers had been aware of this analogy the progress of both these methods would, no doubt, have been faster. For example, electrofocusing of proteins was introduced in 1954 by Kolin[17] and in a more sophisticated version by Svensson (Rilbe) in 1961[18], but it was not until 1978 that chromatofocusing, the chromatographic equivalent of electrofocusing, was first described[19]. Characteristic of both methods is the zone-sharpening effect (Fig. 5), *i.e.*, the final separation pattern is to a great extent independent of the volume of the sample. For chromatofocusing this attractive feature is illustrated in Fig. 6, which shows that a fixed amount of protein gave the same chromatogram when the volume in which the protein was dissolved was varied

3200-fold. This focusing effect (which also can be demonstrated by applying the sample in aliquots; see Fig. 7) has, of course, many advantages, but it may also create problems: the calculated high concentration of proteins in a focused zone is not always attainable because the solubility of many proteins at their isoelectric points is low, resulting in precipitation of the proteins. The presence of such precipitates may decrease the resolution and the recovery considerably and reduce the lifetime of a column. The risk of precipitation can be suppressed if the experiments are performed in the presence of ethylene glycol or a mild neutral detergent such as G3707, heptaoxyethylene lauryl ether[20]. Ethylene glycol has, furthermore, the favourable effect of stabilizing labile proteins (enzymes)[21]. However, the addition of these agents to the buffers did not increase the recovery of activity (89%) of β-galactosidase in the experiments described herein, whereas the mass recoveries of ovalbumin and serum albumin were excellent (about 100%) even in the absence of these agents.

Titration and protein capacity

Sluyterman and Wijdenes[22] found that agarose beads derivatized with polyethyleneimine and used for conventional low-pressure chromatography had a lower titration capacity at basic pH, whereas the column used in this study exhibited the lowest titration capacity in the acidic range (see Fig. 1c). We have no explanation for this discrepancy. In this connection we emphasize that the titration capacity of an ion exchanger is not related to the protein capacity in a simple way, since many of the titrated groups are not available to proteins for steric reasons.

Resolution as a function of the concentration of the eluting buffer

A decrease in the concentration of the eluting Polybuffer affected the resolution favourably (Fig. 3a). Wagner and Regnier[23] did not observe such an effect in their chromatofocusing experiments on Synchropac AX-300. The polyethyleneimine-based anion exchanger used in this study gave a satisfactory separation even when the Polybuffer was diluted as much as 160-fold (see Fig. 3b), which is considerably more than has been reported for other ion exchangers[23]. This is of practical importance, since the high price of Polybuffer limits the usefulness of chromatofocusing, particularly in large-scale operations. However, at a dilution of 1:160 the proteins were eluted at a virtually constant pH (Fig. 3b). The separative mechanism at this extremely high dilution is therefore not based on chromatofocusing but rather on conventional ion-exchange chromatography.

Macroporous vs. deformed non-porous agarose beads

An obvious advantage of conducting chromatofocusing in the HPLC mode as described herein is that columns as short as 3 cm can be used without loss in resolution. The analysis times can accordingly be reduced. However, additional advantages are gained when the macroporous beads used in the experiments described herein are exchanged for non-porous, deformed beads (see the following paper[24]). For instance, the decrease in resolution with an incrase in flow-rate demonstrated in Fig. 2 is in accordance with the van Deemter equation[25], but is not observed on columns packed with the non-porous beads.

The residence time

The time between the first and last injection of the sample in the experiment illustrated in Fig. 6c was about 50 min. Since the focusing patterns in Fig. 6a, b and c are very similar one can conclude that the residence time of proteins on the column will not influence the appearance of the chromatograms; in other words, the adsorption is not time-dependent, which is characteristic also of agarose-based hydrophobic interaction and ion-exchange chromatography[7,9].

ACKNOWLEDGEMENTS

This work was financially supported by the Swedish Natural Science Research Council and the Carl Trygger and the Knut and Alice Wallenberg Foundations.

REFERENCES

1 S. Hjertén, *Arch. Biochem. Biophys.*, 99 (1962) 466–475.
2 S. Hjertén and K. Yao, *J. Chromatogr.*, 215 (1981) 317–322.
3 S. Hjertén, *Acta Chem. Scand.*, Ser. *B*, 36 (1982) 203–209.
4 S. Hjertén and K.-O. Eriksson, *Anal. Biochem.*, 137 (1984) 313–317.
5 K.-O. Eriksson, *J. Biochem. Biophys. Methods*, 11 (1985) 145–152.
6 S. Hjertén, Z.-O. Liu and D. Yang, *J. Chromatogr.*, 296 (1984) 115–120.
7 S. Hjertén, K. Yao, K.-O. Eriksson and B. Johansson, *J. Chromatogr.*, 359 (1986) 99–109.
8 S. Hjertén, *Trends Anal. Chem.*, 3 (1984) 87–90.
9 K. Yao and S. Hjertén, *J. Chromatogr.*, 385 (1987) 87–98.
10 S. Hjertén, *Protides Biol. Fluids*, 30 (1983) 9–17.
11 S. Hjertén and D. Yang, *J. Chromatogr.*, 316 (1984) 301–309.
12 S. Hjertén, *Biochim. Biophys. Acta*, 79 (1962) 393–398.
13 S. Hjertén, in Milton T. W. Hearn (Editor), *HPLC of Proteins, Peptides and Polynucleotides*, VCH Publishers, in press.
14 F. Maisano, M. Belew and J. Porath, *J. Chromatogr.*, 321 (1985) 305–317.
15 E. A. Peterson and H. A. Sober, *J. Am. Chem. Soc.*, 78 (1956) 751–755.
16 S. Hjertén, *J. Chromatogr.*, 270 (1983) 1–6.
17 A. Kolin, *J. Chem. Phys.*, 22 (1954) 1628–1629.
18 H. Svensson, *Acta Chem. Scand.*, 15 (1961) 325–341.
19 L. A. AE. Sluyterman and O. Elgersma, *J. Chromatogr.*, 150 (1978) 17–30.
20 S. Hjertén, J.-l. Liao and K. Yao, *J. Chromatogr.*, 387 (1987) 127–138.
21 S. Hjertén, H. Pan and K. Yao, *Protides Biol. Fluids*, 29 (1982) 15–27.
22 L. A. AE. Sluyterman and J. Wijdenes, *J. Chromatogr.*, 206 (1981) 441–447.
23 G. Wagner and F. E. Regnier, *Anal. Biochem.*, 126 (1982) 37–43.
24 S. Hjertén, J.-P. Li and J.-L. Liao, *J. Chromatogr.*, 475 (1989) 177–185.
25 J. J. van Deemter, F. J. Zuiderweg and A. Klinkenberg, *Chem. Eng. Sci.*, 5 (1956) 271–289.

Journal of Chromatography, 475 (1989) 177–185
Elsevier Science Publishers B.V., Amsterdam — Printed in The Netherlands

CHROM. 21 512

HIGH-PERFORMANCE CHROMATOFOCUSING OF PROTEINS ON AGAROSE COLUMNS

II. DEFORMED NON-POROUS 12–15 μm BEADS

STELLAN HJERTÉN*, JIN-PING LI[a] and JIA-LI LIAO
Institute of Biochemistry, University of Uppsala, Biomedical Center, P.O. Box 576, S-751 23 Uppsala (Sweden)
(Received March 14th, 1989)

SUMMARY

By shrinkage and cross-linking in organic solvents, macroporous agarose beads were rendered impermeable to proteins. Beads derivatized with polyethyleneimine in an aqueous solution gave a relatively linear pH gradient upon elution with Polybuffer™. The titration capacity was 6–7 and 3–4 mequiv. per 100 ml agarose gel at basic and acidic pH, respectively. The columns were packed at pressures high enough to deform the beads, which increases the resolution owing to the decrease in the distance between the beads. The resolution has been determined as a function of the flow-rate, concentration of eluting buffer (Polybuffer) and sample load. Interestingly, the resolution increased with an increase in flow-rate. The importance of choosing an optimum concentration of Polybuffer was also demonstrated in a series of experiments with human growth hormone, which was fractionated into four components when the Polybuffer was diluted 1:80, but not at a dilution of 1:40. The mass recovery was 96% for human serum albumin and 93% for ovalbumin, whereas the recovery of the activity of β-galactosidase was 90%. In comparison with macroporous beads, the deformed (compressed) non-porous beads have the advantage of permitting a more rapid separation and regeneration and to give a resolution which is independent of or even increases with the flow-rate. The protein capacity of the latter beads is not much lower than that of the macroporous beads.

INTRODUCTION

Recently we have described the preparation of chromatographic columns of deformed non-porous agarose beads and their application to the separation of proteins by high-performance hydrophobic interaction chromatography[1,2], ion-exchange chromatography[1,3] and adsorption chromatography based on interaction

[a] Permanent address: Institute of Radiation Medicine, Beijing, China.

0021-9673/89/$03.50

with metal (hydr)oxides[4,5]. These beads have the attractive property that the resolution is almost independent of or increases with an increase in flow-rate.

The main aim of the present work was to investigate whether the latter feature also applied for chromatofocusing on such beads. The paper is thus an extension of the studies presented in the preceding paper[6], which deals with chromatofocusing on macroporous agarose beads. For a rapid comparison of the two agarose beads we have used the same subtitles, when suitable, in these two papers.

MATERIALS AND METHODS

12% Macroporous agarose beads (dimensions: 15–20 μm) were a gift from Mr. Sten Porrvik, Casco Nobel, Sundsvall, Sweden. The beads were prepared essentially according to a method described in ref. 7. Polyethyleneimine (molecular weight 30 000) and boron trifluoride diethyletherate (BF_3) were from Serva (Heidelberg, F.R.G.). Polybuffer™ was from Pharmacia (Uppsala, Sweden). β-Galactosidase, *o*-nitrophenyl-D-galactopyranoside, Bis-Tris[bis(2-hydroxyethyl)iminotris(hydroxymethyl)methane], 1,4-butanediol diglycidyl ether, conalbumin, ovalbumin and a baker's yeast extract were from Sigma (St. Louis, MO, U.S.A.). Dioxane was from Fisons (Loughborough, U.K.). Sodium borohydride and chloroform were from E. Merck (Darmstadt, F.R.G.) and dimethylformamide from BDH Chemicals (Poole, U.K.). γ-Glycidoxypropyltrimethoxysilane was a gift from Mr. H. Gustafsson, Sikema, Stockholm, Sweden; human growth hormone from Professor P. Roos (this institute) and human serum albumin and transferrin from Dr. L.-O. Andersson (KabiVitrum, Stockholm, Sweden). Alcohol dehydrogenase activity was determined essentially as described in ref. 8, with the main modifications that the substrate was ethanol and that the assay was performed at pH 8.5 (this reference deals with the activity measurement of glucose-6-phosphate dehydrogenase).

All solutions were prepared with Milli Q pure water and degassed before use.

INSTRUMENTATION

The chromatographic equipment was as described in Part I[6].

The column tubes were made of Plexiglas with an inner diameter of 0.6 cm (for design details, see ref. 9). They were packed in water at a flow-rate higher than that used in the subsequent experiments and sufficiently high to deform the beads strongly. The movable piston was then pressed down to make contact with the upper surface of the gel bed to prevent the compressed bed from expanding upon reduction of the flow-rate for chromatographic experiments.

EXPERIMENTAL AND RESULTS

Preparation of non-porous agarose beads

The macroporous agarose beads were shrunk and cross-linked in organic solvents[1,2]. Briefly, 5 g of agarose beads were washed with distilled water by centrifugation at 1000 *g* for 2 min (these centrifugation conditions were used in all subsequent washings) and then transferred to dioxane by washing three times with water–dioxane (1:1) and three times with dioxane. Finally, 5 ml of a mixture of dioxane–chloroform

(1:1) was added. This washing procedure was repeated twice. The volume of the beads was then about 1/3 of that originally. The shrunken beads were suspended in 25 ml of chloroform. With stirring, 4 ml of the cross-linker, γ-glycidoxypropyltrimethoxysilane, was added followed by 0.9 ml of BF_3 in 15 ml of chloroform as a catalyst for activation of the epoxide groups in the cross-linker. After 30 min the beads were transferred back to water by centrifugation and washing with dioxane, dioxane–water (1:1) and water. The beads, thus prepared, were impenetrable to proteins[1–3]. The diameters of the shrunken, cross-linked beads were 12–15 μm.

Coupling of polyethyleneimine to non-porous beads and determination of the titration capacity

This coupling was performed essentially as described in refs. 10 and 11 with some modifications. A 1-g amount of the cross-linked non-porous agarose beads was suspended in 1.0 ml of 0.5 *M* sodium bicarbonate (pH 8.0) containing 6 mg of sodium borohydride, and 1.0 ml of polyethyleneimine was then added. This imine has been used previously for the preparation of ion exchangers suitable for chromatofocusing[12]. The mixture was stirred at room temperature for 4 h. The beads were then transferred to chloroform and cross-linked once more with γ-glycidoxypropyltrimethoxysilane according to the procedure described in the preceding section.

The titration capacity was determined in the presence of 0.5 *M* sodium chloride as described in Part I[6]. The result is presented in Fig. 1. Curve A was obtained for beads prior to the second cross-linking and curve B afterwards. Beads corresponding to curve B were used in this study, because they permitted higher flow-rates, even though the capacity was lower than that of the beads cross-linked only once (curve A). Higher titration capacity was accomplished by prolonging the time of reaction with polyethyleneimine, but at the expense of the rigidity of the beads.

Coupling in an organic solvent (dimethylformamide) was carried out as follows: 1 g of cross-linked non-porous agarose beads was transferred to dimethylformamide by repeated centrifugation and washing steps. After the last washing, 10 ml of dimethylformamide and then 1.0 ml of polyethyleneimine were added, followed by 30 mg of $SnCl_4$ as a catalyst[13]. The mixture was stirred at room temperature for 1 h. The gel had an higher total titration capacity but the capacity within different pH intervals

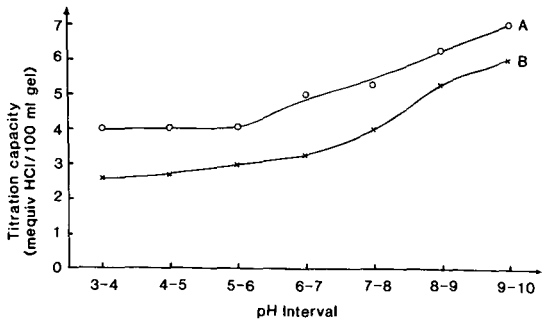

Fig. 1. The titration capacity within different pH intervals. A 3-mg amount of gel in 10 ml of 0.5 *M* NaCl solution was titrated with 0.1 *M* HCl. (A) Cross-linked gel coupled with 1.0 ml of polyethyleneimine per gram gel for 4 h; (B) gel (A) cross-linked again.

varied in a non-regular way and the resolution on these beads was not satisfactory. Therefore they were not used further.

Estimation of protein recovery

Human serum albumin (HSA) and ovalbumin were employed as samples for estimation of mass recovery. HSA (0.2 mg) dissolved in 100 μl of the starting buffer (0.025 *M* Bis-Tris–HCl, pH 5.5) was applied to the column (5.0 cm × 0.6 cm I.D.) and eluted with Polybuffer 74 (diluted 1:40)–HCl, pH 4.0, at a flow-rate of 2 ml/min. Ovalbumin was treated in the same way, but the amount of protein was 1 mg. The volumes of the eluted fractions were measured along with their absorption at 280 nm. From these data, the mass recovery of HSA was estimated at 96% and that of ovalbumin at 93%.

A sample of β-galactosidase (500 μg in 100 μl of the starting buffer) was subjected to chromatofocusing under the same experimental conditions, although the bed height was 2.5 cm and the flow-rate 1 ml/min. The recovery of the enzyme activity was 90%.

Resolution as a function of flow-rate and Polybuffer concentration

A Plexiglas column with an inner diameter of 0.6 cm was packed in water at a flow-rate of 5.0 ml/min to a height of 3.0 cm with the 12% shrunken non-porous agarose beads (see Instrumentation). The bed was equilibrated with 0.025 *M* Bis-Tris–HCl, pH 6.5.

Human transferrin (0.25 mg) was dissolved in 50 μl of the equilibration buffer (starting buffer) and applied to the column. The sample was desorbed at a flow-rate of 4.8 ml/min with Polybuffer 74 (diluted 1:40)–HCl, pH 5.0. Similar experiments were performed at the flow-rates 2.4, 1.2 and 0.6 ml/min. Two transferrin peaks were obtained. The resolution, R_s, between them was calculated at different flow-rates from eqn. 1 in Part I[6].

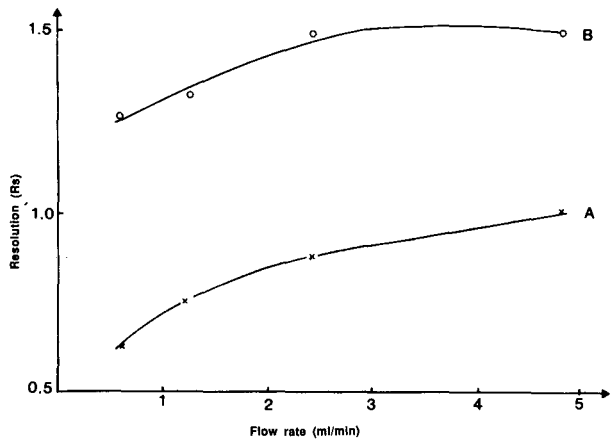

Fig. 2. Resolution as a function of flow-rate and dilution of Polybuffer. After application of 0.25 mg of human transferrin in 50 μl of starting buffer the column (3.0 cm × 0.6 cm I.D.) was eluted at the flow-rates 4.8, 2.4, 1.2 and 0.6 ml/min. (A) Polybuffer diluted 1:40; (B) Polybuffer diluted 1:80. The resolution was determined for the two transferrin peaks obtained.

The results are presented in Fig. 2, curve A. The experiment was then repeated, with the difference that the Polybuffer was diluted 1:80 (see Fig. 2, curve B).

Resolution as a function of sample load

The sample consisted of 0.25 mg of human transferrin dissolved in 100 μl of the buffer, 0.025 *M* Bis-Tris–HCl, pH 6.5. Following equilibration of the column bed (2.5 cm × 0.6 cm I.D.) with this buffer, the sample was applied and then eluted at a flow-rate of 2.0 ml/min with Polybuffer 74 (diluted 1:80)–HCl, pH 5.0. The resolution was calculated as in the previous section. The column was then washed with 2 *M* sodium chloride. Following equilibration of the column, a similar experiment was carried out with 0.5 mg of transferrin. In the same way, the resolution was determined for 1.0 and 2.0 mg of the same protein. A plot of the resolution against the sample load is presented in Fig. 3.

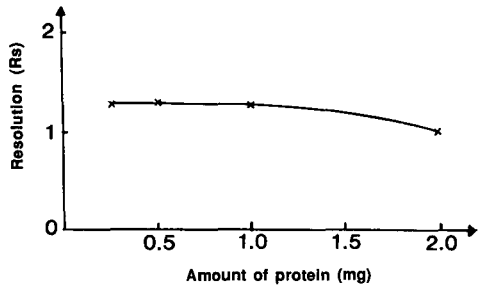

Fig. 3. Resolution as a function of sample load. Samples of human transferrin (0.25, 0.5, 1.0 and 2.0 mg in 100 μl of starting buffer) were applied on the column (2.5 cm × 0.6 cm I.D.) and eluted at a flow-rate of 2.0 ml/min. The resolution was calculated for the two transferrin peaks obtained.

Demonstration of the effect of elution buffer concentration on separation of human growth hormone components

The experiments were performed under the same conditions as given in *Resolution as a function of flow-rate and Polybuffer concentration,* with the difference that the flow-rate was constant at 2.0 ml/min. The column was equilibrated with starting buffer, 0.025 *M* Bis-Tris–HCl, pH 5.5. About 0.5 mg of human growth hormone (HGH) dissolved in the starting buffer were applied to the column and eluted with Polybuffer 74 (1:40)–HCl. After washing with 2 *M* NaCl and reequilibration with the starting buffer, the same amount of HGH was applied and eluted with 80-fold diluted Polybuffer 74–HCl, pH 4.0; the experiment was then repeated with 160-fold diluted Polybuffer 74–HCl, pH 4.0. The chromatograms are shown in Fig. 4.

Chromatofocusing of conalbumin

Since this protein has been used previously as a model substance in methodological studies of chromatofocusing[14], it was of interest to see how it behaved in our chromatographic system. The column (3.0 cm × 0.6 cm I.D.) was equilibrated with 0.025 *M* Bis-Tris–HCl, pH 6.0. Conalbumin (200 μg) was dissolved in 100 μl of this buffer and injected onto the column. Elution was accomplished with Polybuffer 74 (diluted 1:40)–HCl, pH 5.2, at a flow-rate of 1 ml/min (Fig. 5). The continuous

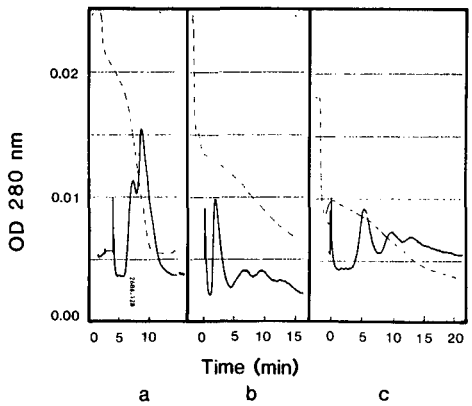

Fig. 4. Chromatofocusing of human growth hormone at different dilutions of the eluting buffer. Sample amount: 0.5 mg. (a) Polybuffer diluted 1:40; (b) Polybuffer diluted 1:80; (c) Polybuffer diluted 1:160. Column: 3.0 cm × 0.6 cm I.D. Flow-rate: 2.0 ml/min. The pH was measured continuously (the dashed curves).

increase in background absorption was probably caused by contaminating substances in the Polybuffer.

Purification of alcohol dehydrogenase from baker's yeast

Following equilibration of the column (4.0 cm × 0.6 cm I.D.) with 0.005 *M* Bis-Tris–HCl, pH 6.5, 400 μg of a yeast extract dissolved in 100 μl of this buffer was applied. For desorption we employed Polybuffer 74 (diluted 1:40)–HCl, pH 4.0. Fractions of 1 ml were collected and their alcohol dehydrogenase (ADH) activity was determined (Fig. 6). The recovery of enzyme activity was 100%, half (52%) being eluted in a peak close to the void peak and half (48%) at a pH around 4.8.

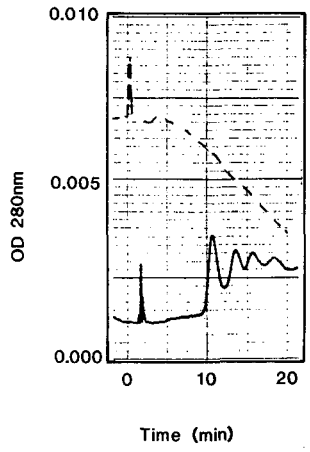

Fig. 5. Chromatofocusing of conalbumin. The column (3.0 cm × 0.6 cm I.D.) was equilibrated at pH 6.0. Conalbumin (200 μg) was eluted with Polybuffer 74 (1:40)–HCl, pH 5.2. Flow-rate: 1 ml/min.

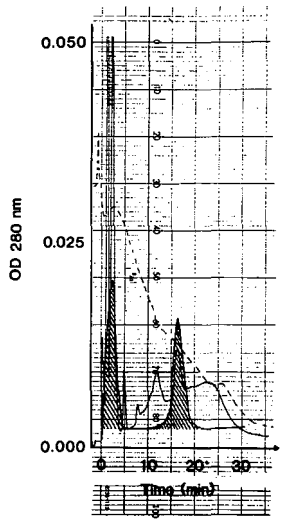

Fig. 6. Purification of alcohol dehydrogenase by chromatofocusing. After equilibration of the column at pH 6.5, 400 μg of the sample (yeast extract) was eluted with Polybuffer 74 (1:40)–HCl, pH 4.0. Enzyme activity was traced to the shaded peaks. Flow-rate: 1 ml/min.

DISCUSSION

Titration capacity

Fig. 1 shows that the titration capacity in different pH intervals of an ion exchanger synthesized from non-porous agarose beads has the same profile as that based on macroporous beads (Fig. 1 in Part I[6]), *i.e.*, the capacity is higher at basic than at acidic pH in contrast to the result reported by Sluyterman and Wijdenes[12]. The titration capacity was higher for the macroporous beads (compare Fig. 1 with Fig. 1c in Part I).

Protein capacity

The non-porous agarose beads were prepared from the macroporous beads used in the experiments described in Part I[6]. After shrinkage and cross-linking, the volume of the beads was about one third that of the original non-shrunken beads[2]. A bed of shrunken beads thus contains many more beads per unit than does a bed of non-shrunken beads. Furthermore, the surface area of a shrunken bead might be about the same as that of a non-shrunken bead, although the surface of the shrunken beads is more creased to judge from scanning electron microscopy pictures. These considerations indicate that the capacity of a bed of non-porous shrunken agarose beads, expressed in terms of the amount of protein adsorbed per ml bed, need not necessarily be much lower than that of a bed of macroporous beads (compare Fig. 3 with Fig. 2 in Part I[6]). The lower capacity is compensated by a shorter regeneration time (see below) and the possibility to operate a column packed with deformed non-porous beads at higher flow-rates without loss in resolution (Fig. 2). The throughput (amount of protein purified per unit time) may therefore be similar. An advantage of the non-porous beads from the viewpoint of preparation is that they can be relatively

large (15–50 μm in diameter) and have a wide size distribution and still give high resolution[1–3].

Resolution as a function of flow-rate

In chromatofocusing[15] as well as in other chromatographic methods based on the use of conventional beds the resolution decreases with an increase in flow-rate. We have shown in several papers that compressed beds of non-porous agarose beads are unique in the sense that they do not follow this rule. These beads have the same attractive feature when utilized for chromatofocusing, as shown in Fig. 2. Some possible explanations for this anomalous behaviour have been treated only briefly[1]. A more thorough discussion will be given elsewhere. Since the resolution increases with the flow-rate upon chromatofocusing on deformed non-porous agarose beads the experiments can be conducted very rapidly without any drawbacks (Fig. 2).

Resolution as a function of the concentration of the eluting buffer

In chromatofocusing on deformed non-porous agarose beads (as for macroporous beads) (see Part I[6]) the resolution increases (Fig. 2) upon dilution of the Polybuffer (although the peaks became broader) and even at dilutions as high as 1:40–1:160 where the buffer capacity is low there was no shoulder in the region of the pH gradient where the proteins were eluted (Figs. 4 and 5). This finding is of practical importance, since Polybuffers are expensive.

Time for regeneration

The macroporous and non-porous agarose beads used for chromatofocusing require 10–15 and 5 bed volumes of the equilibration buffer, respectively, for regeneration. A 1-ml column packed with the latter beads can therefore be regenerated in somewhat more than 1 min at a flow-rate of 4 ml/min.

pI Values

Isoelectric focusing of human growth hormone gives four main peaks with the p*I* values of 4.9, 4.8, 4.7 and 4.6[16]. The chromatofocusing experiments shown in Fig. 4 gave similar p*I* values.

A short comparison between high-performance isoelectric focusing in capillary tubes and high-performance chromatofocusing on deformed non-porous agarose beads

If the flow-rates in the experiments shown in Figs. 5 and 6 are increased to 4 ml/min the analysis times will be about 5–10 min, which are normal in free high-performance isoelectric focusing in capillary tubes with an inner diameter in the range 0.025–0.1 mm[17,18]. This method (which is the electrophoretic counterpart of chromatofocusing) has, however, an higher resolution than chromatofocusing because the separation medium in a carrier-free electrophoresis method (an aqueous solution) is more homogeneous than that in any chromatographic method (a non-uniformly packed bed). In this comparison between isoelectric focusing and chromatofocusing we have considered free high-performance isoelectric focusing (HPIF) in capillary tubes and high-performance chromatofocusing (HPCF) on deformed non-porous agarose beads. This might be justified, since HPIF and HPCF are among the most rapid and most highly resolving methods based on electrophoretic and chromato-

graphic focusing, respectively. The former method has the disadvantage of permitting separation only on a micro-scale.

ACKNOWLEDGEMENTS

This work was financially supported by the Swedish Natural Science Research Council and the Carl Trygger and the Knut and Alice Wallenberg Foundations.

REFERENCES

1 S. Hjertén, K. Yao and Jia-li Liao, *Makromol. Chem., Macromol. Symp.*, 17 (1988) 349–357.
2 S. Hjertén and Jia-li Liao, *J. Chromatogr.*, 457 (1988) 165–174.
3 Jia-li Liao and S. Hjertén, *J. Chromatogr.*, 457 (1988) 175–182.
4 S. Hjertén, I. Zelikman, J. Lindeberg, Jia-li Liao, K.-O. Eriksson and J. Mohammad, *J. Chromatogr.*, in press.
5 S. Hjertén, I. Zelikman and J. Lindeberg, *J. Chromatogr.*, in press.
6 S. Hjertén and Jin-ping Li, *J. Chromatogr.*, 475 (1989) 167–175.
7 S. Hjertén, *Biochim. Biophys. Acta*, 79 (1964) 393–398.
8 P. Cohen and M. A. Rosemeyer, *Eur. J. Biochem.*, 8 (1969) 1–7.
9 S. Hjertén, in M. T. W. Hearn (Editor), *HPLC of Proteins, Peptides and Polynucleotides*, VCH, Weinheim, in press.
10 F. Maisano, M. Belew and J. Porath, *J. Chromatogr.*, 321 (1985) 305–317.
11 K. Yao and S. Hjertén, *J. Chromatogr.*, 385 (1987) 87–98.
12 L. A. Æ. Sluyterman and J. Wijdenes, *J. Chromatogr.*, 206 (1981) 441–447.
13 S. Hjertén, K. Yao, Z.-Q. Liu, D. Yang and B.-L. Wu, *J. Chromatogr.*, 354 (1986) 203–210.
14 G. Wagner and F. E. Regnier, *Anal. Chem.*, 126 (1982) 37–43.
15 *FPLC™ Ion-Exchange and Chromatofocusing*, Pharmacia Laboratory Separation Division, Uppsala, 1985, pp. 132–133.
16 P. Roos, personal communication.
17 S. Hjertén, Jia-li Liao and K. Yao, *J. Chromatogr.*, 387 (1987) 127–138.
18 S. Hjertén, K. Elenbring, F. Kilàr, Jia-li Liao, A. J. C. Chen, S. Siebert and M.-D. Zhu, *J. Chromatogr.*, 403 (1987) 47–61.

Journal of Chromatography, 475 (1989) 187–194
Elsevier Science Publishers B.V., Amsterdam — Printed in The Netherlands

CHROM. 21 542

HYDROLYZED MACROPOROUS GLYCIDYL METHACRYLATE–ETHYLENE DIMETHACRYLATE COPOLYMER WITH NARROW PORE SIZE DISTRIBUTION

A NOVEL PACKING FOR SIZE-EXCLUSION HIGH-PERFORMANCE LIQUID CHROMATOGRAPHY

T. B. TENNIKOVA[a], D. HORÁK and F. ŠVEC*
Institute of Macromolecular Chemistry, Czechoslovak Academy of Sciences, 162 06 Prague (Czechoslovakia)
M. B. TENNIKOV
Science and Technology Corporation, Academy of Sciences of the U.S.S.R., 198 103 Leningrad (U.S.S.R.)
and
E. E. KEVER and B. G. BELENKII
Institute of Macromolecular Compounds, Academy of Sciences of the U.S.S.R., Leningrad 199 004 (U.S.S.R.)
(First received January 6th, 1989; revised manuscript received March 31st, 1989)

SUMMARY

By means of chromatographic methods and mathematical treatment, commercial inorganic and polymeric packings were compared with macroporous glycidyl methacrylate–ethylene dimethacrylate copolymers prepared by the usual polymerization techniques. It was found that the pore size polydispersity of the usual polymeric sorbents is several times higher than that of the inorganic sorbents. For this reason, they are better suited for the separation of mixtures of macromolecules with freely mobile chains than of globular proteins. This was demonstrated by the separation of eleven polystyrene standards and benzene, which was identical with that which can be accomplished only by using a mixed sorbent consisting of several types of silica. Purposeful interferences with the polymerization mixture, *i.e.*, a change in the porogenic mixture, allowed synthesis of polymeric beads in which the pore size distribution was almost identical with that of inorganic packings.

INTRODUCTION

Macroporous polymeric sorbents for size-exclusion (high-performance) liquid chromatography (SEC) are relatively often used in the separation, purification and analysis of proteins, polysaccharides, polynucleotides and other natural polymers, and

[a] On leave from the Institute of Macromolecular Compounds, Academy of Sciences of the U.S.S.R., Leningrad 199 004, U.S.S.R.

0021-9673/89/$03.50

also of many types of synthetic polymers. Some of the best known commercial products, are Separon HEMA (Tessek, Prague, Czechoslovakia)[1], Bio-Gel TSK and Fractogel TSK, both products of TOSOH Japan (TSK GEL PW) distributed by Bio-Rad (Richmond, CA, U.S.A.)[2] and Merck (Darmstadt, F.R.G.)[3] and based on hydrophilic polymers of the methacrylate or polyether type. Compared with inorganic sorbents, especially porous glass and silica, their advantage consists in an high chemical stability in basic media and in a comparatively large pore volume.

With regard to their application in SEC, decisive roles are played by the pore geometry, specific surface area, the average pore size and the pore distribution. These factors also govern the efficiency and selectivity in the separation of macromolecules[4,5]. The structures of inorganic (except glass) and polymeric matrices do not differ in morphology to any important extent, even though their origins are different, but there are considerable differences between the chromatographic properties of the two types of sorbents. The narrowest pore size distribution can undoubtedly be observed in porous glass, but such materials are not available in the particle sizes needed for HPLC. Silica-based sorbents may also have very similar pore properties[6]. Polymeric macroporous sorbents are manufactured by suspension radical polymerization[7]. In the last two cases the porous structure consists of mutually linked submicroscopic globules, which in the case of silica are completely rigid and non-porous.

The arrangement of globules in an individual polymer particle (bead)[8], their sizes and porosities are the main factors which affect the chromatographic properties of a polymeric sorbent. Decisive roles are played by the polymerization conditions and by the composition of the polymerization mixture. Under the usual conditions, the pore size distribution in macroporous polymers is much broader than that observed with inorganic sorbents. For this reason, synthetic polymeric sorbents can on the whole be successfully employed in the separation of macromolecules having a broad molecular weight distribution[2], but they are not suited to the SEC of globular proteins with a narrow size range of macromolecules. This conclusion is reached by comparing the selectivity of separation on polymeric sorbents (TSK GEL PW) and silica-based sorbents with polymeric coatings (TSK GEL SW)[10].

The porous structure of the sorbents affects the separation not only in SEC, but also when modified sorbents are used in other types of HPLC, *e.g.*, hydrophobic interaction, reversed phase and ion exchange[11]. The presence of pores with diameters below about 10 nm markedly lowers the extent of surface modification, and this is negatively reflected in the chromatographic separation.

Thus, there is a need to obtain a polymeric sorbent for the effective SEC separation of rigid globules of proteins, having porous properties close to those of the narrow pore size of inorganic sorbents, but with the additional advantage of being stable also in basic media. A possible route towards this is a variation of the solvent ratio in the porogenic mixture[12,13], and a means of characterizing the required effect is mathematical treatment of the results of chromatographic measurements, *i.e.*, a procedure which is basically identical with the intended application; the results obtained can be applied directly in chromatography.

EXPERIMENTAL

Macroporous copolymers, glycidyl methacrylate–ethylene dimethacrylate (GMA–EDMA), were prepared by the suspension radical polymerization of the two monomers in the presence of a mixture of cyclohexanol and dodecanol as porogenic solvents, and of azobisisobutyronitrile as an initiator. Porogens cause phase separation during cross-linking polymerization, leaving pores in the structure of the final beads. After polymerization had been completed, they were removed from the polymer by washing. A 1% (w/w) solution of poly(vinyl alcohol) in water, which ensures particles with sizes suitable for application in HPLC, was the dispersing phase. The synthesis has been described in detail elsewhere[7,12,13]. The epoxy groups of the macroporous polymer are relatively hydrophobic, but they are reactive, and their presence may lead to irreversible covalent binding of the substances with the sorbent during the chromatographic separation. This is why, prior to packing of the column, the epoxy groups were hydrolyzed in dilute sulphuric acid[9], which gives rise to two vicinal hydroxy groups, increases the hydrophilicity and prevents any chemical reactions that might take place. The extent of hydrolysis was monitored by IR spectroscopy until all epoxides had disappeared from the sorbent. Fractions of the particles were obtained by using an air classifier Multi-Plex Labor Zick-Zack Sichter A 100 MZR (Alpine, Augsburg, F.R.G.), and their widths were determined by means of a Coulter Counter TA II apparatus (Coulter Electronics, Luton, U.K.).

Chromatographic experiments were performed in a TriRotar SR 2 liquid chromatograph (Jasco, Japan) using a RIDK 101 refractometric detector (Laboratory Instruments, Prague, Czechoslovakia) and a spectrophotometric detector UVIDEC IV (Jasco). The columns, 250 mm × 4.6 mm I.D., were packed with sorbents from a slurry in chloroform or acetone under a pressure of 20 MPa. Polystyrene standards (Waters Assoc., Milford, MA, U.S.A.) in tetrahydrofuran (THF) or chloroform (concentration 0.05%, w/w) and dextran standards (Pharmacia, Uppsala, Sweden) in an aqueous solution, concentration 0.5% (w/w) were used for testing.

The porometric characteristics of the sorbents tested were calculated using an approach described in detail in the literature[14,15]. It is based on the measurement of the distribution coefficient, K_d, which is a measure of changes in the free energy of a macromolecule accompanying its penetration into the pores and depends on the coil radius, r, of the polymer molecule of the standard in the given solvent which is related to the molecular weight. The calculation minimizes the sum of the squares of deviations of experimental points from the theoretical curve by variation of the parameters of the model distribution function while applying the experimental dependence of K_d on r/R, where R is the pore radius. To achieve a better approximation to the real system, a method derived for sorbents with non-uniform porosity was used[15]. In this way, the specific surface area, S_g, and the specific pore volume, V_p, were obtained, along with the average pore radius, D_S, calculated from the specific surface area, and also calculated using the pore volume, D_V, and the normalized pore volume V_p/V_t, where V_t is the total sorbent volume in the column.

Using these values, it is possible to calculate the specific pore volume related to the known sorbent density, $V_\rho = V_p/(V_{col} - V_t)$ where V_{col} is the column volume, or the specific pore volume related to the weight of the sorbent $V_w = V_p/w$, and hence also the density of the polymeric sorbent, ρ. Another characteristic quantity is the

specific surface area, $S_{g\rho}$ and S_{gw}, which is obtained as the product of the specific volume, V_ρ or V_w, and of the slope of the initial part of the curve representing the dependence of K_d on r/R mentioned above[15].

The real mixture of polystyrene standards was separated in a microcolumn chromatograph KHZH 1309 (Science and Technology Corporation, Academy of Sciences of the U.S.S.R., Leningrad, U.S.S.R.) provided with a refractometric detector and fluoroplastic columns 350 mm × 0.5 mm I.D., packed either with the sorbent GMA–EDMA (5:95), or with a mixture of porous narrow-dispersion silica gels having a linear calibration graph[16]. The chromatographic analysis took place in 2-butanone, the concentration of the individual components of the mixture being 0.1% (w/w).

RESULTS AND DISCUSSION

Table I collects the data on the composition of the organic phase, used in the preparation of a series of copolymers differing in their cross-linking under otherwise constant reaction conditions. The epoxy groups of these copolymers were hydrolyzed prior to further application.

The procedure chosen for the evaluation of chromatograms of standard compounds (dextrans, polystyrenes) offers the possibility to compare the porometric characteristics of various sorbents used in HPLC, whether inorganic or polymeric. The comparison is however not restricted to the usual characteristics such as the specific surface area, pore volume, pore size distribution, etc., obtained by the B.E.T. method, solvent regain or porosimetry, and mostly in the dry state, *i.e.*, under conditions very far from those prevailing in real applications in various solvents. Table II summarizes the data which characterize the pore properties of a set of commercial inorganic (silica) and polymer sorbents, comparing them with sorbents based on GMA–EDMA. It is clear that there is a considerable difference between the widths of the pore size distributions of inorganic and of polymeric sorbents as characterized by D_V/D_S. Pores

TABLE I

COMPOSITION OF THE ORGANIC PHASE USED FOR SYNTHESIS OF GLYCIDYL METHACRYLATE–ETHYLENE DIMETHACRYLATE SORBENTS

Reaction conditions for polymerization: aqueous phase, 1% (w/w) solution of poly(vinyl alcohol), 60% (v/v), of feed; polymerization temperature 70°C; time 8 h; monomers to porogen mixture ratio 40:60 (v/v).

Sorbent	*Composition of organic phase (%, v/v)*[a]			
	GMA	*EDMA*	*CyOH*	*DoOH*
G-60	60	40	91	9
G-60-WD	60	40	100	0
G-20	20	80	91	9
G-20-WD	20	80	100	0
G-5	5	95	91	9
G-5[b]	5	95	91	9

[a] Abbreviations: GMA = glycidyl methacrylate; EDMA = ethylene dimethacrylate; CyOH = cyclohexanol; DoOH = dodecanol.

[b] Reproducibility test.

smaller than 10 nm and larger than 75 nm are present in polymeric sorbents to a considerable extent. The presence of very small pores as demonstrated below substantially reduces the pore volume accessible to globular proteins (up to 40% of the nominal pore volume), and thus restricts application in the chromatography of proteins. On the contrary, the presence of very large pores, which is in essence due to defects in the steric arrangement of globules in the particle, has been already demonstrated by scanning electron microscopy (SEM)[13]. They are the reason for a lower selectivity in steric exclusion of macromolecules of any type in the molecular weight range 10^2–10^6. The standard sorbents can be still used with advantage in the analysis of mixtures of synthetic polymers containing components having molecular weights above 10^6. The pore size polydispersity of silica-based sorbents is much lower; D_V/D_S lies in the range 1–2, and is thus three to five times lower than that for the usual organic sorbents. It should be stressed, however, that the fraction of pores in unit sorbent volume, V_p/V_t, is not very different for different sorbents, lying in the range 0.5–0.6 in most cases.

In the chromatographic analysis of polymer mixtures possessing a broad molecular weight distribution the high selectivity of silica-based sorbents for proteins is in fact a disadvantage. To make these sorbents suitable for this purpose, chromatographic columns are packed with a mixture of several types of silica with various exclusion limits; their composition must be calculated so as to make the calibration graph for the column linear over the whole range[16]. Fig. 1 shows the calibration dependence of a mixture of silica gels, and also a similar plot for the GMA–EDMA copolymer (G-5). The two plots are very similar. Hence, the sorbent G-5 may be used directly, instead of a laboriously obtained mixture of silica-based sorbents. It can also be seen in Table I that the properties of G-5 and the "linear mixture" are similar. An important advantage of G-5 over silica is the demonstrated stability of the polymer in basic media at usual temperatures[17], whilst their mechanical properties are similar. Fig. 2 illustrates the chromatographic separation of a mixture of eleven polystyrene standards and benzene in a single column packed with the sorbent G-5, which can be regarded as satisfactory.

In the separation of globular proteins, however, the universality for the whole usual range of molecular weights outlined above is not advantageous. Hence we have a challenging task, namely to reduce the pore size distribution to the level of inorganic sorbents while preserving the original pore volume. It has been demonstrated that, in addition to the concentration of the cross-linking agent and temperature, the morphology of macroporous copolymers GMA–EDMA is also affected by the composition of the porogenic mixture[13]. With increasing amount of dodecanol in a mixture with cyclohexanol the specific surface area (B.E.T.) decreases while the pore volume remains the same (solvent regain); bearing in mind the SEM results, it is seen that the presence of dodecanol in the porogenic mixture leads, in particular, to the formation of large pores. The reason is a poorer thermodynamic quality of the porogenic solvent containing dodecanol, resulting in a rapid precipitation of microgels after the onset of polymerization (so-called nuclei which increases to reach the size of globules during subsequent polymerization). Removal of dodecanol from the polymerization mixture will be reflected in a better packing of globules in the macroporous particle and in the elimination of large pores. Two sorbents denoted WD (without dodecanol) were therefore synthesized under identical conditions (with the

TABLE II

CHARACTERISTICS OF THE POROUS STRUCTURE OF INORGANIC AND POLYMERIC SORBENTS FOR SEC[a]

Sorbent	*Producer*	*Material*	D_S *(nm)*	D_V *(nm)*	D_V/D_S	V_p/V_t	V_p *(ml/g)*	S_{gp} *(m^2/g)*	V_w *(ml/g)*	S_{gw} *(m^2/g)*	ρ *(g/ml)*
Lichrospher Si 300	Merck, F.R.G.	Silica	25.0	34.0	1.35	0.60	2.40	180	2.00	165	2.2[b]
Lichrospher Si 500	Merck, F.R.G.	Silica	35.0	49.0	1.40	0.52	1.34	75	–	–	2.2[b]
MPS 250	Gorkii, U.S.S.R.	Silica	16.5	25.5	1.53	0.38	0.60	70	–	–	2.2[b]
Linear mixture L4	Ref. 14	Silica	11.1	51.3	4.58	0.41	0.64	100	–	–	2.2[b]
TSK SW 3000	Toyo Soda, Japan	Silica	13.0	15.0	1.15	0.60	1.75	260	–	–	–
TSK PW 3000	Toyo Soda, Japan	Polymer	7.2	29.2	4.05	0.44	–	–	–	–	–
Separon HEMA BIO 300	TESSEK, Czechoslovakia	Polymer	8.8	36.8	4.15	0.38	–	–	0.63	140	1.3[c]
Separon HEM BIO 1000	TESSEK, Czechoslovakia	Polymer	16.5	84.6	5.10	0.52	–	–	1.34	165	1.4[c]
G-60		Polymer	16.5	85.6	5.19	0.53	–	–	1.55	150	1.45[c]
G-20		Polymer	10.0	42.7	4.25	0.54	–	–	1.50	300	1.44[c]
G-5		Polymer	8.2	41.9	5.09	0.54	–	–	1.55	375	1.46[c]
G-5[d]		Polymer	8.0	42.0	5.25	0.56	–	–	1.58	375	1.45[c]
G-60-WD		Polymer	17.3	41.5	2.40	0.56	–	–	1.17	135	1.45[c]
G-60-WD[d]		Polymer	16.6	49.3	2.95	0.48	–	–	1.0	120	1.50[c]
G-20-WD		Polymer	9.0	20.6	2.30	0.54	–	–	1.12	255	1.43[c]

[a] For abbreviations see text.
[b] Published data.
[c] Calculated data.
[d] Reproducibility test.

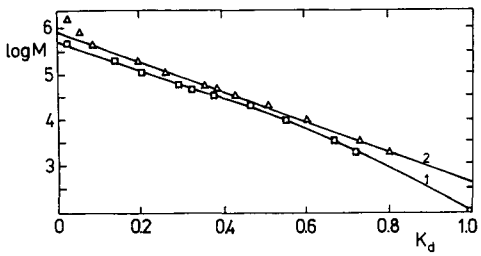

Fig. 1. SEC calibration graphs of the sorbent G-5-(hydrolyzed) (1) and a mixture of silicas (2) for polystyrenes. Conditions: particle size 4–6 μm; metal column 250 mm × 4.6 mm I.D.; eluent THF; elution rate 0.5 ml/min; refractometric detection.

exception of the composition of the porogen). As shown in Table II, the polydispersity of pore size in sorbents of this series does indeed approach that of inorganic sorbents. Fig. 3 demonstrates the pore size distributions of WD sorbents, obtained by mathematical treatment of chromatograms of standards[14,15] and compares them with the distribution of sorbents prepared in the presence of dodecanol. It is clear that the fraction of large pores does indeed considerably decrease but the content of small pores decreases, too. This then leads to a shift of the maximum of the differential distribution curve to somewhat higher values, but the distribution becomes much narrower. The largest fractions in the sorbents G-60-WD and G-20-WD are, respectively, those of pores with sizes 25–27 and 12–16 nm. Pores having radii above 50 nm are hardly present at all in any of the sorbents of the WD series.

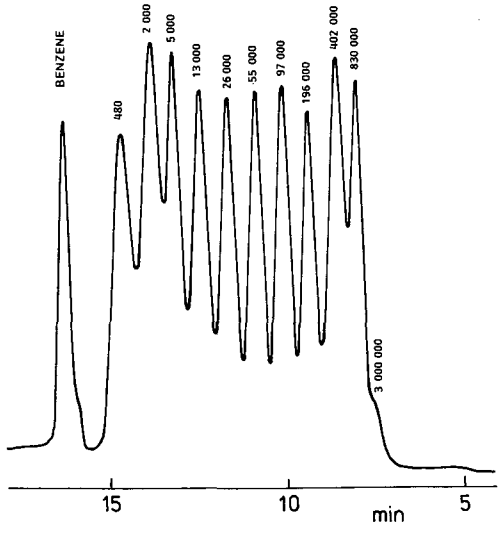

Fig. 2. Size-exclusion HPLC of a mixture of polystyrene standards and benzene. Conditions: sorbent G-5 (hydrolyzed), 4–6 μm; eluent 2-butanone; flow-rate 3 μl/min; PTFE column 350 mm × 0.5 mm I.D.; analysis time 17 min.

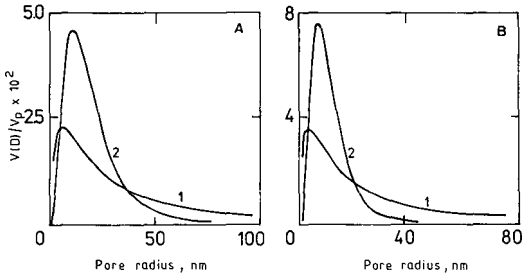

Fig. 3. Effect of the porogenic mixture composition on the pore size distribution of sorbents based on copolymers GMA–EDMA, calculated from chromatographic data. Sorbents: (A) 1 = G-60, 2 = G-60-WD; (B) 1 = G-20, 2 = G-20-WD.

CONCLUSIONS

It has been demonstrated that polymeric sorbents possessing advantageous properties for SEC can be synthesized. A sorbent based on GMA–EDMA (G-5) can replace a mixture of silicas for the separation of polymers with a broad molecular weight distribution. By modifying the composition of the polymerization mixture in the copolymerization of GMA and EDMA, sorbents can be obtained the porous characteristics of which approach those of silica-based commercial sorbents and which have no analogy in commercial polymeric sorbents.

ACKNOWLEDGEMENTS

The authors are indebted to Mr. A. A. Gorbunov for stimulating discussions and to Mr. Z. Plichta, MSc, for his assistance in experimental work.

REFERENCES

1 J. Čoupek, in T. C. Gribnau, J. Visser and R. J. F. Nivard (Editors), *Affinity Chromatography and Related Techniques*, Elsevier, Amsterdam, 1982, p. 165.
2 *Chromatography, Electrophoresis, Immunochemistry, Molecular Biology, HPLC and Liquid Handling*. Catalog N, Bio-Rad Laboratories, Richmond, CA, 1988, p. 52.
3 M. Gurkin and V. Patel, *Am. Lab.*, January (1982) 1.
4 W. W. Yan, J. J. Kirkland, D. D. Bly and H. J. Stoklasa, *J. Chromatogr.*, 125 (1976) 219.
5 J. J. Kirkland, *J. Chromatogr.*, 125 (1976) 231.
6 K. Unger, J. Schick-Kalb and K.-F. Krebs, *J. Chromatogr.*, 83 (1973) 5.
7 F. Švec, J. Hradil, J. Čoupek and J. Kálal, *Angew. Makromol. Chem.*, 48 (1975) 135.
8 Z. Pelzbauer, J. Lukáš, F. Švec and J. Kálal, *J. Chromatogr.*, 171 (1979) 10.
9 T. B. Tennikova, D. Horák, F. Švec, J. Kolář, J. Čoupek, S. A. Trushin, V. G. Maltzev and B. G. Belenkii, *J. Chromatogr.*, 435 (1988) 357.
10 Y. Kato, K. Komiya, H. Sasaki and T. Hashimoto, *J. Chromatogr.*, 193 (1980) 311.
11 T. B. Tennikova, L. V. Vinogradova, V. N. Zgonnik and B. G. Belenkii, *Izv. Akad. Nauk SSSR, Ser. Khim. Nauk*, (1987) 352.
12 D. Horák, F. Švec, M. Ilavský, M. Bleha, J. Baldrian and J. Kálal, *Angew. Makromol. Chem.*, 95 (1981) 117.
13 D. Horák, Z. Pelzbauer, M. Bleha, M. Ilavský, F. Švec and J. Kálal, *J. Appl. Polym. Sci.*, 26 (1981) 411.
14 A. A. Gorbunov, L. Ya. Solovyeva and V. A. Pasechnik, *Vysokomol. Soedin., Ser. A*, 26 (1984) 967.
15 A. A. Gorbunov, L. Ya. Solovyeva and V. A. Pasechnik, *J. Chromatogr.*, 448 (1988) 307.
16 V. V. Nesterov, S. P. Zhdanov, B. I. Venzel, L. Z. Vilenchik, O. I. Kurenbin, T. P. Zhmakina and B. G. Belenkii, *Vysokomol. Soedin., Ser. B*, 26 (1984) 163.
17 J. Hradil and F. Švec, *Reactive Polymers*, 3 (1985) 91.

Journal of Chromatography, 475 (1989) 195–208
Elsevier Science Publishers B.V., Amsterdam — Printed in The Netherlands

CHROM. 21 535

POLYMER-BASED PACKING MATERIALS WITH ALKYL BACKBONES FOR REVERSED-PHASE LIQUID CHROMATOGRAPHY

PERFORMANCE AND RETENTION SELECTIVITY

NOBUO TANAKA*, TOSHIHIRO EBATA, KATSUSHI HASHIZUME, KEN HOSOYA and MIKIO ARAKI

Kyoto Institute of Technology, Department of Polymer Science and Engineering, Matsugasaki, Sakyo-ku, Kyoto 606 (Japan)

(First received February 13th, 1989; revised manuscript received March 29th, 1989)

SUMMARY

Polymer-based packing materials for reversed-phase liquid chromatography, including poly(styrene–divinylbenzene), poly(alkyl methacrylate) and esterified poly (vinyl alcohol), were examined with respect to their performance and retention characteristics for a variety of hydrocarbons in aqueous–organic mobile phases. Materials with alkyl backbones showed performance comparable with silica C_{18} under optimized conditions. The performance is dependent on the molecular shape, rigidity and aromatic character of the solutes as well as on the organic solvents in the mobile phase. Better performance was generally seen with alkyl compounds, compared with aromatic compounds. In a mobile phase containing tetrahydrofuran, in which most packing materials showed better performance than in methanol–water, packing materials with aromatic functionality showed lower efficiencies only for planar polynuclear aromatic hydrocarbons. All the polymer-based packing materials showed preferential retention of aromatic solutes, especially for those with rigid, planar structure rather than flexible, bulky compounds, when these packing materials are compared with a silica C_{18} phase. Polystyrene and poly(vinyl alcohol)-based packing materials showed a greater preference than did the other alkyl-type polymer gels, although this preference was reduced in tetrahydrofuran–water. The retention selectivity and the differences in column performance of the polymer-based phase were explained by the biporous structure of the polymer gels and the solvation of the polymer chains with organic solvents.

INTRODUCTION

An increasing demand for packing materials more stable than silica C_{18} in reversed-phase liquid chromatography (RPLC) has prompted the recent development of polymer-coated silica packings[1–3] and organic polymer-based packing materials, such as poly(styrene–divinylbenzene) (PS)[4–6], poly(alkyl methacrylate) (PAM)[7],

0021-9673/89/$03.50

esterified poly(vinyl alcohol) (PVA)[8,9], alkylated poly(acrylamide)[10] and poly-(hydroxyalkyl acrylate or methacrylate) (PHA), which can be substituted for silica C_{18} when appropriate.

Among the modern polymer-based phases, the most popular PS gels have been used in RPLC for a decade, mainly for the separation of basic compounds and biopolymers[11]. These separations often need severe separation conditions, which may dissolve silica gels. Although PS packing materials sometimes showed lower efficiencies for aromatic solutes than did silica-based packing materials, the performance was adequate for many separations of small molecules and excellent in the separations of polar compounds and polypeptides[12–19].

The performance and retention characteristics of PS have been studied with various mobile phase compositions, temperatures, organic solvents and pore sizes of packing materials. The results were explained in terms of the aromatic character and the solvation of the polymer structures as well as the microporosity in the gel structure[20–32].

We recently showed that alkylated PHA and PVA gels provided preferential retention of rigid, planar compounds rather than bulky flexible solutes compared with silica C_{18}[33]. It is agreed that the biporous structures, microporous primary structures composing macroporous particles, are responsible for the potentially poor performance and preferential retention of rigid solutes shown by polymer gels[22,25,33,34].

Recently some new polymer-based packing materials for RPLC have become available. They include octadecanoylated PVA gel, commercially available as Asahipak ODP-50, PAM gel, available as Shodex DE-613 (described as short alkyl methacrylate by the manufacturer), and alkylated PHA gel, available as TSK C_{18}-4PW. It was thought desirable to assess the performance and retention characteristics of these packing materials, and compare them with those of PS gel and silica C_{18}. Accordingly we examined four polymer-based packing materials, one PS gel and three polymer gels with alkyl backbones, as well as silica C_{18}, with respect to their performance and retention characteristics for a wide range of hydrocarbons with various sizes, shapes, rigidities and planarities. Each polymer-based packing material showed different retention characteristics and performance which are explained by the chemical as well as the micropore structures of these polymer gels.

EXPERIMENTAL

The high-performance liquid chromatography (HPLC) system consisted of an 880 PU pump, 875 UV detector, 830 refractive index (RI) detector (JASCO, Tokyo, Japan) and a 7000A data processor (System Instruments, Tokyo, Japan). The column packing materials, PLRP-S 300 (Polymer Laboratories, Church Stretton, U.K.) and TSK Octadecyl-4PW (abbreviated as C_{18}-4PW; Tosoh, Tokyo, Japan), and the packed columns (both 15 cm × 6 mm I.D.) of Shodex RS pak DE-613 (Showa Denko, Tokyo, Japan) and Asahipak ODP-50 (Asahi, Kawasaki, Japan) were gifts from the suppliers. Silica-based packing materials were prepared as previously described[33]. Silica C_{18}, C_8, PLRP-S and TSK C_{18}-4PW were packed into stainless-steel columns (10 cm × 4.6 mm I.D.).

Samples used for the examination of the effect of molecular shape on the reten-

tion and column performance include pentane (1), hexane (2), heptane (3), octane (4), decane (5), cyclohexane (6), adamantane (7), *trans*-decalin (8), naphthalene (9), anthracene (10), pyrene (11), benz[*a*]pyrene (12), diphenylmethane (13), 1,2-diphenylethane (14), *o*-terphenyl (15), triphenylene (16), triptycene (17), triphenylmethane (18), fluorene (19), benzene (20), toluene (21), ethylbenzene (22), propylbenzene (23), butylbenzene (24) and amylbenzene (25). (Structures were shown in a previous report[33].) Polystyrene standard materials were obtained from Pressure Chemicals (Pittsburg, PA, U.S.A.). Chromatographic measurement and size-exclusion chromatographic (SEC) analysis of the pore size distribution were performed as reported previously[33,35]. Nitrogen adsorption measurement was carried out at the Shiseido Toxicological and Analytical Research Center (Yokohama, Japan).

RESULTS AND DISCUSSION

Table I lists the results of nitrogen adsorption measurement with polymer-based packing materials as well as with some silica gel particles with 30–50 nm pores. The surface areas of the polymer gels were generally larger than those of silica particles of similar pore sizes, although some of the silica particles were found to be mixtures of particles of different pore sizes[35]. The pore size distribution can be measured by SEC[36–38] as well as by the nitrogen adsorption method for these highly cross-linked organic polymer gels. All the polymer gels showed the presence of micropores less than 3 nm diameter in both methods. Fair agreement between the results of the two methods including a micropore region was seen for all the packing materials, as shown in Fig. 1.

In SEC, all the polymer-based packing materials showed selective permeation, or a second plateau, in molecular weight–elution volume curves, at a molecular weight range less than 500 in tetrahydrofuran (THF)[35]. The mean pore size in the meso- and macropore regions decreases in the order TSK C_{18}-4PW, PLRP-S 300, Asahipak ODP-50 and Shodex DE-613. The fraction of the pore volume occupied by

TABLE I

POLYMER AND SILICA-BASED PACKING MATERIALS[a]

Packing material	*Surface area (m^2/g)*	*Pore size (nm)*	*Pore volume (ml/g)*	*Particle size (μm)*
Shodex DE-613	(354)		(0.41)	6
TSK C_{18}-4PW	(48)	(50)	(0.60)	7
Asahipak ODP	(421)	(25)	(1.06)	5
PLRP-S 300	(380)	30 (60)	(1.26)	8
LiChrospher 500[b]	50	50	0.8 (0.90)	10
Nucleosil 300[b]	100 (109)	30	0.8 (0.81)	5
Hypersil 300[b]	60	30	0.6	5
Spherisorb 300[b]	190	30	1.5	5
Vydac TP[b]	80	30	0.6	10

[a] Specifications given by the suppliers (results experimentally obtained by nitrogen adsorption are given in parentheses).

[b] The results for the silica particles are reported in ref. 35.

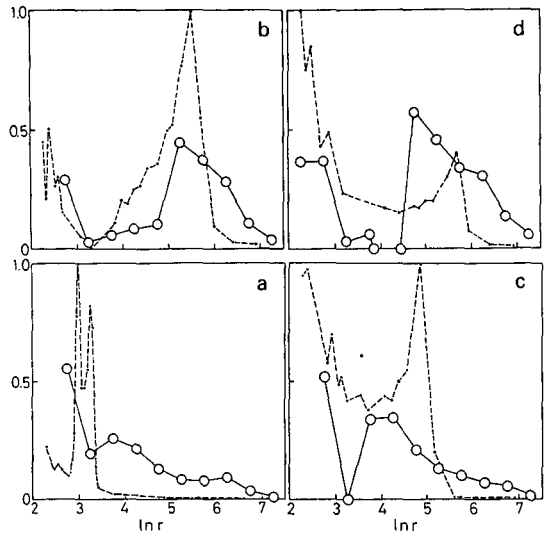

Fig. 1. Pore size measurement by nitrogen adsorption (– – –) and SEC (———). (a) Shodex DE-613; (b) TSK C_{18}-4PW; (c) Asahipak ODP-50; (d) PLRP-S 300. The vertical axis corresponds to the fraction of pore volume, normalized in the case of inverse SEC, and the abscissa corresponds to the logarithm of the pore radius (Å).

micropores increases in the order PLRP-S 300, TSK C_{18}-4PW, ODP-50 and DE-613, as shown in Fig. 1.

The nitrogen adsorption measurement stresses the presence of micropores on ODP-50 and PLRP-S particles. The size of the meso- or macropores determined by nitrogen adsorption increases in the order Shodex DE-613, Asahipak ODP-50, TSK C_{18}-4PW and PLRP-S 300, in fair agreement with the results of SEC. The difference between the results of the two pore-size determination methods in the micropore region is presumably due to the presence of THF in SEC. The results imply that some micropores of ODP-50 and PLRP-S 300 allowed nitrogen to enter, but not larger molecules in SEC. THF causes swelling of these highly cross-linked gels and at the same time fills the micropores[22]. The about 10–15% increases in flow resistance observed with polymer-packed columns compared with silica-packed columns with a change in mobile phase from 80% methanol to 70% acetonitrile or 40% THF, shown in Table II, indicate that these polymers gels are swollen to some extent in these solvents.

As shown in Table II, polymer-based packing materials with C_{18} derivatization possess less hydrophobic properties than does silica C_{18}, presumably due to the presence of hydrophilic functional groups. The hydrophobic selectivity estimated by comparing $\alpha(CH_2)$ values[39], or the retention increase caused by one methylene group, is greater in 80% methanol than in 40% THF with silica C_{18} and PLRP-S, while the opposite result was obtained with DE-613, C_{18}-4PW and ODP-50 having hydrophilic functional groups as well as silica C_8 and C_1. Incorporation of THF molecules into these less hydrophobic stationary phases resulted in an increase in hydrophobic property. The relatively hydrophilic polymer gels, however, showed considerable retention

TABLE II

PROPERTIES OF POLYMER PACKING MATERIALS RELATED TO THE MOBILE PHASE

	Silica			*Shodex DE-613*	*TSK C_{18}-4PW*	*Asahipak ODP-50*	*PLRP-S 300*
	C_1	C_8	C_{18}				
Hydrophobicity [retention increment for one methylene group, $a(CH_2)$][a]							
80% Methanol	0.098	0.142	0.183	0.094	0.114	0.133	0.146
	(0.54)	(0.78)	(1.0)	(0.51)	(0.62)	(0.73)	(0.80)
70% Acetonitrile	0.083	0.127	0.170	0.068	0.126	0.133	0.144
	(0.49)	(0.75)	(1.0)	(0.40)	(0.74)	(0.78)	(0.85)
40% THF	0.144	0.159	0.164	0.103	0.150	0.139	0.125
	(0.88)	(0.97)	(1.0)	(0.63)	(0.91)	(0.85)	(0.76)
Retention of phenyl group, b[a]							
80% Methanol	−0.570	−0.182	−0.029	0.206	−0.330	0.148	0.435
	(−0.54)	(−0.15)	(0)	(0.24)	(−0.30)	(0.18)	(0.46)
70% Acetonitrile	−0.137	0.082	0.187	0.291	−0.396	0.105	0.270
	(−0.32)	(−0.11)	(0)	(0.10)	(−0.58)	(−0.08)	(0.08)
40% THF	0.499	0.634	0.736	0.850	0.363	0.647	0.579
	(−0.24)	(−0.10)	(0)	(0.11)	(−0.37)	(−0.09)	(−0.16)
Flow resistance (column back pressure at 1 ml/min)[b]							
80% Methanol	92	86	94	46	85	92	54
	(1.0)	(1.0)	(1.0)	(1.0)	(1.0)	(1.0)	(1.0)
70% Acetonitrile	50	47	52	28	47	59	34
	(0.54)	(0.55)	(0.55)	(0.61)	(0.55)	(0.64)	(0.63)
40% THF	137	129	140	76	142	153	88
	(1.49)	(1.50)	(1.49)	(1.65)	(1.67)	(1.66)	(1.63)

[a] Calculated from the linear relationship between the log k' values and the carbon number of alkylbenzenes, ethylbenzene to amylbenzene: $\log k' = a(CH_2)C_n + b$. The slope, $a(CH_2)$, indicates the hydrophobic property of the stationary phase, and the intercept, b, the retention of an imaginary phenyl group. Relative values are indicated in parentheses taking the values on silica C_{18} as the standard.

[b] Column back pressure (kg/cm^2) at a flow-rate of 1 ml/min calculated by plotting pressure reading against flow-rate. Relative back pressure, taking the pressure in 80% methanol as a standard for each packing material, in parentheses.

of rigid planar hydrocarbons, as shown by the retention of the phenyl group in Table II. The results indicate the wide variation of the polymer gels and the participation of solvent molecules incorporated in polymer gels in solute retention.

Table III lists the k' values in methanol–water of hydrocarbons with structural features. The greatest selectivity based on molecular shape was seen in methanol–water as the mobile phase which provides the least solvation of the polymer chains. Polymer-based packing materials showed much less retention of alkanes than did silica C_{18}. Decane has no functional groups, and is expected to undergo minimum specific interactions with the stationary phase except hydrophobic interaction. All the polymer phases except DE-613 showed a clear preference for rigid, planar polynuclear aromatic hydrocarbons (PAHs) compared with the bulky aromatic compounds with rotational freedom of phenyl groups, which in turn were retained more favourably than saturated hydrocarbons, when compared with silica C_{18}. The retention of PAHs on polymer gels is very strong, taking into account the low hydrophobic prop-

TABLE III

RETENTION CHARACTERISTICS OF POLYMER-BASED PACKING MATERIALS IN 80% METHANOL

Packing material	*k'(α)*[a]				
	Decane	*Adamantane*	*Pyrene*	*Triphenylmethane*	*Triptycene*
Silica C_{18}	31.7	11.3 (0.36)	7.29 (0.23)	7.24 (0.23)	3.01 (0.10)
Shodex DE-613	3.48	4.58 (1.32)	15.0 (4.31)	16.7 (4.80)	12.5 (3.58)
TSK C_{18}-4PW	4.68	2.54 (0.54)	5.16 (1.10)	2.46 (0.53)	2.05 (0.44)
Asahipak ODP-50	14.8	7.23 (0.49)	7.90 (1.21)	11.3 (0.76)	6.97 (0.47)
PLRP-S 300[b]	10.5	7.18 (0.68)	33.3 (3.17)	19.4 (1.84)	5.67 (0.54)

[a] The α values (given in parentheses) were calculated by dividing the *k'* values of each solute by the *k'* value of decane.

[b] In 90% methanol.

TABLE IV

SOLUBILITY PARAMETERS OF SOLVENTS AND POLYMERS[45]

	Poly(methyl methacrylate)	*PS–DVB*[a]	*Poly(vinyl alcohol)*	*Methanol*	*Aceto-nitrile*	*THF*	*Water*
Solubility parameter	9.0–9.5	9.1	12.6	14.5	11.9	9.1	23.4

[a] Copolymer of styrene and divinylbenzene.

erties of the polymer-based packing materials. Cycloalkanes were also favoured by the polymer-based phases compared with linear alkanes having more flexibility. This tendency can be generalized as the preference by polymer gels toward solutes with rigid, compact structure and aromatic character[33].

In the case of alkyl-bonded silica-based phases, the preference for planar solutes was related to the alkyl chain length[40] and the surface density of the bonded moieties[41] as well as the functionality of the silylating reagent[42]. Aromatic groups bonded to the silica gel surface also showed preference for aromatic compounds[43]. Such preference on the polymer-based stationary phases, however, was not affected by the alkyl chain length of the stationary phase or the size of the macropores of the polymer packing materials[33]. DE-613 and C_{18}-4PW, or the polymer gels with alkyl backbones, showed preferential retention of aromatic compounds in spite of their saturated structures. The preference toward rigid compounds over flexible ones was also seen with saturated compounds having no functional group such as adamantane. Therefore the shape selectivity associated with polymer gels can be attributed, at least partially, to the structural matching between the solute and the polymer chain structure, or the micropores[22,33].

In order to show the difference in selectivity of the polymer-based packing materials more clearly, the log *k'* values on the polymer-based packing materials are plotted against those on silica C_{18}, and also against those on Shodex DE-613 in Fig. 2. A group of compounds with similar structural features behaved similarly. These

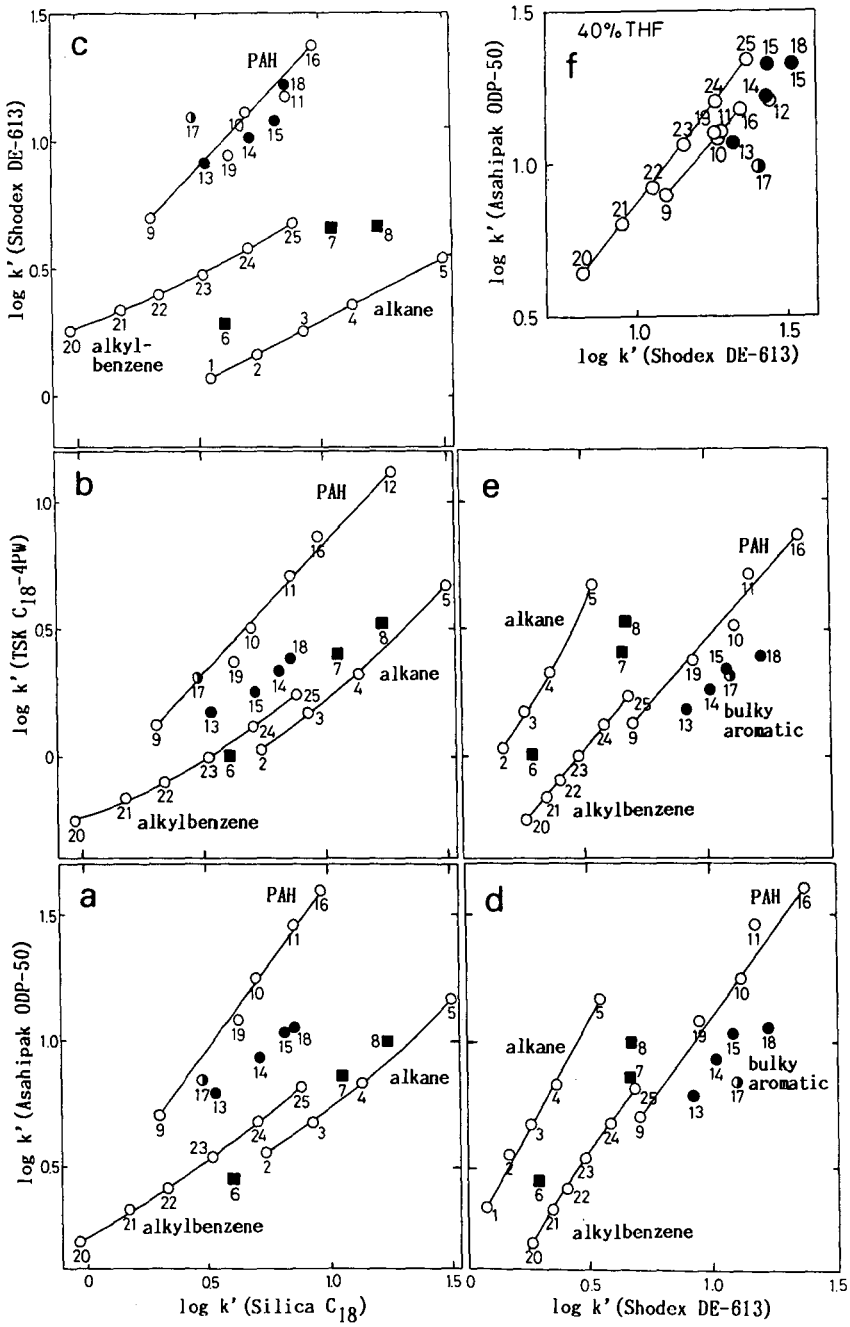

Fig. 2. Comparison of retention selectivity. Plots of log k' values on Asahipak ODP-50, TSK C_{18}-4PW and Shodex DE-613 against log k' values on silica C_{18}, (a), (b) and (c), respectively, and plots of log k' values on Asahipak ODP-50 and TSK C_{18}-4PW against log k' values on Shodex DE-613, (d) and (e), respectively in 80% methanol. Plots of log k' values on ODP-50 against log k' values on DE-613 in 40% THF (f). All measurements were carried out at 30°C. Curves are drawn to indicate the location of a group of compounds of similar structural features. Solid circles indicate aromatic compounds with phenyl groups having rotational freedom, or bulky compounds, and solid squares, cycloalkanes. See Experimental for the identification of the solutes.

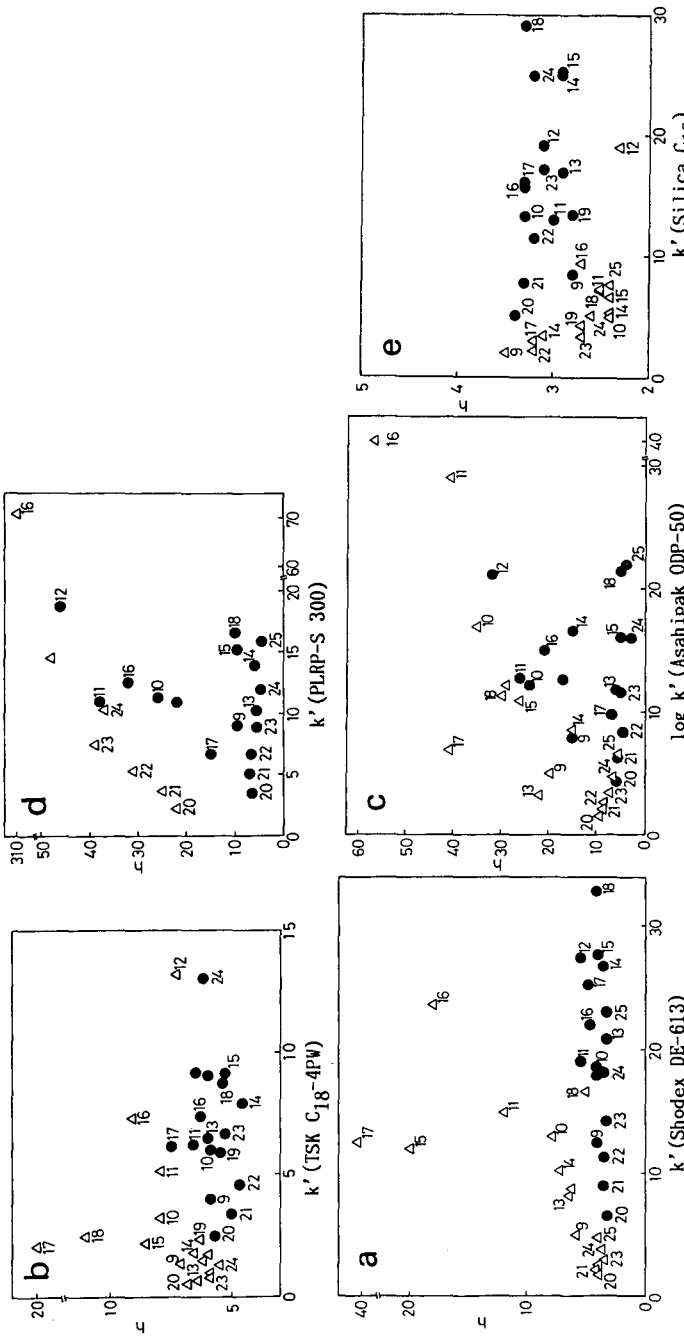

Fig. 3. Plots of reduced plate heights, h, against retention, k', of hydrocarbons on Shodex DE-613 (a), TSK C_{18}-4PW (b), Asahipak ODP-50 (c), PLRP-S 300 (d) and silica C_{18} (e), in 80% methanol (△) and in 40% THF (●). Values of h at a flow-rate of 1 ml/min for each column. See Experimental for the identification of the solutes.

plots can afford more reliable information about the selectivity of packing materials than simple comparisons of k' values of individual compounds. The polymer-based phases showed considerably different solute selectivities from silica C_{18} and from each other, which must be related to the chemical and the three-dimensional structure of these polymer gels. For example, DE-613 showed preference for aromatic compounds having more than one phenyl group compared to alkylbenzenes and for cycloalkanes compared to linear alkanes, while ODP-50 showed clear preference for planar PAHs compared to bulky aromatic compounds (13–15, 18), when these packing materials are compared with silica C_{18}. The selectivity of polymer-based packings is very similar to that of a 2-(1-pyrenyl)ethyl-bonded silica phase which possesses very rigid pyrene rings on the silica surface[43]. The polymer gels with alkyl backbones are supposed to provide such selectivity based on the rigid polymer network. The C_{18} type polymer packings, ODP-50 and C_{18}-4PW, showed greater retention of alkyl compounds than did DE-613 having short alkyl groups, as shown in Fig. 2d and e.

The preference for plánar solutes over bulky solutes increases in the order silica C_{18}, Shodex DE-613, TSK C_{18}-4PW, Asahipak ODP-50 and PLRP-S 300. The PAM gel, Shodex DE-613, actually showed favourable retention of bulky aromatic compounds such as triptycene (17) compared to PLRP-S 300, C_{18}-4PW and ODP-50. The results indicate a looser micropore structure of the polymer-based packing materials from alkyl monomers, especially with DE-613, than of PVA or PS gel. The results also indicate that the nitrogen adsorption measurements better explain the structural selectivity in 80% methanol based on the presence of micropores. Although the bulky solutes were preferentially retained by DE-613 compared to ODP-50, the structural selectivity was reduced in 40% THF as shown in Fig. 2f. The effect of the polymer structure is not so obvious in THF in both SEC and in RPLC.

A change in mobile phase resulted in a greater change in the selectivity on the polymer-based packing materials than on the silica C_{18}. As seen in Table II, the retention of a phenyl group on PLRP-S or ODP-50 in 40% THF relative to silica C_{18} was much less than in 80% methanol. Similarly, PLRP-S and ODP-50 showed a large decrease in retention of PAHs, 10–12 and 16, upon changing the mobile phase from 80% methanol to 40% THF, as shown in Fig. 3. This change was accompanied by an increase in retention of other aromatic compounds with bulkiness or flexibility such as 15 and 17. In the case of DE-613, the same change in the mobile phase from 80% methanol to 40% THF resulted in a similar extent of retention of PAHs, and a much greater increase for other aromatic compounds.

The greater preference for planar PAHs shown by ODP-50 and PLRP-S 300 than by other packing materials in methanol–water, and the loss of such a preference in THF–water, suggest that the retention of PAHs on PLRP-S and ODP-50 in methanol–water is dominated by the contribution of the polymer network structure. In agreement with this, nitrogen adsorption measurement indicates the presence of narrower pores on ODP-50 and PLRP-S 300 than on the other materials. The mobile phase effects are understandable in terms of the combination of the facts that microscopic swelling occurs in polymer gels in THF due to better solvation which would favour the retention of bulky compounds, and that THF selectively binds to micropores which otherwise would preferentially bind rigid, planar compounds[22,25]. A structural matching between the polymer chain structure and the solutes, in other words a steric compatibility, seems to exist, especially with PLRP-S, which may lead

to slower diffusion, or lower column performance for aromatic compounds in methanol–water.

When the column performance was examined, the silica C_{18} phase showed a good performance for all the solutes tested in the three mobile phases, 80% methanol, 80% acetonitrile and 40% THF. In 80% methanol, C_{18}-4PW, DE-613 and ODP-50 showed similar plots. While consistent reduced plate height, h, values were obtained for alkanes and alkylbenzenes, increases in h were seen with increasing k' values for PAHs, and more so for bulky aromatic compounds. The efficiency of PLRP-S 300 is considerably lower than those of the other materials in this mobile phase, but still showed a similar tendency. The results are understandable in terms of the restricted diffusion of bulky solutes in the polymer network structure.

In 40% THF, however, evidently different features in column performance were seen between the two groups of polymer-based packing materials. DE-613 and C_{18}-4PW, alkyl ester type gels, showed consistently good performance for all the hydrocarbons tested as did silica C_{18}, although the h values were slightly larger than those on silica C_{18} at comparable flow-rates. Conversely, ODP-50 and PLRP-S 300 showed poorer performance, that is an increase in h values with increasing k' values, only for planar PAHs in THF–water and in acetonitrile–water. In the same mobile phases, these packing materials showed better performance for more bulky compounds, such as *o*-terphenyl (15), triptycene (17) and triphenylmethane (18) than in methanol–water.

Note that ODP-50 and PLRP-S showed better performance for bulky molecules than for PAHs in THF–water, while this was not the case with DE-613 and C_{18}-4PW. The difference between the two groups of packing materials was also seen in the mobile phase effect on the retention selectivity and in the pore-size distribution determined by nitrogen adsorption, as mentioned above.

The differences in the structural effect of the solutes on column performance can be explained based on the differences in the chemical structure of the polymer chains. DE-613 and C_{18}-4PW are alkyl-type gels, containing no aromatic functionality, while PLRP-S contains aromatic groups and ODP-50 contains a cyclic cross-linking reagent, an isocyanuric derivative which assumes a planar structure[44]. These functionalities can provide interactions with aromatic compounds via π-electrons, especially when the solutes are planar. The fact that the retention of bulky compounds on ODP-50 and PLRP-S is relatively weaker than that of PAHs compared with DE-613 and C_{18}-4PW in similar mobile phases indicates that the latter possess looser network structures than does ODP-50, and are well solvated with THF to give consistent h values.

On the contrary, ODP-50 possesses a smaller, more rigid micropore structure which restrict bulky hydrocarbons from entering into the micropores to give higher preference for PAHs in methanol–water, as is the case with PS gel[22]. With better solvation in THF–water and in acetonitrile–water, only PAHs showed slightly lower performance due to the interaction with the polymer backbones of ODP-50 and PLRP-S containing aromatic groups. With alkyl monomers and alkyl cross-linking reagents, C_{18}-4PW and DE-613 did not show such an effect.

As shown in Fig. 4, higher h values were obtained with polymer packings in 80% methanol than with silica C_{18}, although the efficiencies of the alkyl-type gels are much better than that of PS-based gel in this mobile phase. The differences are much

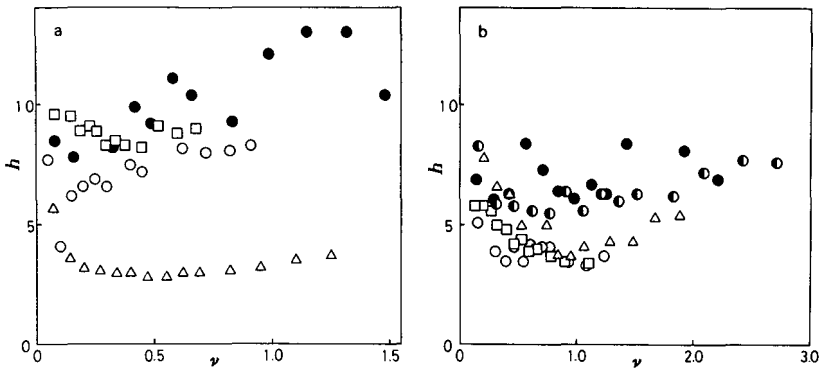

Fig. 4. Dependence of reduced plate heights, h, on the reduced velocity of the mobile phase, v, in 80% methanol (a) and in 40% THF (b). Solute: propylbenzene. Packing materials: silica C_{18} (△); Shodex DE-613 (○); TSK C_{18}-4PW (●); Asahipak ODP-50 (□); PLRP-S 300 (◐).

smaller, especially at low flow-rates, in 40% THF. The results agree well with those obtained by others on PS-based packing materials[22,25,32]. The performance of the alkyl-type gels was comparable with that of silica C_{18}, as shown in Fig. 5. This suggests that these packing materials can have wide applicability in RPLC, although the scope of application is yet to be explored.

It is commonly accepted that polymer gels show lower performance with increasing solute retention. This is shown to be true for a series of compounds with common structural features such as rigidity and planarity which match the chemical and dimensional structure of the polymer micropores. Such an effect strongly depends on the structures of the organic solvent and of the solute.

The PVA-based gel ODP-50 showed excellent performance for alkyl compounds in all the solvent systems, as reported earlier[8,9]. Although h values for polyaromatic compounds are larger than those for alkyl compounds on this stationary phase, the performance was significantly improved in THF–water and more so in

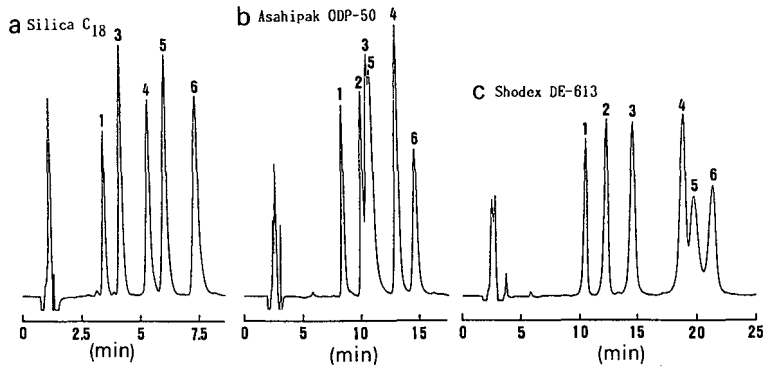

Fig. 5. Performance of polymer-based packing materials for hydrocarbons. Mobile phase: 50% THF. Flow-rate: 1 ml/min. Temperature: 30°C. (a) Silica C_{18}; (b) ODP-50; (c) DE-613. Solutes: benzene (1); toluene (2); naphthalene (3); diphenylmethane (4); triptycene (5); *o*-terphenyl (6).

acetonitrile–water, which gave the best results for this packing material. Solvation of the polymer chains reflected in the matching of solubility parameters seems to be important in determining the performance in each system. The solubility parameter of PVA is similar to that of acetonitrile, as seen in Table IV[45]. The two C_{18}-type polymer packings, ODP-50 and C_{18}-4PW, showed relatively similar retention selectivity, although ODP-50 showed slightly greater retention of aromatic compounds than did C_{18}-4PW. The differences in retention selectivity and structure dependency of the column efficiency are most likely caused by the cross-linking reagents used in these polymer gels. These packing materials showed selectivities similar to that of silica C_{18} in the presence of acetonitrile or THF.

Although PLRP-S 300, a PS gel, showed relatively poor performance for aromatic hydrocarbons, especially for PAHs in 80% methanol, the performance was much better in 40% THF. In spite of the lower performance than for the other alkyl-type polymer-based phases for low-molecular-weight aromatic compounds, PLRP-S gels have been widely used for the separations of basic compounds and polypeptides, where stability of stationary phases is required[11]. This material is reported to show excellent performance for high-molecular-weight compounds such as polypeptides which cannot enter into the micropores[18,19].

The present results suggest that the abundance of micropores which barely permit the slow diffusion of solutes causes band broadening. The results of the pore-size determination provide evidence to support this interpretation. The actual pore volume in the micropore region existing in a column is the largest with DE-613 in a solvating medium, followed by ODP-50, C_{18}-4PW and PLRP-S 300 in this order. Yet DE-613, C_{18}-4PW and ODP-50 showed much better performance than did PLRP-S 300. The latter, with a very small pore volume in this region, showed a very large effect of microporosity on the retention and performance for PAHs due to the presence of styrene and divinylbenzene units as well as the polymer gel structure allowing the solute to be trapped[22]. Column performance is related more to the chemical as well as the three-dimensional structures of the micropores than to the total volume of such micropores in the polymer gels.

CONCLUSION

Determination of the pore size by nitrogen adsorption and SEC provides useful information about the performance and retention selectivity of polymer-based packing materials for RPLC. Polymer-based packing materials, including PS, PAM and esterified PVA, showed selective retention of solutes with structural rigidity compared with silica C_{18}, the preference order being PAHs, flexible aromatic compounds, cycloalkanes and linear alkanes. The column efficiencies provided by polymer gels with alkyl backbones are much better than those of PS-packed columns, and comparable with those provided by silica-based phases under optimized conditions. The change in mobile phase from methanol–water to acetonitrile–water or THF–water resulted in higher column efficiencies and loss of structural selectivity accompanied by slight swelling of gels. The results can be explained by the contribution of chemical as well as the three-dimensional structures of the polymer micropores. As more stable packing materials are desired for RPLC[46], the use of polymer-based packing materials will increase with understanding of their chromatographic properties.

ACKNOWLEDGEMENTS

We thank Dr. Y. Kato of Tosoh, Dr. M. Komuro of Showa Denko, Dr. K. Noguchi of Asahi Chem. Ind. and Ms. L. L. Lloyd of Polymer Laboratories for gifts of packing materials and columns. We also thank Dr. Y. Ohtsu of Shiseido for nitrogen adsorption measurements. This work was supported by Grant No. 61470038 from the Ministry of Education.

REFERENCES

1 G. Schomburg, A. Deege, J. Kohler and U. Bien-Vogelsang, *J. Chromatogr.*, 282 (1983) 27.
2 H. Figge, A. Deege, J. Kohler and G. Schomburg, *J. Chromatogr.*, 351 (1986) 393.
3 Y. Ohtsu, H. Fukui, T. Kanda, K. Nakamura, M. Nakano, O. Nakata and Y. Fujiyama, *Chromatographia*, 24 (1987) 380.
4 D. P. Lee, *J. Chromatogr. Sci.*, 20 (1982) 203.
5 J. V. Dawkins, L. L. Lloyd and F. P. Warner, *J. Chromatogr.*, 352 (1986) 157.
6 Y. B. Yang and M. Verzele, *J. Chromatogr.*, 387 (1987) 197.
7 Y. Tanaka, H. Sato, K. Miyazaki and Y. Yamada, *J. Chromatogr.*, 407 (1987) 197.
8 K. Yasukawa, Y. Tamura, T. Uchida, Y. Yanaghara and K. Noguchi, *J. Chromatogr.*, 410 (1987) 129.
9 Y. Yanaghara, K. Yasukawa, U. Tamura, T. Uchida and K. Noguchi, *Chromatographia*, 24 (1987) 701.
10 J. V. Dawkins, N. P. Gabbott, L. L. Lloyd, J. A. McConville and F. P. Warner, *J. Chromatogr.*, 452 (1988) 145.
11 N. Tanaka, *Adv. Chromatogr. (N.Y.)*, 29 (1989) in press.
12 K. Aramaki, T. Hanai and H. F. Walton, *Anal. Chem.*, 52 (1980) 1963.
13 D. P. Lee and J. H. Kindsvater, *Anal. Chem.*, 52 (1980) 2425.
14 T. Isobe, Y. Kurosu, Y. Fang, N. Ishioka, H. Kawasaki, N. Takai and T. Okuyama, *J. Liq. Chromatogr.*, 7 (1984) 1101.
15 L. L. Lloyd, Z. Dryzek, D. B. Harrison and F. P. Warner, *10th International Symposium on Column Liquid Chromatography, San Francisco, May, 1986.*
16 K. A. Tweeten and T. N. Tweeten, *J. Chromatogr.*, 359 (1986) 111.
17 D. P. Lee, *J. Chromatogr.*, 443 (1988) 143.
18 W. G. Burton, K. D. Nugent, T. K. Slattery, B. R. Summers and L. R. Snyder, *J. Chromatogr.*, 443 (1988) 363.
19 W. G. Burton, K. D. Nugent, T. K. Slattery, B. F. Johnson and L. R. Snyder, *J. Chromatogr.*, 443 (1988) 381.
20 D. H. Freeman and I. C. Poinescu, *Anal. Chem.*, 49 (1977) 1183.
21 F. Nevejans and M. Verzele, *Chromatographia*, 20 (1985) 173.
22 F. Nevejans and M. Verzele, *J. Chromatogr.*, 406 (1987) 325.
23 R. V. Vivilecchia, B. G. Lightbody, N. Z. Thimot and H. M. Quinn, *J. Chromatogr. Sci.*, 15 (1977) 424.
24 E. Ozaki, K. Saitoh and N. Suzuki, *J. Chromatogr.*, 177 (1979) 122.
25 L. D. Bowers and S. Pedigo, *J. Chromatogr.*, 371 (1986) 243.
26 R. M. Smith, *J. Chromatogr.*, 291 (1984) 372.
27 S. Bitteur and R. Rosset, *J. Chromatogr.*, 394 (1987) 279.
28 D. H. Freeman and S. B. Schram, *Anal. Chem.*, 53 (1981) 1235.
29 F. V. Warren and B. A. Bidlingmeyer, *Anal. Chem.*, 56 (1984) 950.
30 S. Mori, *Anal. Chem.*, 50 (1978) 745.
31 S. Coppi, A. Betti and S. Caldari, *J. Chromatogr.*, 395 (1987) 159.
32 S. Coppi, A. Betti, C. Bighi, G. P. Cartoni and F. Coccioli, *J. Chromatogr.*, 442 (1988) 97.
33 N. Tanaka, K. Hashizume and M. Araki, *J. Chromatogr.*, 400 (1987) 33.
34 M. Hirukawa, Y. Arai and T. Hanai, *J. Chromatogr.*, 395 (1987) 481.
35 N. Tanaka, M. Araki, H. Tsuchiya, A. Okuno, K. Iwaguchi, S. Ohnishi and N. Takai, *J. Chromatogr.*, 448 (1988) 95.
36 I. Halasz and K. Martin, *Angew. Chem., Int. Ed. Engl.*, 17 (1978) 901.
37 J. H. Knox and H. P. Scott, *J. Chromatogr.*, 316 (1984) 311.
38 A. A. Gorbunov, L. Ya. Solovyova and V. A. Pasechnik, *J. Chromatogr.*, 448 (1988) 307.

39 N. Tanaka and E. R. Thornton, *J. Am. Chem. Soc.*, 99 (1977) 7300.
40 N. Tanaka, K. Sakagami and M. Araki, *J. Chromatogr.*, 199 (1980) 327.
41 K. Kimata, K. Iwaguchi, S. Onishi, K. Jinno, R. Eksteen, K. Hosoya, M. Araki and N. Tanaka, *J. Chromatogr. Sci.*, in press.
42 S. A. Wise and W. E. May, *Anal. Chem.*, 55 (1983) 1479.
43 N. Tanaka, Y. Tokuda, K. Iwaguchi and M. Araki, *J. Chromatogr.*, 239 (1982) 761.
44 H. Wada, *Chromatographia*, 22 (1986) 194.
45 J. Brandrup and E. H. Immergut (Editors), *Polymer Handbook*, Wiley, New York, 2nd ed., 1975, p. IV–340.
46 J. J. Kirkland, J. L. Glajch and R. D. Farlee, *Anal. Chem.*, 61 (1989) 2.

Journal of Chromatography, 475 (1989) 209–217
Elsevier Science Publishers B.V., Amsterdam — Printed in The Netherlands

CHROM. 21 495

ION CHROMATOGRAPHY ON METHACRYLATE ION EXCHANGERS

J. HRADIL* and F. ŠVEC
Institute of Macromolecular Chemistry, Czechoslovak Academy of Sciences, 162 06 Prague 6 (Czechoslovakia)
and
A. A. ARATSKOVA, L. D. BELJAKOVA, V. I. ORLOV and Ya. I. YASHIN
Institute of Physical Chemistry, Academy of Sciences of the U.S.S.R., 117071 Moscow (U.S.S.R.)
(First received December 12th, 1988; revised manuscript received March 14th, 1989)

SUMMARY

The preparation and properties of ion chromatography sorbents based on glycidyl methacrylate–ethylene dimethacrylate macroporous copolymers are described. Anion exchangers were suitable for the separation of inorganic anions and possessed a high selectivity towards the NO_3^- anion. Alkaline metal cations and NH_4^+ were separated under the conditions of non-suppressed ion chromatography. In general, the addition of organic compounds (methanol, ethanol and acetone) increased the retention of cations in the column.

INTRODUCTION

At present, ion chromatography is carried out with modified silica and sorbents based on macroporous styrene–divinylbenzene copolymers[1]. Strongly acidic sulpho groups or strongly basic trimethylammonium groups are used as the exchange groups[2]. These groups are introduced into the polymer by a consecutive chemical transformation[3], by splitting off or blocking (poisoning) of the excess exchange groups[4] and also of dynamically or statically coated polyelectrolytes present at low concentrations on the polymer matrix[5–7]. Ion exchangers based on methacrylate copolymers were prepared containing sulphonate and trimethylammonium groups and possessing sufficient hydrolytic stability, which can undergo more than 100 exchange cycles without any essential decrease in their exchange capacity[8,9]. A more common strongly basic group bonded to the methacrylate matrix is triethylammonium. The ion exchangers used in ion chromatography have a very low exchange-site concentration[1], 2–3 orders of magnitude lower than those employed in ion exchange or ion-exchange chromatography. The concentration of ion-exchange groups in most exchangers is 1 mmol/g and higher, which may perhaps be used in suppression columns, but not in ion chromatography.

As far as we know, ion exchangers based on methacrylates have not yet been employed in ion chromatography. We therefore thought it worthwhile to examine the behaviour of modified methacrylate copolymers in ion chromatography.

0021-9673/89/$03.50

TABLE I

PROPERTIES OF MACROPOROUS METHACRYLATE ION EXCHANGERS FOR ION CHROMATOGRAPHY

Ion exchange[a]	*Sample No.*	*Ratio between agent and sorbent (mmol/g)*	*Conversion (%)*	*Solvent*	*Particle size (μm)*	*Exchange-site concentration*		
						Elemental analysis	*Titrimetrically*	*Chromato-graphically*
Anion exchangers, P–$N(CH_3)_3^+$	1	20.120	–	None	19–25	2.26	1.51	–
	2	1.007	–	Water	19–25	1.33	0.94	
	3	0.250	–	Diethyl ether	17–20	0.15	Undeterminable	0.02
	4	0.013	–	Diethyl ether	19–35	0.07	Undeterminable	0.007
Cation exchangers, P–SO_3^-	5	2.000	5.48		19–25	0.75	–	–
	6	0.312	17.6		19–25	0.42	–	0.1
	7	0.083	71.5		17–20	0.13	–	0.02
	8	0.036	53.2		19–35	0.11	–	0.02

[a] P– denotes polymeric matrix.

EXPERIMENTAL

The starting copolymers used in the preparation of ion exchangers were prepared by the suspension radical copolymerization of glycidyl methacrylate (GMA) (60 wt.-%) and ethylene dimethacrylate (EDMA) (40 wt.-%) in the presence of cyclohexanol–dodecanol (91:9) as a porogenic agent[10]. The specific surface area and the pore volume of the copolymers were 66 m^2/g and 1.16 cm^3/g, respectively.

The preparation of anion exchangers was a two-stage process, as shown in Scheme 1. First, the copolymer was reacted with dimethylamine in ethanol. After washing and drying, the intermediate was alkylated with methyl iodide in nitromethane[11].

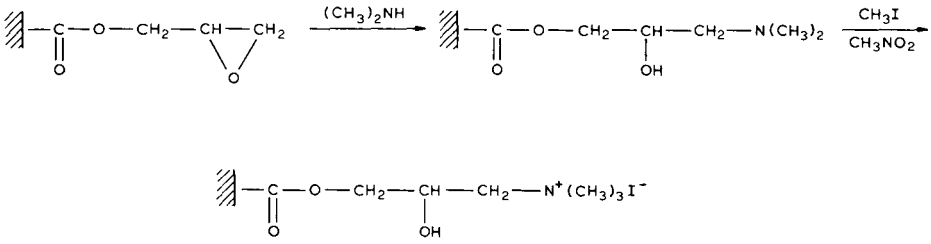

Scheme 1.

Cation exchangers were also prepared in two stages, as shown in Scheme 2. The epoxy groups of the copolymer were hydrolysed with 0.05 mol/l sulphuric acid[12], then modified by reaction with 1,3-propane sultone in an alkaline medium[13,14].

The preparation conditions and properties of the ion exchangers are summarized in Table I.

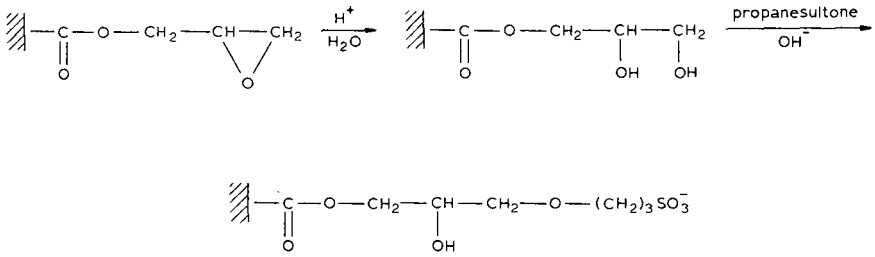

Scheme 2.

Analysis

The exchange-site concentration in the ion exchangers was determined by the elemental analysis of nitrogen or sulphur, and also chromatographically[1] according to the equation

$$c_0 = \frac{H_i^{1/z_i} c_1}{K_i} \tag{1}$$

where c_0 is the exchange-site concentration (mmol/g), z_i is the ion charge, c_1 is the concentration of the elution agent (mol/l), K_i is the equilibrium constant of the ion exchange ($K_{Na-H} = 1.2$, $K_{Cl-OH} = 4.32$) and the adsorption coefficient H_i (ml/g) is defined by

$$H_i = \frac{(t - t_0)u}{w_i} \tag{2}$$

where t is the elution time (min), t_0 is the elution dead time (min), u is the flow-rate of the eluent (ml/min) and w_i is the weighed amount of the ion exchanger in the column.

Using the ion exchangers thus prepared, columns 15 cm (or 10 cm) long and with I.D. 3.3 or 6 mm were filled by employing the slurry technique in a stream of distilled water under a pressure of up to 20 MPa. The anion exchangers were converted into the OH^- form with 0.5 mol/l potassium hydroxide solution, the cation exchangers were converted into the H^+ form with 0.1 mol/l nitric acid, and both were washed with distilled water, until the conductivity of the eluate had fallen below 10 μS.

The ion separation was investigated using a system consisting of an HPP 4001 high-pressure pump, a CDLC 1 conductimetric detector and a CI 100 computing integrator (Laboratory Instruments, Prague, Czechoslovakia). The samples were injected by means of an LCI 20 injection head using the stop-flow method, in a volume between 5 and 35 μl. The standard mixture of anions contained 10 mg/l F^- and Cl^-, 50 mg/l PO_4^{3-} and SO_4^{2-}, 15 mg/l NO_2^- and 25 mg/l NO_3^-. A suppressor column containing a strong acid cation exchanger in the H^+ form was placed behind the separation column.

The standard mixture of cations consisted of 25 mg/l Li^+, Na^+, K^+ and NH_4^+. The suppressor column was not needed in the separation of cations.

RESULTS AND DISCUSSION

The anions were separated using macroporous methacrylate copolymers containing various amounts of trimethylammonium groups (Scheme 1) as given in Table I. High-capacity anion exchangers (2.8 and 1.3 mmol/g) can be used as packings of suppressor columns able to reduce the conductivity of the eluent (0.001 mol/l nitric acid) during the separation of cations from 700 μS to less than 20 μS. Anion exchangers with a lower exchange-site concentration (0.15 and 0.07 mmol/g) were suitable for use in the separation of anions (F^-, Cl^-, PO_4^{3-}. NO_2^-, SO_4^{2-} and NO_3^-). Fig. 1 shows the dependence of the retention of the particular anions on the concentration of sodium hydrogencarbonate in the eluent, *i.e.*, in a solution of sodium carbonate (2.4 mmol/l). The retentions of all anions decrease with increasing content of sodium hydrogencarbonate. The retention of sulphate varies most. Ions from the anion exchanger containing 0.07 mmol/g of groups are eluted with the solution of sodium hydrogencarbonate alone, although this solution has a lower eluting power than the solution containing sodium carbonate. The dependence of the retention of the individual anions on this anion exchanger is shown in Fig. 2. The largest decrease in retention, depending on the concentration of sodium hydrogencarbonate in the eluent, was observed with SO_4^{2-} and PO_4^{3-}, in accordance with their higher valency.

Fig. 3 shows chromatograms of the separation of a mixture of anions on anion

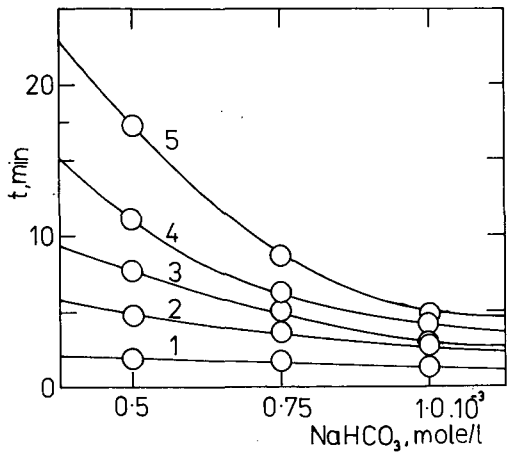

Fig. 1. Dependence of the retention of anions on the concentration of $NaHCO_3$. Column, 10 × 0.6 cm I.D.; flow-rate of eluent, 2 ml/min; sorbent No. 4. 1, F^-; 2, Cl^-; 3, PO_4^{3-}; 4, NO_2^-; 5, SO_4^{2-}.

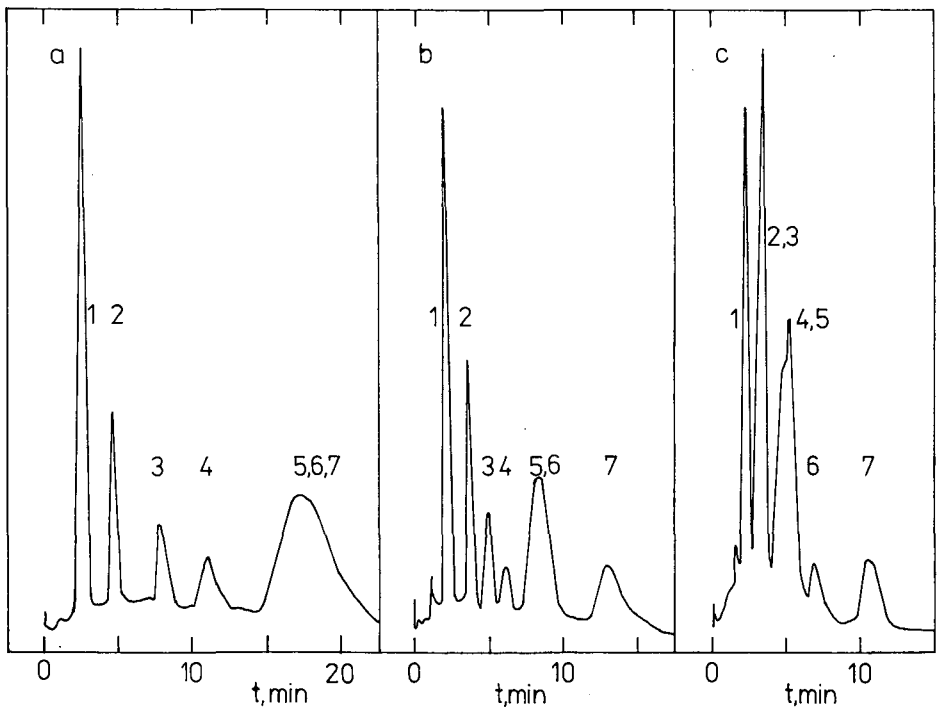

Fig. 2. Chromatogram of the separation of anions at various concentrations of $NaHCO_3$ in the eluent. Column, 10 × 0.4 cm I.D.; eluent, 2.4 mmol/l Na_2CO_3; flow-rate, 2 ml/min; sorbent No. 4. Peaks: 1, F^-; 2, Cl^-; 3, PO_4^{3-}; 4, NO_2^-; 5, SO_4^{2-}; 6, Br^-; 7, NO_3^-.

TABLE II

CHARACTERISTICS OF SEPARATION POWER OF METHACRYLATE ION EXCHANGERS

$n = 5.54\,(t/\omega)^2$ plates/m, where t is the retention time and ω is the peak width at half-height; HETP in mm; R_s is the resolving power, $R_s = (t_2 - t_1)/(\omega_1 + \omega_2)$, given here for adjacent peaks.

Ion	*Anion exchanger and eluent*[a]											
	No. 4, 0.0005 M $NaHCO_3$			*No. 4, 0.00075 M $NaHCO_3$*			*No. 4, 0.001 M $NaHCO_3$*			*No. 3, 0.0024 M Na_2CO_3*		
	n	*HETP*	R_s	*n*	*HETP*	R_s	*n*	*HETP*	R_s	*n*	*HETP*	R_s
F^-	1121	0.89		1385	0.72		1994	0.50		2164	0.46	
Cl^-	4002	0.25	2.00	3116	0.32	1.25	1737	0.57	1.25	4740	0.21	4.08
PO_4^{3-}	3327	0.30	2.33	2463	0.40	1.00	—	—	2.00			
NO_2^-	4290	0.23	1.44	8656	0.11	1.00	556	1.80	0.08			
SO_4^{2-}	1140	0.88	1.25	1887	0.53	1.25	678	1.47	0.67	4409	0.23	2.00
Br^-				—	—	—	4787	0.22	1.67	9245	0.11	1.56
NO_3^-				4163	0.24	1.42	2714	0.37		—	—	—

	Cation exchanger No. 8 and eluent[b]								
	HNO_3 (pH 2.5)			*HNO_3 (pH 2.5)–CH_3OH (2:1)*			*HNO_3 (pH 2.5)–CH_3OH (1:1)*		
	n	*HETP*	R_s	*n*	*HETP*	R_s	*n*	*HETP*	R_s
Li^+	2713	0.37		3693	0.27		7706	0.13	
Na^+	2828	0.35	0.67	5771	0.17	1.74	4743	0.21	1.67
NH^+	3693	0.27	2.86				3693	0.27	0.86
K^+	3246	0.31	0.69	4469	0.22	2.19	6051	0.16	2.86

[a] Column, 10 × 0.6 cm I.D.; flow-rate of eluent, 2 ml/min.
[b] Column, 15 × 0.4 cm I.D.; flow-rate of eluent, 2 ml/min.

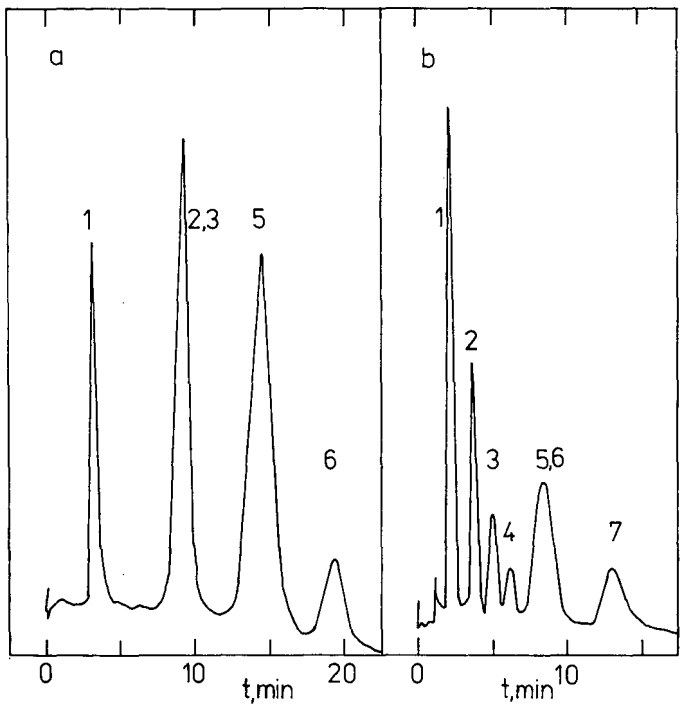

Fig. 3. Chromatogram of the separation of anions. (a) Sample No. 3 (exchange-site concentration 0.15 mmol/g); eluent, 2.4 mmol/l Na_2CO_3. (b) Sample No. 4 (exchange-site concentration 0.07 mmol/l); eluent, 0.75 mmol/l $NaHCO_3$. Other conditions and peaks as in Fig. 2.

exchangers having exchange-site concentrations 0.15 and 0.07 mmol/g. As can be seen (Fig. 3a), on the sorbent with the higher concentration of strongly basic groups the anions are retained longer than on that with the lower concentration. The anion F^- is separated better. On the sorbent with the lower exchange-site concentration (Fig. 3b) all anions, with the exception of SO_4^{2-} and Br^-, are separated within 13 min, with NO_3^- having the highest retention.

Table II shows the resolving powers R_s, defined by

$$R_s = \frac{t_2 - t_1}{\omega_2 + \omega_1} \tag{3}$$

where t_2 and t_1 are the retention times of ions eluted next to each other and ω_1 and ω_2 are their respective peak widths at half-height. The resolving power observed on methacrylate anion exchangers was higher than that with styrene–divinylbenzene[1]. Good stability of methacrylate anion exchangers was also confirmed under chromatographic conditions; the resolving power of the column remained virtually the same during 6 months of use.

The separation of cations by ion chromatography was carried out using macroporous methacrylate copolymers with the strongly acid groups (Scheme 2) bound to them. The procedure used in the synthesis allows the groups to be introduced

predominantly on the surface of globulus of the sorbent, thus accelerating the sorption and desorption process. The cation exchanger with the highest content of sulpho groups could be employed in the suppressor column in the separation of anions; the 20 × 0.6 cm I.D. column decreases the conductivity of the eluent containing 2 mmol/l sodium hydrogencarbonate and 4 mmol/l sodium carbonate from 2000 to 35–40 μS. The cation exchanger having an exchange-site concentration of 0.42 mmol/g, which cannot be used in the suppressor column, separates the individual cations but the retention values are too high.

In the separation of cations on the cation exchanger having an exchange-site concentration of 0.11 mmol/g (sorbent No.8) using nitric acid as the eluent, the cations were separated within 20 min in the order Li^+, Na^+, NH_4^+ and K^+ (Fig. 4).

Fig. 5 shows the effect of the addition of organic solvents (methanol, acetone and ethanol) to the eluent (nitric acid of pH 2.5). The addition of organic compounds generally increase the retention of cations in the column. Methanol at a concentration of 30–50 vol.-% increases the retention of K^+ considerably, that of Li^+ and Na^+ less and that of NH_4^+ only insignificantly. This can be explained by the lower dissociation of cations of alkali metal ions bound on the ion exchanger compared with the ammonium ion. A complete separation of these four cations was achieved within 20 min in with nitric acid (pH 2.5)–methanol (1:1) (Fig. 5). The separation of NH_4^+ and K^+ is characterized by a good resolving power (R_s = 2.9). The column efficiency is 9000 theoretical plates per metre, which can be regarded as satisfactory with respect to the particle size used in the experimental arrangement (19–25 μm).

The results show that owing to their easy modification with ionogenic groups

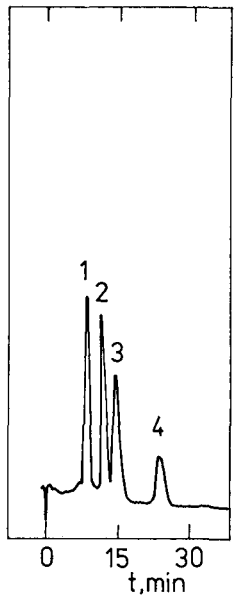

Fig. 4. Chromatograms of the separation of cations of alkali metals on sample No. 8 (exchange-site concentration 0.11 mmol/g). Column, 15 × 0.3 cm I.D.; eluent, HNO_3 (pH 2.5)–methanol (1:1); flow-rate, 1 ml/min. Peaks: 1, Li^+; 2, Na^+; 3, NH_4^+; 4, K^+.

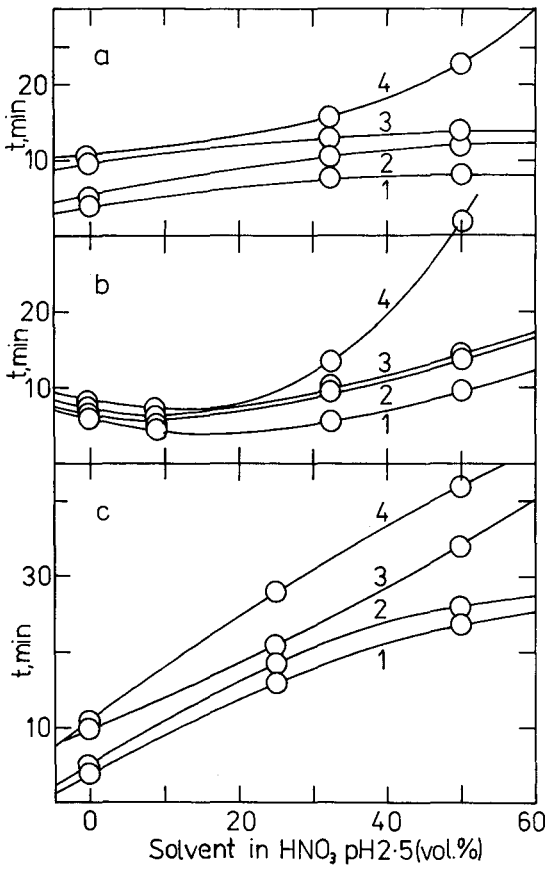

Fig. 5. Dependence of the retention of cations of sample No. 8 (exchange-site concentration 0.11 mmol/g) on the content of solvent in HNO_3 (pH 2.5). Conditions and cations as in Fig. 4, except eluent: (a) HNO_3 (pH 2.5)–methanol; (b) HNO_3 (pH 2.5)–acetone; (c) HNO_3 (pH 2.5)–ethanol.

and sufficient hydrolytic stability, glycidyl methacrylate matrices can be used as column packings in the ion chromatography of both cations and anions. This new hydrophilic type of matrix allows the selectivity of separation to be altered.

REFERENCES

1 J. S. Fritz, D. T. Gjerde and Ch. Pohlandt, *Ion Chromatography*, Hüthig, Heidelberg, 1982.
2 G. J. Sevenich and J. S. Fritz, *React. Polym.*, 4 (1985) 195.
3 R. E. Barron and J. S. Fritz, *J. Chromatogr.*, 284 (1984) 13.
4 D. T. Gjerde, J. S. Fritz and G. J. Schmuckler, *J. Chromatogr.*, 186 (1979) 509.
5 A. M. Dolgonosov, *Zh. Fiz. Khim.*, 58 (1985) 1989.
6 Ch. A. Phol and S. C. Papanu, *Eur. Pat. Appl.*, 134 099 (1985); *C.A.*, 103 (1985) 46047325.
7 D. L. Duval and J. S. Fritz, *J. Chromatogr.*, 295 (1985) 89.
8 J. Hradil and F. Švec, *Angew. Makromol. Chem.*, 135 (1985) 85.
9 A. V. Azanova, J. Hradil, F. Švec and E. F. Panarin, to be published.
10 F. Švec, J. Hradil, J. Čoupek and J. Kálal, *Angew. Makromol. Chem.*, 48 (1975) 135.
11 F. Švec, H. Hrudková, D. Horák and J. Kálal, *Angew. Makromol. Chem.*, 63 (1977) 23.
12 H. Hrudková, F. Švec and J. Kálal, *Br. Polym. J.*, (1977) 238.
13 C. M. A. Ribeiro, J. Hradil, F. Švec and J. Kálal, *Angew. Makromol. Chem.*, 87 (1980) 119.
14 J. Hradil and F. Švec, *Polym. Bull.*, 6 (1982) 565.

Journal of Chromatography, 475 (1989) 219–227
Elsevier Science Publishers B.V., Amsterdam — Printed in The Netherlands

CHROM. 21 573

IMPROVED HIGH-SPEED COUNTER-CURRENT CHROMATOGRAPH WITH THREE MULTILAYER COILS CONNECTED IN SERIES

I. DESIGN OF THE APPARATUS AND PERFORMANCE OF SEMIPREPARATIVE COLUMNS IN 2,4-DINITROPHENYL AMINO ACID SEPARATION

YOICHIRO ITO* and HISAO OKA[a]
Laboratory of Technical Development, National Heart, Lung, and Blood Institute, Bethesda, MD 20892 (U.S.A.)
and
JIMMIE L. SLEMP
Biomedical Engineering and Instrumentation Branch, National Institutes of Health, Bethesda, MD 20892 (U.S.A.)
(First received February 27th, 1989; revised manuscript received April 4th, 1989)

SUMMARY

A compact desktop model of a high-speed counter-current chromatograph holds three identical multilayer coils in the symmetrical positions around the rotary frame to maintain perfect balance of the centrifuge system without the use of a counterweight. These multilayer coils are connected in series to make up a total capacity of 400 ml while the unique gear arrangement on the rotary frame establishes a twist-free mechanism of the flow tubes so that continuous elution can be performed without the use of rotary seal. The high performance of the present system was successfully demonstrated in separations of 10–250 mg of 2,4-dinitrophenyl amino acid mixtures in a two-phase solvent system composed of chloroform–acetic acid–0.1 *M* hydrochloric acid (2:2:1, v/v/v).

INTRODUCTION

High-speed counter-current chromatography (HSCCC) is the most advanced form of the CCC technology which is characterized by rapid and efficient separation on both analytical and preparative scales[1]. As in other centrifugal CCC systems, the partition efficiency of HSCCC can be improved by using a greater length of the coild column. The original HSCCC apparatus is equipped with a column holder on one side of the rotor and the counterweight on the opposite side of the rotor to balance the centrifuge system[1–3]. The use of a single column holder not only limits the column

[a] Visiting scientist from Aichi Prefectural Institute of Public Health, Nagoya, Japan.

0021-9673/89/$03.50

capacity, hence the partition efficiency, but also necessitates careful adjustment of the counterweight mass according to the density of the solvent system applied for separation. Recently, efforts were successfully made to solve these problems by mounting two identical multilayer coils symmetrically, one on each side of the rotary frame, and connecting these columns in series to double the column capacity[4].

The present paper introduces a novel design of the apparatus which holds three multilayer coils symmetrically around the rotary frame. These columns are interconnected in series on the rotary frame to triple the column capacity. The unique mechanical design of the present centrifuge system permits single passage of flow tubes; the flow tube enters from one side and leaves from the other side of the centrifuge without twisting. Performance of the apparatus was evaluated by separations of 2,4-dinitrophenyl (DNP) amino acid samples in a set of three semipreparative multilayer coils.

APPARATUS

The design principle of the present apparatus is illustrated in Fig. 1 where three cylindrical column holders are symmetrically arranged around the centrifuge axis. Each holder undergoes an identical synchronous planetary motion: revolution around the centrifuge axis and rotation about its own axis at the same angular velocity in the same direction as indicated by arrows. These holders are connected in series with flow tubes in the following manner: the inflow tube enters the centrifuge system from the right along the centrifuge axis and is bent to enter the first holder (bottom) on the left side. The connecting tubing running between the first and the second holders leaves the first holder on the right side and is arched around to the left side of the centrifuge and via another bend reaches the second holder (middle) on the left side. The connecting tubing from the second holder similarly reaches the third holder (top) on the left side. The return flow tube from the third holder leaves the holder on the right side and is arched reaching the left side of the centrifuge where it exits the centrifuge system along the central axis of the centrifuge.

In order to prevent twisting the flow tubes, the horizontal portions of the flow tubes on the rotary frame should be counter-rotated synchronously with the rotation of the holder as indicated by arrows. If these requirements are fulfilled, the system

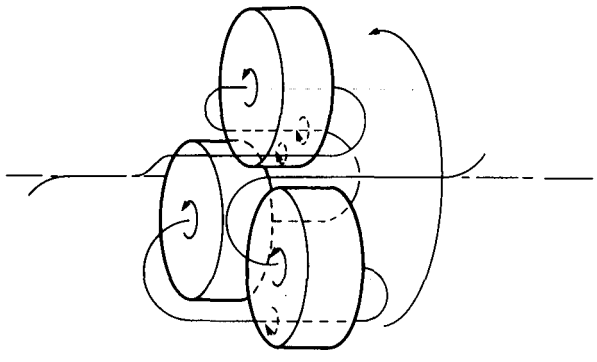

Fig. 1. Orientation and motion of column holders and flow tubes in the present apparatus.

permits flow in and out through the rotating columns without the use of a rotary seal which would become a source of leakage and contamination.

The planetary motion of the column holders and the counter-rotation of the flow tubes above described can be accomplished by the use of a set of 10 identical gears, as shown in Fig. 2, where one stationary sun gear (S) is held on the central axis of the centrifuge and surrounded by 9 planetary gears, *i.e.*, 3 double gears (C) each mounted on the column holder shaft and 3 single gears (T) each affixed to the tube holder shaft. The left half of each double gear interlocks to the stationary sun gear and the right half, to the single planetary gear, while the sun gear is entirely free from the single planetary gears. With this gear arrangement, rotation of the rotary frame around the stationary sun gear causes synchronous rotation of the double gears on the rotary frame and this motion is further conveyed to each single planetary gear to counter-rotate the tube holder shaft holding the flow tube. The number of gears required may be reduced to 8 or 7 but this will sacrifice the symmetry of the gear arrangement in the present design.

Fig. 3 shows a cross-sectional view of the apparatus through the central axis of the centrifuge with a plane across the center of the first column holder. For simplicity, the figure shows a column holder (bottom) and a tube holder shaft (top) on the rotary frame while all other structures behind the scene (including the second column holder, a tube holder shaft, and links) are omitted from the diagram. The motor (right side behind the centrifuge case, as indicated by an arrow) drives the rotary frame around the central stationary pipe via a pair of toothed pulleys coupled with a toothed belt. The rotary frame consists of a pair of aluminum discs rigidly bridged together with multiple links and holds three sets of column holders and tube holder shafts symmetrically at 7.5 cm from the central axis of the centrifuge all through sealed ball bearings. Each column holder is equipped with two identical plastic gears put together on the holder shaft. The first gear on the left side is coupled with the identical stationary sun gear mounted on the central axis of the centrifuge around the stationary pipe. This gear arrangement produces a desired planetary motion of the column

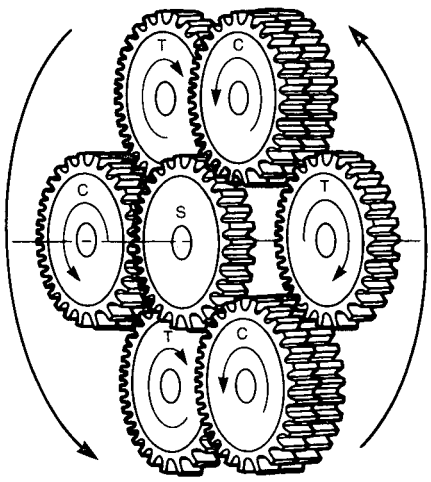

Fig. 2. Gear arrangement of the present apparatus.

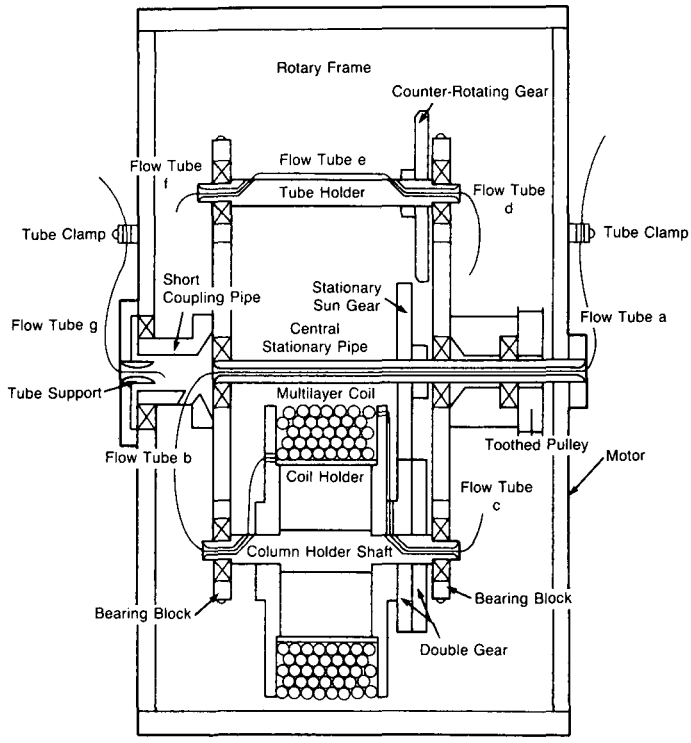

Fig. 3. Cross-sectional view of the apparatus.

holder: revolution around the central axis of the centrifuge and rotation about its own axis at the same angular velocity in the same direction. The second gear on the right side of the column holder shaft is engaged with the identical gear mounted on the tube holder shaft to produce synchronous counter-rotation of the flow tubes, thus fulfilling all the requirements described earlier (see Figs. 1 and 2).

In order to facilitate preparation of multilayer coils, the column holders are designed to be easily removed from the rotary frame by loosening a pair of screws on each bearing block. Each separation column was made by winding a single piece of 1.6 mm I.D. standard wall (0.4 mm thick) PTFE (polytetrafluoroethylene) tubing (Zeus Industrial Products, Raritan, NJ, U.S.A.) directly onto the holder hub of 7.5 cm diameter, forming nine layers of coils between a pair of flanges spaced 5 cm apart. The total capacity of each column measures approximately 135 ml. The β value of the multilayer coil measures 0.5 at the internal terminal to 0.75 at the external terminal. Here, β is given by the ratio of the rotational radius (distance from the holder axis to the coil) to the revolutional radius (distance between the holder axis and the central axis of the centrifuge) and represents an important parameter to govern hydrodynamic distribution of the two solvent phases in the rotating coil[5]. In order to prevent dislocation of the multilayer coil on the holder, the whole column and flanges were covered by heat shrunk vinyl wrapping.

The present centrifuge system requires flexible narrow-bore flow tubes which

can maintain their integrity under repetitive flexing. Each terminal of the multilayer coil was connected to a flow tube of 0.85 mm I.D. and 0.46 mm wall thickness in the following manner: about 1 cm length of the flow tube was inserted into the coil terminal and the junction was covered with several turns of copper wire of about 0.7 mm diameter. The application of this copper wire is to limit heat expansion of the junction, thus forcing the overlapping two tube walls to contact under high pressure. Then, heat was locally applied with a heat gun until the whole junction becomes transparent and fused together. After cooling, the copper wire was removed from the junction. The fused joint thus formed usually can hold the pressure up to several hundred p.s.i. If space is available, the connection can also be made with commercial adaptors on the outside of the flanges.

Interconnection of three multilayer coils were made with flow tubes in such a manner that the external terminal of the first column joins the internal terminal of the second column and, similarly, the external terminal of the second column joins the internal terminal of the third column. In this way all multilayer coils are subjected to the identical elution modes.

The arrangement of the tubing is partially indicated in Fig. 3 (tube a–g); the whole passage is schematically shown in Fig. 1. The inflow tube enters the centrifuge from the right side through the opening of the central stationary pipe, and it passes the side hole of the short coupling pipe at the left end of the rotary frame where it forms an arch to reach the first column holder. Interconnection flow tube between the first and the second columns leaves the first column holder from the right side and, after forming an arch, it runs along the first tube holder towards the left across the rotary frame. On the left side of the rotary frame, the flow tube again forms an arch to reach the second column holder through the center hole on the holder shaft. The interconnection flow tube between the second and the third columns similarly runs through the second tube holder shaft. The outflow tube from the third column leaves the holder from the right side and, after passing through the third tube holder shaft, it reaches the left side of the rotary frame where it enters another side hole of the short coupling pipe to reach the stationary tube support projecting from the left wall of the centrifuge.

These flow tubes on the rotary frame were secured onto each tube holder with a pair of nylon ties while inflow and outflow tubes were each firmly held onto the centrifuge wall with a silicone-rubber-padded clamp. These flow tubes were lubricated with silicone grease and protected with a sheath of tygon tubing where supported or secured to prevent direct contact with metal parts. With this precaution, the flow tubes can maintain their integrity for many months of operation.

The apparatus can be operated up to the maximum revolutional speed of 1500 rpm with a speed control unit (Bodine Electric Co., Chicago, IL, U.S.A.). In the present studies, a Beckman Accu-Flo pump was used to pump the solvents, an LKB Uvicord S (2.5 mm light path) and a six-channel recorder to monitor the absorbance at 275 nm, and an LKB fraction collector to obtain fractions.

EXPERIMENTAL

Reagents

Chloroform was of glass distilled chromatographic grade containing 1% etha-

nol preservative (Burdick and Jackson Labs., Muskegon, MI, U.S.A.) while glacial acetic acid (J. T. Baker, Phillipsburg, NJ, U.S.A.) and 1 *M* hydrochloric acid (Fisher Scientific, Pittsburgh, PA, U.S.A.) were both reagent grade. All DNP amino acids were reagent grade (Sigma, St. Louis, MO, U.S.A.) and include N-DNP-L-aspartic acid (DNP-asp), N-DNP-DL-glutamic acid (DNP-glu), N,N-diDNP-L-cystine [diDNP-$(cys)_2$], N-DNP-L-alanine (DNP-ala), and N-DNP-L-valine (DNP-val).

Preparation of two-phase solvent system and sample solutions

A two-phase solvent system used in the present study consisted of chloroform, glacial acetic acid and 0.1 *M* hydrochloric acid at a volume ratio of 2:2:1. The solvent mixture was thoroughly equilibrated in a separatory funnel by repeating vigorous shaking and degassing several times and the two solvent phases separated shortly before being applied to the column.

Two sample solutions were prepared, one for the runs with the lower non-aqueous phase used as the mobile phase and the other for the runs with the upper aqueous phase mobile. In the experiment with the lower phase mobile, a sample mixture consisting of 100 mg of DNP-val, 100 mg of DNP-ala, 20 mg of diDNP-$(cys)_2$, and 200 mg of DNP-glu was dissolved in the upper stationary phase for a final volume of 42 ml at a concentration of 1% (w/v). Similarly, in the experiment with the upper phase mobile, a mixture of DNP-asp, DNP-glu, diDNP-$(cys)_2$, and DNP-ala at a weight ratio of 5:5:1:10 was dissolved in the lower stationary phase at a concentration of 1% (w/v). In both series of experiments, various sample volumes of 1 ml (10 mg), 5 ml (50 mg), and 25 ml (250 mg) were charged to the column.

Separation procedures

The separations were performed according to the standard procedure used for HSCCC as follows: in each experiment, the entire column (including the dead space in the flow tubes) was filled with the stationary phase. This was followed by injection of the sample solution through the sample port. Then, the centrifuge was rotated at 1250 rpm while the mobile phase was pumped into the column at a flow-rate of 4 ml/min in the proper elution mode, *i.e.*, from the head toward the tail for the lower phase and from the tail toward the head for the upper phase. The effluent from the outlet of the column was continuously monitored with a Uvicord S at 275 nm and fractionated with a fraction collector to obtain 3 ml fractions. After all peaks were eluted from the column, the centrifuge run was terminated, and the column inlet was connected to a pressured N_2 line (100 p.s.i.) to collect the column contents into a graduated cylinder to measure the volume of the stationary phase retained in the column. During the collection of the column contents, the column was rotated at about 200 rpm in the tail-to-head elution mode to accelerate the process. The column was then washed by pumping with methanol and water (each about 100 ml in volume) while slowly rotating the column in the tail-to-head elution mode. Finally, the column-coil was flushed and dried with N_2 prior to the next experiment.

Analysis of fractions

An aliquot of each fraction containing the colored sample was diluted with a known amount of methanol and the absorbance was determined at 430 nm with a Zeiss PM6 spectrophotometer.

RESULTS AND DISCUSSION

The capability of the present apparatus was examined in separation of DNP amino acid samples in a two-phase solvent system composed of chloroform, acetic acid, and 0.1 *M* hydrochloric acid at a 2:2:1 volume ratio using both the upper and the lower phases as the mobile phase. All separations were performed under the optimum experimental condition using a flow-rate of 4 ml/min and a revolutional

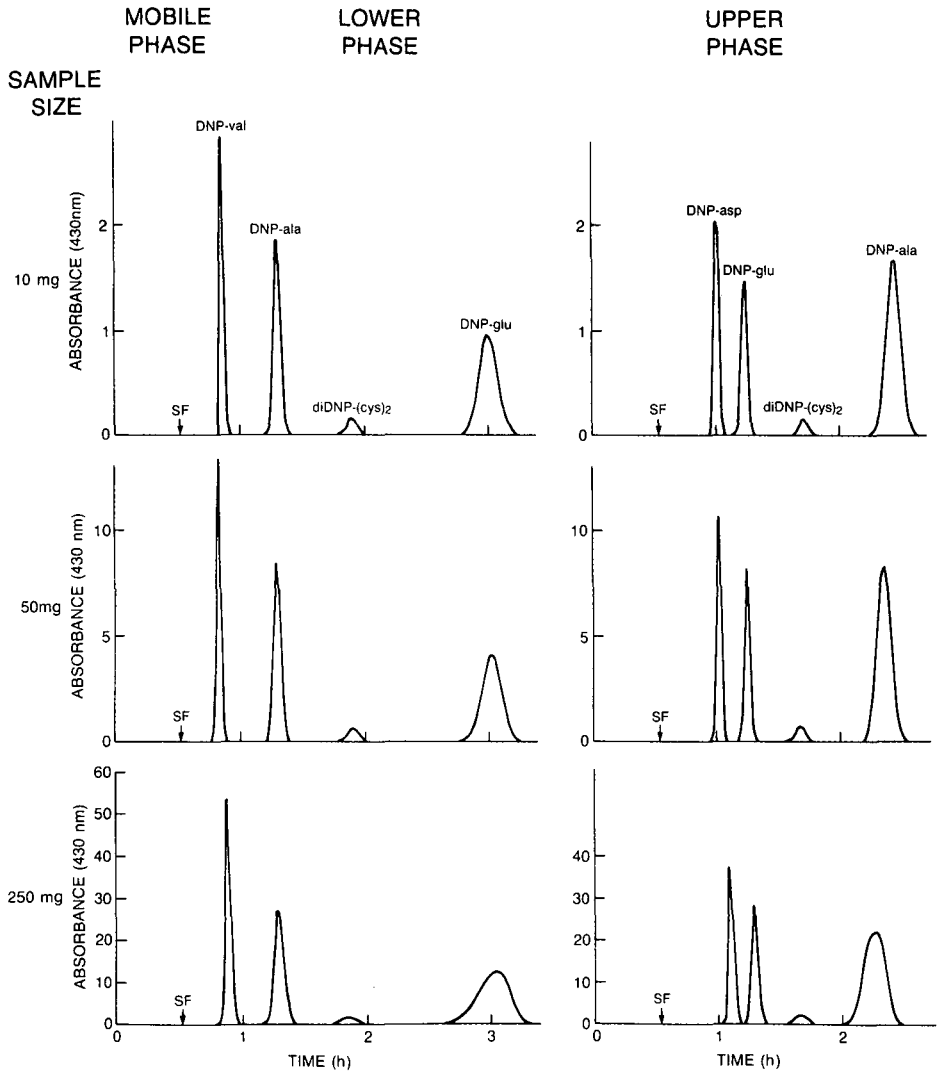

Fig. 4. Chromatograms of DNP amino acids obtained from the present apparatus. Experimental conditions are as follows: Two-phase solvent system: chloroform–acetic acid–0.1 *M* hydrochloric acid (2:2:1, v/v/v); elution mode: head-to-tail for the lower phase of the mobile phase (left column) and tail to head for the upper phase (right column): flow-rate: 240 ml/h; revolution: 1250 rpm.

speed of 1250 rpm. The results are summarized in Fig. 4 where a set of chromatograms is arranged according to the choice of the mobile phase and the applied sample size. In all chromatograms, four components are completely separated and eluted within 4 h.

Partition efficiency of these srparations can be estimated according to the conventional gas chromatographic equation

$$N = (4R/W)^2 \quad (1)$$

where N is the partition efficiency expressed in terms of theoretical plates (TP); R is the retention time or volume of the peak maximum; and W is the peak width expressed by the same unit as R.

The results show that the highest partition efficiencies are found in the 10-mg sample group where the average value for the lower phase of the mobile phase is 2100 TP and that for the upper phase is 2400 TP. These figures are so far the highest among the results obtained with the existing HSCCC instruments. As the sample size is increased to 250 mg, the average partition efficiencies decrease to 1100 TP for the lower phase of the mobile phase and 1400 TP for the upper phase. Using these TP values, the partition efficiencies of the present system can be expressed in various ways such as the length of tubing per TP (cm/TP), TP number produced by each helical turn of the column (TP/turn), and the time required to yield one TP (s/TP) as listed in Table I.

The multilayer coils of the present apparatus, consisting of about 600 helical turns of a 200-m length of tubing, can produce one TP in every 10 cm of the tubing or each helical turn yields 3–4 TP which is comparable to other HSCCC schemes. These results clearly indicate that the use of multilayer coils connected in a series on the rotary frame yields the partition efficiency increased in proportion to the tubing length or total number of helical turns as demonstrated in the previous studies with a pair of multilayer coils[4]. The degree of speed in the separation can be expressed by the time required to produce one TP which is computed by dividing the retention time of the solvent front by the experimental TP value. The present column produces a high partition rate of one second/TP, while the classical counter-current distribution appa-

TABLE I

SUMMARY OF EXPERIMENTAL RESULTS

Exp.[a] *No.*	*Mobile phase*	*Sample size (mg)*	*Partition efficiency (TP)*					*cm/TP*	*TP/turn*	*s/TP*	*Retention (%)*
			P-1[b]	*P-2*	*P-3*	*P-4*	*Mean*				
1	LP	10	2300	2200	2300	1800	2125	9.4	3.5	0.9	62.6
2	LP	50	2000	1900	1800	1400	1775	11.2	3.0	1.0	62.5
3	LP	250	1600	1200	1000	700	1125	17.5	1.9	2.0	63.5
4	UP	10	2800	2800	2300	1800	2425	8.2	4.0	0.9	56.1
5	UP	50	2700	2500	2300	1700	2300	8.6	3.9	1.0	51.6
6	UP	250	1800	1900	1100	800	1400	14.2	2.3	1.7	44.5

[a] See Fig. 4 for experimental conditions.

[b] Peak. For identity of peaks see Fig. 4.

ratus generally requires a few minutes for each transfer which corresponds to one plate, and the droplet CCC developed 10–20 years ago produces one TP in every 45 seconds[6].

One important characteristic feature of HSCCC is its unique ability to produce a highly efficient separation under a relatively low column pressure compared with other CCC schemes. All DNP amino acid separations described above were obtained at the maximum back pressure of 80 p.s.i. for the head-to-tail elution and 30 p.s.i. for the tail-to-head elution as measured with a pressure gauge mounted at the outlet of the pump. Being a rotary-seal-free flow-through mechanism, the present system can safely function against several hundred p.s.i., and the critical pressure which causes leakage may be substantially increased by the use of thick-wall separation columns. Therefore, the partition efficiency of the present apparatus can be further increased several times without a risk of leakage simply by increasing the width of the column holder and/or applying multilayer coils with a smaller I.D. tubing.

The overall results of our studies indicated that the present apparatus can separate hundred milligram quantities of samples at a high partition efficiency in several hours of elution. The results also suggest that small quantities of material can be isolated from the bulk of impurities with a high recovery rate as demonstrated in the separation of diDNP-cystine from the rest of the components. Preliminary applications of the present apparatus to various natural products will be described in Part II.

REFERENCES

1 Y. Ito, *CRC Crit. Rev. Anal. Chem.*, 17 (1986) 65.
2 Y. Ito, *J. Chromatogr.*, 214 (1981) 122.
3 Y. Ito, J. Sandlin and W. G. Bowers, *J. Chromatogr.*, 244 (1982) 247.
4 Y. Ito and F. E. Chou, *J. Chromatogr.*, 454 (1988) 382.
5 Y. Ito, *J. Chromatogr.*, 301 (1984) 387.
6 T. Tanimura, J. J. Pisano, Y. Ito and R. L. Bowman, *Science (Washington, D.C.)*, 169 (1970) 54.

Journal of Chromatography, 475 (1989) 229–235
Elsevier Science Publishers B.V., Amsterdam — Printed in The Netherlands

CHROM. 21 533

IMPROVED METHOD FOR CONTINUOUS UV MONITORING IN HIGH-SPEED COUNTER-CURRENT CHROMATOGRAPHY

HISAO OKA[a] and YOICHIRO ITO*

Laboratory of Technical Development, National Heart, Lung, and Blood Institute, Building 10, Room 5D12, 9000 Rockville Pike, Bethesda, MD 20892 (U.S.A.)

(First received January 25th, 1989; revised manuscript received March 28th, 1989)

SUMMARY

Continuous UV monitoring of the effluent in high-speed counter-current chromatography often encounters difficulty mainly due to the thermolabile nature of the mobile phase which tends to develop turbidity in the flow cell under a slight shift of the ambient temperature. This problem was effectively solved by inserting a fine PTFE tube (3 m × 0.46 mm I.D.) between the column outlet and the UV monitor and immersing a large portion of the tube into a waterbath heated at 30°C. A similar tube was applied at the outlet of the UV monitor to create back pressure which suppressed gas bubble generation from the mobile phase. By the combined use of these devices, noiseless UV tracing was successfully demonstrated in two model experiments using thermolabile two-phase solvent systems: separation of flavonoids from the sea buckthorn ethanol extract with chloroform–methanol–water (4:3:2, v/v/v) and separation of bacitracin components with chloroform–ethanol–water (5:4:3, v/v/v).

INTRODUCTION

High-speed counter-current chromatography (HSCCC) using a multi-layer coiled column is a unique liquid–liquid partition technique that does not require the use of solid supports[1]. The use of two immiscible solvent phases in an open column free of solid support matrix can eliminate various complications associated with conventional liquid chromatography such as tailing of solute peaks, adsorptive sample loss and deactivation, and sample contamination. On the other hand, it is usually difficult to obtain stable continuous UV monitoring of the effluent from a CCC separation and, therefore, the elution curve is usually drawn manually by the spectrophotometric analysis of individual fractions after the effluent is fractionated with a fraction collector[2–4]. In order to avoid the above laborious procedure, it is highly desirous to establish a CCC monitoring system which produces stable UV tracing of the elution curves comparable to those obtained from other chromatographic methods.

Problems in direct UV monitoring of the effluent in CCC may be classified into

[a] Visiting scientist from Aichi Prefectural Institute of Public Health, Nagoya, Japan.

0021-9673/89/$03.50

the following four categories: (1) steady carryover of the stationary phase due to an improper choice of the elution mode and/or the application of an excessively high flow-rate of the mobile phase; (2) migration of the stationary phase into the flow cell which is caused by various conditions such as fluctuations of revolutional speed, vibration of the centrifuge system, and overloading of the sample (which may cause local alteration of the phase volume ratio and the physical properties of the two phases); (3) turbidity of a thermolabile mobile phase in the flow cell due to altered ambient temperature; (4) gas bubble formation from the effluent under reduced pressure in the periphery of the flow passage. Among those, the first two problems can be avoided by a proper choice of the experimental conditions, whereas a suitable modification of the UV monitoring system is essential to overcome the remaining problems[5].

The present paper describes a simple and effective method for continuous UV monitoring of the effluent in HSCCC to yield noiseless tracing comparable to that in high-performance liquid chromatography.

EXPERIMENTAL

Apparatus

The high-speed counter-current chromatograph used in this study was the commercial model of a flow-through coil planet centrifuge called "Ito Multi-layer Coil Separator-Extractor" (P.C. Inc., Potomac, MD, U.S.A.). The column holder is positioned at a distance of 10 cm from the central axis of the centrifuge. The separation column was prepared by winding a long piece of PTFE tubing, 1.6 mm I.D. and 0.3 mm wall thickness, directly onto the holder hub of 10 cm diameter making multiple coiled layers. The β value (the ratio of the rotational radius to the revolutional radius) ranges from 0.5 at the internal terminal to 0.8 at the external terminal. The total capacity of the multi-layer coil measures about 280 ml. This apparatus is equipped with an ACCU-FLO-pump (Beckman, Palo Alto, CA, U.S.A.) and a speed controller (Bodine, Chicago, IL, U.S.A.). Continuous UV monitoring was performed with an LKB 2138 Uvicord S UV monitor (LKB, Bromma, Sweden) operated at 254 nm and a Pharmacia 482 recorder (Pharmacia, Uppsala, Sweden). On the flow line between the coiled column and the UV monitor, a fine PTFE tube of 3 m × 0.46 mm I.D. (Zeus, Raritan, NJ, U.S.A.) was inserted, which can be heated in a water bath at a desired temperature. A similar tube was also applied at the outlet of the UV monitor to prevent a sudden pressure drop which would generate gas bubbles from the mobile phase.

Reagents

Organic solvents including *n*-hexane, ethyl acetate, chloroform, *n*-butanol, *sec.*-butanol, and methanol were all of glass-distilled chromatographic grade (Burdick and Jackson Labs., Muskegon, MI, U.S.A.) while 95% ethanol (Warner-Graham, Cockeysville, MD, U.S.A.) and glacial acetic acid (J. T. Baker, Phillipsburg, NJ, U.S.A.) were of reagent grade. Dried sea buckthorn ethanol extract was obtained from China by the courtesy of Professor Tian You Zhang at Beijing Institute of New Technology Application, Beijing, China, and bacitracin was purchased from Sigma, St. Louis, MO, U.S.A.

Procedure for thermostability test of solvent systems

From the above organic solvents, 11 pairs of solvent systems with a broad spectrum in hydrophobicity (see Table I for their composition) were examined for their thermostability. Each solvent mixture, ranging 3–5 ml in volume, was delivered in a test tube (100 mm × 13 mm O.D.) and a polyethylene plug was applied to the tube. Then, the contents were thoroughly mixed to bring the phases to equilibrium at room temperature (*ca.* 22°C). The mixing was repeated until two clear layers were obtained.

TABLE I

EFFECTS OF TEMPERATURE ON TWO-PHASE EQUILIBRIUM

No.	*Solvent systems*	*Effects of temperature*[a]			
		Cooling		*Warming*	
		UP	*LP*	*UP*	*LP*
1	Hexane–methanol	+	+	−	−
2	Hexane–methanol–water (2:1:1, v/v/v)	−	±	−	−
3	Hexane–ethyl acetate–methanol–water (1:1:1:1, v/v/v/v)	±	+	−	−
4	Ethyl acetate–water	+	−	−	+
5	Ethyl acetate–acetic acid–water (4:1:4, v/v/v)	±	−	−	−
6	Chloroform–water	−	+	−	−
7	Chloroform–methanol–water (5:4:3, v/v/v)	+	+	−	−
8	Chloroform–acetic acid–water (2:2:1, v/v/v)	+	+	−	−
9	*n*-Butanol–water	+	−	−	+
10	*n*-Butanol–acetic acid–water (4:1:5, v/v/v)	+	−	−	−
11	*sec.*-Butanol–water	−	−	+	+

[a] UP = upper phase; LP = lower phase; + = development of turbidity; − = no change in transparency.

In the first series of experiments, each tube was immersed in ice water for 5–10 s to observe turbidity in the upper and/or the lower phases. The second series of experiments was similarly performed with the same set of solvent systems pre-equilibrated at room temperature by immersing each tube into warm water (*ca.* 40°C) for 5–10 s to observe development of turbidity in each phase. All experiments were repeated at least twice to ensure reproducibility of the results.

Preparation of solvent systems and sample solutions

Two different two-phase solvent systems were prepared: chloroform–methanol–water (4:3:2, v/v/v) for separation of flavonoids from the sea buckthorn ethanol extract and chloroform–ethanol–water(5:4:3, v/v/v) for separation of bacitracin components. Each solvent mixture was thoroughly equilibrated in a separatory funnel at room temperature by repeated vigorous shaking and degassing by opening the stopcock, and the two phases were separated shortly before use.

The sample solutions of sea buckthorn ethanol extract and bacitracin were similarly prepared by dissolving 50 mg of each sample in 4.5–4.8 ml of the above solvent mixture used for the separation.

Separation procedure

In each experiment, the coiled column was first entirely filled with the upper aqueous stationary phase, and the sample solution containing 50 mg of the sample was injected into the head of the column through the sample port. (The head–tail relationship of the rotating coil is conventionally defined by an Archimedean screw force which acts on each phase to different extents but in the same direction, namely, towards the head of the coil) Then, the coil planet centrifuge was rotated at the optimal speed of 800 rpm, while the mobile phase was pumped into the head of the column at a flow-rate of 180 ml/h. Effluent from the outlet of the column was continuously monitored with a Uvicord S at 254 nm to record the elution curve. In order to prevent trapping the stationary upper phase within the flow cell, the effluent (lower phase) was passed through the flow cell in an upward direction. During the elution, the fine tube on the flow line between the column outlet and the monitor was immersed in a water bath at the desired temperature which was maintained with a heating rod and a thermal controller (Fisher, Pittsburgh, PA, U.S.A.).

RESULTS AND DISCUSSION

Phase compositions of the two-phase solvent system used in CCC are in a subtle equilibrium at room temperature. Any change in the ambient temperature may cause one or both phases to develop a cloudy appearance; when this occurs in the flow cell of

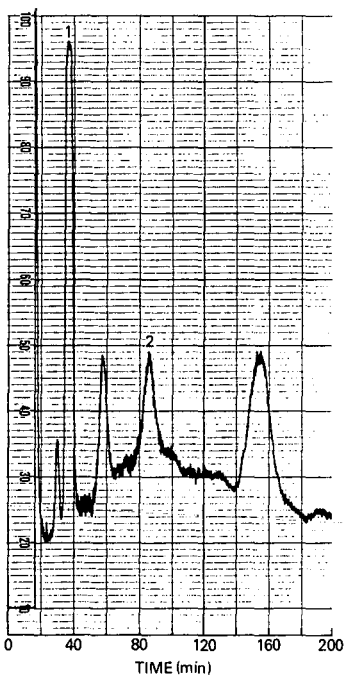

Fig. 1. UV tracing chart in flavonoid separation obtained with the conventional monitoring for HSCCC. Experimental conditions: Monitor, LKB Uvicord S; flow cell, rectangular type, 2.5-mm light path, 10 μl capacity; wavelength, 254 nm; recorder, Pharmacia Model 482 recorder; chart speed, 0.5 mm/min. Peaks: 1 = isorhamnetin; 2 = quercetin.

the UV monitor, it results in an intensive noise and raised base line in the elution curve tracing. The effects of cooling and warming on each phase of 11 selected solvent systems are summarized in Table I where positive signs indicate development of turbidity and negative signs, no change in transparency. The results clearly show that in the majority of these solvent systems cooling tends to develop turbidity in the organic phase, *i.e.*, the lower phase in the chloroform systems, both phases in the non-aqueous hexane–methanol system, and the upper phase in the remaining solvent systems. On the other hand, warming gives no change in transparency except for some binary systems including *sec.*-butanol–water, *n*-butanol–water and ethyl acetate–water. These results strongly suggest that warming the effluent not only prevents development of the turbidity in the effluent, but it may also enable the mobile phase to absorb some amounts of the stationary phase carried over from the separation column. Hence, warming serves to maintain high transparency of the effluent passing through the flow cell in the UV monitor.

In the present studies, these observations were applied to the separation of natural products on two different chloroform solvent systems both utilizing the thermolabile lower non-aqueous phase as the mobile phase. Fig. 1 shows a typical chromatogram of flavonoids in the sea buckthorn ethanol extract with a solvent system of chloroform–methanol–water (4:3:2, v/v/v) obtained by the conventional monitoring method for HSCCC. The effluent was continuously passed upward through a straight standard flow cell held vertically in the Uvicord S where the absorbance was monitored at 254 nm. The thermolabile nature of the lower mobile

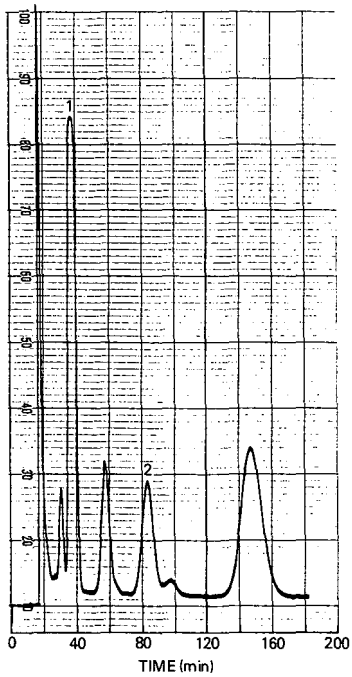

Fig. 2. UV tracing chart in flavonoid separation obtained by heating the effluent. The effluent from the separation column was passed through a fine tube immersed into a water bath maintained at 30°C. Other experimental conditions as in Fig. 1.

phase led to a UV tracing of the elution curve which was disturbed by intensive noise and irregular elevation of the base line. The overall effect was to obscure a minor peak in the chromatogram.

Fig. 2 shows a chromatogram obtained under similar experimental conditions except that the effluent from the separation column was first passed through a narrow tube heated to 30°C in a water bath before entering the UV monitor. The results clearly demonstrate a radical improvement in UV tracing as evidenced by a stable flat base line and smooth tracing of the elution curve. A minor peak, which was obscured by noise in Fig. 1, is now clearly observed in the chromatogram. A slight thickening of the base line was found to be caused by periodical passage of gas bubbles through the flow cell.

Formation of gas bubbles in the peripheral portion of the separation column is a common complication in both liquid chromatography and CCC. This undesirable phenomenon can be effectively controlled by applying a narrow-bore tube at the outlet of the monitor to maintain sufficient back-pressure. A chromatogram of flavonoids shown in Fig. 3 was obtained from a Uvicord S UV monitor equipped with a fine tube (3 m × 0.46 mm I.D.) at the outlet without heating the effluent. This simple method produced a substantial improvement in tracing over the control run (Fig. 1) by eliminating high-frequency noise which was apparently caused by the passage of gas bubbles through the flow cell.

Finally, the experiment was performed by applying both modifications, *i.e.*, heating the effluent to 30°C near the inlet of the monitor and attaching a narrow-bore

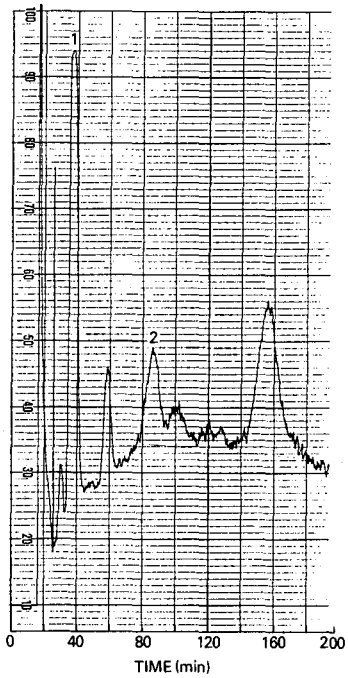

Fig. 3. UV tracing chart in flavonoid separation obtained by applying a fine tube at the outlet of the monitor. Other experimental conditions as in Fig. 1.

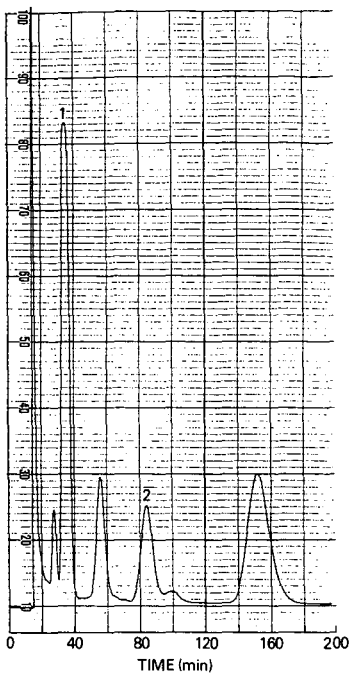

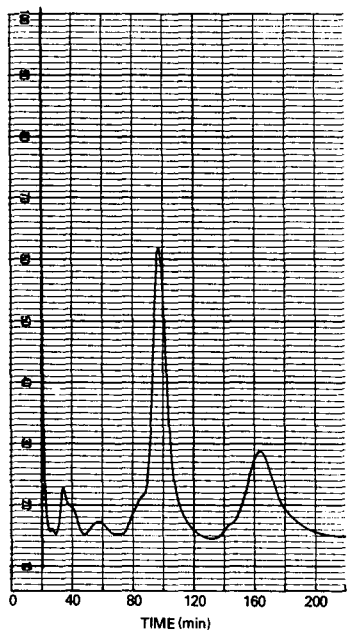

Fig. 4. UV tracing chart in flavonoid separation obtained by the present method. The effluent from the separation column was heated to 30°C before entering the monitor, and a fine tube was applied to the outlet of the monitor to create back pressure.

Fig. 5. UV tracing chart in bacitracin separation by the present method. UV monitoring conditions as in Fig. 4.

tube at the outlet of the monitor. Fig. 4 shows the counter-current chromatogram of flavonoids which was obtained by the present method. As expected, the method yielded a noiseless UV tracing of the elution curve that is comparable in quality to those obtained from HPLC. The chromatogram was found to be almost identical to the elution curve manually drawn after the spectrophotometric analysis of individual fractions without the use of the present device. The above method was also successfully applied to the separation of bacitracin with a two-phase solvent system composed of chloroform–ethanol–water (5:4:3, v/v/v) using the lower nonaqueous phase as the mobile phase (Fig. 5).

As described above, we have established a simple method for stable continuous UV monitoring of effluent from HSCCC. The method may also be effectively applied for other CCC schemes. All elements used in the present device, including fine PTFE tubing, a heater, and a thermoregulator, etc., will be incorporated in the future design of a UV monitor for CCC.

REFERENCES

1 Y. Ito, *CRC Crit. Rev. Anal. Chem.*, 17 (1986) 65.
2 Y. Ito, J. Sandlin and W. G. Bowers, *J. Chromatogr.*, 244 (1982) 247.
3 T. Y. Zhang, D. G. Cai and Y. Ito, *J. Chromatogr.*, 435 (1988) 159.
4 T. Y. Zhang, X. Hua, R. Xiao and S. Kong, *J. Liq. Chromatogr.*, 11 (1988) 233.
5 A. Berthod and D. W. Armstrong, *J. Liq. Chromatogr.*, 11 (1988) 1457.

Journal of Chromatography, 475 (1989) 237–245
Elsevier Science Publishers B.V., Amsterdam — Printed in The Netherlands

CHROM. 21 492

GAS CHROMATOGRAPHIC DETECTION BY ELECTRON IMPACT-INDUCED FLUORESCENCE SPECTROMETRY OF MOLECULAR FRAGMENTS

L. F. GUILBAULT, RONALD HOHMANN and E. L. WEHRY*
Department of Chemistry, University of Tennessee, Knoxville, TN 37996-1600 (U.S.A.)
(First received December 12th, 1988; revised manuscript received March 13th, 1989)

SUMMARY

Detection in gas chromatography (GC) via measurement of fluorescence of fragment species formed by 100-eV electron impact (EI) of compounds as they elute from the column is described. The detector is both selective (generating fragment species diagnostic of functional groups present in the parent molecule) and universal (producing a signal for all analytes). Figures of merit (limits of detection, linearity and precision) for EI-induced fragment fluorescence detection in GC are reported.

INTRODUCTION

Molecular fluorescence spectrometry exhibits two important characteristics (the ability to detect very small quantities of compounds and the generation of information useful for compound identification) that cause the technique to be of considerable potential utility for detection in gas chromatography (GC)[1]. Numerous detection systems for GC based on the measurement of molecular fluorescence have been described[2–13], some of which use supersonic expansion or matrix isolation techniques[7,9,11–13].

A major shortcoming of molecular fluorescence in chromatographic detection is that most molecules do not exhibit sufficiently high fluorescence quantum yields to be detectable at realistic concentrations. This difficulty has been surmounted in liquid chromatography by the widespread application of derivatization reactions that convert non-fluorescent analytes to fluorescent products[14]. Analogous procedures for GC detection have been much slower to develop.

Virtually any non-fluorescent molecule in the gas phase can be fragmented to form fluorescent species; such common molecular fragments as OH, NH, CN, CH and SH (as well as many atomic fragments) are intensely fluorescent, and their spectroscopic characteristics are well known[15]. The most common techniques for converting non-fluorescent molecules to fluorescent fragments are photolysis[16–21] and electron impact (EI)[19,22–25]. With the use of electronic array detectors, fluorescence spectra of fragments formed from compounds eluting from a GC column are measurable "on-the-fly".

0021-9673/89/$03.50

In 1984, Gierczak *et al.*[24] discussed the characteristics of EI-induced fragmentation as a means of generating emissive fragments from a variety of non-fluorescent organic molecules and considered its potential advantages as a technique for detection in GC. However, these investigators did not interface their EI-fluorescence apparatus to a gas chromatograph, and were thus unable directly to assess its performance as a GC detector. The present report describes techniques for interfacing electron impact-fragmentation fluorescence spectrometry (EI-FFS) to a gas chromatograph and the characteristics of EI-FFS as a GC detector.

EXPERIMENTAL

Instrumentation

A schematic diagram of the apparatus is shown in Fig. 1. A gas chromatograph (Perkin-Elmer Sigma 3) is equipped with a glass capillary column (30 m × 0.5 mm O.D.). The end of the column is connected, via a union fitting, to a glass capillary tube of the same diameter as the column, which is threaded through a heated glass-lined stainless-steel transfer line (15 cm × 0.6 cm O.D.) that passes the column eluent into a vacuum chamber. No splitters or other interface devices are used; the entire GC eluent is transferred through the glass capillary tube to the vacuum chamber. The chamber comprises a two-compartment stainless-steel cross, having a total volume of 4 l, differentially pumped by two Balzers TSU 331 turbomolecular pumps (pumping speeds: 330 l/s for helium). The pressure in the chamber is $3 \cdot 10^{-8}$ Torr or less in the absence of sample.

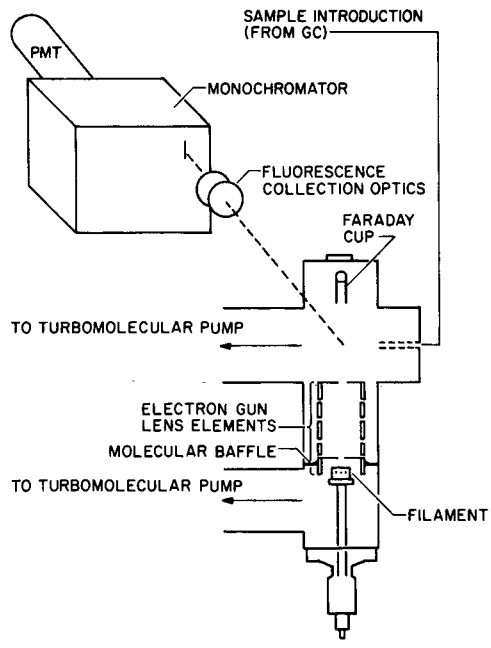

Fig. 1. Schematic diagram of EI-FFS detector, using a photomultiplier tube (PMT) to detect fluorescence.

The two compartments of the chamber are separated by the lens assembly of an electron gun constructed to the design of Erdman and Zipf[26]. The gun comprises a nickel grid, three gold-plated copper electron lenses (separated from one another by an assembly of sapphire balls), and a filament that serves as the electron source. From among the various filament materials available, 1% thoriated tungsten (Scientific Instrument Services, Ringoes, NJ, U.S.A.) appears least susceptible to corrosion in the presence of a wide variety of organic compounds. The filament is operated at 2.5 A and −100 V. The electron lens elements direct the 100-eV electron beam to its point of intersection with the GC eluent, where its current is approximately 1 mA ($6 \cdot 10^{15}$ electrons/s) and its diameter is 1 cm.

Fluorescence exits the chamber through a quartz viewport and is focused by two fused-silica lenses (focal lengths: 15 and 20 cm) onto either of two detection systems. For acquisition of fragment fluorescence spectra "on-the-fly", an EGG PAR OMA-II system, consisting of a Model 1420 intensified silicon diode array mounted to a Model 1225 0.25-m polychromator, is used. With 0.25-mm entrance and exit slits, a total spectral range of 130 nm is dispersed across the 700 intensified elements in the diode array, giving rise to an effective spectral resolution of 0.2 nm. The diode array is cooled to a temperature of 258 K. In all cases, any fluorescence background contributed by the carrier gas is subtracted.

For fluorescence measurements at fixed wavelength, an RCA 8850 photomultiplier tube mounted on a 0.25-m monochromator (Kratos GM-250), is used as a photon counter with EGG ORTEC modular photon-counting electronics. The photomultiplier tube is operated at room temperature at 1750 V. Using 0.70-mm entrance and exit slits, the spectral bandpass of the monochromator is 2 nm. Fluorescence spectra or gas chromatograms are plotted by an X–Y recorder.

Chromatographic techniques

The GC column is a 30 m × 0.32 mm I.D. glass capillary using, as bonded stationary phase, methyl-3,3,3-trifluoropropyl polysiloxane (J&W Scientific). Helium is used as carrier gas. The column can be operated isothermally or can be temperature programmed. Both for isothermal and temperature-programmed operation, the range of column temperatures used in this work was 300–365 K.

RESULTS AND DISCUSSION

Fragment fluorescence spectra

EI-FFS spectra for a large number of compounds have been obtained; representative example spectra are shown in Fig. 2. Table I lists the most intense fragment emissions, and their wavelength maxima, for a number of monofunctional organic compounds. As noted previously by Gierczak *et al.*[24], EI-FFS spectra of organic molecules tend to be very rich in hydrogen atomic emission lines. Other prominent fluorescent fragments include CN (from nitriles and amines), OH (from alcohols), SH^+ (from thiols), CO (from carbonyl compounds and ethers) and Cl^+ (from chlorinated compounds). In Table II are compiled the most intense fragment emissions produced by EI of a series of bifunctional organic compounds. In most cases, fragment emissions diagnostic of both functional groups are observed (*e.g.*, OH and SH^+ from 2-mercaptoethanol).

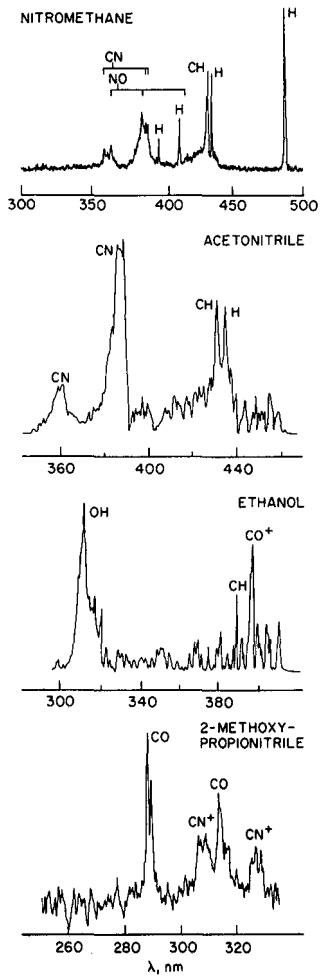

Fig. 2. EI-FFS spectra at 100 eV of nitromethane, acetonitrile, ethanol and 2-methoxypropionitrile. Major fragment emissions are identified in each case.

Using the definitions of Ettre[27], EI-FFS is a "selective" detector; *i.e.*, it identifies classes of compounds, but cannot be expected generally to produce conclusive identification of specific molecules. For example, the EI-FFS spectrum of an unknown aliphatic amine provides unambiguous identification of the compound class, but fails to identify the specific compound.

Unlike most "selective" detectors, EI-FFS can be used either in "selective" or "universal" modes, depending on whether single- or multiple-wavelength detection of fluorescence is utilized. If fixed-wavelength detection is used (*e.g.*, a monochromator or filter plus a photomultiplier tube), element- or compound-class selective detection is achieved by measuring the fluorescence of a single fragment as compounds elute from the column. For example, if fluorescence is monitored only at 337 nm (the wavelength of NH $A^3\Pi \rightarrow X^3\Sigma$ fluorescence), the EI-FFS detector is selective for primary amines;

TABLE I

FRAGMENTS OBSERVED IN THE EI-FFS SPECTRA OF MONOFUNCTONAL ORGANIC COMPOUNDS

Parent compound	*Fragments (positions of emission lines, nm)*[a]
Acetone	H(486,434,410,397), CH(431,389), CO(314)
Acetonitrile	CN(388), H(486,434,410), CH(431)
Carbon tetrachloride	Cl^+(439,460), CCl(460c,278)[b]
Chloroform-*d*	C^2H(431), ^2H(436,434), Cl^+(439)
Dichloromethane	CH(431,388), H(486,434,410), Cl(439,359)
Diethylamine	H(486,434), CH(431), CN(388)
Ethanethiol	H(486,434,410,397), CH(431, 388), SH^+(360)
Ethanol	H(486,434,410), OH(306), CH(431,389), CO^+(397)
n-Hexane	H(486,434,410), CH(431,388)
Nitrobenzene	H(486,434,410,397), CH(431), CN(388,359), NO(386)
Nitromethane	H(486,434,410,397), CH(431), NO(386,364,354), CN(388,359)
Tetrahydrofuran	H(486,434,410), CO(389,438), CH(431), CO^+(397,395)

[a] Fragments listed in decreasing order of their intensity in EI-FFS spectrum.
[b] c denotes a broad continuum in the EI-FFS spectrum.

if fluorescence is monitored at 388 nm (CN $B^2\Sigma^+ \rightarrow X^2\Sigma^+$ fluorescence), the EI-FFS detector responds to any organic molecule containing a C–N bond. The detector also responds selectively to organometallics; metal atom fluorescence is usually produced[28].

On the other hand, if fluorescence is monitored simultaneously at many wavelengths (using a diode array detector), the EI-FFS detector generates a signal for all compounds, and the individual fragment fluorescences can be used to identify the principal functional groups present in each eluting compound.

Limits of detection

The limit of detection is defined as the minimum quantity of analyte, injected into the chromatograph, required to produce a fluorescence signal twice that of the

TABLE II

FRAGMENTS OBSERVED IN THE EI-FFS SPECTRA OF DIFUNCTIONAL ORGANIC COMPOUNDS

Parent compound	*Fragments (positions of emission lines, nm)*[a]
1-Bromo-3-chloropropane	H(486), CH(431,388), Cl^+(386)
3-Chloro-1-propanol	H(486), OH(306), CH(431), Cl^+(386)
Chlorodifluoromethane	CH(431), H(486,434,410,397), HCl^+(351,359)
2-Mercaptoethanol	H(486,434,410,397), CH(431), OH(306), SH^+(335,360), CS (280,260)
Methoxyacetone	H(486,434), CH(431,388), CO(438)
2-Methoxyethylamine	H(486,434,410), CH(431), CN(388), NH(337), CO(292,313,302)
2-Methoxypropionitrile	H(486,434,410), CH(431), CN(388,359), CO(292,313,302), CN^+(306,318,295)
4-Nitrobutyronitrile	H(486,434), CN(388), CH(431)
2-Nitro-1-propanol	H(486,434,410,397), OH(306), CH(431), CN(388)

[a] Fragments listed in decreasing order of their intensity in EI-FFS spectrum.

TABLE III
LIMITS OF DETECTION FOR EI-FFS DETECTION OF ORGANIC COMPOUNDS

Compound	*Limit of detection (μg)*	*Optical detector*
Acetonitrile	0.8	Photomultiplier tube
	10	Intensified diode array
Chloroform	2	Photomultiplier tube
	45	Intensified diode array
Dichloromethane	0.9	Photomultiplier tube
Nitromethane	1	Photomultiplier tube
	10	Intensified diode array
1-Nitropropane	2	Photomultiplier tube
	25	Intensified diode array
2-Nitropropane	2	Photomultiplier tube
	25	Intensified diode array

background noise observed in the presence only of carrier gas; in each case, the fluorescence measurement is made at the wavelength maximum of the EI-FFS spectrum (usually H_β fluorescence, 486 nm). The results are compiled in Table III, wherein it is noted that the limits of detection obtained using the photomultiplier tube as detector are invariably superior to those obtained using the diode array detector. These results are indicative of the relative detectivities of our diode array and photomultiplier systems, and cannot be generalized to conclude that photomultiplier detection is invariably superior to use of an array detector.

Linearity

EI-FFS measurements are generally linear in the partial pressure of parent compound in the vacuum chamber from the limit of detection (typically *ca.* 10^6 Torr) to an upper pressure limit (*ca.* 10^{-3} Torr) which exceeds that ever reached using a capillary GC column[19]. It is therefore expected that the analytical calibration curve for GC detection by EI-FFS should be linear over at least three decades in quantity of analyte. This prediction was verified for nitromethane (measuring the H emission at 486 nm), for which the calibration plot was linear over the range 1 μg–2 mg. Accordingly, quantitative calibration techniques for which linear analytical curves are desirable (*e.g.*, standard addition) should be readily applicable to GC using EI-FFS detection.

Precision

One of the major advantages of EI is that beam currents from heated-filament electron guns can be regulated with much higher precision than the outputs of most photon sources used in conventional fluorescence spectrometry. Typical relative standard deviations for repetitive measurements of fragment intensities in EI spectra of pure compounds introduced into the vacuum chamber by bulb (rather than GC) are 1.0% or less[19]. Hence, for EI-FFS in GC detection, the precision is determined by the reproducibility with which samples are injected onto the column, rather than that of fragment production and fluorescence detection.

Dead volume

An important characteristic of a chromatographic detector is the extent to which its dead volume degrades the apparent efficiency of the chromatographic column. Obviously, the vacuum chamber used in EI-FFS detection has a much greater volume than many conventional GC detectors. However, the total volume of the capillary tube used to transport the column eluent to the vacuum chamber is very small, and the flow-rate of gas through the vacuum chamber is such that the residence times of eluent molecules in the observation region are very short. For capillary column GC, the base widths of chromatographic peaks increased by an average factor of 1.012 when EI-FFS detection was used, compared with those obtained using a conventional flame ionization detector. The largest increase in peak base width observed for EI-FFS detection, relative to that obtained using the flame ionization detector, was a factor of 1.02. Hence, despite the relatively large volume of the EI-FFS detector, only minor peak broading is introduced. An example chromatogram of a eight-component mixture, using H atom fluorescence at 486 nm, is shown in Fig. 3.

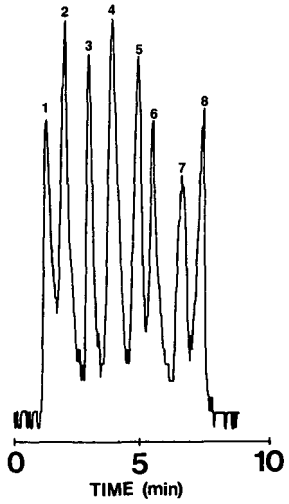

Fig. 3. EI-FFS chromatogram of eight-component mixture measured at 486 nm (H_β fluorescence). Compounds: 1 = methanol; 2 = 2-propanol; 3 = acetone; 4 = acetonitrile; 5 = nitromethane; 6 = 2-pentanone; 7 = 2-nitropropane; 8 = 1-nitropropane. Conditions: isothermal at 25°C for 3 min, then programmed at 18°/min to a final temperature of 80°C.

Universality and choice of carrier gas

EI is a universal fragmentation technique; any compound eluting from a GC generates an EI-FFS spectrum. Unfortunately, the carrier gas also generates fluorescence; for example, the EI-induced fluorescence of N_2^+ can serve as the basis of a sensitive technique for detection of N_2[29]. Because bombardment with 100-eV electrons causes electronic excitation[22], even an atomic carrier gas, such as helium, generates background emission. The EI-induced spectrum of helium contains many atomic emission lines. Nonetheless, for single-wavelength detection using a mono-

chromator–photomultiplier system, a wavelength can be found for any common fragment at which the background emission produced by helium is small (< 700 counts/s in the photon-counting mode). In the case of "on-the-fly" acquisition of spectra using an array detector, it is necessary to subtract the helium fluorescence background (as was done routinely in this work, including the spectra shown in Fig. 2), causing some degradation in the signal-to-noise ratio (S/N). This problem could be alleviated by interposing an interface device, analogous to those used in GC–mass spectrometric systems[30], between the column exit and vacuum chamber (at the cost of additional instrumental complexity and loss of some analyte in the interface).

Possible improvements of EI-FFS detector

The relative simplicity of the EI-FFS detector is an attractive feature. At the cost of increasing complexity, two strategies could be used to improve limits of detection. First, use of a pulsed-electron gun coupled with gated detection (analogous to use of a pulsed laser[31]) should improve S/N; very high instantaneous currents (analogous to the very high peak powers of pulsed laser) can be produced using pulsed-electron guns[32]. Second, not all fragments generated by 100-eV EI of a parent molecule are formed in emissive excited states. Those fragments formed in the ground state by EI can subsequently be excited by a pulsed laser, generating enhanced fragment fluorescence signals[33].

CONCLUSION

As previously emphasized by Gierczak *et al.*,[24] a GC detector based on EI-FFS can be operated as either a universal or a selective detector. Any organic or organometallic compound containing hydrogen produces hydrogen atomic fragment emission at 486 nm; use of a single-wavelength detector (*e.g.*, an interference filter–photomultiplier combination) would enable operation as a universal detector. At the same time, different classes of compounds produce different major fragments (Tables I and II), endowing the EI-FFS detector with substantial selectivity and ability to identify functional groups present in unknown compounds. Interference by co-eluting compounds of dissimilar chemical nature[27] can accordingly be circumvented. Spectra generated by EI-FFS are considerably less useful for identification of specific compounds than those produced by a mass spectrometer; the molecular mass, for example, cannot be obtained from an EI-FFS spectrum. On the other hand, the EI-FFS system described here is less expensive and easier to use than a mass spectrometer.

ACKNOWLEDGEMENT

This work was supported in part by the National Science Foundation (Grant CHE-8317000).

REFERENCES

1 P. Froehlich and E. L. Wehry, in E. L. Wehry (Editor), *Modern Fluorescence Spectroscopy*, Vol. 3, Plenum Press, New York, 1981, p. 79.
2 M. C. Bowman and M. Beroza, *Anal. Chem.*, 40 (1968) 535.

3 H. P. Burchfield, R. J. Wheeler and J. B. Bernos, *Anal. Chem.*, 43 (1971) 1976.
4 D. J. Freed and L. R. Faulkner, *Anal. Chem.*, 44 (1972) 1194.
5 J. Mulik, M. Cooks, M. F. Guyer, G. M. Semeniuk and E. Sawicki, *Anal. Lett.*, 8 (1975) 511.
6 R. P. Cooney and J. D. Winefordner, *Anal. Chem.*, 49 (1977) 1057.
7 J. M. Hayes and G. J. Small, *Anal. Chem.*, 54 (1982) 1202.
8 L. C. Thomas and A. K. Adams, *Anal. Chem.*, 54 (1982) 2597.
9 V. B. Conrad, W. J. Carter, E. L. Wehry and G. Mamantov, *Anal. Chem.*, 55 (1983) 1340.
10 B. Galle and P. Grennfelt, *J. Chromatogr.*, 279 (1983) 643.
11 T. Imasaka, T. Okamura and N. Ishibashi, *Anal. Chem.*, 58 (1986) 2152.
12 B. V. Pepich, J. B. Callis, D. H. Burns, M. Gouterman and D. A. Kalman, *Anal. Chem.*, 58 (1986) 2825.
13 S. W. Stiller and M. V. Johnston, *Anal. Chem.*, 59 (1987) 567.
14 H. Lingeman, W. J. M. Underberg, A. Takadate and A. Hulshoff, *J. Liq. Chromatogr.*, 8 (1985) 789.
15 R. W. B. Pearse and A. G. Gaydon, *The Identification of Molecular Spectra,* Wiley, New York, 1963.
16 J. B. Halpern, W. M. Jackson and V. McCrary, *Appl. Opt.*, 18 (1979) 590.
17 J. B. Halpern, E. B. Koker and W. M. Jackson, *Anal. Chem.*, 55 (1983) 2000.
18 R. C. Oldenborg and S. L. Baughcum, *Anal. Chem.*, 58 (1986) 1430.
19 E. L. Wehry, R. Hohmann, J. K. Gates, L. F. Guilbault, P. M. Johnson, J. S. Schendel and D. A. Radspinner, *Appl. Opt.*, 26 (1987) 3559.
20 R. C. Sausa, A. J. Alfano and A. W. Miziolek, *Appl. Opt.*, 26 (1987) 3588.
21 J. Schendel, R. Hohmann and E. L. Wehry, *Appl. Spectrosc.*, 41 (1987) 640.
22 M. L. Robin, G. K. Schweitzer and E. L. Wehry, *Appl. Spectrosc. Rev.*, 17 (1981) 165.
23 R. N. Compton and J. N. Bardsley, in I. Shinamura and K. Takayanagi (Editors), *Electron–Molecule Collisions,* Plenum Press, New York, 1984, p. 275.
24 C. A. Gierczak, M. A. Heindorf and J. Allison, *Anal. Chem.*, 56 (1984) 2966.
25 G. K. Schweitzer and I. Ishii, *Spectrosc. Lett.*, 17 (1984) 472.
26 P. W. Erdman and E. C. Zipf, *Rev. Sci. Instrum.*, 53 (1982) 225.
27 L. S. Ettre, *J. Chromatogr. Sci.*, 16 (1978) 396.
28 J. Schendel and E. L. Wehry, *Anal. Chem.*, 60 (1988) 1759.
29 D. A. Radspinner and E. L. Wehry, *Talanta*, 34 (1987) 963.
30 G. M. Message, *Practical Aspects of Gas Chromatography/Mass Spectrometry,* Wiley, London, 1984.
31 G. D. Boutilier, J. D. Bradshaw, S. J. Weeks and J. D. Winefordner, *Appl. Spectrosc*, 31 (1977) 301.
32 M. B. Das, S. Bose and R. Bhattacharya, *J. Phys. E,* 19 (1986) 454.
33 H. Kawazumi and T. Ogawa, *Chem. Lett.*, (1985) 925.

Journal of Chromatography, 475 (1989) 247–260
Elsevier Science Publishers B.V., Amsterdam — Printed in The Netherlands

CHROM. 21 501

RADIOLYTIC SYNTHESIS OF HIGH-MOLECULAR-WEIGHT ALKANES FOR CHROMATOGRAPHIC CHARACTERIZATION AND IDENTIFICATION PURPOSES

DOMINIQUE STIENLET, ANNE VERVLOESSEM and JAN CEULEMANS*
Department of Chemistry, University of Leuven, Celestijnenlaan 200-F, B-3030 Leuven (Belgium)
(First received July 4th, 1988; revised manuscript received March 14th, 1989)

SUMMARY

A radiolytic variant of the Wurtz and Wurtz–Grignard coupling reactions is described, requiring only very small amounts of haloalkane reactants and enabling synthesis of high-molecular-weight alkanes for chromatographic characterization and identification purposes. The method consists in the γ-irradiation at room temperature of dilute solutions of chloro- or bromoalkanes in *cis*- or *trans*-decalin. Chromatograms obtained after irradiation consisted of an easily recognizable pattern, that is characteristic for irradiated *cis*- or *trans*-decalin, containing either chloro- or bromoalkanes. Superimposed on this pattern was a very limited number of peaks that are dependent on the exact identity of the chloro- or bromoalkane. These extra peaks can easily be unambiguously assigned and may thus be used for chromatographic characterization and identification purposes. Under the conditions of the experiments, no radical isomerization was observed.

INTRODUCTION

Chromatographic identification may be accomplished by direct comparison of retention times in analyses performed under identical conditions or by comparison with retention indices taken from the literature. Also, more sophisticated equipment may be used, such as gas chromatographs coupled to mass or other spectrometers, allowing comparison of mass spectra or other types of spectra. Unfortunately, the number of compounds that is commercially available is restricted and the same applies to appropriate information available in the literature. Especially for high-molecular-weight compounds, neither the compounds themselves nor the appropriate literature information is often available. For a definite assignment of chromatographic peaks to specific compounds, these compounds must therefore be synthesized. This is not only time consuming; the high cost of the reactants involved and the relatively large amounts of products required (>1 ml) may also make it prohibitively expensive in a number of cases.

In this work, a radiolytic variant of the Wurtz and Wurtz–Grignard coupling reactions is described that is easy to apply and that requires only very small amounts of

0021-9673/89/$03.50

the haloalkane reactants. Only minute amounts of the high-molecular-weight alkanes are obtained by this method, but these are sufficient for chromatographic characterization and identification purposes.

PRINCIPLE OF THE METHOD

The method consists in the γ-irradiation at room temperature of the chloro- and bromoalkane reactants in low concentration in *cis*- or *trans*-decalin (decahydronaphthalene) solutions. Primarily, this irradiation mainly leads to excitation and ionization of decalin, since absorption of ionizing radiation by matter is non-selective:

$$\text{Decalin} \xrightarrow{\sim} \text{Decalin}^* \tag{1}$$

$$\xrightarrow{\sim} \text{Decalin}^+ + e^- \tag{2}$$

Due to the low ionization energy of decalin with respect to that of most chloro- and bromoalkanes[1,2], no hole transfer to these compounds occurs. Chloro- and bromoalkanes are however quite efficient electron scavengers and react with electrons by dissociative electron attachment[3], yielding neutral alkyl radicals:

$$RX + e^- \longrightarrow R^\cdot + X^- \tag{3}$$

(Excitation energy transfer, if occurring, also yields this radical.) The so-formed neutral radicals may react with radicals originating from the radiolysis of decalin, *e.g.*, formed by dissociation of excited decalin molecules or they may react mutually by disproportionation and combination. Combination leads to the formation of an alkane compound, containing twice as many carbon atoms as the chloro- or bromoalkane reactant:

$$R^\cdot + R^\cdot \longrightarrow R\text{–}R \tag{4}$$

By use of decalin solutions, containing two different chloro- or bromoalkanes, cross-combination products may also be obtained:

$$R_1X + e^- \longrightarrow R_1^\cdot + X^- \tag{5}$$

$$R_2X + e^- \longrightarrow R_2^\cdot + X^- \tag{6}$$

$$R_1^\cdot + R_2^\cdot \longrightarrow R_1\text{–}R_2 \tag{7}$$

In view of the above, it is expected that different chloro- or bromoalkanes affect the radiolysis of decalin in a similar way. The only appreciable difference anticipated is the nature of the alkyl radical formed by dissociative electron attachment and the products that originate from it by subsequent reactions. Chromatograms of irradiated

solutions may therefore be expected to consist of (i) a characteristic pattern that is identical for different solutions of either chloro- or bromoalkanes and (ii) a few peaks that are different and that are due to compounds originating from reactions of the alkyl radicals formed by dissociative electron attachment to the haloalkane reactant. In the high-molecular-weight region of the chromatogram, these may be anticipated to be products formed by mutual combination (and cross-combination if the solution contains two different haloalkanes) and by combination with neutral radicals originating from the radiolysis of decalin. As far as these are concerned and in view of the bicyclic nature of decalin, only $C_{10}H^{\bullet}_{17}$ radicals resulting from carbon–hydrogen bond scission are expected to be present in appreciable amounts; carbon–carbon bond scission leads to the formation of a biradical that disappears by mutual reaction of the two radical sites. The anticipated predominance of $C_{10}H^{\bullet}_{17}$ radicals is confirmed by the experimental observation that in the gamma radiolysis of liquid decalin the yield of C_1–C_5 hydrocarbons is very low[4]. The number of products that are specific for a particular chloro- or bromoalkane may therefore be expected to be quite small. Also, differentiation of the mutual combination product of the alkyl radicals formed by dissociative electron attachment to the haloalkane reactant, from combination products with $C_{10}H^{\bullet}_{17}$ radicals, should generally be easy to accomplish.

If all this corresponds to reality and if no radical isomerization occurs, then the combination product may be utilized for chromatographic characterization and identification purposes. The results presented in this paper show that this is indeed the case.

EXPERIMENTAL

Reagents used in this study were *cis*- and *trans*-decalin from Merck-Schuchardt, 1-chlorooctane, 1-bromoheptane and 1- and 2-bromooctane from Fluka and 3-bromooctane from K&K. The decalins were purified by passing through a column containing silica gel, which had been activated immediately prior to use by heating at 250°C for over 24 h. The other products, which were used as additives, were used as received.

Solutions, prepared by conventional techniques, were contained in cylindrical tubes made of quartz. Oxygen was removed by bubbling with argon for 30 min. After deoxygenation, samples were carefully sealed. Irradiations with ^{60}Co γ-rays were carried out at room temperature at the Institute for Radioelements at Fleurus. The absorbed dose was $6.7 \cdot 10^{20}$ eV g^{-1}.

Chromatographic analyses were performed on a Sigma 3 gas chromatograph (Perkin-Elmer) equipped with an inlet-splitting capillary injector and a flame ionization detector. A SCOT column (52 m × 0.5 mm I.D.) made of glass and coated with OV-101 was employed and helium was used as the carrier gas throughout the study.

RESULTS

Chromatograms obtained at a column temperature of 140°C after irradiation of *cis*-decalin containing respectively 1 mole-% 1-bromoheptane, 1-bromooctane and 2-bromooctane are shown in Fig. 1. They consist of an easily recognizable pattern, that

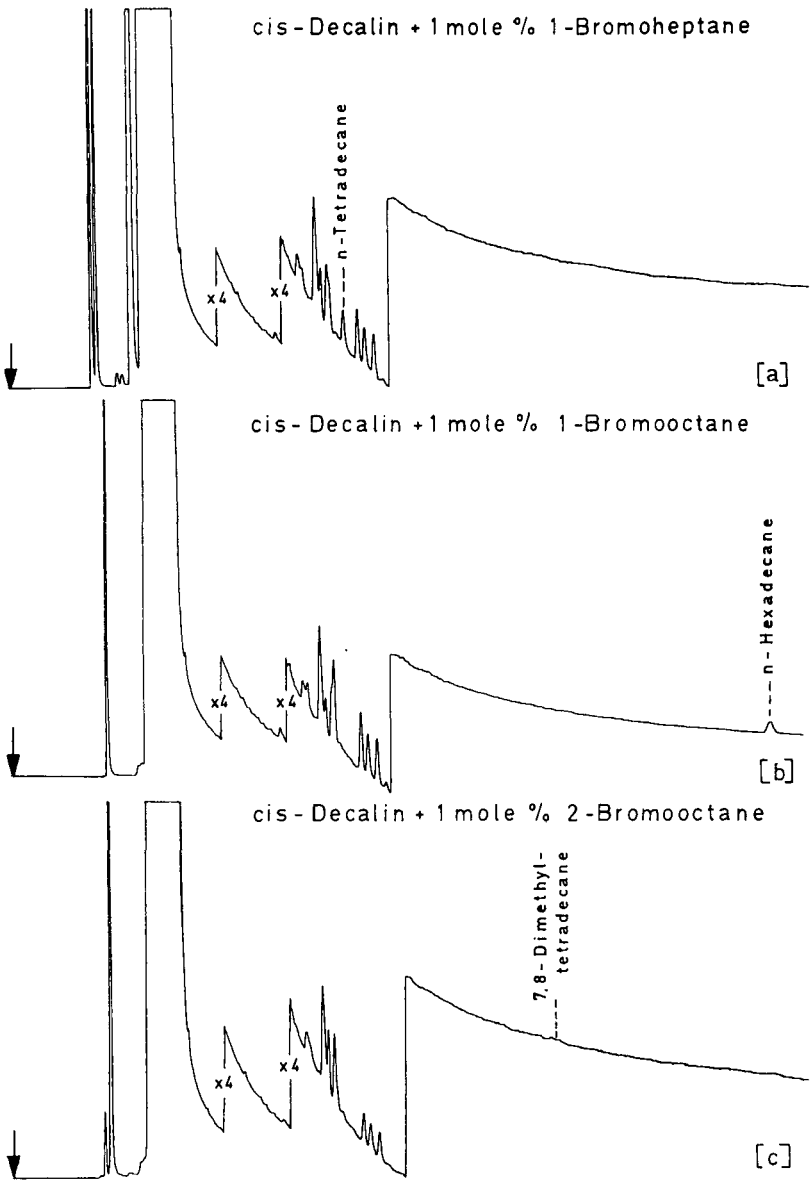

Fig. 1. Chromatograms obtained at a column temperature of 140°C after irradiation of *cis*-decalin, containing respectively 1 mole-% 1-bromoheptane (a), 1-bromooctane (b) and 2-bromooctane (c).

is quite analogous in all three cases. In addition to this characteristic pattern, one extra peak (marked respectively *n*-tetradecane and *n*-hexadecane) is observed after the elution of decalin in solutions containing 1-bromoheptane and 1-bromooctane. In the case of *cis*-decalin solutions, containing 2-bromooctane, the extra peak (marked 7,8-dimethyltetradecane) is both double and very weak.

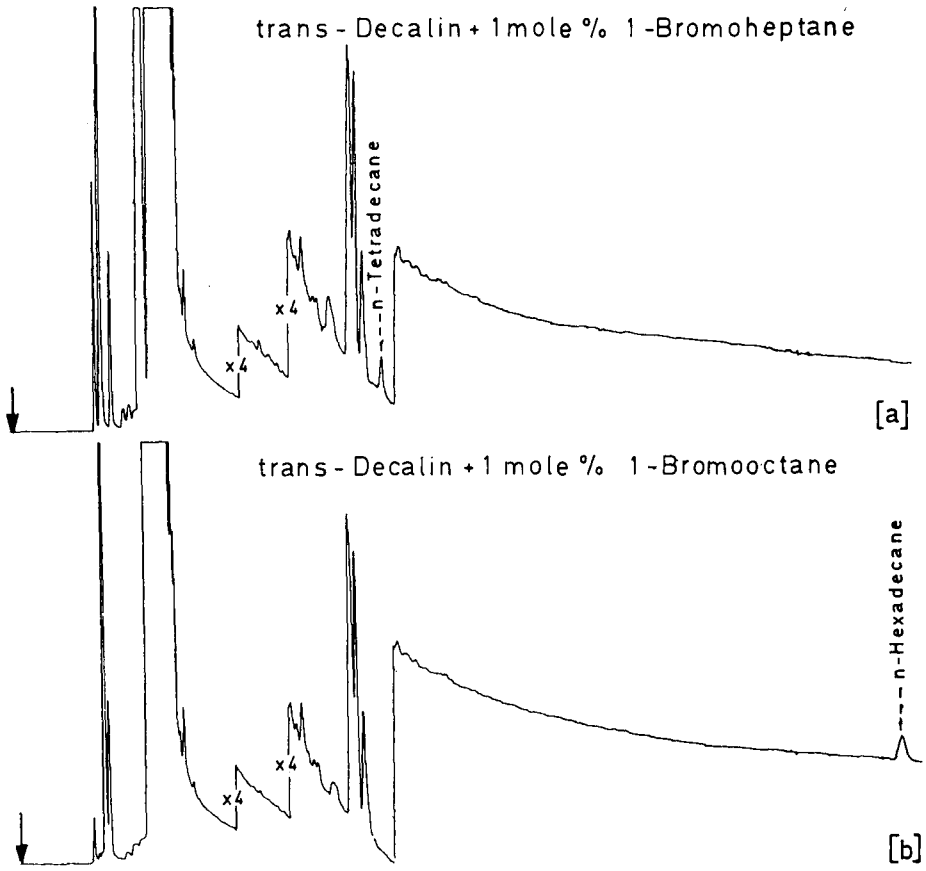

Fig. 2. Chromatograms obtained at a column temperature of 140°C after irradiation of *trans*-decalin, containing respectively 1 mole-% 1-bromoheptane (a) and 1-bromooctane (b).

Chromatograms obtained at a column temperature of 140°C after irradiation of *trans*-decalin containing respectively 1 mole-% 1-bromoheptane and 1-bromooctane are shown in Fig. 2. They again exhibit an easily recognizable pattern common to each case and one extra peak (after the elution of decalin) depending on the bromoalkane present.

Chromatograms obtained at a column temperature of 200°C after irradiation of *cis*-decalin containing respectively 1 mole-% 1- and 2-bromooctane are shown in Fig. 3. Two very prominent groups of peaks are observed in these chromatograms, the first one being dependent on the bromoalkane present and the second one being the same in each case. In addition, an early peak is present (after the elution of decalin) in the case of 1-bromooctane solutions, which is not observed for 2-bromooctane solutions.

Chromatograms obtained at a column temperature of 200°C after irradiation of *trans*-decalin containing respectively 1 mole-% 1-bromoheptane and 2-bromooctane are shown in Fig. 4. Again, two very prominent groups of peaks are observed in each case, the first one being dependent on the bromoalkane present and the second one being the same in each case.

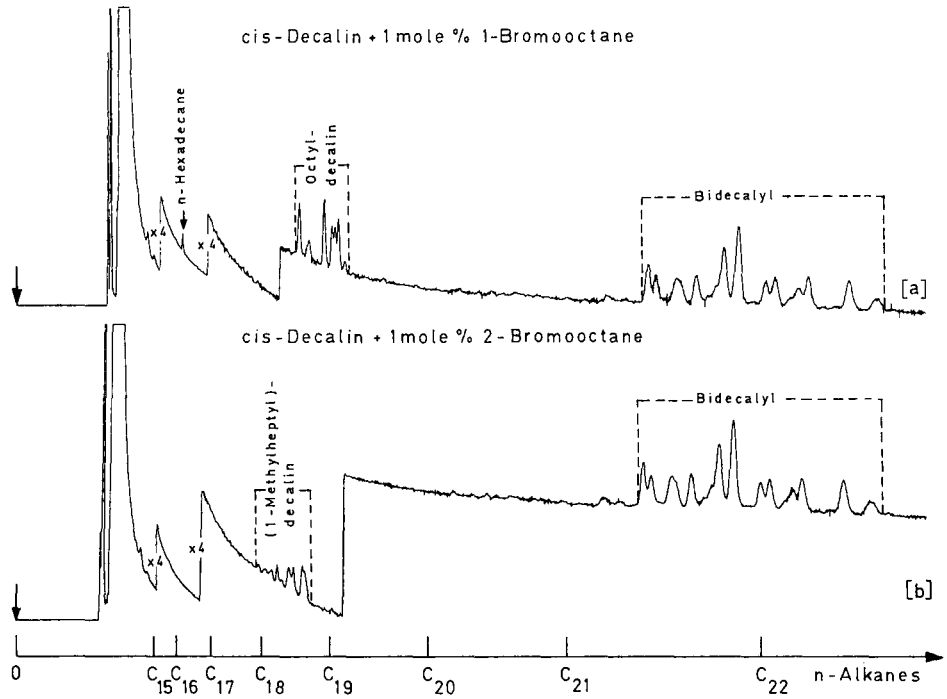

Fig. 3. Chromatograms obtained at a column temperature of 200°C after irradiation of *cis*-decalin, containing respectively 1 mole-% 1-bromooctane (a) and 2-bromooctane (b); the scale indicates the retention characteristics of *n*-alkanes.

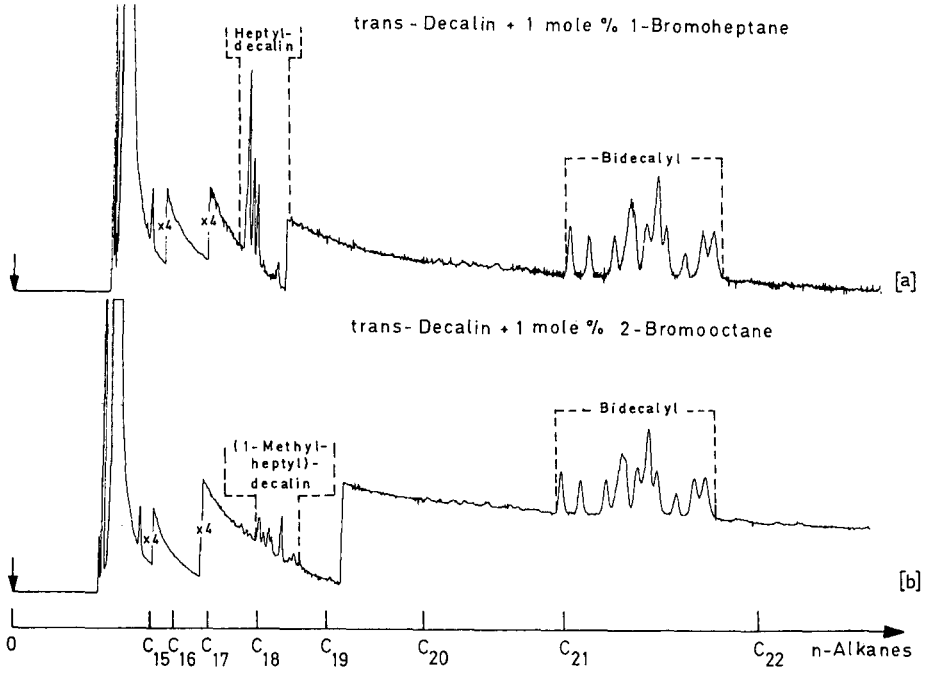

Fig. 4. Chromatograms obtained at a column temperature of 200°C after irradiation of *trans*-decalin, containing respectively 1 mole-% 1-bromoheptane (a) and 2-bromooctane (b); the scale indicates the retention characteristics of *n*-alkanes.

Chromatograms obtained after irradiation of *cis*-decalin containing 1 mole-% 1-chlorooctane at column temperatures of 140 and 200°C are shown in Fig. 5. The chromatogram at 140°C differs considerably from the one obtained after irradiation of *cis*-decalin containing 1 mole-% 1-bromooctane, but the extra peak associated with the presence of the latter compound is also present in this case. The chromatogram obtained at 200°C, on the other hand, corresponds very well with the one obtained after irradiation of *cis*-decalin containing 1 mole-% 1-bromooctane, though the relative importance of some of the peaks is somewhat different and the resolution is less good.

The chromatogram obtained at a column temperature of 140°C after irradiation of *cis*-decalin, containing 0.5 mole-% of both 1-bromoheptane and 1-bromooctane, is shown in Fig. 6. In addition to the characteristic pattern of irradiated *cis*-decalin, containing a bromoalkane, three extra peaks are observed. Chromatograms obtained at a column temperature of 140°C after irradiation of *cis*-decalin, containing 0.5 mole-% of both 1- and 2-bromooctane and 0.5 mole-% of both 1- and 3-bromooctane, are shown in Fig. 7. In addition to the characteristic pattern of irradiated *cis*-decalin, containing a bromoalkane, two extra peaks can easily be discerned in each case.

The concentrations of the high-molecular-weight compounds formed by irradiation may evidently be increased by removal of part (about 80%) of the decalin

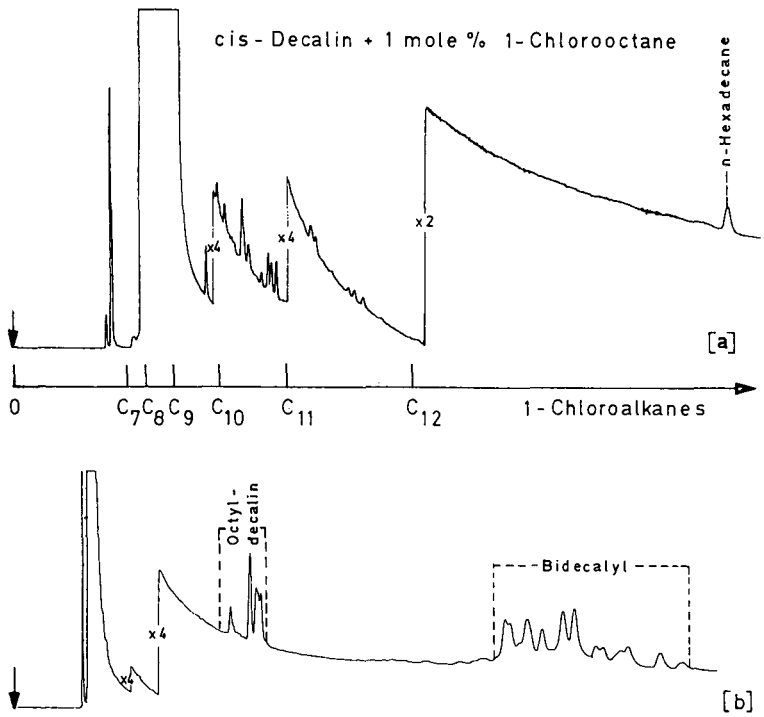

Fig. 5. Chromatograms obtained at a column temperature of respectively 140 (a) and 200°C (b) after irradiation of *cis*-decalin containing 1 mole-% 1-chlorooctane; the scale indicates the retention characteristics of 1-chloroalkanes at 140°C.

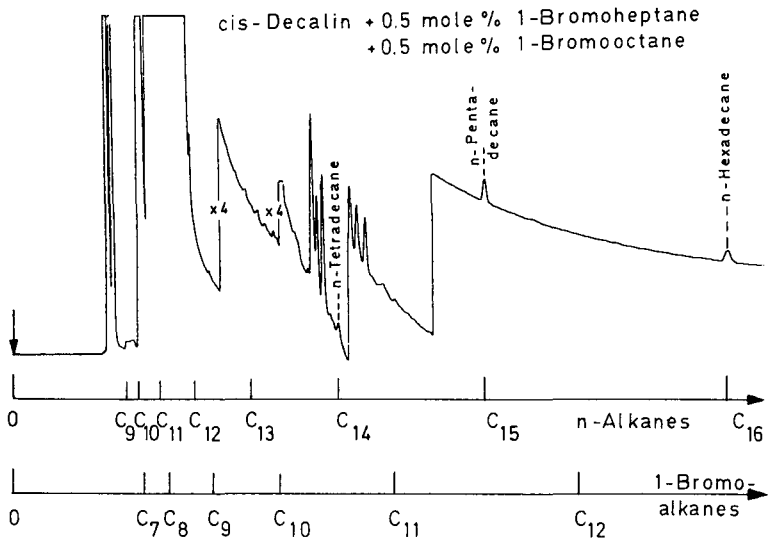

Fig. 6. Chromatogram obtained at a column temperature of 140°C after irradiation of *cis*-decalin, containing 0.5 mole-% of both 1-bromoheptane and 1-bromooctane; the scales indicate the retention characteristics of *n*-alkanes and 1-bromoalkanes.

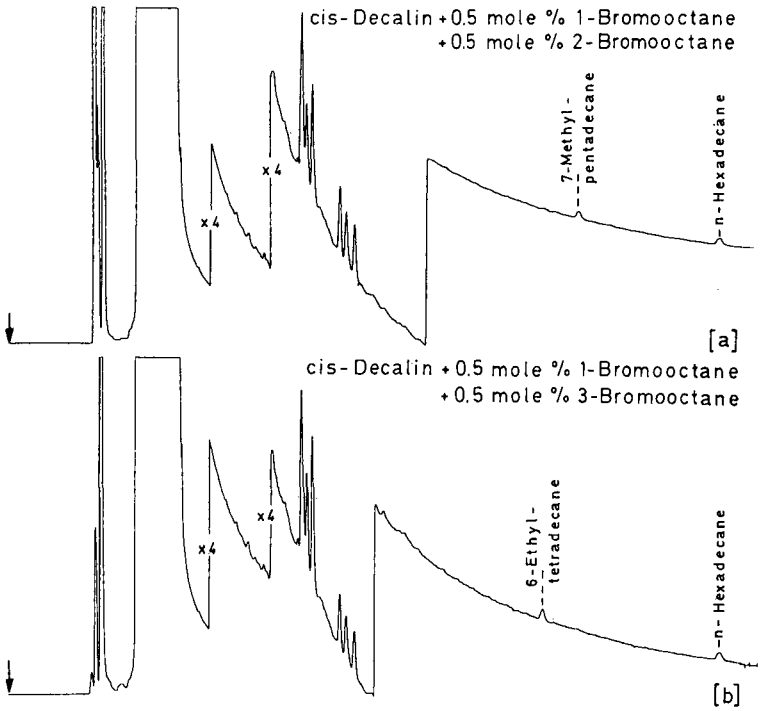

Fig. 7. Chromatograms obtained at a column temperature of 140°C after irradiation of *cis*-decalin, containing respectively 0.5 mole-% of both 1- and 2-bromooctane (a) and of both 1- and 3-bromooctane (b).

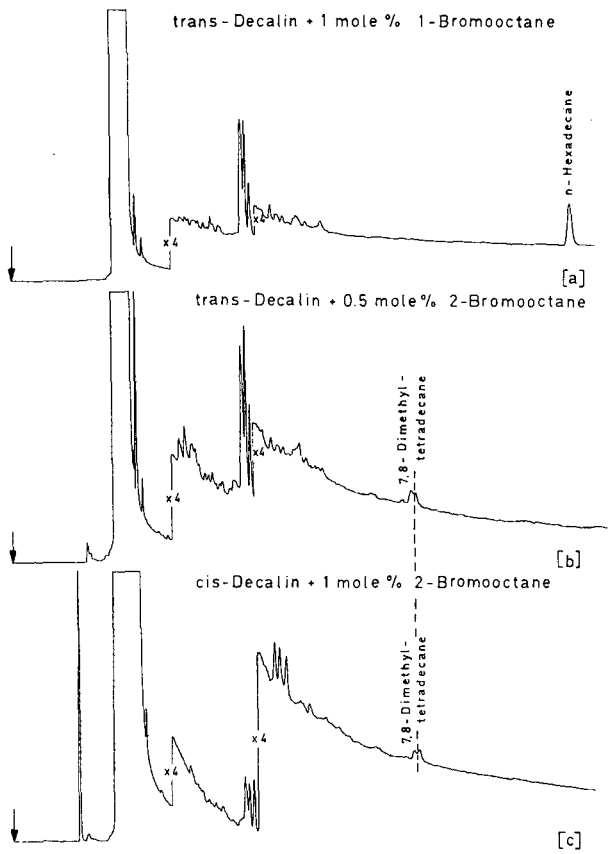

Fig. 8. Chromatograms obtained at a column temperature of 140°C after irradiation and subsequent evaporation by vacuum distillation of *trans*-decalin, containing respectively 1 mole-% 1-bromooctane (a) and 0.5 mole-% 2-bromooctane (b) and of *cis*-decalin containing 1 mole-% 2-bromooctane (c).

solvent by vacuum distillation. Chromatograms obtained at a column temperature of 140°C, after irradiation and subsequent evaporation by vacuum distillation of *trans*-decalin containing either 1 mole-% 1-bromooctane or 0.5 mole-% 2-bromooctane, and of *cis*-decalin containing 1 mole-% 2-bromooctane, are shown in Fig. 8. The two upper chromatograms correspond reasonably well, exhibiting a pattern that is characteristic for irradiated and evaporated *trans*-decalin containing a bromoalkane. In addition to this characteristic pattern, one extra peak is observed in the first chromatogram and a double peak is observed in the second one. The chromatogram obtained after irradiation and subsequent evaporation by vacuum distillation of *cis*-decalin containing 1 mole-% 2-bromooctane largely corresponds with the characteristic pattern obtained after simple irradiation of *cis*-decalin containing a bromoalkane. In addition, the double peak that is superimposed on the characteristic pattern in the chromatogram obtained after irradiation and evaporation of *trans*-decalin containing 0.5 mole-% 2-bromooctane also is observed in this case.

The validity of the method for synthesis of higher-molecular-weight alkanes was

TABLE I

RADIOLYTIC SYNTHESIS AND RETENTION INDICES OF DIFFERENT METHYLEICOSANES

Column temperature: 200°C.

Synthesis product	*Reactants*	*Retention index*
3-Methyleicosane	1-Bromoheptadecane + 2-bromobutane	[a]
4-Methyleicosane	1-Bromohexadecane + 2-bromopentane	2058.8
5-Methyleicosane	1-Bromopentadecane + 2-bromohexane	2054.4
6-Methyleicosane	1-Bromotetradecane + 2-bromoheptane	2048.4
7-Methyleicosane	1-Bromotridecane + 2-bromooctane	2044.8

[a] Synthesis product coincides with 1-bromoheptadecane.

tested by a study of different methyleicosanes. Data obtained are given in Table I. The results clearly show that the method can be extended without problems to higher-molecular-weight alkanes.

DISCUSSION

Assignment of the peaks observed

The chromatograms obtained after irradiation of *cis*- and *trans*-decalin, containing chloro- or bromoalkanes, exhibit two series of peaks. One series is characteristic for irradiated *cis*- or *trans*-decalin, containing either chloro- or bromoalkanes, and is independent of the specific identity of the chloro- or bromoalkane. The compounds responsible for these peaks are of no real relevance to this work and their identification is therefore only briefly discussed. The second series of peaks, on the other hand, is dependent on the specific identity of the chloro- or bromoalkane and constitutes the subject of this study. The compounds responsible for these peaks may be utilized for chromatographic characterization and identification purposes.

Insight into the identity of some of the compounds responsible for the first series of peaks may be obtained by comparison of chromatograms of irradiated *cis*-decalin containing either 1-chlorooctane or 1-bromooctane. Towards the end of the chromatograms obtained at a column temperature of 200°C a very characteristic pattern is observed consisting of at least twelve peaks, which is analogous for 1-chlorooctane and 1-bromooctane. This group of peaks undoubtedly is due to bidecalyls, formed by combination of decalyl radicals. Their retention is in the range of C_{22} aliphatic alkanes, which may at first sight seem high for C_{20} products. These retention characteristics are however not at all abnormal, if one considers the boiling point and vapour pressure characteristics of decalins. The boiling point of *cis*-decalin (195°C), for instance, corresponds with that of undecane (195°C) rather than with that of decane (174°C). On the column employed, the retention time of *cis*-decalin also nearly

corresponds with that of undecane. It is not surprising therefore that the retention characteristics of bidecalyls, which of course contain two decalyl groups, correspond with those of C_{22} rather than with those of C_{20} aliphatic alkanes. The formation of bidecalyls by irradiation results in the appearance of a number of peaks (at least twelve), which is due to both structural and stereoisomerism.

The characteristic pattern in the chromatograms obtained at a column temperature of 140°C cannot be assigned as easily to specific compounds. Comparison of chromatograms, obtained after irradiation of *cis*-decalin containing either 1-chlorooctane or 1-bromooctane, reveals that in the former case some peaks are eluted at considerably shorter times which indicates that they are due to chlorinated decalins and that the corresponding peaks in the latter chromatogram are due to brominated decalins. Some of the minor common peaks, on the other hand, are in all likelihood due to alkyl derivatives of decalin, since processes involving scission of two carbon–carbon bonds in the same molecule apparently occur to some extent in the gamma radiolysis of liquid decalin[4]. A definite assignment can however difficultly be made on the basis of the information available. Knowledge of the exact identity of the compounds responsible for this characteristic pattern is not essential for the applicability of the method, however. The method is based on the extra peaks that are dependent on the chloro- or bromoalkanes present in small concentration and these can be identified unambiguously.

In the high-molecular-weight region of the chromatograms, extra peaks that are dependent on the chloro- or bromoalkanes present in small concentration are due to two different types of products. The first type results from mutual combination of alkyl radicals, formed by dissociative electron attachment to the chloro- or bromoalkanes. In the present work, they are always found in the chromatograms obtained at a column temperature of 140°C. The presence of 1-bromoheptane, for instance, results in the formation of *n*-tetradecane, the presence of 1-bromooctane in the formation of *n*-hexadecane and the presence of both 1-bromoheptane and 1-bromooctane in the same sample in the formation of *n*-tetradecane, *n*-pentadecane and *n*-hexadecane. The second type of extra peaks, that are dependent on the chloro- or bromoalkanes present in small concentration, also is dependent on the nature of the decalin (*cis* or *trans*). These peaks may be assigned to products resulting from combination of alkyl radicals, formed by dissociative electron attachment to the chloro- or bromoalkanes, with decalyl radicals formed by radiolysis of decalin. In the present work, they are always found in the chromatograms obtained at a column temperature of 200°C. Due to the presence of both structural and stereoisomers, a number of peaks are observed for this type of products.

The situation for the first type of extra peaks, which are characteristic for secondary chloro- or bromoalkanes present in small concentration, appears at first sight less simple and rational than in the case of primary chloro- or bromoalkanes. After irradiation of *cis*-decalin containing 1 mol % 2-bromooctane, no clear extra peak is observed at a column temperature of 140°C (see Fig. 1). Also, after irradiation of *cis*-decalin containing both either 1- and 2-bromooctane or 1- and 3-bromooctane, only two extra peaks in each case are observed in the chromatogram obtained at a column temperature of 140°C (see Fig. 7). By removing part (about 80%) of the decalin after irradiation by vacuum distillation, the missing peaks may be made to appear, however. This is clearly seen in Fig. 8, for 2-bromooctane in both *cis*- and

trans-decalin. A clear peak for 7,8-dimethyltetradecane is now observed, which is actually a double peak as a result of optical isomerism; two asymmetric carbon atoms are present in this compound, resulting in the occurrence of diastereomers that are partly separated in the analysis. It thus appears that alkanes formed by mutual combination of secondary alkyl radicals are formed less efficiently than alkanes resulting from the combination of secondary with primary alkyl radicals and from the mutual combination of primary alkyl radicals. This undoubtedly is due to differences in the rate constant ratios for disproportionation to combination. Such ratios are indeed considerably larger for secondary than for primary alkyl radicals[5]. The effect may not be due to inefficient formation of secondary alkyl radicals by dissociative electron attachment, since the yields of cross-combination products of primary and secondary alkyl radicals are comparable to those of compounds formed by mutual combination of primary alkyl radicals. The effect is, on the other hand, not restricted to secondary alkyl radicals. In view of trends in the rate constant ratios for disproportionation to combination, similar but even stronger effects are expected for tertiary alkyl radicals. It thus appears that the radiolytic synthesis method is most easily applied to combination and cross-combination products, whereby at least one of the alkyl radicals is primary. This already covers a wide range of combinations. Other combinations may also be studied if a subsequent vacuum distillation is carried out. The assignment of the radiolytic synthesis product may however be more difficult in this case.

Absence of radical isomerization

The results obtained clearly indicate that radical isomerization is not important under the conditions of the experiments, which is of fundamental importance to the applicability of the radiolytic synthesis method. Kossiakoff and Rice[6] originally postulated that long-chain alkyl radicals can undergo unimolecular isomerization by hydrogen atom transfer reactions involving cyclic transition states. Important results have been reported on isomerizations of vibrationally excited alkyl radicals, resulting from the addition of hydrogen atoms to olefins[7]. Only processes involving transition states with ring sizes of five and larger were observed. The isomerizations are characterized by activation energies[8,9] that are of the same order of magnitude as for those for hydrogen transfer reactions from alkanes to alkyl radicals. In the case of isomerizations involving five-membered ring activated complexes, the activation energy is higher as a result of ring strain energy[7–9]. Radicals formed by addition of hydrogen atoms to olefins contain considerable amounts of excess internal energy from the exothermicity and activation energy of the addition reaction. In contrast, radicals formed by dissociative electron attachment of thermal or near-thermal electrons to chloro- or bromoalkanes have little excess internal energy. Indeed, the electron affinity of chlorine atoms[10] is about equal to the strength of carbon–chlorine bonds in chloroalkanes[11]. Similarly, the electron affinity of bromine atoms[10] is not much larger than the strength of carbon–bromine bonds in bromoalkanes[11]. Electron swarm studies indicate[12], on the other hand, that while the attachment rates of some lower bromoalkanes peak at considerable electron energies (about 0.75 eV), those of higher bromoalkanes peak at quite low electron energies, *i.e.*, 0.2 eV for 1-bromo-octane and thermal energies for 1-bromodecane, so that higher alkyl radicals are formed with little excess energy. Isomerization is on the other hand quite unlikely for lower alkyl radicals because of ring restrictions (see above).

In the radiolytic synthesis method, combination products of radicals directly formed by dissociative electron attachment are observed but not of radicals subsequently formed by isomerization. This indicates that in this method radicals generally have no time to isomerize before they react with another radical or disappear by other means. This may be due to: (i) the low excess internal energy the radicals possess upon their formation as indicated above and the ease with which they can dissipate this energy because experiments are performed in the condensed state; (ii) the relatively low temperature at which the irradiations are performed (room temperature) and/or (iii) a relatively high (local) concentration of radicals making radical recombination occur quicker than in the pyrolytic and photolytic studies mentioned above. It may be interesting in this regard to remark that, in contrast to pyrolytic and photolytic experiments, energy deposition by absorption of high-energy ionizing radiation is inhomogeneous. Electrons ejected as a consequence of the ionization produced by radiation may themselves be sufficiently energetic to produce further ionization and excitation. If the energy of these secondary electrons is relatively small, less than about 100 eV, their range in liquid or solid materials will be short and any secondary ionizations and excitations they produce will be situated close to the original ionization, giving a small cluster or spur of excited and ionized species. Thus, local radical concentrations at some points are likely to be higher than the average radical concentration.

All these considerations make the experimental observation, that no radical isomerization is observed in the radiolytic synthesis method, quite understandable.

Comparison with other synthesis methods

The main advantage of the method described in this work, with respect to different synthesis methods described in the literature[13], consists in the fact that in the radiolytic synthesis method only very small amounts of the haloalkane reactants are required. Many of the high-molecular-weight haloalkane reactants required are commercially available but their cost is often so high as to make it prohibitively expensive to use them in the classical synthesis methods. Due to the fact that, by irradiating decalin containing two different haloalkanes, cross-combination products may be obtained by the radiolytic synthesis method and to the fact that only very small amounts of haloalkane reactants are required, information on a great number of high-molecular-weight alkanes may by this method be obtained from one particular high-molecular-weight haloalkane; for the second haloalkane reactant a number of inexpensive low-molecular-weight haloalkanes may be utilized. The amount of high-molecular-weight alkane obtained is of course very small as well, but is sufficient for chromatographic characterization and identification purposes. The irradiation facilities required for the radiolytic synthesis method evidently are not available in every laboratory, but in many countries nowadays irradiations are commercially performed for a reasonable fee, making the method accessible to many scientists.

CONCLUSIONS

Chromatograms obtained after γ-irradiation at room temperature of dilute solutions of chloro- or bromoalkanes in *cis*- or *trans*-decalin consist of an easily recognizable pattern, that is characteristic for irradiated *cis*- or *trans*-decalin,

containing either chloro- or bromoalkanes. Superimposed on this pattern is a very limited number of peaks that are dependent on the exact identity of the chloro- or bromoalkane. These extra peaks can easily be unambiguously assigned and may thus be used for chromatographic characterization and identification purposes. In the high-molecular-weight region they are due to (i) an alkane compound resulting from mutual combination of alkyl radicals that are formed by dissociative electron attachment to the chloro- or bromoalkanes and (ii) alkyl decalins resulting from combination of these alkyl radicals with decalyl radicals formed by radiolysis of decalin. A cross-combination product is also formed when two different chloro- or bromoalkanes are present during irradiation. The method is most easily applied to combination and cross-combination products, whereby at least one of the alkyl radicals is primary. Under the conditions of the experiments, no radical isomerization is observed.

REFERENCES

1 H. M. Rosenstock, K. Draxl, B. W. Steiner and J. T. Herron, *J. Phys. Chem. Ref. Data*, 6, Suppl. 1 (1977) I-1.
2 R. D. Levin and S. G. Lias, *Ionization Potential and Appearance Potential Measurements, 1971–1981*, National Bureau of Standards, Washington, DC, 1982.
3 L. G. Christophorou, D. L. McCorkle and A. A. Christodoulides, in L. G. Christophorou (Editor) *Electron–Molecule Interactions and Their Applications*, Vol. 1, Academic Press, New York, 1984, p. 477.
4 W. Stachowicz, Z. Kecki and S. Minc, *Nukleonika*, 13 (1968) 187.
5 J. A. Kerr, in J. K. Kochi (Editor), *Free Radicals*, Vol. I, Wiley-Interscience, New York, 1973, p. 1.
6 A. Kossiakoff and F. O. Rice, *J. Am. Chem. Soc.*, 65 (1943) 590.
7 E. A. Hardwidge, C. W. Larson and B. S. Rabinovitch, *J. Am. Chem. Soc.*, 92 (1970) 3278; and references cited therein.
8 L. Endrenyi and D. J. Le Roy, *J. Phys. Chem.*, 70 (1966) 4081.
9 K. W. Watkins and L. A. Ostreko, *J. Phys. Chem.*, 73 (1969) 2080.
10 A. A. Christodoulides, D. L. McCorkle and L. G. Christophorou, in L. G. Christophorou (Editor), *Electron–Molecule Interactions and Their Applications*, Vol. 2, Academic Press, New York, 1984, p. 423.
11 J. A. Kerr and A. F. Trotman-Dickenson, in R. C. Weast and S. M. Selby (Editors), *Handbook of Chemistry and Physics*, The Chemical Rubber Co., Cleveland, OH, 48th ed., 1967, p. F-149.
12 A. A. Christodoulides and L. G. Christophorou, *J. Chem. Phys.*, 54 (1971) 4691.
13 See for instance, J. D. Downer and K. I. Beynon, in S. Coffey (Editor), *Rodd's Chemistry of Carbon Compounds*, Elsevier, Amsterdam, 2nd ed., 1964, p. 359.

Journal of Chromatography, 475 (1989) 261–272
Elsevier Science Publishers B.V., Amsterdam — Printed in The Netherlands

CHROM. 21 500

PREPARATION, STABILITY AND QUANTITATIVE ANALYSIS BY GAS CHROMATOGRAPHY AND GAS CHROMATOGRAPHY–ELECTRON IMPACT MASS SPECTROMETRY OF *tert.*-BUTYLDIMETHYLSILYL DERIVATIVES OF SOME ALKYLPHOSPHONIC AND ALKYL METHYLPHOSPHONIC ACIDS

J. GARFIELD PURDON*[a], JACK G. PAGOTTO and RAYNOR K. MILLER
Chemical Detection and Decontamination Section, Protective Sciences Division, Department of National Defence, Defence Research Establishment Ottawa, Ottawa, Ontario K1A OZ4 (Canada)
(First received August 30th, 1988; revised manuscript received March 9th, 1989)

SUMMARY

Studies of *tert.*-butyldimethylsilylation of several alkyl methylphosphonic, alkylphosphonic and chlorine-substituted alkylphosphonic acids by several derivatizing reagents under differing reaction conditions are reported and a simple procedure for formation of these derivatives is identified. Determination of the stabilities of representative derivatives are reported and capillary column gas chromatographic (GC) retention data for all the derivatives studied are tabulated. General sensitivities for detection and quantitation of these compounds by GC–flame photometric detection and GC–electron impact mass spectrometry in both full-scan and multiple-ion detection modes are presented.

INTRODUCTION

To facilitate the negotiations of disarmament treaties in support of a potential ban on the development, production and stockpiling of chemical warfare (CW) weapons, sensitive methods of detection and analysis are required for verification of the use of these compounds. Consequently, it will be necessary *a priori* to have in place methods for the recovery, work-up and analysis of samples suspected of containing chemical warfare agents and their degradation products[1]. The sensitive identification and verification of the presence of organophosphorus nerve agents and similar materials by methods such as gas chromatography (GC) and gas chromatography–mass spectrometry (GC–MS) is generally a straightforward procedure after separation from the environmental matrix has been effected[1–9]. Due to their instability in water, however, these compounds hydrolyse readily to form alkyl methylphosphonic acids and, ultimately, methylphosphonic acid[3,8,10–13]. These materials cannot be chromato-

[a] Present address: Department of National Defence, Defence Research Establishment Suffield, Ralston, Alberta T0J 2NO, Canada.

graphed readily because of their low volatility and polar nature. Therefore, chemical derivatization is necessary if GC is to be employed. Similar restrictions apply to the analysis of agricultural organophosphorus compounds which form alkylphosphoric acids on hydrolysis[12].

Traditionally, the derivatization procedure employed is diazoalkylation to form the alkyl esters which then can be chromatographed[3,4,11–17]. This approach, while effective, employs reagents which are hazardous and potentially explosive[11,15]. In addition, there have been reports that the methylation, at least in the case of alkyl methylphosphonic acids, may be incomplete[13].

Another approach which has also been used is trimethylsilylation of phosphorus acids or salts, although this has the disadvantage that the trimethylsilyl derivatives are readily hydrolysed by traces of moisture sometimes requiring that a carefully-sealed reaction vessel be used for quantitative measurements[18–21].

A third approach which has been examined is that of pentafluorobenzylation[8,13]. The advantages include enhanced sensitivity for electron-capture detectors in GC, for ultraviolet detectors in high-performance liquid chromatography (HPLC), and for negative ion chemical ionization in MS. The derivatization reaction however, requires the use of sodium hydride and 18-crown-6 at 45°C for several hours to ensure complete conversion[8].

Liquid chromatographic analysis has also been reported[22]. By employing *p*-bromophenacyl bromide derivatization, Bossle *et al.*[22] could detect levels of alkyl methylphosphonic acids down to 40 ng and analyse for the materials in aqueous media, a desirable feature for the analysis of disarmament-related samples.

We report here the application of an improved approach to derivatization for this class of compounds. *tert.*-Butyldimethylsilylation has been applied to the GC, GC–MS and MS analyses of compounds such as prostaglandins[23,24], deoxynucleosides[25], fatty acids[26], steroids[27–30] and recently, to inorganic oxyanions such as sulfates, phosphites and phosphates[31]. *tert.*-Butyldimethylsilyl (TBDMS) derivatives offer the benefits of hydrolytic stability, ease of preparation, and high sensitivity for MS detection[31]. Recently we reported a GC–MS investigation of the TBDMS derivatives of several alkyl methylphosphonic- and alkylphosphonic acid derivatives[32]. It was shown that the electron impact mass spectra of these compounds are dominated by 3–4 peaks which account for more than 40% of the total ionization of the molecule[32]. In addition, most of these dominant ions occur at relatively high m/z, suggesting that sensitive detection of these classes of compounds by GC–MS multiple ion detection (MID) methods should be free from interference. In this investigation, we report on methods of preparation and GC analysis of these compounds as well as their stabilities and detection sensitivities by GC–flame photometric detection (FPD) and GC–electron impact (EI)MS in both full-scan and MID modes.

EXPERIMENTAL

Reagents and instruments

N-Methyl-N-(*tert.*-butyldimethylsilyl)trifluoroacetamide (MTBSTFA) and MTBSTFA with 1% *tert.*-butyldimethylsilyl chloride (TBDMSCl) were obtained from Regis (Morton Grove, IL, U.S.A.). Derivatization kits (1 ml) of TBDMSCl and imidazole (1:2.5 mol/mol) in dimethylformamide (DMF)[23] were obtained from

Applied Science Division (State College, PA, U.S.A.). Silylation-grade acetonitrile, DMF, and toluene were obtained from Pierce (Rockford, IL, U.S.A.). Methylphosphonic (MPA), ethylphosphonic (EPA), *n*-propylphosphonic (nPPA) and *n*-butylphosphonic (nBPA) acids were obtained from Fairfield Chemical (Blythewood, SC, U.S.A.) while samples of ethyl methylphosphonic (EMPA) and isopropyl methylphosphonic (iPMPA) acids were provided courtesy of Dr. E. W. Sarver (Chemical Research, Development and Engineering Center, Aberdeen Proving Ground, MD 21010, U.S.A.). Samples of pinacolyl methylphosphonic acid (PinMPA) were generated by controlled hydrolysis of the corresponding fluoridate using aqueous hydrochloric acid for purposes of retention time determination and mass spectral generation. Diisopropyl methylphosphonate (DPMP), used as an internal standard in some experiments, and 2-chloroethylphosphonic acid were obtained from Fairfield Chemical.

GC analyses were carried out on a Varian Model 3700 gas chromatograph equipped with Varian dual flame photometric and flame ionization detectors, a fused-silica capillary column (30 m × 0.322 mm I.D.) DB5-30N (J&W Scientific, Rancho Cordova, CA, U.S.A.) and, in some preliminary studies, a shorter column (15 m × 0.32 mm I.D.) SE-30 (Varian). Injections were effected using a Varian Model 8000 autosampler adjusted to deliver 1-μl samples into a Varian fused-silica capillary direct injector body (Model 1085). Integration and instrument control were performed on Varian 111 CDS data systems. Conditions for analysis were typically: carrier gas, helium at 2.4 ml/min at 250°C; injector, 220°C; detector, 250°C; column oven program, 60°C for 2 min, 10°/min to 230°C and hold for the 30 m column; and 50°C for 2 min, 25°/min to 100°C followed by 5°C/min to 250°C and hold for the shorter column.

GC–MS analyses were carried out on a Finnigan 4023 gas chromatograph–mass spectrometer–data system equipped with a fused-silica capillary column (30 m × 0.258 mm I.D.) DB5-30N (J&W Scientific). Injections were effected manually using the Finnigan split/splitless Grob injector in the splitless mode. Conditions for analysis were typically: carrier gas, helium at 1.4 ml/min at 50°C; injector, 260°C; transfer line, 270°C; ion source, 190°C; column oven program, 50°C for 1.6 min, 22°/min to 140°C, 5°/min to 200°C, 10°/min to 260°C and hold, injection at 0.8 min, split at 1.6 min; full scan parameters were sensitivity, 10^{-7} V/A; scanning 45–1000 a.m.u. at 2.5 s/scan; MID parameters were: sensitivity, 10^{-8} V/A; scanning 1 mass unit window for 0.105 s each with a total of 0.25 s for two ions with time delay/settling time.

Derivatization procedure

Generally, derivatization involved combining carefully-measured quantities of the materials in the Reactivials, heating for specific periods of time at constant temperature and allowing to cool, followed by analysis and storage. Volumetric measurements were made using Hamilton syringes and sample preparation and storage were carried out in screw cap glass vials with PTFE/silicone septa (Pierce). Heating and temperature control were effected in a Pierce Reacti-therm heating/stirring module. No precautions were taken to exclude air or moisture from the vials and no extraction or clean-up was carried out. Stability experiments involved storage at room temperature and at 0°C.

RESULTS AND DISCUSSION

Derivatization reactions

The reagent often employed for TBDMS-derivative syntheses has been a mixture of TBDMSCl and imidazole in DMF[23–30]. The introduction of imidazole as a catalyst and DMF as the reagent solvent was found to increase the reactivity of TBDMSCl considerably when used to derivatize alcohols[23]. Recently other reagents and approaches have become available including MTBSTFA in acetonitrile[31,33], in DMF[31] and in tetrahydrofuran (THF)[31,33]. Accordingly, several derivatization procedures were examined to determine the effect of solvent, temperature, time, and reagents on the yields of TBDMS derivatives of alkyl methyl- and alkylphosphonic acids in organic solvents.

(A) MTBSTFA + 1% TBDMSCl in acetonitrile and toluene. Samples of EMPA and iPMPA (42 ng/μl) in acetonitrile were treated with an excess of MTBSTFA + 1% TBDMSCl both at 60°C and at room temperature for 1 h. GC analyses using the shorter column revealed two sharp peaks not present in blank derivatization solutions whose areas were similar for treatments at both temperatures. GC–MS analysis of the 60°C sample, although indicating that the components contained ions expected for TBDMS derivatives of these compounds[32], was inconclusive because of poorly-shaped GC peaks. Mixtures of MPA, EPA, nPPA and nBPA (*ca.* 50 ng/μl) were treated with the MTBSTFA–TBDMSCl combination in acetonitrile at 60°C for 30 min and, again, GC–MS indicated that TBDMS derivatives of all the acids had been formed but poorly-shaped GC peaks were observed. Subsequently, it was determined that increasing the initial column temperature to above 100°C significantly improved the chromatography and that substitution of toluene for acetonitrile as the predominant solvent resulted in clean well-separated peaks, provided that the solvent mixture contained at least 90% toluene.

Mixtures of iPMPA (to represent alkyl methylphosphonic acids) and MPA (to represent alkylphosphonic acids) (*ca.* 40–60 ng/μl each) were employed to examine the extents of derivatization and to define optimum reaction conditions in the toluene–acetonitrile (90:10) solvent system. Reactions were carried out at room temperature, and at 60°C for 30-, 60- and 150-min periods; yields are summarized in Table I. The quantities produced at 60°C and 60 min using no catalyst (see B below) are taken as representing 100% conversion for basis of comparison. Within the margin of analytical error, derivatization of both acids at both temperatures and all three reaction times appears to be complete.

(B) MTBSTFA in toluene. A mixture of the phosphonic acids (excluding pinacolyl methyl- and chloroethylphosphonic acids), some originally prepared in acetonitrile, some in chloroform, was reacted with MTBSTFA in an excess of toluene (toluene > 95%, v/v; final concentrations approximately 45 ng/μl) for 1 h at 60°C. Sharp, well-defined peaks were obtained and complete mass spectra corresponding to the acid derivatives were recorded[32]. Derivatizations of iPMPA and MPA mixtures (40–60 ng/μl) were carried out using MTBSTFA in toluene–acetonitrile (100:1) at both room temperature and at 60°C for 30-, 60- and 150-min periods; yields are given in Table I. As in A above, both phosphorus acids appear to be quantitatively derivatized at both temperatures and all three reaction times.

Derivatization of a sample of pinacolyl methylphosphonic acid in acetonitrile

TABLE I

EFFECTS OF REACTION TIME AND TEMPERATURE ON DERIVATIZATION OF ISOPROPYL METHYLPHOSPHONIC (iPMPA) AND METHYLPHOSPHONIC ACID (MPA) MIXTURES IN TOLUENE USING MTBSTFA WITH/WITHOUT 1% *tert.*-BUTYLDIMETHYLSILYL CHLORIDE

Reaction temperature (°C)	*Reaction duration (min)*	*Yields of derivatives (%)*[a]	
		iPMPA	*MPA*
24.5	30	97 [98]	95 [97]
24.5	60	95 [97]	93 [96]
24.5	150	102 [96]	101 [94]
60	30	99 [98]	99 [102]
60	60	100 [96]	100 [98]
60	150	101 [100]	97 [97]

[a] Values for solutions with added catalyst given in square brackets.

was carried out using MTBSTFA in an excess of toluene at 60°C for 1 h and formation of the PinMPA derivative confirmed by GC–MS analysis[32]. Separation of the two stereoisomers of the derivative on the capillary column was essentially baseline and both isomers of the unhydrolysed fluoridate as well as some MPA derivative, the final product of complete hydrolysis of the fluoridate ester, were detected.

A sample of 2-chloroethylphosphonic acid, dissolved in acetonitrile, was derivatized by reaction with MTBSTFA in an excess of toluene at 60°C for 1 h; GC–MS analysis confirmed the formation of this derivative as well[32].

(C) TBDMSCl–imidazole in DMF. Derivatizations using a combination of TBDMSCl–imidazole (1:2.5) in DMF were attempted at 60 and at 160°C for 1 h using iPMPA (22.5 ng/μl) and MPA (32.4 ng/μl) in DMF–acetonitrile (DMF > 95%) containing the internal standard DPMP. A parallel reaction using MTBSTFA in toluene–acetonitrile (100:1), carried out at 60°C for 1 h, served as a basis of comparison. Yields of iPMPA and MPA derivatives were found to be only 37 and 80% at 60°C and 72 and 48% at 160°C, respectively. Gas chromatograms of the solutions resulting from the TBDMSCl–imidazole reaction indicated the presence of a number of other components.

Derivatization of these acids using either MTBSTFA with/without 1% TBDMSCl catalyst is very effective. In both cases, reactions appear to be complete at room temperature, and at 60°C, in 30 min, although there is a suggestion that higher yields may have resulted at the higher temperature. In contrast, although TBDMS derivatives were formed when TBDMSCl–imidazole reagent was used in DMF, the conversion is incomplete under both similar and more severe conditions. Increasing the reaction temperature in this case improves the formation of the iPMPA derivative but appears to reduce the conversion of MPA derivative. Without further study, it is unclear whether the MPA derivative yield decreased because of subsequent decomposition or because of other factors, although instability of silylation product mixtures using this reagent have been reported[33]. In addition, the presence of other byproducts using this approach could present problems for quantitation of the derivatives by non-specific detection such as FID or FPD. Attempts to remove or reduce the levels of these materials by extraction or adsorption cleanup would complicate the analysis and

possibly decrease sample recovery. In summary, the first two methods of derivatization possess clear advantages over the last approach both in simplicity and completeness.

GC separation

A typical reconstructed GC–MS ion chromatogram of a mixture of six of the acid derivatives (excluding that for PinMPA and 2-chloroethylphosphonic acid) is shown in Fig. 1. The solution was prepared by derivatizing a mixture of the acids (43–47 ng/μl) with MTBSTFA for 1 h at 60°C in a toluene–acetonitrile–chloroform (100:10:1) mixed solvent. The minor components are traces of the original solvents employed to dissolve the acids. The identifications of the various components, confirmed by GC–MS[32], are listed in Table II along with retention times of all derivatives and other materials identified in the GC–MS and GC studies. Baseline resolution of the two alkyl methylphosphonic acid derivatives was achieved in a GC–MS analysis using a DB-5 capillary column, an on-column injector (J&W Scientific), a 1-m length of silylated precolumn/retention gap and an oven temperature program of 110°C for 1 min followed by a rise of 20°/min to 260°C. In summary, clean separation of the derivatives can readily be achieved using toluene as the major solvent component for splitless injection. Similar GC results can be accomplished by direct- or cool on-column injection techniques using toluene and acetonitrile as co-solvents.

The poor chromatography observed in the analysis of catalysed derivatizations (see A above) can be ascribed to solvent polarity (acetonitrile) and the method and temperature of injection being employed. The effects of using polar compounds such as methanol, water, and acetonitrile as solvents on the chromatographic elution of a variety of compounds on bonded non-polar columns, DB-1 and DB-5, have been reported[34]. On-column injection with acetonitrile as solvent led to very severe peak splitting unless the injection was effected rapidly. Co-injection of a non-polar solvent such as benzene with the polar solvent, especially if the two form an azeotrope, nearly eliminated the problem and varying the temperature of the injection improved the

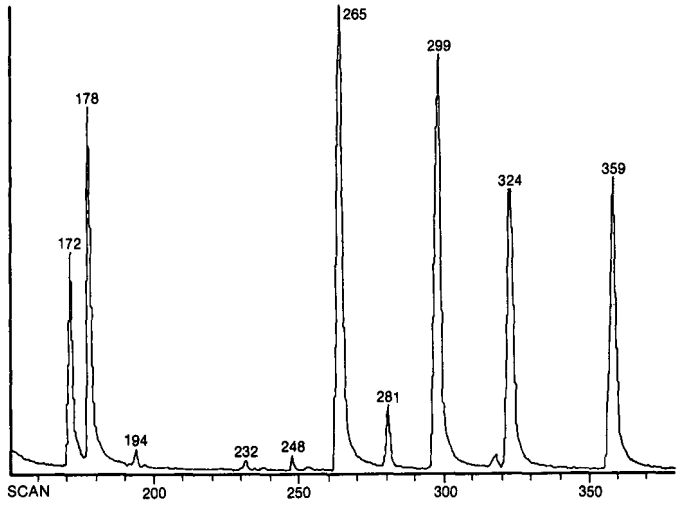

Fig. 1. GC–MS analysis of a sample of TBDMS derivatives of alkyl methyl- and alkylphosphonic acids.

TABLE II

GAS CHROMATOGRAPHIC RETENTION DATA FOR SELECTED TBDMS DERIVATIVES OF ALKYL METHYL- AND ALKYLPHOSPHONIC ACIDS

Oven program: (GC–MS), 50°C for 1.6 min, 22°/min to 140°C, 5°/min to 200°C, 10°/min to 260°C and hold, injection at 0.8 min, split at 1.6 min; (GC), 60°C for 2 min, 10°/min to 230°C and hold.

Compound name	*Scan (No.)*[a]	*Retention time (min)*	
		GC–MS	*GC*
Diisopropyl methylphosphonate[b]	–	–	8.82
Ethyl methylphosphonic acid derivative	172	7.17	12.15
Isopropyl methylphosphonic acid derivative	178	7.42	12.53
Pinacolyl methylphosphonic acid derivative[c]	–	–	15.30
Methylphosphonic acid derivative	265	11.03	15.78
1,3,5-Trimethylbenzene[d]	281	–	–
Ethylphosphonic acid derivative	299	12.45	16.71
n-Propylphosphonic acid derivative	324	13.50	17.33
n-Butylphosphonic acid derivative	359	14.95	18.18
2-Chloroethylphosphonic acid derivative	–	–	18.65

[a] GC–MS results (See Fig. 1).

[b] Internal standard employed in some GC analyses.

[c] Pinacolyl methylphosphonic acid derivative synthesized by hydrolysis of the corresponding fluoridate ester and analysed separately *in situ*; retention time quoted is for first stereoisomer.

[d] Impurity found in toluene.

chromatography[34]. Another study noted that splitting of the GC peaks could be eliminated by injecting at temperatures higher than the boiling point of the solvent[35]. In the present study, elimination of the poor peak shapes when acetonitrile was used as the solvent in the splitless injector by the use of toluene as the predominant solvent (>90%) and when the injector temperature was increased, are consistent with the reported investigations[34,35]. In conclusion, GC separation of phosphonic acid TBDMS derivatives is best achieved using an excess of non-polar solvent for on-column injection or high injector temperatures for splitless or direct injection.

GC retention times

Generally, retention times increase linearly with molecular weight of the derivative within a class. For a GC analysis with a linear temperature program, the retention times of the alkyl methylphosphonic- and the alkylphosphonic acid derivatives display similar straight line relationships with molecular weight, the latter being slightly shifted to longer retention times (Fig. 2). The 2-chloroethylphosphonic acid derivative appears to fall on the line of the other alkylphosphonic acid derivatives. This linear behaviour could permit the prediction of retention times for other homologues in the two series to aid in identification of other phosphonic acid derivatives. However, although the retention times were very reproducible thus providing a possible basis for a useful screening tool for the detection of these compounds, samples submitted for verification purposes would contain an assortment of environmental components, some of which could interfere with and weaken identifications based solely on retention indices. An improvement could be realised by

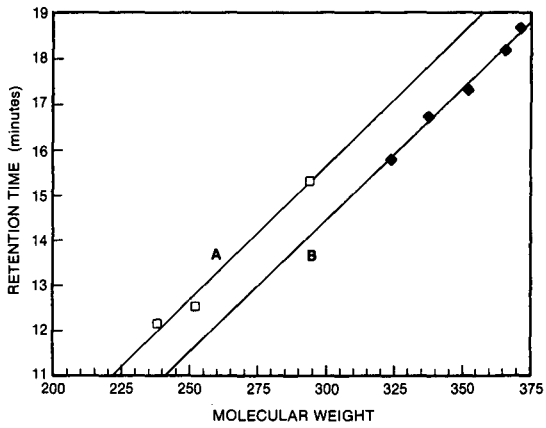

Fig. 2. Capillary column GC retention times of (A) alkyl methylphosphonic, and (B) alkylphosphonic acid TBDMS derivatives as a function of their molecular weight.

use of an FPD system with a phosphorus filter which would reduce the interference problem, compared to FID which responds to a greater number of materials. MS is clearly superior due to its unequivocal identification capability.

Derivative stabilities

Mixtures of iPMPA (22.5 ng/μl), MPA (32.4 ng/μl) and an internal standard of DPMP were derivatized using MTBSTFA in toluene–acetonitrile (100:1) at 60°C for 1 h. The resulting solution was stored at room temperature without cleanup, reactant removal, or addition of drying agent. GC analyses were carried out over a period of six days at which time the solution was stored in a freezer at 0°C for a further period of 22 days; results are given in Table III.

TABLE III

STABILITIES OF ISOPROPYL METHYLPHOSPHONIC- AND METHYLPHOSPHONIC ACID DERIVATIVES

Based on GC–FPD analyses; formation reaction conditions were 60°C for 60 min using MTBSTFA in toluene.

Elapsed time (h)	*Isopropyl methylphosphonic acid derivative (% change)*	*Methylphosphonic acid derivative (% change)*
0.0	–	–
4.0	+5	−7
4.5	+4	−8
27.5	−5	+3
98.25	+1	−7
98.75	−2	−9
119.75	−2	−11
120.5	−7	+2
143.5	−3	−8
672 (freezer, 22 days)	+3	−3

A separate examination of the 2-chloroethylphosphonic acid derivative stability, conducted by reacting 2-chloroethylphosphonic acid (23.1 ng/μl) with MTBSTFA in toluene–acetonitrile (20:1) at 60°C for 1 h and analyzing by GC, demonstrated a stability of better than 96% over 24 h at room temperature. However, after a period of 4 days, the solution yellowed and a fine precipitate formed; no analysis of the latter solution was undertaken.

The behaviour observed with the iPMPA and MPA derivatives indicates that long term stability of these materials can be expected even when in contact with the derivatization reagents. Over a storage period of six days at room temperature and in a freezer for a further three weeks in a closed air atmosphere with no added drying agent, neither derivative displayed significant degradation. From the single examination of the stability of the 2-chloroethylphosphonic acid derivative, however, there is an indication that it may be less stable than its alkyl counterpart; further tests would be required to verify its behaviour.

Sensitivity and linearity

For a derivative to be useful in trace analysis, a low detection limit and a wide range of linearity of response are important characteristics. Consequently, a limited investigation of these factors was undertaken. Employing iPMPA and MPA as representatives of the two compound classes and DPMP as an internal standard, derivatives were formed using MTBSTFA in toluene–acetonitrile (100:1) at 60°C for 1 h. Solutions were prepared by successive dilution with toluene and analysed by GC. The responses to the phosphonic acid derivatives, corrected for injection volume variation using the internal standard as a reference, are displayed in Fig. 3. Each point is the average of at least four injections at each concentration.

For GC–FPD, responses for all three compounds are strictly linear over the range with correlation coefficients of greater than 0.999 and minimum detectable limits of less than 500 pg for each derivative. The response remains linear to amounts exceeding 20 to 30 ng although actual upper limits were not determined. A limited GC–MS study was conducted in both full-scan and MID EI modes. In the former,

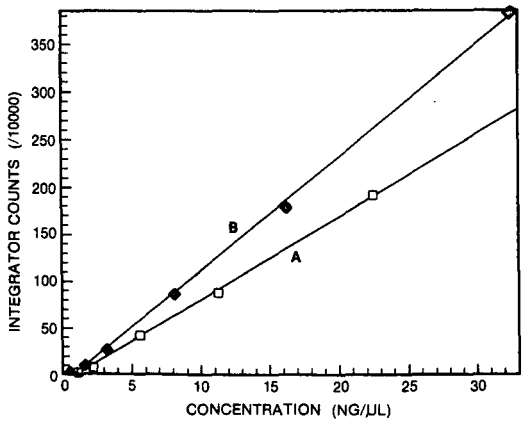

Fig. 3. Linearity and sensitivity of flame photometric capillary column gas chromatography to representative TBDMS derivatives of phosphonic acids. (A) iPMPA, (B) MPA.

a sample containing iPMPA (0.34 ng) and MPA (0.49 ng) derivatives still produced background-subtracted spectra containing sufficient information to perform library searches for identification (Fig. 4). Using these full-scan spectra, single ion chromatograms at *m/z* 153 (iPMPA derivative) and 267 (MPA derivative) indicate that accurate quantitation would be possible down to less than 200 pg and 350 pg, respectively. EI-MS in the full-scan mode, possessing approximately equivalent sensitivity to the GC–FPD, has the important advantage of simultaneous unequivocal MS identification of the compound.

Under GC–MS MID conditions monitoring the two most intense ions for each derivative, *m/z* 153 and 195 (iPMPA) and *m/z* 225 and 267 (MPA) and quantitating on the more intense for each, quantities down to less than 17 and 24 pg respectively at a signal-to-noise ratio of 2:1 were determined without special instrumental tuning precautions. Although the useful limits for analysis performed in this manner are conservatively 30 and 60 pg respectively, monitoring single ions for each compound coupled with accurate retention time data to verify the identification, could further reduce these limits.

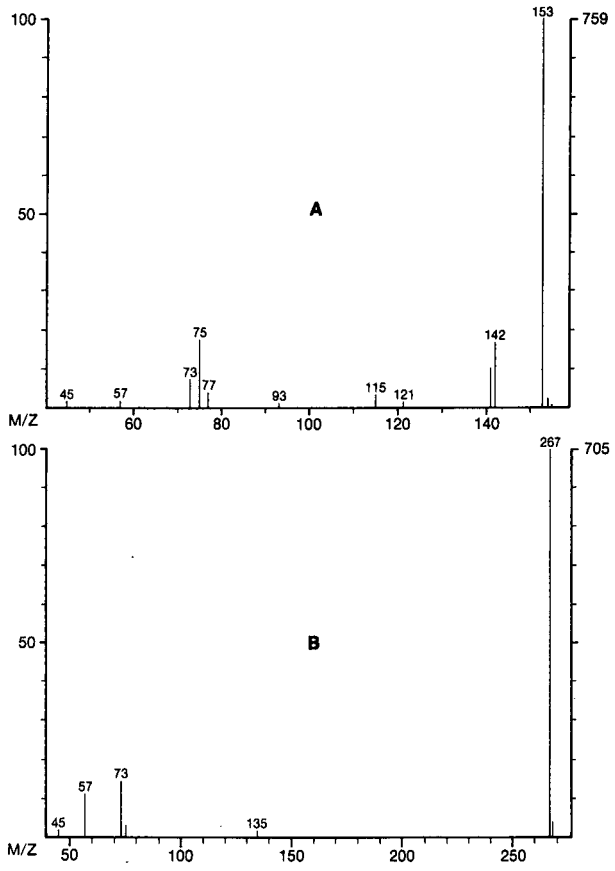

Fig. 4. Background-corrected electron impact mass spectra of (A) the iPMPA TBDMS derivative at 0.34 ng, (B) the MPA TBDMS derivative at 0.49 ng.

CONCLUSION

tert.-Butyldimethylsilyl derivatization possesses significant advantages in ease of formation, stability, excellent detection sensitivity, and clean chromatography over methylation or trimethylsilylation for the GC analysis of alkyl methylphosphonic-, alkylphosphonic and chlorinated alkylphosphonic acids. Derivatization without the use of drying agents or inert atmosphere is readily effected by the addition of commercially-available MTBSTFA, either with or without catalyst (1% TBDMSCl), to the sample and heating to 60°C for 30 min. GC analysis can be carried out immediately by direct injection of the reaction solution without further cleanup. The derivatized solutions of chlorinated alkylphosphonic acids may be safely stored without significant degradation for up to 24 h at room temperature while those of alkyl methyl- and alkylphosphonic acids can be stored for up to 6 days at room temperature or at least a month in a freezer.

GC separation of the phosphonic acid TBDMS derivatives examined in this study is readily achieved on a non-polar capillary column, provided that more than 90% of the solvent employed is non-polar for on-column injection, or high injector temperatures are employed for splitless or direct injection. Linear correlations of the retention times for each class of phosphonic acid derivative with molecular weight are excellent, permitting accurate predictions of retention times for other homologues. Quantitation down to 500 pg is possible using GC–FPD, while with EI-MS, quantitation can be carried out down to 300–500 pg for the full-scan mode and down to 30–60 pg using MID.

REFERENCES

1 J. K. Miettinen, in P.-G. Jonsson, B. Lenntorp, R. Palmaeus, K. Pearsson, J. Santesson and J. Schyllander (Editors), *Proceedings of the International Symposium on Protection Against Chemical Warfare Agents, Stockholm, June 6–9, 1983*, FOA Report C40171, National Defence Research Institute, Umea, pp. 85–86 and suppl. pp. 47–53.
2 A. Verweij, E. Burghardt and A. W. Koonings, *J. Chromatogr.*, 54 (1971) 151.
3 A. Verweij and H. L. Boter, *Pestic. Sci.*, 7 (1976) 355.
4 S. Bergek, *FOA Rapport C40086-C2*, Oktober (1978) (in Swedish).
5 S. Sass, T. L. Fisher, R. J. Steger and G. A. Parker, *J. Chromatogr.*, 238 (1982) 445.
6 J. K. Miettinen, P. Hirsjärvi and L. Pirilä (Editors), *Chemical and Instrumental Verification of Organophosphorus Warfare Agents*, Ministry of Foreign Affairs of Finland, Helsinki, 1977, pp. 24–62.
7 J. K. Miettinen, P. Hirsjärvi and L. Pirilä (Editors), *Identification of Potential Organophosphorus Warfare Agents, An Approach for the Standardization of Techniques and Reference Data*, Ministry of Foreign Affairs of Finland, Helsinki, 1979, pp. 1–4, 20–50 and appendices.
8 P. Hirsjärvi, J. K. Miettinen, J. Paasivirta and E. Kanolahti (Editors), *Trace Analysis of Chemical Warfare Agents. I. An Approach to the Environmental Monitoring of Nerve Agents*, Ministry of Foreign Affairs of Finland, Helsinki, 1981, pp. 27, 28, 37–39, 59–64, 72–79, 90–99.
9 S. Sass and T. L. Fisher, *Org. Mass Spectrom.*, 14 (1979) 257.
10 J. Epstein, *Science (Washington, D.C.)*, 170 (1970) 1396.
11 A. Verweij, C. E. A. M. Degenhardt and H. L. Boter, *Chemosphere*, No. 3 (1979) 115.
12 A. Verweij, H. L. Boter and C. E. A. M. Degenhardt, *Science (Washington, D.C.)*, 204 (1979) 616.
13 P. Hirsjärvi, J. K. Miettinen and J. Paasivirta (Editors), *Identification of Degradation Products of Potential Organophosphorus Warfare Agents. An Approach for the Standardization of Techniques and Reference Data*, Ministry of Foreign Affairs of Finland, Helsinki, 1980, pp. 3–10, 18–30 and appendices.
14 J. Askew, J. H. Ruzicka and B. B. Wheals, *J. Chromatogr.*, 41 (1969) 180.
15 A. M. Kadoum, J. Agric. Food Chem., 17 (1969) 1178.

16 M. T. Shafik, D. Bradway and H. F. Enos, *Bull. Environ. Contam. Toxicol.*, 6 (1971) 55.
17 W. P. Cockrane, R. Greenhalgh and N. E. Looney, *J. Assoc. Off. Anal. Chem.*, 59 (1976) 617.
18 M. Zinbo and W. R. Sherman, *Tetrahedron Lett.*, (1969) 2811.
19 D. R. Matthews, W. D. Shults, M. R. Guerin and J. A. Dean, *Anal. Chem.*, 43 (1971) 1582.
20 L. G. Sanchez, R. B. Pinero, A. R. Caceres and M. M. Munoz, *Junta Energ. Nucl. (Spain)*, 425 (1978).
21 G. Bauer and W. Vogt, *Anal. Chem.*, 53 (1981) 917.
22 P. C. Bossle, J. J. Martin, E. W. Sarver and H. Z. Sommer, *J. Chromatogr.*, 267 (1983) 209.
23 E. J. Corey and A. Venkateswarlu, *J. Am. Chem. Soc.*, 94 (1972) 6190.
24 J. T. Watson and B. J. Sweetman, *Org. Mass Spectrom.*, 9 (1974) 39.
25 K. K. Ogilvie, *Can. J. Chem.*, 51 (1973) 3799.
26 G. Phillipou, D. A. Bigham and R. F. Seamark, *Lipids*, 10 (1975) 714.
27 G. Phillipou, D. A. Bigham and R. F. Seamark, *Steroids*, 26 (1975) 516.
28 R. W. Kelly and P. L. Taylor, *Anal. Chem.*, 48 (1976) 465.
29 M. A. Quilliam and J. B. Westmore, *Steroids*, 29 (1977) 579.
30 M. A. Quilliam and J. B. Westmore, *Anal. Chem.*, 50 (1978) 59.
31 T. P. Mawhinney, *J. Chromatogr.*, 257 (1983) 37.
32 J. G. Purdon, J. G. Pagotto, R. K. Miller and T. L. Stewart, *DREO Report*, No. 910, Defence Research Establishment Ottawa, Ottawa, 1985 (unclassified/unlimited).
33 T. P. Mawhinney and M. A. Matson, *J. Org. Chem.*, 47 (1982) 3336.
34 R. G. Jenkins, in R. E. Kaiser (Editor), *Proc. 4th. Int. Symp. Capillary Chromatography, Hindelang, May 3–7, 1981*, Huthig, Heidelberg, 1981, Paper No. 40, p. 803.
35 C. A. Saravalle, F. Munari and S. Trestianu, *J. Chromatogr.*, 279 (1983) 241.

Journal of Chromatography, 475 (1989) 273–281
Elsevier Science Publishers B.V., Amsterdam — Printed in The Netherlands

CHROM. 21 497

IDENTIFICATION OF SOME HUMAN URINARY METABOLITES OF THE INTOXICATING BEVERAGE KAVA

A. M. DUFFIELD*,[a]
Biomedical Mass Spectrometry Unit, The University of New South Wales, P.O. Box 1, Kensington, N.S.W. 2033 (Australia)
D. D. JAMIESON
School of Physiology and Pharmacology, The University of New South Wales, P.O. Box 1, Kensington, N.S.W. 2033 (Australia)
and
R. O. LIDGARD, P. H. DUFFIELD and D. J. BOURNE
Biomedical Mass Spectrometry Unit, The University of New South Wales, P.O. Box 1, Kensington, N.S.W. 2033 (Australia)
(First received February 8th, 1989; revised manuscript received March 6th, 1989)

SUMMARY

Methane chemical ionization (CI) gas chromatography–mass spectrometry (GC–MS) has been used to identify some of the human urinary metabolites of the kava lactones following ingestion of kava prepared by the traditional method of aqueous extraction of *Piper methysticum*. All seven major, and several minor, kava lactones were identified in human urine. Observed metabolic transformations include the reduction of the 3,4-double bond and/or demethylation of the 4-methoxyl group of the α-pyrone ring system. Demethylation of the 12-methoxy substituent in yangonin (or alternatively hydroxylation at C-12 of desmethoxyyangonin) was also recognised. This product was isolated by high-performance liquid chromatographic analysis of crude urine extracts and characterised by methane CI GC–MS. In contrast to the situation prevailing in the rat no dihydroxylated metabolites of the kava lactones, or products from ring opening of the 2-pyrone ring system, were identifed in human urine. GC–MS analysis of urine can be readily utilised to determine whether donors have recently consumed kava.

INTRODUCTION

Kava, the intoxicating beverage of the Pacific Islands[1,2] has recently become a drug of abuse amongst some of the aboriginal communities of the Northern Territory of Australia[3–6]. *Piper methysticum* is imported mainly from Fiji and Vanuatu and aqueous extraction of the commercially dried plant material is used for

[a] Present address: Australian Jockey Club Laboratory, P.O. Box 3, Randwick, N.S.W. 2031, Australia.

0021-9673/89/$03.50

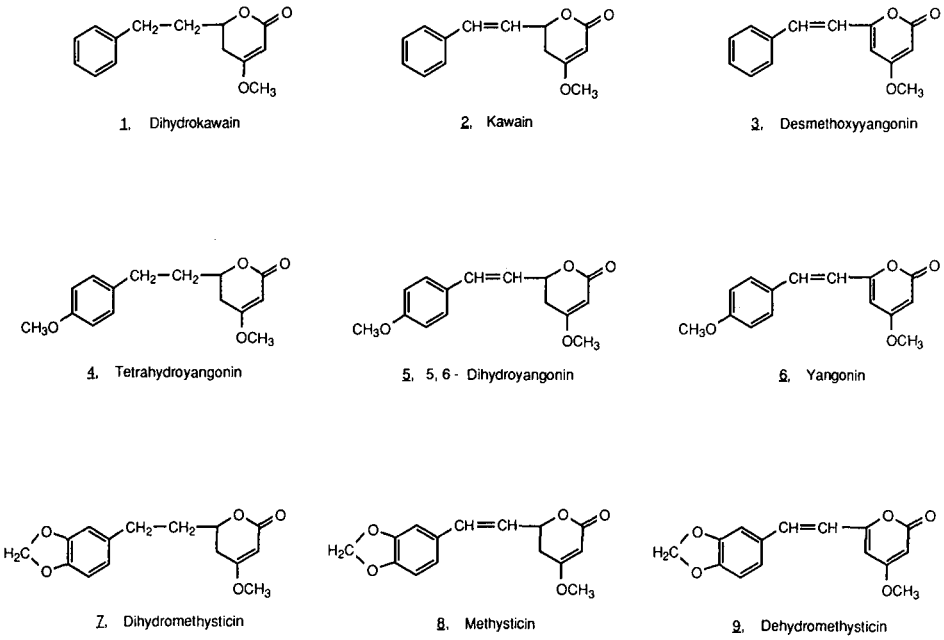

Fig. 1. Chemical structures and names of the major components of kava resin. Compounds **5** and **9** are present in only trace amounts.

the preparation of kava. The chemical structures of the lipid constituents of kava, often referred to as kava resin, and conveniently isolated by solvent extraction of *Piper methysticum*, have been defined (see Fig. 1)[1,2,7,8]. We have recently described[7,8] the application of gas chromatography–mass spectrometry (GC–MS) to the identification of known major, and several previously undetected minor constituents, of this resin.

One report has appeared[9] on the metabolism of kava lactones in the rat. This involved GC–MS analysis of urine from rats given, by stomach tube, an aqueous suspension of selected pure kava lactones. In the case of dihydrokawain (**1**) and kawain (**2**) the major urinary metabolite resulted from *p*-hydroxylation of the phenyl ring accompanied by smaller amounts of a further hydroxylation product. In addition minor metabolites arising from ring opening of the unsaturated 4-methoxy-2-pyrone ring system were recognised[9]. In contrast methysticin (**8**) produced only trace amounts of urinary metabolites resulting from rupture of the methylenedioxy ring system to a catechol structure, with and without concommitant reduction of the 7,8-double bond. Yangonin (**6**) and its 7,8-dihydro analogue yielded no identifiable urinary metabolites from rupture of the 2-pyrone ring system but were demethylated at C-12 to a phenol which was the precursor of other hydroxylated metabolites[9].

In addition to these metabolic transformations rat urine also contained unchanged kava lactones, which in the case of dihydrokawain (**1**), amounted to a 48% recovery of an administered dose after 48 h[9]. We now wish to report on the complex mixture of metabolites, and unchanged kava lactones, which are excreted in human urine after ingestion of kava prepared by the traditional method of water extraction of commercial *Piper methysticum*.

EXPERIMENTAL

Preparation of kava

Commercial *Piper methysticum* (450 g), was immersed (muslin bag) in water (3 l) at room temperature and after squeezing (5 min) "kava" was obtained. The beverage was consumed by healthy male subjects in about 100-ml aliquots. Typically 1 l was consumed in a period of about 1 h before sleeping and no physiological effects were apparent after consumption of this dose. Urine samples were collected before sleep and again on rising in the morning.

Urine sample work-up for direct GC–MS

All solvents were distilled prior to use. Urine (100 ml) was acidified (pH 1) with 2 *M* hydrochloric acid and extracted with chloroform (3 × 30 ml), centrifuged to break persistent emulsions, and the combined organic phase washed with 5% aqueous sodium carbonate (2 × 20 ml), water (20 ml) and then the chloroform layer was dried over anhydrous sodium sulphate. Filtration and removal of the chloroform *in vacuo* provided a residue 10% of which was derivatised in a Reactivial with bis(trimethylsilyl)trifluoroacetamide (BSTFA) (50 μl) (Pierce, Rockford, IL, U.S.A.) at 80°C for 30 min and aliquots (1–2 μl) used for GC–MS analysis.

GC–MS

MS instrumentation consisted of a Finnigan Model 3200 CI GC–MS system interfaced to a Finnigan-Incos Model 2300 data system. It was operated under the conditions previously described[7]. GC separations were made with a quartz BP-10 capillary column (25 m × 0.3 mm I.D.; helium flow, 1 ml/min; Scientific Glass Engineering, Melbourne, Australia). Samples were injected at an initial oven temperature of 100°C which was temperature programmed at 6°C/min to a final temperature of 300°C. The CI mass spectrometer was scanned in 1 s between *m/z* 60 and 460 during these analyses. Methane served as the CI reactant gas at an ion source pressure of 1 Torr.

HPLC

Gradient purifications were carried out with a Waters Model 510 pump fitted with a U6K injector, a Waters M45 pump and a Model 660 solvent programmer. Reversed-phase purifications utilized an Econosil C_{18} column (250 mm × 4.6 mm I.D., particle size 5 μm) (Alltech Assoc., Homebush, Australia). The detection system included a Hewlett Packard 1040A diodearray interfaced with a HP 9000 series 300 computer and a HP 9133 disc drive. Chromatograms were recorded at 220, 260 and 360 nm with a bandwidth of 4 nm. The reference wavelength was set at 550 nm with a bandwidth of 100 nm. UV spectra and chromatograms were hard-copied using either a HP Model 7470A plotter or a HP Thinkjet printer.

Urine extraction and HPLC separation

Urine (50 ml) was extracted with chloroform (3 × 20 ml) as described above and the neutral residue dissolved in methanol (0.5 ml) which was then fractionated into two separate injections under the above HPLC conditions. A linear gradient was used, programmed from 10% methanol in 0.2% aqueous acetic acid to 100% methanol

during 30 min. The fraction eluting between 28 and 29 min was collected and evaporated to dryness for characterisation by methane CI MS.

The chloroform extract from the urine of a second volunteer was chromatographed using the same column but a different mobile phase consisting of 45% acetonitrile in 0.2% aqueous acetic acid. The eluent from a single injection of this extract was collected between retention times of 2 and 10 min and evaporated to dryness. This residue in methanol was re-injected under the same conditions. The peak displaying the *trans*-yangonin chromophore (Fig. 3) was trapped (retention time 8–9 min) and the solvent removed. This material was then characterised by methane CI MS and shown to be identical with that isolated by high-performance liquid chromatography (HPLC) using the methanol based solvent system.

*Hydrogenation of dihydrokawain to 3,4,7,8-tetrahydrokawain (**10a**)*

Dihydrokawain (10 mg) in ethyl acetate (10 ml) was hydrogenated at 55–60°C for 5 h over a 10% Pd/C catalyst (5 mg). Solvent was added as necessary to maintain the reaction mixture at a volume of between 5 and 10 ml. The catalyst was filtered off and the residue shown by methane CI MS to have an $[MH]^+$ at *m/z* 235 and its mass spectrum and retention time was similar to that recorded for **10a** in Table II and Fig. 2.

*Hydrogenation of tetrahydroyangonin (**4**)*

In a similar experiment **4** was hydrogenated to 3,4,5,6,7,8-hexahydroyangonin identified by its methane CI mass spectrum[a] as **10b:** $[MH]^+$ *m/z* 265 (55%), *m/z* 247 (15%), *m/z* 233 (40%), *m/z* 215 (11%), *m/z* 187 (4%), *m/z* 173 (6%), *m/z* 147 (28%),

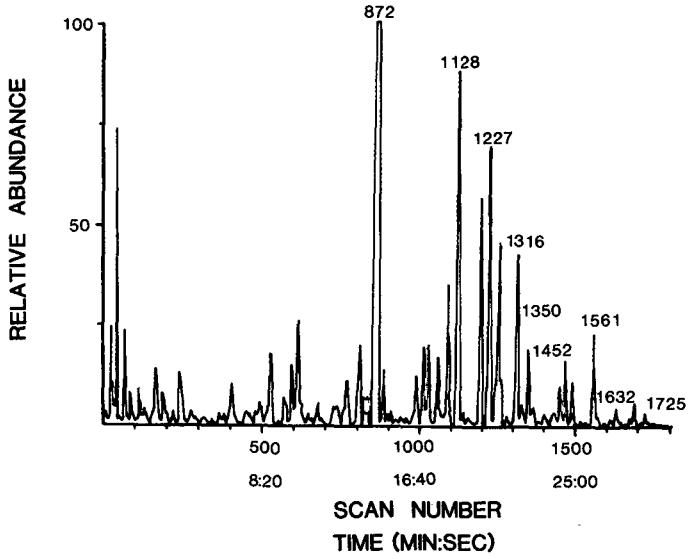

Fig. 2. Methane CI GC–MS total ion current record of a derivatised (TMS) urine extract after human consumption of kava. The GC conditions were as follows: BP-10 column (25 m × 0.3 mm O.D.) which was temperature programmed from 100 to 300°C at 6°C min^{-1} 1.5 min after sample injection.

[a] Unless indicated to the contrary all $[MH]^+$ ions were accompanied by the methane adduct species $[M+C_2H_5]^+$ and $[M+C_3H_5]^+$, respectively.

m/z 121 (100%) and *m/z* 103 (8%). We were unable to detect by methane CI GC–MS the presence of this compound in extracts of kava urine.

RESULTS AND DISCUSSION

Caffeine provided a focal point (scan number 872 in Fig. 2) in the GC–MS analysis of TMS derivatised residues from human urine after consumption of kava. All the identified kava resin components and their metabolites had longer GC retention times than caffeine. The major unchanged kava lactones whose structures are summarised in Fig. 1 (**1–4**, **6–8**) were readily identified from their methane CI mass spectra[7] and their identity and scan number in Fig. 2 are recorded in Table I.

TABLE I

IDENTIFICATION IN FIG. 2 OF UNCHANGED KAVA LACTONES PRESENT IN HUMAN URINE AFTER DRINKING KAVA

Compound	*Scan number*	*$[MH]^+$ m/z*
Dihydrokawain (**1**)	1195	233
Kawain (**2**)	1316	231
Desmethoxyyangonin (**3**)	1350	229
Tetrahydroyangonin (**4**)	1452	263
Dihydromethysticin (**7**)	1561	277
11-Methoxytetrahydroyangonin	1612	293
Yangonin (**6**)	1632	259
Methysticin (**8**)[a]	1645	275
Dehydromethysticin (**9**)	1725	273

[a] Methysticin (**8**) was not detected in Fig. 2. Other analyses of kava urine extracts did give a positive identification for **8** at this retention time (immediately following yangonin). The GC column must be relatively new and free of decomposition products to transmit methysticin to the MS ion source[7].

The first identified kava metabolite eluted at scan number 1060 (Fig. 2) and had a protonated molecular ion ($[MH]^+$) at *m/z* 235 and its mass spectrum is summarised in Table II. This metabolite corresponds to saturation of the 3,4-double bond of dihydrokawain (**1**) so that the metabolite would be **10a**. This was confirmed by synthesis of **10a** from catalytic hydrogenation of dihydrokawain. We did not detect analogues of **10a** corresponding to methoxyl (**10b**, $[MH]^+$, *m/z* 265) or methylenedioxy ($[MH]^+$, *m/z* 279) substitution of the phenyl ring [*i.e.*, metabolites of tetrahydroyangonin (**4**) and dihydromethysticin (**7**) respectively].

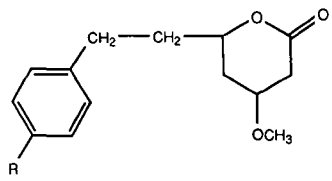

10a, R = H, $[MH]^+$, *m/z* 235
10b, R = OCH_3, $[MH]^+$, *m/z* 265

TABLE II

METHANE CI MASS SPECTRA OF THE TMS DERIVATIVES OF KAVA LACTONE METABOLITES IDENTIFIED IN HUMAN URINE

Scan No.	*Structure*	*$[MH]^+$ m/z*	*Mass spectrum*[a]
1060	**10a**	235	235,100; 217,27; 203,70; 185,65; 157,17; 143,68; 117,23; 103,27; 91,5
1092, 1129[b]	**11a**	293	293,18; 277,6; 275,10; 243,2; 233,3; 231,7; 203,65; 185,69; 161,55; 157,22; 143,100; 117,20; 91,16
1365	**11b**	323	323,6; 251,12; 233,35; 215,11; 191,10; 173,8; 161,22; 147,15; 121,100; 75,7; 73,9
1436, 1470[b]	**11c**	337	337,6; 336,4; 321,7; 275,6; 247,68; 229,24; 205,12; 187,35; 161,95; 135,100; 75,18; 73,13
1227, 1255[b]	**12a**	291	291,1; 275,1; 201,70; 189,12; 183,20; 161,100; 157,9; 155,28; 145,9; 143,7; 141,12; 131,6; 117,11; 101,10; 91,23; 75,28; 73,30
1332	**12b**	321	321, 100; 305,12; 231,48; 215,8; 207,12; 121,40; 91,8; 75,4; 73,8
1677	**13**	317	317,100; 301,9; 245,6; 125,25

[a] *m/z*, % relative intensity.

[b] Relative intensity variations in *m/z* values between each isomeric pair was within 10%.

The next urinary metabolites to be recognised eluted (Fig. 2) at scans 1092 and 1128 and they had very similar methane CI mass spectra with $[MH]^+$ ions of *m/z* 293 (Table II). These products formally correspond to structure **11a** and may be C_4 epimers.

Two methylenedioxy substituted metabolites with identical mass spectra ($[MH]^+$, *m/z* 337) appear at scan numbers 1436 and 1470 respectively in Fig. 2 and structure **11c** is consistent with the mass spectral evidence (Table II). Presumably these metabolites **11a** + **11c** would be derived from either dihydrokawain (**1**), or kawain (**2**), and either dihydromethysticin (**7**) or methysticin (**8**), respectively. Interestingly only one isomer of the methoxylated version, **11b** ($[MH^+$, *m/z* 323) was identified (Table II, scan number 1365 in Fig. 2) in all the urine samples investigated and presumably this arose from metabolism of the tetrahydroyangonin (**4**) content of kava.

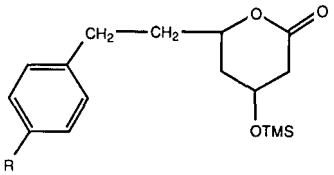

11a, R = H, $[MH]^+$, *m/z* 293
11b, R = *p*-OCH_3, $[MH]^+$, *m/z* 323
11c, R = 11,12-O-CH_2-O-, $[MH]^+$, *m/z* 337

Another metabolite ($[MH]^+$, *m/z* 291) was detected as two isomers with similar methane CI mass spectra at scan numbers 1223 and 1255 (Fig. 2) and formally correspond to the demethylation product (**12a**) of dihydrokawain (**1**). Tetramethylsilyl

(TMS) derivatisation of the 1,3-diketo metabolite would be expected to yield[10] a mixture of 2- and 4-OTMS structures. The methoxylated analogue (**12b**) [presumably the metabolite of tetrahydroyangonin (**4**)] elutes (Fig. 2) at scan number 1332 ($[MH]^+$, *m/z* 321). The anticipated second isomer of **12b** may co-elute with desmethoxyyangonin (**3**) around scan number 1350 but the relatively large amount of **3** did not allow positive clarification of this point. Only weak responses were detected corresponding to the methylenedioxy metabolite (**12c**) ($[MH]^+$, *m/z* 335) in some urine analysis but insufficient ion current was available for definitive identification.

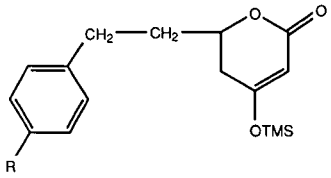

12a, R = H, $[MH]^+$, *m/z* 291
12b, R = *p*-OCH_3, $[MH]^+$, *m/z* 321
12c, R = 11,12-O-CH_2-O–, $[MH]^+$, *m/z* 335

Scan 1677 in Fig. 2 is a kava metabolite ($[MH]^+$ at *m/z* 317) which corresponds to the product of demethylation (**13**) of the 12-methoxyl group of yangonin (**6**) or, alternatively, from hydroxylation at C-12 of desmethoxyyangonin (**3**). This metabolite was isolated from crude urine extracts by HPLC using multivariate UV detection. The UV spectrum of the material collected from HPLC analysis was very similar to yangonin (Fig. 3) and its properties are consistent with its assignment as 12-desmethylyangonin (**13**). This was confirmed from solid probe methane CI-MS which yielded a single product, {$[MH]^+$, *m/z* 245 (base peak)} with a fragment of *m/z* 125 (15% relative abundance). This fragmentation behaviour is similar to yangonin[7] and the fragment at *m/z* 125 confirms the presence of the 2-pyrone ring system in the metabolite[7]. Derivatisation (TMS) of the product collected from HPLC afforded a compound ($[MH]^+$, *m/z* 317) whose methane CI GC mass spectrum was identical to that obtained (Fig. 2) from direct TMS derivatisation of the crude urine extract.

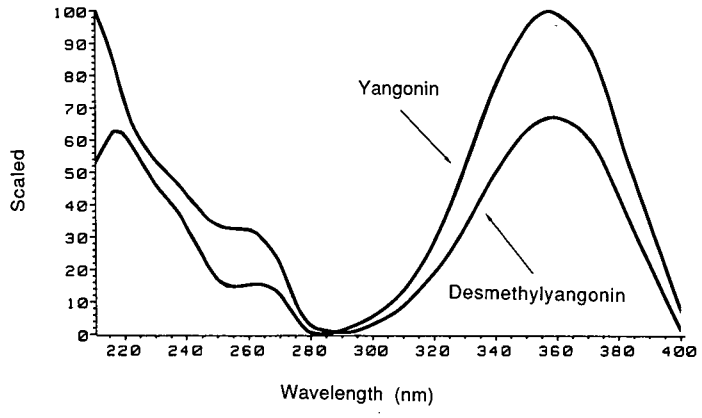

Fig. 3. UV spectra of yangonin (**6**) and a metabolite isolated by HPLC and identified as 12-desmethylyangonin (**13**).

C-12-Desmethylyangonin (**13**) was identified[9] as a metabolite of yangonin (**6**) in rat urine.

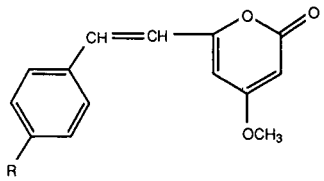

13, R = OH, $[MH]^+$, *m/z* 245
R = OTMS, $[MH]^+$, *m/z* 317

In contrast to the situation pertaining to the metabolism by rodents of kava lactones[9] we did not detect in human urine products resulting from opening of the 2-pyrone ring of the kava lactones (Fig. 1). These products would have been removed in the 5% sodium carbonate wash employed in the urine work-up. Acidification of this aqueous extract and solvent extract isolated a crude acidic fraction which was then derivatised as its TMS ester/ether analogues. GC–MS of this derivatised fraction failed to identify any mass spectra compatible with pyrone ring opened metabolites of the kava lactones. Other metabolites of the kava lactones are present in human urine but their identity could not be determined on the evidence currently available.

This methane CI GC–MS analysis was used to screen over 80 urine samples collected from aboriginal donors in the Northern Territory. We were able to define those individuals who had not taken kava (no kava lactones or metabolites detected), those who had previously, but not recently, consumed kava (trace to small amounts of marker lactones observed) and those who had recently consumed a quantity of kava (identification of relatively large amounts of kava lactones and there metabolites). Our analysis of these samples correlated with the results of a questionnaire completed by the urine donors regarding their recent use of kava. This work demonstrated that it is relatively easy to define by urine analysis those individuals who have consumed kava and this may be of interest to forensic analysts.

ACKNOWLEDGEMENTS

We wish to thank the National Health and Medical Research Council of Australia for supporting this research and Professor John Mathews of the Menzies School of Medical Research, Darwin, for providing us with urine samples collected from aboriginal donors in the Northern Territory.

REFERENCES

1 A. T. Shulgin, *Bull. Narc.*, 25 (1973) 59–74.
2 F. Keller and M. W. Klohs, *Lloydia*, 26 (1963) 1–15.
3 J. Cawte, *Aust. N.Z. J. Psychiatry*, 19 (1985) 83–87.
4 J. Cawte, *Aust. N.Z. J. Psychiatry*, 20 (1986) 70–76.
5 S. Sotheeswaran, *Chem. Aust.*, 54 (1987) 377–378.

6 M. W. Klohs in D. H. Efron, B. Holmstedt and N. S. Kline (Editors), *Ethnopharmacological Search for Psychoactive Drugs,* Public Healt Service Publication 1645, U.S. Government Printing Office, Washington, DC, 1967, pp. 126–132.
7 A. M. Duffield, R.O. Lidgard and G. K.-C. Low, *Biomed. Environ. Mass Spectrom.*, 13 (1986) 305–313.
8 A. M. Duffield and R. O. Lidgard, *Biomed. Environ. Mass Spectrom.*, 13 (1986) 621–626.
9 A. K. Rasmussen, P. R. Scheline, E. Solheim and R. Hänsel, *Xenobiotica,* 9 (1979) 1–16.
10 D. Herbst, W. B. Mors, O. R. Gottlieb and C. Djerassi, *J. Am. Chem. Soc.*, 81 (1959) 2427–2430.

Journal of Chromatography, 475 (1989) 283–292
Elsevier Science Publishers B.V., Amsterdam — Printed in The Netherlands

CHROM. 21 521

CARRIER AMPHOLYTE-MEDIATED OXIDATION OF PROTEINS IN ISOELECTRIC FOCUSING

GIANFRANCO COSSU, MARIA GAVINA PIRASTRU and MARIANNA SATTA
Laboratory of Immunohematology, Ospedale A. Segni, Ozieri 07041, Sassari (Italy)
and
MARCELLA CHIARI, CLAUDIA CHIESA and PIER GIORGIO RIGHETTI*
Chair of Biochemistry, Faculty of Pharmacy and Department of Biomedical Sciences and Technologies, University of Milan, Via Celoria 2, Milan 20133 (Italy)
(Received March 20th, 1989)

SUMMARY

It has been found that all commercially available carrier ampholytes (the amphoteric buffers used to create and stabilize the pH gradient in isoelectric focusing, IEF) (*e.g.*, Ampholine, Pharmalyte) are extensively oxidized by persulphate during gel polymerization. These oxidized species are formed for all pH ranges, from acidic to basic, and exhibit chromophoric peaks in the 300–360 nm range. It is believed that these oxidized products are N-oxides (possibly even nitrosamines). Owing to their high redox potentials during IEF, especially in alkaline pH ranges, they are able to capture two H^+ and two electrons and be reduced, while oxidizing in proteins SH group of Cys to –S–S– (possibly even to cysteic acid). This generates artefactual band heterogeneity, not present in the starting sample, which could never be eliminated as, on rerunning the zone, additional oxidation will take place. In such cases, the presentation of proof of sample homogeneity to agencies such as the FDA, for recombinant DNA products for human consumption, might be impossible. Such a cause of artefactual sample heterogeneity can be virtually eliminated by simply not exposing the carrier ampholytes to persulphate. In the proposed IEF protocol, "empty" gels are polymerized, washed, dried and reswollen in the desired pH interval.

INTRODUCTION

For at least a decade users of the isoelectric focusing (IEF) technique have debated extensively on potential artefacts arising from its very principle, *i.e.*, isoelectric condensation of amphoteric macroions. It was believed that if proteins, during migration to the p*I* position, were to bind to the carrier buffers (CA) [a multitude of oligoamino, oligocarboxylic amphoteric species, having M_r from 600 (the most basic) to 900 Da (the most acidic)][1], multiple equilibria would then ensue, a pattern of $n + 1$ zones being generated, representing n complexed states with n different CA species plus one uncomplexed protein zone originally in equilibrium with all the others[2].

0021-9673/89/$03.50

Our group has extensively analysed these phenomena over the years. Indeed, Galante *et al.*[3], on the basis of variations of melting points of tRNA in presence of Ampholine, have demonstrated that the mechanism of IEF fractionation of nucleic acids is strong complex formation between them and the CA species used to generate and stabilize the pH gradient in IEF. The complex is strongly pH dependent: it is almost non-existent at neutral pH (7.4), weak at pH 5.4 and very strong at pH 4.2 and lower, *i.e.*, in the typical pH range of the apparent isoelectric fractionation of tRNAs and mRNAs.

Subsequently, in the analysis of heparin (a carboxylated and sulphated polysaccharide), Righetti and co-workers[4,5], on the basis of spectra taken in solution and in focused gels, of repeated runs of isolated, focused bands, of IEF fractionations performed in the presence and absence of urea, at variable Ampholine-to-heparin ratios and with heparins with varying degrees of substitution, demonstrated the IEF heparin profile to be artefactually elicited by interaction with carrier ampholytes. It was thus found that the 21 IEF heparin fractions were indeed 21 different complexes of the same macromolecule with 21 specific Ampholine molecules determining the apparent p*I* of the focused zone. It was then understood[6] that the anomalous fractionations of nucleic acids and heparin were just particular cases of a more general phenomenon, by which all polyanions (*e.g.*, polyphosphates, polysulphates, polycarboxylates and even acidic dyes[7]) would elicit complex formation with carrier ampholytes in the range 3–5, with a strongly pH-dependent affinity, being *ca.* 10 000 fold greater at pH 3 than at pH 7.

Correspondingly, at the opposite extreme of the pH scale, it was found that polycations were able to complex CAs too, although only poly-Arg could form stable complexes, poly-Lys and poly-His exhibiting no appreciable binding[8].

The situation described above would appear to be hopeless; on the contrary, the artefacts here reported are unique examples and refer to limiting structures, *i.e.*, mostly to polyanions and polycations, which, lacking counter ions in their chemical framework, have to bind any other counter ion available in solution. There is no evidence that CAs will elicit the same multimodal distribution by interacting with proteins. In fact, according to Rilbe[9], in IEF a protein should be both isoelectric and isoionic, the latter term indicating that the isoelectric protein is stripped free of any other counter ions available in the surrounding buffer, except from protons deriving from the protolytic equilibria due to its amino acid composition. This is made possible by the fact that both proteins and carrier ampholytes are amphoteric species, so that at their respective isoelectric points they can form an "inner" salt, with no tendency to bind to foreign ions. This is certainly not the case in zone electrophoresis with conventional buffers. For example, it is known that, by electrophoresis in borate buffers, bovine serum albumin (BSA) is always split into two bands, representing the equilibrium[10] free BSA $\rightleftharpoons$ borate–BSA.

If IEF is then a safe fractionation procedure, are there any instances in which artefactual bands can be generated? We report here an undesirable phenomenon that must have plagued the technique since at least 1971, when gel IEF was first described[11]: when focusing proteins, free SH groups can be oxidized during the run, producing zones with higher p*I*. The oxidation power comes from the carrier buffers themselves, oxidized by the persulphate during the gel polymerization step. The phenomenon is described here and remedies are proposed.

EXPERIMENTAL

Materials

Repel- and Bind-Silane, Gel Bond PAG, the Multiphor 2 chamber, Multitemp thermostat and Macrodrive power supply were from LKB (Bromma, Sweden) and Pharmalyte and Ampholyte buffers and a protein p*I* marker kit were purchased from Pharmacia (Uppsala, Sweden). Acrylamide, N,N′-methylenebisacrylamide (Bis), N,N,N′,N′-tetramethylethylenediamine (TEMED), ammonium persulphate and Coomassie Brilliant Blue R-250 were from Bio-Rad Labs. (Richmond, CA, U.S.A.) and dithiothreitol (DTT) and urea from Merck (Darmstadt, F.R.G.). Human globin chains were prepared by the acetone–acid method of Clegg *et al.*[12].

Spectrophotometric analyses

UV–VIS spectrophotometry was performed with a Cary 219 instrument (Varian, Palo Alto, CA, U.S.A.). Ampholine and Pharmalyte pH ranges were analysed for potential oxidation by persulphate during the gel polymerization step. Solutions of 1.5% of the pH intervals used for haemoglobulin focusing (pH 6–9) were prepared in 100 m*M* buffer (phosphate, titrated to neutral pH) and standard amounts of catalysts were added (1 μl of TEMED and 1 μl of 40% ammonium persulphate per 1 ml of gelling solution) in the absence of gelling monomers (acrylamide and Bis). As a blank, the same amounts of TEMED and persulphate, diluted in 100 m*M* phosphate buffer (pH 7.0) were used. All cuvettes were subjected to the standard treatment utilized for gel polymerization (1 h, 50°C) and then spectra were taken at room temperature in the range 280–450 nm at 2 A full-scale, with automatic baseline correction.

Conventional IEF in carrier ampholytes

Human globin chains were taken as a model for the potential oxidation of SH groups duing focusing. Three types of gels were prepared. In one, the gel was polymerized directly in the presence of 2.5% carrier ampholytes (CA; a 1:1 mixture of pH 6–8 and pH 7–9 ranges plus a small amount of pH 3–10) and 8 *M* urea and used as such with a 30-min prerun.

A second gel type was polymerized in the absence of any additive ("empty" gel), washed first in 100 m*M* ascorbic acid for 30 min, then twice in distilled water, dried and reswollen in the presence of 2.5% CA and 8 *M* urea. This gel was run using also 100 m*M* ascorbic acid as anolyte.

A third gel type was treated exactly as the second gel, except that it was run using 50 m*M* phosphoric acid as anolyte. All gels were made to contain a 5%T, 4%C matrix and were polymerized with the same amounts of catalysts (1 μl of TEMED and 1 μl of 40% ammonium persulphate per 1 ml of gelling solution) at 50°C for 1 h. Human globin chains, freshly dissolved in 8 *M* urea, 2% CA in the pH range 6–8 and 5% 2-mercaptoethanol, were applied in pockets precast at the anode in amounts ranging from 15 to 20 μg. Focusing was performed at 10 W (maximum) and 1500 V (at equilibrium) for 2–4 h. Staining was made in Coomassie Blue in the presence of copper(II) sulphate[13]. The globin chain focusing technique is essentially as described by Righetti *et al.*[14], except that addition of detergent to the sample and gel layer was omitted, as it was not the aim of this work to separate the A_γ and G_γ chains.

RESULTS

Action of persulphate on carrier ampholytes

Fig. 1 shows the results of incubating carrier ampholytes with persulphate, under conditions mimicking those used for preparing standard polyacrylamide gels. The spectra of the *ca.* neutral pH ranges (pH 6–8 Ampholine and pH 5–8 Pharmalyte) show that, in the two controls, essentially no chromophores are apparent, whereas on contact with AP, strong chromophores appear. Ampholine exhibits a bimodal distribution, with peaks centred on 300 and 345 nm, whereas Pharmalyte produces a single strong chromophore centred on 316 nm.

Action of oxidized carrier ampholytes on proteins

The presence of these oxidation products in Ampholine and Pharmalyte could be deleterious to protein fractionation because, even in the absence of persulphate (*e.g.*,

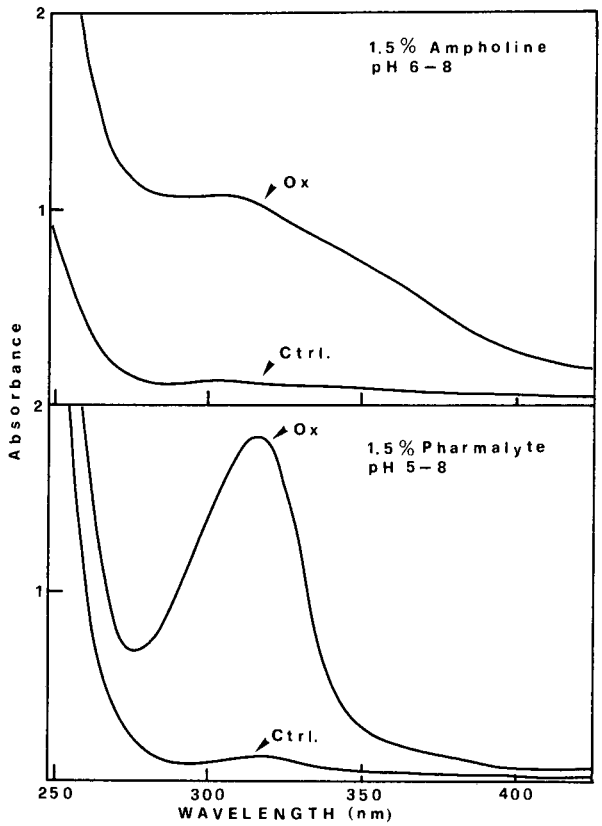

Fig. 1. Oxidation of carrier ampholytes by persulphate; 1.5% solutions of either Ampholine (pH 6–8) or Pharmalyte (pH 5–8) in 100 m*M* phosphate buffer (pH 7.0) were incubated for 1 h at 50°C either as such (control, Ctrl.) or in presence of 0.04% ammonium persulphate and TEMED (oxidized, Ox). Note, in this last instance, the formation of strong chromophores in the 300–360 nm region, which we attribute to the formation of N-oxides.

even if the gel had been extensively pre-run to discharge persulphate and its degradation products to the anode), the focusing gel could bear an intrinsic oxidation power present all along the pH gradient as oxidized buffering species. When focusing in alkaline pH ranges, proteins could be directly oxidized, while reducing the oxidized buffers present along the migration path. That this could be the case is shown in Fig. 2A: when globin chains are focused in an Ampholine gel (containing oxidized Ampholine species) the α-globin chains are clearly split into two bands, the upper zone (representing oxidized α-chains, as discussed below) constituting *ca.* 40% of the two components. Even β-globin chains are split into two bands, whereas foetal chains are resolved into a single component. If the run is performed in presence of Pharmalyte,

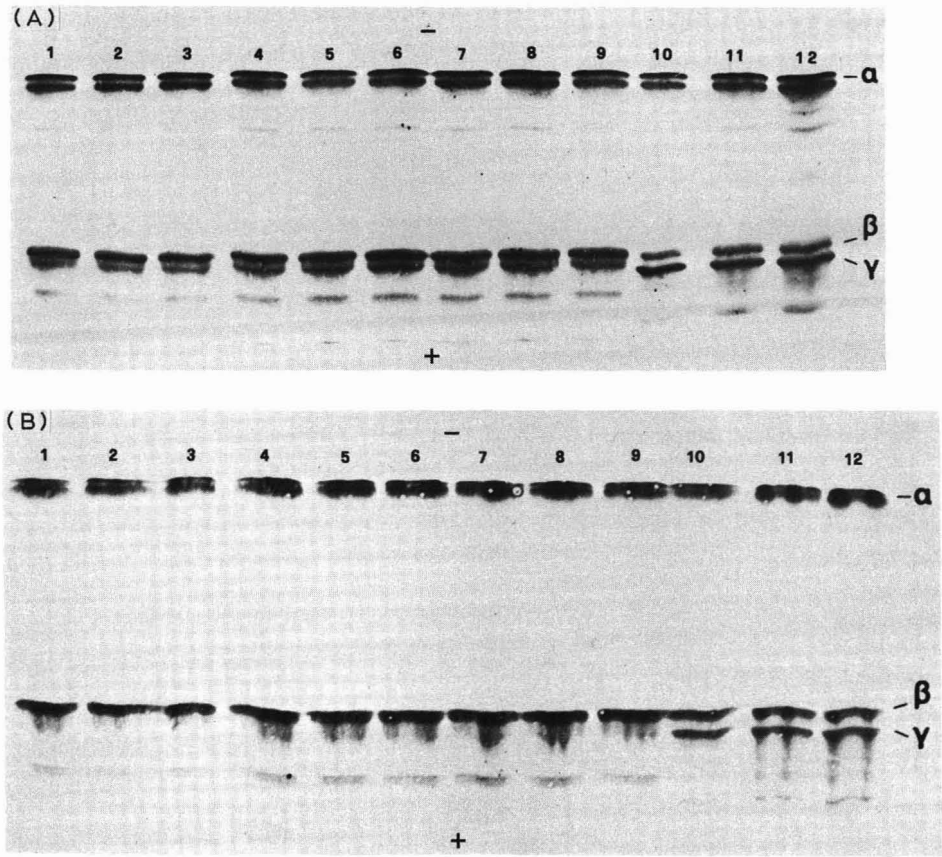

Fig. 2. Focusing of human globin chains. Gels: 5%T, 4%C polyacrylamide, in the presence of 8 *M* urea and 2.5% carrier ampholytes. (A) Gel containing a total of 2.5% Ampholines in the pH ranges 6–8, 7–9 and 3.5–10, in the ratio 45:45:10. (B) Gel containing a total of 2.5% Pharmalytes in the pH ranges 6–8, 6.5–9 and 3–10 in the ratio 45:45:10. Both gels were polymerized directly in the presence of urea and carrier ampholytes with 0.04% persulphate and TEMED. Samples: 1–9, globin chains from normal human adults; 10–12, globin chains from umbilical cord blood. The samples were applied anodically at a concentration of *ca.* 20 μg total protein. The gels were prefocused for 30 min at 400 V and the run was continued for 2 h at 1100 V and an additional 30 min at 1800 V. Staining with Coomassie Brilliant Blue in Cu^{2+}. Note the splitting of α-chains into two bands, more pronounced in Ampholine IEF.

the α-chains are still split into two components, whereas the β-globins appear as a single zone (Fig. 2B). In both instances, the foetal chains are unaffected by the presence of oxidized carrier ampholyte species.

In order to check the above hypothesis (oxidation of globin chains by oxidized carrier ampholyte species), a control experiment was run as follows: an empty gel was prepared (in the absence of ampholytes and urea), washed first in ascorbic acid and then in distilled water, and dried. The dried gel was then reswollen in the presence of urea and either Ampholine or Pharmalyte. As shown in Fig. 3A, now α-globins focus as a single zone, indicating the absence of oxidation products, whereas β-chains are still resolved into two fractions. However, if the experiment is performed with Pharmalytes, both α- and β-globins focus as single zones (Fig. 3B). In both instances, the foetal chains are unaffected and always focus as a single component.

The ability of persulphate to oxidize globin chains (mediated by the present of oxidized carrier ampholyte species during the IEF run) was investigated by running a series of gels polymerized with different levels of persulphate. Three types of gels were

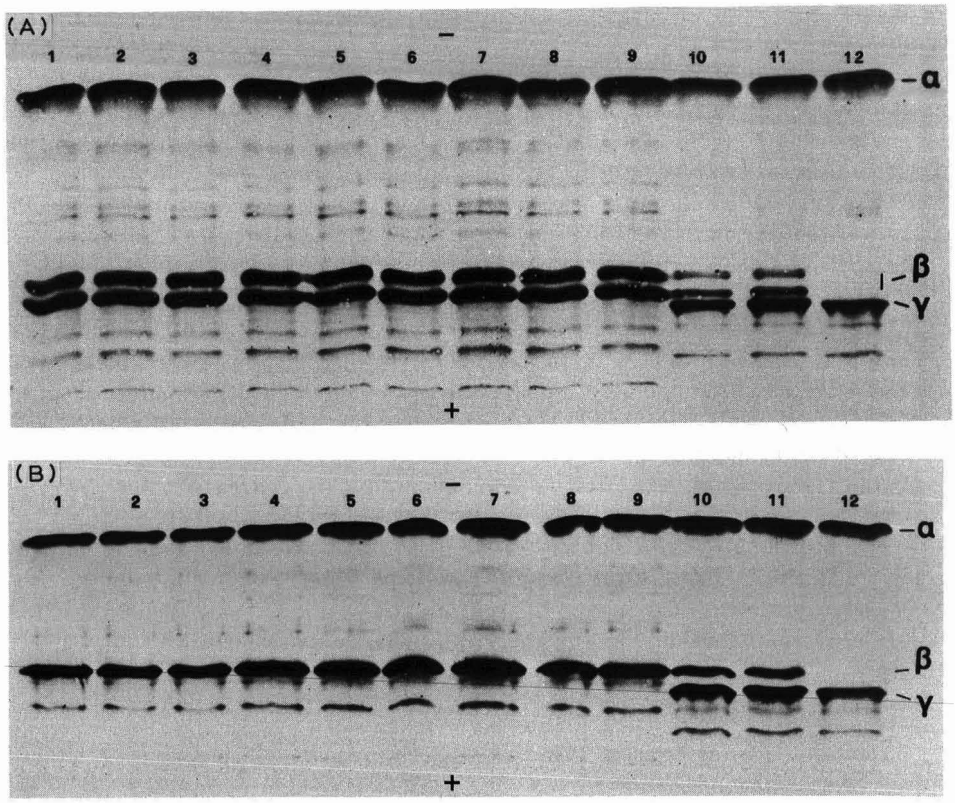

Fig. 3. Focusing of human globin chains. Gels as in Fig. 2, except that "empty" matrices were polymerized, washed once (45 min) with 100 m*M* ascorbic acid (pH 4.5) and then twice for 45 min with distilled water. After drying, the matrices were reswollen in the presence of 8 *M* urea and either 2.5% Ampholine (A) or 2.5% Pharmalyte (B) in the ratios given in Fig. 2. Other experimental conditions as in Fig. 2. Note the disappearance of oxidized α-chains in both instances. Samples 1–11 as in Fig. 2; No. 12 is from a homozygous β°-thalassemic.

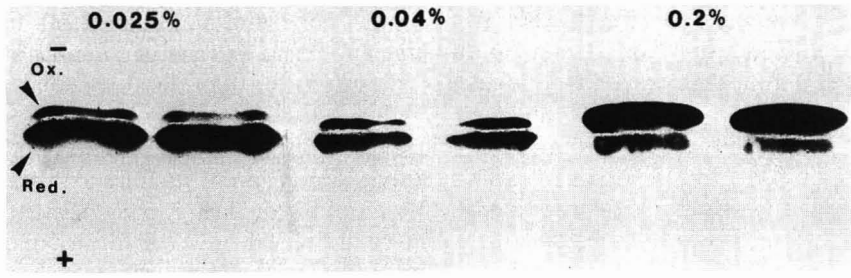

Fig. 4. Oxidation of α-globin chains as a function of persulphate levels during gel polymerization. Three different gels were polymerized (in the presence of Ampholine and urea) with either 0.025, 0.04 or 0.2% persulphate. Focusing and other experimental conditions as in Fig. 2. After staining. the ratio α_{ox}/α_{red} was evaluated by densitometry and found to be 15:85, 35:65 and 80:20, respectively.

investigated: containing 0.025% persulphate (AP) (the minimum level for obtaining a reasonable gel polymerization), or 0.04% persulphate (the amount routinely used in most laboratories) or 0.2% persulphate (definitely an excess, seldom used in routine work). The gels were then prerun for 45 min and reduced globin chains applied anodically. As shown in Fig. 4, the amount of oxidized α-globin chains is directly proportional to the initial amount of persulphate used in gel polymerization. At the lowest AP level (0.025%) the ratio α_{ox}/α_{red} is only 15:85; at the normal AP levels (0.04%) this ratio is increased to 35:65, whereas at the highest AP level, the oxidized α-chain clearly predominates (α_{ox}/α_{red} = 80:20).

DISCUSSION

We had recently become aware, in our studies on immobilized pH gradients (IPG) (for a review, see Righetti and Gianazza[15]) that, when focusing in alkaline pH gradients, strange phenomena occurred with cysteine-rich protein molecules. For example, with pro-urokinase (a 46 kDa protein containing 24 Cys out of a total of 411 amino acids and exhibiting a p*I* of *ca.* 9.8), a size-homogeneous preparation would be resolved, in IPGs, into an extremely large number of bands (at least ten major and ten minor bands focusing in the pH range 7–10)[16]. Having ruled out common sources of polydispersity, such as different degrees of glycosylation or IEF artefacts, such as binding to carrier ampholytes or carbamylation by urea, we attributed this phenomenon to the coexistence among species in the –SH, –S–S– and SO_3^- states. This equilibrium could remain undetected in most instances, as two thirds of the known proteins have isoelectric points failing in the acidic portion of the pH scale[17]. Given the mildly alkaline p*K* of the SH group of Cys (p*K* = 8.3), the presence of an –SH rather than an –S–S– group would go undetected in acidic proteins, as neither would contribute to the surface charge. However, in urokinase-like molecules, owing to the high isoelectric point of the "native" forms and to the presence of an unusually large number of Cys, an equilibrium between –SH and –S–S– states would be immediately visible by producing a series of charge-altered species. For example, the disappearance of two –SH groups, with the formation of a single –S–S– bridge, would produce species with a net loss of two negative charges because, at the high p*I* (9.8) of the "native" protein molecules, such groups would be fully ionized. The high-p*I* pro-urokinase was

found to have almost no titratable SH groups (less than 1 mol/mol of protein), in agreement with literature data, whereas the low-p*I* components had a larger number of available SH groups. However, this number was much lower than the theoretically expected amount of 24–SH groups/mol of protein. As an answer we had proposed that oxidation of Cys could proceed to an irreversible state, *i.e.*, cysteic acid. From the point of view of charge, high-p*I* molecules carrying a free –SH group or its fully oxidized cysteic acid derivative should be indistinguishable, as both would carry a net negative charge. However, titration with Ellman reagent would reveal only the former and ignore Cys residues converted into cysteic acid and in fact lower p*I* pro-urokinases had very few extra SH groups that could be titrated.

Indeed, this phenomenon of Cys oxidation was described so long ago that it has probably been forgotten. Thus, as early as 1971, Jacobs[18,19] first reported the partial modification of Cys and Met to cysteic acid and methionine sulphoxide, on prolonged IEF, in bovine ribonuclease (also an alkaline protein). These oxidation phenomena could be largely suppressed by removal of oxygen from the IEF column (at that time most IEF experiments were run in a vertical column in a sucrose density gradient) and by addition of antioxidants, such as thiodiglycol and ascorbic acid. With the advent of open-face IEF gels, both of these remedies were abandoned as impractical (thiol groups are inhibitors of gel polymerization). However, with the modification proposed here, such remedies can easily be exploited again, as an "empty" IEF gel can be polymerized, washed and dried and can be reswollen in the solvent of choice (including any desired reducing agent).

More recently, when exploring the chemistry of the Immobiline chemicals, we discovered that these buffers also were easily oxidized by persulphate during the polymerization process[20]. In the light of these observations, it became clear that such redox reactions occurred during the IPG run itself and that the IPG matrix was directly responsible for oxidation of Cys residues in proteins[20]. The alkaline Immobilines themselves (oxidized during the polymerization process by persulphate) act as electron acceptors in this redox process. We therefore suggested that, during the IPG run, two reactive Cys residues in a protein would release two protons and two electrons which were captured by an oxygen atom bound to the tertiary amine, thus reducing the latter and forming a molecule of water. If this were the mechanism, it became clear that protection against oxidation should be obtained by direct reduction of the matrix. In fact, washing the matrix in 100 m*M* ascorbic acid, at pH 4.5, afforded full protection against oxidation of Cys residues in proteins[20].

What happens to the four alkaline Immobilines when they are exposed to ammonium persulphate could simply be the addition of oxygen to the tertiary amino group giving amine oxides ($R_3N^+O^-$). It is known that this reaction is facile and usually occurs readily at room temperature in water, alcohol or benzene solvents in presence of even dilute solutions of organic peracids[21]. The mechanism of tertiary amine oxide formation has not been studied in detail but, by analogy with primary amines, the reaction must involve attack by the electrophilic peroxidic oxygen on the amine lone pair, followed by anion elimination and proton loss, according to the following scheme:

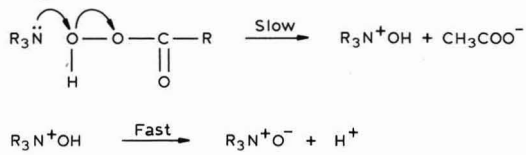

In accord with this conclusion, the reactions are first order with respect to each reactant, and the protonated amine is unreactive.

Some comments remain to be made also about the oxidizing power of carrier ampholytes in conventional IEF. It is clear from the present data (see Fig. 4) that carrier ampholytes have an oxidizing power with respect to Cys residues which is even greater than that exhibited by Immobilines. When using high persulphate levels, in fact, almost all of the α-globin chains exist as oxidized species. We believe that this oxidation could occur on the Cys-104 residue of α-chains, according to the following equilibrium (at pH > 7.5):

$$2\alpha\text{-SH} \rightleftharpoons \alpha\text{-S–S-}\alpha$$

Are there any examples of such phenomena in the literature? Except for the data of Jacobs[18,19] (who, however, never postulated the existence of oxidized carrier ampholytes), not really; however, we can recall here that in the 1970s the Ampholine chemicals (at that time produced only by LKB) had a distinct yellowish colour (especially in the pH range 3.5–5) and produced peaks in the UV region, with maxima around 320 and 368 nm[22]. Moreover, ampholytes synthesized by us in the laboratory exhibited two chromophores in a pH-dependent equilibrium (maxima at 315 and 368 nm, isosbestic point at 335 nm) with an associated protolytic function having an apparent pK of 1.1. We had attributed this pK value to the sixth nitrogen atom in pentaethylenehexamine[23] and had hypothesized oxidation of these amines with the formation of nitrogen heterocyclic structures. Judging from the present results it must have been these species that were responsible for the oxidative phenomena reported by Jacobs[18,19].

A possible explanation for the observed α-chain oxidation is as follows: as the redox potential in reactions involving nitrogen is of the order of +0.5 V, whereas that of similar reactions involving sulphur is of the order of −0.5 V, it is clear that the N-oxides formed on the carrier ampholytes during gel polymerization will act as oxidizing agents, at alkaline pH values, on free –SH groups (possibly even on –S–S– bridges) producing species of higher oxidation level.

As a guideline for future developments in carrier ampholyte chemistry, we believe that Ampholines should be discontinued, as they are more extensively oxidized than Pharmalytes, thus producing larger amounts of oxidized protein bands during the IEF run. In addition, as a disturbing phenomenon, they appear, even in the reduced state, to produce a splitting of the β-chains into two bands (whose origin is not understood), whereas this splitting is never observed with Pharmalyte chemicals.

ACKNOWLEDGEMENTS

This work was supported in part by a grant from Progetto Finalizzato "Biotecnologie e Biosensori", CNR, Rome (P.G.R.) and by a grant from Regione Sardegna (G.C.).

REFERENCES

1 A. B. Bosisio, R. S. Snyder and P. G. Righetti, *J. Chromatogr.*, 209 (1981) 265–272.
2 J. R. Cann, in P. G. Righetti, C. J. Van Oss and J. W. Vanderhoff (Editors), *Electrokinetic Separation Methods*, Elsevier, Amsterdam, 1979, pp. 369–387.
3 E. Galante, T. Caravaggio and P. G. Righetti, *Biochim. Biophys. Acta*, 442 (1976) 309–315.
4 P. G. Righetti and E. Gianazza, *Biochim. Biophys. Acta*, 532 (1978) 137–146.
5 P. G. Righetti, R. P. Brown and A. L. Stone, *Biochim. Biophys. Acta*, 542 (1978) 232–244.
6 E. Gianazza and P. G. Righetti, *Biochim. Biophys. Acta*, 540 (1978) 357–364.
7 P. G. Righetti, E. Gianazza, O. Brenna and E. Galante, *J. Chromatogr.*, 137 (1977) 171–181.
8 E. Gianazza and P. G. Righetti, in B. J. Radola (Editor), *Electrophoresis '79*, Walter de Gruyter, Berlin, 1980, pp. 129–140.
9 H. Rilbe, *Ann. N.Y. Acad. Sci.*, 209 (1973) 11–22.
10 J. R. Cann, *Biochemistry*, 5 (1966) 1108–1112.
11 P. G. Righetti and J. W. Drysdale, *Biochim. Biophys. Acta*, 236 (1971) 17–28.
12 J. B. Clegg, M. A. Naughton and D. J. Weatherall, *J. Mol. Biol.*, 19 (1966) 91–100.
13 P. G. Righetti and J. W. Drysdale, *J. Chromatogr.*, 98 (1974) 271–321.
14 P. G. Righetti, E. Gianazza, A. M. Gianni, P. Comi, B. Giglioni, S. Ottolenghi, C. Secchi and L. Rossi-Bernardi, *J. Biochem. Biophys. Methods*, 1 (1979) 45–57.
15 P. G. Righetti and E. Gianazza, *Methods Biochem. Anal.*, 32 (1987) 215–278.
16 P. G. Righetti, B. Barzaghi, E. Sarubbi, A. Soffientini and G. Cassani, *J. Chromatogr.*, 470 (1989) 337–350.
17 P. G. Righetti, G. Tudor and K. Ek, *J. Chromatogr.*, 220 (1981) 115–194.
18 S. Jacobs, *Protides Biol. Fluids, Proc. Colloq.*, 19 (1971) 499–502.
19 S. Jacobs, *Analyst (London)*, 98 (1973) 25–33.
20 P. G. Righetti, M. Chiari, E. Casale and C. Chiesa, *Applied and Theoretical Electrophoresis*, 1 (1989) 115–121.
21 B. C. Challis and A. R. Butler, in S. Patai (Editor), *The Chemistry of the Amino Group*, Wiley-Interscience, New York, 1975, pp. 326–327.
22 E. Galante, T. Caravaggio and P. G. Righetti, in P. G. Righetti (Editor), *Progress in Isoelectric Focusing and Isotachophoresis*, Elsevier, Amsterdam, 1975, pp. 3–12.
23 P. G. Righetti, M. Pagani and E. Gianazza, *J. Chromatogr.*, 109 (1975) 341–356.

Journal of Chromatography, 475 (1989) 293–309
Elsevier Science Publishers B.V., Amsterdam — Printed in The Netherlands

CHROM. 21 539

PREPARATIVE PROTEIN PURIFICATION IN A MULTI-COMPARTMENT ELECTROLYSER WITH IMMOBILINE MEMBRANES

PIER GIORGIO RIGHETTI*
Department of Biomedical Sciences and Technologies, University of Milano, Via Celoria 2, Milan 20133 (Italy)
ELISABETH WENISCH
Institute of Applied Microbiology, University of Agriculture and Forestry, Peter-Jordan Strasse 82, A-1190 Vienna (Austria)
and
MICHEL FAUPEL
Exploratory Research and Services, Chromatography Laboratory, Pharmaceutical Division, Ciba Geigy Ltd., Basle (Switzerland)
(Received March 23rd, 1989)

SUMMARY

Preparative electrophoresis in gel phases, including isoelectric focusing, is characterized by low load limits (only a few milligrams of protein per millilitre of matrix), low recoveries (rarely exceeding 70%) and heavy contamination from neurotoxic gel material (unreacted monomers and ungrafted oligomers). A multi-compartment electrolyser is described based on the principle of highly buffering Immobiline membranes of well defined isoelectric points (p*I*). Each chamber is delimited by isoelectric membranes having p*I*s encompassing the p*I* value of the components of interest in the mixture to be separated. Such components are transported electrophoretically from chamber to chamber until they collect in the chamber defining their p*I* values. As the sample feed is kept in a number of reservoirs equal to the number of chambers in the electrolysers, at the end of the purification process each reservoir will contain, under ideal conditions, a homogeneous protein fraction. Examples of the purification of r-DNA Eglin C and of monoclonal antibodies are given.

INTRODUCTION

Isoelectric focusing (IEF) in immobilized pH gradients (IPG) was introduced as a method with an extremely high resolving power for protein characterization and analysis[1]. In fact, with a resolving power (Δp*I*, expressed as the p*I* difference between two just resolved proteins) of 0.001 pH unit (compared with Δp*I* = 0.02 in conventional IEF)[2], it was shown to separate easily even neutral mutants bearing no charge difference at the substitution site[3]. Initially, the technique was used only for analysis in narrow pH ranges, but subsequently recipes for wide pH ranges (up to 7 pH units)

0021-9673/89/$03.50

were made available through a computer program developed for this purpose[4]. It was later realized that IPGs coupled a high load ability with their high resolving power[5–7].

However, most preparative techniques in gel phases are bound to fail, as it has been demonstrated that the load ability (in terms of milligrams of protein per millilitre of gel phase) is strongly dependent on the strength of the supporting matrix: only dilute gelatins afford moderately high protein loads. As the %T (grams of total monomers/ml) is increased above 3%, the load ability rapidly decreases as the gel matrix and the protein zone contained therein have to compete for water of hydration[7]. An additional, severe problem is that, when the supporting phase is a polyacrylamide gel, the protein will be eluted heavily contaminated with unreacted monomers and ungrafted oligomers, to such an extent that, at low sample loads, the amount of material recovered is represented mostly by gel contaminants rather than by the applied macromolecule[8]. An exception to this is IEF in granulated gel layers, in which the supporting Sephadex phase can be extensively washed prior to use, and the protein recovered contaminated solely by the soluble amphoteric buffers[9].

Thus, in principle, only free liquid systems could support high protein loads and yield a protein free from gel impurities. In addition to the early, vertical density columns for preparative IEF[10], two systems have been extensively described over the years: (a) multi-compartment electrolysers, as developed by Rilbe's group[11–14], and (b) continuous flow, recycling IEF chambers, as proposed by Bier's group[15–17]. As we are mainly discussing focusing systems, we shall not deal in detail with other preparative systems, such as the continuous flow apparatus of the Hannig type[18] or the Bio stream[19], which work mainly within the framework of zone electrophoretic separations.

Jonsson and Rilbe[14] described a large electrolyser containing 46 separation compartments, having a total volume of 7.6 l and a length of 1 m. The compartments are closed, and internal cooling and stirring are effected by slow rotation of the whole apparatus in a tank filled with cold water. The apparatus is run with an electric load of up to 5 kV, and isoelectric focusing takes 2–3 days. Owing to its very large size and the high cost of the chemicals needed to operate it, this instrument has never become popular. At the opposite extreme, Egen *et al.*[17] developed a small-scale apparatus, available commercially under the trade-name Rotofor (Bio-Rad Labs.), which is a compact, 20-compartment electrolyser, cooled by a central cold finger and also rotating on its axis for zone stabilization (this principle of stabilization of zones by rotating the chamber on its axis was a remarkable achievement of Hjertèn well before the Space Shuttle became available for elimination of gravitational effects in free zone electrophoresis)[20].

Ideally, such multi-compartment electrolysers should contain membranes that are chemically and mechanically resistant, flow-tight, free of electroosmosis and thin. Flow-tight membranes are desirable because (a) they prevent convective remixing of the contents of adjoining compartments during fractionation due to differences in density, (b) they prevent liquid flow forwards and backwards through the electrolyser caused by uneven pressure (*e.g.*, as generated by electrode gases) and (c) they facilitate loading and emptying of the electrolyser. In practice, owing to inherent difficulties with the membrane technology available at the time, neither Rilbe's nor Bier's electrolysers contained flow-tight membranes. In the former instance, a porous poly-

(vinyl chloride) paper membrane was adopted, and in the Rotofor the membrane was simply a nylon net.

In 1987, in a series of papers[21–24], we reported a new technique, called "segmented immobilized pH gradients", with which we opened a "window" in an IPG gel, designed to keep isoelectric in a liquid stream a major component of a mixture under purification. Only the impurities were focused in the lateral gel phases delimiting the "window", whereas the component of interest was kept isoelectric at all times during the focusing process in the initial sample feed, which was continuously recycled orthogonally to the electric field. As originally described, the sample flow cell was flanked by two segments of an immobilized pH gradient; subsequently, these two IPG segments were reduced to membranes of well defined p*I* values, able to buffer and titrate a single protein to its p*I*, while allowing all other impurities to migrate through and simply be lost in the electrodic compartments[25].

We have now realized that such a mono-compartment electrolyser is not ideally suited in practice, as researchers often have a need to isolate and characterize more than just a single fraction in their preparations. We therefore describe here a multi-compartment electrolyser based on the principle of Immobiline membranes. As the unique feature of such a system is the Immobiline membrane technology, in that such membranes possess a buffering power, an extremely well defined p*I* value and are able to quench electroosmosis[26], we shall give here guidelines on the successful preparation and characterization of such membranes.

EXPERIMENTAL

Materials

Repel- and Bind-Silane, Gel Bond PAG, the Multiphor 2 chamber, Multitemp thermostat and Macrodrive power supply were from LKB (Bromma, Sweden), Pharmalyte and Ampholyte buffers and the protein p*I* marker kit were purchased from Pharmacia (Uppsala, Sweden), the multi-channel peristaltic pump was from Ismatec (Zurich, Switzerland), the glass microfibre filters (GF/D) were purchased from Whatman (Clifton, NJ, U.S.A.) and light paraffin oil (Art. 7160) from Merck (Darmstadt, F.R.G.). Acrylamide, N,N′-methylenebisacrylamide (Bis), N,N,N′,N′-tetramethylethylenediamine (TEMED), ammonium persulphate and Coomassie Brilliant Blue R-250 were from Bio-Rad Labs. (Richmond, CA, U.S.A.), dithiothreitol (DTT) and urea from Merck and r-DNA N-acetyl Eglin C (*ca.* 90% pure) from Ciba Geigy (Basle, Switzerland). Monoclonal antibodies against the gp41 from AIDS virus were prepared and purified by Jungbauer *et al.*[27].

Analytical IPGs

To follow the progress of the purification of monoclonal antibodies, analytical IPG gels in the pH range 8.5–10 were made according to Gelfi *et al.*[28]. The samples were loaded in pockets precast at the anodic side in a pH 8.5 plateau gel segment (2 cm long). About 40 μl, with up to 50 μg of protein, were loaded and focusing was continued for 25 000 V h as described by Sinha and Righetti[29]. The gels were stained with Coomassie Brilliant Blue R-250 in Cu^{2+}.

Analytical IEF

For monitoring the purification of Eglin C, Ampholine PAG plates in the pH range 3.5–9.5 (4%T, 3%C, 2.2% Ampholine concentration) were used. A total of 200 μg of protein was applied (in volumes up to 20 μl, at the anodic side) and then focusing was performed at 10 W limiting, 10 mA and 1000 V at equilibrium (at 10°C). The analytical runs were usually terminated within 2 h and then the gels were stained with Coomassie Brilliant Blue R-250 in Cu^{2+}.

Description of the apparatus

Basically, the multi-compartment electrolyser consists of a stack of chambers sandwiched between an anodic and a cathodic reservoir. Fig. 1 shows one of these chambers, provided with two inlets and outlets for sample recycling, an O-ring for ensuring flow-tight connections and four holes for threading four long metal rods which can be tightened by hand-driven butterfly nuts for assembling the apparatus. We have built several versions of these cells, capable of housing Immobiline mem-

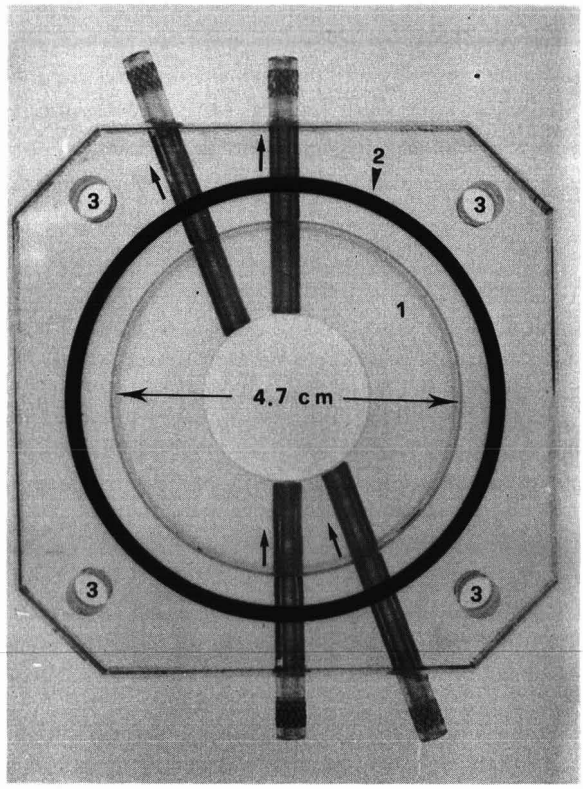

Fig. 1. A chamber of the multi-compartment electrolyser. A Perspex square of dimensions 7.5 cm with a central depression of 4.7 cm is used for housing the Immobiline membrane sandwiched between two flat caoutchouc rings of 1.2 cm width. 1 = Membrane housing; 2 = O-ring for a flow-tight connection when assembling the entire apparatus; 3 = four holes for threading four metal rods used to hold together the electrolyser. The arrows indicate inlets and outlets for sample flow. All chambers, including the electrodic reservoirs, have identical cross-section and hold equal volumes (5 ml).

branes from 4.7 cm (the present apparatus) up to 9 cm in diameter. The pH-controlling membranes are housed in the central depression between two 1-cm-wide rings of caoutchouc. After assembling and tightening the apparatus, each compartment is flow-tight, so that no net liquid bulk flow ensues (except, when applicable, as generated by electroosmosis).

Fig. 2 shows one of the terminal parts of the electrolyser, housing the platinum wire bathed by the electrolyte solution. This rests on a rectangular Perspex mounting, which will act as one of the legs of the electrolyser, once the entire stack of cells is assembled (see Fig. 3). The distance between adjacent cells is only 10 mm, so that each chamber holds *ca.* 5 ml of liquid. Fig. 3 shows the entire assembled apparatus; in this particular experiment, four fractions were collected, so that the electrolyser is built with a stack of six cells, the two extreme ones acting as anodic and cathodic chambers. All solutions, including anolyte and catholyte, are continuously recycled from larger reservoirs. Two additional chambers, not needed in this experiment, are shown assembled outside the electric field, to the left of the apparatus. Two of the four metal

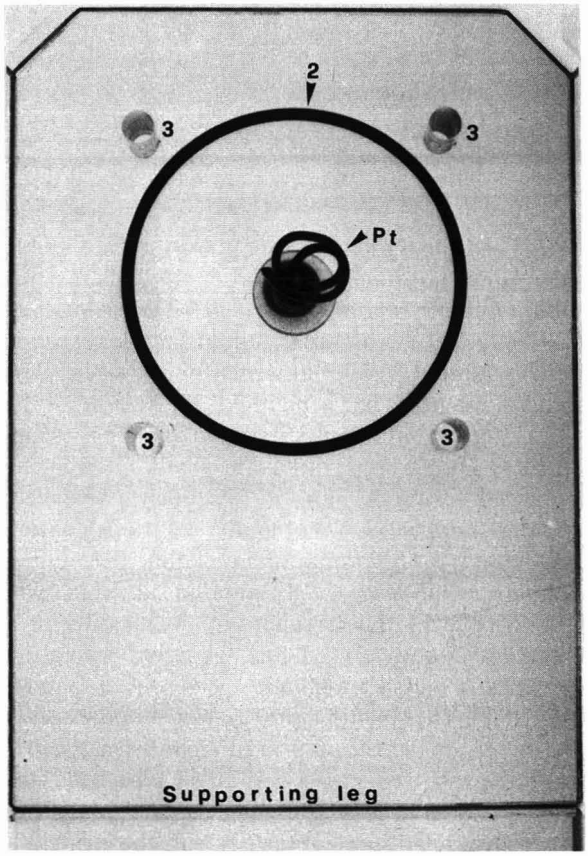

Fig. 2. Terminal part of the electrolyser and electrode support. The platinum wire is mounted on a rectangular (10 × 14 cm) Perspex slab which also acts as one of the two legs supporting the apparatus (see Fig. 3). When piling the different chambers on it (see Fig. 3), the first one will become the electrode reservoir. Numbers as in Fig. 1.

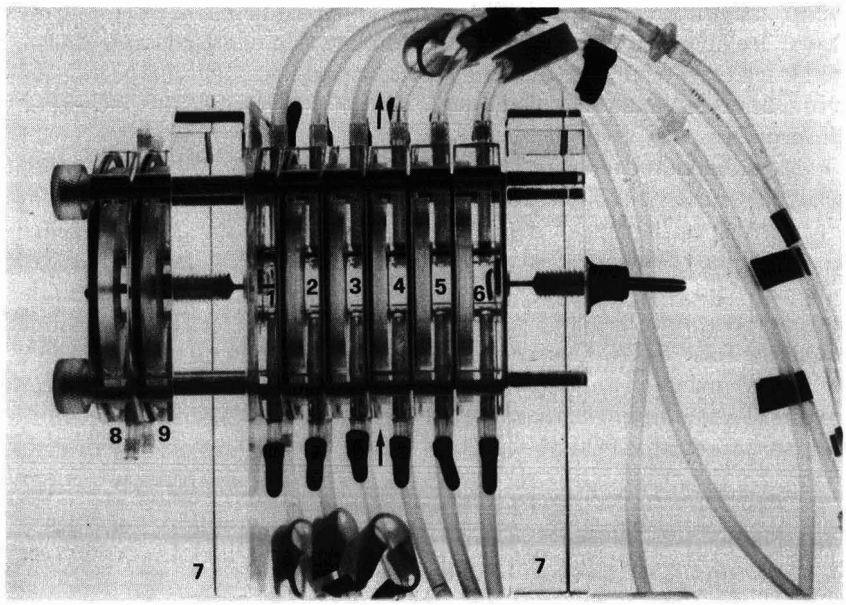

Fig. 3. View of the mounted multi-chamber electrolyser. 1, 6 = Electrode compartments; 2–5, 8, 9 = sample flow chambers (two, not in use, are mounted outside); 7 = electrode mounting units and supporting legs. The arrows indicate sample and electrolyte flow.

rods (with two nuts), needed for assembling and tightening the electrolyser, are visible in front of the apparatus. Inlets and outlets not in use are stoppered by black caps.

Fig. 4 shows one of the sample reservoirs that we have built. They consist of three-necked flasks, bearing holes in the lateral caps for insertion of sample recycling tubing. The one shown in Fig. 4 holds a total of 25 ml, but vessels of any size can be built according to experimental needs. A magnetic bar is placed at the bottom of the vessel for keeping the solutions under gentle, continuous stirring to avoid electrode-cantation. An important feature of these sample reservoirs is the small outlet at the bottom of the vessel. This is kept plugged during the run, but it is opened to collect the sample at the end of the run, so as to avoid collection of lighter solutions floating on the liquid surface during the run. In fact, for fractionation in alkaline pH ranges, the sample liquid surface is flooded with a thin film of light paraffin oil, which will prevent adsorption of carbon dioxide (which will ruin the separation by introducing a new "Immobiline", carbonate, with pK 10.5 and 6.3)[30]. Thus, when harvesting the sample from the bottom outlet, the paraffin oil is left behind.

Fig. 5 shows the operational assembly (not including the power supply): to the left is the multi-compartment electrolyser, in the centre a multi-channel peristaltic pump and to the right the sample and electrolyte reservoirs resting on a large-surface magnetic stirrer. As very little joule heating is generated during the run in an IPG gradient we find it adequate, for proper temperature control, to run the entire assembly in a cold room. At a standard temperature of 4–5°C in a cold room, the solutions during the run will be prevalently at 8–9°C. Once assembled, the apparatus can be run for long periods without any damage to the membranes or any leakage. We have performed runs continuously for up to 10 days.

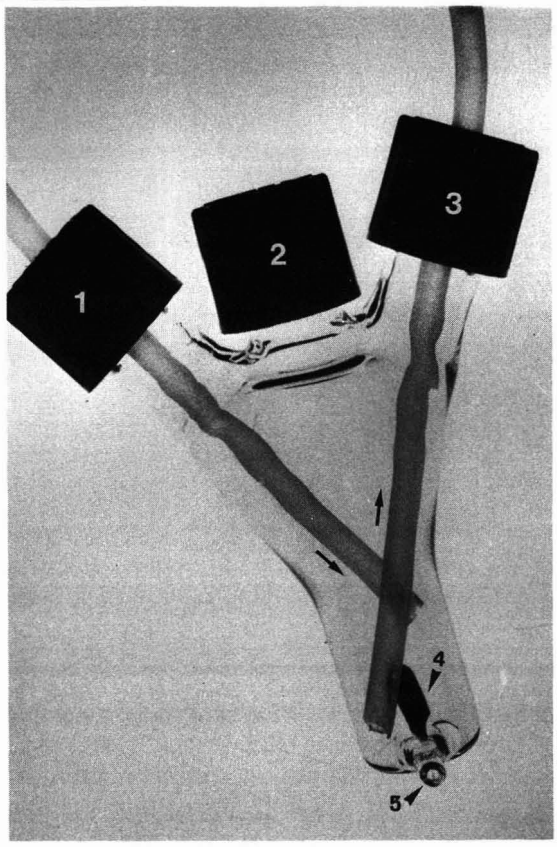

Fig. 4. Sample flow chamber. 1, 3 = Inlet and outlet for sample flow; 2 = opening for sampling; 4 = magnetic bar; 5 = bottom outlet for collecting paraffin-oil-protected liquid. The tubes are secured in place via a hole in the stoppers.

Membrane preparation

This is perhaps the most delicate part of the entire apparatus. The real novelty of this instrument is the concept of isoelectric, highly buffering Immobiline membranes. Hence the separation will only be as good as the membranes that have been prepared and will act by buffering and keeping isoelectric any desired protein within each chamber of the electrolyser. The membranes *per se* are made with the Immobiline technology, *i.e.*, by mixing neutral monomers (acrylamide and Bis) and charged species (the weak acids and bases constituting the Immobiline family; we have recently described the properties of nine such chemicals, plus two strong titrants)[31,32], in such ratios as to define unequivocally a given pH value in the entire membrane. This pH value will be the isoelectric point of the membrane, which, by virtue of its considerable buffering power, will be able to titrate macroions in contact with it. There is only one safe way to define the desired p*I* of a set of membranes: it consists in running an analytical IPG gel containing exactly the amount and types of Immobiline chemicals which will later be utilized in the preparative run. If any additives are needed to keep the protein in solution (*e.g.*, glycerol, neutral or zwitterionic detergents, urea),

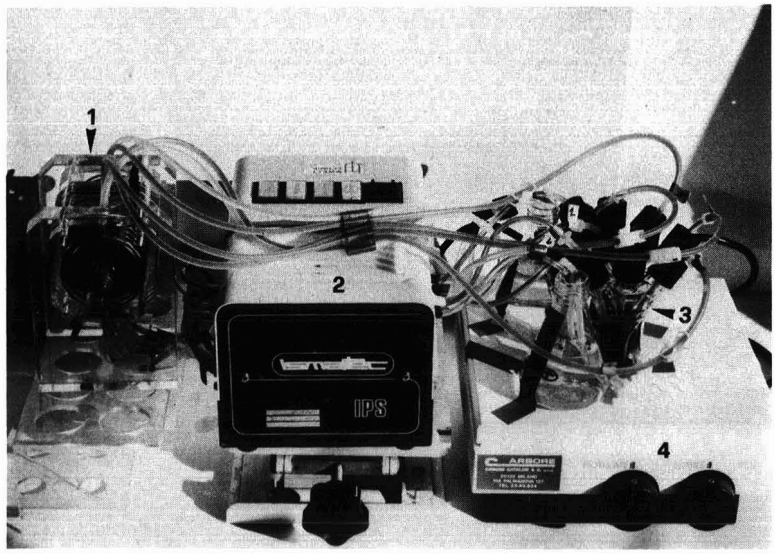

Fig. 5. View of the experimental assembly. 1 = Multi-chamber electrolyser; 2 = multi-channel peristaltic pump; 3 = block of sample flow chambers; 4 = magnetic stirrer (power supply not shown).

they should also be present in the analytical IPG run. After focusing and on staining the gel, the positions of the bands of interest will be noted and their p*I* values measured accurately by linear interpolation of the pH value along the gel matrix. pH points will then be selected just above and below the p*I* of the protein of interest, in such a way as to exclude the p*I* values of the nearest contaminants. These pH points (or values) will then be used to calculate the composition of the anodic and cathodic membranes (in terms of molarity of buffering and titrant Immobilines) needed to keep isoelectric that particular protein band. This calculation will be repeated for any other band of interest whose purification is sought (as an example of such an interpolation, see Fig. 11 in ref. 33).

Such polyacrylamide membranes are not self-supporting, and would tear apart during the run. We have investigated a number of fabrics for buttressing the buffering, isoelectric gel stratum (see also Wenger *et al.*[26]). We have found the best candidate to be glass microfibre filters from Whatman (see also Discussion). A housing is machined in a Perspex block, just 1 mm deep and having the same diameter as that of the membrane (see Fig. 6A). This housing is filled with the gelling solution having a given p*I* value and then the glass filter is gently lowered on to it, so that it will absorb the liquid from its lower face while expelling any trapped air from its upper surface. After placing the filter in position, the chamber is closed with a 3-mm thick glass and the assembled polymerization cell (see Fig. 6B) is placed in a forced-ventilation oven for a 1-h polymerization cycle at 50°C. After gelling, the chamber is gently pried open, any excess gel trimmed from the filter perimeter with a surgical blade and the membrane subjected to several washing cycles in distilled water until all unpolymerized material and catalysts have been removed. As the total membrane thickness (gel phase and glass filter) is barely 1 mm, ten washing cycles (each 1 h long) are

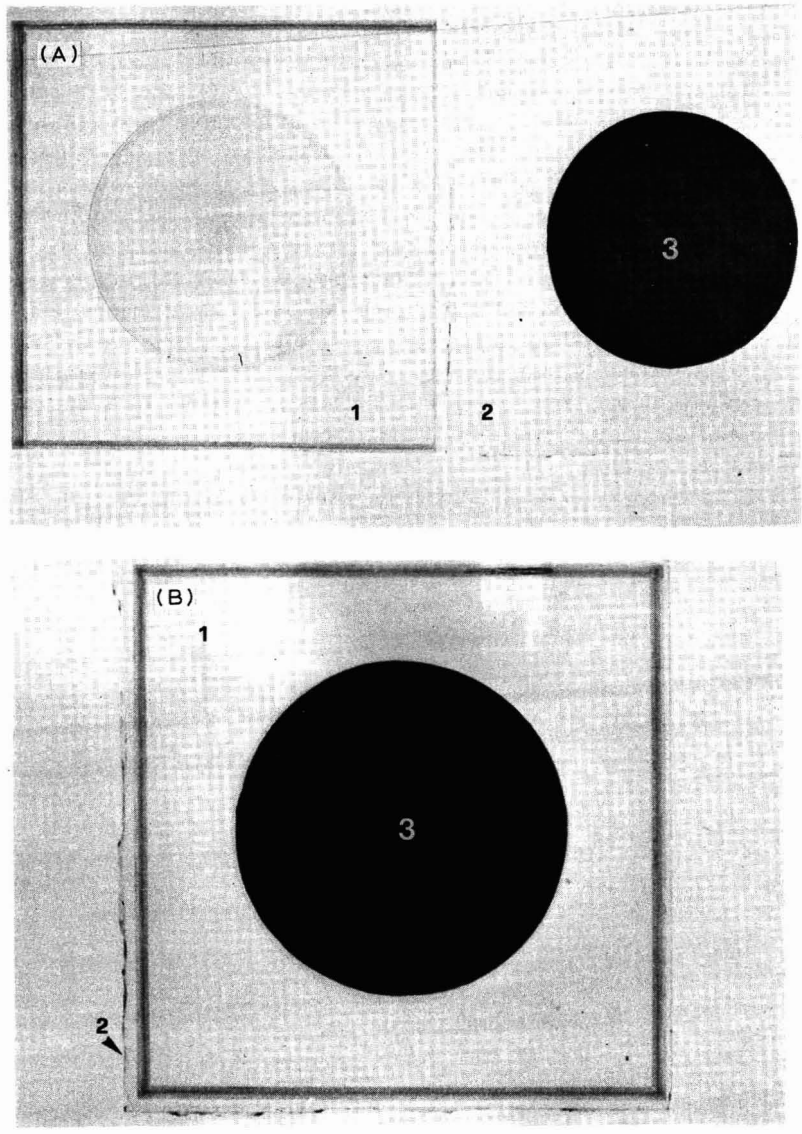

Fig. 6. Membrane polymerization cassette. (A) A Perspex block (7.5 × 7.5 cm) is machined to accommodate a central, circular housing (1 mm deep) of 4.7 cm diameter (1); 2 = cover-glass; 3 = Whatman GF/D glass microfibre filter. (B) Assembled cassette during Immobiline membrane polymerization.

sufficient to ensure virtually complete elimination of unpolymerized material (no free acrylamide could be detected in the washings down to the femtomole level).

RESULTS

Purification of N-acetyl Eglin C

This protein was produced in *E. coli* by recombinant DNA (r-DNA) techniques at Ciba Geigy[36] and was *ca.* 90% pure when given to us to be treated in the multi-

compartment electrolyser. This was a special purification problem because, by analytical IEF, we had seen that some contaminants had ΔpI values of *ca.* 0.01 pH unit. Therefore, in order to ensure complete elimination of these impurities, the pI of Eglin C was measured in several runs (pI = 5.5 ± 0.01) and both the anodic and cathodic membranes were made so as to define a pH = 5.5. Thus, whereas in most IPG runs we work under the condition $pI_{am} < pI_p < pI_{cm}$, here we have defined the most stringent restraint, $pI_{am} = pI_p = pI_{cm}$, where the subscripts am, p and cm denote anodic membrane, protein and cathodic membrane, respectively. In this instance, we used a large apparatus with a membrane diameter of 9 cm and with only one sample flow chamber, as we had no interest in collecting the anodic and cathodic impurities. A 5-g amount of Eglin C, dissolved in 250 ml of "Baker" water, was recycled in the electrolyser at a constant 12 W in a cold room. At hourly intervals, 100 μl were sampled and kept at 4°C for subsequent analysis. The experiment was terminated with the last sampling after 5 h and the aliquots were analysed in a pH 3.5–9.5 Ampholine PAG plate. As shown in Fig. 7A, all impurities having pI values $\geqslant$ 0.01 pH unit on either side of the pI 5.5 value of Eglin C were completely removed. Considering that, during

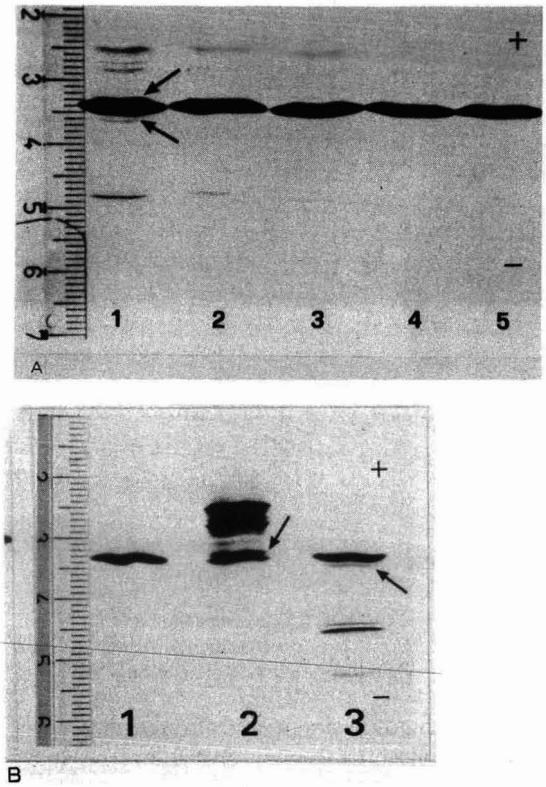

Fig. 7. Purification of N-acetyl Eglin C. A 5-g amount of Eglin C (in 250 ml of distilled water) was recycled in a single-chamber apparatus (9 cm diameter) at 12 W, 10°C for 5 h. (A) Analytical CA-IEF gel (pH 3.5–9.5) of 200 μg of protein at (1) time zero (control); (2) 1 h; (3) 2 h; (4) 4 h; (5) 5 h of recycling. (B) Analytical CA-IEF gel of (1) 5-h aliquot, (2) anodic chamber content and (3) cathodic chamber content (the last two samples representing 500-μl aliquots dialysed and lyophilized). The arrows indicate one anodic and one cathodic contaminant with a ΔpI of only 0.01 pH unit removed from Eglin C.

this time period, a total of 5 g of Eglin C were treated, this amounts to a processing rate of 1 g/h of protein, a load ability rarely reported, if at all, in any electrokinetic process ever described.

It might be asked what the mass recovery of Eglin C is, considering that the two boundaries had the same p*I* as the protein under purification. By protein and biological assay, it was found that the amount recovered in the sample flow chamber was 4.750 g, *i.e.*, 95% of the total initial mass input. Aliquots of the anodic and cathodic electrolytes were also collected, dialysed, liophylized and then analysed by analytical IEF. As shown in Fig. 7B, some Eglin C was lost in the two electrolyte reservoirs; most important, it can be shown (see the two arrows) that the two anodic and cathodic impurities (having a Δp*I* of *ca.* 0.01) originally present in the Eglin C preparation have now been completely removed and have leached out in the electrolyte compartments.

Purification of human monoclonal antibody isoproteins

Human monoclonal antibodies, made in a hybridoma cell line, against the transmembrane protein gp41 from the immunodeficiency virus (HIV-1) were prepared by Jungbauer *et al.*[27]. By analytical IPGs, they were found to consist of a family of at least six isoproteins, three major and three minor (see Fig. 8A, last two tracks to the left), with p*I*s of 8.93, 9.04 and 9.18 (the three major) and 8.84, 9.40 and 9.60 (the three minor). This was a challenging separation, as it is known that focusing in alkaline pH ranges, both in CA-IEF and IPGs, is besieged with problems (carbon dioxide absorption, electroosmosis, potential hydrolysis of both the matrix and the Immobiline chemicals). We assembled the apparatus in Fig. 3 with six chambers, the two extreme ones for electrolyte solutions and four sample chambers, delimited by five membranes having isoelectric points of 8.87, 8.98, 9.11, 9.29 and 9.50. A 200-mg amount of protein dissolved in 80 ml of 25% glycerol and 0.5% Tween 20 was recycled for a total of 75 000 V h. The content of each chamber was then analysed by analytical IPGs in the pH range 8.5–10. As seen in Fig. 8A, there is clearly an enrichment of the various isoforms in the different chambers, but not a single homogeneous fraction. The content of chamber 4 was then used in a "cascade" fashion and re-run in the multi-chamber apparatus. As shown in Fig. 8B, fraction 3 now contains an almost pure component. Work on the purification to homogeneity of these monoclonal antibodies will be reported elsewhere.

DISCUSSION

Membrane preparation

The most delicate aspect of multi-compartment electrolysers utilizing isoelectric Immobiline membranes is the production and quality control of such membranes. We shall therefore describe in details the manipulations involved. An extensive study was first made of the properties of different support materials. When first described, Wenger *et al.*[26] had already tried a number of porous sheets, including polyethylene, polypropylene, nylon nets and cotton fabrics. We finally adopted GF/D glass microfibre filters from Whatman, as they appear to be the best supports for isoelectric Immobiline gels in preparative protein purification. First, they are highly resistant to chemical attack (except by hydrofluoric acid and strong alkalis). Resistance to all

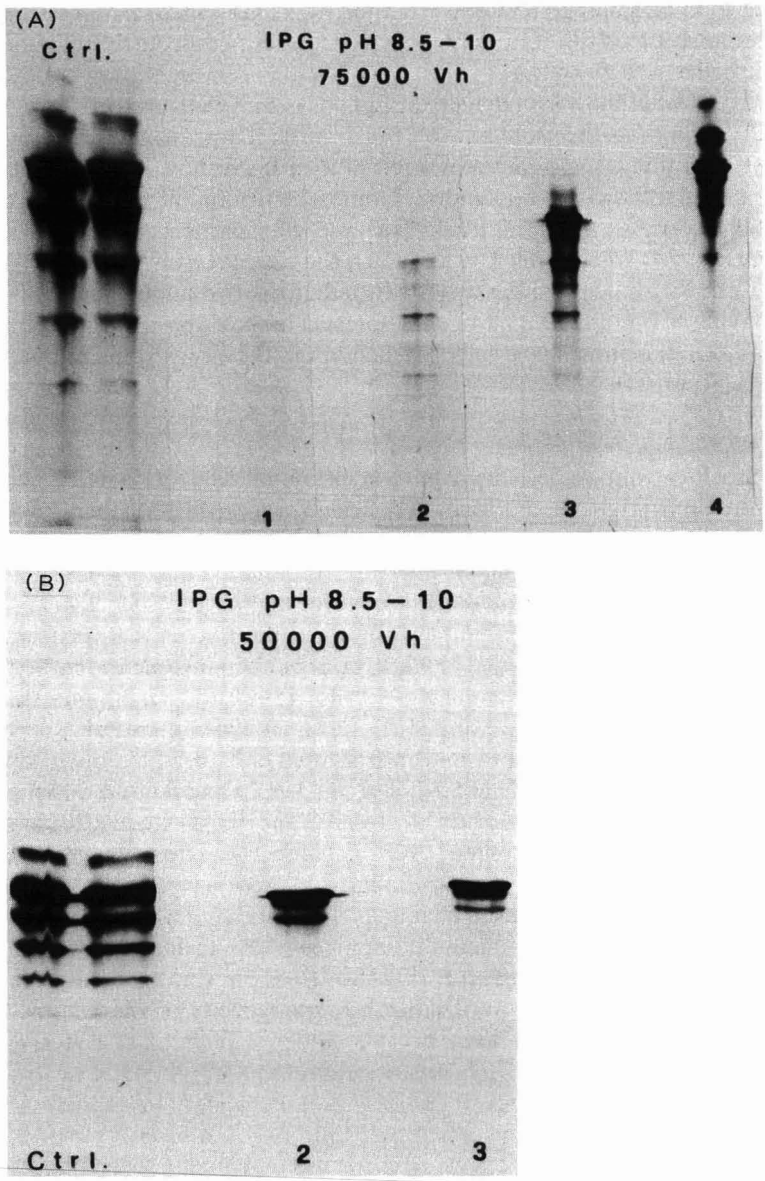

Fig. 8. Purification of human monoclonal antibodies. A 200-mg amount of total antibodies (in a total volume of 80 ml) was purified in an electrolyser with four sample chambers mounted. (A) Ctrl. = starting material; 1–4 = 30-μl aliquots from chambers 1–4, respectively. Sampling taken after 75 000 V h and analysed in an IPG pH 8.5–10 gel. Anodic sample application; Coomassie Brilliant Blue R-250 staining. The cathode is uppermost. (B) The content of chamber 4 in A (50 mg total protein) was distributed over four chambers and re-run for 50 000 V h. Ctrl. = unfractionated, starting material; 2, 3 = aliquots from chambers 2 and 3 of the electrolyser. Even though the fractions are still not homogeneous, note the extensive purification achieved.

other acids is excellent up to 5 *M* concentration. In addition, glass microfibres do not swell in organic solvents or water and do not leach out impurities, as they do not contain any binders. Because of its fine capillary structure, a glass microfibre filter will absorb larger volumes of liquids than cellulose papers of equivalent weight. This is important for the production of Immobiline membranes, as it ensures that more gel volume will be held within the glass fibres, thus allowing a higher buffering capacity of the membrane per unit weight. In addition, Immobiline gels have a very strong adhesivity to glass surfaces, this guaranteeing that no detachment between the gel phase and the glass support will occur. In fact, even on prolonged use (more than 10 days at pH > 9) we have never experienced problems of membrane destruction or even perforation. The glass microfibre filters have remarkable tear strength and burst strength, which probably result from the very large number of weak bonds between the hydrated silica surface of adjacent fibres. Being composed of glass, these filters are virtually non-ageing material and are not subject to weakening and embrittlement even for extreme periods of storage. The composition of borosilicate glass fibres, as given by the manufacturer, is SiO_2 57.9%, B_2O_3 10.7%, Al_2O_3 5.9%, Na_2O 10.1%, K_2O 2.9%, CaO 2.6%, MgO 0.4%, BaO 5.0%, ZnO 3.9% and F 0.6%. The content of leachable material is negligible except for sodium (1710 ppm extracted at 27°C for 24 h).

Membrane composition and storage

For most applications, a 5%T matrix seems to be adequate; it is porous enough to allow transmembrane migration of most proteins (at least up to 200 kDa), yet robust enough to prevent undesirable swelling of the gel due to the content of charged species. In terms of Immobiline content, we prefer to use *ca.* 20 m*M* buffering ion (plus the amount of titrant needed to define the desired p*I* value); under these conditions, and according to the relative p*I* − pK value, the membranes will have a β power ranging from 6 to 10 mequiv. l^{-1} pH^{-1}, which is more than adequate to buffer any amount of protein tangent to the membrane or crossing it. In particular instances up to 50 m*M* buffering ion can be used, but it should be remembered that at high Immobiline molarities there will be two major problems: (a) the gel matrix could swell to the point of bursting and (b) the resulting p*I* value could be erratic because, at high concentrations, the p*K* values in the Immobiline membrane could change.

In the separation of immunoglobulins, we have adopted additional strategies: the membrane was made to contain 5%T, but the amount of cross-linker was increased to 8%C (from a standard value in all gels of 4%C); the higher %C renders the membrane more porous, thus facilitating the transmigration of large proteins, and also tends to reduce swelling of the gel phase, which is more pronounced in alkaline pH ranges. In addition, the two lateral membranes in contact with the electrode solution were made even more robust (10%T), again to prevent swelling due to different osmotic pressures generated by pH and conductivity steps at the separation chamber/electrolyte boundaries. When making alkaline membranes, there could be the problem of how long to store them; if not utilized immediately, the membranes can be stored for at least 3 weeks in 20 m*M* acetate buffer (pH 5). It is known that mildly acidic pH values ensure maximum stability of all Immobiline chemicals[34]. Then, just prior to use, they are extensively washed in distilled water (or in any additive needed for the separation).

When casting the membranes, the following precautions should be taken: (a) coat the cover-glass extensively with Repel-silane so that, on opening the cassette, the Immobiline membrane will not adhere to it, with the risk of tearing the gel phase; (b) avoid trapping air bubbles; even when minute, air bubbles embedded in the filter can swell during the run and bore holes in the membrane; (c) degas the gelling solution (conventional IPG gels are not degassed, but here it is essential) and prepare enough of it so that it slightly overflows when poured into the polymerization chamber (see Fig. 6). An excess of gelling solution will reduce the risk of trapping air bubbles when lowering the glass cover into the chamber to seal it against atmospheric oxygen.

Running the electrolyser

Some precautions should be taken here also. In alkaline pH ranges, avoidance of carbon dioxide absorption is essential. If not properly shielded, the apparatus will act as a carbon dioxide trap, with a continuous background of HCO_3^- ions migrating from the cathode through the intermediate sample chambers to the anode, where they would be discharged back in the atmosphere at pH < 6. To prevent this phenomenon, we float light paraffin oil (density = 0.88) on the surface of the liquid pumped in each chamber (including catholyte and, when necessary, also anolyte). For this reason, we have made special sample reservoirs containing an outlet at the bottom (see Fig. 4), so that at the end of the experiment the sample can be collected from this outlet while leaving the paraffin oil behind. In alkaline pH ranges, we have found it to be important, for correct maintenance of pH in each chamber, to have electrode solutions with pH values approaching as close as possible the pH range in which fractionation takes place. For this reason, we have used as the anolyte a 1 m*M* solution of HEPES + pH 8.5–10 carrier ampholytes to pH 6.8 and as the catholyte a 0.1 m*M* solution of sodium hydroxide (pH 10). Alternatively, isoelectric Lys (pH 9.8) could be used. In general, dilute acids and bases should be used in the electrode compartments, *e.g.*, in the Eglin C run, 1 m*M* acetic acid and 1 m*M* sodium hydroxide solution were used as anolyte and catholyte, respectively.

Sample pretreatment

For optimum performance, the way in which the sample is treated before the IPG run is important. We had already demonstrated[23] that, in IPG runs, any amount of salt present in the sample is deleterious to the fractionation process. In particular, salts made from strong acids and bases should be avoided (*e.g.*, sodium chloride, but also a phosphate buffer) because, on passage of the current, the anions and cations present therein produce strongly acidic and basic boundaries which can rapidly denature proteins by a pH shock[35]. Thus, ideally, an already desalted sample zone should be preferentially used as the initial feed. If that is not possible, the sample should be equilibrated in buffers formed from weak acids and bases (*e.g.*, Tris–acetate will be acceptable, but Tris–HCl will not), or if strong species are present, additional weak counter ions should be added (typically carrier ampholytes, able to buffer in the transient state any strong anion or cation migrating out of the sample zone). In any event, the amount of salts present in the initial sample feed should be kept to a minimum, as the macroions will not be able to migrate until all the small ions have vacated the sample zone[23,35].

From this point of view, it is of interest to note the effect of carrier ampholytes

(CA) on the progress of separation. At least in alkaline pH ranges, and with immunoglobulins, we have noted that, rather than helping the separation, CA chemicals are in fact detrimental. They seem to induce a strong electroosmotic flow and in addition they could bind to the macroions, thus altering their p*I* values. In our early experiments, when the immunoglobulins were fractionated in the presence of small amounts of CAs, we had to recalculate the p*I* values of the different membranes, as the proteins had altered their apparent p*I* values and were focusing in the wrong chambers. There is definitely an effect of CAs on the p*I* values of alkaline proteins, which usually results in a lowering of the apparent p*I* of the protein, as measured in an IPG gel in the absence of CAs. The Δp*I* in presence or absence of CAs is, in our case, as much as 0.2 pH unit, but it could be even higher. Given the small differences in isoelectric points in the various immunoglobulin fractions, such p*I* alterations are deleterious to the fractionation process. Thus, we have recently come to the conclusions that, whenever possible, addition of CA buffers should be avoided altogether. If the protein input is high enough (concentrations of the order of 10 mg ml^{-1}), the macroions will act as buffering species, so that no extra buffers need to be added to the liquid phase for pH control; the isoelectric protein will take care of this. For example, we had calculated that, at a concentration of 10 mg ml^{-1}, and at pH = p*I*, human haemoglobin as a β power = 1 μequiv. l^{-1} pH^{-1}, which, albeit low, is adequate to ensure pH control in the absence of small ions moving through the system[6].

It is in general believed that an isoionic protein would have a very low solubility. However, in most instances, this solubility is high enough to avoid protein precipitation. So far we have not experienced any isoelectric protein precipitation in our membrane apparatus. Often, slightly changing the composition of the liquid phase is sufficient to keep the protein in solution. For example, in the case of immunoglobulin fractionation, the proteins are fully soluble, even at high concentrations, in the presence of 25% glycerol and small amounts of neutral detergent (0.5% Tween 20). In some instances, though, addition of urea might be needed. It is true that, in conventional IEF, severe protein precipitation has often been observed (for a review, see Righetti[2]). However, on close scrutiny, we can observe that in those instances the initial sample input consisted of a highly unpurified protein mixture. In any focusing system, in the absence of buffer or salt ions, acidic and basic proteins present initially will tend to form aggregates which will neutralize each other and induce massive precipitation. In our system (and we believe as a general rule in electrokinetic separations), the input protein should already be at an advanced stage of purification (it should be at least 50% pure, preferably 70–80%). Under these conditions, risks of precipitation with unlike proteins will be minimized.

Electrical conditions

The speed of the separation process will depend on, among other factors, the voltage applied and the lateral cross-sectional area of the membrane (see the mass transport equation in ref. 25). Because, for any multi-compartment electrolyser built, the geometry is fixed, given a constant membrane surface area, the other way to speed up the purification process will be to increase the voltage gradient over the separation chamber. At the beginning, in the "segmented IPG" technology utilizing pH gradients on both sides of the flow chamber, we were limited, by the joule heat that developed and by the need to perform the run in the presence of CAs, to barely 50 V

cm^{-1}. In the present membrane apparatus, and in the absence of foreign ions except the protein macroions, considerably higher voltage gradients can be applied. For example, in the purification of monoclonal antibodies, when the sample feed was devoid of salts and carrier ampholytes were not added, once residual traces of ions had been removed in an initial low-voltage run (100–150 V cm^{-1}), much higher voltages could be applied (up to 800 V/cm). Even at such high voltages, the total wattage did not exceed 5 W, and the temperature rise in the liquid compartment, simply by air cooling in a cold room, was barely 4–5°C above the standard cold-room temperature of 4–5°C. However, salt-containing samples should be run initially at low voltage gradients until the ion boundaries have been eliminated, otherwise two undesirable phenomena will occur: (a) thermal sample denaturation due to joule heat and (b) pH denaturation due to the formation of strongly acidic and basic ion boundaries[35].

CONCLUSIONS

We have accumulated 2 years of experience first with the "segmented IPG" principle and now with multi-compartment electrolysers exploiting isoelectric Immobiline membranes. We are confident that this could become one of the leading techniques in the near future for purifying r-DNA proteins to homogeneity and we hope that these experimental observations will serve as guidelines for scientists eager to exploit this novel technique. We emphasize that, so far, IPGs appear to be the only technique coupling an extremely high load capacity with an extremely high resolving power, which is not lost in the scaling-up process.

ACKNOWLEDGEMENTS

This work was supported in part by a grant from Progetto Finalizzato Biotecnologie e Biosensori, Consiglio Nazionale delle Ricerche, Rome, Italy. E.W. is on leave of absence from the University of Agriculture and Forestry, Vienna, Austria.

REFERENCES

1 B. Bjellqvist, K. Ek, P. G. Righetti, E. Gianazza, A. Görg, R. Westermeier and W. Postel, *J. Biochem. Biophys. Methods*, 6 (1982) 317–339.
2 P. G. Righetti, *Isoelectric Focusing: Theory, Methodology and Applications*, Elsevier, Amsterdam, 1983.
3 G. Cossu and P. G. Righetti, *J. Chromatogr.*, 398 (1987) 211–216.
4 P. G. Righetti and E. Gianazza, *Methods Biochem. Anal.*, 32 (187) 215–278.
5 K. Ek, B. Bjellqvist and P.G. Righetti, *J. Biochem. Biophys. Methods*, 8 (1983) 134–155.
6 C. Gelfi and P.G. Righetti, *J. Biochem. Biophys. Methods*, 8 (1983) 157–172.
7 P. G. Righetti and C. Gelfi, *J. Biochem. Biophys. Methods*, 9 (1984) 103–119.
8 P. G. Righetti, K. Ek and B. Bjellqvist, *J. Chromatogr.*, 291 (1984) 31–42.
9 B. J. Radola, *Ann. N.Y. Acad. Sci.*, 209 (1973) 127–143.
10 O. Vesterberg, T. Wadström, K. Vesterberg, H. Svensson and B. Malmgren, *Biochim. Biophys. Acta*, 133 (1967) 435–445.
11 H. Rilbe, *Protides Biol. Fluids*, Proc. Colloq., 17 (1970) 369–372.
12 H. Rilbe, *Ann. N.Y. Acad. Sci.*, 209 (1973) 80–93.
13 H. Rilbe, A. Forcheimer, S. Pettersson and M. Jonsson, in P. G. Righetti (Editor), *Progress in Isoelectric Focusing and Isotachophoresis*, Elsevier, Amsterdam, 1975, pp. 51–63.
14 M. Jonsson and H. Rilbe, *Electrophoresis*, 1 (1980) 3–14.

15 M. Bier and N.B. Egen, in H. Haglund, J. C. Westerfield and J. T. Ball, Jr. (Editors), *Electrofucus/78*, Elsevier, Amsterdam, 1979, pp. 35–48.
16 M. Bier, N. B. Egen, T. T. Allgyer, G. E. Twitty and R. A. Mosher, in E. Gross and J. Meienhofer (Editors), *Peptides: Structure and Biological Function*, Pierce, Rockford Il, 1979, pp. 79–89.
17 N. B. Egen, W. Thormann, G. E. Twitty and M. Bier, in H. Hirai (Editor), *Electrophoresis '83*, Walter de Gruyter, Berlin, 1984, pp. 547–550.
18 K. Hannig, in J. R. Norris and D. W. Ribbons (Editors), *Methods in Microbiology*, Vol. 5B, Academic Press, London, 1971, pp. 513–520.
19 A. R. Thompson, in C. F. Simpson and M. Whittaker (Editors), *Electrophoretic Techniques*, Academic Press, London, 1983, pp. 253–274.
20 S. Hjertèn, *Chromatogr. Rev.*, 9 (1967) 122–219.
21 M. Faupel, B. Barzaghi, C. Gelfi and P. G. Righetti, *J. Biochem. Biophys. Methods*, 15 (1987) 147–162.
22 P. G. Righetti, B. Barzaghi and M. Faupel, *J. Biochem. Biophys. Methods*, 15 (1987) 163–176.
23 B. Barzaghi, P. G. Righetti and M. Faupel, *J. Biochem. Biophys. Methods*, 15 (1987) 177–188.
24 P. G. Righetti, B. Barzaghi, M. Luzzana, G. Manfredi and M. Faupel, *J. Biochem. Biophys. Methods*, 15 (1987) 189–198.
25 P. G. Righetti, B. Barzaghi and M. Faupel, *Trends Biotech.*, 6 (1988) 121–125.
26 P. Wenger, M. de Zuanni, P. Javet, C. Gelfi and P. G. Righetti, *J. Biochem. Biophys. Methods*, 14 (1987) 29–43.
27 A. Jungbauer, C. Tauer, F. Steindl, E. Wenisch, M. Purtscher, M. Reiter, F. Unterluggauer, A. Buchacher, K. Uhl and H. Katinger, *J. Biochem. Biophys. Methods*, (1989) in press.
28 C. Gelfi, M.L. Bossi, B. Bjellqvist and P. G. Righetti, *J. Biochem. Biophys. Methods*, 15 (1987) 41–48.
29 P. K. Sinha and P. G. Righetti, *J. Biochem. Biophys. Methods*, 15 (1987) 199–206.
30 C. Gelfi and P. G. Righetti, *Electrophoresis*, 5 (1984) 257–262.
31 M. Chiari, E. Casale, E. Santaniello and P. G. Righetti, *Theor. Appl. Electrophoresis*, 1 (1989) 99–102.
32 M. Chiari, E. Casale, E. Santaniello and P. G. Righetti, *Theor. Appl. Electrophoresis*, 1 (1989) 103–107.
33 P. G. Righetti, *J. Chromatogr.*, 300 (1984) 165–223.
34 P. Pietta, E. Pocaterra, A. Fiorino, E. Gianazza and P. G. Righetti, *Electrophoresis*, 6 (1985) 162–170.
35 P. G. Righetti, M. Chiari and C. Gelfi, *Electrophoresis*, 9 (1988) 65–73.
36 H. Rink, M. Liersch, P. Sieber, F. Meyer, *Nucleic Acids Res.*, 12 (1984) 63–69.

Journal of Chromatography, 475 (1989) 311–319
Elsevier Science Publishers B.V., Amsterdam — Printed in The Netherlands

CHROM. 21 561

HIGH-PERFORMANCE LIQUID CHROMATOGRAPHIC ANALYSIS OF FLUORESCENT DERIVATIVES OF ADENINE AND ADENOSINE AND ITS NUCLEOTIDES

OPTIMIZATION OF DERIVATIZATION WITH CHLOROACETALDEHYDE AND CHROMATOGRAPHIC PROCEDURES

SHIGENORI SONOKI*, YUMI TANAKA, SHIN HISAMATSU and TSUGUO KOBAYASHI
College of Environmental Health, Azabu University, Fuchinobe, Sagamihara, Kanagawa 229 (Japan)
(First received August 30th, 1988; revised manuscript received April 10th, 1989)

SUMMARY

The use of chloroacetaldehyde (CAA) as a potential precolumn fluorimetric labelling reagent for adenine compounds was examined in detail. The reaction kinetics was greatly influenced by parameters such as the pH, temperature and CAA concentration. These parameters were optimized with regard to the reaction yield. The resulting procedure for CAA derivatization of adenine compounds was found to be excellent for quantitative analysis. Because the CAA derivatives of the adenine compounds studied were markedly stable, precise quantitative results were easily obtained using high-performance liquid chromatography. CAA derivatives of the five adenine compounds, *i.e.*, 1,N^6-etheno-adenine, -adenosine, -adenosine 5′-monophosphate, -adenosine 5′-diphosphate and -adenosine 5′-triphosphate were separated. The detection limits for the 1,N^6-etheno derivatives were 0.5–1.7 pmol per 10-μl injection. Due to its simplicity, speed, sensitivity and selectivity, this procedure is recommended for use in studies on the metabolism and biology of adenine compounds.

INTRODUCTION

Purine and pyrimidine bases, nucleosides and nucleotides are not only components of nucleic acids and coenzymes, but also play a rôle as mediators of hormone action. The analysis of purine and pyrimidine compounds in biological materials is essential for understanding nucleic acid metabolism. With the advent of high-performance liquid chromatography (HPLC), precise determination and high resolution of these compounds was made feasible[1–12]. Notwithstanding this radical development, very little attempt has been made to develop detection procedures with high sensitivity and selectivity. Nevertheless, some results on the specific detection of adenine compounds and cytidine as fluorescent derivatives have been reported, wherein chloroacetaldehyde (CAA) was used as the fluorimetric labelling reagent[13–19]. The essential features of the reaction of CAA and the application of its derivatized nucleo-

0021-9673/89/$03.50

tides and coenzymes to biological functions have been independently reviewed by Kost and Ivanov[20] and by Leonard[21].

In this paper, data on the optimization of the CAA derivatization of adenine compounds and their chromatographic separation are presented. In addition, the first successful application of a method developed to measure adenine compounds in rat serum is described.

EXPERIMENTAL

Apparatus

A Japan Spectroscopic (JASCO) Model 800-MP-15 high-performance liquid chromatograph with a JASCO FP-210 spectrofluoro monitor was used. Chromatograms were recorded on a JASCO Model 805-GI graphic integrator, while fluorescence spectra were obtained on a JASCO FP-770 spectrofluorometer.

HPLC columns

The properties of the following columns were examined: silica gel Finepak Sil (250 mm × 4.6 mm) and octadecylsilane-bonded silica gel Finepak Sil C_{18}T-5 (reversed phase, 250 mm × 4.6 mm) (both from JASCO); vinyl alcohol copolymers Asahipak GS-320H (dual mode of adsorption and gel permeation chromatography, 250 mm × 7.6 mm) (Asahi, Tokyo, Japan).

Chemicals

Adenine (Ade), adenosine (Ado), adenosine 5′-monophosphate (AMP), adenosine 5′-diphosphate (ADP) and adenosine 5′-triphosphate (ATP) were obtained from Sigma (St. Louis, MO, U.S.A.), chloroacetaldehyde solution (40%, practical grade) from Wako (Osaka, Japan). All other chemicals used were of analytical grade from commercial sources. Standard solutions were freshly prepared by dissolving the carefully weighed adenine compounds in distilled water to a concentration of 1 mg/ml. These standard solutions were diluted to the target concentrations in distilled water and stored at 4°C.

Chromatographic conditions

Separations were performed at a flow-rate of 1.0 ml/min at 40°C. The eluting solvents were: A, 0.2 *M* phosphate buffer (pH 5.0); B, 0.2 *M* phosphate buffer (pH 5.0)–methanol (70:30, v/v). Elution was carried out for 5 min with solvent A, followed by solvent B for 25 min. The column effluent was monitored fluorometrically at an excitation wavelength of 290 nm and at an emission wavelength of 415 nm.

Preparation of CAA derivatives

A 0.1 *M* CAA solution was prepared by diluting a commercial chloroacetaldehyde solution (40% CAA) in distilled water. Unless specified otherwise, the following procedure was used. To 100 μl of serum sample or 100 μl of diluted standard solutions in a reaction tube, 100 μl each of 0.2 *M* phosphate buffer (pH 5.0) and 0.1 *M* CAA were added. The reaction tube was stoppered hermetically and heated at 100°C for 30 min. The pH of the reaction mixture after derivatization was 4.5. Thereafter the mixture was diluted to 2 ml by adding 1.7 ml of 0.1 *M* Tris–HCl buffer (pH 7.4)

resulting in a pH of 7.0. Immediately after dilution, an equal volume of water-saturated diethyl ether was added to the mixture to remove the excess of CAA by extraction. A 5–10 μl aliquot of the aqueous phase was injected into the HPLC system.

Preparation of the sample fluid from rat serum

Blood samples were obtained individually from eight male rats (age, 3 months; strain, Sprague-Dawley). After 2 h at room temperature, erythrocytes were removed from the collected blood by centrifugation at 1500 *g* for 10 min. The resulting serum was deproteinized using an equal volume of cold 12% trichloroacetic acid solution. After a 5-min incubation in an ice-bath, the mixture was centrifuged at 1500 *g* for 10 min and the supernatant was collected. Trichloroacetic acid was removed using water-saturated diethyl ether. The supernatant was adjusted to pH 4.5 by titrating with 0.1 *M* KOH. The protein-free supernatants were stored at −20°C until analysis. Sample volumes of 100 μl of the protein-free supernatants were sufficient for analysis by the above-mentioned procedure.

RESULTS

Fluorescence spectra of 1,N^6-etheno derivatives

Standard samples containing 1 μg each of the 1,N^6-etheno derivatives of the adenine compounds were analyzed. The fluorescence spectra are given in Fig. 1. As can be deduced, all 1,N^6-etheno derivatives exhibited similar fluorescence emission spectra patterns, however the fluorescence excitation intensities at 223 nm increased in the order of 1,N^6-ethenoadenine, 1,N^6-ethenoadenosine, 1,N^6-etheno-AMP, 1,N^6-etheno-ADP and 1,N^6-etheno-ATP. For HPLC analysis, the fluorescence intensity was measured using excitation at 290 nm and emission at 415 nm for simultaneous analysis of the 1,N^6-etheno derivatives of the five adenine compounds.

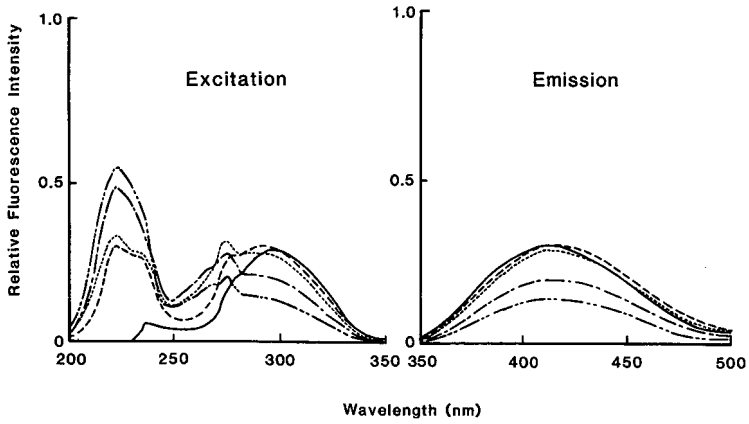

Fig. 1. Fluorescence spectra of 1,N^6-ethenoadenine (———), 1,N^6-ethenoadenosine (– – –), 1,N^6-etheno-AMP (------), 1,N^6-etheno-ADP (– · –) and 1,N^6-etheno-ATP (– · · –). Emission was measured at an excitation wavelength of 290 nm, while excitation was measured at an emission wavelength of 415 nm.

Separation of 1,N^6-etheno derivatives by HPLC

Three columns were examined for their ability to separate 1,N^6-etheno derivatives: Finepak Sil, Sil C_{18}T-5 and Asahipak GS-320H. A significantly better separation was obtained using the Asahipak GS-320H column. Hence, the latter was used throughout the present study and all results presented were obtained on this column.

The separation of the 1,N^6-etheno derivatives of the adenine compounds is shown in Fig. 2A, while Fig. 2B shows the separation of non-derivatized adenine compounds as monitored by UV absorbance at 260 nm. The 1,N^6-etheno derivatives were more sharply separated from each other *vis-à-vis* the separation of the non-derivatized adenine compounds.

The effect of the pH of the eluting solvents (see Experimental) on the separation of 1,N^6-etheno derivatives was examined. Following an increase from pH 5 to 7, a worsening in the separation of each derivative was noted. A value of 5.0 was selected as the pH of the eluting solvents A and B, because of the good separation of the 1,N^6-etheno derivatives of five adenine compounds.

Assay linearity and detection limit

Calibration graphs were constructed by analyzing a series of serum samples containing adenine compounds of know concentrations. Each concentration was studied in triplicate. The fluorescence intensities, measured as peak areas, were linear over a range of detection limits up to 40 pmol per 10-μl injection. The detection limits for 1,N^6-ethenoadenine, 1,N^6-ethenoadenosine, 1,N^6-etheno-AMP, 1,N^6-etheno-ADP and 1,N^6-etheno-ATP were 1.7, 0.5, 0.6, 0.9 and 1.3 pmol per 10-μl injection respectively, at a signal-to-noise ratio of about five. Conversely, the detection limits for non-derivatized adenine compounds monitored by UV absorbance at 260 nm were 10–30 pmol per 10-μl injection. This is taken to indicate that the fluorimetric analyses were approximately 10- to 30-times more sensitive than the UV-monitoring method.

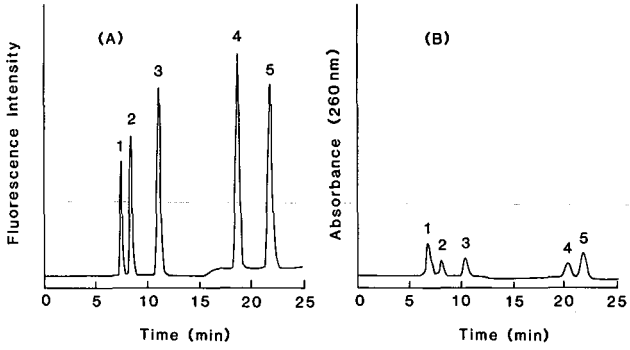

Fig. 2. Chromatograms of 1,N^6-etheno derivatives of adenine compounds (11.4 ng of each per 10-μl injection) (A) and of non-derivatized adenine compounds (49.4 ng of each per 10-μl injection) monitored by UV absorbance at 260 nm (B). Peaks: (A) 1 = 1,N^6-etheno-ATP; 2 = 1,N^6-etheno-ADP; 3 = 1,N^6-etheno-AMP; 4 = 1,N^6-ethenoadenosine; 5 = 1,N^6-ethenoadenine; (B) 1 = ATP; 2 = ADP; 3 = AMP; 4 = adenosine; 5 = adenine.

Assay precision

The intra-assay precision was determined by analyzing, on the same day, a set of five replicate serum samples containing various amounts of adenine compounds. The inter-assay precision was determined by analyzing serum samples containing various amounts of adenine compounds for 5 days over a period of 2 weeks. As regards the intra-assay precision, all coefficients of variation were below 4%; higher coefficients of variation were found for the inter-assay precision (2.7–8.1%).

Recovery

The extraction recoveries of the adenine compounds were determined by comparing the fluorescence intensities obtained by direct injection of $1,N^6$-etheno derivatives with those obtained after extraction of the spiked adenine compounds (10 μg/ml) from rat serum. The extraction recoveries of Ade, Ado, AMP, ADP and ATP were 93.8 ± 5.1, 92.2 ± 6.1, 87.6 ± 5.8, 91.4 ± 5.6 and 93.8 ± 5.8% (mean ± S.D., $n = 5$), respectively.

Effect of pH on the derivatization reaction

To examine the effect of the pH in the reaction mixture on the reaction yield, standard samples containing 1 μg of each adenine compound in the reaction mixture were derivatized using 0.2 *M* phosphate buffers (pH 3.2–6.0) for pH adjustments. As shown in Fig. 3, the effect on the derivatization of pH values below 4.5 was small, however the fluorescence intensities decreased markedly above pH 4.5.

Effect of reaction temperature and reaction time on the derivatization yield

The derivatization with CAA was carried out using the procedure described in the Experimental, except that the reaction temperature was varied from 60 to 120°C. A reaction temperature of 100°C was found to be the most effective. The effect of the

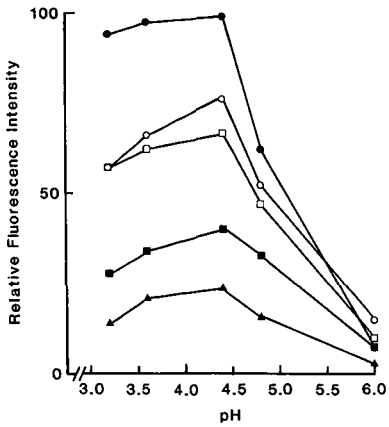

Fig. 3. Effect of the pH in the reaction mixture on chloroacetaldehyde derivatization of adenine compounds. ○, $1,N^6$-Ethenoadenine; ●, $1,N^6$-ethenoadenosine; □, $1,N^6$-etheno-AMP; ■, $1,N^6$-etheno-ADP; ▲, $1,N^6$-etheno-ATP. Each point represents the mean of triplicate determinations of the fluorescence intensity of each peak of the CAA derivative separated on the Asahipak GS-320H column. Chromatographic conditions similar to those in Fig. 2.

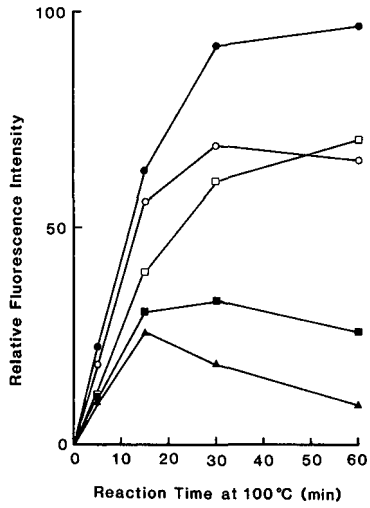

Fig. 4. Effect of reaction time at 100°C on chloroacetaldehyde derivatization of adenine compounds. For details see Fig. 3.

reaction time at 100°C was examined over a period of 60 min. The results, Fig. 4, clearly indicate that the fluorescence intensities of 1,N^6-ethenoadenosine and 1,N^6-etheno-AMP increased with reaction time, whereas those of 1,N^6-ethenoadenine, 1,N^6-etheno-ADP and 1,N^6-etheno-ATP gradually decreased. Hence, for the simultaneous analysis of the five adenine compounds, the derivatization was performed at 100°C for 30 min.

Effect of CAA concentration on quantitative analysis

The molar ratio of CAA to total adenine compounds was varied from $0.7 \cdot 10^2$ to $70 \cdot 10^2$. The total amount of adenine compounds present was always 0.018 μmol. A minimum molar ratio of $7 \cdot 10^2$ of CAA to adenine compounds is required for quantitative analysis. When the ratio fell below this minimum the assay response always became non-linear. Therefore, samples containing high concentrations of adenine compounds had to be diluted prior to derivatization in order to ensure a linear response.

Stability of CAA derivatives

The stability of the derivatives as a function of pH was examined at pH 4.5 and 7.0. The pH of the reaction mixture was adjusted by adding the appropriate buffer after the CAA derivatization reaction. The results obtained are shown in Fig. 5. At pH 4.5, 1,N^6-etheno-AMP, 1,N^6-etheno-ADP and 1,N^6-etheno-ATP were stable throughout the investigation period, although 1,N^6-ethenoadenosine underwent up to 40% decomposition within 7 days. During this time, the fluorescence response of 1,N^6-ethenoadenine increased by approximately the same percentages. At pH 7.0 (Fig. 5B), the fluorescence intensity of 1,N^6-ethenoadenosine increased slightly. Due to the rapid decomposition of 1,N^6-ethenoadenosine at pH 4.5, the reaction mixture was adjusted to pH 7.0 immediately after the reaction.

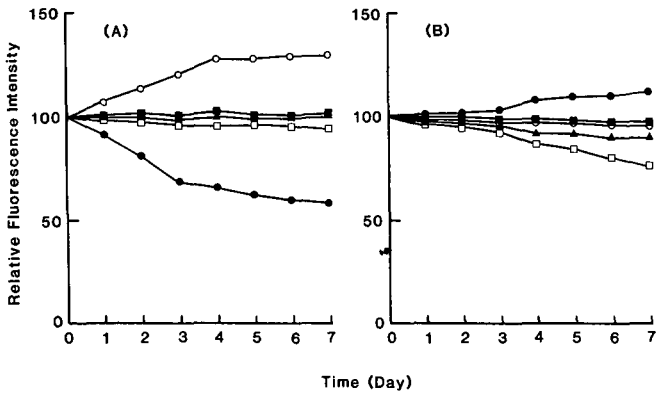

Fig. 5. Stability of 1,N^6-etheno derivatives of adenine compounds at pH 4.5 (A) and 7.0 (B). Details as in Fig. 3.

Specificity

The reaction specificity was examined not only with the major bases, but also with their nucleosides and nucleotides. Under conditions similar to those used in this study, no fluorescent CAA derivatives were detected with guanine, cytosine, thymine and uracil, as well as with their respective nucleosides and nucleotides.

Application to biological fluid

Typical chromatograms showing analyses of CAA derivatives in serum samples with and without addition of standards prior to extraction and CAA derivatization are shown in Fig. 6A and B, respectively. Chromatograms showing analyses of non-derivatized serum samples with monitoring of the absorbance at 260 nm are given in

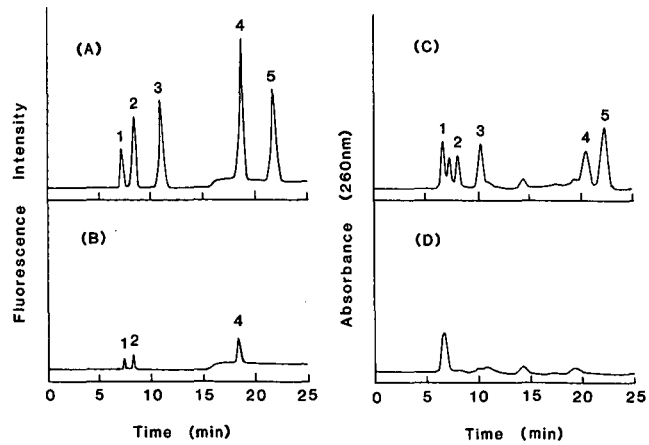

Fig. 6. Typical chromatograms of 1,N^6-etheno derivatives (A) in a serum sample spiked with adenine compounds (10 μl of 1 mg/ml of each) prior to extraction and derivatization and (B) in a blank serum sample. Chromatograms obtained from analyses of non-derivatized serum samples with (C) and without (D) addition of adenine compounds by monitoring the UV absorbance at 260 nm are shown for comparison. Peak notations are similar to those in Fig. 2.

TABLE I

CONCENTRATIONS OF ADENINE COMPOUNDS IN RAT SERUM

Compound	*Concentration (nmol/ml serum)*
Adenosine	2.21 ± 0.79
ADP	0.47 ± 0.14
ATP	0.41 ± 0.14

Fig. 6C and D. There was no interference by the matrix in the separation in chromatogram A, although some interference was evident in the separation in chromatogram C. Ado, ADP and ATP were detected as 1,N^6-etheno derivatives in blank serum samples, as shown in Fig. 6B. Except for interference, no adenine compounds were detected by monitoring the absorbance at 260 nm, as shown in Fig. 6D. The concentrations of adenine compounds detected in rat serum are summarized in Table I. The results are given as mean values ± standard deviation for eight male rats. Ade and AMP were not detected by the method described.

DISCUSSION

In studies of nucleic acid metabolism, the microanalysis of nucleic acid components with high sensitivity and selectivity is required.

To cite a few references, Secrist *et al.*[14,15] found that fluorescent 1,N^6-etheno derivatives of adenosine and its nucleotide were obtained by the reaction with CAA. Similarly, Barrio *et al.*[15] reported that cytidine reacted more rapidly with CAA when near pH 3.5, while 4.5 was the optimum pH required for reaction with adenosine. Also, Kochetkov *et al.*[13] have revealed a dependence of the selectivity of the CAA reaction on pH. Moreover, Sattsangi *et al.*[22] have reported that the synthesis of the fluorescent N^2,3-ethenoguanine by sterically hindering the reaction of CAA at N-1 of the guanine ring. Yoshioka and Tamura[17] reported the determination of Ade, Ado, AMP and cyclic AMP as their 1,N^6-etheno derivatives by HPLC, using a porous polystyrene column.

In the present study, we attempted to optimize the CAA derivatization and chromatographic separation of adenine compounds. Likewise, we have proposed a procedure having some advantages for the analysis of adenine and related compounds, as summarized below. (1) The 1,N^6-etheno derivatives of the adenine compounds were distinctly separated from each other using an Asahipak GS-320H column, as compared with the previous method[17–19]. Hence, simultaneous quantitative analysis of Ade, Ado, AMP, ADP and ATP was possible. The solid phase of the Asahipak GS-320H column is a hydrophilic hard gel composed of copolymers of vinyl alcohol. (2) The 1,N^6-etheno derivatives were deemed to be more stable at pH 7.0, hence precise analysis was possible. Upon degradation of 1,N^6-ethenoadenosine at pH 4.5, a gradual increase in the fluorescence intensity of 1,N^6-ethenoadenine was observed. This seems to be caused by hydrolysis of 1,N^6-ethenoadenosine by an acid, thereby yielding 1,N^6-ethenoadenine. At pH 7.0, the fluorescence intensity of 1,N^6-ethenoadenosine increased slightly. In this case, gradual dephosphorylation of 1,N^6-

etheno-AMP yielded 1,N^6-ethenoadenosine. (3) The CAA derivatization was found to be specific for the adenine compounds. Although CAA derivatization of cytidine and guanine had been reported[15,22], under the conditions used in this study, however, no fluorescent derivatives were detected with cytosine and guanine, as well as with their nucleosides and nucleotides. This discrepancy is apparently due to differences in the reaction conditions such as pH, temperature and CAA concentration.

This study was primarily undertaken to develop an analytical method for measuring adenine compounds in biological materials. The significance of the concentrations of adenine compounds found in rat serum remains to be elucidated. Suffice it to say that the developed methodology should enhance not only the possibility of measuring other adenine compounds, but also the study of the metabolism and biological roles of adenine compounds.

REFERENCES

1 M. Zakaria and P. R. Brown, *J. Chromatogr.*, 226 (1981) 267.
2 P. R. Brown (Editor), *HPLC in Nucleic Acid Research*, Marcel Dekker, New York, 1984, p. 247.
3 R. A. Hartwick, A. M. Krstulovic and P. R. Brown, *J. Chromatogr.*, 186 (1979) 659.
4 G. A. Taylor, P. J. Dady and K. R. Harrap, *J. Chromatogr.*, 183 (1980) 421.
5 A. McBurney and T. Gibson, *Clin. Chim. Acta*, 102 (1980) 19.
6 R. J. Simmonds and R. A. Harkness, *J. Chromatogr.*, 226 (1981) 369.
7 R. Boulieu, C. Bory, P. Baltassat and C. Gonnet, *Anal. Biochem.*, 129 (1983) 398.
8 D. M. Tidd and D. S. Dedhar, *J. Chromatogr.*, 145 (1978) 237.
9 R. Meyer and K. G. Wagner, *Anal. Biochem.*, 148 (1985) 269.
10 R. Boulieu and C. Bory, *J. Chromatogr.*, 339 (1985) 380.
11 K. Nakano, K. Shindo, T. Yasaka and H. Yamamoto, *J. Chromatogr.*, 343 (1985) 21.
12 P. Rotllan, A. Liras and P. Llorente, *Anal. Biochem.*, 159 (1986) 377.
13 N. K. Kochetkov, V. N. Shibaev and A. A. Kost, *Tetrahedron Lett.*, (1971) 1993.
14 J. A. Secrist, III, J. R. Barrio, N. J. Leonard and G. Weber, *Biochemistry*, 11 (1972) 3499.
15 J. R. Barrio, J. A. Secrist, III and N. J. Leonard, *Biochem. Biophys. Res. Commun.*, 46 (1972) 597.
16 G. Avigad and S. Damle, *Anal. Biochem.*, 50 (1972) 321.
17 M. Yoshioka and Z. Tamura, *J. Chromatogr.*, 123 (1976) 220.
18 J. F. Kuttesch, F. C. Schmalstieg and J. A. Nelson, *J. Liq. Chromatogr.*, 1 (1978) 97.
19 G. C. Mills, F. C. Schmalstieg, K. B. Trimmer, A. S. Goldman and R. M. Goldblum, *Proc. Natl. Acad. Sci. U.S.A.*, 73 (1976) 2867.
20 A. A. Kost and M. V. Ivanov, *Chem. Heterocycl. Compd.*, 16 (1980) 209.
21 N. J. Leonard, *CRC Crit. Rev. Biochem.*, 15 (1984) 125.
22 P. D. Sattsangi, N. J. Leonard and C. R. Frihart, *J. Org. Chem.*, 42 (1977) 3292.

Journal of Chromatography, 475 (1989) 321–329
Elsevier Science Publishers B.V., Amsterdam — Printed in The Netherlands

CHROM. 21 560

REVERSED-PHASE THIN-LAYER AND HIGH-PERFORMANCE LIQUID CHROMATOGRAPHY OF AROMATIC ALKOXY AND HYDROXY ACIDS

MARGIT BIDLÓ-IGLÓY
Institute for Drug Research, P.O. Box 82, H-1325 Budapest (Hungary)
(First received November 29th, 1988; revised manuscript received April 4th, 1989)

SUMMARY

The R_M and log k' values of aromatic alkoxy and hydroxy acids showed a linear correlation with the methanol and acetonitrile concentration of the mobile phases in reversed-phase thin-layer and high-performance liquid chromatography. Values of R_M and log k' extrapolated to 0% organic solvent content, however, were different in mobile phases containing methanol and acetonitrile, respectively. Correlations of log k' values with the corresponding R_M values were linear in both solvent systems. The elution order was examined with respect to the structures of the acids. Linear correlations of the chromatographic parameters with the carbon atom number of the substituent alkyl group in the molecules was found in the case of homologous compounds. However, the chromatographic parameters of di- and trimethoxy acids could not be predicted on the basis of the corresponding parameters of the monomethoxy acids. Experimental data were used to optimize the separation of the acids.

INTRODUCTION

The detection, identification and determination of organic acids, including alkoxy acids, by chromatography is an important field of organic analysis. Several methods are given in the literature for the separation of such compounds by reversed-phase high-performance liquid chromatography (HPLC) and for studying their structure–retention correlations[1–9].

Several authors investigated the log k'–R_M correlation of different compounds in reversed-phase chromatography[10–13]. Recently, Pietrogrande *et al.*[14] compared the retention data of several compounds of pharmaceutical interest using reversed-phase HPLC and thin-layer chromatography (TLC). They pointed out the difference in retention when using methanol or acetonitrile as a mobile phase component. With the aid of R_M–log k' correlations, the chromatographic parameters measured by different chromatographic techniques can be compared. On the other hand, HPLC separation can be modelled by rapid, simple TLC tests.

In previous work[15] HPTLC of aromatic alkoxy acids on reversed phases and silica gel was studied. The object of the present paper is to compare reversed-phase

0021-9673/89/$03.50

TABLE I

EXPERIMENTALLY MEASURED R_M AND log k' VALUES AT DIFFERENT PERCENTAGES OF METHANOL IN MOBILE PHASES OF PHOSPHATE BUFFER 0.1 *M* (pH 2)

Acid	*90% methanol*		*80% methanol*		*70% methanol*		*60% methanol*		*50% methanol*		*40% methanol*	
	R_M	*log k'*	R_M	*log k'*	R_M	*log k'*	R_M	*log k'*	R_M	*log k'*	R_M	*log k'*
Benzoic	−0.659	−0.68	−0.432	−0.47	−0.176	−0.241	0.105	0.096	0.347	0.367	0.753	0.674
2-Methoxybenzoic	−0.689	−0.759	−0.477	−0.645	−0.347	−0.470	−0.052	−0.078	0.269	0.236	0.602	0.463
3-Methoxybenzoic	−0.550	−0.614	−0.347	−0.398	−0.213	−0.169	0.158	0.198	0.501	0.453	0.865	0.824
4-Methoxybenzoic	−0.630	−0.600	−0.410	−0.417	−0.231	−0.191	0.158	0.175	0.477	0.481	0.826	0.796
2,4-Dimethoxybenzoic	−0.954	−1.060	−0.689	−0.980	−0.575	−0.718	−0.327	−0.333	−0.017	−0.078	0.269	0.192
3,4-Dimethoxybenzoic	−0.689	−0.782	−0.550	−0.646	−0.288	−0.427	−0.070	0.039	0.288	0.208	0.630	0.536
3,4,5-Trimethoxybenzoic	−0.659	−0.759	−0.524	−0.598	−0.213	−0.345	0.017	0.031	0.327	0.317	0.689	0.673
4-Butoxy-3,5-dimethoxybenzoic	−0.158	−0.268	−0.087	−0.019	0.347	0.346	0.865	0.826	–	–	–	–
4-Decyloxy-3,5-dimethoxybenzoic	0.501	0.440	0.865	1.058	–	–	–	–	–	–	–	–
4-Oxybenzoic	−0.865	−1.019	−0.788	−0.914	−0.525	−0.718	−0.347	−0.330	−0.052	−0.116	0.194	0.168
3-Methoxy-4-oxybenzoic	−0.753	−1.019	−0.720	−0.914	−0.550	−0.699	−0.327	−0.305	−0.035	−0.085	0.288	0.213

TLC and HPLC retention data and to examine the correlation between the elution orders and chemical structures of the compounds studied. The knowledge obtained can be used for an improved separation of isomeric acids. Since some of these compounds are possible intermediates, decomposition products or metabolites of pharmaceutically active products, the improved HPLC separation system can be used in purity and stability control.

EXPERIMENTAL

The following acids were tested: benzoic, 2-methoxy-, 3-methoxy-, 4-methoxy-, 2,4-dimethoxy-, 3,4-dimethoxy-, 3,4,5-trimethoxy-, 4-hydroxy-, 4-hydroxy-3-methoxy-, 4-*n*-butoxy-3,5-dimethoxy- and 4-*n*-decyloxy-3,5-dimethoxybenzoic acid.

Benzoic acid (purum) was obtained from Reanal (Budapest, Hungary), the mono- and dialkoxy acids (purum) from Fluka (Buchs, Switzerland); trialkoxy acids were synthesized in this institute.

TLC tests were carried out on RP-18 F_{254s} (Merck, Darmstadt, F.R.G.) 20 cm × 10 cm plates. The plates were developed in a sandwich chamber. HPLC measurements were performed on an LKB (Bromma, Sweden) liquid chromatograph, with a 2150 Model HPLC pump and UV detection at 240 nm (LKB variable wavelength detector). A Nucleosil C_{18} 5-μm column (200 mm × 4 mm; Bio-Separation Techniques, Budapest, Hungary) was used. The mobile phases consisted of mixtures of 0.1 *M* phosphate buffer (pH 2) and acetonitrile, and 0.1 *M* phosphate buffer (pH 2) and methanol, respectively. The concentration of acetonitrile ranged from 20 to 45% (v/v), that of methanol from 40 to 90% for the methoxy acids. Acids containing *n*-butoxy and *n*-decyloxy groups were tested only in buffer–methanol mixtures containing 80 and 90% methanol. The flow-rate was 1 or 1.5 ml/min. Solvents used in the mobile phases were HPLC grade (Interchemia, Budapest, Hungary). Measurements were replicated three times.

RESULTS AND DISCUSSION

Values of $R_M = \log [(1 - R_F)/R_F]$ and $\log k' = \log [(t_R - t_0)/t_0$ for acids were determined by chromatography in different mobile phases. The t_0 values were measured by injecting aqueous potassium dichromate solution and measuring the retention time, as described in the literature[11]. Tables I and II present the experimentally measured R_M and $\log k'$ values at different methanol and acetonitrile concentrations in the mobile phase. The R_M values in 20% acetonitrile were not taken into consideration in the correlation calculations because of the low R_F values and elongated spots of most of the acids. From these data the correlation equations were obtained (Table III).

Considering the correlation equations, it is seen that, using methanol in the mobile phases, the slopes are approximately 1 and the intercepts are approximately zero in the R_M–$\log k'$ correlation. The change of the buffer concentration was not taken into consideration when examining the dependence of the retention of organic solvent concentration in the mobile phase. Preliminary experiments showed that a two-fold dilution of the buffer in this concentration range caused only slight changes in the retention of these acids; the change in organic solvent concentration was much more important.

TABLE II

EXPERIMENTALLY MEASURED R_M AND log k' VALUES AT DIFFERENT PERCENTAGES OF ACETONITRILE IN MOBILE PHASES CONSISTING OF PHOSPHATE BUFFER 0.1 *M* (pH 2)

Acid	*45% methanol*		*35% methanol*		*30% methanol*		*25% methanol*		*20% methanol*	
	R_M	*log k'*	R_M	*log k'*	R_M	*log k'*	R_M	*log k'*	R_M	*log k'*
Benzoic	−0.087	0.120	0.250	0.443	0.525	0.722	0.602	0.719	0.885	
2-Methoxybenzoic	−0.105	0.049	0.140	0.327	0.477	0.605	0.501	0.584	0.741	
3-Methoxybenzoic	0.0	0.163	0.327	0.521	0.630	0.813	0.630	0.838	1.057	
4-Methoxybenzoic	−0.035	0.129	0.327	0.488	0.630	0.780	0.630	0.806	1.025	
2,4-Dimethoxybenzoic	−0,288	−0.010	−0.052	0.270	0.308	0.551	0.389	0.515	0.664	
3,4-Dimethoxybenzoic	−0.250	0.046	0.070	0.263	0.389	0.564	0.477	0.562	0.767	
3,4,5-Trimethoxy-benzoic	−0.176	0.049	0.105	0.369	0.477	0.674	0.602	0.696	0.937	
4-Hydroxybenzoic	−0.368	−0.250	−0.194	0.007	0.087	0.32	0.122	0.248	0.377	
4-Hydroxy-3-methoxybenzoic	−0.347	−0.250	−0.158	0.022	0.105	0.336	0.140	0.270	0.319	

The R_M and log k' values extrapolated to zero organic solvent content, $R_{M,0}$ and log k'_0, respectively, are different in most cases, when approached by the methanol and acetonitile containing mobile phase series, respectively. This is in accord with the literature[12,14]. The $R_{M,0}$ and log k'_0 values of 2,4-dimethoxybenzoic acid, however, were practically equal when measured in methanol or acetonitrile containing mobile phases.

Values of $R_{M,0,CH_3OH}$, $R_{M,0,CH_3CN}$, log k'_{0,CH_3OH} and log k'_{0,CH_3CN} are presented in Table IV. From these data the following correlations were calculated:

$$R_{M,0,CH_3OH} = 1.115\ R_{M,0,CH_3CN} + 0.147\ (r = 0.913)$$

$$\log k'_{0,CH_3OH} = 0.968 \log k'_{0,CH_3CN} + 0.241\ (r = 0.938).$$

The linear correlation makes it possible to convert R_M values measured by TLC into HPLC log k' values.

Considering the individual retention data, it was seen that for HPLC separation of methoxy acids, mobile phases with lower acetonitrile concentration are suitable.

Fig. 1 and 2 show the HPLC separation of aromatic acids containing one or more methoxy groups. When interpreting the elution orders of these acids on the basis of $R_{M,0}$ and log k'_0 values, respectively, some problems arise. Considering the effect of the substituent groups on the retention, the polar hydroxy group, as expected, reduced the retention of 4-hydroxy- and 3-methoxy-4-hydroxybenzoic acid compared to that of benzoic or 3-methoxybenzoic acid. The effect of the methoxy group, however, is not unambiguous. When comparing the retention data with those of benzoic acid it is seen that the 2-methoxy group decreases but the 3- and 4-methoxy groups increase the retention. The retention of 2,4- and 3,4-dimethoxy-benzoic acids, however, is less than that of benzoic acid. 3,4,5-Trimethoxybenzoic acid shows nearly equal retention properties to those of benzoic acid, although it contains three substituent groups, which individually increase retention. None of the R_M or log k' values of di- and trimethoxy acids can be calculated on the basis of additivity of ΔR_M or Δ log k'

Fig. 1. HPLC separation of aromatic monomethxoy acids. Column: Nucleosil C_{18}, 5 μm, 200 × 4 mm. Mobile phase: acetonitrile–0.1 *M* phosphate buffer (pH 2) (20:80). Flow-rate: 1.5 ml/min. Detection: UV at 240 nm. Elution order: 2-methoxybenzoic, benzoic, 4-methoxybenzoic and 3-methoxybenzoic acid at 6.8, 9.1, 11.79 and 12.81 min respectively.

Fig. 2. HPLC separation of aromatic acids containing more than one methoxy group. Conditions as in Fig. 1. Elution order: 2,4-dimethoxy-, 3,4-dimethoxy- and 3,4,5-trimethoxybenzoic acid at 5.92, 7.01 and 9. 72 min respectively.

TABLE III

CORRELATION EQUATIONS FOR MOBILE PHASES CONTAINING METHANOL OR ACETONITRILE CALCULATED FROM EXPERIMENTALLY OBTAINED R_M VALUES

c_{CH_3OH} is the concentration of methanol; c_{CH_3CN} is the concentration of acetonitrile in the mobile phase, respectively.

Compound	*Correlation equations*
Mobile phases containing methanol	
Benzoic acid	$R_M = -0.027\ c_{CH_3OH} + 1.75$ ($r = 0.997$); $\log k' = -0.027\ c_{CH_3OH} + 1.74$ ($r = 0.995$); $\log k' = 1.009\ R_M - 0.026$ ($r = 0.998$)
2-Methoxybenzoic acid	$R_M = -0.025\ c_{CH_3OH} + 1.46$ ($r = 0.989$); $\log k' = -0.026\ c_{CH_3OH} + 1.49$ ($r = 0.987$); $\log k' = 1.013\ R_M - 0.092$ ($r = 0.993$)
3-Methoxybenzoic acid	$R_M = -0.028\ c_{CH_3OH} + 1.92$ ($r = 0.986$); $\log k' = -0.029\ c_{CH_3OH} + 1.93$ ($r = 0.996$); $\log k' = 1.027\ R_M - 0.006$ ($r = 0.996$)
4-Methoxybenzoic acid	$R_M = -0.030\ c_{CH_3OH} + 1.95$ ($r = 0.992$); $\log k' = -0.029\ c_{CH_3OH} + 1.90$ ($r = 0.994$); $\log k' = 0.964\ R_M - 0.045$ ($r = 0.971$)
2,4-Dimethoxy-benzoic acid	$R_M = -0.023\ c_{CH_3OH} + 1.11$ ($r = 0.993$); $\log k' = -0.027\ c_{CH_3OH} + 1.24$ ($r = 0.989$); $\log k' = 1.103\ R_M - 0.075$ ($r = 0.985$)
3,4-Dimethoxybenzoic acid	$R_M = -0.024\ c_{CH_3OH} + 1.49$ ($r = 0.985$); $\log k' = -0.027\ c_{CH_3OH} + 1.61$ ($r = 0.989$); $\log k' = 1.018\ R_M - 0.063$ ($r = 0.986$)
3,4,5-Trimethoxybenzoic acid	$R_M = -0.027\ c_{CH_3OH} + 1.71$ ($r = 0.993$); $\log k' = -0.029\ c_{CH_3OH} + 1.79$ ($r = 0.994$); $\log k' = 1.076\ R_M - 0.048$ ($r = 0.997$)
4-Hydroxybenzoic acid	$R_M = -0.021\ c_{CH_3OH} + 1.01$ ($r = 0.993$); $\log k' = -0.025\ c_{CH_3OH} + 1.13$ ($r = 0.987$); $\log k' = 1.137\ R_M - 0.032$ ($r = 0.990$)
4-Hydroxy-3-methoxybenzoic acid	$R_M = -0.021\ c_{CH_3OH} + 1.06$ ($r = 0.980$); $\log k' = -0.026\ c_{CH_3OH} + 1.22$ ($r = 0.988$); $\log k' = 1.165\ R_M - 0.064$ ($r = 0.986$)

Mobile phases containing acetonitrile

Benzoic acid	$R_M = -0.030\ c_{CH_3CN} + 1.36$ ($r = 0.984$); $\log k' = -0.029\ c_{CH_3CN} + 1.48$ ($r = 0.988$); $\log k' = 0.968\ R_M + 0.181$ ($r = 0.995$)
2-Methoxybenzoic acid	$R_M = -0.028\ c_{CH_3CN} + 1.21$ ($r = 0.975$); $\log k' = -0.031\ c_{CH_3CN} + 1.43$ ($r = 0.985$); $\log k' = 0.892\ R_M + 0.165$ ($r = 0.993$)
3-Methoxybenzoic acid	$R_M = -0.031\ c_{CH_3CN} + 1.46$ ($r = 0.984$); $\log k' = -0.032\ c_{CH_3CN} + 1.68$ ($r = 0.985$); $\log k' = 1.027\ R_M + 0.178$ ($r = 0.999$)
4-Methoxybenzoic acid	$R_M = -0.032\ c_{CH_3CN} + 1.49$ ($r = 0.982$); $\log k' = -0.032\ c_{CH_3CN} + 1.65$ ($r = 0.985$); $\log k' = 0.995\ R_M + 0.165$ ($r = 0.999$)
2,4-Dimethoxybenzoic acid	$R_M = -0.031\ c_{CH_3CN} + 1.14$ ($r = 0.977$); $\log k' = -0.027\ c_{CH_3CN} + 1.24$ ($r = 0.965$); $\log k' = 0.802\ R_M + 0.259$ ($r = 0.976$)
3,4,5-Trimethoxybenzoic acid	$R_M = -0.035\ c_{CH_3CN} + 1.46$ ($r = 0.966$); $\log k' = -0.035\ c_{CH_3CN} + 1.63$ ($r = 0.985$); $\log k' = 0.847\ R_M + 0.234$ ($r = 0.987$)
4-Hydroxybenzoic acid	$R_M = -0.023\ c_{CH_3CN} + 0.71$ ($r = 0.978$); $\log k' = -0.026\ c_{CH_3CN} + 0.93$ ($r = 0.943$); $\log k' = 1.079\ R_M + 0.176$ ($r = 0.987$)
4-Hydroxy-3-methoxybenzoic acid	$R_M = -0.023\ c_{CH_3CN} + 0.73$ ($r = 0.981$); $\log k' = -0.024\ c_{CH_3CN} + 0.88$ ($r = 0.917$); $\log k' = 1.137\ R_M + 0.168$ ($r = 0.983$)

TABLE IV
VALUES OF $R_{M,0,CH_3OH}$, $R_{M,0,CH_3CN}$, $\log k'_{0,CH_3OH}$ AND $\log k'_{0,CH_3CN}$ FOR THE ACIDS

Acid	$R_{M,0,CH_3OH}$	$R_{M,0,CH_3CN}$	$log\ k'_{0,CH_3OH}$	$log\ k'_{0,CH_3CN}$
Benzoic	1.75	1.36	1.74	1.48
2-Methoxybenzoic	1.46	1.21	1.49	1.43
3-Methoxybenzoic	1.92	1.46	1.83	1.68
4-Methoxybenzoic	1.95	1.49	1.90	1.65
2,4-Dimethoxybenzoic	1.11	1.14	1.24	1.24
3,4-Dimethoxybenzoic	1.49	1.31	1.61	1.33
3,4,5-Trimethoxybenzoic	1.71	1.46	1.79	1.63
4-Hydroxybenzoic	1.01	0.71	1.13	0.93
4-Hydroxy-3-methoxybenzoic	1.06	0.73	1.22	0.88

increments of the substituents. This anomaly was not observed in the silica gel TLC of these compounds[15]. The elution order on silica gel can be predicted on the basis of additivity of ΔR_M increments. Probably, steric effects are more important in reversed-phase chromatographic retention, than in silica gel chromatography.

The acids containing butoxy and decyloxy groups were chromatographed only in mobile phases containing 80 and 90% methanol because of their strong mutual interaction with the reversed stationary phase. Together with 3,4,5-trimethoxybenzoic acid, they can be considered as members of the following homogous series:

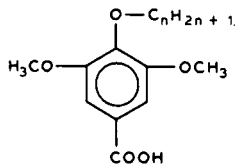

$n=1$ 3,4,5-trimethoxybenzoic acid
$n=4$ 4-*n*-butoxy-3,5-dimethoxybenzoic acid
$n=10$ 4-*n*-decyloxy-3,5-dimethoxybenzoic acid

The R_M and $\log k'$ values were determined in buffer–methanol mixtures and 90% methanol and correlated with the carbon atom number, n_C. Linear correlations were observed:

90% methanol: $R_M = 0.126n_C - 0.736$ ($r=0.993$)
$\log k' = 0.131n_C - 0.851$ ($r=0.996$)
80% methanol: $R_M = 0.148n_C - 0.674$ ($r=0.999$)
$\log k' = 0.183n_C - 0.770$ ($r=0.999$)

REFERENCES

1 B. A. Charpentier and J. R. Cowles, *J. Chromatogr.*, 208 (1981) 132.
2 M. C. Spanjer and C. L. de Ligny, *J. Chromatogr.*, 253 (1982) 32.
3 E. Burtscher, H. Binder, R. Concin and O. Bobleter, *J. Chromatogr.*, 252 (1982) 167.
4 K. V. Casteele, H. Geiger and Ch. F. Van Sumere, *J. Chromatogr.*, 258 (1983) 111.

5 J. M. Andersen and W. B. Pedersen, *J. Chromatogr.*, 259 (1983) 131.
6 T. Hanai and J. Hubert, *J. High Resolut. Chromatogr. Chromatogr. Commun.*, 7 (1984) 524.
7 J. G. Buta, *J. Chromatogr.*, 295 (1984) 506.
8 C. A. Chang and Q. Wu, L. Tan, *J. Chromatogr.*, 361 (1986) 199.
9 J. Macek and E. Smolková-Keulemansová, *J. Chromatogr.*, 333 (1985) 309.
10 U. A. Th. Brinkman and G. de Vries, *J. Chromatogr.*, 192 (1980) 331.
11 M. Bieganowska and E. Soczewiński, *J. Chromatogr.*, 205 (1981) 451.
12 K. Glowniak and M. Bieganowska, *J. Chromatogr.*, 370 (1986) 281.
13 M. C. Guerra and A. M. Barbaro, *J. Chromatogr.*, 320 (1985) 281.
14 M. C. Pietrogrande, P. A. Borea and G. L. Biagi, *J. Chromatogr.*, 447 (1988) 404.
15 M. Bidló-Iglóy, in H. Kalász and L. S. Ettre (Editors), *Chromatography 85'*, Publishing House of the Hungarian Academic of Sciences, Budapest, 1986, p. 453.

Journal of Chromatography, 475 (1989) 331–341
Elsevier Science Publishers B.V., Amsterdam — Printed in The Netherlands

CHROM. 21 531

ION CHROMATOGRAPHIC DETERMINATION OF NITRITE IN THE PRESENCE OF A LARGE AMOUNT OF CHLORIDE

PAOLO PASTORE
Department of Inorganic, Metallorganic and Analytical Chemistry, University of Padova, Via Marzolo 1, 35131 Padova (Italy)
IRMA LAVAGNINI
Institute of Industrial Chemistry, University of Padova, Via Marzolo 9, 35131 Padova (Italy)
and
ANDREA BOARETTO and FRANCO MAGNO*
Department of Inorganic, Metallorganic and Analytical Chemistry, University of Padova, Via Marzolo 1, 35131 Padova (Italy)
(First received January 20th, 1989; revised manuscript received March 23rd, 1989)

SUMMARY

Different procedures for the quantitation of nitrite in the presence of a large excess of chloride are described. The results obtained show that, in general, solutions characterized by NO_2^-/Cl^- ratios of about 1/10 000 can very easily be analyzed. The best results were obtained with amperometric detection in conjunction with NaCl as the eluent which allows ratios down to about 1/700 000 to be employed. One of the procedures investigated was successfully applied to the analysis of samples of sea-water from fish breeding pools.

INTRODUCTION

The use of different detectors, *i.e.*, conductometric, spectrophotometric and amperometric, has widened the application of ion chromatography (IC) to the determination of inorganic ions in a variety of aqueous matrices[1]. Nitrite ion, in particular, can be determined by the universal conductometric procedure[2], by oxidation at a glassy carbon electrode[3] and by UV absorbance detection[4]. The determination of nitrite ion is indeed of particular importance since it is largely used in the food industry and because it is able to reveal, in environmental analyses, organic contaminations[5]. Samples, on the other hand, often have an high content of other interfering ions so that the direct use of IC can be severely limited. The presence of a large amount of chloride is a typical drawback in the determination of traces of nitrite since the tail of the chloride peak can obscure the nitrite peak. The present paper reports on the problem of determining, following different approaches, traces of nitrite at very low nitrite to chloride concentration ratios. In particular, the potential of different procedures employing always the same general purpose column was tested

0021-9673/89/$03.50

and compared: a mixed H_3BO_3–Na_2CO_3 eluent with an anion membrane suppressor followed by a conductivity detector, UV and glassy carbon amperometric detectors in conjunction with different eluents. Moreover, an application to real sea-water samples drawn from fish-breeding pools was performed.

EXPERIMENTAL

Chemicals and reagents

Unless otherwise stated, all chemicals were of analytical reagent grade. Demineralized water was passed through a Millipore cartridge (GS 0.22 μm) for final purification and deaerated. Nitrite standards (1000 ppm and lower concentrations) were prepared according to the literature[6]. The following set of solutions were used as eluents in the chromatographic tests: 1.8 m*M* Na_2CO_3–1.7 m*M* $NaHCO_3$; 0.5 m*M* Na_2CO_3–2 m*M* H_3BO_3; 20 m*M* NaCl; 25 m*M* H_2SO_4 for regenerating the anion membrane suppressor. For the preparation of the sodium chloride eluent, an high quality reagent, 99.999% Aldrich NaCl, was used to avoid problems due to traces of more strongly retained anions, I^-, etc.

Apparatus and procedure

A Dionex Model 2010i ion chromatograph was used throughout this study. Chromatograms were recorded either on an AMEL x–y recorder or on a Spectra-Physics Model 4290 integrator. The column, obtained from Dionex, was a general purpose 250 mm × 4.0 mm AS4A column in conjunction with a 50 mm × 4.0 mm AG4A guard column. A 50-μl sample loop was used for all injections. A Dionex conductivity detector, a variable wavelength Model 8987 UV–VIS Knauer detector and an EG&G PAR Model 400 detector were employed. Preliminary UV spectra were recorded by using a Perkin-Elmer Model Lamda 5 spectrophotometer and an EG&G PAR Model 273 potentiostat was used in the unitial electroanalytical investigations. The pH of the eluent solutions was measured with a Metrohm Model 654 pH meter. In order to obtain the data for deconvolution of the overlapped peaks of Cl^- and of NO_2^-, the experimental curves obtained with the H_3BO_3 eluent were digitalized by a graphic digitalizer, Houston instruments "True Grid" Model 1017. The two contributors to the detector response were described by a suitable mathematical model. A gaussian function

$$y = a_1 \exp - \frac{1}{2}[(x - a_2)/a_3]^2 \tag{1}$$

(where x is the time and y the response of the conductometric detector) was used to represent the nitrite peak, while an hyperbola

$$y = a_4 \cdot \frac{1}{x - a_5} + a_6 \tag{2}$$

was fitted to the chloride tail. The parameters of the mathematical model

$$y(x, \bar{a}) = a_1 \exp - \frac{1}{2}[(x - a_2)/a_3]^2 + a_4 \cdot \frac{1}{x - a_5} + a_6 \tag{3}$$

were obtained by means of a non-linear regression routine, the Simplex procedure[7], which minimized the sum of the squares of the differences between the experimental and computed data points. The programs used, written in FORTRAN IV, were run under a RT-11 operating system on a PDP 11/23 Digital computer equipped with a Tektronix Model 4662 plotter.

RESULTS AND DISCUSSION

Preliminary considerations

The determination, by ion chromatography, of traces of nitrite in the presence of a large amount of chloride is usually accomplished by eliminating, on a silver-loaded cation-exchange resin, the excess of chloride ions[8]. This procedure, however, can be quite tedious, expensive and potentially harmful to the chromatographic column since traces of heavy metals are strong poisons of it. Even when addition of NaI to the analyte solution eliminated the above mentioned danger, owing to the very low value of the solubility product of AgI, attempts were made to overcome all the drawbacks either by finding a new eluent able to produce a better separation between chloride and nitrite, or by employing different detection procedures.

H_3BO_3–Na_2CO_3 eluent and conductivity detection

Literature data[1] indicate that different pH values of the eluent, that is different ratios between $NaHCO_3$ and Na_2CO_3, do not affect appreciably the ratio of the capacity factors, k', for nitrite and chloride ions. Therefore the strong tailing of the chloride peak always prevents the detection of a small nitrite peak. The presence of H_3BO_3 in the eluent implies, on the other hand, two different effects, namely a slight

TABLE I

CAPACITY FACTORS AND PEAK WIDTHS (4σ) OF NO_2^- FOR DIFFERENT Na_2CO_3–H_3BO_3 CONCENTRATIONS IN THE PRESENCE OF A LARGE AMOUNT OF Cl^- (500 ppm)

Chromatographic conditions: sample volume, 50 μl; flow-rate, 2 ml min^{-1}; detector, suppressed conductivity.

Eluent (M)		*Capacity factor, k'*	*Peak width (s)*
Na_2CO_3	H_3BO_3		
$2.5 \cdot 10^{-4}$	$2 \cdot 10^{-3}$	29.11	72.5
$5 \cdot 10^{-4}$	$2 \cdot 10^{-3}$	14.11	34
$1 \cdot 10^{-3}$	$2 \cdot 10^{-3}$	7.44	17.5
$2 \cdot 10^{-3}$	$2 \cdot 10^{-3}$	—[a]	—[a]
$5 \cdot 10^{-4}$	$1 \cdot 10^{-3}$	11.44	20
$5 \cdot 10^{-4}$	$2 \cdot 10^{-3}$	14.11	34
$5 \cdot 10^{-4}$	$3 \cdot 10^{-3}$	17.22	44
$5 \cdot 10^{-4}$	$4 \cdot 10^{-3}$	19.88	52.5
$2.5 \cdot 10^{-4}$	$1 \cdot 10^{-3}$	22.11	44
$5 \cdot 10^{-4}$	$2 \cdot 10^{-3}$	14.11	34
$1 \cdot 10^{-3}$	$4 \cdot 10^{-3}$	10.22	27.5

[a] No separation.

increment in the difference between the k' values and mainly a strong effect in reducing the tail of the chloride peak. On the basis of these findings, H_3BO_3 was added to the eluent, to improve the separation by modifying the shape of the larger peak. Several tests, performed with different concentrations of H_3BO_3 and Na_2CO_3 (see Table I), indicated that a suitable composition of the eluent was 2 mM H_3BO_3 and 0.5 mM Na_2CO_3 which results in a pH of 8.4. Fig. 1 shows, via a logarithmic diagram, that the main species present in the eluent solution are H_3BO_3 and HCO_3^-. Therefore the active ionic species in the eluent is HCO_3^-, while H_3BO_3 plays the rôle of a fronting agent. Since the analytical column works best with a low ionic loading of the sample solution, high chloride to nitrite ratios can be analyzed only by reducing, by proper dilution, the overall concentration and taking advantage of the high sensitivity of the detector. A chromatogram of a sample containing only 0.1 p.p.m. of NO_2^- is still well developed (see Fig. 2a) with a coefficient of variation of about 3%. By adding 500 ppm of Cl^- to 0.1 ppm of NO_2^- a complete resolution was not achieved (Fig. 2b), but deconvolution of the data as described above gave the response shown in Fig. 2d. The correctness of the mathematical model (eqn. 3) is demonstrated by the fitted curve shown in Fig. 2c, which is quite close to that in Fig. 2b. It is evident that the deconvolution method adopted allows the area of the nitrite peak to be evaluated by means of the eqn. 1. Therefore, the limiting Cl^- to NO_2^- ratio for this procedure is about 500/0.05, which results in a precision quite close to that of the analysis of NO_2^- alone.

Of interest is that the retention times for NO_2^- alone and in presence of a large amount of Cl^- do not coincide. This difference, about 1 min, can be explained by taking into account the weaker eluent strength of Cl^- in comparison with HCO_3^-. With a large chloride loading, it can be assumed that HCO_3^- is substituted as the eluent ion by Cl^- in the neighbourhood of the NO_2^- band. Fig. 3 compares the responses at six different nitrite concentrations, in the range 0.1–1 ppm, obtained in absence and in

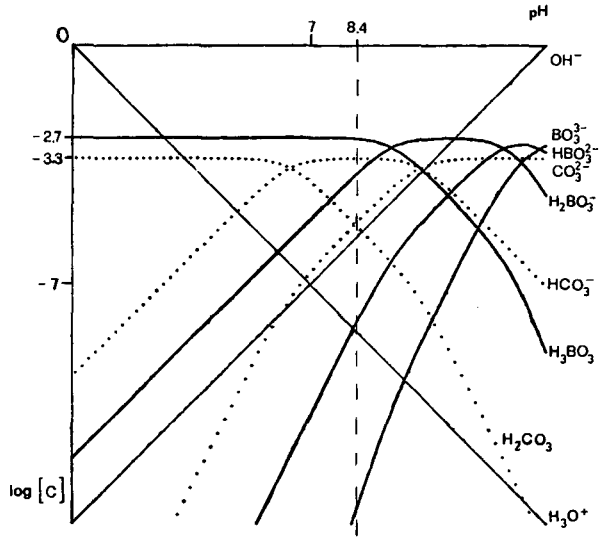

Fig. 1. Logarithmic diagram (pH *vs.* log[C]) for the Na_2CO_3–H_3BO_3 eluent. Eluent composition: 2 mM H_3BO_3 and 0.5 mM Na_2CO_3.

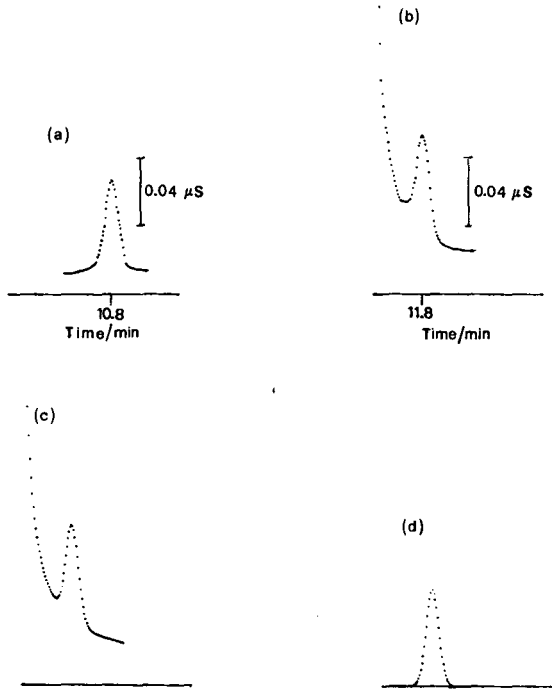

Fig. 2. (a) Digitalized ion chromatographic response of a 0.1 ppm aqueous solution of NO_2^-. (b) Digitalized ion chromatographic response of a 0.1 ppm aqueous solution of NO_2^- in the presence of 500 ppm Cl^-. (c) Fitted chromatogram of an aqueous solution containing 0.1 ppm NO_2^- and 500 ppm Cl^-. The model used was a Gaussian function plus an hyperbola. The parameters were estimated by a Simplex algorithm. (d) Peak of NO_2^- after deconvolution of the two components as described in (c). Chromatographic conditions: sample volume, 50 μl; flow-rate, 2 ml min^{-1}; detector, suppressed conductivity; mobile phase, 2 m*M* H_3BO_3 and 0.5 m*M* Na_2CO_3 in water.

the presence of chloride after the data handling. The fact that the points lie on a straight line of unit slope indicates that the chloride excess does not influence the nitrite peak. Two disadvantages, however, have to be mentioned. Some ions, SO_4^{2-} or PO_4^{3-} for instance, are retained too strongly with the H_3BO_3–Na_2CO_3 eluent and the performance of the analysis is obviously strongly dependent on the behaviour of the column. An aged column, yielding markedly shortened retention times, prevents a satisfactory resolution of the peaks.

$NaHCO_3$–Na_2CO_3 eluent and spectrophotometric detection

Using the classical $NaHCO_3$–Na_2CO_3 eluent, the selectivity of the spectrophotometric detector allows the determination at 210 nm of traces of nitrite in the presence of a large amount of chloride, since chloride absorbs weakly in the UV region only below 200 nm. As reported in the literature[4] and also demonstrated by us, the suppressor membrane, besides decreasing the high background electrical conductance of the eluent, also decreases the high background absorbance of the eluent in the range 190–220 nm because the extinction coefficient of a solution of H_2CO_3 is lower than

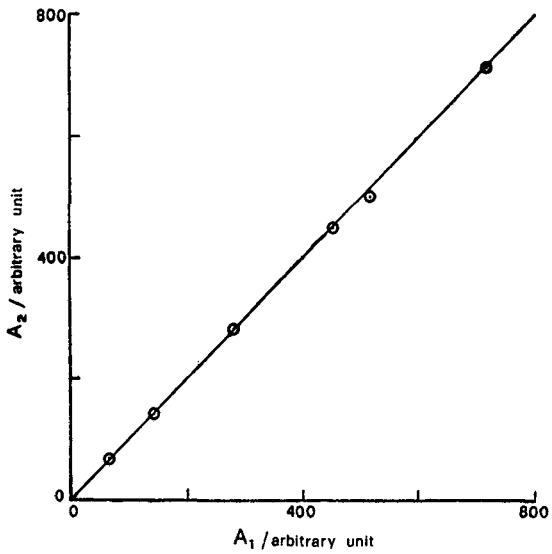

Fig. 3. Plot of the peak areas of NO_2^-, A_2, *vs.* the peak areas of NO_2^- in the presence of 500 ppm Cl^-, A_1. Concentration range of NO_2^-: 0.1–1.0 ppm. The areas were computed after the fitting procedure described in Fig. 2c. Regression plot: $A_2 = a + bA_1$; $a = 1.39 \pm 4.67$; $b = 0.99 \pm 0.1$; $\rho = 0.9998$. Chromatographic conditions as in Fig. 2.

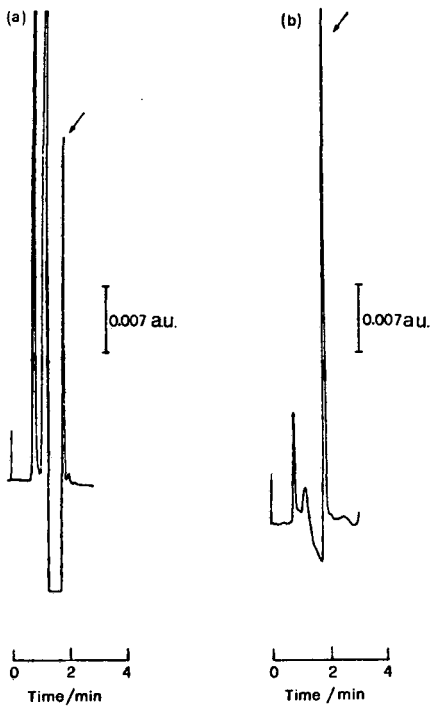

Fig. 4. Ion chromatographic responses of 1 ppm. NO_2^- and of 500 ppm Cl^- without (a) and with (b) the suppressor membrane and UV detection. Chromatographic conditions: sample volume, 50 μl; flow-rate, 2 ml min^{-1}; wavelength, 210 nm; mobile phase, 1.8 m*M* Na_2CO_3 and 1.7 m*M* $NaHCO_3$ in water.

that of one of HCO_3^--CO_3^{2-}. Therefore, the configuration with the UV detector inserted after the membrane suppressor was adopted for higher sensitivity and higher reproducibility. Fig. 4a and b shows two chromatograms obtained without and with the suppressor. It is seen that the broad negative peak due to the chloride ion eluted before NO_2^- is strongly reduced, as expected on the basis of the above arguments, upon insertion of the membrane suppressor. Since NO_2^- is only one of the pollutants potentially present in sea-water, the experimental device described was also tested to determine whether it were possible to measure other contaminants, like NO_3^- and PO_4^{3-}, in the same chromatographic analysis, which is a strong requirement advanced by environmental analysts[9]. The approach described gives quite good results for NO_3^- but, of course, does not allow the determination of PO_4^{3-} as a consequence of its lack of absorption. This ion, however, does not suffer any interference from the presence of chloride because of its long retention time, so that the use of the conductometric detector, connected in series with the UV detector, is suggested for the determination of PO_4^{3-} (ref. 10). Fig. 5a and b shows the chromatographic responses relative to a mixture of 0.25 ppm of NO_2^-, NO_3^- and PO_4^{3-} in the presence of 1000 ppm of Cl^- obtained with UV (Fig. 5a) and conductometric (Fig. 5b) detectors. The eluent in this case was 0.002 *M* Na_2CO_3 aqueous solution. It was chosen because of the requirement of using the lowest concentration of H_2CO_3 which gave the smallest dip while

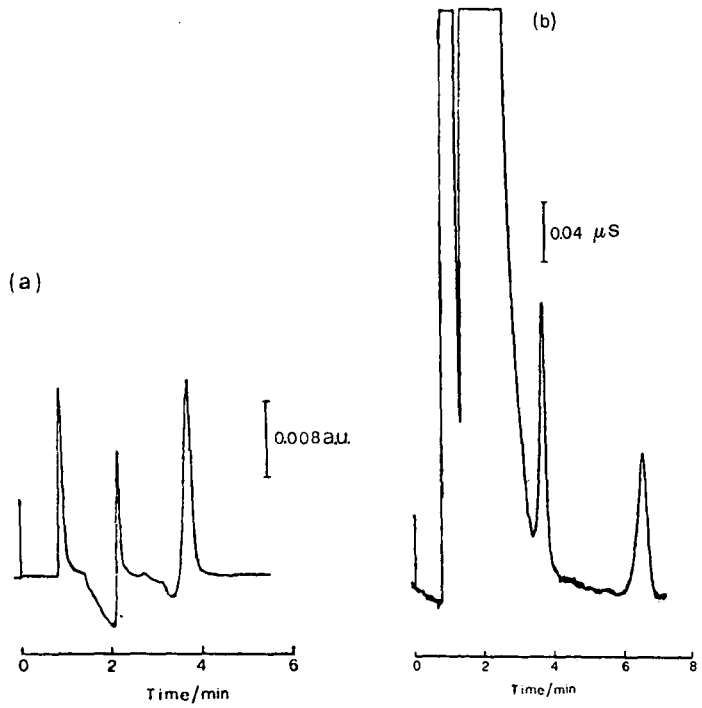

Fig. 5. Ion chromatographic response of 0.25 ppm of NO_2^-, 0.25 ppm NO_3^- and 0.25 ppm PO_4^{3-} in the presence of 1000 ppm of Cl^- obtained with UV (a) and conductometric detection (b). Chromatographic conditions: sample volume, 50 μl; flow-rate, 2 ml min^{-1}; wavelength, 210 nm (a); mobile phase, 0.002 *M* Na_2CO_3 in water.

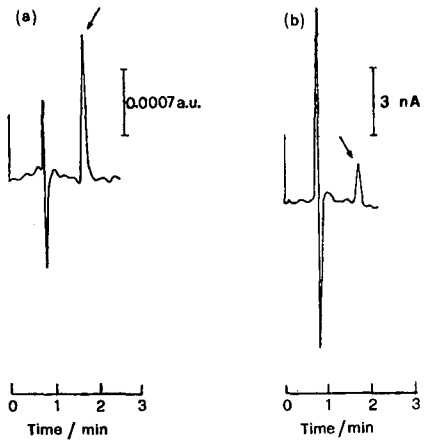

Fig. 6. (a) Ion chromatographic response of 0.03 ppm NO_2^- in the presence of 500 ppm. Cl^- obtained by UV detection. Chromatographic conditions: sample volume, 50 μl; flow-rate, 2 ml min^{-1}; wavelength, 210 nm; mobile phase, 0.02 *M* NaCl in water. (b) Ion chromatographic response of 0.007 ppm NO_2^- in the presence of 500 ppm Cl^- obtained by amperometric detection. Chromatographic conditions: sample volume, 50 μl; flow-rate, 2 ml min^{-1}; E = 1 V; mobile phase, 0.01 *M* NaCl in water; working electrode, glassy carbon; counter electrode, Pt; reference electrode Ag/AgCl saturated KCl.

maintaining a good eluent strength. According to the procedure reported in ref. 11, the detection limit for NO_2^- (as 3σ of the baseline noise) was 0.01 ppm so that the limiting ratio for NO_2^-/Cl^- is 1/50 000.

NaCl eluent and spectrophotometric and amperometric detection

Since the excess of chloride in the sample solution can cause instability of the analytical column (broad positive and negative preceding peaks), the use of the chloride ion itself as the eluent was taken into account. With this new eluent the baseline has to be best possible and with an appropriate concentration (0.02 *M*) the retention time of NO_2^- is practically equal to that obtained with HCO_3^-–CO_3^{2-} as the eluent. Fig. 6a shows a chromatogram of 500 ppm of Cl^- and 0.03 ppm of NO_2^-. However, caution must be exercised in using this eluent. The usual analytical reagent grade NaCl contains traces of I^- and other ions which are more strongly retained on the column. For this reason, after several hours of elution, they are removed from the column causing an undesired flicker noise in the baseline and ghost peaks with both detectors. When no instability occurs, the limiting ratio obtainable by this procedure is determined only by the detection limit relative to NO_2^-. Since the detection limit of NO_2^- is[11] about 0.005 ppm with a spectrophotometric detector at 210 nm, the limiting ratio Cl^-/NO_2^- can decrease to 1000/0.005, *i.e.*, 200 000/1. With the amperometric detector, working at an appropriate oxidation potential (*ca.* 900 mV *vs.* Ag/AgCl saturated KCl), not only the selectivity with respect to NO_2^- is maintained but also an advantage is obtained from the ability of chloride ion to enhance the electrochemical reversibility of many oxidation processes[12]. Fig. 6b shows a chromatogram of 500 ppm of Cl^- and 0.007 ppm of NO_2^-. On the basis of the above considerations, it can be stated that a detection limit of about 0.0014 ppm is easily achieved and consequently

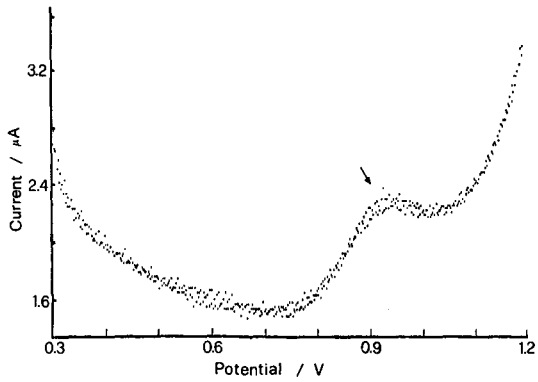

Fig. 7. Square wave voltammetric response of 0.9 ppm NO_2^- in 2500 ppm Cl^- in aqueous solution. Conditions: step height, 2 mV; pulse amplitude, 50 mV; frequency, 20 Hz. Electrodes as in Fig. 6b. The arrow indicates NO_2^-.

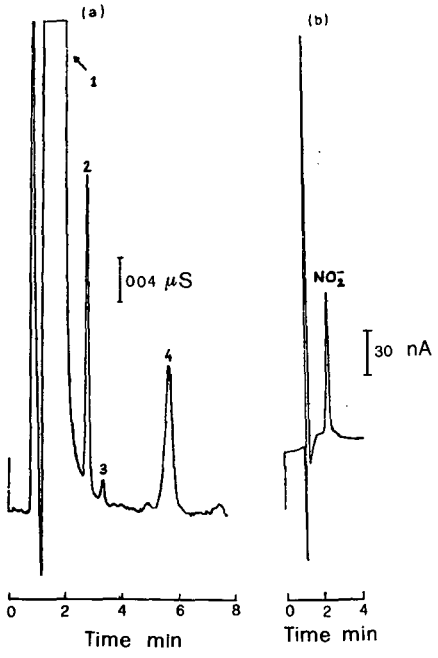

Fig. 8. (a) Ion chromatographic response obtained with conductometric detection for a real sample of sea-water diluted 20-fold. Peaks: 1 = Cl^- and NO_2^-; 2 = Br^-; 3 = NO_3^-; 4 = PO_4^{3-}. Chromatographic conditions: sample volume, 50 μl; flow-rate, 2 ml min^{-1}; detector, suppressed conductivity; mobile phase, 0.002 *M* Na_2CO_3 in water. (b) Ion chromatographic response obtained with amperometric detection of the same sample. Chromatographic conditions: sample volume, 50 μl; flow-rate, 2 ml min^{-1}; E = 1 V; mobile phase, 0.02 *M* NaCl in water; working electrode, glassy carbon; counter electrode, Pt; reference electrode, Ag/AgCl/saturated KCl.

the limiting ratio is about 715 000/1. In this connection it can be noted that a sensitive electroanalytical technique, namely square wave voltammetry, gives a detection limit for NO_2^- of only about 0.9 ppm as shown in Fig. 7. This is in accord with the general statement that, on passing from an unstirred solution to a flowing solution, using an appropriate thin-layer detector, a relevant enhancement in sensitivity is generally obtained[13]. One drawback has been pointed out for the suggested analytical system. After some hours of elution, a quite slow passivation of the electrode surface causes an increasing loss of sensitivity of the detector. For this reason the internal standard method is more suitable than the use of a calibration graph. However, the usual polishing with Al_2O_3 restores the optimum performance of the detector.

Analysis of real samples

The quality control of water in fish breeding plants is of obvious importance and NO_2^- is one of the most important species whose concentration has to be monitored. For this kind of analysis the approaches described above have been utilized. Since the real samples contained about 20 000 ppm of Cl^- (sea-water) and very low concentrations of NO_2^- we used the amperometric detector. This procedure was quite satisfactory as demonstrated by Fig. 8 which compares the responses of a real sample diluted 1 to 20 recorded with the conductometric (Fig. 8a) and the amperometric (Fig. 8b) detectors. In the first case the tail of the chloride peak overlaps the bromide one, while the amperometric detector exhibits an excellent response which gives a value of 0.35 ppm NO_2^- with a coefficient of variation of less than 0.5%.

CONCLUSIONS

The results in Table II clearly indicate that the analytical procedures examined are suitable for the quantitation of NO_2^- in the presence of a large excess of chloride ion, even when using a general purpose analytical column. Concentrations of NO_2^- higher than those reported are, of course, easier to determine owing to the general linear response of NO_2^- (up to 10 ppm) even in the presence of the large excess of Cl^-. Dedicated experimental devices, *i.e.*, spectrophotometric and amperometric detectors with NaCl as the eluent, give the best performance, allowing the determination of NO_2^- in sea-water at very low concentrations, but quite satisfactory results can be still obtained when only the eluent composition is changed and the general purpose conductivity detector is employed.

TABLE II

DETECTION LIMITS (DL) IN THE PRESENCE OF CHLORIDE AND LIMITING RATIOS FOR THE DIFFERENT ELUENT–DETECTOR COMBINATIONS INVESTIGATED

Eluent	*Conductometric*		*UV*		*ED*	
	DL NO_2^- *(ppm)*	Cl^-/NO_2^-	*DL* NO_2^- *(ppm)*	Cl^-/NO_2^-	*DL* NO_2^- *(ppm)*	Cl^-/NO_2^-
HCO_3^-–CO_3^{2-}	0.1	200	0.01	50 000	–	–
H_3BO_3–CO_3^{2-}	0.05	10 000	–	–	–	–
NaCl	–	–	0.005	200 000	0.0014	715 000

ACKNOWLEDGEMENTS

Financial aid from the Italian National Research Council (CNR) and the Ministry of Public Education is acknowledged.

REFERENCES

1 J. Weiss, *Handbook of Ion Chromatography*, Dionex, Sunnyvale, CA, 1986.
2 *Determination of Tracer Ions in Oilfield Drilling Fluids and Geological Brines*, Application Note 3, Dionex, Sunnyvale, CA, 1987.
3 J. E. Newbery and M. Pilar Lopez de Haddad, *Analyst (London)*, 110 (1985) 81.
4 R. J. Williams, *Anal. Chem.*, 55 (1983) 851.
5 S. De Fulvio, *Metodi Analitici per le Acque*, Vol. 1, Multigrafica Editrice, Roma, 1979.
6 P. J. Naish, *Analyst (London)*, 109 (1984) 809.
7 S. N. Deming and S. L. Morgan, *Anal. Chem.*, 45 (1973) 278A.
8 R. M. Merril, *The Analysis of Anions in Geological Brines using Ion Chromatography*, Sandia National Laboratories, Albuquerque, 1985.
9 P. Cescon, personal communication, 1988.
10 P. Pastore, I. Lavagnini, A. Boaretto and F. Magno, work in progress.
11 Analytical Methods Committee, *Analyst (London)*, 112 (1988) 199.
12 J. Wang and L. D. Hutching, *Anal. Chim. Acta*, 167 (1985) 325.
13 K. Stulik and V. Pacakova, *Electroanalytical Measurements in Flowing Liquids*, Ellis Horwood, Chichester, 1987.

Journal of Chromatography, 475 (1989) 343–351
Elsevier Science Publishers B.V., Amsterdam — Printed in The Netherlands

CHROM. 21 520

HIGH-PERFORMANCE LIQUID CHROMATOGRAPHIC ANALYSIS OF ALDEHYDES AT TRACE LEVEL AS THEIR 3-METHYLBENZOTHIAZOLONE AZINE DERIVATIVES

GIUSEPPE CHIAVARI*, M. CRISTINA LAGHI and GIANCARLO TORSI
Dipartimento di Chimica "G. Ciamician", Università di Bologna, Via F. Selmi 2, Bologna 40126 (Italy)
(First received July 18th, 1988; revised manuscript received March 21st, 1989)

SUMMARY

The high-performance liquid chromatographic analysis of some simple carbonyl compounds as their 3-methylbenzothiazolone derivatives was studied. The detection was performed by means of an ultraviolet–visible spectrophotometric detector. All compounds except formaldehyde gave two isomers of the type *E* and *Z*. The derivatization was quantitative only for formaldehyde, acetaldehyde and benzaldehyde. The chromatographic conditions were optimized to solve the problem due to the presence of two isomers. The low detection limits obtained for these compounds make this method a competitive alternative to dinitrophenylhydrazine and lutidine methods.

INTRODUCTION

Carbonyl compounds are a major class of air pollutants. In particular, formaldehyde is the most abundant carbonyl compound in the atmosphere, while other aldehydes, such as acetaldehyde and benzaldehyde, have also been detected, and their concentrations may be comparable to that of formaldehyde[1].

Formaldehyde is a combustion product originating from many sources[2,3] and is used as a raw material in numerous industries. It has been identified as a suspected carcinogen of class A2[4], and for this reason in the U.S.A. the maximum tolerable limit in air has recently been reduced to 1.2 mg/m^3. Carbonyls are also considered as an important class of compounds in atmospheric chemistry because of their role in gas and liquid phase reactions[5].

Of particular interest in the dispersed liquid phase (fog, clouds, rain) is the reaction of carbonyl compounds with S(IV), leading to the formation of highly acidic compounds like hydroxyalkanesulphonic acids.

Concern about environmental pollution and occupational hazards due to the presence of formaldehyde has led to the development of analytical methods for the determination of aldehydic compounds at trace level. The two commonly used spectrophotometric methods are the Nash method (involving lutidine derivatives)[6] and the methylbenzothiazolone hydrazone (MBTH) method[7]. The Nash method is

0021-9673/89/$03.50

specific for formaldehyde, while the MBTH method is non-selective because it measures total aldehydes as their formaldehyde equivalent. Both methods show no response to ketones. Several other techniques have been reported for the separation and/or determination of various aldehydes or their derivatives. They include thin-layer chromatography (TLC)[8,9], gas chromatography[10] and especially high-performance liquid chromatography (HPLC)[11–19].

The best known method for the separation and quantitation of carbonyl compounds at trace levels by HPLC is that proposed by Selim[11] which uses 2,4-dinitrophenylhydrazones as reactants. Several applications of this method have been reported involving both spectrometric[12–14] and electrochemical detection[15].

In previous papers we studied the possibility of using lutidine derivatization[17] and the first step of the classical method with MBTH, *i.e.*, azine formation, see Fig. 1[18] for the analysis of carbonyl compounds by HPLC using electrochemical detection. In both cases picogram quantities were detected. The advantage of the revised MBTH method is due to a more simple reaction and the possibility of analysing ketones. However the reaction can lead to the formation of two isomers (*Z* and *E*) with the possibility, in HPLC, of peak splitting and consequent problems when a quantitative analysis is sought.

The presence of two isomers was verified in a previous paper[18] using a C_{18} bonded phase. The two isomers have been further investigated by UV analysis and TLC. Moreover the HPLC behaviour of these compounds has been studied using different columns. Finally, microscale derivatization experiments have been carried out using standard mixtures in order to determine the yield and the detection limit of the method under conditions similar to those encountered with real samples.

EXPERIMENTAL

The LC equipment consisted of a quaternary solvent Perkin-Elmer (Norwalk, CT, U.S.A.) Model 410 system with a 6-μl Rheodyne 7125S injector was employed. Detection was performed with a Perkin-Elmer dual beam LC95 variable wavelength detector and with a Coulchem electrochemical detector, ESA Model 5100A (Bedford,

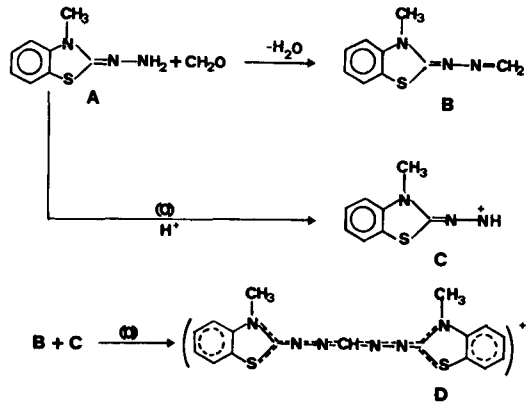

Fig. 1. Mechanism of the MBTH derivatization reaction with and without oxidant. The azine is compound B. (O) = (Oxygen).

MA, U.S.A.). The UV spectra (Fig. 2) were obtained with an Hewlett-Packard Model 1090 (Palo Alto, CA, U.S.A.) with a diode array detector, an HP integrator Model 79995-6A and a colour plotter Model 7440A. The UV spectra of MBTH derivatives were obtained with a Perkin-Elmer 551 UV–VIS spectrometer.

The following columns were tested: (a) silica gel Hypersil (HPLC Technology, Macclesfield, U.K.), 5 μm, 150 mm × 4.6 mm, fully porous spherical adsorbent; (b) Hypersil ODS (HPLC Technology), 5 μm, 150 mm × 4.6 mm reversed-phase material with a monolayer coverage of dimethyloctadecylsilyl groups; (c) Hypersil C_1 (HPLC Technology), 5 μm, 150 mm × 4.6 mm reversed phase with a trimethyl chain; (d) Spherisorb C_6 (Phase Separation, Queensferry, U.K.), 5 μm, 150 mm × 4.6 mm, bonded phase resulting from the highest possible coverage with an hexyl carbon chain.

A solution of 0.02 *M* potassium dihydrogenphosphate containing various amounts of methanol (HPLC grade; Carlo Erba, Milan, Italy) was used as the mobile phase. The pH was adjusted to the desired value by adding sulphuric acid. The mobile phase was first filtered with a 0.2-μm nylon membrane and then degassed. The flow-rate was held at 1 ml/min and all experiments were carried out at room temperature.

The TLC measurements were carried out by applying 3 μl of methanolic solutions (3 mg/ml) of the MBTH azine derivatives to a start line 1 cm from the bottom of the plate. The plates used were: (a) Merck 60, F_{254} precoated TLC plates, 10 cm × 5 cm, layer thickness 0.25 cm, developed with ethyl acetate-cyclohexane (20:80, v/v), spots of the separated azines developed by exposure to iodine vapours; (b) RP C_{18}, Merck precoated TLC plates, 10 cm × 5 cm, layer thickness 0.25 mm, developing system 0.02 *M* potassium dihydrogenphosphate solution–methanol (90:10, v/v), spot visualization by exposure to air.

The microscale derivatization was carried out by adding 1 ml of MBTH hydrochloride, 0.5% in water (Fluka, Buchs, Switzerland) to a known volume of a solution of the carbonyl compounds of known concentration. The solution was kept for 1 h at 95°C in a closed vessel and after cooling it was extracted with 4 ml of isooctane. The organic phase was then directly injected into the column.

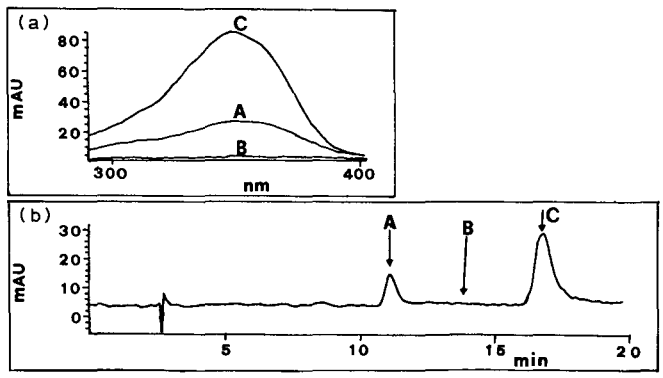

Fig. 2. HPLC separation of the *E* and *Z* isomers of the benzaldehyde derivative at λ = 350 nm (a), and UV spectra of the isomers (b). Chromatographic conditions: column, Hypersil ODS; eluent, 0.02 *M* KH_2PO_4 in water–methanol (30:70).

RESULTS AND DISCUSSION

In a previous paper the peak splitting of the compounds in reversed-phase (RP) chromatography was ascribed to the formation of isomers *Z* and *E* during the derivatization[17]. Evidence in support of this hypothesis was provided by the results obtained with an electrochemical detector (equal potential *vs.* current curves) as well as by the interconversion of one isomer into the other[18].

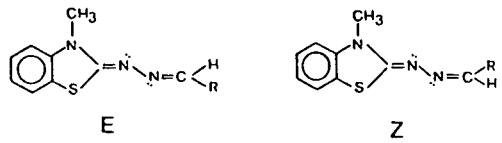

E Z

Another experimental result which suggests the presence of isomers has been obtained by analysing the spectra of the two peaks with a multi-diode array detector (see Fig. 2 for the spectrum of the benzaldehyde derivative). The λ_{max} and ε values of the most important azines so obtained are summarized in Table I.

The presence of double peaks, as already mentioned, is however not desired in analytical measurements since there is always a chance of peak overlapping. Moreover, for quantitation, both peaks must be considered. A survey of azine determination by TLC[8,9] gave no indication of peak splitting. For this reason the TLC measurements were repeated both with silica gel and RP C_{18} plates. The most significant results are reported in Table II. It is seen that, on RP plates, the isomers of aliphatic derivatives are not resolved, whereas the unsaturated ones are separated. The different compounds can easily be separated but there is overlapping when the number of compounds present is high. On the contrary, on silica gel plates, the isomers can easily be resolved with the exception of methyl ethyl ketone.

The same general trend is observed in HPLC when similar stationary phases are used. The chromatographic parameters relevant to the three RP columns are reported in Table III. No significant difference is observed. The peak splitting increases with the

TABLE I

VALUES OF λ_{max} AND ε FOR THE MOST IMPORTANT MBTH CARBONYL DERIVATIVES

MBTH derivative	λ_{max} *(nm)*	$\varepsilon \cdot 10^4$ *(l mol^{-1} cm^{-1})*
MBTH reagent	290	0.10
(a) Formaldehyde	308	2.78
(b) Acetaldehyde	305	2.48
(c) Propionaldehyde	308	1.59
(d) *n*-Butyraldehyde	308	2.13
(e) *n*-Valeraldehyde	308	1.55
(f) Acrolein	334	3.56
(g) Crotonaldehyde	327	3.45
(h) Benzaldehyde	346	4.80
(i) Acetone	309	2.32
(j) Methyl ethyl ketone	308	2.73
(k) Acetophenone	343	3.25

TABLE II

TLC SEPARATION OF MBTH AZINES

MBTH derivative	*RP-18*		*Silica*	
	R_{F1}	R_{F2}	R_{F1}	R_{F2}
(a) Formaldehyde	0.44		0.26	
(b) Acetaldehyde	0.40		0.26	0.38
(c) Propionaldehyde	0.35		0.32	0.42
(d) *n*-Butyraldehyde	0.31		0.34	0.50
(e) *n*-Valeraldehyde	0.25		0.36	.54
(f) Acrolein	0.41	0.43	0.28	0.40
(g) Crotonaldehyde	0.34	0.39	0.26	0.36
(h) Benzaldehyde	0.21	0.32	0.22	0.40
(i) Acetone	0.48		0.32	
(j) Methyl ethyl ketone	0.32		0.44	
(k) Acetophenone	0.18	0.32	0.48	

aromaticity of the carbonyl compound and with the aliphatic content of the bonded phase.

Fig. 3 shows a chromatogram of a standard mixture in which a compromise as been made between good separation and low or no peak splitting. A good resolution of acetone, acrolein and propionaldehyde was not achieved. However, acrolein can be determined selectively at 350 nm where only unsaturated derivatives have a significant response (Fig. 4).

TABLE III

SEPARATION OF MBTH DERIVATIVES ON DIFFERENT COLUMNS

Eluents: 0.02 *M* KH_2PO_4 with 77% (1), 70% (2) and 65% methanol (3). k_1 and k_2 are the capacity factors of the isomers.

MBTH derivative	*Hypersil ODS (1)*		*Spherisorb (2)*		*Hypersil* C_1 *(3)*	
	k_1	k_2	k_1	k_2	k_1	k_2
(a) Formaldehyde	0.80		0.71		0.66	
(b) Acetaldehyde	1.11		0.94		0.94	
(c) Propionaldehyde	1.87		1.46		1.54	
(d) *n*-Butyraldehyde	2.79		1.99		2.25	
(e) *n*-Valeraldehyde	4.26		2.89		3.36	
(f) Acrolein	1.55	1.72	1.14	1.26	1.46	
(g) Crotonaldehyde	1.92	2.29	1.45	1.62	1.80	2.00
(h) Benzaldehyde	2.75	4.75	2.13	2.92	2.86	3.66
(i) Acetone	1.61		1.10		1.35	
(j) Methyl ethyl ketone	2.79		1.80		1.99	
(k) Acetophenone	3.73	7.13	2.36	3.50	3.24	5.18

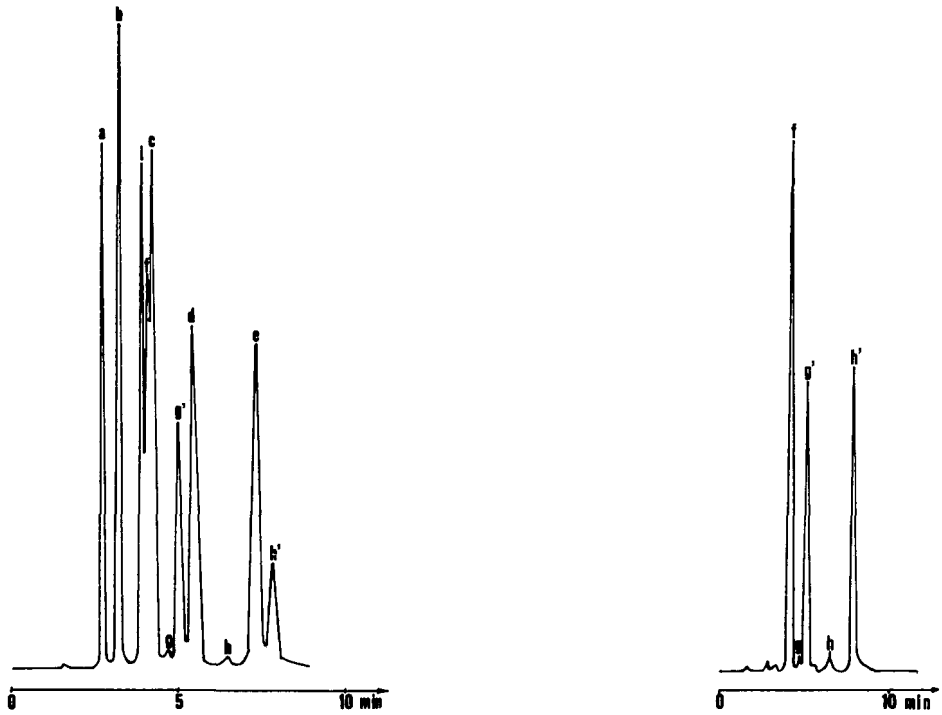

Fig. 3. Separation of azines on an Hypersil C_1 column. Chromatographic conditions: mobile phase, 0.02 *M* KH_2PO_4 in water–methanol (35:65); detection, λ = 308 nm. For peak identification, see Table I.

Fig. 4. As in Fig. 3, but with λ = 350 nm.

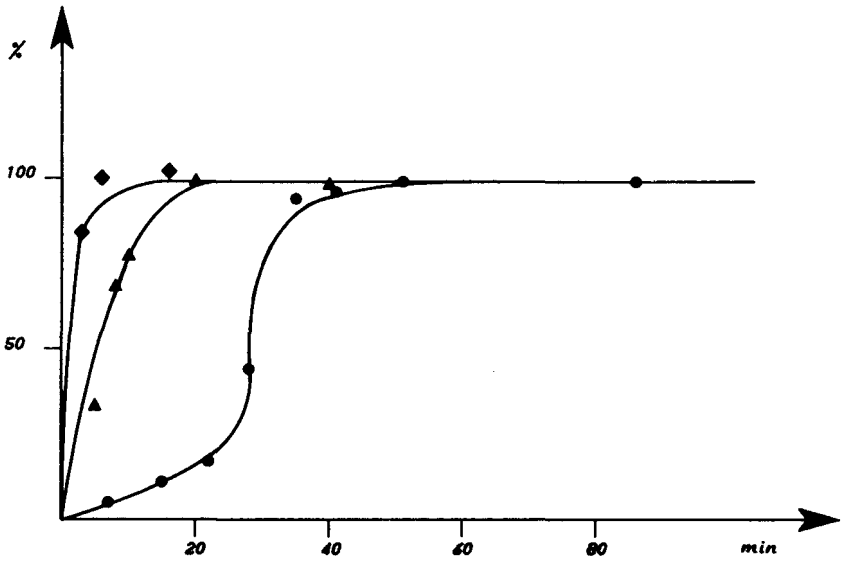

Fig. 5. Reaction yield *vs.* time of formaldehyde derivatization at different temperatures: (●) 25, (▲) 50 and (◆) 95°C.

TABLE IV

PERCENT YIELD OF DIFFERENT AZINES AFTER A REACTION TIME OF 1 h AT 95°C

MBTH derivative	*Yield (%)*
(a) Formaldehyde	100
(b) Acetaldehyde	100
(c) Propionaldehyde	45
(d) *n*-Butyraldehyde	45
(e) *n*-Valeraldehyde	40
(f) Acrolein	70
(g) Crotonaldehyde	70
(h) Benzaldehyde	100
(i) Acetone	20
(j) Methyl ethyl ketone	10
(k) Acetophenone	10

Derivatization results

To demonstrate the applicability of the proposed method to real samples such as fog and rain, we have evaluated the microscale derivatization yield in the concentration range 0–100 μM.

Fig. 5 shows the kinetics of azine formation from formaldehyde (10 μM) and a charge excess of MBTH at different temperatures. The percent yield of different azines after a reaction time of 1 h at 95°C is reported in Table IV. Since the extraction yield for all compounds is above 95%, the data of Table IV represent a rough measure of the reaction velocities of the different carbonyls with MBTH and therefore of the applicability of the method, if a reaction time of 1 h is considered a limit for the analysis. Based on the above argument, the proposed method is quite reliable for analysing formaldehyde, acetaldehyde and benzaldehyde. The calibration graph with microderivatization for formaldehyde is shown in Fig. 6 where the height of the

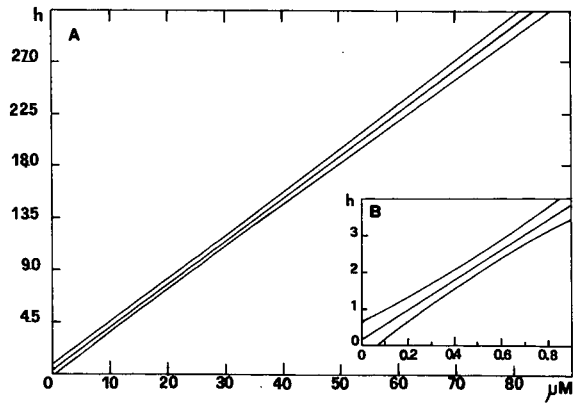

Fig. 6. Calibration graph for formaldehyde in the concentration range 0–100 μM obtained with microderivatization (A) and in the concentration range 0–1 μM (Insert B). The outer lines represent the 95% confidence limits.

TABLE V

COMPARISON OF DETECTION LIMITS (μM) FOR DIFFERENT CARBONYL DERIVATIVES OBTAINED WITH DIFFERENT METHODS

A = Spectrophotometric method; B = HPLC method with amperometric detector; MD = microscale derivatization; C = HPLC method with UV–VIS detector; D = HPLC method with coulometric detector.

Method		*Formaldehyde*	*Acetaldehyde*	*Benzaldehyde*
Nash	A[20]	5.5		
	B[17]	1.5		
DNPH	B[15]	0.19	0.48	0.15
	MD[15]	0.48	0.48	0.36
MBTH	A[9]	30.3	22.7	3.45
	B[18]	0.04	0.13	0.47
	C[a]	0.07	0.08	0.19
	D[a]	0.13	0.14	1.60
	MD[a]	0.29	0.47	0.34

[a] This work.

relevant peak is plotted *vs.* the concentration of the test solution. The limit of detection obtained from data at concentrations lower than 1 μM (insert of Fig. 6) calculated according to Miller and Miller[21] is reported in Table V. In the same table the detection limits obtained with different methods given in literature are also presented for comparison. It is seen that the proposed method has the lower limit of detection for all the compounds studied.

Work is in progress to apply this method to real atmospheric samples.

ACKNOWLEDGEMENT

This work was supported by a grant (40%) from Ministera della Pubblica Istruzione.

REFERENCES

1 D. Grosjean, *Environ. Sci. Technol.*, 16 (1982) 254.
2 P. L. Magill and R. W. Benoliel, *Ind. Eng. Chem.*, 44 (1952) 1347.
3 D. F. Magin, *J. Chromatogr.*, 202 (1960) 255.
4 *IARC Monographs on the Evaluation of Carcinogenic Risks to Humans*, Vol. 7, International Agency for Research on Cancer, Lyon, 1987, p. 211.
5 J. G. Alvert, L. Lazrus, G. L. Kok, B. G. Heikes, J. G. Walega, J. Lind and C. A. Cantrel, *Nature (London)*, 317 (1985) 27.
6 T. Nash, *Biochem. J.*, 55 (1953) 416.
7 E. Sawicki, T. R. Hauser, T. W. Stanley and W. Elbert, *Anal. Chem.*, 33 (1961) 93.
8 F. C. Hunt, *J. Chromatogr.*, 35 (1968) 111.
9 V. Carunchio, G. De Angelis, A. M. Girelli and A. Messina, *Talanta*, 29 (1985) 47.
10 H. Kallio, R. R. Linko and J. Kaitaranta, *J. Chromatogr.*, 65 (1972) 355.
11 S. Selim, *J. Chromatogr.*, 136 (1977) 271.
12 K. Kuwata, M. Uebori and H. Yamasaki, *J. Chromatogr. Sci.*, 17 (1979) 262.
13 K. Funk and D. Grosjean, *Anal. Chem.*, 53 (1981) 168.
14 W. A. Jacob and P. T. Kissinger, *J. Liq. Chromatogr.*, 5 (1982) 669.

15 G. Chiavari and C. Bergamini, *J. Chromatogr.*, 318 (1985) 427.
16 M. C. Facchini, G. Chiavari and S. Fuzzi, *Chemosphere*, 15 (1986) 667.
17 G. Chiavari, M. C. Facchini and S. Fuzzi, *J. Chromatogr.*, 333 (1985) 262.
18 G. Chiavari, M. C. Facchini and S. Fuzzi, *J. Chromatogr.*, 387 (1987) 459.
19 D. G. Mitchell and J. S. Garden, *Talanta*, 29 (1982) 921.
20 R. V. Smith and P. W. Erhardt, *Atmos. Environ.*, 47 (1975) 2462.
21 J. C. Miller and J. N. Miller, *Statistics for Analytical Chemistry*, Wiley, Chichester, 1984.

Journal of Chromatography, 475 (1989) 353–361
Elsevier Science Publishers B.V., Amsterdam — Printed in The Netherlands

CHROM. 21 579

ISOLATION OF DRUG RESIDUES FROM TISSUES BY SOLID PHASE DISPERSION

STEVEN A. BARKER*, AUSTIN R. LONG and CHARLES R. SHORT
Department of Physiology, Pharmacology and Toxicology, School of Veterinary Medicine, Louisiana State University, Baton Rouge, LA 70803 (U.S.A.)
(First received January 17th, 1989; revised manuscript received April 17th, 1989)

SUMMARY

A new method based on solid phase dispersion of tissue for the subsequent isolation of drugs is reported. By blending tissues with a polymeric phase bound to a solid support one obtains a semi-dry material which can be used as a column packing material from which one can isolate drugs in a stepwise fashion based on the solubility characteristics of the drugs in this matrix. The applicability of this approach for multidrug residue extraction from a single sample is demonstrated for compounds representing the organophosphate, benzimidazole anthelmintic and β-lactam antibiotic drug classes.

INTRODUCTION

The isolation of drug and metabolite residues from tissues is often a complex and laborious task. This is due to the nature of the matrix, containing significant quantities of connective tissues, proteins, lipids, etc., of a compartmentalized and difficult to disrupt nature. Classical methology has, in general, approached the isolation of drugs and metabolites from this matrix in the following manner: (1) mincing and/or mechanical homogenization of the tissue in an aqueous solvent; (2) addition of acids, bases or salts to precipitate protein and remove cellular debris; (3) centrifugation; (4) transfer of the supernatant and adjustment of pH; (5) counter-current extraction of the sample, often leading to intractable emulsions; (6) back-extraction to assist in purification of the sample. Homogenization in and repeated extraction of tissues by organic solvents has also proven to be a useful approach but generates large volumes of solvents which must be evaporated and usually requires back-extraction[1,2].

A portion of this labor may be eliminated by the use of solid phase extraction (SPE) columns wherein a supernatant, obtained as described through step 4 above for example, is added to a SPE column appropriate for the analysis and the compounds of interest are isolated from other sample components based on interaction with the column polymer phase. This process eliminates emulsion formation and much of the sample manipulation required by classical methods (for example see refs. 3–7). How-

0021-9673/89/$03.50

ever, the process of sample homogenization, centrifugation, precipitation, etc., remains labor intensive and contributes, through sample manipulation and the entrainment or electrostatic binding of some drugs to tissue debris, to lower than ideal recoveries.

We present here a new approach to the isolation of drugs and their metabolites from tissues that appears to eliminate many of these difficulties. This approach employs the use of a lipophilic solid phase packing material (C_{18}) to disperse tissues onto a solid support and, thus, to produce a semi-dry, easy to handle column packing material from which individual drugs, a class of drugs or several classes of drugs may be isolated from a single sample. This approach and the underlying concepts are examined using spiked tissues.

EXPERIMENTAL

Bulk C_{18} (octadecylsilane-coated silica bead, 40 μm, end capped, 18% load) SPE column packing material was obtained from Analytichem, Harbor City, CA, U.S.A. The material was washed prior to use by placing 24 g of the packing in an emptied 50-ml Chem-Elut column (Analytichem), attaching the column to a vacuum box and successively adding 50 ml each of HPLC grade hexane, benzene, ethyl acetate and methanol to remove contaminants inherent in manufacture. Tissues (bovine muscle) were obtained from commercial food markets and were kept frozen at -5°C until utilized. Thawed tissues (0.5 g) were injected (10-μl syringe) with drugs dissolved in dimethyl sulfoxide or dimethylformamide at various concentrations for analysis. Blank samples were injected with the corresponding solvents used to dissolve the drug standards.

The following classes of compounds were examined: (1) organophosphates (phenthion, crufomate, coumaphos and famphur); (2) benzimidazole anthelmintics [fenbendazole (FBZ), oxfendazole (FBZSO), sulfonyl FBZ ($FBZSO_2$), *p*-hydroxy-FBZ (FBZOH), mebendazole (MEB), thiabendazole (THI) and albendazole (ALB)]; (3) β-lactam antibiotics (penicillin, ampicillin and cephapirin). The concentrations examined are shown in Table I.

Sample preparation

Samples were prepared in the following manner: Tissue blanks or spiked tissues (0.5 g) were added to 2.0 g of prewashed C_{18} packing material in a glass mortar. The sample was gently blended with a glass pestle for 30 s to produce a semi-dry, homogenous appearing material. This was added to a syringe barrel-column (10 ml) containing a frit (0.45 μm) and 0.50 g of clean C_{18} packing at the bottom. Clean packing (0.25 g) was added to the top of the column and the column was lightly tamped to remove air pockets. A retainer was placed on top of the material and a syringe plunger was used to compress the sample to a volume of 4 ml. A 100-μl disposable pipette tip was attached to the end of the column and the column was placed in a rack, ready for elution (see Fig. 1). The following elution profile, collecting each fraction separately, was performed; hexane, benzene, ethyl acetate and methanol (8 ml of each, respectively). The four fractions were evaporated to dryness under dry nitrogen and an appropriate solvent was added to solubilize the residue. (1) Hexane and benzene fractions, 500 μl *n*-hexane. (2) Ethyl acetate fraction, 50 μl acetonitrile and 450 μl of

TABLE I

LIST OF COMPOUNDS EXAMINED

Range of concentrations (μg/g) analyzed, eluting solvent wherein drug was obtained, correlation coefficients (r, ± standard deviation, S.D., 6 points) for standard curves, recoveries (calculated for all concentrations, ± S.D., inter- and intra-assay variabilities (mean of n determinations). Data were obtained as described in Experimental.

Compound	*Fraction collected*	*Concentration (μg/g) range examined*	*r ± S.D. (n = 4)*	*Recovery ± S.D. (n = 20)*	*Inter-assay variability (n = 20)*	*Intra-assay variability (n = 5)*
Fenthion	Hexane	0.1–2	0.997 ± 0.003	85.62 ± 7.50	8.40	3.01
Coumaphos	Hexane	0.1–2	0.998 ± 0.007	76.57 ± 7.87	20.62	7.08
Famphur	Benzene	0.4	–	82.10 ± 8.78	10.70	5.50
Cruformate	Benzene	0.1–2	0.992 ± 0.006	93.64 ± 6.38	6.82	6.05
Thiabendazole	Ethyl acetate	0.2–4.0	0.9975 ± 0.0019	63.82 ± 9.57	6.91	2.74
FBZSO	Ethyl acetate	0.2–4.0	0.9912 ± 0.0019	82.86 ± 9.48	7.08	3.79
FBZOH	Ethyl acetate	0.2–4.0	0.9900 ± 0.0081	68.35 ± 10.5	13.31	8.18
$FBZSO_2$	Ethyl acetate	0.2–4.0	0.9962 ± 0.0009	85.67 ± 15.04	5.01	3.01
Mebendazole	Ethyl acetate	1.0	–	63.01 ± 4.24	8.10	4.37
Albendazole	Ethyl acetate	0.2–4.0	0.9975 ± 0.0017	73.92 ± 7.99	3.07	3.95
FBZ	Ethyl acetate	0.2–4.0	0.9842 ± 0.0099	73.97 ± 11.82	7.29	5.65
Cephapirin	Methanol	0.2–5	0.992 ± 0.007	72.37 ± 26.48	10.23	6.90
Penicillin	Methanol	0.2–5	0.994 ± 0.005	86.29 ± 6.12	17.88	4.99
Ampicillin	Methanol	2.0	–	59.75 ± 9.75	27.82	8.61

0.05 N phosphoric acid. The sample was vortexed and filtered through a 0.45-μm disposable filter (Bio-Rad). (3) Methanol fraction, 500 μl of 0.05 N phosphoric acid. The resulting suspension was centrifuged (5 min at 17 000 g) and the supernatant was filtered through a 0.45-μm disposable filter. The compounds detected in each fraction are shown in Table I.

Sample analysis

Organophosphates. Analyses were conducted by gas chromatography (GC) using a Varian Vista 6000. Column, DB-5 (J & W Scientific), 25 m × 0.25 mm I.D., 0.25-mm coating. Temperature program, 150°C for 1 min, increasing at 10°C/min to 300°C and holding for 2 min. Splitless injection was used with the purge function being activated at 0.75 min post injection. Injection port temperature, 250°C. Detection was accomplished using a nitrogen–phosphorus detector at 300°C, 6.0 mV at 10^{-12} sensitivity setting.

Benzimidazoles. Analyses were conducted by high-performance liquid chromatography (HPLC) with photo diode-array detection (Hewlett-Packard 1090). Col-

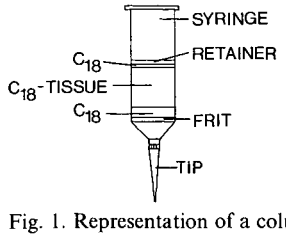

Fig. 1. Representation of a column constructed for conducting analyses as described.

umn, octadecylsilane, 12.5 cm × 0.5 cm I.D., 10 μm particle size (Varian Assoc., MCH-10). Solvent system, isocratic (0.75 ml/min), 0.05 *N* phosphoric acid–acetonitrile (67:33, v/v). Column temperature, 45°C. Detection and quantitation were conducted at 290 nm (20 nm band width, reference spectrum range of 200–350 nm). Full UV spectra were used to determine, in part, the identity of each benzimidazole and the purity of each peak.

β-Lactams. Analyses were conducted as described above using a detection wavelength of 230 nm and a solvent system (isocratic, 1.0 ml/min) of 0.05 *N* phosphoric acid–acetonitrile (80:20) and a column temperature of 35°C.

Recoveries for all compounds were determined from comparison of the data obtained from extracted samples to the data obtained by direct analysis of each compound at the respective concentrations without extraction.

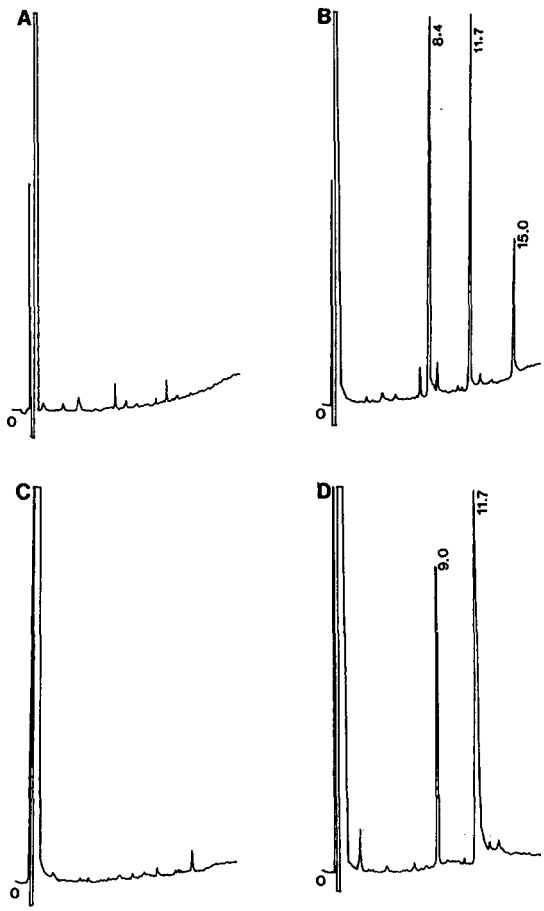

Fig. 2. Representative gas chromatograms from the analysis of the solvent eluate fractions obtained as described in Experimental. (A) Tissue blank, hexane fraction; (B) hexane fraction from tissue spiked with the drugs listed in Table I, showing the presence of phenthion (8.4 min, 0.4 μg/g), famphur (added as an external standard at 0.4 μg/g of sample, 11.7 min) and coumaphos (15.0 min, 0.4 μg/g); (C) tissue blank, benzene fraction; (D) benzene fraction from spiked tissues showing the presence of crufomate (0.1 μg/ml, 9.0 min) and famphur (internal standard, 0.4 μg/ml, 11.7 min).

RESULTS

Table I shows the levels of each compound examined, the fraction in which it was obtained, the recoveries for each compound, correlation coefficients of standard curves and the inter- and intra-assay variability obtained for analyses so conducted. Fig. 2A–D illustrate the GC–nitrogen–phosphorus detection analyses of blank tissue extracts obtained from the hexane and benzene eluates (A and C, respectively) and that obtained for spiked tissues (B and D, respectively). The organophosphates phenthion and coumaphos were detected in the hexane fraction, whereas the compounds crufomate and famphur were observed to elute in the benzene fraction. Famphur was used as an internal standard in these studies, being spiked in all samples prior to extraction at a level of 0.4 μg/g and was added as an external standard for the analysis of the hexane fraction.

The presence of a small quantity of lipid was noted in the hexane and benzene fractions but its presence did not interfere with the analyses of the organophosphates in any manner. Analyses of the hexane and benzene fractions by HPLC gave no indication of the presence of even trace levels of the benzimidazole anthelmintics. No further sample cleanup was required for the analysis of the organophosphates in these fractions.

Analysis of the ethyl acetate fraction by HPLC (Fig. 3A–B) showed that all of the benzimidazoles examined here are eluted in this fraction. The compound mebendazole (MEB) served as an internal standard for these analyses. Under the conditions used no interfering substances were noted, eliminating the need for back-extraction or further cleanup of the sample prior to analysis. Analysis of the ethyl acetate fraction by the HPLC method described for β-lactams gave no indication that the β-lactams

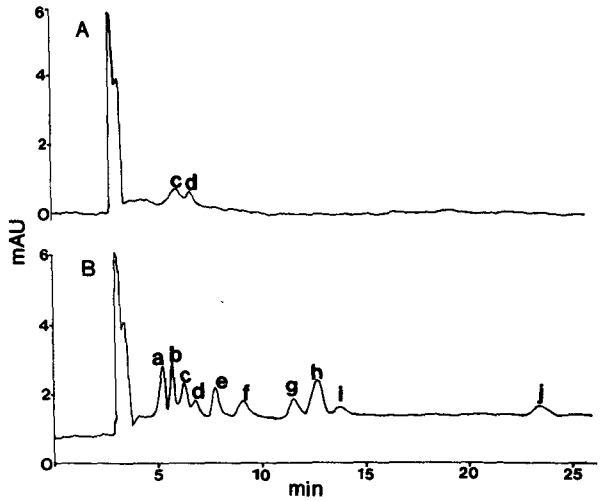

Fig. 3. Representative chromatograms obtained from the HPLC–diode-array analysis of the ethyl acetate eluate fraction of (A) a tissue blank and (B) from that obtained from a spiked (0.2 μg/g) tissue. Peaks: a = THI (retention time 5.2 min), b = unknown sample component (5.6 min), c and d = background contaminants (6.2 and 6.7 min), e = FBZSO (7.7 min), f = FBZOH (9.0 min), g = $FBZSO_2$ (11.5 min), h = MEB, internal standard (1.0 μg/g) (12.5 min), i = ALB (13.6 min), j = FBZ (23.4 min).

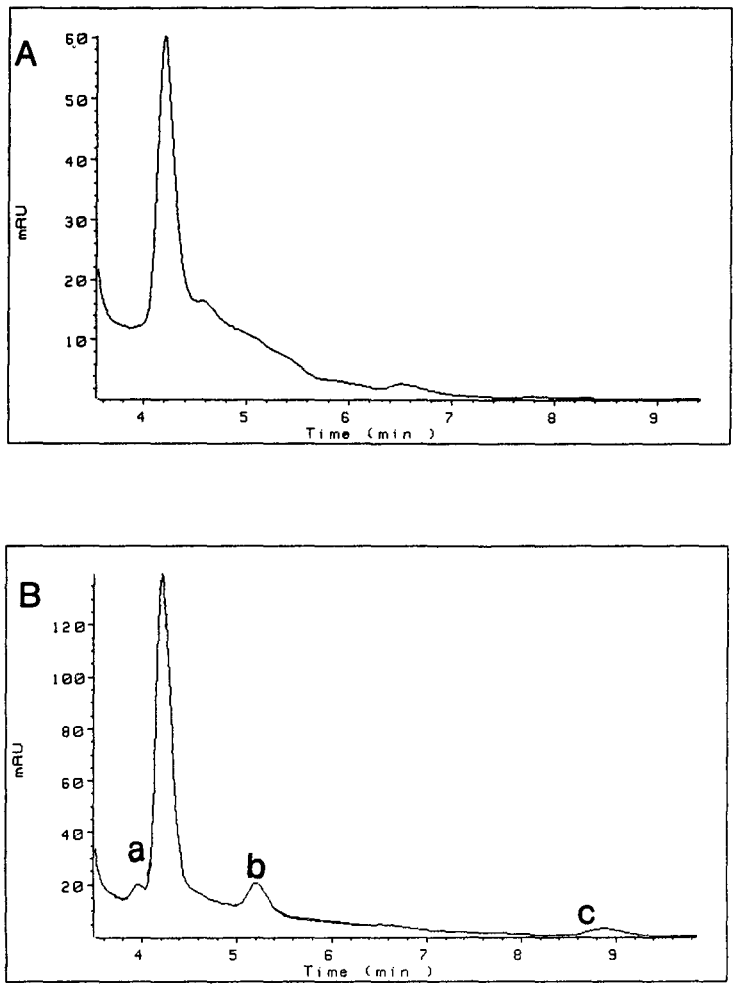

Fig. 4. Representative chromatograms obtained from the HPLC–diode-array analysis of the methanol eluate fraction from (A) a tissue blank and (B) from that obtained from a spiked (1.0 μg/g) tissue sample. Peaks: a = cephapirin; b = ampicillin (internal standard, 2.0 μg/g); c = penicillin.

are eluted in this fraction. Elution of the columns with methanol yielded, upon evaporation, a white residue which, upon testing with ninhydrin, was determined to consist mainly of proteins. Addition of 0.05 *N* phosphoric acid, vortexing and centrifugation (17 000 *g*) of the resulting suspension produced a relatively clean supernatant, low in proteinaceous material. Analysis of the resultant samples by HPLC (Fig. 4A–B) indicated that, for the analysis of penicillin and cephapirin, using ampicillin as an internal standard, no further sample cleanup was necessary. Analysis of the methanol extract by the method for benzimidazoles gave no evidence for the presence of any of the benzimidazoles in this fraction.

DISCUSSION

The application of SPE technology to the isolation of a specific drug or class of drugs from various matrices has grown tremendously in the last decade. Much of this growth has been due to the relative ease of sample handling with samples being poured directly to the column with little or no prior preparation, and the wide range of polymer phases bound to solid supports currently available for a variety of applications. Further, elution profiles for the compound(s) of interest from the matrix employed has a high degree of flexibility and can be readily varied for a given analytical problem. The use of SPE also avoids the formation of emulsions, a common occurrence with counter-current extraction, and, in most cases, reduces the volume of solvents required for efficient isolation of the compound(s) of interest. However, the use of SPE for the isolation of drugs, environmental contaminants and natural compounds from tissues has heretofore required sample homogenization and removal of tissue debris prior to column application. Addition of homogenates directly to the top of a column invariably leads to the cessation of flow from the plugging of the frit or upper layers of the column packing. We have previously reported a partial solution to this problem through the blending of homogenized tissues with diatomaceous earth (DE), for the isolation of the benzimidazole anthelmintics and their metabolites from liver tissue[8] as well as other matrices[9]. By mixing dry DE with homogenized tissues one obtains a semi-dry column packing material from which the benzimidazoles can be eluted with ethyl acetate. Through mixing the homogenate with DE one eliminates the need for precipitation of cellular components and centrifugation of the sample to pellet the debris. Further, the surface area of the sample exposed to the solvent is increased and the entire sample, proteins, connective tissue, etc., is exposed to extractive elution. However, we have observed that the use of DE is limited in application in terms of providing a more generic matrix from which several classes of compounds can be isolated from a single sample. While neutral and moderately polar compounds can be isolated from the DE matrix, compounds of greater polarity (β-lactams for example) are highly retained. This property has advantages of its own but does not truly provide a multi-residue extraction capability.

Classical methodologies have on occasion employed the use of surfactants or detergents to disrupt or, otherwise, dissolve tissue cell membranes so as to liberate internal components of cells and to remove protein and other cellular components from the lipid membrane matrix. The use of such detergents often leads to their interfering in the isolation procedure or subsequent analysis and additional steps must often be taken to assure their removal, which can also be a laborious task. The approach presented here can be seen as an extension of this concept; the use of a lipid solubilizing material to disrupt cell membranes and to, essentially, disperse tissues, but with the dispersing agent being bound to a solid support[10]. We envision this process as disrupting the cell membrane through solubilization of the component phospholipids and cholesterol into the C_{18} polymer matrix, with more polar substituents directed outward, perhaps forming a hydrophilic outer surface on the bead. If this is the case then the process could be viewed as essentially turning the cells inside-out and forming an inverted membrane with the polymer bound to the solid support. This process would create a pseudo-ion exchange/reversed phase for the separation of added components. Thus, the C_{18} polymer would be modified by cell

membrane phospholipids, interstitial fluid components, intracellular components, cholesterol, etc., and would possess elution properties that would be dependent on the tissue used, the ratio of C_{18} to tissue employed and the elution profile performed. We have observed this to be the case in our preliminary examination of other tissues, wherein the elution profile is altered by the type of tissue used and may be further modified by changing the ratio of C_{18} to tissue.

Preliminary examinations of the blended materials by scanning electron microscopy indicate that complete disruption of the cells does occur and that this process of disruption may be further modified by the use of a solvent to blend the tissues, as determined from preliminary studies.

The blending of tissue with C_{18}-coated silica beads by the use of a mortar and pestle proceeds rapidly and smoothly, producing a semi-dry, homogenous appearing material. This has been observed to be the case with either fat, liver or muscle tissues. The mechanical forces applied during homogenization may be sufficient to lead to fracturing of some of the beads. However, to which degree this may occur, it does not appear to effect the flow of solvent through the column or lead to active sites wherein compounds may be lost. The effect of active site formation may not become evident except at lower concentrations (< 100 ng/g) and may limit the extension of this approach.

The range of compounds examined here lends credence to the proposition that this approach may provide a generic technique for multiresidue analysis of drugs and their metabolites in tissues. Further, this approach eliminates the need to conduct tissue homogenization, precipitation, centrifugation, pH adjustments and sample transfers. While examined here as a multiresidue approach, the results imply that such a methodology may be applied to a specific class of compounds or a single compound, whether of exogenous or endogenous origin. We have further observed that tissue "dissolution" onto a solid support can also be conducted with C_3, C_8, C_3 sulfonic, as well as other polymer phases, with the major criterion being the presence of a lipid solubilizing polymer phase. Each of the various phases available may be useful in more specific applications. The concept of blending a sample with a solid support, producing a column packing material unique to each sample matrix, is also feasible, such as the use of microcrystalline cellulose to blend and extract cellulosic materials.

In the case of the drugs examined here, little or no further sample cleanup was necessary prior to analysis. This may, of course, not be the case for other drugs or for other tissues and depends, in part, on the compound to be isolated and the instrumentation used for detection. Nevertheless, a major portion of the isolation of a compound from tissue may be performed by this technique and be followed by appropriate back-extraction or other cleanup steps to sufficiently purify the sample prior to analysis.

The results presented here are based on spiked tissues, much as would be required or obtained for the preparation of standard curves or for conducting recovery studies, for the quantitative analysis of tissue residues incurred from the administration of these drugs. The purpose of the present research was to demonstrate the application of solid phase dispersion for the isolation of the fourteen drugs examined here from a single sample. While the use of tissues from animals actually administered these drugs would be ideal it was outside the scope and practicality of the present

research. Such studies are currently being conducted on these and other classes of compounds seperately, examining incurred residues in muscle as well as other tissues obtained from animals used in drug depletion studies, with the assistance of the United States Food and Drug Administration.

This approach may be applied to the isolation of drugs and their metabolites from edible tissues, as occurs in food safety monitoring programs, for toxicological examination of *post-mortem* tissues for drugs, or for the isolation of naturally occurring compounds from various tissue sources. The adaptability of the method, in terms of the stated variables, should make this approach useful for these and other applications.

ACKNOWLEDGEMENTS

This research was supported by Cooperative Agreements 5V01-FD-01319 and FD-U-000235 with the Food and Drug Administration.

REFERENCES

1 F. Tishler, J. L. Sutter, S. N. Bathish and H. F. Hagman, *J. Agr. Food Chem.*, 16 (1968) 50–53.
2 W. Horowitz, *J. Assoc. Off. Anal. Chem.*, 64 (1981) 104–130.
3 G. Musch and D. L. Massart, *J. Chromatogr.*, 432 (1988) 209–222.
4 F. T. Delbeke, M. Debackere, N. Desmet and F. Maertens, *J. Chromatogr.*, 426 (1988) 194–201.
5 S. H. Wong, *Clin. Chem.*, 34 (1988) 848–855.
6 C. T. Wehr, *J. Chromatogr.*, 418 (1987) 27–60.
7 R. W. Giese, *Clin. Chem.*, 29 (1983) 1331–1343.
8 S. A. Barker, T. McDowell, B. Charkhian, L. Hsieh and C. R. Short, *J. Assoc. Off. Anal. Chem.*, submitted for publication.
9 S. A. Barker, L. Hsieh and C. R. Short, *Anal. Biochem.*, 155 (1986) 112–118.
10 S. A. Barker, A. R. Long and C. R. Short, in W. Huber (Editor), *Proceedings of the 6th Biennial Symposium of the American Academy of Veterinary Pharmacology and Therapeutics, Blacksburg, VA, June 1988*, American Academy of Veterinary Pharmacology and Therapeutics, Blacksburg, VA.

Journal of Chromatography, 475 (1989) 363–372
Elsevier Science Publishers B.V., Amsterdam — Printed in The Netherlands

CHROM. 21 517

PURIFICATION OF RABBIT LIVER ALDEHYDE OXIDASE BY AFFINITY CHROMATOGRAPHY ON BENZAMIDINE SEPHAROSE 6B

J. G. P. STELL*, A. J. WARNE and C. LEE-WOOLLEY
The School of Pharmacy (Pharmaceutical Chemistry), University of Bradford, Bradford BD7 1DP (U.K.)
(First received November 15th, 1988; revised manuscript received March 20th, 1989)

SUMMARY

Highly purified rabbit liver aldehyde oxidase was prepared in high yield using affinity chromatography on Benzamidine Sepharose 6B. Rabbit liver was homogenised, heat treated and ammonium sulphate was added to the supernatant to give a crude preparation of the enzyme. Aliquots of the crude preparation were chromatographed on a Benzamidine Sepharose 6B column at pH 9 and the aldehyde oxidase was eluted by a benzamidine containing buffer. This single affinity step resulted in a 38-fold increase in purity over the crude preparation with an 84% recovery of enzyme activity. Further purification on a Mono Q ion-exchange column gave an additional 1.7-fold increase in specific activity to yield a highly purified preparation of the enzyme. The new method described is considerably simpler and faster than ones hitherto employed and gives a much better yield of the highly purified enzyme.

INTRODUCTION

Rabbit liver is a rich source of the molybdenum containing enzyme aldehyde oxidase (EC 1.2.3.1). Methods usually employed for its isolation and purification are based on that originally described by Rajagopalan *et al.*[1] and subsequently modified by Felsted *et al.*[2]. In the initial steps of this process, the tissue homogenate is subjected to a brief heat treatment, followed by centrifugation and ammonium sulphate precipitation to yield a crude preparation of the enzyme. Up to this stage there is little loss in enzyme activity and an approximately six-fold gain in specific activity. Further purification requires a number of stages, involving acetone precipitation, adsorption onto calcium phosphate gel, ion-exchange and gel permeation chromatography. Application of these techniques yields a product with a further 40–50 fold increase in specific activity and which is regarded as the pure enzyme[2]. However during this long involved procedure approximately 80% of the original enzyme activity present is lost. Recently Yoshihara and Tatsumi[3] improved the yield slightly by including an FMN Sepharose 4B affinity chromatography step in their isolation of the enzyme from guinea pig liver.

The present article describes a rapid affinity chromatography method for the

0021-9673/89/$03.50

purification of rabbit liver aldehyde oxidase in high yield using Benzamidine Sepharose 6B.

EXPERIMENTAL

Materials

The following materials were obtained from the suppliers as listed below. *p*-Dimethylaminocinnamaldehyde (DMAC), benzamidine, *p*-aminobenzamidine, xanthine, xanthine oxidase (grade 1 from buttermilk) from Sigma (Poole, U.K.). Benzamidine Sepharose 6B, Sephadex G-25M, PD-10 columns, Mono Q™ HR 5/5 anion-exchange column, from Pharmacia (Milton Keynes, U.K.). Bio-Rad Protein Assay Kit from Bio-Rad Labs. (Watford, U.K.). Millex-GV 0.22-μm filters, from Millipore (Harrow, U.K.). All buffer solutions used throughout this study were prepared from standard reagent grade chemicals and all contained EDTA at a concentration of 10^{-4} *M*.

Enzyme purification

Preliminary purification steps. Partially purified aldehyde oxidase was prepared from the livers of New Zealand White female rabbits. The livers were weighed then liquidised in an Atomix liquidiser in three volumes of ice-cold 0.1 *M* pH 7 phosphate buffer solution to give a 25% homogenate. The suspension was rapidly heated to 55–60°C on a water bath, maintained at this temperature for 10 min then rapidly cooled in an ice bath and centrifuged (15 000 *g*, 45 min, 4°C). To the clear supernatant, sufficient ammonium sulphate was added to give 50% saturation. The solution was stirred slowly on an ice bath for 20 min and the precipitate obtained collected by centrifugation (6000 *g*, 20 min, 4°C). The precipitate was dissolved in 0.01 *M* pH 7, phosphate buffer using 1 ml of buffer solution for every 10 g of original liver wet weight. The partially purified enzyme prepared in this manner was divided into small portions and frozen in liquid nitrogen until required.

Affinity chromatography on Benzamidine Sepharose 6B. All chromatographic operations were carried out in a refrigerated cabinet maintained at 4–6°C and using a Pharmacia dual pump fast protein liquid chromatography (FPLC) system equipped with a Pharmacia UV-M monitor and FRAC-100 fraction collector. The eluent was monitored at 436 nm.

Portions (1–2 ml) of the partially purified aldehyde oxidase preparation were passed down a small column of G-25M Sephadex (Pharmacia PD-10). Prior equilibration and elution being carried out with a 0.1 *M* pH 9 glycine–sodium hydroxide buffer solution containing 0.1 *M* sodium chloride. This removes contaminating ammonium sulphate and adjusts the sample to the starting conditions for the next operation. The protein containing eluent from the G-25M column was then applied to a column containing Benzamidine Sepharose 6B (60 mm × 15 mm I.D.) which had been equilibrated with the pH 9 glycine buffer–sodium chloride solution. Elution was carried out with the same buffer–sodium chloride solution until a large non-active protein peak had been clearly eluted from the column. The eluting solvent was then changed to one containing 6 m*M* benzamidine in the above pH 9 glycine buffer–sodium chloride solution to elute the aldehyde oxidase. The flow-rate was 1 ml/min throughout and 1-ml fractions were collected. Fractions containing aldehyde

oxidase activity were pooled and treated as below or passed down a PD-10, G-25M Sephadex column to adjust to pH 7 (using 0.067 *M* phosphate buffer) and remove the benzamidine present in the eluent from the affinity column. The purified enzyme preparation was used for further studies immediately or frozen and stored in liquid nitrogen until required.

Ion-exchange chromatography on the Mono Q column. An 11-ml volume of the ammonium sulphate fraction was chromatographed on the benzamidine sepharose column as described above using three separate applications of *ca.* 3.7 ml and the fractions containing aldehyde oxidase activity collected in each case. These were combined and ammonium sulphate added to 50% saturation. The resulting precipitate was collected by centrifugation (7000 *g*, 20 min, 4°C) and dissolved in 1 ml of pH 7 0.067 *M* phosphate buffer. Aliquots of this solution (0.5 ml) were passed down a Sephadex G-25M column (PD-10) to remove excess ammonium sulphate and equilibrate to the starting buffer to be used on the Mono Q column. After filtration (Millex-GV, 0.22 μm) the sample was applied to the Mono Q anion-exchange column via a superloop and eluted as follows. The start buffer (A) consisted of 20 m*M* Bis–Tris propane, pH 6.85. The gradient buffer (B) consisted of 20 m*M* Bis–Tris propane, pH 6.7 containing 1.0 *M* sodium chloride. The flow-rate was 2 ml/min, the temperature was 4°C and detection was performed at 280 nm. Elution profile: 0.0 to 10.5 ml, 0% B, 100% A; 10.5 to 30.5 ml, 0% B to 35% B (linear gradient); 30.5 to 34.5 ml, 35% B to 100% B (linear gradient). Fractions were collected and assayed for enzyme activity and protein content. The UV–VIS absorption spectrum was recorded of fractions containing the major portion of enzyme activity and the A_{280} to A_{450} ratio determined.

Enzyme assay

Aldehyde oxidase activity was determined by adding a suitable volume of the enzyme solution (usually 20 or 50 μl) to DMAC as substrate (25 μM) in pH 7 phosphate buffer (0.067 *M*) and monitoring the decrease in absorbance at 398 nm due to disappearance of the substrate[4]. All determinations were carried out using a Pye Unicam SP8-200 spectrophotometer with cuvettes of 1-cm light path and thermostated at 30°C. Protein estimation was by the method of Bradford[5] using a Bio-Rad Protein Assay Kit in accordance with the manufacturers instructions and bovine serum albumin as standard. Specific activity was calculated as the number of enzyme units per mg of protein, one unit of activity being defined as the amount of enzyme which oxidised 1.0 μmol of *p*-dimethylaminocinnamaldehyde per min at 30°C. A molar extinction coefficient of 30 500 at 398 nm[4] being used to convert absorbance units to moles of substrate oxidised.

Inhibitor studies

The rate of reaction at pH 7 and pH 9 was observed using two different concentrations of DMAC (20 and 10 μM) and several different concentrations of the amidines (0.0625–1.0 m*M*) to ascertain the degree of inhibition produced by the latter compounds. Rates of reaction were also measured over a range of DMAC concentrations (2–20 μM) using a suitable concentration of the amidine in order to determine the type of inhibition occurring at pH 7 and pH 9. The rate of oxidation of xanthine (7, 14 and 28 μM) by xanthine oxidase in the presence and absence of benzamidine (1.0 m*M*) at pH 7, 8 and 9 was determined by following the change in absorbance at 298 nm which accompanies the oxidation of xanthine to uric acid[6].

Polyacrylamide gradient gel electrophoresis

Polyacrylamide gel electrophoresis (PAGE) was carried out on Pharmacia "PhastGel" Gradient 8–25 ultrathin microelectrophoresis gels using a Pharmacia "Phastsystem" in accordance with the manufacturer's instructions. Samples of the purified material obtained from the benzamidine Sepharose column and the final preparation from the Mono Q column were run on both native and sodium dodecyl sulphate (SDS)-PAGE along with a sample of the crude ammonium sulphate preparation (native PAGE) and molecular weight marker proteins (SDS-PAGE). The samples to be run on SDS-PAGE were first diluted with an equal volume of a solution containing 5% SDS and 10% β-mercaptoethanol and then placed on a boiling water bath for 5 min. The amount of material applied to the gels was in the range 165–480 ng of protein for the purified preparations and 5 μg for the crude ammonium sulphate preparation. On completion of electrophoresis the gels were stained with Pharmacia PhastGel Blue R (Coomassie Brilliant Blue R) to locate the proteins.

RESULTS AND DISCUSSION

Benzamidine Sepharose 6B has been used as an affinity chromatography medium for the purification of trypsin[7] and a number of aromatic amidine compounds have been shown to be potent inhbitors of this enzyme[8,9]. Benzamidine bears some structural resemblance to certain α-aminoazaheterocyclic compounds which we have found to be competitive inhibitors of aldehyde oxidase, *e.g.*, 2-aminoquinoline[10,11], 1-aminoisoquinoline and 6-aminophenanthridine[11]. A study was therefore under-

TABLE I

INHIBITION OF ALDEHYDE OXIDASE CATALYSED OXIDATION OF DMAC BY BENZAMIDINE (BA) AND *p*-AMINOBENZAMIDINE (PABA) AT pH 7 AND pH 9

pH	*DMAC* (μM)	*Percentage inhibition*					K_i[a] (M)
		[BA] (mM)					
		0.0625	*0.125*	*0.25*	*0.5*	*1.0*	
9	20	–	22	35	52	68	$1.65 \cdot 10^{-4}$
	10	–	28	43	61	76	
7	20	–	5	10	19	32	$1.04 \cdot 10^{-3}$
	10	–	7	13	23	38	
		[PABA] (mM)					
		0.0625	*0.125*	*0.25*	*0.5*	*1.0*	
9	20	22	37	54	70	–	$8.0 \cdot 10^{-5}$
	10	30	46	63	77	–	
7	20	4	10	18	31	–	$5.75 \cdot 10^{-4}$
	10	6	13	23	37	–	

[a] Inhibitor (I) constant (K_i), calculated from Dixon ($1/v$:[I]) plots. v is the rate of oxidation of DMAC in μmol l^{-1} min^{-1}.

taken to see if benzamidine possessed any inhibitory properties towards aldehyde oxidase and to investigate the possible application of Benzamidine Sepharose 6B as an affinity chromatography material for the purification of this enzyme. The less readily

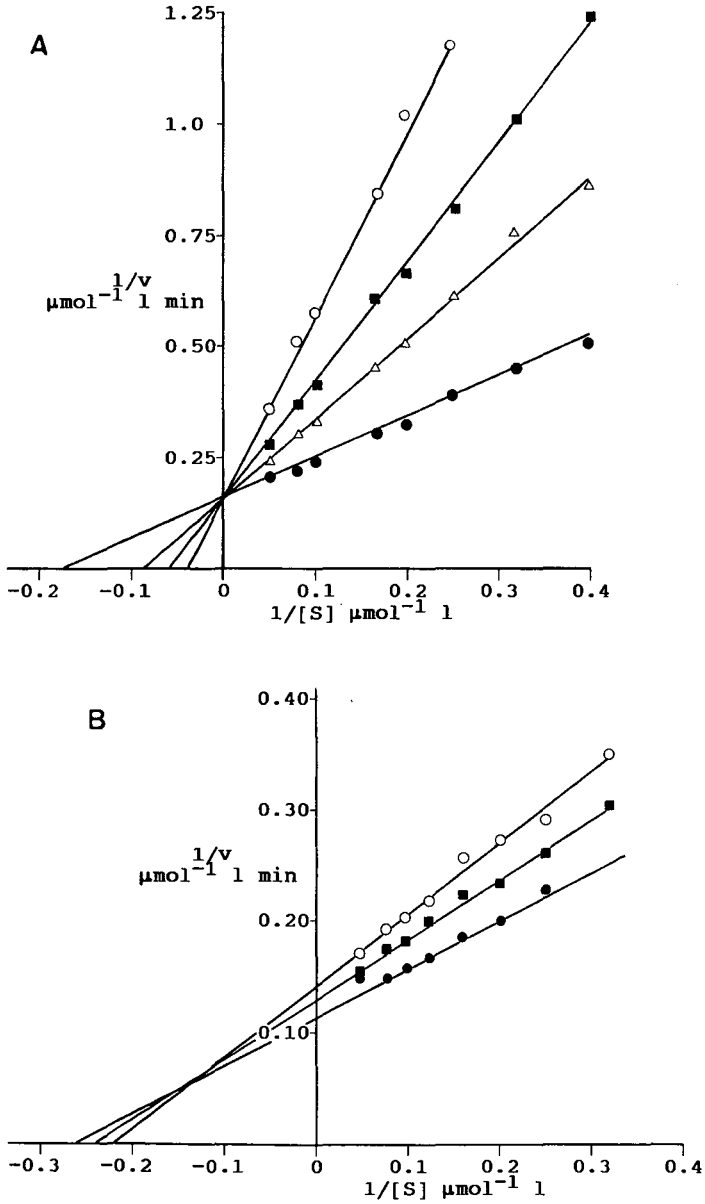

Fig. 1. Double reciprocal plots showing the effect of different concentrations of benzamidine on the rate of oxidation of DMAC by aldehyde oxidase. (A) Reaction carried out in pH 9, 0.1 *M* glycine–sodium hydroxide buffer in the presence of 0.00 (●); 0.125 (△); 0.25 (■); and 0.5 m*M* (○) benzamidine. (B) Reaction carried out in pH 7, 0.067 *M* phosphate buffer in the presence of 0.00 (●); 0.50 (■); and 1.00 m*M* (○) benzamidine.

available and considerably more expensive *p*-aminobenzamidine, which is the actual ligand on the Sepharose 6B, was also tested but to a more limited extent.

Preliminary experiments were carried out using the partially purified aldehyde oxidase from the ammonium sulphate precipitation stage to ascertain the effect different concentrations of the two benzamidines had on the rate of oxidation of DMAC by the enzyme between pH 7 and pH 9.

The enzyme is reasonably stable over this pH range and DMAC which is an excellent substrate with high extinction coefficient can also be used at these pH values. The results presented in Table I, show benzamidine to be an effective inhibitor of aldehyde oxidase with the inhibitory properties being much more pronounced at the higher pH values.

Kinetic determinations showed that at pH 9 the inhibition was purely competitive in nature (Fig. 1A) whereas at pH 7 a mixture of competitive and non-competitive inhibition appeared to be occuring (Fig. 1B).

The behaviour of *p*-aminobenzamidine was similar in all respects to that of benzamidine but was approximately twice as effective with respect to its inhibitory properties (Table I). Benzamidine was also tested to see if it had any inhibitory properties towards the closely related xanthine oxidase but no inhibition was observed over the pH range 7 to 9 in the presence of 1 m*M* benzamidine. These results suggested that Benzamidine Sepharose 6B ought to be an eminently suitable affinity chromato-

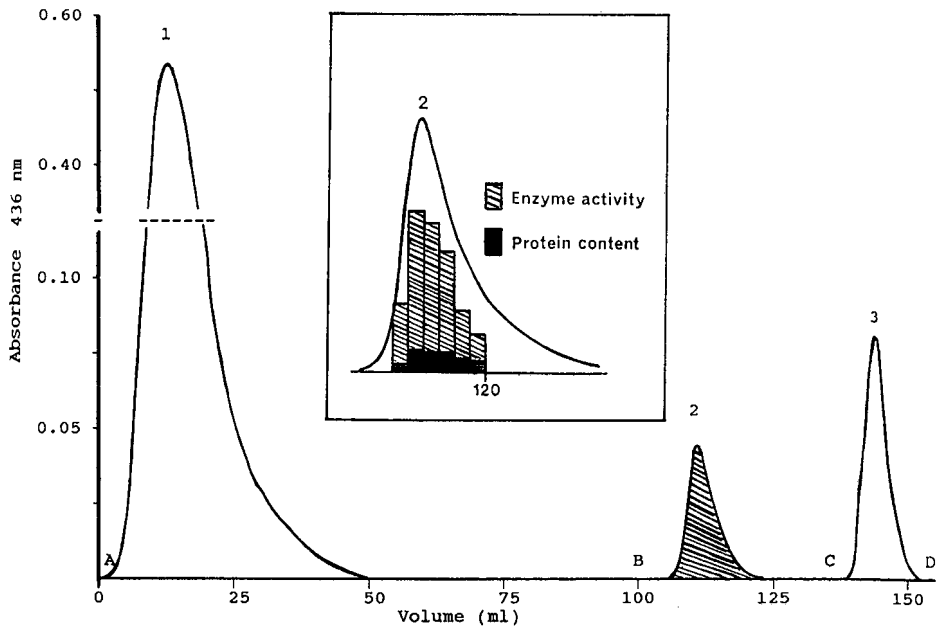

Fig. 2. Elution profile of crude ammonium sulphate fraction from rabbit liver on Benzamidine Sepharose 6B. Shaded area (peak 2) indicates enzyme activity. Eluting buffers: A to B, pH 9, 0.1 *M* glycine buffer + 0.1 *M* sodium chloride. B to C, as A to B + 6 m*M* benzamidine. C to D, pH 4, 0.067 *M* phosphate buffer + 0.5 *M* sodium chloride. Inset box: peak 2 (scale enlarged) showing levels of enzyme activity and protein content of fractions, conditions as in text.

graphy material for the purification of aldehyde oxidase. The affinity of material for the enzyme would be expected to be reasonably high at pH 9 but the binding not being so tight as to make displacement from the affinity ligand difficult, *e.g.*, either by lowering the pH or incorporating benzamidine in the eluting buffer. To test this hypothesis trial experiments were performed whereby small samples of the partially purified aldehyde oxidase in pH 9 buffer were applied to a short column containing a little Benzamidine Sepharose 6B (*ca.* 1 ml volume of the gel). On carrying out elution with a pH 9 glycine buffer–sodium chloride solution a considerable amount of non-active protein material passed rapidly through the column while all the aldehyde oxidase activity was retained on the affinity gel. It was found that the enzyme could be displaced from the gel by lowering the pH to 6.5 with 0.1 *M* phosphate buffer or more efficiently by incorporating benzamidine (6 m*M*) in the pH 9 eluting solution. A larger column of the Benzamidine Sepharose 6B was therefore prepared and samples of the partially purified aldehyde oxidase preparation chromatographed as described in the experimental section. The elution profile for a typical separation is shown in Fig. 2. On assaying the fractions it was found that virtually all the enzyme activity resided in the second smaller peak that was eluted by the benzamidine containing buffer. Owing to the strong UV absorption of benzamidine at 280 nm it was necessary to monitor the eluent at 436 nm where the enzyme still has a reasonable absorption and the benzamidine does not interfere. The contaminating benzamidine was easily removed from fractions containing enzyme activity by passage through a short column of G-25M sephadex. Specific activity measurements on these active fractions indicated a 38-fold increase in purification over the ammonium sulphate preparation (Table II). This high degree of purification had not only been achieved in essentially one relatively simple chromatographic operation but with a striking 84% recovery of enzyme activity. However despite the high specific activity, spectroscopic measurements indicated that some contaminating protein material was still present as the A_{280} to A_{450} ratio was somewhat higher at approximately 8.5 than the value of 5.2–5.3 quoted by Felsted *et al.*[2] for the exhaustively purified enzyme. Further purification was therefore attempted using a Mono Q anion-exchange column as described in the Experimental section. The elution profile is shown in Fig. 3. All the aldehyde oxidase activity was present in the large peak eluting between 24 and 33% concentration of the gradient eluting buffer B. The recovery of enzyme activity was 83% and the specific activity had increased to 2.83 units per mg of protein, *i.e.*, by a factor of 1.7 over the product from the affinity column, and consequently raised the purification factor to

TABLE II

PURIFICATION OF ALDEHYDE OXIDASE FROM RABBIT LIVER ON BENZAMIDINE SEPHAROSE 6B

Fraction	*Volume (ml)*	*Total protein (mg)*	*Protein concentration (mg/ml)*	*Total activity (units)*[a]	*Specific activity (units/mg)*	*Yield (%)*	*Purification factor*
Crude ammonium sulphate	4.65	165	36	7.28	0.044	100	1
Benzamidine Sepharose purified	22	3.36	0.15	6.10	1.68	84	38

[a] One unit of activity = amount of enzyme that converts one μmol of DMAC per min at pH 7 at 30°C.

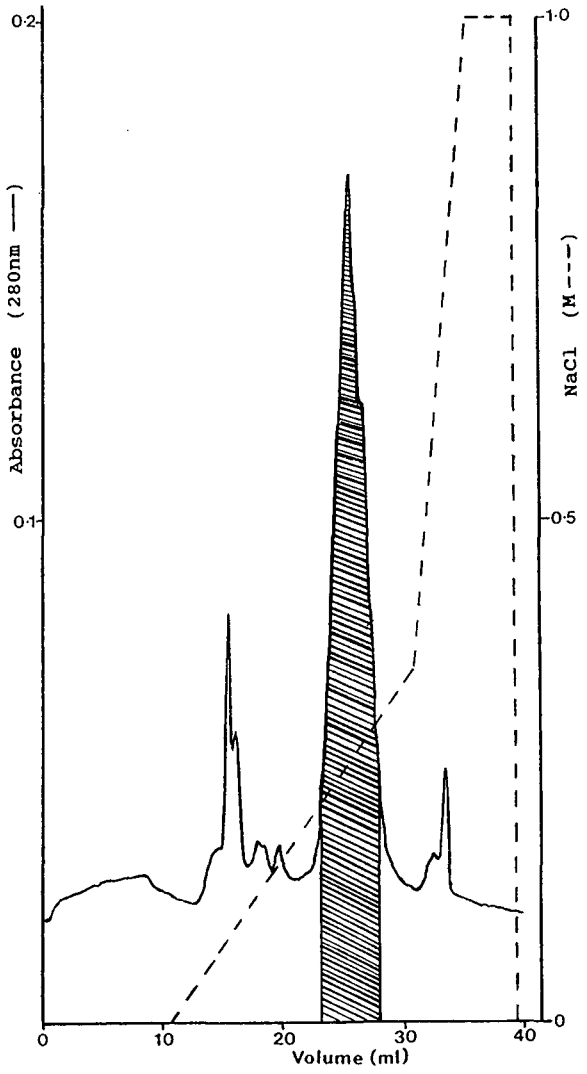

Fig. 3. FPLC on the Mono Q HR 5/5 anion-exchange column of active material from Benzamidine Sepharose 6B affinity column. Shaded area indicates enzyme activity.

a value of 64 when compared to the crude ammonium sulphate preparation. As the latter shows an approximately 6-fold increase in specific activity with respect to the initial homogenate[1,2] then the overall purification in the present study is of the order of 350–400 fold.

Native polyacrylamide gel electrophoresis (Fig. 4a) of the Mono Q purified material showed only a single band even at high sample loading (480 ng), corresponding in position to a band present in the crude ammonium sulphate preparation. The material from the benzamidine sepharose column showed a similar

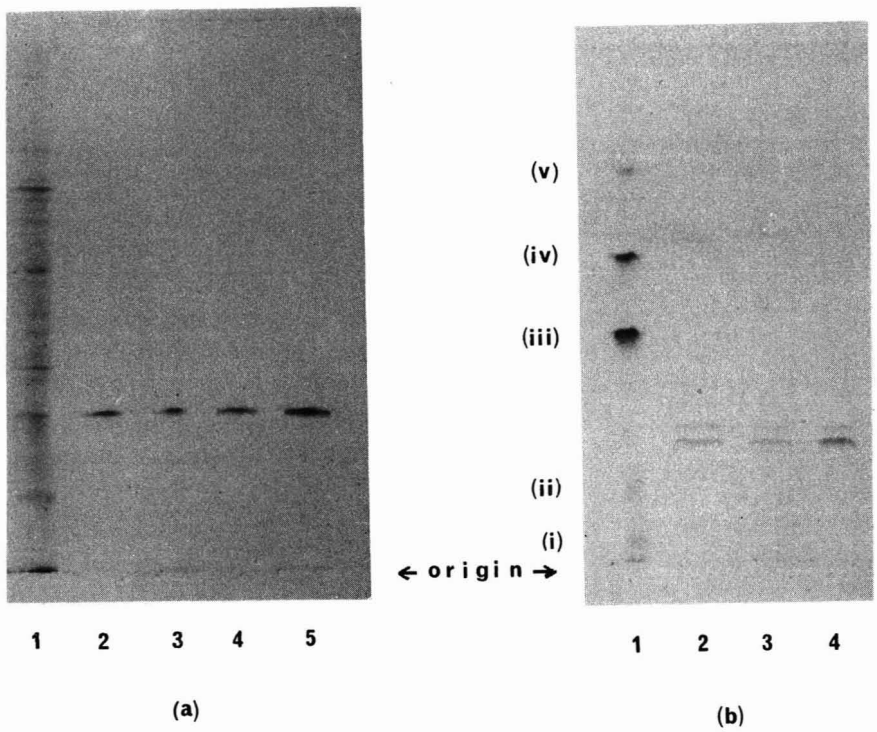

Fig. 4. (a) Native PAGE. Lane 1, crude ammonium sulphate preparation (5 μg). Lanes 2 and 3, material eluted from Benzamidine Sepharose 6B column (2 and 3 = 330 ng). Lanes 4 and 5, material eluted from Mono Q column (4 = 240 ng; 5 = 480 ng). (b) SDS-PAGE. Lane 1, marker proteins; (i) thyroglobulin (330 000), (ii) ferritin (220 000), (iii) albumin (67 000), (iv) lactate dehydrogenase (36 000), (v) ferritin (18 500). Subunit molecular weight in parentheses. Lanes 2 and 3, material eluted from the Benzamidine Sepharose 6B column (2 and 3 = 165 ng). Lane 4, material eluted from Mono Q column (240 ng).

intense band in the same position, but in this sample an additional faint band at $R_F \approx 0.7$ was also present.

On electrophoresis in the presence of SDS (Fig. 4b) both of the purified preparations showed a major band corresponding to a subunit molecular weight of approximately 144 000 and a minor band at approximately 130 000 (estimated from log MW to R_F plot of the marker proteins). These results are very similar to those obtained by Yoshihara and Tatsumi[3] for purified guinea pig aldehyde oxidase. No other bands were present in the Mono Q preparation but the material from the benzamidine sepharose column showed an additional four very faint bands of lower molecular weight material. Further confirmation of the high degree of purity of the aldehyde oxidase prepared in the above manner is afforded by the absorption spectrum (Fig. 5) and a value of 5.4 for the A_{280}/A_{450} ratio, both of which are comparable to those reported by Felsted *et al.*[2] for the pure enzyme.

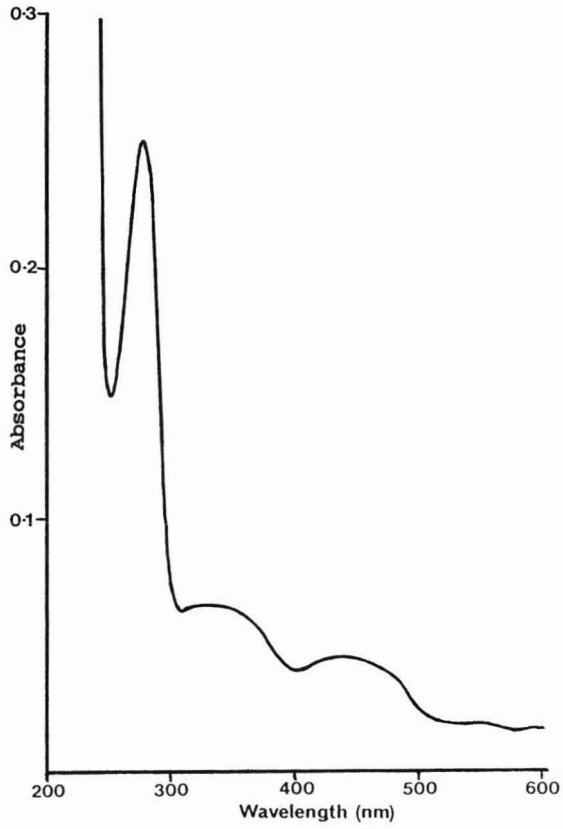

Fig. 5. Absorption spectrum of the purified aldehyde oxidase eluted from the Mono Q column.

CONCLUSION

The work presented in this paper describes a new affinity ion-exchange chromatography method for the isolation of aldehyde oxidase from rabbit liver. The method has the advantage of being considerably simpler and faster than methods hitherto employed and produces a much higher yield of the highly purified enzyme.

REFERENCES

1 K. V. Rajagopalan, I. Fridovich and P. Handler, *J. Biol. Chem.*, 237 (1962) 922.
2 R. L. Felsted, A. E. Chu and S. Chaykin, *J. Biol. Chem.*, 248 (1973) 2580.
3 S. Yoshihara and K. Tatsumi, *Arch. Biochem. Biophys.*, 242 (1985) 213.
4 J. Kurth and A. Kubiciel, *Biomed. Biochim. Acta*, 43 (1984) 1223.
5 M. Bradford, *Anal. Biochem.*, 72 (1976) 248.
6 L. Greenlee and P. Handler, *J. Biol. Chem.*, 239 (1964) 1090.
7 H. F. Hixson and A. Nishikawa, *Arch. Biochem. Biophys.*, 154 (1973) 501.
8 M. Mares-Guia and E. Shaw, *J. Biol. Chem.*, 240 (1965) 1579.
9 J. D. Geratz, *Experentia*, 25 (1969) 1254.
10 R. Banoo, *Ph.D. Thesis*, University of Bradford, Bradford, 1980, p. 171.
11 J. G. P. Stell and B. Fisher, in preparation.

Journal of Chromatography, 475 (1989) 373–379
Elsevier Science Publishers B.V., Amsterdam — Printed in The Netherlands

CHROM. 21 555

EXTRACTION OF BUTYLTIN SPECIES AND THEIR GAS CHROMATOGRAPHIC DETERMINATION AS CHLORIDES IN A SEDIMENT CERTIFIED REFERENCE MATERIAL FOR TRACE METALS, PACS-1[a]

K. W. M. SIU*, P. S. MAXWELL and S. S. BERMAN
Division of Chemistry, National Research Council of Canada, Montreal Road, Ottawa, Ontario K1A 0R9 (Canada)
(Received April 6th, 1989)

SUMMARY

A gas chromatographic method has been developed for the determination of butyltin species in sediment. The butyltin species are separated as chlorides by using a DB-608 open tubular column after their extraction from the sediment using a combination of sonication in methanolic HCl and solvent extraction. Two extractants are possible: toluene–isobutyl acetate–tropolone and hexane–isobutyl acetate. The efficiencies for the first extractant are: tributyltin, 94.4 ± 4.7%; dibutyltin, 94.9 ± 2.2%; and monobutyltin, 86.3 ± 4.2%. The absolute detection limits are about 30 pg tin. Using a 1-g sample, the relative detection limits are about 30 ng tin per g sediment. These may be lowered to 3 ng tin per g by starting with a 4-g sample and adding a concentration step. The reference material PACS-1 was found to contain 1.08 ± 0.31 μg tin per g of tributyltin and 1.13 ± 0.30 μg tin per g of dibutyltin.

INTRODUCTION

Due to their significant environmental impact, the butyltin species are under intense scrutiny. Gas chromatography (GC) with flame photometric or electron-capture detection is often the analytical method of choice because of its speciation capability, high sensitivity and general availability. Although many versions of butyltin species extraction from complex environmental matrices have been developed, they almost always involve releasing and extracting the butyltin species into an organic solvent as chlorides and/or tropolone complexes[1–9]. It is general belief that the butyltin chlorides are not sufficiently volatile or inert for successful GC, and derivatization to more inert forms such as hydrides[3–6,9] and tetraalkyl forms[1,2] is necessary. This belief appears justified considering the proliferation of reports on hydridization and Grignard reactions[1–6,9].

Yet, some of the earliest work on the GC of organotin species was on the separation of organotin halides[10,11]. It was evident that organotin halides with alkyl

[a] NRCC 30230.

groups containing a few carbon atoms, such as butyltin halides, are volatile enough for GC. However, it was also quite apparent that on-column adsorption and degradation, particularly those of the more ionic mono- and dibutyltin chlorides, were appreciable. These effects could be minimized by extensive silylation/deactivation carried out frequently[11]. The GC of organotin halides took a quantum leap after the significance of hydrogen halide doping was realized[7,8,12,13]. Flinn and co-workers[12,13] added hydrogen halide, either in solution or gaseous form, into the carrier gas stream of the chromatograph. A hydrogen halide steady state established between the gas and liquid phases. Organotin compounds injected were derivatized, on-column, to the halides and eluted as such. Degradation of the organotin halides was minimized by the presence of a large excess of hydrogen halide which shifted the equilibrium in favour of organotin halides. This allowed the separation of sub-microgram amounts of mono-, di- and tributyltin halides and detection of 1 pg of tripropyltin and tributyltin chloride[12,13].

This study aims to: (1) test the chromatography of butyltin halides on the more inert and yet more delicate open tubular columns, (2) apply this chromatographic technique to the determination of butyltin species in a sediment sample, and (3) develop compatible extraction techniques for butyltin species.

EXPERIMENTAL

Instrumentation

A Varian VISTA 6000 gas chromatograph modified for megabore open tubular columns was used. Two columns were tried; these were DB-1 (J&W Scientific, 100% methylsilicone) and DB-608 (also from J&W Scientific, 40–45% phenyl-, 60–55% methylsilicone). Most work, however, was done on the DB-608 column. Nitrogen (Linde, ultra-high-purity grade) further purified by passing sequentially through a molecular sieve 5A trap and a heated oxygen scavenger unit (Supelco) was used as carrier gas at 16 ml/min. The injector temperature was 200°C. To separate the butyltin chlorides on the DB-608 column, the following temperature program was used: initial 80°C, hold 2 min; temperature ramp 10°C/min; final 135°C, hold 4 min. For the analysis of sediment extracts, a second temperature gradient of 10°C/min to 180°C for 4 min was added to elute concomitant sulphur compounds. The detector was the Varian dual-flame photometric detector. For tin detection, optimal response was obtained with single flame operation. In this mode, no air was supplied to the lower burner and only the upper burner was lit. The column effluent mixed with hydrogen (104 ml/min) at the base of the flame jet and burned in an atmosphere of air (154 ml/min). The red SnH emission was monitored using a 40-nm band pass filter centred on 600 nm (Ealing Optics). The photomultiplier current was processed by the Varian dual-flame photometric detector electrometer whose output was smoothed by a long-pass filter (Spectrum 1021A) before recorded by a strip-chart recorder (Fisher Recordall 5000).

Reagents

Butyltin compounds were purchased (from Alfa). Their purity was confirmed by high-performance liquid chromatography–inductively coupled plasma mass spectrometry (HPLC–ICPMS). Solutions of these were usually made up in methanol and

refrigerated when not in use. Sediment samples were certified reference materials PACS-1 and MESS-1 (National Research Council of Canada). PACS-1 was collected from Esquimalt Harbour in British Columbia, while MESS-1 was from the Miramichi River estuary in New Brunswick.

Extraction of sediment samples

A 1-g amount of sediment plus any butyltin chloride spikes was sonicated with 2 ml of 10 *M* hydrochloric acid and 1 ml of methanol for 1 h. The suspension was then extracted with 1 ml of hexane–isobutyl acetate (80:20), or 1 ml of toluene–isobutyl acetate (80:20) containing 1.5% (w/v) tropolone after addition of 7 ml of water. Both extractions required vigorous mechanical shaking. Maximum transfer of butyltin chlorides required about 10 min of shaking for hexane–isobutyl acetate while 1 h for toluene–isobutyl acetate–tropolone. The phases were separated by centrifugation at about 700 *g* for 10 min. A 1 μl volume of the water immiscible phase was injected into the chromatograph.

HCl doping

Hydrochloric acid was introduced into the GC system by either discrete injections of 0.5 *M* HCl in methanol or continuous doping of a few ml/min of 1% HCl gas in nitrogen. For HCl solution injections, the gas chromatograph was conditioned by a daily 3-μl injection prior to analysis. To ensure proper butyltin chloride elution, 1 μl of HCl solution was co-injected with every sample injection.

RESULTS AND DISCUSSION

GC of butyltin chlorides

Fig. 1 shows a typical separation of butyltin trichloride, dibutyltin dichloride and tributyltin chloride, each containing 2 ng of tin, using the more polar DB-608 column. The DB-1 column yields a comparable pattern. Without HCl treatment, tributyltin chloride, the most covalent species, elutes with no apparent degradation; the dibutyltin dichloride peak exhibits significant tailing and is about 50% its normal

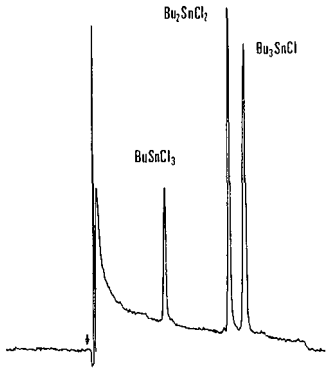

Fig. 1. Temperature programmed separation of butyltin trichloride, dibutyltin dichloride and tributyltin chloride standards, each containing 2 ng of tin (Bu = butyl). The arrow indicates the point of injection. Conditions are given in the Experimental section.

height on the DB-608 column, while only about 10% on the DB-1 column; butyltin trichloride does not elute on either column. With HCl, all species elute as almost symmetrical peaks.

The butyltin chloride peaks as eluted by using temperature programming are expected to be similar in height in the absence of degradation or irreversible adsorption assuming that their carbon quenching effects on the tin emission are comparable. The fact that the butyltin chloride peak is only about 50% of the dibutyltin dichloride and tributyltin chloride peaks, which are comparable, indicates that some degradation and/or irreversible adsorption of that species takes place even with HCl doping. This percentage is variable and has been seen to change from 30 to 100%. Generally, it is higher when the column is new and presumably more inert, and becomes progressively lower as the column ages. As well, it also appears somewhat influenced by the sample matrix. The magnitude of these effects, however, are deemed tolerable for quantitation of relatively high concentrations of butyltin trichloride using standard additions method.

The effectiveness of gas phase and solution phase HCl doping are rated similar. However, in HCl solution introduction, no hardware modification is necessary. Further, the acid is only added with each sample injection resulting in less overall stress on the GC system. The open tubular columns hold well in the presence of HCl. Our last DB-608 column withstood approximately 2000 injections over a span of six months. As well, the gas chromatograph exhibits no ill-effects from HCl use.

The flame photometric detector is a sensitive detector for tin. Our detection limit (signal to noise = 2, SnH emission centred on 600 nm) is about 30 pg tin. Optimal sensitivity was obtained under single flame operation. An attempt to improve the detection limit by using a more red sensitive photomultiplier tube (Hamamatsu R928) was unsuccessful, indicating that the limiting noise arose from the flame. No efforts were made to use the more sensitive but less reproducible blue tin emission[14].

Extraction of butyltin species as chlorides from sediments

In the earlier phases of this study, various published sediment extraction methods[1,5] were tried and found unquantitative for MESS-1 and PACS-1. The extraction methods reported here, whose emphases are on extraction efficiency, speed and simplicity, were subsequently developed for these two sediments. The toluene–isobutyl acetate–tropolone procedure is preferred as it extracts all three butyltin species efficiently —di- and tributyltin quantitatively while monobutyltin almost quantitatively (Table I). The efficiencies were determined by spiking micrograms per gram amounts of butyltin chlorides to MESS-1, which contains negligible amounts of butyltin species. The hexane–isobutyl acetate combination extracts 60–70% of the more nonpolar dibutyltin dichloride and tributyltin chloride, but only a small fraction of butyltin trichloride.

Sonication of the sediment with methanolic HCl releases butyltin most probably as chlorides. However, a significant fraction of tributyltin appears to sorb on the sediment —removal of the sediment phase prior to extraction resulted in low tributyltin recovery. Inclusion of the methanolic HCl digestion step is imperative, without which very low recovery of butyltin ensues. Maximum extraction of butyltin chlorides occurs under relatively high hydrochloric acid concentration for hexane–isobutyl ace-

TABLE I

EXTRACTION EFFICIENCIES FOR THE TOLUENE–ISOBUTYL ACETATE–TROPOLONE PROCEDURE

Species	*Recovery*[a]
Tributyltin	94.4 ± 4.7[b]
Dibutyltin	94.9 ± 2.2
Monobutyltin	86.3 ± 4.2

[a] $n = 4$.

[b] Standard deviation.

tate while under relatively low concentration for toluene–isobutyl acetate–tropolone. For the former extractant, hydrochloric acid is required to shift the equilibria to favour undissociated butyltin chlorides which are extracted; for the latter, relatively low acidity favours formation of the tropolone complexes of butyltin which dissolve preferentially in toluene. Of the two extractants, hexane–isobutyl acetate is the more efficient getter of tributyltin. Maximum transfer of tributyltin requires only about 10 min of vigorous shaking for hexane–isobutyl acetate while about 1 h for toluene–isobutyl acetate–tropolone. On the contrary, transfer of butyltin to toluene–isobutyl acetate–tropolone as well as dibutyltin to both extractants is rapid.

Determination of butyltin species in sediments

A 1-μl volume of the extractant was injected into the chromatograph for analysis. Aside from causing the build-up of a black deposit on the injector lining which required periodic cleaning, introduction of the crude extracts did not appear to degrade chromatography or column performance. Owing to the selectivity of the dual-flame photometric detector, very few non-tin peaks were seen: MESS-1 had none,

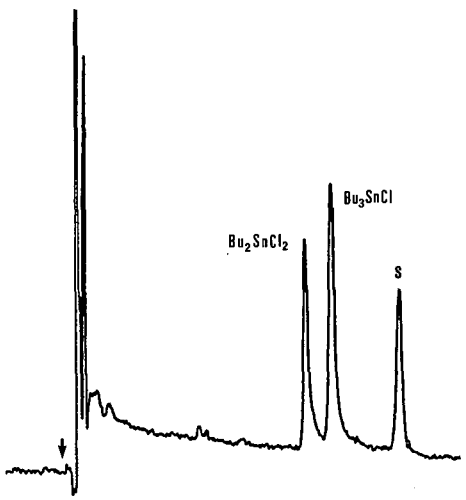

Fig. 2. Typical chromatogram of a toluene–isobutyl acetate–tropolone extract of PACS-1 showing the presence of di- and tributyltin. S = Concomitant sulphur compound.

TABLE II

DETERMINATION OF DIBUTYLTIN AND TRIBUTYLTIN IN PACS-1

Values are ± standard deviations. Number of replicate analyses is given in parentheses.

Technique	*μg tin per g dry weight*	
	Dibutyltin	*Tributyltin*
GC–FPD		
hexane–isobutyl acetate	1.07 ± 0.31 (8)	1.14 ± 0.27 (8)
toluene–isobutyl acetate–tropolone	1.08 ± 0.31 (6)	1.11 ± 0.33 (7)
HPLC–ICPMS	1.18 ± 0.15 (9)	1.61 ± 0.27 (8)
ISMS–MS		1.29 ± 0.07 (5)
Certified value	1.16 ± 0.18[a]	1.27 ± 0.22[a]

[a] 95% confidence interval.

while PACS-1 exhibited three sulphur-containing peaks all eluting later than the butyltin chlorides and causing no interference. There is little doubt that the butyltin species are injected as either chlorides or tropolone complexes into the chromatograph. The exact form matters little as any non-chloride butyltin species are rapidly derivatized by HCl *in situ* to butyltin chlorides[12,13].

MESS-1 contains no detectable butyltin species (less than 30 ng tin per g) and was studied here only for use as a sediment matrix for assessing butyltin extraction efficiencies. On the contrary, PACS-1 contains significant amounts of dibutyltin and tributyltin (Fig. 2). Quantitation of these two species was carried out by using standard additions employing both sediment extraction methods, whose results are comparable. These and results obtained by using HPLC–ICPMS and ion spray mass spectrometry–mass spectrometry (ISMS–MS) are listed in Table II. Agreement amongst the different methods is good.

Improving relative detection limits

The relative detection limits for dibutyltin and tributyltin in this method are about 30 ng tin per g sediment, sufficiently sensitive for PACS-1. For the analysis of

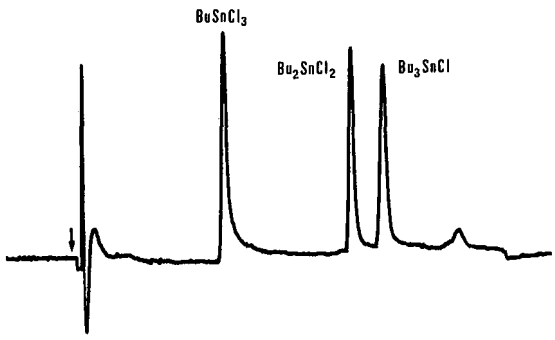

Fig. 3. Chromatogram of a toluene–isobutyl acetate–tropolone extract of MESS-1 spiked with 0.1 μg tin per g of butyltin chlorides.

sediments containing lower butyltin concentrations, the relative detection limits may be lowered by inserting a concentration step. This is demonstrated as follows. A 4-g sample of MESS-1 spiked with butyltin species at levels of 0.1 μg tin per g sediment was extracted in the usual fashion with 4 ml of toluene–isobutyl acetate–tropolone. The extract was evaporated to dryness with a stream of nitrogen and dissolved in 40 μl of methanol. A 1-μl volume of this solution was injected for analysis. Fig. 3 shows a typical chromatogram. The relative detection limits have been lowered to 3 ng tin per g sediment.

CONCLUSION

The open tubular columns tested work well for GC of butyltin chlorides. A method for determining butyltin species in sediment has been developed. The butyltin species are extracted in an efficient procedure as either chlorides or tropolone complexes, which are derivatized on column to chlorides. The accuracy of this method is assured by two other independent techniques.

ACKNOWLEDGEMENTS

We thank B. Kinsella, Curtin University of Technology, Bentley, Australia, for initiating extraction studies on sediments, and W. A. Aue, Dalhousie University, Halifax, Canada, as well as J. H. Weber, University of New Hampshire, Durham, NH, U.S.A., for helpful discussions on various aspects of butyltin species determination.

REFERENCES

1 R. J. Maguire, *Environ. Sci. Technol.*, 18 (1984) 291.
2 M. D. Mueller, *Fresenius' Z. Anal. Chem.*, 317 (1984) 32.
3 Y. Hattori, A. Kobayashi, S. Takemoto, K. Takami, Y. Kuge, A. Sugimae and M. Nakamoto, *J. Chromatogr.*, 315 (1984) 341.
4 T. Tsuda, H. Naganishi, T. Morita and J. Takebayashi, *J. Assoc. Off. Anal. Chem.*, 69 (1986) 981.
5 L. Randall, J. S. Han and J. H. Weber, *Environ. Technol. Lett.*, 7 (1986) 571.
6 T. Tsuda, H. Nakanishi, S. Aoki and J. Takebayashi, *J. Chromatogr.*, 387 (1987) 361.
7 M. Takeuchi, K. Mizuishi, H. Yamanobe and Y. Watanabe, *Bunseki Kagaku*, 36 (1987) 138.
8 G. A. Junk and J. J. Richard, *Chemosphere*, 16 (1987) 61.
9 K. Takami, H. Yamamoto, T. Okumura, A. Sugimae and M. Nagamoto, *Anal. Sci.*, 3 (1987) 63.
10 T. R. Compton, *Gas Chromatography of Organometallic Compounds*, Plenum Press, New York, 1982, p. 344.
11 W. O. Gauer, J. N. Seiber and D. G. Crosby, *J. Agric. Food Chem.*, 22 (1974) 252.
12 C. G. Flinn, *Ph.D. thesis*, Dalhousie University, Halifax, 1979.
13 W. A. Aue, B. J. Flinn, C. G. Flinn, V. Paramasigamani and K. A. Russell, *Can. J. Chem.*, 67 (1989) 402.
14 C. G. Flinn and W. A. Aue, *Can. J. Spectrosc.*, 25 (1980) 141.

Journal of Chromatography, 475 (1989) 381–389
Elsevier Science Publishers B.V., Amsterdam — Printed in The Netherlands

CHROM. 21 564

STABILITY-INDICATING CAPILLARY GAS–LIQUID CHROMATOGRAPHIC ASSAY OF DICYCLOMINE HYDROCHLORIDE IN SOME PHARMACEUTICAL FORMULATIONS

HENRY S. I. TAN* and YA-PING YAN
College of Pharmacy, University of Cincinnati Medical Center, Cincinnati, OH 45267 (U.S.A.)
and
ALAN P. THIO
Division of Regulatory Services, College of Agriculture, University of Kentucky, Lexington, KY 40546 (U.S.A.)
(First received January 30th, 1989; revised manuscript received April 12th, 1989)

SUMMARY

A stability-indicating assay method for some dicyclomine hydrochloride formulations was developed utilizing capillary gas–liquid chromatography. A methanolic extract of the sample, containing phenacetin as internal standard, was chromatographed by temperature programming on a 15 m × 0.524 mm I.D., DB-17 column with nitrogen carrier gas and flame ionization detection ($1 \cdot 10^{-10}$ A). The dicyclomine hydrochloride was well resolved from phenacetin with retention times of *ca.* 9 and 7 min, respectively. Dicyclomine hydrochloride–internal standard peak area ratio was linear over 0.1–1.0 μg of dicyclomine hydrochloride injected ($r = 0.999$). Under the experimental conditions the limit of detection was 0.025 μg of dicyclomine hydrochloride injected. Validation studies with synthetic capsules, tablets and injectables covering a range of 5–25 mg of dicyclomine hydrochloride per unit gave an overall percent recovery (± relative standard deviation, $n = 9$) of 99.9 ± 1.7%. The method was successfully applied to the assay of commercial formulations. Stability tests indicated that degradation products of dicyclomine, formed upon acid treatment, did not interfere with the dicyclomine and internal standard peaks. They further showed that dicyclomine is fairly stable in base.

INTRODUCTION

Dicyclomine hydrochloride [(bicyclohexyl)-1-carboxylic acid 2-(diethylamino)-ethyl ester hydrochloride] is a widely used anticholinergic agent. Based on its antispasmodic effect it is applied in the treatment of functional disturbances of gastrointestinal motility without affecting gastric secretion. For many years the official assay method for its pharmaceutical formulations was based on titrimetry using a chloroform–water system with sodium lauryl sulfate as titrant and methyl yellow as indicator[1]. Because the titration end point was difficult to observe and the titrant need-

0021-9673/89/$03.50

ed to be restandardized prior to use, other assay procedures have been proposed, many from drug regulatory laboratories. This has lead to the replacement of the official method by a high-performance liquid chromatography (HPLC) procedure which became official in Supplement 6 of USP XXI[2]. This new compendial method is identical to the procedure published by Jee[3,4] who utilized UV detection at 215 nm without an internal standard and did not address any stability-indicating aspects of the method. Dicyclomine does not have a distinct absorption spectrum and measurement at 215 nm is done in a region where many compounds, *e.g.* dosage form ingredients, show absorptions.

A nuclear magnetic resonance spectroscopic method[5] was published for the assay of dicyclomine hydrochloride. Because this method required an analytical sample containing 200 mg of the compound, it cannot be applied to single dose analysis for content uniformity test purposes. Dicyclomine has also been assayed by gas–liquid chromatography (GLC). The published methods, however, required the preparation of several reagents and were lengthy[6–8]. This paper reports a simple, stability-indicating assay method for dicyclomine hydrochloride in capsules, tablets and injectables based on capillary GLC.

EXPERIMENTAL

Apparatus

The following apparatus were used: Varian Model 3300 microprocessor-controlled gas chromatograph with a flame ionization detector, a Model 1040 megabore injector and Model 4270 electronic integrator (Varian Instruments, Walnut Creek, CA, U.S.A.). Injections were made with 5-μl Hamilton Series 900 syringes and gas flow-rates were measured with an Optiflow 520 digital flow meter (Fairfield, CA, U.S.A.). A Model 145 Isotemp dry bath (Fisher Scientific, Pittsburgh, PA, U.S.A.) was used for the stability tests.

Reagents and materials

The following reagents were used: dicyclomine hydrochloride (courtesy Merrell-Dow Pharmaceuticals, Cincinnati, OH, U.S.A.); phenacetin (Eastman-Kodak, Rochester, NY, U.S.A.), methanol (Optima or HPLC grade, Fisher Scientific, Fairlawn, NJ, U.S.A.), and Extrelut QE solid phase extraction cartridges (E.M. Science, Cherry Hill, NJ, U.S.A.). Ultra-high purity 99.999% nitrogen and hydrogen, and zero-grade air (total hydrocarbons < 0.1 ppm) were obtained from AGA Gas (Waumee, OH, U.S.A.). All other chemicals were analytical grade.

GLC conditions

A 15 m $\times$ 0.524 mm I.D. fused-silica, 1 μm DB-17 column (J & W Scientific, Folsom, CA, U.S.A.) was used with nitrogen carrier gas delivered at a flow-rate of 2.0 ml/min with a total make up gas of 30 ml/min. The flow-rates for hydrogen and air were about 30 and 300 ml/min, respectively. The injector port and detector were heated at 250°C. The temperature of the column oven was maintained at 160°C for 2 min, then programmed at 20°C/min for 4 min and held at the final temperature of 240°C for 5 min. A flame ionization detection (FID) current of $1 \cdot 10^{-10}$ A was used. The integrator was set at an attenuation of 16.

Internal standard solution

About 125 mg of phenacetin was transferred into a 50-ml volumetric flask, dissolved and diluted to volume with methanol.

Standard solution preparation

About 100 mg of dicyclomine hydrochloride was transferred into a 100-ml volumetric flask, dissolved and diluted to volume with methanol. Exactly 2.0 ml of the solution was transferred into a 10-ml volumetric flask and after addition of 2.0 ml of internal standard solution, the mixture was diluted to volume with methanol.

Sample solution preparation

Tablets. Twenty tablets were accurately weighed and pulverized. An aliquot of the powder, equivalent to about 20 mg of dicyclomine hydrochloride, was transferred into a 50-ml volumetric flask. After addition of 10.0 ml of internal standard solution, the mixture was diluted to volume and filtered, discarding the first 5 ml of filtrate. Exactly 5.0 ml of the filtrate was diluted to 10.0 ml in a volumetric flask.

Capsules. The contents of twenty capsules were quantitatively removed from the capsules, thoroughly mixed, and accurately weighed. An aliquot of the powder, equivalent to about 10 mg of dicyclomine hydrochloride, was transferred into a 50-ml volumetric flask and subjected to the same steps as described for tablets beginning with "addition of 10.0 ml of internal standard solution".

Injectables. A volume, equivalent to 5.0 mg of dicyclomine hydrochloride, was carefully pipetted onto a dry Extrelut cartridge. Elution of the compound was done four times with 4-ml, 2-ml, 2-ml and 2-ml portions of chloroform. The eluates were collected in a 25-ml volumetric flask. After addition of 5.0 ml of internal standard solution, the mixture was diluted to volume with methanol.

Chromatographic procedure

Using a 5-μl syringe, 2.0 μl of the sample solution or standard solution was injected into the gas chromatograph under the operating conditions described above. Quantitation was based on relating the dicyclomine hydrochloride–internal standard peak area ratio of the sample to that of the standard.

Stability tests

(a) Three samples, each containing about 15 mg of dicyclomine hydrochloride in 10 drops of water, were prepared by sonication (30 s). The solutions were heated at 80°C with 1 ml of 9 *M* sulfuric acid in separate tubes with PTFE-lined screw caps for 15, 30 and 45 min, respectively. At the end of each heating period, the mixture was poured over about 2 g of crushed ice and extracted first with ether and then with chloroform. The ether and chloroform extracts were evaporated to dryness under a gentle nitrogen stream, the residues were each reconstituted in 1.0 ml of methanol and chromatographed.

(b) Three samples were prepared and subjected to the same steps described in (a) above except that the solutions were heated with 1 ml of 1 *M* sodium hydroxide. Following the chloroform extraction, the aqueous solution was acidified with 1 *M* hydrochloric acid to pH 1 and then extracted with ether. The ether extract was evaporated to dryness under a gentle nitrogen stream, the residue was reconstituted in 1 ml of methanol, and chromatographed.

RESULTS AND DISCUSSION

Under the proposed experimental conditions dicyclomine hydrochloride and phenacetin eluted as fairly symmetrical sharp peaks and were well-separated from one another (Fig. 1). The approximate retention times were 7 min for phenacetin and 9 min for dicyclomine with capacity factors, k', of about 8.4 and 11.1, respectively, and height equivalent to a theoretical plate (HETP) values ($\pm$ standard deviation, S.D., $n = 10$) of 0.38 $\pm$ 0.13 mm and 0.512 $\pm$ 0.05 mm, respectively.

The relationship between dicyclomine hydrochloride–internal standard peak area ratio and amount of dicyclomine hydrochloride injected was established. Linearity was obtained between 0.1 and 1.0 μg of dicyclomine hydrochloride injected ($r = 0.999$). A typical regression equation was $A = 1.03C - 0.01$, where A = area ratio of dicyclomine hydrochloride–internal standard and C = amount of dicyclomine hydrochloride injected in micrograms.

Validation studies were performed on synthetically prepared capsules, tablets and injectables. Capsule placebos contained calcium sulfate, starch, lactose, gelatin, magnesium stearate, titanium oxide, FD&C Blue No. 1 and FD&C Red No. 3[9]. Tablet placebos contained acacia, dibasic calcium phosphate, starch, lactose, sucrose, magnesium stearate and FDC Blue No. 1[9]. The injectables contained chlorobutanol and sodium chloride. The gas chromatograms were similar to those of standard solutions. The capsule and tablet placebos did not show peaks between 1 and 10 min

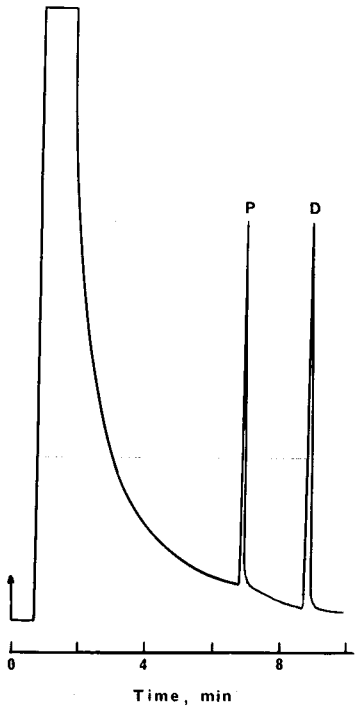

Fig. 1. Gas chromatogram of a standard solution run under conditions described in text. P = phenacetin; D = dicyclomine hydrochloride.

TABLE I

RECOVERY DATA FROM SYNTHETIC FORMULATIONS

Sample	*Dicyclomine hydrochloride*		
	Amount weighed (mg/unit[b])	*Amount found[a] (mg/unit[b])*	*Recovery (%)*
Capsule	5.3	5.4	101.9
Capsule	15.2	15.2	100.0
Capsule	25.3	25.2	99.6
Tablet	5.0	4.9	98.0
Tablet	14.5	14.2	97.9
Tablet	24.7	24.4	98.8
Injectable	4.9	5.0	102.0
Injectable	14.6	14.5	99.3
Injectable	25.1	25.6	102.0
Overall recovery (%)			99.9
R.S.D. (%)			1.67

[a] Average of duplicate assays.
[b] Unit = capsule, tablet or ml.

after injection. Table I shows the recovery data from these simulated formulations. The overall percent recovery (± relative standard deviation, R.S.D.) was (n = 9) 99.9 ± 1.7%. The validation studies were performed over a range of 5–25 mg of dicyclomine hydrochloride per capsule, tablet or ml. This corresponds to a range of 50% below and 150% above the usual label amounts in capsules and injectables of 10 mg per capsule or ml, respectively. Since tablets usually contain 20 mg per tablet, the range corresponds to 75% below and 25% above the label claim.

The method was applied to the assay of commercial capsules, tablets, and injectables. Fig. 2 is a typical gas chromatogram for the methanolic extract from tablets. The chlorobutanol preservative in injectables did not interfere with the dicyclomine and internal standard peaks because it coeluted with the solvent. Fig. 3 shows the gas chromatogram of a solution of chlorobutanol in carbon disulfide. The recovery data (Table II) showed quantitative recovery as percent label claims of greater than 97% were obtained. The USP XXI potency limits were 93.0–107.0% of label claim for these formulations[1].

The proposed assay method was designed to allow individual dosage unit assay, particularly for the capsules and tablets, because USP XXI requires that these two formulations meet the content uniformity test. In addition, the limit of detection was determined for qualitative analysis purposes. The sensitivity, as determined by the method of Kaiser[10], was $7.2 \cdot 10^{-11}$ M or 25 ng of dicyclomine hydrochloride injected under the described experimental conditions.

Dicyclomine (I) is an ester that may undergo hydrolysis into dicyclohexylcarboxylic acid (II) and diethylaminoethanol (III) according to the reaction shown in Fig. 4. A stability test was conducted by heating the compound with 9 M sulfuric acid and with 1 M sodium hydroxide to determine if these hydrolysis products, when formed, interfere with the dicyclomine and/or internal standard peaks. The worked-

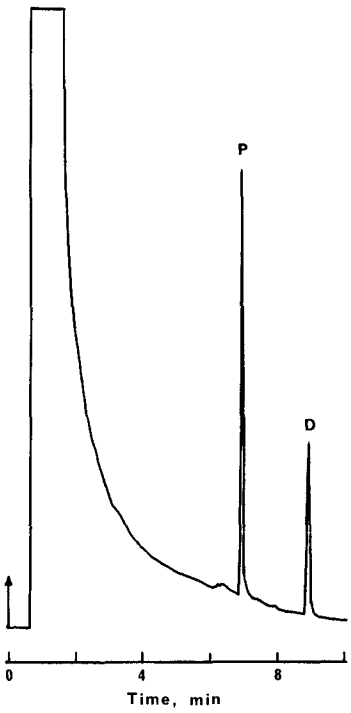

Fig. 2. Gas chromatogram of methanol extract from a commercial tablet run under conditions described in text. P = phenacetin; D = dicyclomine hydrochloride.

up ether extracts from the described 15 and 30 min 9 *M* sulfuric acid treatment gave upon gas chromatography a peak with a retention time of about 6 min. Although no identification was made, the peak was presumably that of dicyclohexylcarboxylic acid. Diethylaminoethanol and dicyclomine were not observed in the chromatogram because they were in the protonated forms and remained in the acidic aqueous phase.

TABLE II

RECOVERY DATA FROM COMMERCIAL FORMULATIONS

Sample	*Dicyclomine hydrochloride*		
	Label claim (mg/unit[b])	*Amount found[a] (mg/unit[b])*	*Label claim (%)*
Capsule A	10	9.76	97.6
Capsule B	10	9.63	96.3
Tablet A	20	19.96	99.8
Tablet B	20	19.92	99.6
Injectable A	10	10.09	100.9
Injectable B	10	10.12	101.2

[a] Average of duplicate assays.
[b] Unit = capsule, tablet or ml.

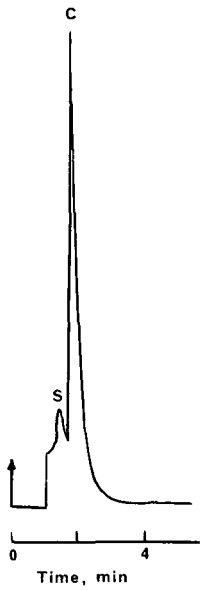

Fig. 3. Gas chromatogram of chlorobutanol (C) in carbon disulfide (S) run under conditions described in text.

Subsequent extraction with chloroform gave, however, after evaporation and chromatography of the reconstituted solution of the residue, the intact dicyclomine with a peak area somewhat smaller than that of control. Protonated dicyclomine is soluble in chloroform because of the higher polarity of chloroform compared to that of ether. The acid hydrolysis in 15 and 30 min produced only small quantities of the decomposition products. Since the FID response factor for diethylaminoethanol is low, this compound was not observed in the chromatograms. However, the worked-up ether extract from the 45-min acid treatment gave two peaks with retention times of about 5 and 6 min. The peak at 5 min was probably that of the diethylaminoethanol product which in 45 min was produced in sufficiently large quantities. Although it was protonated the large quantity was enough to distribute it into the ether phase, as dictated by the partition coefficient, in such amount that was observable in the chromatogram. The more extensive hydrolysis of dicyclomine hydrochloride in 45 min was confirmed by the appearance of a dicyclomine hydrochloride peak with a peak area much small-

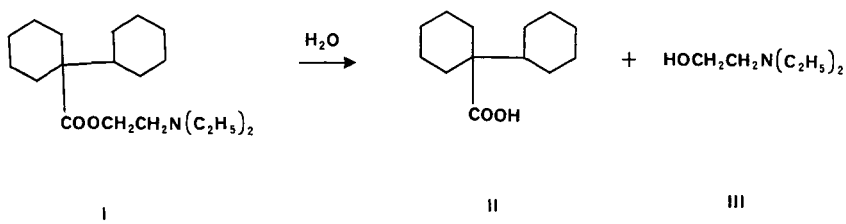

Fig. 4. Hydrolysis reaction of dicyclomine.

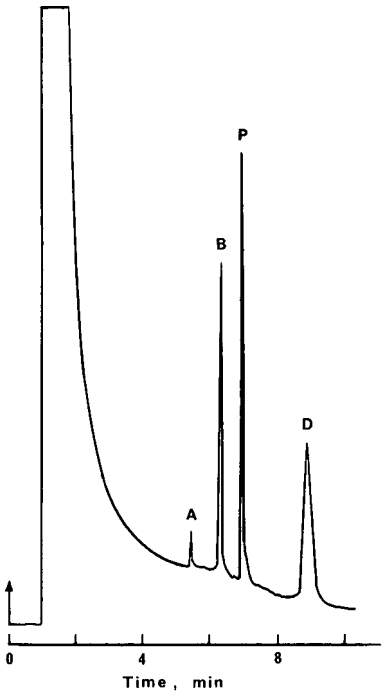

Fig. 5. Gas chromatogram of a mixture of acid decomposition products (A and B) with dicyclomine (D) and phenacetin (P).

er than that of control in the chromatogram of the subsequent chloroform extract. Fig. 5 is the chromatogram of the reconstituted solution in methanol from the 45-min ether extract which was spiked with a relatively large amount of dicyclomine hydrochloride and phenacetin to determine the locations of the hydrolysis products, the dicyclomine hydrochloride and phenacetin peaks. This chromatogram clearly shows that the hydrolysis products do not interfere with the peaks of interest.

Surprisingly, dicyclomine hydrochloride remained fairly stable upon heating with 1 *M* sodium hydroxide. Because dicyclomine is an ester, the compound is expected to hydrolyze also upon heating with aqueous base. The chromatograms of the worked-up ether extracts after 45 min heating showed only the peak of intact dicyclomine with an area of similar size as that of control. The subsequent chloroform extract showed only trace quantities of dicyclomine because this compound was already removed in the ether extraction. When the remaining basic solution was acidified with hydrochloric acid to pH 1 and then extracted with ether, the worked-up ether extract showed only a trace of the purported dicyclohexylcarboxylic acid.

The above results indicate that the assay method is stability-indicating for dicyclomine as far as interference by hydrolysis decomposition products are concerned. The method is simple, no reagents are necessary, the assay is quantitative, and it is applicable for single unit dosage assay.

ACKNOWLEDGEMENTS

The authors thank Merrell Research Institute of Merrell-Dow Pharmaceuticals, Cincinnati, OH, U.S.A. for supplying the dicyclomine hydrochloride powder.

REFERENCES

1 *The United States Pharmacopeia,* Mack Publishing Co., Easton, PA, 21st rev., 1985, p. 316 ff.
2 *The United States Pharmacopeia,* The United States Pharmacopeial Convention, Rockville, MD, 21st rev., Suppl. 6, p. 2558 ff.
3 J. M. Lee, *FDA Lab. Info. Bull.,* 1 (1985) 2943.
4 J. M. Lee, *FDA Lab. Info. Bull.,* 2 (1986) 3083.
5 G. M. Hanna, *J. Assoc. Off. Anal. Chem.,* 67 (1984) 222.
6 F. L. Fricke, *J. Assoc. Anal. Chem.,* 55 (1972) 1162.
7 C. R. Brownell and L. L. Alber, *J. Assoc. Off. Anal. Chem.,* 62 (1979) 1116.
8 T. Daldrup, F. Susanto and P. Michalke, *Fresenius' Z. Anal. Chem.,* 308 (1981) 413.
9 *Physicians' Desk Reference,* Medical Economics Co., Oradell, NJ, 42nd ed., 1988, p. 1119.
10 H. Kaiser, *Anal. Chem.,* 42 (1970) 26A.

Journal of Chromatography, 475 (1989) 391–399
Elsevier Science Publishers B.V., Amsterdam — Printed in The Netherlands

CHROM. 21 530

ELECTROCHEMICAL DETECTION OF MERCAPTURIC ACID DERIVATIVES AFTER SEPARATION BY HIGH-PERFORMANCE LIQUID CHROMATOGRAPHY

TOSHIMASA TOYO'OKA*, TAKASHI SUZUKI, YUKIO SAITO and ATSUSHI TAKAHASHI
National Institute of Hygienic Sciences, 1-18-1 Kamiyoga, Setagaya-ku, Tokyo 158 (Japan)
(First received November 7th, 1988; revised manuscript received February 9th, 1989)

SUMMARY

Mercapturic acid derivatives were separated by isocratic elution on a high-performance liquid chromatography column (Inertsil ODS) and detected electrochemically at various applied potentials (+0.60–+0.85 V). The responses of the electrochemical detector gradually increased with increasing potential but a plateau value was not obtained for all samples tested. When methanol was employed as a modifier of the eluents instead of acetonitrile, the response curves (current *vs.* voltage) were shifted to higher voltages for all mercapturic acid derivatives. Both the linearity ($r > 0.998$) and the reproducibility (coefficient of variation < 3.5%) of the detector response were consistent. The strength of the detector response depended on the atomic configuration near the sulphur atom in the mercapturic acid derivatives. The detection limits of eleven mercapturic acid derivatives at +0.80 V were in the range 0.21 [S-(3-hydroxybutyl)mercapturic acid] to 8.3 pmol [S-(2-O-acetylbutyl)mercapturic acid methyl ester].

INTRODUCTION

Baumann and Preusse[1] and Jaffe[2] demonstrated in 1879 that certain sulphur-containing compounds appeared in dog urine after administration of halogenated aromatic compounds like bromobenzene. These compounds, identified as N-acetylcysteine conjugates, were called mercapturic acids. There have since been a number of reports concerning the detection of mercapturic acids, many of which involved non-selective methods[3–7]. In the simplest assay procedure, the concentration of thiols, formed by alkaline hydrolysis of the thioether bond, is measured indirectly after their reaction with dithiobis(nitrobenzoic acid) to form 2-nitrobenzoic acid (yellow dye)[8]. This has been used to determine thioether compounds including mercapturic acids in urine samples[3–5]. High background values and large variations in individual values were found in all these studies, however. These were mainly due to high urinary concentrations of endogenous sulphur-containing compounds such as cysteine and cystine. Therefore, selective methods allowing a more specific detection of the mercapturic acid metabolites are needed. A gas chromatography–mass spectrometry

0021-9673/89/$03.50

(GC–MS) method which includes the derivatization of the COOH group with an alkylating agent, *e.g.*, diazomethane was recently developed which gave a selective and sensitive detection for this type of compounds in urine[9–13]. Numerous mercapturic acids have since been isolated from biological samples by use of this method, *e.g.*, ethylmercapturic acid[14] and 3-oxobutyl- and 3-hydroxybutylmercapturic acid[15] have been identified from rat urine after administration of urethane and tributylphosphate, respectively.

This paper reports attempts to separate and detect some mercapturic acid derivatives by high-performance liquid chromatography (HPLC) and electrochemical detection (ED). The aim of the research was the development of a simple, selective and sensitive detection method.

EXPERIMENTAL

Materials

S-Ethylmercapturic acid (a in Table I) and S-ethoxycarbonylmercapturic acid (m) were prepared by the method of Boyland and Nery[14]. Other mercapturic acid (MA) derivatives (b–l in Table I) were synthesized according to previous reports[15,16]. Phosphoric acid was of biochemical reagent grade (Wako Pure Chemicals, Osaka, Japan). Water, acetonitrile and methanol were of HPLC grade (Wako Pure Chemicals). All other chemicals were of analytical reagent grade and were used without further purification.

HPLC and ED

The HPLC–ED system is shown schematically in Fig. 1. A Shimadzu (Kyoto, Japan) LC-6A high-performance liquid chromatograph equipped with a Rheodyne injector (Model 7125; Cotati, CA, U.S.A.) was used. The signal from the electro-

TABLE I

STRUCTURES OF MERCAPTURIC ACID DERIVATIVES TESTED

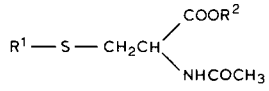

	Derivative	R^1	R^2
a	S-Ethylmercapturic acid	CH_2CH_3	H
b	S-Butylmercapturic acid	$CH_2CH_2CH_2CH_3$	H
c	S-(3-Hydroxybutyl)mercapturic acid	$CH_2CH_2CH(OH)CH_3$	H
d	S-(2-Oxobutyl)mercapturic acid	$CH_2COCH_2CH_3$	H
e	S-(3-Hydroxybutyl)mercapturic acid methyl ester	$CH_2CH_2CH(OH)CH_3$	CH_3
f	S-(3-Oxobutyl)mercapturic acid methyl ester	$CH_2CH_2COCH_3$	CH_3
g	S-(2-Hydroxybutyl)mercapturic acid methyl ester	$CH_2CH(OH)CH_2CH_3$	CH_3
h	S-(2-Oxobutyl)mercapturic acid methyl ester	$CH_2COCH_2CH_3$	CH_3
i	S-*sec.*-Butylmercapturic acid methyl ester	$CH(CH_3)CH_2CH_3$	CH_3
j	S-(4-O-Acetylbutyl)mercapturic acid methyl ester	$CH_2CH_2CH_2CH_2OCOCH_3$	CH_3
k	S-(3-O-Acetylbutyl)mercapturic acid methyl ester	$CH_2CH_2CH(OCOCH_3)CH_3$	CH_3
l	S-(2-O-Acetylbutyl)mercapturic acid methyl ester	$CH_2CH(OCOCH_3)CH_2CH_3$	CH_3
m	S-Ethoxycarbonylic mercapturic acid	$COOCH_2CH_3$	H

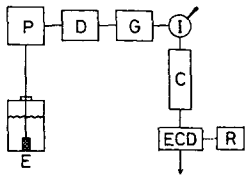

Fig. 1. Schematic diagram of the HPLC-ED system for mercapturic acid derivatives. E = Eluent reservoir; P = pump; D = damper; G = guard cell; I = injector; C = analytical column; ECD = coulochemical detector; R = recorder.

chemical detector was recorded on a C-R6A Chromatopac (Shimadzu). An analytical column, Inertsil ODS (150 mm × 4.6 mm I.D., 5 μm) (Gaskuro Kogyo, Tokyo, Japan), was maintained at 40°C in a column oven (Gaskuro Kogyo). The electrochemical cell (Model 5010) of a coulometric detector (Model 5100A; ESA, Bedford, MA, U.S.A.) was placed after the analytical column. The guard cell (Model 5020) of the detector was placed between the pump and the injector. In a separate experiment, a Shimadzu SPD-6A UV spectrophotometer equipped with an 8-μl flow cell was used for the detection of the eluates from the column at 210 nm. All the eluents used as mobile phases were degassed with an ultrasonicator prior to use. The flow-rate of the eluent was 1.0 ml/min.

Sample preparation

A 4 m*M* stock solution of each mercapturic acid derivative in methanol was prepared. The various concentrations (1.0–10 μ*M*) of MA derivatives were prepared by dilution in water. A fixed volume of the mixed solution was injected into the HPLC column.

RESULTS AND DISCUSSION

HPLC separation of mercapturic acid (MA) derivatives

HPLC separation of MA derivatives was performed on a reversed-phase column before ED. The effect of both the acetonitrile concentration and pH in the eluents on the separation was investigated by isocratic elution on an Inertsil ODS column. Since the MA derivatives tested have hydrophilic COOH and OH groups, many peaks corresponding to the MA derivatives (a–i) were eluted near the void volume in neutral and alkaline solutions (pH 4–8), and complete separation was difficult (data not shown). The separation was gradually improved with decreasing pH (4 to 2), and was efficient at pH 2.2 with 0.15 *M* H_3PO_4. The capacity factor, k', of each compound, however, increased as the concentration of acetonitrile decreased (Table II). Effective separation was achieved by isocratic elution with CH_3CN–0.15 *M* H_3PO_4 (15:85) (eluent I). However, 31 min were required for the elution of the hydrophobic MA methyl esters, *e.g.*, i and l. To overcome this disadvantage, the separation was also attempted with various concentrations of methanol in 0.15 *M* H_3PO_4. At the same modifier concentrations, elutions with solvents containing methanol were slower than those with acetonitrile. A complete separation in a short time was impossible by isocratic elution in all eluents containing methanol. Although complete separation in a relatively short time may be provided by gradient or step-

TABLE II

CAPACITY FACTORS, k', OF MERCAPTURIC ACID DERIVATIVES UNDER VARIOUS CONDITIONS

ND = Not determined; UV detection at 210 nm; $k' = t - t_0/t_0 = 2.0$ min. The void volume of the column was measured with acetone as a marker, eluted with 100% methanol.
Eluents: I CH_3CN–0.15 *M* H_3PO_4 (15:85); II CH_3CN–0.15 *M* H_3PO_4 (13:87); III CH_3CN–0.15 *M* H_3PO_4 (10:90); IV CH_3CN–0.15 *M* H_3PO_4 (8:92); V CH_3CN–0.15 *M* H_3PO_4 (20:80); VI CH_3CN–0.15 *M* H_3PO_4 (18:82); VII CH_3CN–0.15 *M* H_3PO_4 (17:83); VIII CH_3OH–0.15 *M* H_3PO_4 (20:80); IX CH_3OH–0.15 *M* H_3PO_4(18:82); X CH_3OH–0.15 *M* H_3PO_4 (33:67); XI CH_3OH–0.15 *M* H_3PO_4 (35:65); XII CH_3OH–0.15 *M* H_3PO_4 (40:60); XIII CH_3OH–0.15 *M* H_3PO_4 (45:55); XIV CH_3OH–0.15 *M* H_3PO_4 (50:50).

MA	*k'*													
	I	*II*	*III*	*IV*	*V*	*VI*	*VII*	*VIII*	*IX*	*X*	*XI*	*XII*	*XIII*	*XIV*
c	0.61	0.80	1.39	2.04	ND	ND	ND	1.60	1.93	ND	ND	ND	ND	ND
a	1.03	1.33	1.95	2.75	ND	ND	ND	2.05	2.35	ND	ND	ND	ND	ND
d	1.11	1.44	2.25	3.11	ND	ND	ND	1.79	2.13	ND	ND	ND	ND	ND
e	1.44	1.97	3.46	4.98	ND	ND	ND	3.41	4.17	ND	ND	ND	ND	ND
f	1.65	2.14	3.46	4.98	ND	ND	ND	2.55	3.10	ND	ND	ND	ND	ND
g	1.95	2.63	4.53	6.71	ND	ND	ND	4.33	5.30	ND	ND	ND	ND	ND
h	2.53	3.31	5.33	7.51	ND	ND	ND	3.71	4.52	ND	ND	ND	ND	ND
b	7.92	11.1	ND	ND	3.87	5.06	5.85	ND	ND	5.39	4.56	2.99	1.94	1.35
j	9.27	13.7	ND	ND	4.20	5.59	6.56	ND	ND	4.54	3.71	2.25	1.43	0.94
k	9.78	14.4	ND	ND	4.52	5.99	7.01	ND	ND	4.72	3.89	2.37	1.50	0.94
l	13.0	19.3	ND	ND	5.92	7.92	9.29	ND	ND	6.11	4.99	2.99	1.94	1.35
i	14.5	19.2	ND	ND	6.96	9.02	10.39	ND	ND	7.52	6.29	4.04	2.64	1.80

wise elution, the solvent exchange during an analysis with ED causes a large difference in background current. Therefore, ED of the MA derivatives was carried out in three groups (group A: a, c and f; B: d, e, g and h; C: b, i–l) according to the elution times.

ED of MA derivatives

A coulometric electrochemical cell (Model 5010) attached to a Coulochem 5100A (ESA) has dual series working electrodes made of porous graphite. The guard cell (Model 5020) placed between the pump and the injector pre-oxidizes the mobile phase, reducing the background currents at the working electrodes. For example, with the guard cell operating at +0.85 V, the background current detected with the second electrode (+0.80 V) dropped to 18.1 μA, a value which was 67.7% of that obtained with the guard cell off [eluent used, CH_3CN–0.15 *M* H_3PO_4 (2:8)]. The guard cell has no effect on the electrochemical oxidation of MA derivatives. However, the eluent may be oxidized by the cell judging from the rising baseline level at 210 nm with increasing potential.

The electrochemical responses obtained with each injection of MA derivatives were plotted against the potential difference applied to the working electrode (second or down-flow electrode). The potential of the first (or up-flow) electrode was fixed at +0.60 V, because all the MA derivatives gave no response at this potential. In the analysis of biological samples, *e.g.*, urine, the use of the first electrode seems to be advantageous for the removal of endogenous compounds oxidized at potentials lower than +0.60 V.

As depicted in Fig. 2, the ED responses increased exponentially with applied potential, however a current plateau was not obtained at all the points tested (+0.64–0.85 V). Although the use of potentials higher than +0.85 V may result in high currents, the background current based on the eluents must also increase, as judged by the results shown in Fig. 3. In addition, the elevated potentials will reduce the lifetime of the cell and so applied potentials higher than +0.85 V were not examined in all the experiments.

When CH_3OH–0.15 *M* H_3PO_4 (18:82) was used as the eluent, the currents at certain potentials were lower than those in CH_3CN–0.15 *M* H_3PO_4 (10:90), and the current–voltage (*C–V*) curves shifted to higher voltages for all MA derivatives tested (Fig. 2C). The currents for compounds a and c (Fig. 2C) in CH_3OH–0.15 *M* H_3PO_4 (18:82) were almost the same at all voltages, in contrast to the results obtained in CH_3CN–0.15 *M* H_3PO_4 (10:90) (Fig. 2A). The background currents were reduced compared with those in CH_3CN–0.15 *M* H_3PO_4 (20:80) (Fig. 3). Since the response in the eluent containing acetonitrile was higher than those in methanol at the same voltage, acetonitrile was selected as the modifier for ED of MA derivatives in subsequent experiments.

The ED response to various concentrations of MA derivatives injected was also determined. As shown in Fig. 4, different concentrations gave a linear current passing through the origin ($r > 0.998$). The coefficient of variation (C.V.) of the ED response at +0.80 V was tested at two different concentrations (50 and 250 pmol) and was reproducible and lower than 3.5% (Table III).

The *C vs. V* curves in Fig. 2A and B indicate that the derivatives having COOH groups (a–c) but not d were relatively sensitive to electrochemical oxidation. The effect of the substituent groups –OH and –C=O at the same position was not obvious from a comparison between compounds e and f or between g and h. The existence of certain groups adjacent to the sulphur atom reduced the electrochemical responses (g and h against e and f). Therefore, the ED responses seem to depend on the distance of the particular group from the sulphur atom. A similar phenomenon was also ob-

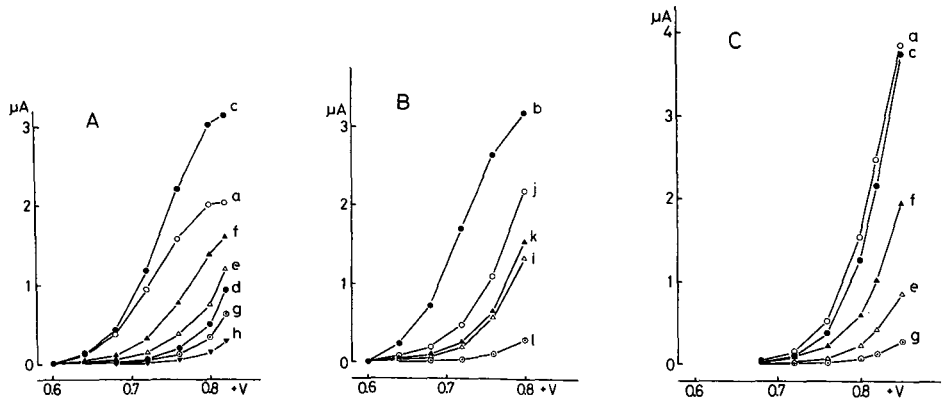

Fig. 2. Current *vs.* voltage (*C vs. V*) curves for mercapturic acid derivatives. Compounds a–l in Table I. Up-flow potential: +0.60 V. Guard cell potential: +0.85 V. (A) CH_3CN–0.15 *M* H_3PO_4 (10:90) (eluent III); (B) CH_3CN–0.15 *M* H_3PO_4 (20:80) (eluent V); (C) CH_3OH–0.15 *M* H_3PO_4 (18:82) (eluent IX). Other HPLC conditions as in Experimental section.

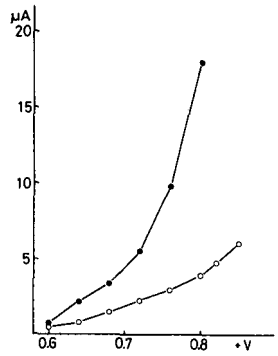

Fig. 3. Change of background current with applied potential. ●-●, CH_3CN–0.15 *M* H_3PO_4 (20:80) (eluent V); ○-○, CH_3OH–0.15 *M* H_3PO_4 (18:22) (eluent IX). HPLC and ED conditions as in Fig. 2.

served by comparison of O-acetyl esters (order of response, j> k> l). Steric hindrance also decreased the ED response (i in Fig. 2). On the other hand, S-ethoxycarbonylmercapturic acid (m), having both an amide group ($NHCOCH_3$) and an ethoxycarbonyl group (S–$COOCH_2CH_3$), showed no response to ED at any potential (+0.60–0.85 V). The above data suggest that the amide group is not responsible for the electrochemical oxidation, but the sulphur is oxidized by the electrochemical cell.

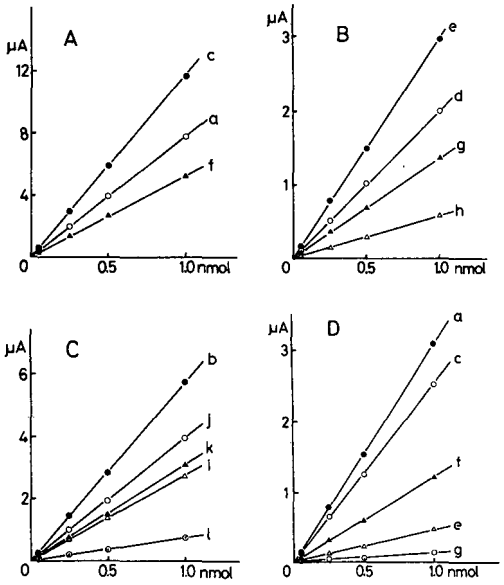

Fig. 4. Linearity of electrochemical response for various amounts of mercapturic acid derivatives. Up-flow potential: +0.60 V. Down-flow potential: +0.80 V. Guard cell potential: +0.85 V. (A) and (B) CH_3CN–0.15 *M* H_3PO_4 (10:90) (eluent III); (C) CH_3CN–0.15 *M* H_3PO_4 (20:80) (eluent V); (D) CH_3OH–0.15 *M* H_3PO_4 (18:82) (eluent IX). Other HPLC conditions as in Experimental section.

TABLE III

REPRODUCIBILITY OF ED RESPONSE

Eluents as in Table II. HPLC and ED conditions as in Fig. 4.

		C.V. (%), n = 5	
MA	*Eluent*	*50 pmol injected*	*250 pmol injected*
c	III	2.1	0.25
a	III	1.8	0.14
f	III	1.8	0.21
d	III	3.5	0.40
e	III	2.6	0.45
g	III	3.4	1.8
b	V	1.3	1.2
j	V	1.8	1.9
k	V	2.1	2.0
l	V	1.4	1.8
i	V	3.2	2.9

Typical chromatograms obtained with both UV detection at 210 nm and ED at +0.80 V in eluents III and V are depicted in Fig. 5. At 210 nm, similar peak heights for various MA derivatives were obtained in each chromatogram, whereas the ED responses at +0.80 V were different for the individual MA derivatives. The detection limits for the derivatives under the proposed conditions were estimated as 0.21–8.3 pmol, lower than those with UV detection at 210 nm (1.2–3.9 pmol) except for compounds h and l (Table IV). The detection limits may be improved by recycling of the eluents which may make the baseline more stable, and by a decrease in phosphoric acid concentration in the eluents in order to reduce the background current.

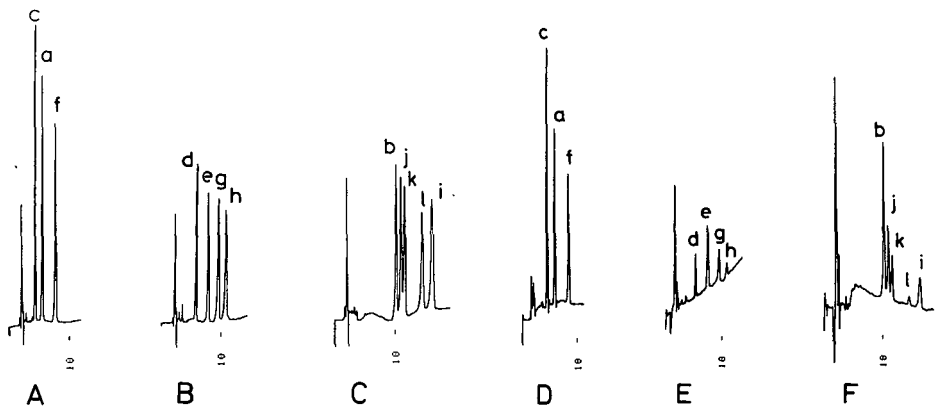

Fig. 5. Chromatograms of mercapturic acid derivatives obtained by UV and ED detections. (A)–(C) UV detection at 210 nm (250 pmol each); (D)–(F) ED at +0.80 V (up-flow potential, +0.60 V; guard cell potential, +0.85 V) (25 pmol each). (A), (B), (D) and (E) CH_3CN–0.15 *M* H_3PO_4 (10:90) (eluent III); (C) and (F) CH_3CN–0.15 *M* H_3PO_4 (20:80) (eluent V). Other HPLC conditions as in Experimental section.

TABLE IV

COMPARISON OF DETECTION LIMITS BETWEEN UV AND ED

ND = Not determined. Eluents as in Table II. HPLC and ED conditions as in Fig. 4.

MA	*Detection limit (S/N = 2) (pmol)*			
	UV (210 nm)		*ED (+0.80 V)*	
	III	*V*	*III*	*V*
c	1.2	ND	0.21	ND
a	1.4	ND	0.31	ND
f	1.8	ND	0.42	ND
d	2.7	ND	1.2	ND
e	3.3	ND	0.82	ND
g	3.5	ND	1.7	ND
h	3.9	ND	4.0	ND
b	ND	2.6	ND	0.47
j	ND	2.9	ND	1.1
k	ND	3.1	ND	1.8
i	ND	3.1	ND	2.4
l	ND	3.6	ND	8.3

Most mercapturic acids have been identified as urinary metabolites originating from xenobiotic compounds[17]. Therefore, the mercapturic acid assay will help to assess human exposure to harmful chemicals, if there is a quantitative relationship between the values in urine and the degree of exposure. Generally speaking, when the urinary MA excretion is extremely low, the assay is difficult due to interference from endogenous compounds. The proposed method in combination with HPLC and ED is sensitive enough (Table IV). Furthermore, the method is simple and does not require the derivatization used in GC methods. Therefore, with a suitable pretreatment, the HPLC–ED method may be useful for the routine analysis of MAs in biological samples. The application of this method is currently being evaluated and the results will be reported elsewhere.

ACKNOWLEDGEMENTS

The authors thank K. Hashiguchi, Nico Bio Science Co. Ltd., for his valuable comments. This work was supported in part by a Grant-in-Aid for Encouragement of Young Scientists from the Ministry of Education, Science and Culture of Japan, and by a Grant-in-Aid from the Ministry of Health and Welfare for the Comprehensive 10-Year Strategy for Cancer Control.

REFERENCES

1 E. Baumann and C. Preusse, *Ber. Dtsch. Chem. Ges.*, 12 (1879) 806–810.
2 M. Jaffe, *Ber. Dtsch. Chem. Ges.*, 12 (1879) 1092–1098.
3 F. Buffoni, G. Santoni, V. Albanese and P. Dolara, *J. Appl. Toxicol.*, 3 (1983) 63–65.
4 F. Seutter-Berlage, H. L. van Dorp, H. G. J. Kosse and P. T. Henderson, *Int. Arch. Occup. Environ. Health*, 39 (1977) 45–51.

5 H. Vainio, H. Savolainen and I. Kilpikari, *Br. J. Ind. Med.*, 35 (1978) 232–234.
6 K. H. Summer, K. Rozman, F. Coulston and H. Greim, *Toxicol. Appl. Pharmacol.*, 50 (1979) 207–212.
7 R. van Doorn, R. P. Bos, R. M. E. Brouns, C.-M. Leijdekkers and P. T. Henderson, *Arch. Toxicol.*, 43 (1980) 293–304.
8 G. L. Ellman, *Arch. Biochem. Biophys.*, 82 (1959) 70–77.
9 T. Seutter-Berlage, L. P. C. Delbressine, F. L. M. Smeets and H. C. J. Ketelaars, *Xenobiotica*, 8 (1978) 413–418.
10 P. J. van Bladeren, D. D. Breimer, G. M. T. Rotteveel-Smijs, R. A. W. de Jong, W. Buijs, A. van der Gen and G. R. Mohn, *Biochem. Pharmacol.*, 29 (1980) 2975–2982.
11 J. D. Osterloh, B.-S. Cohen, W. Popendorf and S. M. Pond, *Arch. Environ. Health*, 39 (1984) 271–275.
12 W. Dekant, M. Metzler and D. Henschlar, *Biochem. Pharmacol.*, 35 (1986) 2455–2458.
13 W. Onkenhout, P. P. J. Mulder, P. J. Boogaard, W. Buijs and N. P. E. Vermeulen, *Arch. Toxicol.*, 59 (1986) 235–241.
14 E. Boyland and R. Nery, *Biochem. J.*, 94 (1965) 198–208.
15 T. Suzuki, K. Sasaki, M. Takeda and M. Uchiyama, *J. Agric. Food Chem.*, 32 (1984) 1278–1283.
16 T. Suzuki, K. Sasaki, M. Takeda and M. Uchiyama, *J. Agric. Food Chem.*, 32 (1984) 603–610.
17 L. F. Chasseaud, *Adv. Cancer Res.*, 29 (1979) 175–275.

Journal of Chromatography, 475 (1989) 400–403
Elsevier Science Publishers B.V., Amsterdam — Printed in The Netherlands

CHROM. 21 551

Note

Studies on 1-(2-phenethyl)-4-(N-propionylanilino)piperidine (fentanyl) and related compounds

III. Effect of methyl group introduction into fentanyl on sensitivity enhancement in gas chromatography with surface ionization detection

SHIN-ICHI SUZUKI*
National Research Institute of Police Science, 6, Sanban-cho, Chiyoda-ku, Tokyo 102 (Japan)
HITOSHI TSUCHIHASHI
Forensic Science Laboratory, Osaka Prefectural Police Head Quarters, 9, Otemaeno-cho, Higashi-ku, Osaka 540 (Japan)
and
HIROMI ARIMOTO
Analytical Application Department, Shimadzu Corporation, Nishinokyo, Nakagyo-ku, Kyoto 604 (Japan)
(First received January 30th, 1989; revised manuscript received April 6th, 1989)

Fentanyl is an important analgesic used widely in surgical operation, and recently numerous reports have been published on modified fentanyl-related compounds as a "Designer Drug"[1–3]; these substances were characterized by their pharmaceutical activities and by structural modification of control compounds. The amounts of dosage of fentanyl are quite low and the clarification of its use is difficult by reason of its low concentration in blood and urine. There have been some reports on the identification of this drug in blood upon death by overdose[4,5]. In these cases the concentrations of fentanyl in blood, urine and bile were 4–13 ng/ml. The structures of the compounds, α-methylfentanyl, 3-methylfentanyl, *p*-tolylfentanyl, *n*-propylfentanyl, isopropylfentanyl and fentanyl, studied in this report are summarized in Fig. 1.

Some kinds of fentanyl analogues, such as the 3-methyl and α-methyl derivatives, are more potent and the safety margin narrower than that of fentanyl[3,6], so the lethal concentrations of some fentanyls were considered lower than those reported. Furthermore, methods to screen lower concentrations in biological fluids are needed to clarify fentanyl abuse.

The extraction and detection of this kind of compounds in pharmacokinetic studies were performed by complicated methods. Several screening methods of analysis of fentanyls have been reported, such as radioimmunoassay (RIA)[7,8] and gas chromatography with nitrogen sensitive detection (GC–NPD) on a packed column by Woenstenbourghs[9] and also on a capillary column by Watts and Caplan[10].
Surface ionization detection (SID) was introduced in 1985 by Fujii and Arimoto[11] and this method is characterized by its high sensitivity and specificity especially to tertiary amino compounds. We have reported the discrimination of 3- and α-methylfentanyl[12] by several spectroscopic and chromatographic methods and the GC–Fourier trans-

0021-9673/89/$03.50

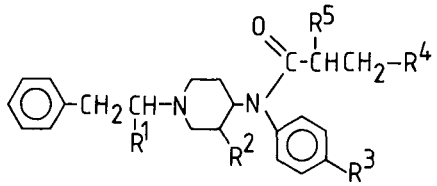

Compound name	R^1	R^2	R^3	R^4	R^5
Fentanyl	H	H	H	H	H
α-Methylfentanyl	CH_3	H	H	H	H
3-Methylfentanyl	H	CH_3	H	H	H
p-Tolylfentanyl	H	H	CH_3	H	H
n-Propylfentanyl	H	H	H	CH_3	H
i-Propylfentanyl	H	H	H	H	CH_3

Fig. 1. Structures of monomethylated fentanyl-related compounds.

form infra-red (FT-IR) analysis of monomethylated fentanyl isomers[13]. In this report, the relationship between the introduction of methyl groups in several positions of fentanyl and the enhancement of the sensitivity of SID is discussed.

EXPERIMENTAL

Materials

Five monomethylated fentanyl-related compounds were prepared by the method of Van Bever *et al.*[6], and fentanyl citrate was obtained from Sankyo (Tokyo, Japan) and examined as its free base.

GC conditions

A Shimadzu GC-14A chromatograph was used with a CBP-1 fused-silica capillary column (film thickness 0.50 μm, 50 m × 0.33 mm I.D.). The GC conditions were: column temperature, 100–320°C (10°C/min); injection temperature, 330°C; carrier gas (helium) flow-rate, 3.5 ml/min; splitless injection. The data obtained were processed with a Shimadzu data processor C-R5A.

SID

The SID conditions were: platium emitter current, 2.2 A; emitter temperature, *ca.* 600°C; ring electrode bias voltage, +200 V with respect to the collector electrode.

Analytical procedures

Each sample (5 pg–100 ng) was injected as a methanol solution into the GC device, and the detection was performed with conventional flame ionization (FID) and SID. The sensitivities of five monomethylated fentanyls and fentanyl itself with these detectors were compared using the peak areas calculated by the C-R5A.

RESULTS AND DISCUSSION

The sensitivity of SID to fentanyl isomers was higher than that of FID. For

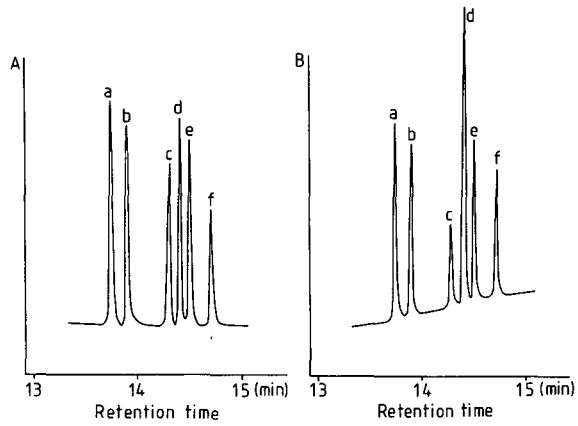

Fig. 2. Gas chromatograms of monomethylated fentanyl isomers by FID (A) and SID (B). Peaks: a = isopropylfentanyl; b = fentanyl; c = 3-methylfentanyl; d = α-methylfentanyl; e = *n*-propylfentanyl; f = *p*-tolylfentanyl.

example, fentanyl was detectable at about 5 pg per injection; on the other hand, by FID analysis, the detection limit was about 10 ng per injection (signal-to-noise ratio, S/N > 10).

The sensitivities of the fentanyls were enhanced unequally. Fig. 2 shows typical chromatograms of fentanyl and five monomethylated fentanyl isomers obtained by using FID (A) and SID (B). For SID, 100 pg of each compound were injected as a methanol solution, and for FID, 100 ng of each.

The calculated peak areas and the sensitivity enhancement relative to fentanyl are summarized in Table I. About 300–1000 times greater sensitivity was observed with SID compared to FID.

There were differences in the sensitivity enhancement of these compounds using SID, especially in the case of α-methyl- and 3-methylfentanyl. Introduction of the methyl group in the α-position of the N-phenethyl group (α-methylfentanyl) was more effective for the enhancement of sensitivity than with other fentanyls. However, introduction of a methyl group into the 3-position of the piperidine ring (3-methyl-

TABLE I

SENSITIVITY ENHANCEMENT RATIOS OF MONOMETHYLATED FENTANYL ISOMERS TO FENTANYL

Compound	*Peak area*		*Sensitivity enhancement*	*Ratio to enhancement of fentanyl*
	FID (counts/0.1 μg)	*SID (counts/0.1 ng)*		
Fentanyl	11457 ± 382	7013 ± 107	612.1	1.00
α-Methylfentanyl	11125 ± 431	11376 ± 365	1022.6	1.67
3-Methylfentanyl	8895 ± 225	2462 ± 82	297.0	0.44
p-Tolylfentanyl	7124 ± 296	5082 ± 116	713.4	1.17
n-Propylfentanyl	9737 ± 183	6288 ± 183	645.8	1.06
Isopropylfentanyl	13140 ± 516	8256 ± 203	628.3	1.03

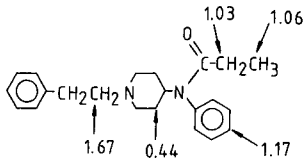

Fig. 3. Sensitivity enhancement induced by methyl group introduction into fentanyl.

fentanyl) reduced the enhancement of sensitivity compared with that for fentanyl. Introduction into the propionyl side chain (*n*-propyl- and isopropylfentanyl) and the *para* position of the anilino group (*p*-tolylfentanyl) resulted in little difference compared with fentanyl.

This phenomena can be explained as follows. In the case of α-methylfentanyl, the electron donating effect of the α-methyl group makes the surface ionization easier than with the other compounds. On the contrary, surface ionization of 3-methylfentanyl was not easy, and this phenomena was presumed to be caused by its steric effect. Since other fentanyl-related compounds, *n*-propyl-, isopropyl- and *p*-tolylfentanyl, did not have these electron donating and/or steric effects, their sensitivity enhancement was nearly equal to that of fentanyl.

The sensitivity enhancement compared to fentanyl is summarized in Fig. 3.

From these results, the important site of surface ionization of fentanyl and related compounds was assumed to be the 1-position of the piperidine ring.

In conclusion, GC–SID was highly sensitive and specific and would be suitable for the detection of these compounds and of use in forensic science. The method has been applied to biological samples, such as blood, and the results will be the subject of a subsequent report.

REFERENCES

1 T. C. Kram, D. A. Cooper and A. C. Allen, *Anal. Chem.*, 53 (1981) 1379.
2 R. Baum, *Chem. Eng. News*, 9 (1985) 7.
3 S. Suzuki and T. Inoue, *Forensic Toxicol. News*, 9 (1985) 7.
4 J. C. Garriott, R. Rodriguez and V. J. M. Di Maio, *J. Anal. Toxicol.*, 8 (1984) 288.
5 R. J. Matejczyk, *J. Anal. Toxicol.*, 12 (1988) 236.
6 W. F. M. Van Bever, C. J. E. Niemegeers and P. A. J. Janssen, *J. Med. Chem.*, 17 (1974) 1047.
7 M. Michiels, R. Hendriks and J. Heykants, *Eur. J. Clin. Pharmacol.*, 12 (1977) 153.
8 G. L. Henderson, *Clin. Pharmacol. Ther.*, 23 (1978) 188.
9 R. J. Woestenbourghs, D. R. Stanski, J. C. Scott and J. J. Heykants, *Anesthesiology*, 67 (1987) 85.
10 V. Watts and Y. Caplan, *J. Anal. Toxicol.*, 12 (1988) 246.
11 T. Fujii and H. Arimoto, *Anal. Chem.*, 57 (1985) 2625.
12 S. Suzuki, T. Inoue and C. Kashima, *Chem. Pharm. Bull.*, 34 (1986) 1340.
13 S. Suzuki, *Forensic Sci. Int.*, in press.

Journal of Chromatography, 475 (1989) 404–411
Elsevier Science Publishers B.V., Amsterdam — Printed in The Netherlands

CHROM. 21 608

Note

Isocratic separation of seven benzimidazole anthelmintics by high-performance liquid chromatography with photodiode array characterization

AUSTIN R. LONG, LILY C. HSIEH, CHARLES R. SHORT and STEVEN A. BARKER*
Department of Veterinary Physiology, Pharmacology and Toxicology, School of Veterinary Medicine, Louisiana State University, Baton Rouge, LA 70803 (U.S.A.)
(First received January 25th, 1989; revised manuscript received April 18th, 1989)

The benzimidazole anthelmintics are used in animal production to control internal worm parasites and are of concern since foods derived from treated animals may contain residues of these drugs and their metabolites that exceed maximal (800 ng/g, fenbendazole) legal levels[1]. In this regard the United States Department of Agriculture Food Safety Inspection Service (USDA-FSIS) has included five benzimidazoles in its National Residue Program over the past ten years (albendazole, fenbendazole, mebendazole, oxfendazole and thiabendazole) for monitoring[2]. However, the analytical methodology has varied greatly for each and no single approach has been proven to be adequate for the extraction, separation, detection and quantitation of these compounds as a class in a single analysis.

This laboratory has reported methods for the analysis of the anthelmintic fenbendazole and its major metabolites (oxfendazole, fenbendazole sulfone and *p*-hydroxyfenbendazole) in samples of urine, feces and tissue homogenates (S9) obtained from *in vivo* and *in vitro* metabolism studies[3–8]. This approach utilized a modified solid phase extraction method for isolation of the drugs, a high-performance liquid chromatographic (HPLC) method for their separation and ultraviolet detection (UV, 290 nm) for their quantitation. However, fixed-wavelength UV detection, which has been used to detect and quantitate many of the benzimidazoles[3–8], does not provide sufficient information about a peak. Thus, the analyst must rely on retention times of suspect peaks compared to those of standard benzimidazoles in making decisions for further action. This difficulty may be overcome by the coupling of HPLC with photodiode array UV detection, providing for a means by which one may separate and characterize benzimidazoles based on retention times and UV spectra. The practical application of this approach is that it has the potential of minimizing suspect peaks in sample extracts and could greatly reduce the number of samples requiring further analysis or attempts at confirmation. The use of column heating may also facilitate these separations and has not been utilized in previous work on benzimidazoles[3–8].

We have analyzed seven benzimidazole compounds under various HPLC conditions, varying solvent composition and column temperature, in order to determine the best separation scheme for a particular analysis. An examination of the

0021-9673/89/$03.50

ability of chromatographic retention parameters and characteristic diode array UV spectra to provide a dual criteria by which one can characterize benzimidazoles was also undertaken. We report here a method for the isocratic separation and photodiode array UV characterization of seven benzimidazole anthelmintics that should prove useful for the screening of food extracts for these compounds.

MATERIALS AND METHODS

Chemicals and expendable materials

Solvents were obtained from a commercial source (Fisher Scientific, Pittsburgh, PA, U.S.A.) at the highest purity (HPLC-grade) available and were used without further purification. HPLC-grade water was obtained by passing triple distilled water through a Modulab Water Polisher I (Continental Water Systems Co., San Antonio, TX, U.S.A.) water purification system. Oxfendazole, fenbendazole, fenbendazole sulfone and *p*-hydroxyfenbendazole were obtained from Hoechst (Frankfurt, F.R.G.). Mebendazole was supplied by Janssen Pharmaceutical (Piscataway, NJ, U.S.A.). Thiabendazole was obtained from Merck Sharp & Dohme (Rahway, NJ, U.S.A.) and albendazole from Dr. J. O'Rangers (Center for Veterinary Medicine, Rockville, MD, U.S.A.) Stock solutions (1 mg/ml) were prepared by dissolving standard benzimidazoles with dimethylformamide (DMF). A standard stock mixture was prepared by adding an aliquot of each stock solution (except mebendazole, MBZ) to a single vial and diluting with DMF to the desired concentration. Samples for HPLC analysis were prepared by placing an aliquot (10 μl) of standard stock mixtures (3.12, 6.25, 12.5, 25, 50 and 100 μg/ml; 12.5 μg/ml mebendazole internal standard) into separate vials and removing the DMF by passing a steady flow of dry nitrogen gas over the vial contents maintained at 30°C in a water bath. The residue was solubilized in 0.5 ml of mobile phase [0.017 *M* H_3PO_4– acetonitrile (60:40, v/v)] and an aliquot (20 μl) was analyzed by HPLC.

Chromatographic conditions and measurements

Analyses were performed on a Hewlett Packard Model 1090 HPLC/Chemstation system equipped with a photodiode array detector set at 290 nm with a bandwidth of 20 nm, 100–350 nm reference spectrum and sensitivity of 0.1 ma.u.f.s. The column dimensions were 30 cm × 4 mm I.D., octadecylsilyl derivatized silica, 10-μm ODS Varian MicroPak (Sunnyvale, CA, U.S.A.). The temperature was varied according to experimental design. Peak area ratio curves for the concentrations (62.5–2000 ng/ml) examined were determined by dividing integrated areas of each peak by that of the internal standard (mebendazole).

RESULTS

Fig. 1 shows the structures of the benzimidazoles studied. Fig. 2 is a representative chromatogram showing the separation of the seven benzimidazoles. Fig. 3 shows the UV spectra (photodiode array, 1000 ng/ml and 250 ng/ml, smoothed; 20 μl injection volume) of thiabendazole, oxfendazole, *p*-hydroxyfenbendazole, fenbendazole sulfone, mebendazole, albendazole and fenbendazole. Table I lists the compounds examined, concentrations, column temperatures and standard curve

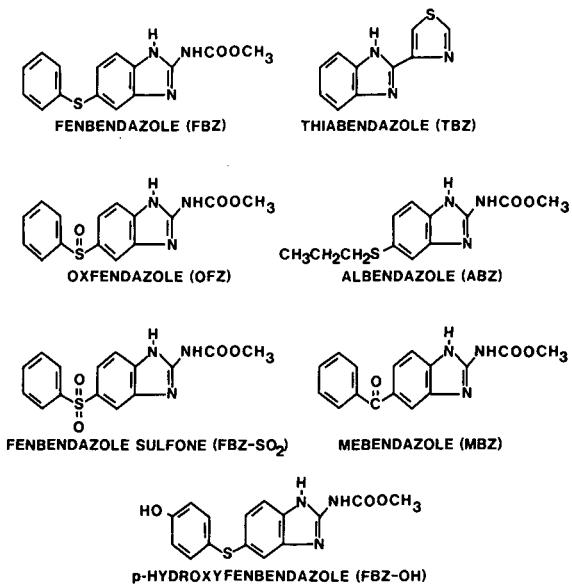

Fig. 1. Structures of the benzimidazoles examined.

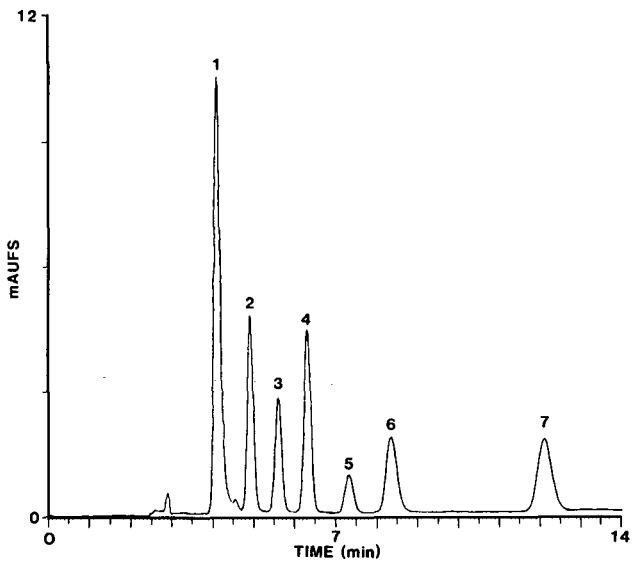

Fig. 2. Representative chromatogram (photodiode array, 290 nm) showing the separation of the seven benzimidazoles examined (1000 ng/ml, 20 μl injection) using 0.017 M H_3PO_4–acetonitrile, (60:40, v/v) as the mobile phase. The column temperature was 45°C. Order of elution: (1) thiabendazole, (2) oxfendazole, (3) *p*-hydroxyfenbendazole, (4) fenbendazole sulfone, (5) mebendazole, (6) albendazole and (7) fenbendazole.

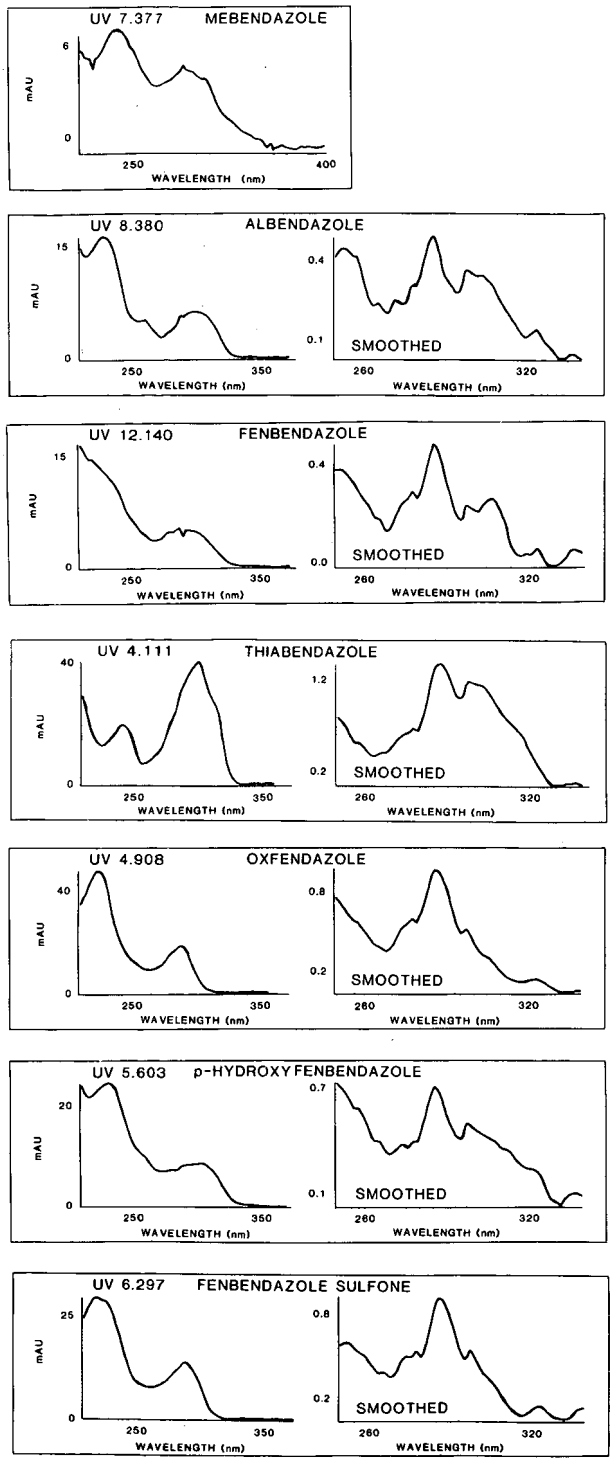

Fig. 3. UV (photodiode array, 290 nm) spectra (1000 ng/ml, 20 μl injection volume) and smoothed spectra (250 ng/ml, 20 μl injection volume) of the seven benzimidazoles examined. The UV numbers represent the retention times where each spectrum was acquired.

TABLE I

PEAK AREA RATIO STANDARD CURVE CORRELATION COEFFICIENTS ACHIEVED FOR COLUMN TEMPERATURES FROM 35 TO 60°C FOR EACH BENZIMIDAZOLE ANALYZED

The concentrations were 62.5, 125, 250, 500, 1000 and 2000 ng/ml. The injection volume was 20 μl. The mobile phase consisted of 0.017 *M* H_3PO_4–acetonitrile (60:40, v/v) at a flow-rate of 1 ml/min. The internal standard was mebendazole (MBZ) at a concentration of 250 ng/ml. Abbreviations: TBZ = thiabendazole; OFZ = oxfendazole; FBZ-OH = *p*-hydroxyfenbendazole; FBZ-SO_2 = fenbendazole sulfone; ABZ = albendazole; FBZ = fenbendazole; I.S. = internal standard.

Column temperature (°C)	*Benzimidazole*						
	TBZ	*OFZ*	*FBZ-OH*	*FBZ-SO_2*	*MBZ*	*ABZ*	*FBZ*
35	0.9998	0.9999	0.9999	0.9999	I.S.	0.9999	0.9999
40	0.9999	0.9999	0.9999	0.9999	I.S.	0.9999	0.9999
45	0.9999	0.9998	0.9999	0.9999	I.S.	0.9998	0.9998
50	0.9997	0.9997	0.9996	0.9995	I.S.	0.9992	0.9994
55	0.9972	0.9975	0.9976	0.9982	I.S.	0.9995	0.9987
60	0.9981	0.9986	0.9989	0.9996	I.S.	0.9995	0.9982

correlation coefficients determined. Table II lists retention data for separations at solvent strengths from 30 to 50 % acetonitrile. Table III lists retention data for separations at column temperatures from 35 to 60°C.

DISCUSSION

Baseline separation of the seven benzimidazoles (Fig. 1) examined was accomplished utilizing an isocratic 0.017 *M* H_3PO_4–acetonitrile (60:40, v/v) mobile

TABLE II

RETENTION DATA (k') FOR BENZIMIDAZOLES SEPARATED AT DIFFERENT SOLVENT STRENGTHS

Benzimidazole concentrations were 500 ng/ml (20 μl injection). The mobile phase consisted of 0.017 *M* H_3PO_4–acetonitrile. Column temperature: 45°C. $k' = (t_R - t_0)/t_0$, where t_R = retention time and t_0 the retention time of the unretained compound (2.89 min). Abbreviations as in Table I.

Compound	*Acetonitrile (%)*				
	30	*35*	*40*	*45*	*50*
TBZ	0.56	0.47	0.43	0.40	0.40
OFZ	1.49	0.99	0.69	0.53	0.40
FBZ-OH	2.11	1.34	0.93	0.70	0.55
FBZ-SO_2	2.95	1.82	1.16	0.80	0.55
MBZ	3.37	2.19	1.52	1.13	0.86
ABZ	3.81	2.57	1.90	1.47	1.20
FBZ	7.66	4.71	3.22	2.30	1.60

TABLE III

RETENTION DATA (k') FOR BENZIMIDAZOLES AT DIFFERENT COLUMN TEMPERATURES

The mobile phase was 0.017 M H_3PO_4–acetonitrile (60:40, v/v). k' determined as in Table II. Abbreviations as in Table I.

Compound	*Column temperature (°C)*					
	35	*40*	*45*	*50*	*55*	*60*
TBZ	0.47	0.45	0.43	0.41	0.40	0.38
OFZ	0.74	0.73	0.69	0.69	0.66	0.63
FBZ-OH	1.05	1.00	0.93	0.91	0.85	0.79
FBZ-SO_2	1.33	1.26	1.16	1.14	1.04	0.97
MBZ	1.65	1.60	1.52	1.52	1.43	1.34
ABZ	2.06	1.98	1.90	1.88	1.79	1.69
FBZ	3.51	3.37	3.22	3.16	2.94	2.77

phase, producing complete separation (Fig. 2) without resorting to exotic solvent systems or solvent programming, in 13 min. This solvent system was significantly different from that used in earlier studies to obtain separation of fenbedazole and its metabolites[3–8].

The linearity of standard curves (Table I) and the peak shape of each compound (Fig. 2) were maintained at the column temperatures (35–60°C) examined. Retention data (Table III) for separations at different column temperatures indicate there is no advantage in terms of resolution and/or run times at column temperatures above 45°C. In addition, because of the possibility of solvent outgassing at elevated temperatures, benzimidazole separations should be done at column temperatures below 50°C. Thus, a column temperature of 45°C was optimal for benzimidazole separations.

Retention data (Table II) for different acetonitrile concentrations suggested the optimal separation, with a minimal run time, was achieved utilizing a 0.017 M H_3PO_4–acetonitrile (60:40, v/v) mobile phase. Acetonitrile concentrations above 40% resulted in less than optimal separations of thiabendazole and oxfendazole. Baseline separations for the seven benzimidazoles were achieved at acetonitrile concentrations of less than 40% but resulted in lengthy run times. Use of the solvent system water–0.017 M H_3PO_4–acetonitrile (5:15:80) as previously reported[3–8] failed to separate albendazole and thiabendazole from the other compounds.

The utilization of photodiode array detection aided in the screening of suspected peaks in terms of UV characteristics. The photodiode array UV spectra of the compounds (1000 ng/ml, 20 μl injection) examined are shown in Fig. 3. By comparing the UV spectra of suspected sample peaks with known UV spectra, at each respective retention time, one could use these criteria as a preconfirmational screening procedure. UV specra were obtained for these benzimidazoles at the action level of 800 ng/g utilizing the separation conditions outlined and photodiode array detection (20 μl injection of a 500 μl final sample volume, 16 ng on column). However, one must be careful not to overextend this technology. The characteristic UV spectra of these compounds at much lower concentrations (5 ng on column) do not correlate well with the spectra obtained at higher concentrations, as evidenced by a comparison of the

spectra (1000 ng/ml, 20 μl injection) to smoothed spectra at a lower concentration (250 ng/ml, 20 μl injection) in Fig. 3. The spectra for the 250 ng/ml concentration were obtained by utilizing a mathematical smoothing function. The smoothing function can be used cumulatively, however this does not result in the correct UV spectrum. Thus, the characterization of benzimidazoles at low concentrations by photodiode array detection is limited to approximately 5 ng on column or, as assayed here, a level of 250 ng/ml. The absolute limit of detection, based only on the presence of a peak at the correct retention time and having a peak height of greater than three times baseline, was approximately 1.25 ng on column for all of the compounds examined. The minimal detectable limit for mebendazole was not determined. However, lower ng/ml sample concentrations may be determined in this manner by dissolving the final residue for analysis in a smaller volume and/or injecting a volume of greater than 20 μl of the sample.

CONCLUSIONS

The peak shape, detector response and linearity of standard curves for the benzimidazoles studied, at concentrations down to 62.5 ng/ml (20 μl injection volume; minimal detectable limit of 1.25 ng on column) and at column temperatures of less than 50°C, were sufficient to allow for quantitative determinations of these compounds. The method described also allows for preconfirmational screening of the benzimidazoles studied at the action level of 800 ppb[a] (20 μl injection volume; 16 ng on column). However, the UV spectra obtained for samples below 250 ng/ml (20 μl injection volume, 5 ng on column) would perhaps not be suitable for preconfirmational screening purposes. The separation protocol as outlined here has been utilized for quantitative determinations of benzimidazoles isolated from meat[9] and milk[10] and should be applicable as a multiresidue screening method for other benzimidazole determinations.

ACKNOWLEDGEMENTS

This research was supported by Cooperative Agreements 5V01-FD-01-319 and FD-V-000235 with the Food and Drug Administration.

REFERENCES

1 *Fenbendazole Drugs for Animal Use,* Code of Federal Regulations, U.S. Food and Drug Administration, Washington, DC, 1988, Title 21, Part 556:275.
2 *Compound Evaluation and Analytical Capability National Residue Program Plan,* U.S. Department of Agriculture, Food Safety and Inspection Service, Washington, DC, 1988.
3 S. A. Barker, L. C. Hsieh and C. R. Short, *Anal. Biochem.*, 55 (1986) 112–118.
4 C. R. Short, S. A. Barker, L. C. Hsieh, S.-P. Ou, L. E. Davis, M. G. Koritz, C. A. Neff-Davis, R. F. Bevill, I. J. Munsiff and G. C. Sharma, *Am. J. Vet. Res.*, 48 (1987) 811–815.
5 C. R. Short, S. A. Barker, L. C. Hsieh, S.-P. Ou, T. McDowell, L. E. Davis, C. A. Neff-Davis, R. F. Bevill, I. J. Munsiff and G. C. Sharma, *Am. J. Vet. Res.*, 48 (1987) 958–961.

[a] The American billion (10^9) is meant.

6 C. R. Short, S. A. Barker, L. C. Hsieh, S.-P. Ou, W. M. Pedersoli, L. M. Krista and J. S. Spano, *J. Vet. Pharmacol. Ther.*, 11 (1988) 204–209.
7 C. R. Short, S. A. Barker, L. C. Hsieh, S.-P. Ou and T. McDowell, *Res. Vet. Sci.*, 44 (1988) 215–219.
8 C. R. Short, W. Flory, L. C. Hsieh and S. A. Barker, *J. Vet. Pharmacol. Ther.*, 11 (1988) 50–55.
9 S. A. Barker, A. R. Long and C. R. Short, *J. Chromatogr.*, (1989) in press.
10 A. R. Long, L. C. Hsieh, M. S. Malbrough, C. R. Short and S. A. Barker, *J. Assoc. Off. Anal. Chem.*, (1989) in press.

Journal of Chromatography, 475 (1989) 412–415
Elsevier Science Publishers B.V., Amsterdam — Printed in The Netherlands

CHROM. 21 544

Note

Adsorbability to and desorbability from Sephadex G-15 of sodium and phosphate ions

TOSHIHIKO OKADA*
The First Department of Biochemistry, Kanazawa Medical University, Uchinada, Ishikawa 920-02 (Japan)
and
MINORU MIYAKOSHI and MASAO INOUE
Central Research Laboratory, Kanazawa Medical University, Uchinada, Ishikawa 920-02 (Japan)
(Received March 29th, 1989)

Sephadex G-15 is a well known gel having a molecular sieving function. However, the elution volume of an inorganic ion sometimes deviates from the expected value because of ion–gel matrix and ion–ion interactions[1]. One ion–gel matrix interaction is the adsorption of the ion to the gel; this phenomenon has been reported by many workers[2–11]. However, no quantitative analysis of ion adsorption to the gel has been reported. This report describes the results of quantitative adsorption experiments using sodium-22 labelled sodium chloride and phosphorus-32 labelled phosphoric acid.

EXPERIMENTAL

Chemicals

Sodium chloride, monosodium phosphate, $NaH_2{}^{32}PO_4 \cdot 2H_2O$, and disodium phosphate, $Na_2HPO_4 \cdot 12H_2O$, were of analytical grade from Wako (Osaka, Japan). Sodium-22 chloride (61.60 mCi/mg, 99% pure) and phosphorus-32 labelled phosphoric acid (carrier free, 99% pure) in 0.02 *M* HCl were obtained from New England Nuclear (Boston, MA, U.S.A.).

Eluents and samples

Distilled water and 0.025 *M* sodium phosphate buffer (pH 7.0) were used as the eluents.

The sample was $^{22}NaCl$ dissolved in distilled water. Unlabelled NaCl was added at various concentrations to the sample when necessary. Another sample was 0.218 μCi of $H_3{}^{32}PO_4$ ($7.5 \cdot 10^{-18}$ mmol) in either distilled water or sodium phosphate buffer.

Procedures

Sephadex G-15 (Pharmacia; dry particle diameter, 40–120 μm) was packed according to standard procedures in two kinds of glass tubes: a long column (Excel column Type SE-1000, 1000 mm × 19 mm; bed height, 90 cm; porous polystyrene

0021-9673/89/$03.50

support) and a short one (100 mm × 6 mm; bed height, 6 cm; glass wool support). The former contains 85 g of the gel and the latter 0.5 g for the experiments with $^{22}NaCl$, 0.43 g with $H_3{}^{32}PO_4$.

When the long column was used, a peristaltic pump (LKB; gear-box, 3:250) was inserted between the eluent reservoir and the top of the column to maintain a constant flow-rate of 12 ml/h. A 0.6-ml volume of sample solution was applied to the top of the column, and the eluate was collected in 10-min fractions using an LKB7000 Ultrorac fraction collector. The column was operated at 4°C.

A peristaltic pump was not used with the short column. A 1.0-ml volume of sample solution was applied to the column and was collected in 1.0-ml fractions. The column was operated at room temperature.

Quantitation of ions

The sodium-22 ion ($^{22}Na^+$) was counted in an Auto Well Gamma system (Model JDC-751, Aloca), and phosphorus-32 labelled phosphate ion was counted in a liquid scintillation counter (Model LSC-900, Aloca).

RESULTS AND DISCUSSION

Adsorption and desorption of $^{22}Na^+$

When 0.06 μCi of $^{22}NaCl$ ($8.3 \cdot 10^{-9}$ mmol) in distilled water were applied to the long column and eluted with distilled water no radioactivity was found in the eluate. This indicated that almost all of the applied radioactivity was adsorbed to the column. The adsorbed radioactivity was recovered in a single peak using sodium phosphate buffer as an eluent (Fig. 1). On the other hand, when 0.02 μCi of $^{22}NaCl$ in the same buffer were applied to the long column and eluted with buffer, almost all of the radioactivity appeared in a peak (data not shown).

In order to analyze quantitatively the adsorbability of Na^+ to the gel, 10 ml containing 0.02 μCi of $^{22}NaCl$ in 0.5 m*M* cold NaCl were applied to two short columns and eluted with distilled water. No radioactivity appeared in the eluates, and

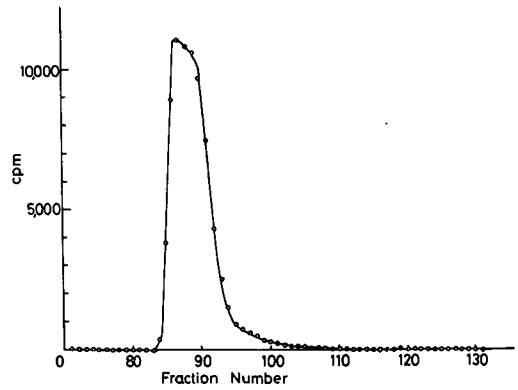

Fig. 1. Elution profile of $^{22}Na^+$ which had been adsorbed to Sephadex G-15. When 0.06 μCi of $^{22}NaCl$ in distilled water were eluted with distilled water from the long column no radioactivity was detected in the eluate. The adsorbed radioactivity was eluted with sodium phosphate buffer.

the gel was taken out from one of the columns and counted. From a count of 35 486 cpm, it was calculated that $3.2 \cdot 10^{-3}$ mmol of Na^+ were adsorbed to 1.0 g of gel. Assuming that all of the adsorbed sodium ion binds to the stray –COOH groups in the gel, the number of such groups to which Na^+ is adsorbed was calculated to be approximately $1.9 \cdot 10^{18}$ per gram of the gel. When the Na^+ adsorbed to the gel in the other short column was eluted with sodium phosphate buffer the eluate gave 40 055 cpm. This means that at least 88% of the radioactivity adsorbed was in the gel, not on the column glass.

Adsorption and desorption of phosphorus-32 labelled phosphate

When carrier-free labelled phosphate (0.218 μCi) in distilled water was applied to the long column and eluted with distilled water no radioactivity appeared in the eluate. This indicated again that the radioactivity was adsorbed to the column. In contrast to the case of Na^+, the adsorbed radioactivity was not recovered appreciably by eluting with either distilled water or sodium phosphate buffer. Therefore, the labelled phosphate seemed to bind tightly to the gel and was exchanged scarcely with the unlabelled phosphate in the eluent.

Pretreatment of the gel with buffer prevents the adsorption of phosphate. Of the 13 229 cpm of labelled phosphate in distilled water applied to the pretreated short column, only 945 cpm were adsorbed (Table I). This value is far less than that obtained (4365 cpm) with the non-treated column. However, when the labelled phosphate dissolved in buffer was applied to the treated short column and eluted with distilled water no radioactivity was adsorbed to the gel (Table I), indicating that unlabelled phosphate from the buffer prevented the adsorption of the labelled phosphate.

In order to determine quantitatively the adsorbability of the labelled phosphate to the gel, 100 μl of $H_3{}^{32}PO_4$ (13 229 cpm) solution were added to 1.0 ml of the buffer which had been diluted 0-, 100-, 1000- or 10 000-fold in distilled water. The samples were eluted with distilled water from the short columns. In every case almost all of the applied radioactivity was recovered in the eluate (Table I). Therefore, 100 μl of $H_3{}^{32}PO_4$ were added to 1.0 ml of distilled water when the solution was applied to the short column and eluted with distilled water, 4365 cpm (33%) were lost in the column

TABLE I

ELUTION BEHAVIOUR OF LABELLED PHOSPHATE ELUTED WITH DISTILLED WATER FROM A SHORT SEPHADEX G-15 COLUMN WHICH WAS EITHER NOT TREATED OR PRETREATED WITH BUFFER

	Non-treated		*Pretreated*	
	Distilled water	*Phosphate buffer[a] (2.5 μM)*	*Distilled water*	*Phosphate buffer*
Sample	13 229	13 229	13 229	13 229
Eluate	8 864	13 611	12 284	13 776
Difference	−4 365	+382	−945	+547

[a] Sodium phosphate buffer diluted 10 000-fold.

(Table I). Since the gel itself gave 4335 cpm, essentially all the labelled phosphate was adsorbed to the gel and not to the glass, *i.e.*, $6.3 \cdot 10^{-12}$ mmol ($3.7 \cdot 10^{9}$ atoms) per gram of gel.

ACKNOWLEDGEMENT

We thank Miss Naoko Kawara for her help in preparing this manuscript.

REFERENCES

1 N. Yoza, *J. Chromatogr.*, 86 (1973) 325.
2 J.-C. Janson, *J. Chromatogr.*, 28 (1967) 12.
3 P. A. Neddermeyer and L. B. Rogers, *Anal. Chem.*, 40 (1968) 755.
4 B. Z. Egan, *J. Chromatogr.*, 34 (1968) 382.
5 N. Yoza, T. Ogata and S. Ohashi, *J. Chromatogr.*, 52 (1970) 329.
6 T. Ogata, N. Yoza and S. Ohashi, *J. Chromatogr.*, 58 (1971) 267.
7 N. Yoza, T. Ogata, Y. Ueno and S. Ohashi, *J. Chromatogr.*, 61 (1971) 295.
8 W. Brown and K. Chittumbo, *J. Chromatogr.*, 63 (1971) 478.
9 M. Sinibaldi and M. Lederer, *J. Chromatogr.*, 107 (1975) 210.
10 T. Deguchi, *J. Chromatogr.*, 108 (1975) 409.
11 G. Kura, A. Koyama and T. Tarutani, *J. Chromatogr.*, 144 (1977) 245.

Journal of Chromatography, 475 (1989) 416–420
Elsevier Science Publishers B.V., Amsterdam — Printed in The Netherlands

CHROM. 21 538

Note

Simultaneous analysis of different species involved in hexaglycine hydrolysis

DEVENDRA S. KALONIA*, SHANKAR MUSUNURI and JARTCHAWAN TANGLERTPAIBUL
School of Pharmacy, 372 Fairfield Road, University of Connecticut, Storrs, CT 06268 (U.S.A.)
(Received February 21st, 1989)

Due to advances in biotechnology and modern methods of synthesis, there is a great interest in developing therapeutic agents that are peptide and protein based[1]. One of the important requirements towards using peptides and proteins as therapeutic agents is an understanding of their nature such as physicochemical properties, enzymatic reactions and transport across membranes. Glycine peptides of different chain lengths have been used as model peptides by many researchers to investigate transport across various membranes[2–5]. Our group is using peptides of 2–6 glycine units to study physicochemical properties and transport behaviour across membranes. The high-performance liquid chromatography (HPLC) assays of various glycine peptides using C_8 bonded phase[6] and NH amino column[7] were found unsatisfactory due to poor separations and long retention times. Another assay for 2–6 amino acid peptides using a C_{18} column with 0.1 *M* phosphate buffer at pH 2.1 or 0.6 *M* perchloric acid at pH 0.2 showed extremely poor retention times for glycine peptides[8].

One of the properties under investigation was the acid-catalyzed hydrolysis which involved the starting material hexaglycine (HG) and different intermediates such as pentaglycine (PG), tetraglycine (FG), triglycine (TG) and diglycine (DG). In order to study the kinetics of this peptide, an effective HPLC assay was required to analyze all intermediates and final products. There were two requirements for the assay. First, the use of an aqueous mobile phase, since the hydrolysis studies were conducted in aqueous media; and second, analyses with HPLC without pretreatment of the samples. This was particularly important because pretreatment could alter the composition of different species in hydrolysis samples.

EXPERIMENTAL

Standard materials

Glycine (G), DG, TG, FG, PG and HG were of high-purity grade and were obtained from Sigma. Pentanesulfonic acid, sodium dihydrogenphosphate and phosphoric acid were used as supplied by Aldrich.

Standard solutions

Stock solutions for all glycine peptides were prepared by using 20 mg of peptide

0021-9673/89/$03.50

in 100 ml of doubly distilled water. A standard solution containing 0.01 mg/ml of HG, PG, FG, TG, DG and 0.1 mg/ml of glycine was prepared by mixing different volumes of stock solutions.

Apparatus

The analytical system consisted of an LDC/Milton Roy ConstaMetric III metering pump with a 20-μl fixed-loop injector and a SpectroMonitor 3000 variable-wavelength detector set at 205 nm and 0.1 a.u.f.s with a signal routed to a Perkin-Elmer programmable integrator for peak area integration.

Columns and HPLC eluents

A Val-U-Pak HP analytical column (Regis, Morton Grove, IL, U.S.A.), 250 × 4.6 mm I.D., packed with 5-μm spherical ODS silica (reversed phase) was used. The eluent consisted of 10 m*M* sodium dihydrogenphosphate and 5 m*M* sodium pentanesulfonate (ion pairing agent) in water which was adjusted to pH 2.7 with phosphoric acid. The flow-rate was adjusted to 1.0 ml/min.

Hydrolysis studies

The hydrolysis studies were conducted at various temperatures (80, 85 and 90°C) in 0.1 *M* HCl. The reaction mixture consisted of a mixture of 50 mg of peptide and 50 ml of 0.1 *M* HCl. Samples of 1 ml were withdrawn at various time intervals (0, 4, 8, 12, . . .100 h). The samples were mixed with 1 ml of ice-cold 0.1 *M* sodium dihydrogenphosphate to stop the reaction by increasing the pH to approximately 3 and decreasing the temperature to below 30°C. (Under these conditions the peptide hydrolysis was negligible for the duration of the analysis.)

RESULTS AND DISCUSSION

A typical chromatogram representing the separation of different compounds is shown in Fig. 1. It can be seen from the chromatogram that the retention time of each component increased with an increase in the number of amino acids in the peptide.

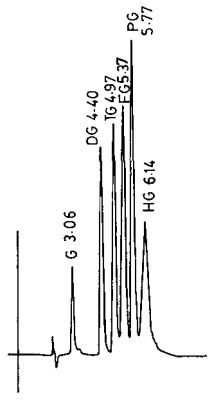

Fig. 1. Chromatogram showing peaks for glycine (G), diglycine (DG), triglycine (TG), tetraglycine (FG), pentaglycine (PG) and hexaglycine (HG).

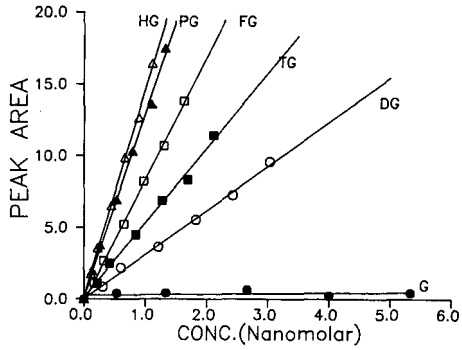

Fig. 2. Calibration curves for different species for peak area *versus* concentration.

The peaks were calibrated with both peak area and peak height as shown in Figs. 2 and 3. The calibration plot of peak area *versus* concentration (Fig. 2) shows that the slope gradually increases as the number of amino acids in the chain increases. On the other hand, the calibration plots of peak height *versus* concentration (Fig. 3) do not show a uniform pattern. This is probably due to broadening of the peaks and a decrease in peak height at longer retention times.

A comparative analysis indicated that both peak height and area under the peak were equally reproducible. The calibration constants obtained by linear regression ($r^2 \geq 0.99$) in area per nmol were as follows: G = 110.12; DG = 3093.84; TG = 5277.08; FG = 8355.2; PG = 12 950.83; HG = 14 648.4; and in height per nmol were G = 962.3; DG = 37 982.1; TG = 63 894.6; FG = 101 520.2; PG = 174 103.9; HG = 89 297.2. A plot of capacity factor, k', *versus* chain length is shown in Fig. 4. The relationship is linear for all peptides except glycine. This is probably due to the zwitterionic and highly polar nature of glycine. The pK_a of glycine is 2.4 and the pH of the mobile phase is 2.7. Therefore, approximately 66% of glycine will be present as zwitterion which has a relatively higher polarity as compared to the other peptides.

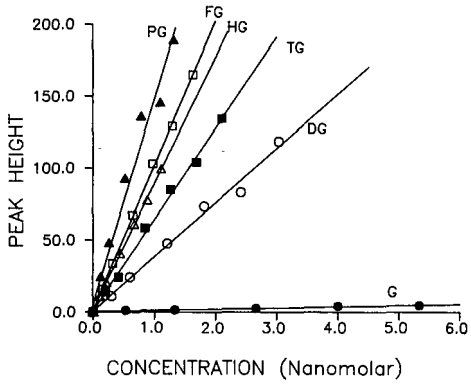

Fig. 3. Calibration curves for different species for peak height *versus* concentration.

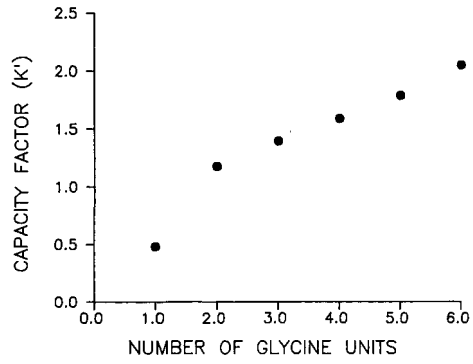

Fig. 4. Capacity factor (k') *versus* number of glycine units.

Application to peptide hydrolysis

The above assay was used to analyze different kinetic samples obtained from hydrolysis studies. A typical set of kinetic data is shown in Fig. 5. The plot shows that the concentration of HG decreases exponentially, whereas the concentrations of PG, FG and TG increase initially, reach a maximum and then decrease exponentially. This indicates that the above compounds are present as intermediates during hydrolysis. The rate of diglycine hydrolysis was found to be much smaller than other rates. Therefore, the concentration profil for diglycine reached a maximum at longer times (approximately 120 h, not shown in the figure) and then decreased exponentially. The concentration of glycine increased exponentially as a function of time. The glycine data were not used in the determination of the rate constants, and hence not shown in the figure. This assay was used for extensive hydrolysis studies of various glycine peptides and results will be reported in a subsequent paper[9]. It was found that for the duration of the assay all species were stable.

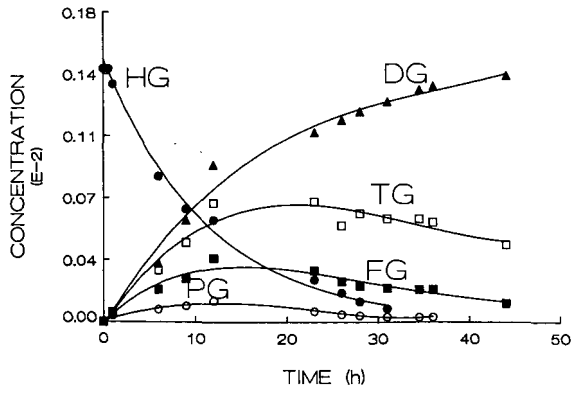

Fig. 5. Concentration *versus* time plots for various species during acid-catalyzed hydrolysis.

CONCLUSIONS

A fast and efficient HPLC assay was successfully developed to analyze glycine peptides. All species were stable during the analysis. The assay was successfully used to study hydrolysis kinetics of hexaglycine. This assay can also be used to study the kinetics of various intermediates independently.

ACKNOWLEDGEMENT

We thank the Merck Foundation for supporting this work in the form of a research fellowship.

REFERENCES

1 V. H. L. Lee, *Pharm. Int.*, 7 (1986) 208.
2 M. Himukai, A. Kameyama and T. Hoshi, *Biochim. Biophys. Acta*, 732 (1983) 659.
3 N. Takuwa, T. Shimada, H. Matsumoto and T. Hoshi, *Biochim. Biophys. Acta*, 814 (1985) 186.
4 V. Ganapathy, J. F. Mendicino and H. Leibach, *J. Biol. Chem.*, 256 (1981) 118.
5 S. A. Adibi and E. L. Morse, *J. Clin. Invest.*, 60 (1977) 1008.
6 E. P. Kroeff and D. J. Pietrzyk, *Anal. Chem.*, 50 (1978) 1353.
7 V. K. Dua and A. Bush, *J. Chromatogr.*, 244 (1982) 128.
8 I. Molnar and Cs. Horváth, *J. Chromatogr.*, 142 (1977) 623.
9 D. S. Kalonia and S. Musunuri, in preparation.

Journal of Chromatography, 475 (1989) 421–425
Elsevier Science Publishers B.V., Amsterdam — Printed in The Netherlands

CHROM. 21 554

Note

Liquid chromatographic determination of planar aromatic sulphur compounds in crude oil

SEIJA SINKKONEN
Department of Chemistry, University of Jyväskylä, Kyllikinkatu 1–3, SF-40100 Jyväskylä (Finland)
(First received January 6th, 1989; revised manuscript received April 4th, 1989)

Little data have been reported concerning the liquid chromatographic (LC) retention characteristics of polycyclic aromatic sulphur heterocycles (PASHs) presumably because of their low concentrations relative to polycyclic aromatic hydrocarbons (PAHs) in environmental samples and the lack of a suitable sulphur-specific LC detector.

No successful method to separate sulphur heterocycles as original compounds from the non-polar aromatic compound fraction has been reported. Adsorption chromatography using silica gel and/or alumina has been generally used as the first step for isolating PASHs. However, the isolation of the PASHs from PAHs has been difficult.

Organic sulphides are known to form adducts with metal cations and with many other substances[1]. Complexation of organic sulphur compounds by means of copper, mercury, palladium and other metal salts is a well known technique and has been applied to coal extracts and coal products[2]. Procedures using these salts have been effective for the isolation of aliphatic sulphides but are generally not applicable to the separation of thiophene compounds. Thiophene compounds can be separated on a silver nitrate-coated silica column[3]. Copper(II) chloride is a good complexing agent for aliphatic thioethers, and $PdCl_2$ for aromatic heterocycles[1,4–7].

The sulphone method described in the literature was applied for gas chromatographic (GC) determination and required reduction of the isolated sulphones back to heterocyclic sulphides[8–14]. The aromatic fraction was treated in benzene–acetic acid (1:1) with H_2O_2 and then fractionated on a silica gel column. The unoxidized aromatic compounds were eluted with benzene and the sulphone/quinone fraction was collected with benzene–methanol (1:1) as the eluent. The latter fraction was reduced with $LiAlH_4$ in diethyl ether and the sulphides were separated from the hydroquinones by elution with hexane on a silica gel column.

The purpose of this study was to develop a method for the separation and determination of the PASHs in crude oil. The method was to be applied to environmental samples in oil residue analysis.

0021-9673/89/$03.50

EXPERIMENTAL

Thin-layer chromatography (TLC)

TLC experiments were performed to see where the heterocyclic aromatic sulphur compounds could be separated from aromatic hydrocarbons in the non-polar aromatic compounds fraction of crude oil. The experiments were done according to the literature[15]. Silica gel (Merck, Kieselgel 60 F_{254}, 20 cm × 10 cm, 0.25 mm) and alumina (Merck, Aluminium oxid 60 F_{254}, Type E, 20 cm × 20 cm, 0.25 mm) plates with a fluorescence indicator were used.

The components tested were biphenyl, dibenzothiophene (DBT) and the non-polar aromatic fraction of a Russian crude oil. Biphenyl and dibenzothiophene were used to see how the addition of a sulphur atom to an aromatic hydrocarbon changes the R_F values in different solvent systems.

Ligand-exchange chromatography

Approximately 10 g of silica gel were mixed with 0.5 g of palladium chloride in an aqueous solution and dried at 140°C in an oven overnight. A 4-g amount was introduced into a glass column (20 cm × 5.0 mm I.D.) and about 200 mg of the non-polar aromatic fraction of the crude oil in 2 ml of hexane were added to the top of column. Hexane, chloroform and benzene were used as the eluents.

Oxidation of dibenzothiophenes to sulphones and analysis by high-performance liquid chromatography (HPLC)

A weighed sample of Russian crude oil was first fractionated into aliphatic hydrocarbons and non-polar aromatic compounds using column chromatography[16]. The non-polar aromatic fraction was oxidized by refluxing with an excess of 30% hydrogen peroxide in glacial acetic acid for 4 h. The mixture was allowed to stand overnight, then extracted with dichloromethane and washed with water to remove acetic acid. Silica gel column chromatography was used to separate the sulphones from the dichloromethane extract. The column contained 6 g of SiO_2. Non-oxidized compounds were eluted with 80 ml of hexane and sulphones with 40 ml of methanol.

Sulphones cannot easily be analysed by GC because they are highly polar, non-volatile and thermolabile[17]. Reversed-phase HPLC is a suitable method. The apparatus used was an Hitachi 655A-11 liquid chromatograph with a 655A variable wavelength UV monitor. An Spherisorb ODS2 column, 5 μm (25 cm × 4.6 mm I.D.), was used. Methanol–water and acetonitrile–water solutions were used as the eluents.

RESULTS AND DISCUSSION

TLC

From the results, it was concluded that the aromatic sulphur heterocycles cannot be separated as a group from aromatic hydrocarbons by TLC on silica gel or alumina plates. The only measurable differences in R_F values for biphenyl and dibenzothiophene on silica gel were detected when light petroleum (b.p. 40–60°C)–diethyl ether–acetic acid (80:15:5), light petroleum (b.p. 40–60°C)–ethyl acetate–acetic acid (80:15:5) or light petroleum (b.p. 40–60°C)–acetone–acetic acid was used as the eluent. Even then the separation was not complete. On alumina, biphenyl and DBT were successfully separated with light petroleum or hexane.

Ligand-exchange chromatography

The sulphur compounds were separated from the non-polar aromatic fraction of the crude oil using silica gel/$PdCl_2$ column chromatography. Hexane and benzene alone did not elute the compounds; rather hexane–chloroform or hexane when a little diethylamine was added.

The fraction obtained was analysed by GC–mass spectrometry (MS) and the presence of C_{0-3}DBT (dibenzothiophenes with 0–3 carbons in side chains) was confirmed by molecular ion mass fragmentography.

Oxidation

The methanol fraction obtained from the oxidation of crude oil was examined by

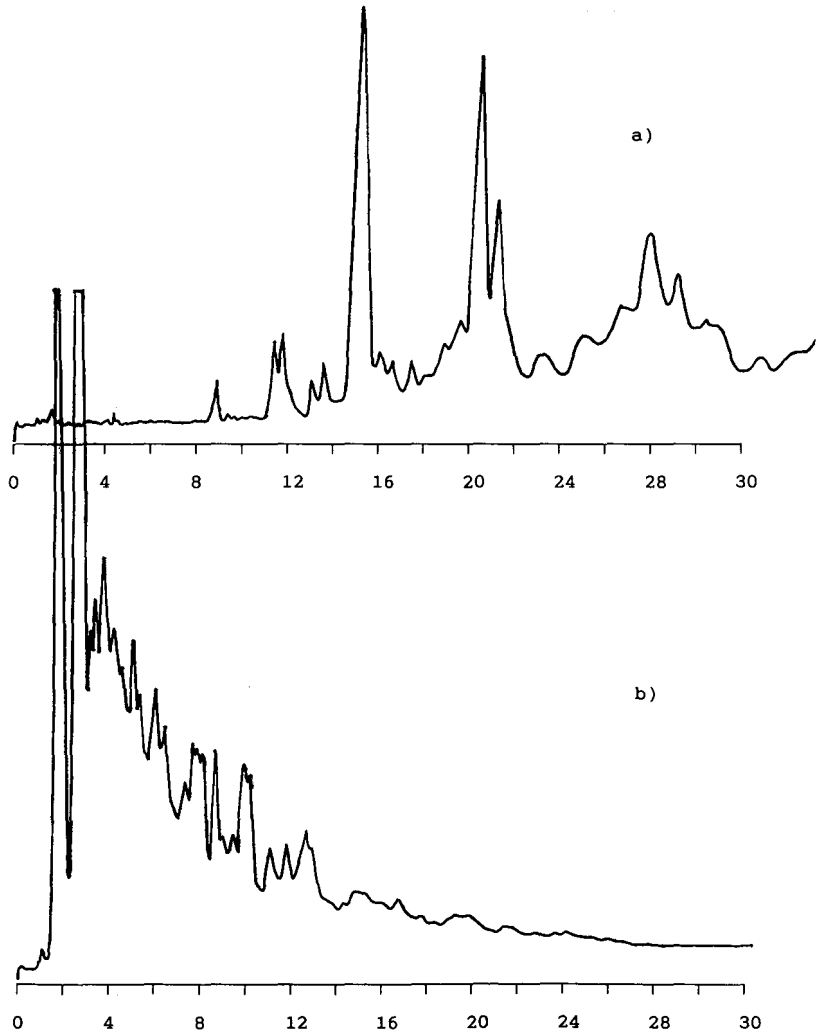

Fig. 1. HPLC chromatograms of (a) the non-polar aromatic compounds fraction of Russian crude oil (28.7 μg) and (b) the sulphone fraction of the same oil (13.8 μg). Column: Spherisorb 5 μm. Mobile phase: acetonitrile–water (60:40); flow-rate 1 ml/min. Detection: UV, 254 nm.

GC–MS using a short SE-54 column and found to contain mainly dibenzothiophene-5,5-dioxide and methylated analogues.

The procedure was also tested with dibenzothiophene, which was oxidized completely to dibenzothiophene-5,5-dioxide and recovered in 90–100% yield after silica gel column chromatography.

In reversed-phase HPLC, sulphones are eluted in a reatively short time when the eluent contains 33–45% water. The retention time of dibenzothiophene-5,5-dioxide was 5.60 min when acetonitrile–water (60:40) was used as the eluent. The sulphones from crude oil were all eluted before 15 min. The non-oxidized dibenzothiophenes and aromatic hydrocarbons have much longer retention times. When the eluent contains less than 35% water the sulphones are not eluted. When the eluent contains more than 45% water the retention times are longer than with 40% of water. The wavelengths used in the UV detection were 225, 231, 240 and 254 nm. At shorter wavelengths the sensitivity increases for sulphones. For example, at 231 nm it is ten times that at 254 nm, but there are disturbing peaks. Therefore the wavelength of 254 nm was chosen for the analysis. The HPLC chromatogram of the non-oxidized non-polar aromatic compound fraction of Russian crude oil and the chromatogram of the same fraction after oxidation and column chromatography are shown in Fig. 1.

CONCLUSIONS

Different TLC adsorbents like silica gel, aluminium oxide and amino silane did not allow the isolation of PASHs.

Column chromatography using silica gel impregnated with palladium chloride produced a moderate separation of PASHs, but the compounds were partly eluted as PASH–$PdCl_2$ complexes which cannot be analyzed by conventional methods.

The oxidation of dibenzothiophenes to the corresponding sulphones was found to be quantitative and the separation of the sulphones from oxidized and unoxidized PAHs was achieved by column chromatography. The oxidation time of 4 h used was long enough to oxidize all of the dibenzothiophenes to the corresponding sulphones, which can be analyzed as such or reduced back to the original sulphur compounds.

The non-polar aromatic fraction was about 28% of the Russian crude oil samples when weighed and the sulphone fraction about 20% of the non-polar aromatic compound fraction.

The sulphones were not determined quantitatively by HPLC because of the lack of a good internal standard. Diphenyl sulphone was tested but it was not sufficiently resolved from other sulphones. The synthesis of model compounds for the analysis of PASHs is underway in our laboratory.

REFERENCES

1 J. Vogh and J. E. Dooley, *Anal. Chem.*, 47 (1975) 816–825.
2 T. Kaimai and A. Matsunaga, *Anal. Chem.*, 50 (1978) 268–270.
3 W. Joyce and P. Uden, *Anal. Chem.*, 55 (1983) 540–543.
4 K. D. Gundermann, H. P. Ansteeg and A. Glitsch, *International Conference on Coal Science, August 15-19, Pittsburg, PA, 1983*, pp. 631–634.
5 M. Nishioka, M. L. Lee and R. N. Castle, *Fuel*, 65 (1986) 390–397.
6 M. Nishioka, R. M. Campell, M. L. Lee and R. N. Castle, *Fuel*, 65 (1986) 270–273.

7 M. Nishioka, D. G. Whiting, R. M. Campell and M. L. Lee, *Anal. Chem.*, 58 (1986) 2251–2255.
8 C. M. White, in A. Björseth (Editor), *Handbook of Polycyclic Aromatic Hydrocarbons,* Marcel Dekker, New York, Basle, 1983, pp. 594–601.
9 W. D. Later, M. L. Lee, K. D. Bartle, R. C. Kong and D. L. Vassilaros, *Anal. Chem.*, 53 (1981) 1612–1620.
10 R. C. Kong, M. L. Lee, M. Iwao, Y. Tominaga, R. Pratap, R. D. Thompson and R. N. Castle, *Fuel*, 63 (1984) 702–707.
11 C. Willey, M. Iwao, R. N. Castle and M. L. Lee, *Anal. Chem.*, 53 (1981) 400–407.
12 M. L. Lee, C. Willey, R. N. Castle and C. M. White, *International Symposium on Analysis, Chem. and Biology, October 1979*, Battelle Press, Columbus, OH, 1980, pp. 59–74.
13 D. M. Jewell, R. G. Ruberto and J. T. Swansiger, *Sulfur Compounds in Petroleum: Isolation and Characterization,* Vol. 19, American Chemical Society, Division of Petroleum Chemistry, 1975, Philadelphia, PA, pp. 19–29.
14 H. V. Drushel and A. L. Sommers, *Anal. Chem.*, 39 (1967) 1819–1829.
15 J. Knuutinen and J. Paasivirta, *J. Chromatogr.*, 194 (1980) 55–61.
16 J. Paasivirta, R. Herzshuh, M. Lahtiperä, J. Pellinen and S. Sinkkonen, *Chemosphere*, 10 (1981) 919–928.
17 V. Vignier, F. Berthou and D. Picart, *J. High Resolut. Chromatogr. Chromatogr. Commun.*, 6 (1983) 661–665.

Journal of Chromatography, 475 (1989) 426–431
Elsevier Science Publishers B.V., Amsterdam — Printed in The Netherlands

CHROM. 21 556

Note

High-performance liquid chromatography of long chain 7-oxo alcohols, acids and their esters[a]

SAJID HUSAIN*, G. PRATAP and R. NAGESWARA RAO
Regional Research Laboratory, Hyderabad-500 007 (India)
(First received September 14th, 1988; revised manuscript received April 6th, 1989)

Long chain fatty alcohols, acids and their derivatives are important intermediates in the manufacture of various oil-field chemicals[1–3], *viz.*, pourpoint depressants, surface active and anticorrosive agents. Their carbon numbers generally vary between C_{12} and C_{22}. A series of 7-oxo alcohols, acids and their esters of carbon numbers C_{12}–C_{22} have recently been synthesized[4,5] in our laboratory for the first time to evaluate the flow improving properties of their comb-like polymers on different crude oils. A method is needed for their identification and purity determination, and a thorough literature survey having revealed that no such method is available.

Generally, fatty alcohols are separated by gas chromatography (GC)[6,7] after converting them into trifluoroacetate/acetate esters. The quantitative separation and identification of oxopentanols in reaction mixtures by gas chromatography–mass spectrometry (GC–MS) and NMR spectroscopy have been reported[8,9]. Short-chain oxo alcohols such as 3-hydroxy-2-octanone, 5-hydroxy-2-hexanone and 4-hydroxypentanone in different fat products have been separated quantitatively by GC[10,11]. However, these methods are tedious and time consuming since they involve a large number of derivatization steps. Subbarao and co-workers[12,13] have described the separation of several fatty alcohols and their oxygenated compounds using thin-layer chromatography (TLC). Weihrauch *et al.*[14] have estimated a variety of long-chain oxo fatty acids, isolated from milk fat, by GC–MS. Methods for the separation of positional isomers of C_{18} and C_{24} oxo acids have also been reported[15,16].

The present paper reports a simple high-performance liquid chromatographic (HPLC) method for the separation and identification of 7-oxo alcohols, acids and their esters in mixtures. It compares the chromatographic behaviour of these compounds with that of the corresponding fatty alcohols, acids and their esters. Further it describes the application of this method to the analysis of long chain saturated alcohols and acids present in different waxes.

EXPERIMENTAL

Apparatus

A high-pressure liquid chromatograph Model ALC/GPC 244 equipped with a

[a] RRL H Communication number: 2255.

0021-9673/89/$03.50

Model M 6000 A reciprocating pump and U6K injector from Water Assoc. (Milford, MA, U.S.A.) was used. It was connected to a refractive index detector and a D 5000 duel channel strip-chart recorder with a Chromatopak E 1A integrator (Shimadzu). A 10-μl syringe (Hamilton, Bonaduz, Switzerland) and a stainless-steel fatty acid column (30 cm × 3.9 mm I.D., 10 μm) were used.

Materials and reagents

7-Oxo alcohols and 7-oxo acids were synthesized in our laboratory according to the procedures reported elsewhere[4,5]. Their purities were checked by TLC. Fatty alcohols and fatty acids obtained from Sigma (St. Louis, MO, U.S.A.) were used as supplied without any purification. The ethyl esters of related carboxylic acids were prepared by a general method[17]. Two different waxes, *viz*, bees-wax and sugar cane wax, were saponified prior to analysis.

All reagents used were of HPLC grade obtained from Spectrochem, India.

Mobile phase

The mobile phase used was water–acetonitrile–tetrahydrofuran (35:45:20, v/v/v). The components were degassed before mixing.

Procedure

A standard mixture of 7-oxo alcohols was injected on to the column by means of a 10-μl Hamilton syringe through a U6K injector using a flow technique. The analysis was carried out under isocratic conditions at a flow-rate of 1.5 ml/min and a chart speed of 1.0 cm/min at room temperature (27°C). The column was stabilized prior to its use.

RESULTS AND DISCUSSION

The long chain 7-oxo alcohols, acids and their esters (series A) were synthesized[4,5] in the laboratory. Corresponding fatty acids and their respective derivatives (series B) were selected for comparative studies. They have been analysed by HPLC. The retention times, t_R, and capacity factors, k', for these compounds are given in Table I. Fig. 1 shows that 7-oxo alcohols ranging in carbon number from C_{12} to C_{22} are completely separated. The peaks were identified from the retention times of individual compounds. As the retention times increase the peaks are broadened progressively with increasing carbon chain length from C_{12} to C_{22}.

The retention data for series A and B (Table I) have been used to find out the kind of molecular interaction involved in their chromatographic separation. Fig. 2 shows plots between log k' and the carbon numbers of these compounds. The plots are linear for the respective series. It can be concluded that partition phenomena play a dominant rôle in the separation of these compounds. Further, it is seen from Table I and Fig. 2 that the trends in the separation of corresponding compounds in series A and B are similar. However, the long-chain 7-oxo derivatives of series A have shorter retention times than the corresponding compounds of equivalent chain length in series B. This may be due to the fact that the 7-oxo substituted compounds are more polar than those compounds having no substitution.

The method developed has great potential for the simultaneous separation and

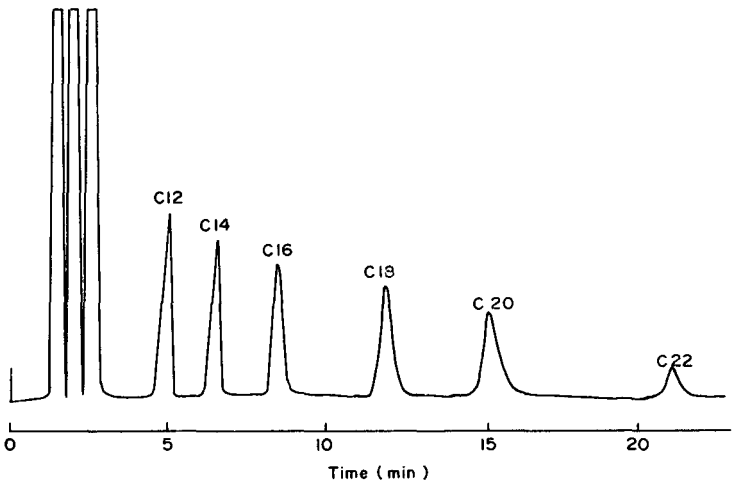

Fig. 1. Chromatogram of C_{12}–C_{22} 7-oxo alcohols. For conditions, see text.

TABLE I

RETENTION DATA FOR SERIES A AND B

Series A: 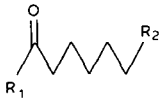

Series B: 

R_1	Carbon number	R_2					
		CH_2OH		$COOH$		$COOC_2H_5$	
		$t_R(s)$	k'	$t_R(s)$	k'	$t_R(s)$	k'
Series A							
$-(CH_2)_4CH_3$	12	346	0.55	335	0.50	435	0.94
$-(CH_2)_6CH_3$	14	402	0.79	386	0.72	505	1.25
$-(CH_2)_8CH_3$	16	478	1.13	445	0.99	625	1.79
$-(CH_2)_{10}CH_3$	18	582	1.60	527	1.35	718	2.48
$-(CH_2)_{12}CH_3$	20	720	2.21	644	1.88	1003	3.48
$-(CH_2)_{14}CH_3$	22	929	3.15	780	2.48	1309	4.84
Series B							
$-(CH_2)_4CH_3$	12	501	1.24	427	0.91	548	1.45
$-(CH_2)_6CH_3$	14	614	1.74	510	1.28	684	2.05
$-(CH_2)_8CH_3$	16	772	2.45	620	1.77	880	2.93
$-(CH_2)_{10}CH_3$	18	1000	3.46	765	2.42	1187	4.30
$-(CH)_2)_{12}CH_3$	20	1271	4.67	927	3.14	1626	6.26
$-(CH_2)_{14}CH_3$	22	1710	6.63	1239	4.53	2175	8.71

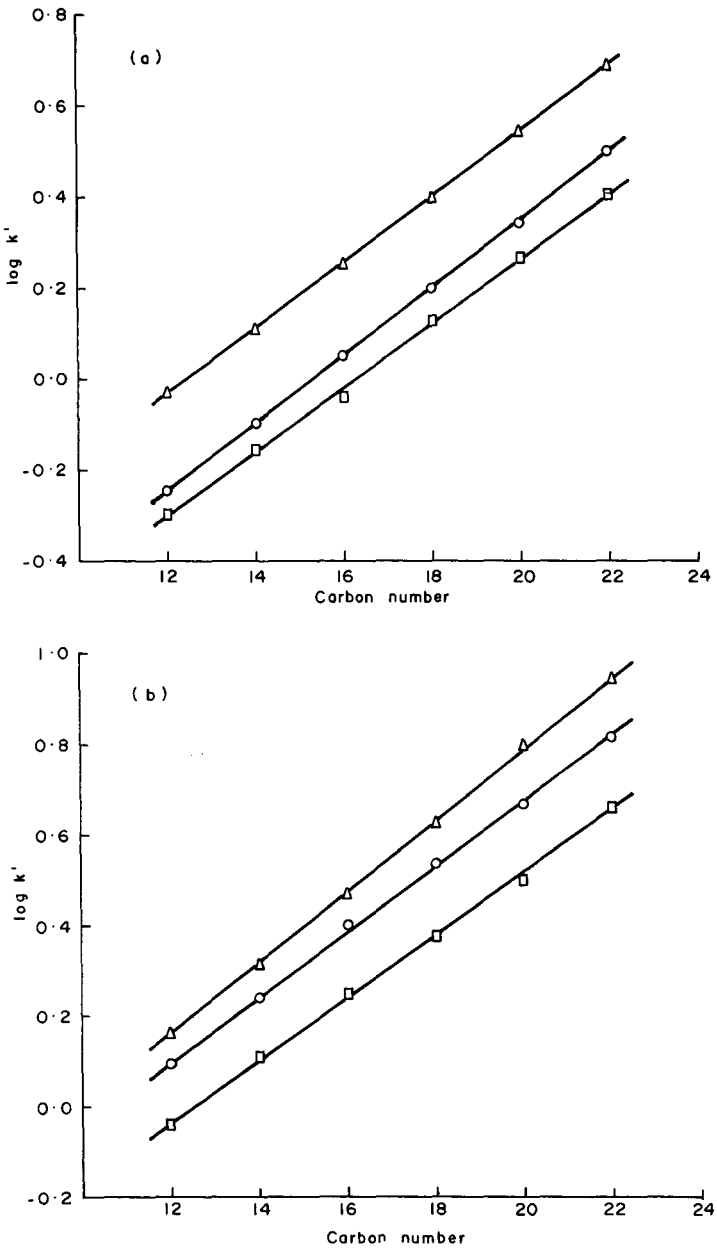

Fig. 2. Plots of log k' *vs.* carbon number for (a) series A and (b) series B. ○, CH_2OH; □, COOH; △, $COOC_2H_5$.

identification of 7-oxo alcohols/acids in mixtures either prepared synthetically or isolated from natural products. Since the 7-oxo alcohols rarely occur in nature, this method cannot be applied for their analysis. However, two different waxes have been saponified first in order to separate fatty alcohols and acids, and then subjected to

TABLE II

COMPOSITION OF FATTY ACIDS AND ALCOHOLS IN COMMERCIAL WAXES

Average of three determinations

Composition (by carbon number)		*Composition (%)*			
		HPLC		*GC*	
		Bees wax	*Sugar cane*	*Bees wax*	*Sugar cane*
C_{14}	acid	1.0 ± 0.1	–	1.1 ± 0.1	–
	alcohol	–	–	–	–
C_{16}	acid	51.4 ± 1.3	3.0 ± 0.1	50.5 ± 1.6	2.9 ± 0.2
	alcohol	–	–	–	–
C_{18}	acid	9.0 ± 0.5	2.0 ± 0.1	8.8 ± 0.7	2.0 ± 0.1
	alcohol	–	–	–	–
C_{20}	acid	1.5 ± 0.2	1.6 ± 0.1	1.0 ± 0.1	1.7 ± 0.3
	alcohol	–	–	–	–
C_{22}	acid	1.5 ± 0.2	3.5 ± 0.1	1.8 ± 0.1	3.8 ± 0.3
	alcohol	–	–	–	–
C_{24}	acid	18.0 ± 0.9	3.4 ± 0.1	17.6 ± 0.6	3.1 ± 0.1
	alcohol	12.5 ± 0.5	0.5 ± 0.1	11.9 ± 0.8	0.6 ± 0.1
C_{26}	acid	4.5 ± 0.4	10.2 ± 0.6	4.9 ± 0.5	10.1 ± 0.9
	alcohol	10.5 ± 0.8	13.2 ± 0.7	10.1 ± 0.8	15.4 ± 0.9
C_{28}	acid	4.0 ± 0.3	56.0 ± 1.3	43.0 ± 0.5	58.5 ± 1.5
	alcohol	13.8 ± 0.7	75.8 ± 1.7	14.2 ± 0.9	76.7 ± 1.9
C_{30}	acid	3.0 ± 0.2	10.5 ± 0.5	3.0 ± 0.3	10.5 ± 0.6
	alcohol	33.6 ± 1.1	8.0 ± 0.3	31.6 ± 1.5	5.2 ± 0.2
C_{32}	acid	5.0 ± 0.3	5.5 ± 0.2	47.0 ± 0.2	5.4 ± 0.4
	alcohol	23.1 ± 1.0	2.5 ± 0.1	23.5 ± 1.4	2.1 ± 0.3
C_{34}	acid	1.1 ± 0.1	4.3 ± 0.1	2.0 ± 0.2	3.9 ± 0.3
	alcohol	6.5 ± 0.3	–	6.0 ± 0.5	–

HPLC analysis. The quantity of each component has been determined by comparing its peak area with the total area of the peaks in the chromatogram. Table II gives the respective compositions obtained by HPLC and GC[18,19]. It can be seen that the results obtained by the two techniques are in good agreement. They clearly demonstrate the suitability of the present method for determining the composition of fatty acids and alcohols in waxes and also wax esters which are a dominant class of lipids in calanoid copepods[20,21]. The method is more simple and rapid than those which involve a number of derivatization steps.

ACKNOWLEDGEMENT

We thank Mr. R. Narasimha of RRL, Hyderabad for technical assistance.

REFERENCES

1 H. H. Naza, E. I. Abou, W. M. Azim, E. I. Aba and M. M. Ahmed, *J. Chem. Tech. Biotechnol.*, 35A (1985) 241.
2 Shell Oil Co., Houston, TX, *U.S. Pat.*, 3,957,659 (1976).

3 K. L. Shanta, G. Pratap and V. S. Bhaskar Rao, *J. Appl. Polym. Sci.*, in press.
4 G. Pratap, K. L. Shanta and V. S. Bhaskar Rao, *Org. Prep. Pro. Int.*, 20 (1988) 593.
5 K. L. Shanta, G. Pratap and V. S. Bhaskar Rao, *Fat Sci. Technol.*, in press.
6 R. Wood and F. Snyder, *Lipids*, 1 (1966) 62.
7 J. W. Farquhar, *L. Lipid. Res.*, 3 (1962) 21.
8 M. Pechal, Z. Cvengrosova, S. Holotik, L. Malik and M. Hrusovsky, *J. Chromatogr.*, 206 (1981) 541.
9 R. Pentti, B. Saara and S. Hekki, *Am. J. Enol. Viticult.*, 21 (1970) 136.
10 J. Suzuki and M. E. Bailey, *J. Agric. Food Chem.*, 33 (1985) 343.
11 A. A. Nomeir and M. B. Abou-Donia, *Anal. Biochem.*, 151 (1985) 381.
12 L. J. Morris, D. H. Wharry and E. W. Hammond, *J. Chromatogr.*, 33 (1968) 471.
13 N. H. Isaiah, R. Subbarao and J. S. Aggarwal, *J. Chromatogr.*, 43 (1969) 519.
14 J. L. Weihrauch, C. R. Brewington and D. P. Schwartz, *Lipids*, 9 (1974) 883.
15 A. P. Tulloch, *J. Am. Oil Chem. Soc.*, 41 (1964) 833.
16 C. R. Smith, *Lipids*, 1 (1966) 268.
17 V. H. Schilokheccht and G. Renner, *Fette, Seifen, Anstrichm.*, 66 (1964) 176.
18 D. T. Downing, Z. H. Kranz, J. A. Lamberton, K. E. Murray and A. H. Redcliffe, *Aust. J. Chem.*, 14 (1961) 253.
19 Z. H. Kranz, J. A. Lamberton, K. E. Murray and A. H. Redcliffe, *Aust. J. Chem.*, 13 (1960) 498.
20 R. G. Ackman, B. A. Links and J. Ringley, *J. Fish. Res. Board Can.*, 31 (1974) 1912.
21 R. F. Lec, J. C. Nevenzel and G. A. Paffenhofer, *Mar. Biol.*, 9 (1971) 99.

Journal of Chromatography, 475 (1989) 432–441
Elsevier Science Publishers B.V., Amsterdam — Printed in The Netherlands

CHROM. 21 557

Note

Residue analysis of the herbicides cyanazine and bentazone in sugar maize and surface water using high-performance liquid chromatography and an on-line clean-up column-switching procedure

ELBERT A. HOGENDOORN* and CHÉRIE E. GOEWIE
National Institute of Public Health and Environmental Protection, P.O. Box 1, NL-3720 BA Bilthoven (The Netherlands)
(First received December 27th, 1988; revised manuscript received April 10th, 1989)

In order to decide about the acceptability of the application of the herbicides bentazone (3-isopropyl-1*H*-benzo-2,1,3-thiadiazin-4-one 2,2-dioxide; CAS No.25057-89-0) and cyanazine [2-(4-chloro-6-ethylamino-1,3,5-triazin-2-ylamino)-2-methylpropionitrile; CAS No. 21725-46-2] to sugar maize in The Netherlands, a field study was carried out in which maize fields were treated with both herbicides. In this paper a high-performance liquid chromatographic (HPLC) method, involving on-line clean-up by means of column switching, is described for the simultaneous determination of these herbicides together with the 6- and 8-hydroxy metabolites of bentazone. Generally this type of work requires limits of determination (LOD) of 0.1 mg/kg.

Cyanazine, a triazine herbicide, can be determined by gas chromatography (GC)[1,2] and also by reversed-phase HPLC (UV detection, 224 nm) using a basic eluent (pH 8)[2,3]. Bentazone can be determined by GC after derivatization with diazomethane[4] or pentafluorobenzoyl chloride[5] or by reversed-phase HPLC (UV detection, 229 nm), using an acidic eluent (pH 3)[6]. In our Institute, a mobility study has been conducted in order to study the behaviour of bentazone and its two metabolites, 6- and 8-hydroxybentazone, in soil columns. The three compounds were analysed by reversed-phase HPLC (UV detection, 229 nm) using an acidic eluent[7]. Liquid–liquid extraction from the acidified effluent was carried out with dichloromethane. Probably owing to adsorption effects, the 6- and 8-hydroxy bentazone metabolites could not be recovered after addition to a soil column.

Cyanazine has been determined in grain[1], soil[2] and surface water[3], after extraction into an organic solvent (both methanol and dichloromethane have been described) followed by subsequent column chromatography over silica gel, Florisil and Bio-Beads. The LOD after HPLC analysis was typically 0.01 mg/kg[2].

Akerblom and Gunborg[8] isolated bentazone from soil and crops using methanol. The extract was cleaned by a complex liquid–liquid extraction procedure, involving three different washing steps, followed by ion-pair extraction of the analyte using tetrabutylammonium hydroxide in dichloromethane. The LOD of the HPLC procedure was 0.02 mg/kg.

From the literature survey, we concluded that the method of choice for the simultaneous determination of the compounds mentioned above is HPLC. In line with

0021-9673/89/$03.50

our previous work[9–11], we decided to develop a clean-up procedure involving precolumn switching for the extracts, in order to increase the speed and reproducibility of the sample clean-up step.

EXPERIMENTAL

Equipment

The HPLC system consisted of the following components: a PROMIS (Spark Holland, Emmen, The Netherlands) autosampler, equipped with a time-programmable high-pressure switching valve, type 7010, one low-pressure switching valve, Type 5300, and an electropneumatic unit, Type 7163 (Rheodyne, Cotati, CA, U.S.A.), two HPLC pumps (Series 10, Perkin-Elmer, Norwalk, CT, U.S.A.) a Kratos (Ramsey, NJ, U.S.A.) Spectroflow 770 UV detector, set at 229 nm, a Kipp (Delft, The Netherlands) recorder and an LDC/Milton Roy (Co. Clare, Ireland) Cl-10 integrator. The precolumn was a 15 × 3.2 mm I.D. Brownlee (Santa Clara, CA, U.S.A.) New Guard cartridge packed with 7-μm RP-18 and the analytical column was a 150 × 4.6 mm I.D. stainless-steel column, packed in-house with 5-μm Hypersil ODS (Shandon, Runcorn, U.K.). The analytical column was kept at 22°C by means of a water jacket.

Chemicals

Cyanazine and bentazone, both of >99% purity, were obtained from BASF (Ludwigshafen, F.R.G.); 6- and 8-hydroxybentazone were a gift from Dr. N. Drescher (BASF). Dichloromethane of analytical quality was bought from Merck (Darmstadt, F.R.G.) and methanol (UV spectrometry grade) and acetonitrile (HPLC quality) from Baker (Deventer, The Netherlands). HPLC water was obtained by filtration of doubly distilled water over a Millipore (Bedford, MA, U.S.A.) Norganic filter, Type CC15 120 00. Anhydrous sodium sulphate and hydrochloric acid (6 *M*) were bought from Baker and orthophosphoric acid (89% pure) and Titrisol buffer (pH 4) from Merck.

HPLC eluents were mixed by volume, and subsequently filtered and degassed by vacuum suction over a 0.5-μm filter (Millipore).

Extraction procedure for maize

Maize kernels were stripped from the cobs and collected. After mixing of the kernels, 50 g were weighed in the cup of a Waring blender and 200 ml of dichloromethane, 4 ml of 6 *M* hydrochloric acid and 100 g of sodium sulphate were added. The mixture was blended for 3 min, then the homogenate was transferred into a tube and centrifuged for 5 min at 7000 *g*. A 100-ml volume of the dichloromethane phase was dried over sodium sulphate and concentrated to 10 ml in a Kuderna Danish apparatus. A 1-ml volume of the dichloromethane extract, containing 2.5 g ml of maize, was pipetted into a calibrated tube, which was placed on a warm water-bath (*ca.* 80°C) and, with the use of a gentle stream of nitrogen, the solvent was removed. The residue was dissolved in hexane, which had been previously saturated with acetonitrile, 1 ml of acetonitrile was added and the tube was shaken for 1 min. The upper layer was removed by pipetting and the acetonitrile was evaporated on a water-bath. The residue was dissolved in 100 μl of methanol, then 1.9 ml of water was added. Aliquots of 100 μl of a solution of the extract in methanol–water (5:95), were further processed automatically by injection on to the precolumn.

Extraction procedure for drinking and surface water (LOD 0.5 μg/l)

A sample of 100 ml of water was placed in a 250-ml round-bottomed flask and concentrated with a rotary film evaporator at 70°C to *ca.* 0.5 ml. About 0.5 ml of distilled water was added and the flask was placed in an ultrasonic bath for 2 min. The concentrate was transferred to a calibrated tube by pipetting. The flask was rinsed with 0.5 ml of water and the final volume in the tube was brought to 2 ml with distilled water. Aliquots of 100 μl of this concentrate were injected on to the precolumn.

Extraction and partial clean-up procedure for drinking water, raw water and rain (LOD 0.01 μg/l)

A 200-ml volume of water was adjusted to pH 10 by dropwise addition of 1 *M* sodium hydroxide solution. The sample was concentrated in a rotary film evaporator at 80°C to *ca.* 3 ml. The sample was transferred to a calibrated tube and, if necessary, the pH was adjusted to 10 by dropwise addition of 1 *M* sodium hydroxide solution. A 2-ml volume of *n*-hexane was added and the tube was shaken vigorously for 30 s. The hexane layer was removed by pipetting. Another 2 ml of *n*-hexane were added and the shaking was repeated. The *n*-hexane was pipetted off and the aqueous layer was acidified by addition of 1.5 ml of 4 *M* hydrochloric acid. Bentazone was extracted with 2 × 2 ml of dichloromethane. The dichloromethane layer was filtered over sodium sulphate into a calibrated tube. The tube was placed on a warm water-bath (*ca.* 60°C) and the solvent was evaporated with a gentle stream of nitrogen. The residue was dissolved in 5% methanol by first adding 20 μl of methanol followed by 180 μl of water. The solution was then pipetted into an autosampler vial and processed further by precolumn switching HPLC.

Precolumn clean-up and HPLC procedure

The set-up for the automated sample clean-up and subsequent HPLC analysis is shown in Fig. 1. The precolumn flushing solvent, A, consisted of methanol–0.03 *M* phosphate buffer (pH 2.70) (5:95), at a flow-rate of 1 ml/min. The eluent for the analytical column, E, was methanol–0.02 *M* phosphate buffer (pH 2.70) (35:65) at a flow-rate of 1 ml/min.

Aliquots of 100 μl were injected by the autosampler (AS) on to the precolumn (PC), using 2.5 ml of flushing solvent for water concentrates and 4.0 ml for maize extracts. The sample was transferred to the analytical column, using 0.5 ml of eluent, by switching the precolumn temporarily in-line with the analytical column.

While the analysis takes place, the precolumn is washed with 5 ml of methanol (B) and reconditioned for the next injection with 10 ml of flushing solvent (A). After every fifth sample injection, an external standard (std. vial) was analysed.

RESULTS AND DISCUSSION

HPLC procedure

Optimization of reversed-phase analysis was carried out on a C_{18} column using methanol and acetonitrile as modifiers and, because of the acidic nature of bentazone (pK_a 3.2), using an acidic aqueous buffer (initially 0.02 *M* phosphate, pH 2.8) to suppress ionization. We observed symmetrical peaks for the analytes when using methanol and serious peak tailing with acetonitrile as the modifier, and therefore continued to work with methanol.

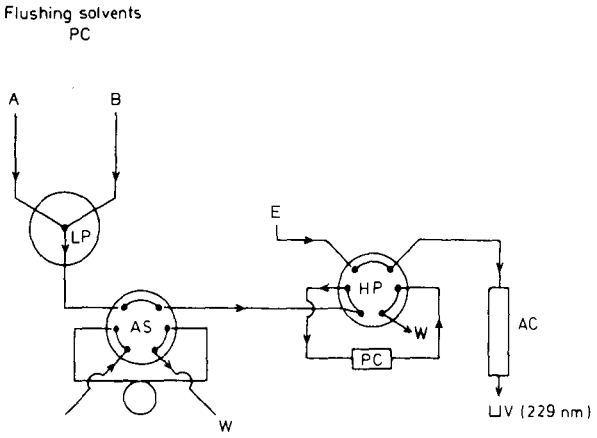

Fig. 1. Schematic representation of the eluent streams and switching valves used for the HPLC analysis. A = Methanol–0.03*M* phosphate buffer (pH 2.70) (5:95); B = 100% methanol; E = methanol–0.03 *M* phosphate buffer (pH 2.70) (35:65); LP = low-pressure three-way selection valve; HP = high-pressure six-port switching valve, equipped with a C_{18} precolumn (PC); AS = autosampler with a 200-μl sample loop; AC = analytical column; W = waste; UV = UV detector.

We studied the behaviour of the analytes and that of a potential interferent, present in maize extracts (see Experimental), as a function of the methanol content of the eluent. The results are presented as ln *k* *vs.* percentage modifier in Fig. 2. It can clearly be seen that the separation of the analytes is easy, but that an unknown component will interfere with either bentazone or cyanazine. Calculation of the R_s values[12] of each of the two peak pairs showed that, in the system used, the resolution is optimal (R_s = 0.91) at 35% methanol.

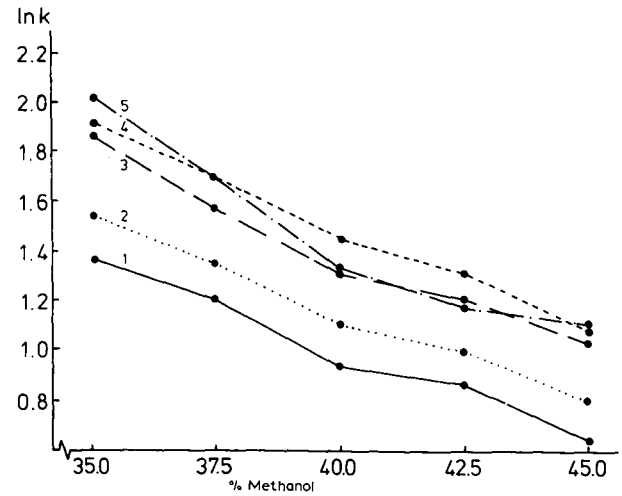

Fig. 2. Logarithmic plot of the capacity factors (*k*) of (3) cyanazine, (4) bentazone, (1) 6- and (2) 8-hydroxybentazone and (5) a unknown matrix compound from maize as a function of the percentage of methanol in the mobile phase. Column: 150 × 4.6 mm I.D. Hypersil ODS. Eluent: methanol in 0.02 *M* phosphate buffer (pH 2.70) (35:65) at a flow-rate of 1 ml/min. For further details, see Experimental.

In order to improve the resolution, we varied the pH of the eluent, keeping the organic modifier composition constant. In this experiment it appeared that pH had a major influence on the behaviour of bentazone and its metabolites. At this stage two new potential interferences appeared in the chromatograms of the maize extract blanks, and these peaks were therefore included in the optimization study.

Fig. 3 shows a plot of the resolution, R_s, as a function of the pH of the buffer in the eluent. It can be seen that no condition can be found where the resolutions for all components is good (*i.e.*, have a value of *ca.* 1.2 or larger). However, as the two interferences are relatively small (corresponding to 0.05 mg/kg of each of the metabolites of bentazone), we decided not to pay much attention to the resolution between the metabolites and the matrix interferences and to select, as a compromise, the conditions that give a good separation between the analytes of interest and some separation between the metabolites and the matrix.

Precolumn clean-up procedure

Initially, we studied the possibility of using disposable cartridges (Baker-10) for clean-up. We tested the ability of cartridges filled with different adsorbents (200 mg of C_8, C_{18} and CN material) to sorb the best retained analyte, bentazone, from an aqueous solution of pH 2.70. None of the cartridges could retain this analyte.

On normal phase material (Baker-10, 500 mg silica) the situation was the opposite: all analytes were very strongly retained. In order to desorb bentazone, 1% of water had to be added to the eluent (methanol–dichloromethane, 50:50). Such a solvent cannot easily be evaporated and therefore this method was rejected.

Analogous to previous work[9–11], we decided to clean redissolved extracts on a reversed-phase precolumn. As the flushing solvent we used the same aqueous buffer

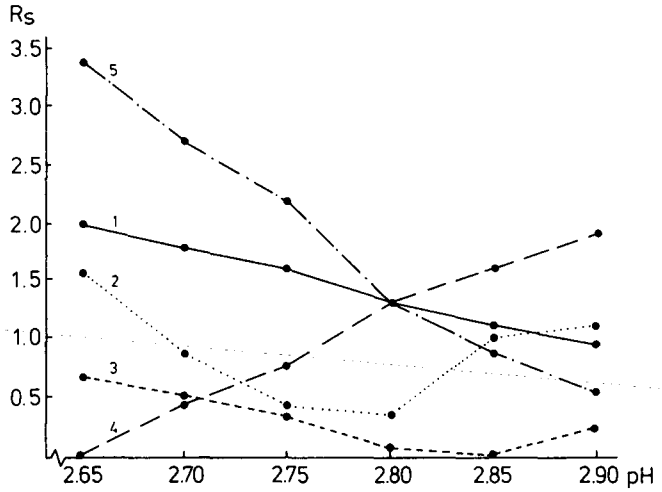

Fig. 3. Resolution (R_s) plotted against pH of the mobile phase for the five peak pairs in Fig. 2. Column: 150 × 4.6 mm I.D. Hypersil ODS. Eluent: methanol in 0.02 *M* phosphate buffer (35:65) at a flow rate of 1 ml/min. For further details see Experimental. 1,6-Hydroxybentazone–8-hydroxybentazone; 2, cyanazine–bentazone; 3,6-hydroxybentazone–interferent 1; 4,8-hydroxybentazone–interferent 2; 5, bentazone–interferent 2.

of pH 2.70 as was used in the HPLC eluent. In order to keep lipophilic matrix residues in solution we added 5% of methanol to this solvent. The flushing solvent was used to transfer the sample from the vial to the precolumn and for clean-up.

We tested three different packing materials in the precolumn: PRP-1 (a divinylbenzene–styrene copolymer), RP-8 and RP-18. We determined the breakthrough volumes of the first-eluted compound, 6-hydroxybentazone, from the flushing solvent [methanol–0.03 *M* phosphate buffer, pH 2.70 (5:95) at a flow-rate of 1 ml/min], and of the last-eluted compound, bentazone, from the transfer or desorption solvent [=eluent of the analytical column: methanol–0.02 *M* phosphate buffer, pH 2.70 (35:65) at a flow-rate of 1 ml/min]. All desorption experiments were carried out in the forward flush mode.

The results are given in Table I. The peak volumes eluted from the precolumn were measured on a recorder as their UV absorbance at 229 nm. In this context, V_{start} and V_{end} are the corresponding starting and end points of the recorder peak in the chromatogram. It can be seen from Table I that on RP-8 there is little retention, and desorption takes place fast; on PRP-1 there is good retention but desorption is slow, which will give rise to undesirable band broadening during analysis. With RP-18, one can concentrate the analytes with 3 ml of flushing solvent, without breakthrough, and desorption can take place with as little as 0.4 ml of eluent.

We used the described procedure with RP-18 to analyse maize extracts spiked with cyanazine, bentazone and the two metabolites. The extracts were found not to contain the metabolites. Further study showed that the concentrations of the metabolites, added to partially cleaned maize extracts, quickly decrease and can no longer be measured after standing for a few hours. Therefore, we concluded that a matrix effect occurs, as had also been observed by Loch[7] in soil, and that attempts to measure the metabolites of bentazone in maize are useless. Our efforts were therefore directed towards the optimization of the analysis of the two herbicides. Clean-up on the precolumn could now be carried out with 4 ml instead of 3 ml of flushing solvent, which made the clean-up in the first part of the chromatogram more efficient. The result is shown in Fig. 4.

TABLE I

BREAKTHROUGH VOLUMES AND ELUTION PROFILES OF 6-HYDROXYBENTAZONE[a] AND BENTAZONE[b] FROM THREE DIFFERENT 7-μm BROWNLEE NEWGUARD (15 × 3.2 mm I.D.) PRECOLUMNS

Packing material in precolumn	*Breakthrough volume of 6-hydroxybentazone (ml)*		*Elution profile of bentazone (ml)*	
	V_{start}	V_{end}	V_{start}	V_{end}
PRP-1	5	>20	0.1	~2
RP-8	0.5	2.5	0.1	0.3
RP-18	3.2	7.0	0.15	0.40

[a] The precolumn flushing solvent was methanol–0.03 *M* phosphate buffer (pH 2.70) (5:95) at a flow-rate of 1 ml/min.

[b] The desorption eluent was methanol–0.02 *M* phosphate buffer (pH 2.70) (35:65), at a flow-rate of 1 ml/min.

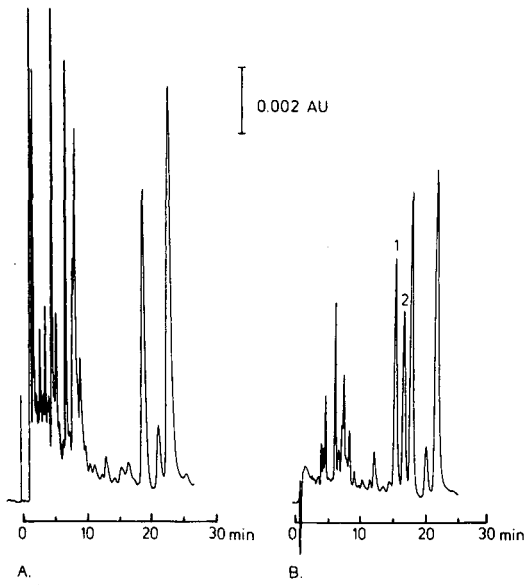

Fig. 4. Effect of the on-line clean-up step described under Experimental; analytical procedure. (A) 125 mg of maize blank analysed without precolumn clean-up; (B) 125 mg of maize with standard addition at a level of 0.46 mg/kg of (1) cyanazine and (2) bentazone, analysed using precolumn clean-up with a 4-ml flushing step.

Quantitative analysis of maize samples

The efficiency of the chromatographic system, including the precolumn switching procedure, was measured with bentazone. The number of theoretical plates, N, was 5200 and the peak asymmetry, measured at 10% peak height ($A_{0.1}$), was 1.1.

The linearity of the calibration graph [standard solutions of compounds in methanol–water (5:95)] was good, with correlation coefficients of over 0.999 for five data points in the range 10–1500 ng injected for each of the four analytes. The repeatablity of the responses of 50-ng injections of standard solutions with the system mentioned above was good. The coefficients of variation were 2.3% for 6-hydroxybentazone, 2.2% for 8-hydroxybentazone, 1.1% for cyanazine and 3.2% for bentazone ($n=8$).

The recoveries of cyanazine and bentazone added to maize at concentrations of 0.1 and 1 mg/kg were excellent (93–97%), as can be seen from Table II. As mentioned above, the two metabolites of bentazone could not be recovered on addition to the raw product, possibly owing to a matrix effect.

The reproducibility of the method was determined during five days, using spike levels of 1.2 mg/kg of each compound. The mean recovery of cyanazine was 91% and for bentazone 98% with corresponding coefficients of variation of 2.9 and 6.7%, respectively ($n=5$).

The LOD of the procedure (calculated from three times the peak-to-peak noise level in the chromatograms) was 0.02 mg/kg for both cyanazine and bentazone. With this procedure, eight samples of maize, four treated with cyanazine and four with bentazone in a supervised trial, were analysed together with four blank samples. In none of the samples could residues of the herbicides be detected.

TABLE II
RECOVERIES OF BENTAZONE AND CYANAZINE ADDED TO MAIZE

Compound	*Spike level (mg/kg)*	*n*[a]	*Mean recovery (%)*	*Standard deviation (%)*
6-Hydroxybentazone	0.096	6	–	–
	0.96	7	–	–
8-Hydroxybentazone	0.16	6	–	–
	1.6	7	–	–
Cyanazine	0.12	6	95	5.8
	1.2	6	93	2.9
Bentazone	0.12	6	97	9.1
	1.2	7	95	5.5

[a] Number of independent analyses.

Water analysis

The method described for maize was applied to the analysis of surface and drinking water which had been concentrated 50-fold by evaporation (see Experimental). The fatty residue in water samples is negligible compared with maize extracts so the liquid–liquid partitioning with *n*-hexane–acetonitrile as a first clean-up step was omitted. For surface water, the limit of determination was 1 μg/l (ppb) and for

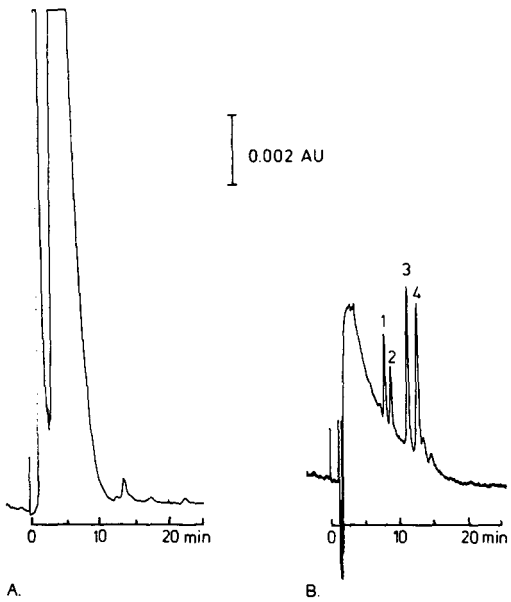

Fig. 5. HPLC of 5 ml of drinking water; (A) Blank, without precolumn clean-up. (B) spiked drinking water with precolumn clean-up at a level of (1) 2.0 μg/l 6-hydroxybentazone, (2) 3.2 μg/l 8-hydroxybentazone and 2.3 μg/l of (3) cyanazine and (4) bentazone. For procedure, see *Extraction procedure for drinking water (LOD 0.5 μg/l).*

drinking water 0.5 μg/l for cyanazine and bentazone. The two hydroxymetabolites of bentazone can be determined at the higher limit of 2 μg/l, owing to a large tail of interferences present in surface water, as can be seen in Fig. 5.

At the 2 μg/l spiking level, the mean recoveries and corresponding coefficients of variation from drinking water were 84 ± 6% for 6-hydroxybentazone, 81 ± 5.2% for 8-hydroxybentazone, 98 ± 2.7% for cyanazine and 99 ± 4.5% for bentazone ($n=6$ for each analyte). At the 10 μg/l level these recoveries were 97 ± 2.7% for 6-hydroxybentazone, 96 ± 2.5% for 8-hydroxybentazone, 100 ± 1.9% for cyanazine and 98 ± 2.1% for bentazone ($n=5$ for each analyte). The recoveries for surface water (Poelpolder, The Netherlands) were determined at spike levels of 10 μg/l and were 44 ± 2.5% for 6-hydroxybentazone, 51 ± 2.2% for 8-hydroxybentazone, 97 ± 3.9% for cyanazine and 97 ± 3.2% for bentazone ($n=5$ for each analyte). The low recoveries for the two polar metabolites of bentazone are probably caused again by matrix compounds, as observed with soil and maize.

In another study, we had been asked by the drinking water authorities to confirm the presence of bentanone in raw water and "purified" water used for the preparation of drinking water and originating from the (polluted) river Rhine, and in rain, both at levels of 0.01 μg/l. In this instance, the method without liquid–liquid partitioning as a clean-up step was insufficient. We therefore introduced an acid–base separation procedure, as described under Experimental.

Bentazene recoveries were determined in "purified" water at spike levels of 0.05–0.15 μg/l to be 73 ± 9.5% ($n=4$) and at 1.1 μg/l to be 77 ± 6.6% ($n=4$) and in rain to be 81 ± 3.1% ($n=6$). In five out of six water samples we found bentazone at levels of 0.1–0.7 μg/l. Our results were also confirmed by gas chromatography–mass spectrometry, using negative ion chemical ionization, after derivatization with pentafluorobenzoyl bromide.

CONCLUSION

An HPLC method for the simultaneous determination of cyanazine and bentazone in sugar maize has been developed using precolumn switching for the automated on-line clean-up of extracts. The method makes use of a reversed-phase HPLC system with UV detection at 229 nm. Compared with the existing methods[2,8], the main advantage is the increase in sample throughput due to the automated process. Because of the reconditioning of the precolumn during the HPLC analysis on the analytical column, many samples (more than 200) can be cleaned on one precolumn, reulting in a cost-effective sample clean-up.

The method is also applicable to the residue analysis of these herbicides in surface and drinking waters at levels down to at least 1 μg/l (ppb). For the specific determination of bentazone in drinking water and rain, the limit of determination was further lowered to 0.01 μg/l (ppb).

REFERENCES

1 H. Roseboom and H. A. Herbold, *J. Chromatogr.*, 202 (1980) 431–438.
2 Y. Xu, W. Lorentz, G. Pfister, M. Bahadir and F. Korte, *Fresenius Z. Anal. Chem.*, 325 (1986) 377–380.
3 H. B. Lee and Y. D. Stokker, *J. Assoc. Off. Anal. Chem.*, 69 (1986) 568–571.

4 US Department of Health and Human Services, *Analytical Methods for Pesticides in Foodstuffs*, Food and Drug Administration, Washington, DC, 1984.
5 J. D. Gaynor and D. C. MacTavish, *J. Agric. Food Chem.*, 29 (1981) 626–629.
6 P. Cabras, P. Diana, M. Meloni, F. M. Pirisi and R. Pirisi, *Pestic. Sci.*, 14 (1983) 130–134.
7 J. P. G. Loch, personal communication.
8 M. Akerblom and A. Gunborg, *J. Assoc. Off. Anal. Chem.*, 67 (1984) 653–655.
9 C. E. Goewie and E. A. Hogendoorn, *Sci. Total Environ.*, 47 (1985) 349–360.
10 C. E. Goewie and E. A. Hogendoorn, *J. Chromatogr.*, 404 (1987) 352–358.
11 C. E. Goewie and E. A. Hogendoorn, *J. Chromatogr.*, 410 (1987) 211–216.
12 C. E. Goewie, *J. Liq. Chromatogr.*, 9 (1986) 1431–1461.

Journal of Chromatography, 475 (1989) 442–446
Elsevier Science Publishers B.V., Amsterdam — Printed in The Netherlands

CHROM. 21 562

Note

Ion-pair chromatographic separation of inorganic sulphur anions including polysulphide[a]

RALF STEUDEL*, GABRIELE HOLDT and THOMAS GÖBEL
Institut für Anorganische und Analytische Chemie, Technische Universität Berlin, Sekr. C 2, D-1000 Berlin 12 (F.R.G.)
(Received March 17th, 1989)

Aqueous sodium sulphide (Na_2S) dissolves elemental sulphur with the formation of polysulphides (Na_2S_n). The maximum average chain length, n, of the anions is *ca.* 5 at 25°C[2,3] and the presence of all polysulphide anions with up to six sulphur atoms has been assumed[2–7]. Owing to the rapid autoxidation of both aqueous monosulphide[8] and polysulphide[9], such solutions usually contain at least traces of sulphite and thiosulphate in addition:

$$Na_2S + \tfrac{1}{2}S_8 \rightarrow Na_2S_5 \quad (1)$$

$$2Na_2S_5 \rightleftharpoons Na_2S_4 + Na_2S_6 \quad (2)$$

$$Na_2S + \tfrac{3}{2}O_2 \rightarrow Na_2SO_3 \quad (3)$$

$$Na_2S_4 + \tfrac{3}{2}O_2 \rightarrow Na_2S_2O_3 + \tfrac{1}{4}S_8 \quad (4)$$

Polysulphide solutions play an important role in a number of technical processes, in environmental chemistry and in the sulphur metabolism of certain sulphur bacteria such as *Chlorobium*[10] and other species[11]. The analysis of such solutions is difficult owing to the air sensitivity and the rapid establishment of equilibria of type 2. UV absorption spectroscopy[2–7] and classical gravimetric and titrimetric techniques[8,12,13] have been applied, but to our knowledge no chromatographic separation has been reported. However, monosulphide, sulphite, sulphate, thiosulphate and thiocyanate have been separated by ion-exchange chromatography[14]. This paper is concerned with the ion-pair chromatographic separation of monosulphide, sulphite, thiosulphate, and polysulphide in aqueous solutions and with the autoxidation of such solutions.

EXPERIMENTAL

The compounds $Na_2S \cdot 7$–$9H_2O$ (Merck), $K_2S_2O_3$ (purum, Fluka) and Na_2SO_3 (puriss. p.a., Fluka) were purchased in the highest available purity. Elemental sulphur

[a] Sulphur compounds, Part 127; for Part 126, see ref. 1.

0021-9673/89/$03.50

(Merck DAB 6) was recrystallized from carbon disulphide and consisted entirely of S_8. To prepare the solutions, either demineralized water ("water 1"), doubly distilled water ("water 2a") or doubly distilled and freshly degassed (in a vacuum) water ("water 2b") was used. The polysulphide solutions were made from freshly recrystallized sodium sulphide (10 g) dissolved in 200 ml of water 2b and 5 g of S_8 by heating and stirring for 2 h under nitrogen. When most of the S_8 had dissolved, 200 ml of water 2b were added and the heating and stirring continued for 1 h, followed by cooling to 20°C and filtration through a glass frit (D2) under nitrogen. To dilute this solution to concentrations suitable for ion chromatography, water 2b that had been adjusted to pH 11 with aqueous sodium hydroxide was used.

The chromatographic equipment consisted of the following components: Varian 5000 pump (microprocessor controlled) or Knauer pump, Valco or Rheodyne loop injector (10 μl), several UV absorbance detectors (Varian UV5 working at 215 nm, GAT-LCD-501 with variable wavelength and Waters 990 diode-array detector with NEC APC III computer), Hewlett-Packard 3390A electronic integrator, Knauer pen recorder and Waters 990 plotter. The following two columns were found to be equally suitable for the ion-pair chromatography: PRP-1 (Hamilton; 150 mm × 4.1 mm I.D., particle size 5 μm) and PLPR-S (Polymer Laboratories; 120 mm × 4 mm I.D., particle size 8 μm).

As the composition and stability of polysulphide solutions depend strongly on the pH, the following alkaline eluent of pH $\approx$ 11 was used: 85% (v/v) water 2a, 15% (v/v) acetonitrile (Promochem Chrom AR), 0.001 mol/l sodium carbonate, 0.002 mol/l tetra-*n*-butylammonium hydroxide (purum, Fluka). This mixture was degassed in a vacuum with application of ultrasound. An increase in the acetonitrile concentration reduces the retention times. The eluent flow-rate was varied between 1 and 2 ml/min.

RESULTS

In Fig. 1 the chromatographic separation of sulphide, sulphite, thiosulphate and polysulphide is shown. The assignment of peaks 1–3 to the first three compounds is based on measurements with the pure substances. Freshly recrystallized commercial sodium sulphide (from water 2a) showed a chromatogram with just one peak (Fig. 1A), the height of which was a linear function of the sulphide concentration in the range 0–1.2 mmol/l. The UV spectrum of this substance showed one peak at 231 nm only (range 200–400 nm). In a similar fashion, the integrated peak areas and the heights of the sulphite and thiosulphate peaks were linear functions of the concentrations of the corresponding anions in the concentration range 0–1 mmol/l (see Fig. 2). Potassium thiosulphate was used as it crystallizes without water, while the exact composition of $Na_2S_2O_3 \cdot 5H_2O$ is always uncertain.

The detection limits of sulphite and thiosulphate in a sodium sulphide sample were approximately 0.02% (by weight) for sulphite and 0.01% or 0.2 μg/ml for thiosulphate. When a solution of elemental sulphur in aqueous sodium sulphide was analysed, the chromatograms shown in Fig. 1B and C were obtained. The assignment of peak 4 to a mixture of polysulphides (S_x^{2-}) is based on the following observations:

(a) the relative height and area of peak 4 increased and simultaneously those of peak 1 decreased when more sulphur was added, which is explained by reaction 1.

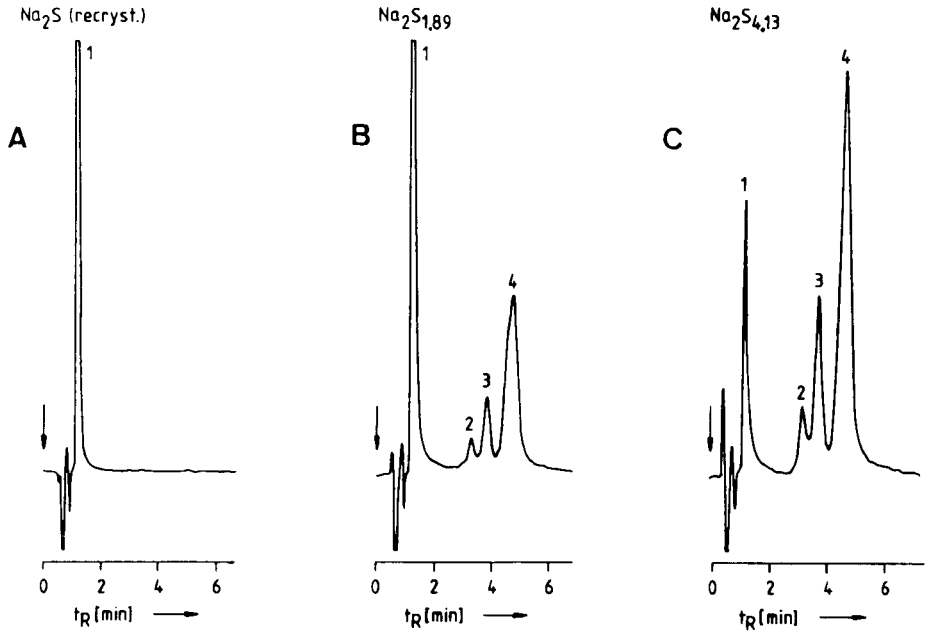

Fig. 1. Chromatograms of (A) freshly recrystallized Na_2S and of two sodium polysulphide solutions of composition (B) $Na_2S_{1.9}$ and (C) $Na_2S_{4.1}$. Ordinate: absorbance at 215 nm. Peaks: 1, HS^-; 2, SO_3^{2-}; 3, $S_2O_3^{2-}$; 4, S_x^{2-}.

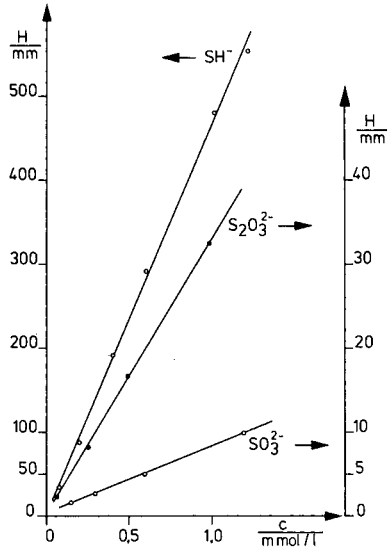

Fig. 2. Calibration functions of sulphide, sulphite and thiosulphate anions; dependence of the chromatographic peak heights as a function of the molar concentrations. As the peak heights also vary with the retention time, the flow-rate and the eluent composition have to be kept constant.

(b) When oxygen was bubbled through the polysulphide solution with simultaneous monitoring of the anion concentrations, it was observed that peaks 1, 2 and 4 decreased and finally dissappeared whereas peak 3 increased, which can be explained by reactions 3, 4 and 5

$$Na_2SO_3 + \tfrac{1}{2}O_2 \rightarrow Na_2SO_4 \quad (5)$$

Sulphate does not absorb at 215 nm and therefore does not show up in the chromatograms.

(c) Using the diode-array detector, an absorption spectrum of the substance represented by peak 4 was recorded (see Fig. 3). The spectrum observed is characteristic of a dilute polysulphide solution[2-7] and distinctly different from the spectrum of S_8[15]. Especially the broad absorption maximum at 285 nm is typical of S_x^{2-}, since S_3^{2-}, S_4^{2-}, and S_5^{2-} absorb at this wavelength with large molar absorptivities[7]. Neither SO_3^{2-} nor $S_2O_3^{2-}$ absorbs at 285 nm.

The assignment of peak 4 to a mixture of polysulphide anions implies that this mixture is not separated due to rapidly established equilibrium reactions of types 2 and 6.

$$S_3^{2-} + S_6^{2-} \rightleftharpoons S_4^{2-} + S_5^{2-} \quad (6)$$

We tried to achieve at least a partial separation by varying the eluent composition and the polysulphide concentration.

Repeatedly a shoulder on either the left or the right wing of peak 4 was observed and several times a separation into two peaks was observed. The other peaks always remained symmetrical with no indications of shoulders or tails. However, these observations were not always reproducible and therefore just indicate that peak 4 represents a mixture of anions which at present cannot be separated. Under these

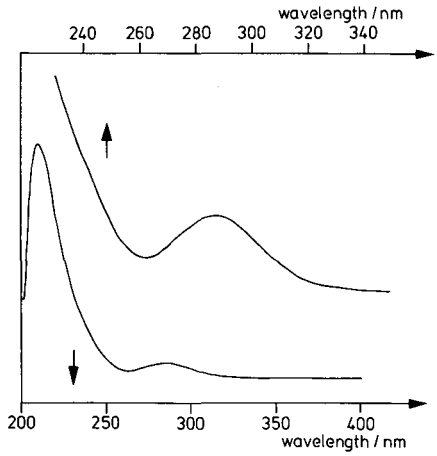

Fig. 3. Absorption spectrum of the substance giving rise to peak 4 in Fig. 1, which is assigned to a mixture of polysulphides, S_x^{2-}. Solvent: acetonitrile–water (15:85, v/v), pH 11. The upper spectrum was recorded with an extended ordinate scale.

circumstances, it does not seem possible to calibrate the height or area of peak 4 *versus* the polysulphide concentration, and only a qualitative and semiquantitative polysulphide analysis is possible.

This chromatographic technique was applied to the analysis of three commercial products of "sodium sulphide, $Na_2S \cdot xH_2O$ (x = 7–9)". These products (Merck) were labelled "reinst", "extra pure" and "pro analysi", respectively. In addition to sulphide, all the samples contained traces of sulphite, thiosulphate and polysulphide. When the samples were dissolved in water 2b and rapidly analysed, between 0.3 and 1.4% (by weight) of thiosulphate and *ca.* 0.2% of sulphite were found. When water 1 was used, slightly higher levels of sulphite and thiosulphate were determined. This indicates that the oxygen dissolved in water 1 produces some additional sulphite and thiosulphate by reactions 4 and 5. This result is in agreement with the observations by Schulek and Körös[8], who observed the formation of sulphite and thiosulphate by autoxidation of sulphide. However, if oxygen was supplied in excess by bubbling it into the sodium sulphide solution through a sintered-glass frit, all the sulphite and thiosulphate disappeared within 90 min (by oxidation to sulphate), as did polysulphide. Obviously reaction 5 is faster than reaction 4 under these conditions. The pH of these solutions was approximately 13.

ACKNOWLEDGEMENTS

We are grateful to Dr. E.-M. Strauss for drawing some of the figures and to the Deutsche Forschungsgemeinschaft and the Verband der Chemischen Industrie for generous support.

REFERENCES

1 R. Steudel, T. Göbel and G. Holdt, *Z. Naturforsch., Teil B*, 44 (1989) 526.
2 A. Teder, *Ark. Kemi*, 31 (1970) 173.
3 A. Teder, *Acta Chem. Scand.*, 25 (1971) 1722.
4 A. Teder, *Ark. Kemi*, 30 (196) 379.
5 W. Giggenbach, *Inorg. Chem.*, 11 (1972) 1201.
6 W. Giggenbach, *Inorg. Chem.*, 13 (1974) 1724.
7 S. Licht, G. Hoder and J. Manassen, *Inorg. Chem.*, 25 (1986) 2486.
8 E. Schulek and E. Körös, *Acta Chim. Acad. Sci. Hung.*, 3 (1953) 111 and 125.
9 R. Steudel, G. Holdt and R. Nagorka, *Z. Naturforsch. Teil B*, 41 (1986) 1519.
10 P. T. Visscher and H. van Gemerden, in J. M. Olson, J. G. Ormerod, J. Amesz, E. Stackebrandt and H. G. Trüper (Editors), *Green Photosynthetic Bacteria*, Plenum Press, New York, 1988, p. 295.
11 J. Then and H. G. Trüper, *Arch. Microbiol.*, 135 (1983) 254.
12 A. V. Manley and F. W. Czech, in J. H. Karchmer (Editor), *The Analytical Chemistry of Sulphur and its Compounds*, Part I, Wiley-Interscience, New York, 1970, p. 347.
13 L. Szekeres, *Talanta*, 21 (1974) 1.
14 R. E. Poulson and H. M. Borg, *J. Chromatogr. Sci.*, 25 (1987) 409.
15 R. Steudel, D. Jensen, P. Göbel and P. Hugo, *Ber. Bunsenges. Phys. Chem.*, 92 (1988) 118.

Journal of Chromatography, 475 (1989) 447–450
Elsevier Science Publishers B.V., Amsterdam — Printed in The Netherlands

CHROM. 21 599

Note

High-performance liquid chromatographic determination of the alkaloids in betel nut

JIU LI HUANG and MICHAEL J. McLEISH*
School of Pharmaceutical Chemistry, Victorian College of Pharmacy Ltd., 381 Royal Parade, Parkville, Victoria 3052 (Australia)
(Received March 10th, 1989)

The nuts of the areca palm, *Areca catechu* L., are commonly chewed by the peoples indigenous to South-Eastern Asia and the Pacific. The nuts have been shown to contain at least six related pyridine alkaloids[1], of which four have been conclusively identified. Arecoline is the major constituent, being present at 0.1–0.5%. The other alkaloids are present in much lower levels[1,2]. The structures of the four major alkaloids are shown in Fig. 1.

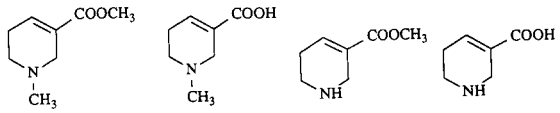

I II III IV

Fig. 1. Structures of the *Areca* alkaloids: (I) arecoline, (II) arecaidine, (III) guvacoline and (IV) guvacine.

Betel nuts have been used for a variety of purposes including appetite suppression[3], increasing stamina and general well-being[2,3], even as a treatment for tapeworm[2,4]. Probably because it is present in the largest quantities most of the effects of chewing betel nuts have been attributed to arecoline, although this has yet to be proved. Arecoline has a stimulating parasympathetic action[5], cardiovascular[6] and ocular[7] effects and as a veterinary preparation it is used as an anthelminthic. More recently it has been suggested that some of the psychic effects observed upon chewing betel nuts may in fact be due to arecaidine and guvacine, which are both potent γ-aminobutyric acid (GABA) uptake inhibitors[8].

It would be of interest to correlate the levels of the individual alkaloids in betel nuts with the observed pharmacological response. Although a gas–liquid chromatographic (GLC) method of quantitation has been described for arecoline in capsule preparations[9] the determination of arecoline levels in nuts has generally involved steam distillation and titration[10]. Paper and thin-layer chromatography have both been used to separate the other related alkaloids[2] however there is no satisfactory method for quantitative analysis. This paper describes the development of a method suitable for the simultaneous determination of the four major alkaloids in betel nuts.

0021-9673/89/$03.50

EXPERIMENTAL

Materials

Arecoline–HBr and arecaidine–HCl were purchased from Sigma (St. Louis, MO, U.S.A.). Guvacoline and guvacine were prepared by N-demethylation of arecoline and arecaidine, respectively. Satisfactory spectral data were obtained for both compounds. All solvents were of analytical reagent or HPLC grade. Water was purified by a Milli-RO4 water purification system or a Milli-Q reagent grade water system (Millipore, Bedford, MA, U.S.A.).

Procedures

Fresh betel nut (2–3 g) was placed in a 50-ml test-tube containing 0.001 *M* orthophosphoric acid (30 ml). Following grinding with an homogenizer (Polytron, Kinematica, Lucerne, Switzerland) the mixture was stirred for 4 h (room temperature) and then centrifuged (2000 *g*) for 10 min. A 1-ml volume of supernatant was mixed with 1 ml 85% orthophosphoric acid and passed through a 0.22-μm filter (Millipore Type GS). This solution was diluted (1:160) into a buffer [0.16% ammonium hydroxide–methanol (60:40)] at pH 3–4. An injection volume of 100 μl was used.

Chromatographic conditions

A Waters Model 510 pump was used in conjunction with a Model 481 variable-wavelength UV detector (Waters Assoc., Milford, MA, U.S.A.). The pump was fitted with a Rheodyne 7125 loop injection system equipped with a 100 μl loop. Peak areas were determined using a Shimadzu C-R4A integrator. Peak heights were measured with the integrator or an Omniscribe recorder. For the stationary phase a cation-exchange column (Whatman Partisil SCX particle size 10 μm, 25 cm × 4.6 mm I.D.) was used at ambient temperature. The mobile phase consisted of 85% orthophosphoric acid–methanol–water (3:400:590), and was adjusted to pH 3.8 with 14% ammonium hydroxide. The flow-rate was 1.8 ml/min and the eluent was monitored at 215 nm.

RESULTS AND DISCUSSION

As there had been no previous reports on the high-performance liquid chromatography (HPLC) of *Areca* alkaloids a number of columns were examined under a variety of conditions. An ion pairing procedure using 1-heptanesulphonic acid and a reversed-phase column showed promising results, however the simplest and best separation was achieved using a strong cation-exchange (SCX) column. The retention times, shown in Table I, are all highly reproducible and demonstrate the ready separation of the four alkaloids.

Calibration graphs were prepared for all four alkaloids. Responses were linear over the range 5–5000 ng/ml (correlation coefficients >0.995). The limits of sensitivity (signal-to-noise ratio of 4) are listed in Table I.

In betel nuts arecoline has been estimated by steam distillation of the nuts followed by titration of the distillate[10]. This procedure involved steam distillation of a solution containing arecoline at pH 9.0–9.1. When this methodology is followed by HPLC both arecoline and guvacoline showed a considerable degree of hydrolysis to

TABLE I
RETENTION TIMES AND SENSITIVITY LIMITS OF ALKALOID STANDARDS

Alkaloid	*Retention time (min)*	*Detection limit (ng/ml)*
Guvacine	3.3	5.2
Arecaidine	4.3	5.2
Guvacoline	5.0	7.9
Arecoline	7.7	12.2

their corresponding acid[11]. These acids are not steam volatile and as a consequence the results obtained using steam distillation methods may be misleading.

To overcome this problem we have developed a mild extraction procedure using dilute (0.001 *M*) orthophosphoric acid. Under these conditions both arecoline and guvacoline are quite stable. Although stirring for 4 h ensures complete extraction, the time may be reduced to 2 h without significant decrease in efficiency. As shown in Fig. 2, this extract does not produce a clean chromatogram, however interfering impurities

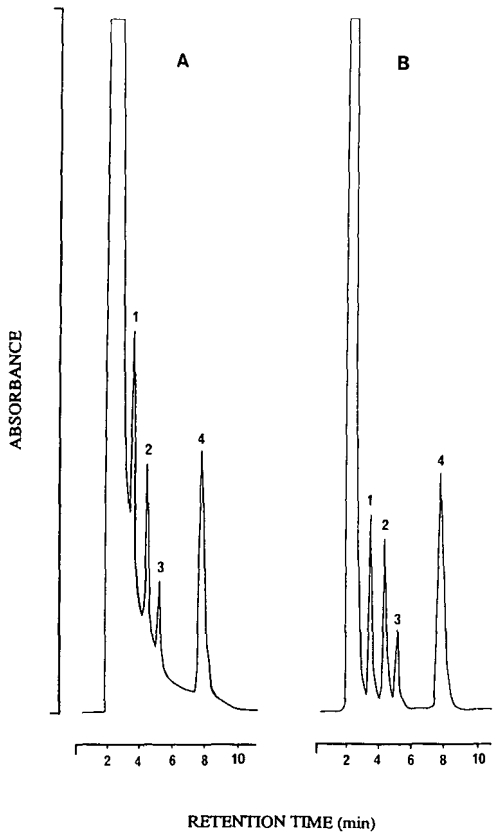

Fig. 2. Chromatogram of the *Areca* alkaloids, (1) guvacine, (2) arecaidine, (3) guvacoline and (4) arecoline, before (A) and after (B) treatment with concentrated orthophosphoric acid. The injection volume was 100 µl. Compounds were detected by UV spectroscopy (λ = 215 nm; 0.05 a.u.f.s.).

may be removed by precipitation with concentrated orthophosphoric acid and subsequent filtration.

Analysis of fresh betel nuts (obtained from Darwin, Australia) showed alkaloid contents of: arecoline (0.30–0.63%), arecaidine (0.31–0.66%), guvacoline (0.03–0.06%) and guvacine (0.19–0.72%). The arecoline levels are marginally higher than those obtained using the steam distillation method for Indian[12] and New Guinea[3] nuts. Individual levels for the other alkaloids have not previously been reported although the total alkaloid content is certainly higher than observed in prior studies[3]. This may be due to seasonal and/or geographical variation. Both possibilities are currently under investigation.

CONCLUSIONS

A simple and rapid HPLC method has been developed for the estimation of *Areca* alkaloids. Levels for the four major alkaloids have been determined in fresh nuts and shown to be higher than previously thought.

ACKNOWLEDGEMENTS

The assistance of Prof. C. Chapman and the staff of the Pharmaceutics Department, Victorian College of Pharmacy is greatly appreciated. Our thanks are also due to George Brown of the Darwin Botanical Gardens for supplying the betel nuts used in this study. One of us (J.L.H.) acknowledges the support of a VCP Centenary scholarship.

REFERENCES

1 R. H. F. Manske and H. L. Holmes (Editors), *The Alkaloids*, Vol. 1, Academic Press, New York, 1950, p. 171.
2 A. M. Mujumdar, A. H. Kapadi and G. S. Pense, *J. Plant. Crops*, 7 (1979) 69.
3 E. R. Farnworth, *Science in New Guinea*, 4 (1976) 85.
4 L. C. Feng, H. C. Ling and J. C. Hwang, *Peking Nat. Hist. Bull.*, 18 (1949) 63.
5 G. B. Leslie, *Nature (London)*, 208 (1965) 1291.
6 C. Heymans, *C.R. Soc. Biol.*, 87 (1922) 1062.
7 T. Kumori, *Chem. Pharm. Bull.*, 9 (1961) 551.
8 G. A. R. Johnstone, P. Krogsgard-Larsen and A. Stephanson, *Nature (London)*, 258 (1975) 627.
9 B. J. Kovensky and C. W. Poole, *J. Pharm. Sci.*, 59 (1970) 1651.
10 E. S. Nambuduri, *J. Assoc. Off. Anal. Chem.*, 51 (1968) 799.
11 J. L. Huang and M. J. McLeish, unpublished results.
12 S. N. Mitra, B. R. Roy and D. Hemnath, *J. Inst. Chem. (India)*, 41 (1969) 154.

Journal of Chromatography, 475 (1989) 451–456
Elsevier Science Publishers B.V., Amsterdam — Printed in The Netherlands

CHROM. 21 516

Note

Adsorption chromatography on cellulose

V. A simple chromatographic system for the identification of inks

M. LEDERER* and M. SCHUDEL
Institut de Police Scientifique et de Criminologie, Université de Lausanne, Place du Château 3, CH-1005 Lausanne (Switzerland)
(Received March 7th, 1989)

In a recent survey of the biomedical applications of chromatography[1], it was pointed out that modern instrumental chromatography is at present beyond the technical, scientific and financial possibilities of many potential users of chromatography, who would welcome simple arrangements for occasional use with their everyday problems. Although these comments were made mainly with reference to medical diagnosis, they are equally valid in other fields, where analytical chemistry plays or should play a role.

We report here some ideas concerning a field which we felt was a challenge in this direction, namely the identification of writing inks on documents in relation to police scientific investigations. The main problem here is that of performing in police stations, which have neither the usual laboratory facilities nor a constant need for such, work usually carried out by graduates of the Institut de Police Scientifique (Lausanne), with a good training in chemical analysis.

A thesis by Tappolet (2) dealt with the high-performance thin-layer chromatographic (HPTLC) analysis of writing inks. It was shown that most commercial inks produce 3–5 zones under good resolution conditions. Hence there seems to be no need to resort to high-efficiency systems for chromatographic recognition.

Horváth[3] stated that "It was particularly irritating that, without getting assurances from the weather bureau that the humidity was in a certain range, it did not make sense to start TLC work that day since the results were greatly affected by the moisture content of the silica". Preliminary work with silica thin layers along the lines of the work of Tappolet[2] indicated the validity of Horváth's comments, so instead of abandoning thin layers, like Horváth, we merely abandoned silica gel and replaced it with paper strips.

EXPERIMENTAL

In developing the system described here, we considered also the availability of the various components used and the environmental acceptability of the eluents, etc., as one can hardly suggest to a police officer that he dispose of poisons or acids down the drain.

0021-9673/89/$03.50

The apparatus consisted of the following items, for which we also indicate the local price, converted to US$. The apparatus can be fitted into a small suitcase.

(1) A simple balance, as can be purchased in shops selling hunting equipment, where it is sold for compounding home-made cartridges. Price US$ 30. It is shown in Fig. 1 and has an accuracy of about 10 mg. Thus in weighing out 1-g amounts the accuracy is 1% or even better.

(2) Chromatography jars were made from large glass coffee jars, to which cork stoppers were fitted with office clips attached to form J-shaped hooks for the paper strips. The price of the corks was about $ 1.

(3) We found that the usual Whatman No. 1 or 3MM papers yielded fairly good chromatograms with aqueous solvents and either of these papers can be used. One large sheet of Whatman No. 1 paper (price *ca.* US$ 0.50) yields enough paper for about 200 individual chromatograms, thus providing another reason for preferring paper strips to silica gel thin layers.

(4) Development: in view of environmental considerations, we used only aqueous eluents. Cellulose eluted with aqueous salt solutions was shown recently[4,5] to be essentially a reversed-phase adsorption system, in which the cellulose functions as a polar stationary phase and adsorption is easily and predictably controlled by the concentration and the type of the salt in the eluent. We obtained good results with solutions of ammonium sulphate, which has the attraction that it is very soluble, but for most separations 1% sodium chloride solution also yields good chromatograms. In electrolyte solutions of reasonable strength the few ions present in tap water cause no measurable changes, so when distilled water is unavailable tap water will suffice. Complete development to the upper border of the paper takes 20–25 min.

(5) Documentation may be effected by merely keeping the developed chromatograms. However, as some dyestuffs in the inks may decompose on storage, we preferred to make a photographic record. Excellent photographic equipment for the recording of thin-layer chromatograms is available, but in view of our aim to keep costs as low as possible we adopted a Polaroid Image System E camera and a "Pola-

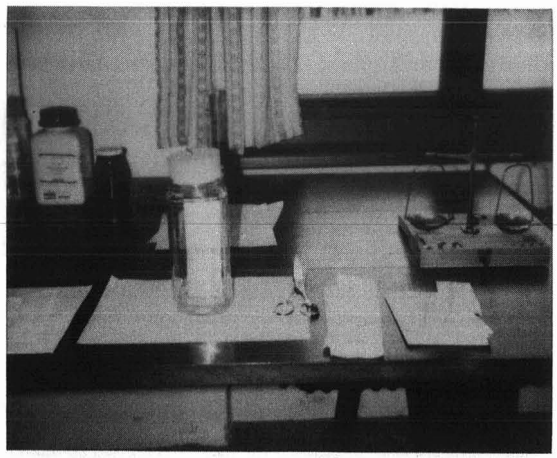

Fig. 1. The entire "laboratory", excluding the camera with which the picture was taken. The equipment can easily be set up on any desk or table.

roid close up Stand", which was principally designed for the copying of photographs on a 1:1 scale. The entire photographic equipment costs about US$ 200 and is therefore the main expense item of the system. The chromatograms of inks yielded poor, pale copies with this system and we found that a Hama Polarisations-Folie, Stärke 0.75 mm, had to be placed in front of the camera lens in order to obtain photographs of the same intensity as the original chromatogram. However, they show a slight brownish tinge in comparison with the original. This can be corrected by placing a colour standard, made with various suitably coloured felt pens, next to the chromatogram, as shown in Fig. 2.

(6) Ultraviolet fluorescence detection: a battery-operated small UV lamp, the "Ultra-violet lamp for Stamps" from Leuchtturm/Lighthouse is available from stamp-dealers at a price of US$ 25 and performs very well in semi-darkness, *e.g.*, inside an open cupboard. Only one of the dyes of the twelve blue and black inks examined is fluorescent in the ultraviolet region; felt pen No.12 (see below) has a pink fluorescent spot, which corresponds to the second slowest spot ($R_F \approx 0.45$). In the case of the set of coloured felt pens (a total of 30 pens) only one fluorescent spot was found.

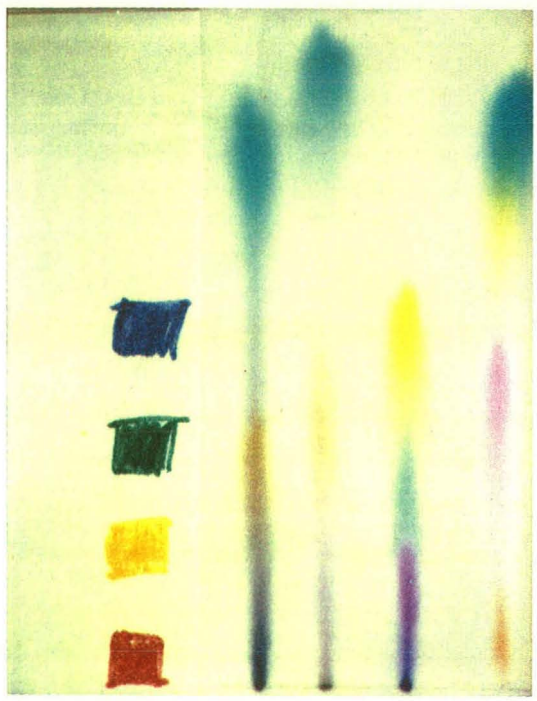

Fig. 2. Polaroid photograph of a chromatogram of four felt pen inks run side by side on a strip of Whatman No.1 paper with 1% sodium chloride as eluent. Colour samples are placed next to the chromatogram, to permit correction for the change in colour due to the photographic process.

RESULTS

The ink of one of the felt pens used for preliminary work was developed with a range of concentrations of ammonium sulphate from 0.005 to 1.3 *M*. The results are shown in Table I. A black ink pen yields a chromatogram with a fast blue spot, then a yellow spot and two red spots in the lower half of the chromatogram (the chromatogram on the right in Fig. 2). It can be seen that increasing the salt concentration lowers the R_F values of all four constituents, as expected. The blue and yellow spots separated well with all eluents, except the very dilute one.

A box of coloured felt pens, as sold for use in schools, was examined (Migros 36 Faserschreiber 7202.335, Switzerland). These pens gave the chromatograms shown schematically in Fig. 3. With many of the colours, the manufacturer employed different ratios of the same yellow and red colours and of the fast-moving blue colour. Some purple constituents yield elongated trails. Only one brick-red dye exhibited UV fluorescence (chromatogram 29). Most chromatograms showed one or two separated spots and the remainder showed three or four spots. Only five pens yielded chromatograms with "comets".

We decided to estimate the number of theoretical plates developed in such a chromatogram. Taking the fast-moving blue spot, we calculated about 1000 theoretical plates. This could certainly be improved by either developing for a longer distance or by using cellulose thin layers instead of paper. Longer development would have made copying more difficult and thin layers would have made the technique more complicated and expensive. We believe neither would have increased the amount of information obtained from such a chromatogram.

We then examined twelve blue and black writing pens: blue, (1) Pental Sign Pen, (2) Pilot Oasis, (3) Pentel "Super Ball" Japan, (4) Pentel Ultra fine S590 Japan (Blue), (5) Markana 33; black, (6) Clici Swiss Made Caran d'Ache 836009, (7) Pentel Sign Pens Japan, (8) Pentel Ultra fine S590 Japan (Black), (9) Pilot Fineliner, (10) Papermate Precise Roller 0.5 mm, (11) Compo, (12) Feutre Bic Porous Pen.

Pens 1 and 3 gave a strongly adsorbed spot at the origin, each with a short forward comet (one purple, the other blackish). Pen 5 gave a single spot at R_F 0. Pens 2, 6, 7 and 8 gave a fast-moving blue spot, and also two or three other constituents, each different from the others. Pen 4 gave the fast-moving blue spot and a slight short forward comet from the origin. Pens 9–12 have already been shown in Fig. 2. Although there are elongated comets in five of the twelve chromatograms, all pens can

TABLE I

R_F VALUES OF THE FOUR SEPARATED DYES FROM A FEUTRE BIC POROUS PEN (BLACK) IN SOLUTIONS OF AMMONIUM SULPHATE AS ELUENTS ON WHATMAN No. 3MM PAPER

Concentration of $(NH_4)_2SO_4$ (M)	*R_F value*			
	Fast blue spot	*Yellow spot*	*Purple spot*	*Red spot*
0.005	0.91	0.80	0.38	0.05
0.05	0.93	0.62	0.39	0.04
0.53	0.66	0.41	0.22	0.02
1.3	0.62	0.37	0.19	0.015

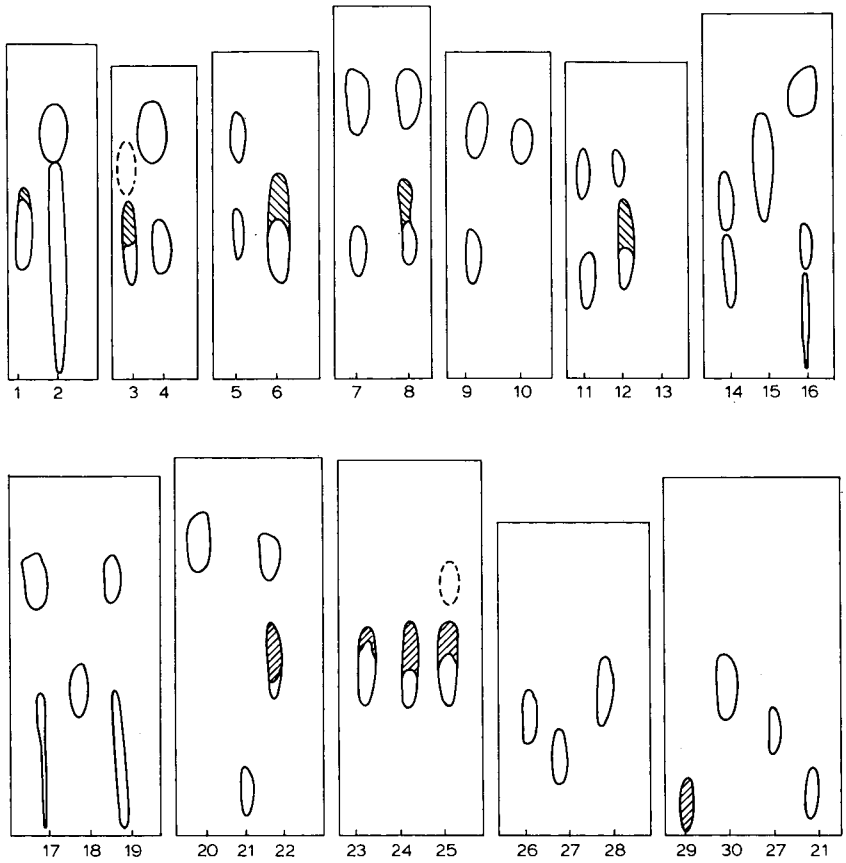

Fig. 3. Schematic representation of 30 chromatograms of coloured felt pens. From left to right: (1) shows a strong yellow spot with an adjacent faster weak red spot (hatched); (2) has a predominant blue fast moving spot and a violet comet from the origin; (3) a strong yellow and a strong red adjacent spot (hatched) and ahead of it a weak blue spot; (4) a strong yellow spot and a fast blue spot; (5) a red spot and a fast blue spot; (6) a yellow spot preceded by a strong red spot (hatched); (7) a violet comet from the origin, a yellow spot and the fast blue spot; (8) the yellow spot preceded by about an equally intense red spot (hatched) and the fast blue spot; (9) a weak yellow spot and a fairly strong blue spot; (10) a single fast blue spot; (11) the same as 9, except with a strong yellow and a weak blue spot; (12) a yellow spot preceded by a very strong red spot (hatched) and a weak blue spot; (13) a violet comet; (14) two red spots, the slower being more purple; (15) a single red spot; (16) a violet comet, the yellow spot and the fast blue spot; (17) almost identical with 16; (18) a single yellow spot; (19) a violet comet and the fast blue spot; (20) a single blue spot; (21) a single dark red spot; (22) a weak yellow spot with an adjacent strong red spot (hatched), preceded by the fast blue spot; (23–25) these are all different ratios of the yellow and the adjacent red (hatched) spot, 25, also has a faint fast blue spot; (26) a single red spot; (27) a single violet spot; (28) a single red spot; (29) a single red spot (UV fluorescent); (30) a single yellow spot.

be readily distinguished from each other by comparing the colour patterns and spot number. Only pen 12 gave one fluorescent spot (the second from the start).

We feel that the system proposed could prove of value in the examination of documents. We have not, so far, dealt with the extraction of the ink from the docu-

ment, or with the problem of the decomposition of inks with time. This will be dealt with by one of us (M.S.) in due course.

The amount of ink placed on the chromatogram in these preliminary studies was a short line of 2–3 mm directly from the pen. Thus a four-letter word would yield enough material for six to eight chromatograms.

We have recently surveyed the literature on paper chromatography with aqueous solvents (to be published) and feel that our system could have applications in various fields, such as the study of anthocyanins and other water-soluble pigments in plants in field work or the detection of some amino acids in urine in cases of amino-aciduria.

REFERENCES

1 M. Lederer, *J. Chromatogr.*, 488 (1989) 5.
2 J. Tappolet, *Thèse de Doctorat*, Université de Lausanne, 1984.
3 Cs. Horváth, in L.S. Ettre and A. Zlatkis (Editors), *75 Years of Chromatography, a Historical Dialogue*, Elsevier, Amsterdam, 1979, p. 154.
4 A. O. Kuhn and M. Lederer, *J. Chromatogr.*, 406 (1987) 389.
5 A. O. Kuhn and M. Lederer, *J. Chromatogr.*, 440 (1988) 165.

Journal of Chromatography, 475 (1989) 457–460
Elsevier Science Publishers B.V., Amsterdam — Printed in The Netherlands

CHROM. 21 610

Note

Measurement of hydroperoxydocosahexaenoic acid in rat brain homogenates by reversed-phase high-performance liquid chromatography

KHURSHED A. ANSARI* and DON W. SHOEMAN
*Department of Neurology, University of Minnesota, School of Medicine and *Neurology Service 127, V.A. Medical Center, 1 Veterans Drive, Minneapolis, MN 55417 (U.S.A.)*
(Received February 10th, 1989)

Free radical induced oxidation of polyunsaturated fatty acids has been implicated in the pathogenesis of tissue changes related to aging[1,2] and to trauma[3] of the nervous system. Because of their instability, the peroxides produced during this process have eluted direct quantitation. Docosahexaenoic acid (DHA), a polyunsaturated fatty acid, appears to be a candidate for oxygenation in the nervous sytem[4] and hydroperoxydocosahexaenoic acid (HPDHA) might be expected to accumulate in nervous tissue under oxidative stress. In this study, we have prepared HPDHA from DHA using soybean lipoxygenase, established its high-performance liquid chromatography (HPLC) characteristics and determined its recovery from brain homogenates. Then, we have attempted to measure the amount of HPDHA in homogenates prepared from rapidly frozen rat brains before and after a 60-min incubation at 37°C in the presence of room air, with or without the addition of the antioxidant butylated hydroxytoluene (BHT), or in the presence of nitrogen. Since HPDHA may be converted into hydroxydocosahexaenoic acid (HDHA), either in tissue or during isolation, we included this compound also in our studies.

MATERIALS AND METHODS

Soybean lipoxygenase [E.C. 1.13.11.12] was obtained from Sigma, St. Louis, MO, U.S.A. Sep-Pak™ silica cartridges were obtained from Rainin, Woburn, MA, U.S.A. and BHT, gold label, was purchased from Aldrich, Milwaukee, WI, U.S.A. Acetonitrile, hexane and water for HPLC were bought from B&J Minneapolis, MN, U.S.A. Reagent-grade glacial acetic acid and ammonium hydroxide, HPLC-grade phosphoric acid and isopropanol, and sodium borohydride were purchased from Fisher Scientific, Pittsburgh, PA, U.S.A. DHA was purchased from Nu Check Prep, Elysian, MN, U.S.A. HPDHA and HDHA were prepared by the method of Hamberg and Samuelsson[5] by using soyban lipoxygenase and purified by using the HPLC system described below. The purified HPDHA and HDHA were analyzed by gas chromatography–mass spectrometry (GC–MS) by using the procedure described previously[6]. Briefly: HPDHA and HDHA, collected during HPLC, were methylated with diazomethane and treated with hydrogen over platinum oxide. Trimethylsilyl derivatives of the reaction products were then analyzed by GC–MS on a Kratos MS-25

0021-9673/89/$03.50

instrument in the electron impact mode at 70 eV. Samples were separated on a 30 m × 0.32 mm I.D. fused-silica capillary column coated with a 0.25-μm film of DB-5. The column, operated in the split mode, was programmed from 200 to 280°C at 10°C/min.

Twelve-month-old, male, S/D retired breeder rats, weighing between 570 and 600 g (obtained from Harlan/Sprague-Dawley, Indianapolis, IN, U.S.A.) were decapitated into liquid nitrogen. Brains were removed while frozen and homogenized in 9 vol. equiv. of 0.05 *M* Tris–HCl. Lipids were extracted from 2 ml of the homogenates with 36 ml of hexane–isopropanol (3:2, v/v) containing 0.005% BHT, either immediately or after incubation for 1 h at 37°C in the presence of room air. In some experiments BHT (0.05%) was added to the homogenates before incubation; in others, nitrogen was substituted for room air.

Free fatty acid fractions were isolated from the hexane–isopropanol extracts by using silica Sep-Pak (TM) cartridges as previously described[7]. Isolated free fatty acid fractions were suspended in 100 μl of methanol and 10-μl aliquots were injected onto a 150 × 4.6 mm I.D. Econosphere™ 5-μm C_{18} cartridge (Alltech, Avondale, PA, U.S.A.). HPLC separations were performed on a Beckman chromatography system including a Model 167 variable-wavelength detector and a Model 506 autosampler. Two Model 110B pumps with a Model 406 analogue interface provided a concave (curve No. 5) gradient from 48 to 100% acetonitrile in 0.1% phosphoric acid over a period of 15 min post injection. The mobile phase was then held at 100% acetonitrile for an additional 5 min, returned to 48% in 2 min and allowed to equilibrate for 3 min before injecting the next sample. Data were collected and analyzed by using the System Gold (TM) software package on an IBM PS/2 Model 30 microcomputer. HPDHA and HDHA were detected at 235 nm. Peak areas were used for quantitation. A standard curve based on varying amounts (10–75 ng) of HPDHA injected onto the column and the corresponding peak areas at 235 nm were constructed (Fig. 1). The coefficient of determination for this curve was 0.98. For recovery experiments, since higher amounts of HPDHA (8.8 μg) were added to brain homogenates, the curve was extended to include amounts up to 216 ng of HPDHA injected onto the column. This curve had a coefficient of determination of 0.99. These curves were then used for quantitation of HPDHA in extracts from homogenates, and the results expressed as μg HPDHA per

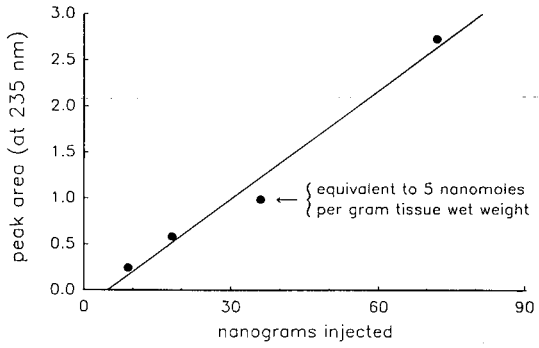

Fig. 1. HPDHA standard curve. Peak areas of absorbance at 235 nm produced by various amounts of HPDHA are plotted against the amount injected. The coefficient of determination for this curve was 0.98.

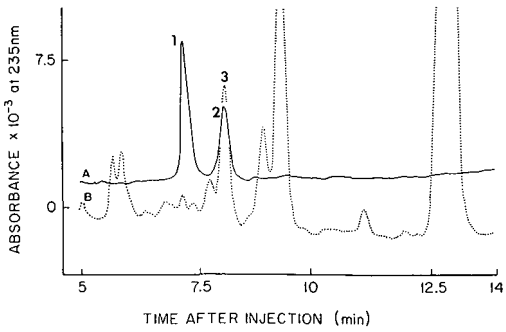

Fig. 2. Chromatograms, monitored at 235 nm of (A) HPDHA and HDHA standards, equivalent to 1.8 and 1.7 μg per gram tissue, wet weight, respectively and (B) the free fatty acid fraction isolated from rat brain homogenate after incubation in the presence of room air for 1 h at 37°C. Peaks: 1 = HDHA; 2, 3 = HPDHA.

gram of tissue, wet weight. This method could detect >0.5 μg of HPDHA per gram wet weight.

RESULTS

A representative HPLC separation of the HPDHA and HDHA standards prepared as described above and used in this study is shown in Fig. 2, tracing A. Under the described conditions adequate baseline separation of the two compounds was achieved. Since these standards were prepared in this laboratory, their identity was verified by GC–MS. The respective peaks were isolated by using HPLC, methylated and hydrogenated. Trimethylsilyl derivatives of these products behaved identically during GC–MS. The fragmentation pattern indicated that the common endproduct was 17-hydroxymethyldocosanoate.

For recovery experiments, 8.8 μg of HPDHA were added to 2 ml of 10% rat brain homogenate and the mixture kept on ice for 10 min prior to extraction of the lipids and their fractionation as described above. The recovery of HPDHA added directly to rat brain homogenate was 78%.

The free fatty acid fraction isolated after rat brain homogenates had been incubated for 1 h in the presence of room air showed a peak corresponding to HPDHA (Fig. 2, tracing B). No HPDHA was found before incubation. Homogenates incubated in the presence of room air for 1 h contained 3.1 ± 0.4 ($n=5$) μg HPDHA per gram of tissue, wet weight. Homogenates incubated for 1 h in the presence of nitrogen or BHT did not contain any HPDHA. None of the samples studied contained any HDHA.

DISCUSSION

Fatty acid hydroperoxides have been considered either unstable[8] or to be immediately reduced after formation *in vivo*[9]. We[7] and others[10,11] found HPDHA to be sufficiently stable to permit its analysis by HPLC. In our previous study[7], where HPDHA (1 mg/ml) was added to brain lipid extracts, the recovery of HPDHA was determined to be 87%. The high extinction coefficient of HPDHA at 235 nm permits

the accurate quantitation of smaller amounts. We now show that the recovery of 8.8 μg HPDHA added to rat brain homogenates before the lipids were extracted is 78%. The somewhat lower recovery seen in the present study could be related to the smaller amounts of HPDHA used.

Our findings would then suggest that RPHPLC could be an important tool for quantitating small amounts of HPDHA. This tool could facilitate studies wherein brain homogenates are investigated for their ability to produce one oxidation product of DHA, namely HPDHA, during oxidative stress.

ACKNOWLEDGEMENTS

This study was supported by the Veteran's Administration. We are indebted to Dr. Tom Krick of the University of Minnesota Mass Spectrometry Lab for his help and advice on the analyses and interpretation of the GC–MS data.

REFERENCES

1 D. Harman, *Proc. Natl. Acad. Sci. U.S.A.*, 78 (1981) 712.
2 D. E. Eddy and D. J. Harman, *Am. Geriatric Soc.*, 15 (1977) 220.
3 D. K. Anderson and E. E. Means, *Free Radicals Biol. Med.*, 1 (1985) 59.
4 N. Salem, Jr., H. Kim and J. A. Yergey, in A. P. Simopoulos, R. R. Kifer and R. E. Martin (Editors), *Health Effects of Polyunsaturated Fatty Acids in Seafoods*, Academic Press, New York, 1986, p. 263.
5 M. Hamberg and B. J. Samuelson, *Biol. Chem.*, 242 (1967) 5329.
6 E. Kaplan and K. A. Ansari, *J. Chromatogr.*, 350 (1985) 435.
7 K. A. Ansari and D. Shoeman, *J. Chromatogr.*, 439 (1988) 453.
8 H. Frank, M. Wiegand, M. Strecker and D. Thiel, *Lipids*, 22 (1987) 689.
9 M. VanRollins and R. C. Murphy, *J. Lipid Res.*, 25 (1984) 507.
10 H. W.-S. Chan and F. A. A. Prescott, *Biochim. Biophys. Acta*, 380 (1975) 141.
11 H. Hughes, C. V. Smith, E. C. Horning and J. R. Mitchell, *Anal. Biochem.*, 130 (1983) 431.

Journal of Chromatography, 475 (1989) 461–466
Elsevier Science Publishers B.V., Amsterdam — Printed in The Netherlands

CHROM. 21 597

Note

Isolation of hydroxy fatty acids from livers of carbon tetrachloride-treated rats by thin-layer chromatography

Z. L. BANDI*,[a] and G. A. S. ANSARI
Department of Pathology, The University of Texas Medical Branch, Galveston, TX 77550 (U.S.A.)
(First received May 18th, 1988; revised manuscript received April 25th, 1989)

Non-enzymatic auto-peroxidation of polyunsaturated fatty acid moieties of glycerophosphatides has been a proposed mechanism of membrane damage induced by several toxins and reactive oxygen intermediates[1–5]. Most studies on the relationship of lipid peroxidation to toxicity have depended either on indirect and non-specific methods for quantification of peroxidation[1–4] or on the identification of some parts of the oxidation products. Hughes *et al.*[5] have identified conjugated double-bond containing peroxidation products of one class of glycerophosphatides, phosphatidylcholines, from the liver of carbon tetrachloride-treated mouse. Consequently, the structure of the *in vivo* lipid peroxidation products and the underlying mechanism are still mostly obscure.

The objective of our work was to isolate all long-chain products of *in vivo* non-enzymatic auto-peroxidation of glycerophosphatide fatty acids which are formed following carbon tetrachloride poisoning. Since the work of Hughes *et al.*[5] indicated that peroxidized lipids were rapidly converted *in vivo* to the corresponding hydroxy acids, we developed a method for isolation of all 12–22 carbons long hydroxy fatty acids, conjugated and not conjugated, from all classes of glycerophosphatides without *in vitro* peroxidation during chemical and chromatographic manipulations of the tissue lipids.

EXPERIMENTAL

All thin-layer chromatography (TLC) plates were pre-coated and were obtained from Analtech, Newark, DE, U.S.A. TLC was carried out at ambient laboratory temperatures (about 22°C) in standard TLC glass chambers (inside dimensions: 7.3 × 27.5 × 26 cm) lined with filter paper. Before chromatography, the solvents were allowed to saturate the chambers for about 10–20 min. Unless otherwise stated, the plates were developed until the solvent front reached the top, about 18 cm from the origin.

[a] Present address: Veteran's Administration Medical Center, Laboratory Services, Temple, TX 76501, U.S.A.

0021-9673/89/$03.50

Extraction of liver lipids[6]

Male Sprague-Dawley rats, weighing 200–250 g, were obtained from Harlen, Houston, TX, U.S.A. Two rats were fasted 12 h overnight prior to receiving carbon tetrachloride (10 mmol/kg) dissolved in mineral oil (1:1, v/v) by gavage. The animals were killed 60 min after dosing by decapitation, exsanguinated, and their livers were excised and kept on ice prior to extraction of lipids. The livers were weighed and total lipids were extracted with 20 volumes of chloroform–methanol (2:1, v/v) containing 0.05% (w/v) 2,6-di-*tert*-butyl-*p*-cresol (BHT). After filtration, the filtrate was washed with 0.2 volume of 0.8% aqueous sodium chloride and centrifuged at 9500 *g* at 4°C to separate the chloroform and water phases. The chloroform layer was removed and concentrated to 2 ml on a rotary evaporator under reduced pressure in oxygen-free nitrogen at 20°C. Water was removed from the lipid extract by repeated addition and evaporation of chloroform. The last 2 ml of chloroform was removed from the lipid extract by addition and evaporation of 50 ml of toluene. The extraction and evaporation procedures were performed in the dark.

Hydrogenation of total-liver lipids

To hydrogenate 700 mg of total-liver lipid extract, 500 mg catalyst (5 or 10 % platinum on charcoal) was placed in a micro hydrogenerator (Supelco, Bellefonte, PA, U.S.A.) and 5 ml of acetic acid–toluene (1:1, v/v) was added. The mixture was stirred by a magnetic stirrer for 15 min under 344.7 kPa (50 lb/in.^{2}) of hydrogen to activate the catalyst. Then, the lipids dissolved in 15 ml of acetic acid–toluene (1:1, v/v) were transferred into the micro hydrogenerator and were hydrogenated at room temperature for 24–48 h under 344.7 kPa (50 lb/in.^{2}) of hydrogen. After hydrogenation, the catalyst was removed by centrifugation and the solvents were removed under reduced pressure by addition and evaporation of toluene.

Isolation of liver phospholipids

Phospholipids were isolated as described earlier[7]. Briefly, to a 2 mm thick, 20 × 20 cm silica gel G TLC plate, about 150–180 mg of hydrogenated total-lipid mixture (0.16 mmol lipid-phosphorus) was applied as a 1 or 2 cm wide band. The plates were developed 3 times by using acetone–chloroform–methanol–acetic acid (50:39:10:1, v/v) as developing solvent. Between developments, the plates were dried for 30 min.

To recover the phospholipids, silica gel was scraped from the place of application and from a 2-cm band above the origin and the phospholipids were eluted with chloroform–methanol–water–acetic acid (50:39:10:1, v/v). After elution, to 100 ml elution solvent, 28 ml of chloroform and 17 ml of 0.85% sodium chloride were added. The mixture was shaken and centrifuged for 40 min at 9500 *g*. The upper phase was removed and the lower phase was evaporated under reduced pressure.

Separation of glycerophosphatides and sphingomyelin[8]

To a 2 mm thick, 20 × 20 cm silica gel H TLC plate, about 100 mg of hydrogenated phospholipids (0.13 mmol lipid-P) were applied. The plates were developed by using chloroform–methanol–water (80:35:5, v/v/v). The position of phospholipids on the plate was detected by spraying the plates with water and comparing the lipid pattern with another plate which was charred after spraying with methanol–sulfuric acid (1:1, v/v) at 100°C.

To recover the glycerophosphatides, silica gel was scraped from the plate from the bottom of the phosphatidylcholine band to the top of the plate and the phospholipids were eluted from the silica gel as described above.

Mild alkaline hydrolysis of glycerophosphatides[9]

An amount of 50 mg of phospholipids was dissolved in 8 ml of chloroform–methanol (1:1, v/v) and 2 ml of 0.5 *M* sodium methoxide in methanol was added. Trans-esterification of glycerophosphatides was allowed to proceed at room temperature for 60 min and then, 2 ml of 0.5 *M* HCl, 1 ml water and 4 ml chloroform were added. The mixture was shaken and centrifuged for 5 min at 9500 *g*. The upper aqueous layer was discarded and the lower phase was evaporated. Water was removed from the lipid residue by repeated addition and evaporation of chloroform.

Isolation of hydroxy fatty acids

The products of alkaline hydrolysis of 100 mg liver glycerophosphatides were applied to a 1 mm thick, 20 × 20 cm silica gel G plate. Both sides of the glass plate were scored 2.5 cm from the vertical edge (Prep-scored uniplate, Analtech, Newark, DE, U.S.A.). The lipids to be fractionated were applied between the two score marks in the middle part of the plate. A mixture of C_{12} and C_{24} hydroxy fatty acid methyl esters was placed on both side of the plate about 1.2 cm from the vertical edge to serve as standards. The plates were developed by using hexane–ether (1:1, v/v) as developing solvent. During the first development, the solvent was allowed to migrate to about 10 cm from the origin. The plates were dried and then developed in the same solvent system once more. After the second development, the 2.5 cm wide strips were snapped off, charred at 100°C after spraying with methanol–sulfuric acid (1:1, v/v) and were compared with the middle part of the plate. The hydroxy fatty acid fraction of the glycerophosphatide hydrolysate, located between the hydroxy fatty acid standards, were scraped off and were eluted from the silica gel with chloroform–methanol, (9:1, v/v).

Synthesis of hydroxy fatty acid methyl ester standards

The hydroxy fatty acid methyl esters used as chromatographic standards were synthesized as described earlier.[10]

RESULTS AND DISCUSSION

Fig. 1 shows the sequence of procedures used for isolation of hydroxy fatty acid moieties of rat liver glycerophosphatides. The described methods had two principle objectives:

(1) To assure that the isolated oxygenated fatty acids of liver glycerophosphatides were peroxidized *in vivo* and not after the lipids were extracted from the livers.

(2) To ensure that the isolated hydroxy fatty acids originated from the glycerophosphatides and not from other lipids of the livers.

To minimize peroxidation of liver lipids during the extraction procedures, the lipids were protected by (i) adding antioxidant (BHT), and (ii) performing the procedures in the dark under nitrogen atmosphere at temperatures below 20°C.

The optional step of hydrogenation of the total-lipid mixture was included to

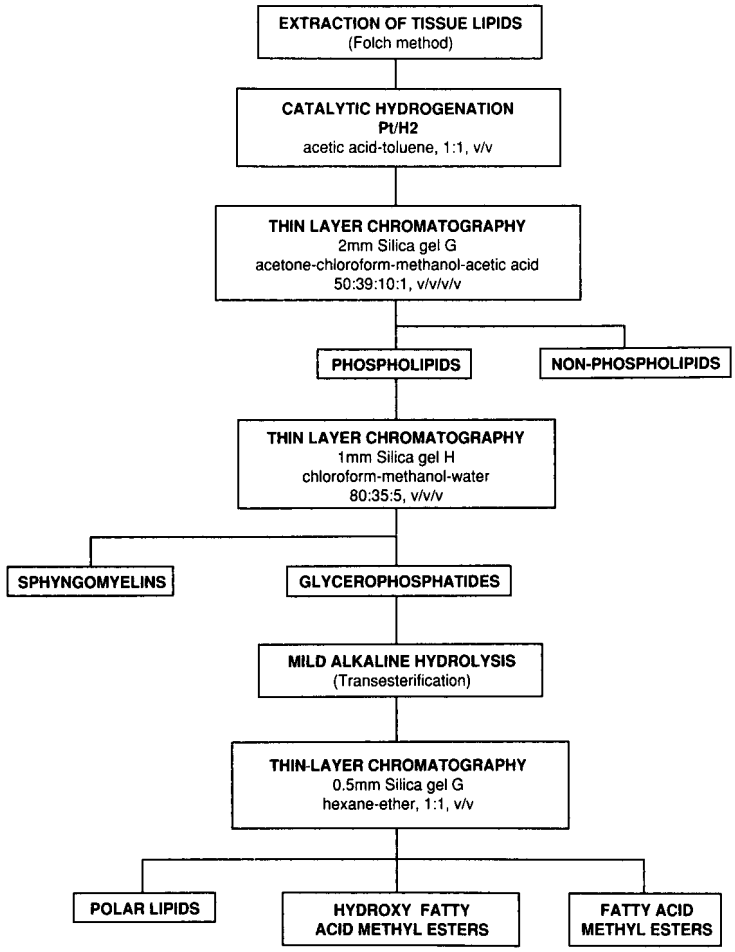

Fig. 1. Isolation of hydroxy fatty acids from rat liver glycerophosphatides.

eliminate the possible peroxidation of the unsaturated fatty acids during chemical and chromatographic procedures. This step is especially useful to determine the trace amounts of hydroxy fatty acids in livers of normal rats[5]. The hydrogenation step, however, could be eliminated if the objective was to determine the position of double bonds in the peroxidized fatty acids.

Following the hydrogenation, vigorous purification of the glycerophosphatides was achieved by two chromatographic procedures. These steps were necessary to assure that hydroxy fatty acids were isolated from glycerophosphatides only. The purification could not be achieved in a single TLC procedure because the rat liver lipids were found to contain trace amounts of some polar compounds. These compounds seemed to contain neither phosphorous nor carbohydrate moieties but they overlapped with glycerophosphatides during TLC[7]. These compounds were removed, together with the neutral lipids, from the glycerophosphatides by the first chroma-

tographic solvent system which contained acetone to prevent the phospholipids migrating away from the origin[7].

Sphingomyelins were separated from the glycerophosphatides because these compounds were known to contain hydroxy fatty acids[11] and because we could not confirm the complete stability of sphingomyelins during the mild alkaline hydrolysis as reported[9]. After repeated purification of the sphingomyelins by combined mild alkaline hydrolysis and TLC, we found trace amounts of unknown compounds that were still released from sphingomyelins during the alkaline hydrolysis.

Fig. 2 demonstrates the isolation of hydroxy fatty acids from alkaline hydrolysate of purified glycerophosphatides. The hydroxy fatty acids thus isolated can be fractionated according to chain length and according to the position of the hydroxyl group by reserved-phase and adsorption high-performance liquid chromatography

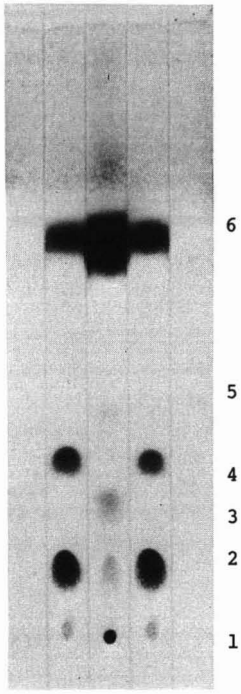

Fig. 2. Isolation of hydroxy fatty acid methyl esters from alkaline hydrolysate of rat liver glycerophosphatides. Developing solvent: hexane–diethyl ether (1:1, v/v). Plate: 0.25 mm thick silica gel G. The plate was charred at 100°C after spraying with methanol–sulfuric acid (1:1, v/v). Lanes A and C are mixtures of chromatographic standards containing C_{12} and C_{24} hydroxy fatty acid methyl esters (methyl 12-OH-dodecanoate and methyl 16-OH-tetracosanoate, respectively) and methyl oleate. Lane B is a sample from the alkaline hydrolysate of glycerophosphatides of carbon tetrachloride dosed rats. (1) is the origin of the chromatogram, containing compounds more polar then C_{12} hydroxy fatty acid methyl ester; (2) in lanes A and B is C_{12} hydroxy fatty acid methyl ester; and (3) in lane B are hydroxy fatty acid methyl esters from the hydrolyzed glycerophosphatides; (4) in lanes A and B is C_{24} hydroxy fatty acid methyl ester; (5) in lane B is trace amounts of unesterified fatty acids; (6) in lanes A and C is methyl oleate and in lane B fatty acid methyl esters from the hydrolyzed glycerophosphatides.

(HPLC), respectively as described earlier[10,12]. The combined chemical and chromatographic properties of the isolated fatty acids (before and after derivatization, TLC purification and reversed-phase HPLC analysis) confirmed the presence of both acyl and hydroxyl groups in the isolated compounds.

The method described for isolation of *in vivo* peroxidized acyl moieties of glycerophosphatides is elaborate but it is more useful than the existing methods because (i) the possible peroxidation of unsaturated fatty acids during manipulation of the lipids is kept to a minimum by hydrogenation of the total liver lipids immediately after extraction from the tissues, (ii) the detection of oxygenated fatty acids does not depend on the presence of conjugated double bonds. The method is able to isolate all long-chain (C_{12}–C_{24}) hydroxy fatty acids, (iii) the procedure can be used for both qualitative and for quantitative analysis (with added internal standards) of the isolated hydroxy fatty acids and (iv) the method can be modified to isolate short-chain hydroxy fatty acids, as esters of butanol, at both micro and preparative scales.

ACKNOWLEDGEMENT

This research was supported by a grant DK27135 awarded by the National Institute of Diabetes, Digestive and Kidney Diseases.

REFERENCES

1 H. Kappus and H. Sies, *Experientia*, 37 (1981) 1233.
2 R. O. Recknagel, E. A. Glende and A. M. Hruszkewycz, in W. A. Pryor (Editor), *Free Radicals in Biology*, Vol. 3, Academic Press, New York, 1977, pp. 97–132.
3 A. L. Tappel, in W. A. Pryor (Editor), *Free Radicals in Biology*, Vol. 4, Academic Press, New York, 1980, pp. 1–47.
4 M. K. Logani and R.E. Davies, *Lipids*, 15 (1980) 485.
5 H. Hughes, C. V. Smith, E. C. Horning and J. R. Mitchell, *Anal. Biochem.*, 130 (1983) 431.
6 J. Folch, M. Lees and G. H. Stanley, *J. Biol. Chem.*, 226 (1957) 497.
7 Z. L. Bandi and G. A. S. Ansari, *J. Chromatogr.*, 435 (1988) 513.
8 P. D. S. Wood and S. Holton, *Proc. Soc. Exp. Biol. Med.*, 115 (1964) 990.
9 G. V. Marinetti, *J. Lipid Res.*, 3 (1962) 1.
10 Z. L. Bandi and E. S. Reynolds, *J. Chromatogr.*, 329 (1985) 57.
11 G. B. Ansell and J.N. Hawthorne (Editors), *Phospholipids*, Elsevier, Amsterdam, 1964, p. 35.
12 Z. L. Bandi and G. A. S. Ansari, *J. Chromatogr.*, 363 (1986) 402.

Author Index

Vol. 475

journal of chromatography news section

NEW BOOKS

HPLC in food analysis, 2nd ed., edited by R. Macrea, Academic Press, London, 1988, 502 pp., price £37.00, ISBN 0-12-464781-2.

Advances in electrophoresis, Vol. 2, edited by A. Chrambach, M.J. Dunn and B.J. Radola, VCH Verlagsgesellschaft, Weinheim, Basle, Cambridge, New York, 1988, X + 456 pp., price DM 178.00. £ 62.00, ISBN 3-527-26946-0.

Advanced scientific computing in BASIC with applications in chemistry, biology and pharmacology (*Data Handling in Science and Technology*, Vol. 4), by P. Valkó and S. Vajda, Elsevier, Amsterdam, Oxford, New York, Tokyo, 1989, XVII + 322 pp., price Dfl. 190.00, US$ 100.00, ISBN 0-444-87270-1, 5.25″ Diskette, price Dfl. 110.00, US$ 58.00, ISBN 0-444-87271-X.

Procédés de séparation par membranes: transport, techniques membranaires, applications, par J.-P. Brun, Masson, Paris, 1988, 288 pp., prix FF 195.00, ISBN 2-225-81573-9.

Polymers in microelectronics, fundamentals and applications, by D.S. Soane and Z. Martynenko, Elsevier, Amsterdam, Oxford, New York, Tokyo, 1989, XIV + 308 pp., price Dfl. 225.00, US$ 95.00, ISBN 0-444-87290-6.

Atmospheric ozone research and its policy implications (*Proceedings of the 3rd US–Dutch International Symposium, Nijmegen, The Netherlands, May 9–13, 1988*), edited by T. Schneider, S.D. Lee, G.J.R. Wolfers and L.D. Grant, Elsevier, Amsterdam, Oxford, New York, Tokyo, 1989, XVIII + 1048 pp., price Dfl. 395.00, US$ 208.00, ISBN 0-444-87266-3.

ANNOUNCEMENTS OF MEETINGS

2nd INTERNATIONAL SYMPOSIUM ON CHIRAL SEPARATIONS, NOTTINGHAM, U.K., SEPTEMBER 12–15, 1989

The Chromatographic Society in conjunction with The Robens Institute are holding the 2nd International Symposium on Chiral Separations at the University of Surrey, Guildford, U.K. from September 12–15, 1989

Among topics to be covered are: metabolic and pharmacokinetic importance of chirality; chiral stationary phases for HPLC, GLC and TLC; preparative approaches; chiroptical detection; applications such as the measurement of drugs, agrochemicals etc.

There will also be a manufacturers exhibition.

Further details are available from: The Executive Secretary, The Chromatographic Society, Trent Polytechnic, Burton Street, Nottingham NG1 4BU, U.K. Tel.: (0602) 418248.

2nd INTERNATIONAL SYMPOSIUM ON HIGH PERFORMANCE CAPILLARY ELECTROPHORESIS, SAN FRANCISCO, CA, U.S.A., JANUARY 29–31, 1990

Following upon the highly successful 1st International Symposium on Capillary Electrophoresis (HPCE '89) held in Boston in April 1989, the 2nd International Symposium (HPCE '90) will be held January 29–31, 1990, at the San Francisco Hilton on Hilton Square, San Francisco, CA, U.S.A.

The three-day program will include lectures, poster presentations and discussion sessions. Topics will include zone electrophoresis, isoelectric focusing, micellar separations, CE–mass spectrometry, gel columns, isotachophoresis, detector design, instrumentation and analytical and micropreparative applications for pharmaceuticals, peptides, proteins, carbohydrates, oligonucleotides, sub-cellular structures and whole cells.

Invited lectures will be presented by Aharon S. Cohen (Northeastern University), Franz M. Everaerts (Eindhoven University of Technology), Andrew G. Ewing (Pennsylvania State University), Eli Grushka (Hebrew University), Jack Henion (Cornell University), Stellan Hjertén (University of Uppsala), James W. Jorgenson (University of North Carolina), Barry L. Karger (Northeastern University), Milos Novotny (Indiana University), Tsuneo Okuyama (Tokyo Metropolitan University), Fred E. Regnier (Purdue University), Pier Giorgio Righetti (University of Milan), Richard D. Smith (Batelle Northwest Labs), Shigeru Terabe (Kyoto University), Edward S. Yeung (Iowa State University), Richard N. Zare (Stanford University) among others to be announced.

Abstracts describing original research in the area of capillary electrophoresis are invited. The deadline for submission of abstracts is September 1, 1989. Papers presented at the symposium will be reviewed for publication in a special volume of the *Journal of Chromatography.* Complete manuscripts will be due at the time of the symposium.

The advance registration fee will be US$ 350, which covers all scientific and social events, admission to the instrumentation exhibit and a copy of the proceedings volume. The registration fee for students and post-doctoral fellows will be US$ 150 and will not include the proceedings volume.

For further information and abstracts forms, please contact: Shirley Schlessinger, Symposium Manager HPCE '90, 400 East Randolph Street, Suite 1015, Chicago, IL 60601, U.S.A. Tel.: (312) 527-2011.

41st PITTSBURGH CONFERENCE AND EXPOSITION ON ANALYTICAL CHEMISTRY AND APPLIED SPECTROSCOPY, NEW YORK, NY, U.S.A., MARCH 5–9, 1990

The 1990 technical program of the Pittsburgh Conference will continue a 40 year tradition of excellent symposia and high quality contributed papers. The largest attendance in conference history is expected at this meeting to be held in the The Jacob K. Javits Convention Center in New York, NY, U.S.A., March 5–9, 1990.

The program features symposia covering a wide range of current topics in chemical analysis and applied spectroscopy arranged by outstanding scientists from diverse disciplines. You are invited to submit an abstract for either a poster or oral presentation in the fields of chemical analysis and applied spectroscopy. A special educational program which includes short courses, UMIX symposia, workshops, and round table discussions will be offered as well. The program committee will be pleased to consider your abstract for the 1990 Pittsburgh Conference technical program. The instructions for submission of abstracts and the deadline are given below.

Original papers may be contributed in all areas of analytical chemistry, spectroscopy and associated fields. One copy of a 250-word abstract must be submitted for review. The deadline for receipt of abstracts is August 4, 1989. All abstracts will be carefully evaluated. The abstract should clearly state (a) the objective of the work, (b) equipment and procedures used, and (c) results and conclusions. Abstracts must include sufficient content for adequate evaluation by the conference program committee. The Pittsburgh Conference reserves the right to accept, put on waiting list, or reject any paper. In November 1989 the designated speaker will be informed of the paper's status: accepted, on the waiting list, or rejected. Specific references to vendor products in the titles of papers are not permitted and will be automatically deleted. No conference proceedings will be published. Authors may publish their papers after the conference. A second abstract will be required for reproduction in book form

for distribution to the conferees. Forms and instructions concerning this second abstract will be sent to the designated speaker with the notification of acceptance of the paper. The abstract for publication will be due December 8, 1989. The title of the paper and the author information originally submitted cannot be changed for the second abstract; therefore, be sure you have the desired title and author information on the original abstracts. The Pittsburgh Conference does not provide financial support to authors of contributed papers.

Authors wishing to present papers in the 1990 Pittsburgh Conference and Exposition Technical Program should submit one copy of a 250-word abstract by August 4, 1989 to: Mrs. Alma Johnson, Program Secretary, The Pittsburgh Conference, 300 Penn Center Blvd., Suite 332, Pittsburgh, PA 15235, U.S.A. Enclose a self-addressed envelope which will be returned to indicate receipt of abstract, but will not indicate acceptance of the abstract for the 1990 Pittsburgh Conference Program.

COLACRO III, 3rd LATIN-AMERICAN CONGRESS ON CHROMATOGRAPHY, SÃO PAULO, BRASIL, MARCH 14–16, 1990

The third Latin-American Congress on Chromatography (COLACRO III) will be held in São Paulo, Brasil, March 14–16, 1990.

COLACRO will cover both pure and applied aspects of chromatographic science (gas chromatography, high-performance liquid chromatography, supercritical-fluid chromatography, gas chromatography–mass spectrometry etc.). The programme includes plenary lectures by invited speakers, poster sessions of submitted papers, workshop seminars and short courses. In conjunction with the congress there will be an exhibition of instruments and accessories by local and international companies. The congress language will be English and Spanish. No simultaneous translation system will be provided.

For further information please contact: Dr. Fernando M. Lanças, Universidade de São Paulo, Instituto de Física e Química de São Carlos, 13560 São Carlos, SP Brasil. Tel.: (0162) 726222, ext. 275; telex: (16) 2374 FQSC BR.

BIOCHEMISCHE ANALYTIK 90, 12th INTERNATIONAL CONFERENCE ON BIOCHEMICAL ANALYSIS, MÜNCHEN, F.R.G., MAY 8–11, 1990

The next conference Biochemische Analytik 1990 is coming forth and, as usual, will be held in the Munich Trade-Fair Centre. The main subjects of this conference will in particular be issues of environmental analytics and modern methods of molecular biology and genetic engineering.

Once again the poster exhibition is to reflect the entire spectrum of analytics within the scope of biosciences. The deadline for submission of posters is November 15, 1989. A special exhibition will be dedicated to current problems of environmental analytics.

As has been the case in previous years, the "Analytica-Forum München" will offer to representatives of the industry the opportunity to present and discuss new apparatus and analytical methods in addition to the trade exhibition.

For further information contact: Ulrike Arnold, Anneli Höhnke, Nymphenburger Strasse 70, D-80000 München 2, F.R.G. Tel.: (089) 1 23 45 00; fax: (089) 18 32 58.

2nd SCIENTIFIC COMPUTING AND AUTOMATION (EUROPE) CONFERENCE AND EXHIBITION, MAASTRICHT, THE NETHERLANDS, JUNE 12–15, 1990

The 2nd Scientific Computing and Automation (SCA) conference and exhibition will be held at the new MECC Centre in Maastricht, The Netherlands, June 12–15, 1990.

The topics for SCA (Europe) will include: chemical applications for supercomputers; sample strategies and experimental design; online databases in chemistry; databases for spectroscopy; dynamic models for catalysis, processes and metabolism; expert systems and statistical tools for the intrepretation of laboratory data; robotic and discrete automation in the laboratory; interfacing tools, soft-

ware and hardware tools; chemical monitoring, multivariate sensors and biosensors; LIMS and LAN strategies for the laboratory; workstations for the scientist, RISC, parallel and traditional; scientific applications for neural networks and fractals; software toolkits for exploratory data analysis and mathematics, computer graphics and image analysis; designing molecules by computer; Europe 1992: implications for standardisation across borders.

Special abstract forms are available for those interested in submitting a paper for the conference. The deadline for abstracts will be February 1, 1990.

There will also be an exhibition giving manufacturers and distributors an unparalleled opportunity to meet delegates and visitors.

For further details contact: SCA (Europe), c/o Reunion International, WG plein 475, 1054 SH Amsterdam, The Netherlands. Tel.: (020) 165151; fax: (020) 890981.

7th SYMPOSIUM ON LIQUID CHROMATOGRAPHY–MASS SPECTROSCOPY (LC–MS, MS–MS, SFC–MS), MONTREUX, SWITZERLAND, OCTOBER 31–NOVEMBER 2, 1990

The 7th Symposium on Liquid Chromatography–Mass Spectroscopy, organized by the International Association of Environmental Analytical Chemistry will be held at the Congress Center in Montreux, Switzerland, October 31–November 2, 1990.

The symposium, devoted to the late Roland W. Frei, will deal with all areas of this topic including technical developments with on-line aspects, theoretical considerations and applications of the techniques in environmental, clinical and pharmaceutical analysis and other fields. Subtopics will be introduced by plenary lectures and invited research lectures followed by brief research presentations and posters. A major portion of the workshop will be devoted to panel and group discussions on the state-of-art of LC–MS, SFC–MS and MS–MS. The symposium will be preceded by a 2-day short course on LC–MS, October 29–30, 1990.

An exhibition will find place during the five days.

Those interested in giving a research lecture or a poster presentation should send an abstract of no more than 200 words to the chairman by November 1, 1989: Professor J. van der Greef, Center for Bioanalytical Sciences, P.O. Box 9502, NL-2300 RA Leiden, The Netherlands.

For preliminary registration contact: M. Frei-Häusler, Strengigässli 20, CH-4123 Allschwil, Switzerland.

5th INTERNATIONAL CONFERENCE ON FLOW ANALYSIS, KUMAMOTO, JAPAN, AUGUST 21–24, 1991

The 5th International Conference of Flow Analysis will be held in Kumamoto, Japan on August 21–24, 1991. It will be organized by The Japanese Association for Flow Injection Analysis.

The scope of the Conference will cover current research on all aspects of continuous flow analysis. The topics will include: instrumentation for flow injection analysis and for continuous segmented and unsegmented flow analysis, inlcuding approaches to total automation; new detector systems and hybrid systems; theory of flow analysis; applications in industrial, environmental and clinical analysis.

The scientific programme will consist of plenary and invited lectures, submitted research papers and posters, and working demonstrations. Authors who wish to present papers should submit abstracts before 28 February 1991. For further information contact: Professor Nobuhiko Ishibashi, Department of Applied Analytical Chemistry, Faculty of Engineering 36, Kyushu University, Hakozaki, Higashiku, Fukuoka 812, Japan.

COURSES

ANALYTICAL CHEMISTRY SHORT COURSES, LOUGHBOROUGH, U.K.

The following short courses will be held in the Department of Chemistry, University of Technology, Loughborough, U.K. during September 1989:
— Basic microbiological methods for the analytical chemist; September 11–15, 1989; fee £510 including residence and all meals. Non-residents £435.
— Immunoassay; September 11–15, 1989; fee £480 including residence and all meals. Non-residents £405 (for both £30 discount if paid in advance).
— Microcomputers in the laboratory; September 11–15, 1989; fee £480 including residence and all meals. Non-residents £405 (for both £30 discount if paid in advance).
— Stability of drugs and formulations; September 18–22, 1989; fee £480 including residence and all meals. Non-residents £405 (for both £30 discount if paid in advance).
— High-performance liquid chromatography; September 18–22, 1989; fee £480 including residence and all meals. Non-residents £405 (for both £30 discount if paid in advance).
Further details may be obtained from: Mrs. J.E. Stirling, Department of Chemistry, Loughborough University of Technology, Loughborough, Leics. LE11 3TU, U.K. Tel.: (0509) 222549.

BIOCHEMICAL SEPARATION METHODS, UPPSALA, SWEDEN, MARCH 27–JUNE 7, 1990

The course on Biochemical Separation Methods (Uppsala Separation School), organized by Professors Stellan Hjertén and Paul Roos, will be held at the Department of Chemistry, University of Uppsala, Uppsala, Sweden, March 27–June 7, 1990.

The course is centered around modern analytical and preparative methods in biochemistry and biotechnology. Methods for the separation of cells, virus, proteins and nucleic acids, and their characterization will be treated. The course consists of lectures and laboratory work dealing with the following methods: moving boundary electrophoresis; free zone electrophoresis; zone electrophoresis in both sieving and non-sieving anticonvection media; two-dimensional polyacrylamide gel electrophoresis (O'Farrell-technique); isoelectric focusing, displacement electrophoresis (isotachophoresis); molecular sieve chromatography; hydroxyapatite chromatography; hydrophobic interaction chromatography; covalent chromatography; bioaffinity chromatography; gas chromatography; HPLC; countercurrent distribution (liquid phase partition); analytical and preparative centrifugation methods (centrifugation in different kinds of density gradients, determination of sedimentation coefficients and of molecular weights); immuno-diffusion; rocket immunoelectrophoresis; crossed immunoelectrophoresis; determination of diffusion coefficients; light scattering; spectrofluorometry; radioimmunoassay and radio receptor assay.

Knowledge of biochemistry and mathematics, corresponding to a basic university degree, is required. Good knowledge of English is necessary. The number of participants is limited to 12, 6 from Sweden and 6 from abroad.

The course fee is U.S.$ 750. Living expenses to cover food and accommodation in student rooms will be a minimum of U.S.$ 1700. No fellowships are available through the organizers.

The closing date for application is January 15, 1990

Application forms can be obtained from: Secretary Ulrika Jansson, Department of Biochemistry, University of Uppsala, Biomedical Center, P.O. Box 576, S-751 23 Uppsala, Sweden.

PUBLICATION SCHEDULE FOR 1989

Journal of Chromatography and Journal of Chromatography, Biomedical Applications

MONTH	J	F	M	A	M	J	J	A	S	
Journal of Chromatography	461 462 463/1	463/2 464/1	464/2 465/1 465/2	466 467/1 467/2	468 469 470/1 470/2	471 472/1 472/2 473/1	473/2 474/1 474/2 475	476 477/1 477/2		The publication schedule for further issues will be published later
Bibliography Section		486/1		486/2		486/3		486/4		
Biomedical Applications	487/1	487/2	488/1 488/2	489/1 489/2	490/1 490/2	491/1	491/2	492 493/1	493/2	

INFORMATION FOR AUTHORS

(Detailed *Instructions to Authors* were published in Vol. 445, pp. 453–456. A free reprint can be obtained by application to the publisher, Elsevier Science Publishers B.V., P.O. Box 330, 1000 AH Amsterdam, The Netherlands.)

Types of Contributions. The following types of papers are published in the *Journal of Chromatography* and the section on *Biomedical Applications:* Regular research papers (Full-length papers), Notes, Review articles and Letters to the Editor. Notes are usually descriptions of short investigations and reflect the same quality of research as Full-length papers, but should preferably not exceed six printed pages. Letters to the Editor can comment on (parts of) previously published articles, or they can report minor technical improvements of previously published procedures; they should preferably not exceed two printed pages. For review articles, see inside front cover under Submission of Papers.

Submission. Every paper must be accompanied by a letter from the senior author, stating that he is submitting the paper for publication in the *Journal of Chromatography*. Please do not send a letter signed by the director of the institute or the professor unless he is one of the authors.

Manuscripts. Manuscripts should be typed in double spacing on consecutively numbered pages of uniform size. The manuscript should be preceded by a sheet of manuscript paper carrying the title of the paper and the name and full postal address of the person to whom the proofs are to be sent. Authors of papers in French or German are requested to supply an English translation of the title of the paper. As a rule, papers should be divided into sections, headed by a caption (*e.g.*, Summary, Introduction, Experimental, Results, Discussion, etc.). All illustrations, photographs, tables, etc., should be on separate sheets.

Introduction. Every paper must have a concise introduction mentioning what has been done before on the topic described, and stating clearly what is new in the paper now submitted.

Summary. Full-length papers and Review articles should have a summary of 50–100 words which clearly and briefly indicates what is new, different and significant. In the case of French or German articles an additional summary in English, headed by an English translation of the title, should also be provided. (Notes and Letters to the Editor are published without a summary.)

Illustrations. The figures should be submitted in a form suitable for reproduction, drawn in Indian ink on drawing or tracing paper. Each illustration should have a legend, all the *legends* being typed (with double spacing) together on a *separate sheet*. If structures are given in the text, the original drawings should be supplied. Coloured illustrations are reproduced at the author's expense, the cost being determined by the number of pages and by the number of colours needed. The written permission of the author and publisher must be obtained for the use of any figure already published. Its source must be indicated in the legend.

References. References should be numbered in the order in which they are cited in the text, and listed in numerical sequence on a separate sheet at the end of the article. Please check a recent issue for the layout of the reference list. Abbreviations for the titles of journals should follow the system used by *Chemical Abstracts*. Articles not yet published should be given as "in press" (journal should be specified), "submitted for publication" (journal should be specified), "in preparation" or "personal communication".

Dispatch. Before sending the manuscript to the Editor please check that the envelope contains three copies of the paper complete with references, legends and figures. One of the sets of figures must be the originals suitable for direct reproduction. Please also ensure that permission to publish has been obtained from your institute.

Proofs. One set of proofs will be sent to the author to be carefully checked for printer's errors. Corrections must be restricted to instances in which the proof is at variance with the manuscript. "Extra corrections" will be inserted at the author's expense.

Reprints. Fifty reprints of Full-length papers, Notes and Letters to the Editor will be supplied free of charge. Additional reprints can be ordered by the authors. An order form containing price quotations will be sent to the authors together with the proofs of their article.

Advertisements. Advertisement rates are available from the publisher on request. The Editors of the journal accept no responsibility for the contents of the advertisements.

Books for the Practising Chromatographer

SELECTIVE SAMPLE HANDLING AND DETECTION IN HIGH-PERFORMANCE LIQUID CHROMATOGRAPHY, PART A

***edited by* R.W. Frei *and* K. Zech**

(Journal of Chromatography Library, 39A)

This is the first of a 2-part work which attempts to treat the sample handling and detection processes in a liquid chromatographic system in an integrated fashion. The need for more selective and sensitive chromatographic methods to help solve the numerous trace analysis problems in complex samples is undisputed, but few workers realize the strong interdependence of the various steps - sample handling, separation and detection - which must be considered if one wants to arrive at an optimal solution. Since the sample handling side, although recognized as a major bottleneck, has been neglected in the chromatographic literature, special emphasis has here been placed on this aspect. Priority is given to the treatment of chemical principles as applied to the topics in this book, rather than to instrumentation.

1988 470 pages US$ 126.25 / Dfl. 240.00 0-444-42881-X

QUANTITATIVE GAS CHROMATOGRAPHY for laboratory analyses and on-line process control

***by* G. Guiochon *and* C.L. Guillemin**

(Journal of Chromatography Library, 42)

This is a book which no chemical analyst should be without!. It explains how quantitative gas chromatography can – or should – be used for accurate and precise analysis. All the problems involved in the achievement of quantitative analysis by GC are covered, whether in the research laboratory, the routine analysis laboratory or in process control. The theory is kept to essentials and presented in a way simple enough to be understood by all analytical chemists, while being complete and up-to-date. A book which should be in the library of universities, instrument companies and any laboratory or plant where gas chromatography is used.

1988 780 pages US$ 165.75 / Dfl. 315.00 0-444-42857-7

NATURAL PRODUCTS ISOLATION: Separation Methods for Antimicrobials, Antivirals and Enzyme Inhibitors

***edited by* G.H. Wagman *and* R. Cooper**

(Journal of Chromatography Library, 43)

This book describes in great detail the recent progress made in the isolation and separation of natural products. Written by experts in their respective fields, it covers antibiotics, marine and plant-derived substances, enzyme inhibitors and interferons. It offers the reader: up-to-date reviews of specific topics in the natural products field not to be found elsewhere; information on new chromatographic methods and techniques - described in sufficient detail to be utilized by investigators in this area of research; and extensive references to enable the serious researcher to pursue particular information. It will appeal to pharmaceutical and natural products researchers and is a valuable acquisition for university chemistry and biochemistry departments.

1989 634 pages US$ 150.00 / Dfl. 285.00 0-444-87147-0

ANALYTICAL ARTIFACTS: GC, MS, HPLC, TLC and PC

***by* B.S. Middleditch**

(Journal of Chromatography Library, 44)

An easy-to-use, encyclopaedic catalogue of the pitfalls and problems encountered by analysts when using various common analytical techniques. Emphasis is on impurities, by-products, contaminants and other artifacts and more than 1100 entries are included. The book is designed to be *used*. It is destined to spend more time on the workbench than on the library shelf.

1989 1058 pages US$ 260.50 / Dfl. 495.00 0-444-87158-6

OPTIMIZATION OF CHROMATOGRAPHIC SELECTIVITY: A Guide to Method Development

***by* P.J. Schoenmakers**

(Journal of Chromatography Library, 35)

"...an important contribution by a worker who has been in the field almost from its inception and who understands that field as well as anyone. If one is serious about method development, particularly for HPLC, this book will well reward a careful reading and will continue to be useful for reference purposes." (LC-GC, Mag. Liquid and Gas Chromatography)

1986 1st repr. 1988 362 pages US$ 113.25 / Dfl. 215.00; 0-444-42681-7

PREPARATIVE LIQUID CHROMATOGRAPHY

***edited by* B.A. Bidlingmeyer**

(Journal of Chromatography Library, 38)

This book adopts a straightforward approach to isolation and purification problems and gives a thorough presentation of preparative LC strategy including the interrelationship between the input and output of the instrumentation, while keeping to an application focus. It stresses the practical aspects of preparative scale separations from TLC isolations through various laboratory scale column separations to very large scale production. Experts in this field have contributed a well-balanced presentation of separation development strategies from preparative TLC to commercial preparative process with practical examples in many application areas such as drugs, proteins, nucleotides, industrial extracts, organic chemicals, enantiomers, polymers, and others.

1987 1st repr. 1989 356 pages US$ 105.25 / Dfl. 200.00 0-444-42832-1

Prepaid orders are despatched postfree.

ORDERS MAY BE PLACED WITH:

ELSEVIER

P.O. Box 211, 1000 AE Amsterdam, The Netherlands

P.O. Box 882, Madison Square Station, New York, NY 10159, USA.

The Dutch guilder price is definitive. US$ prices are valid only in the USA and Canada.